# Synthesis and SAR Evaluation of Novel Imidazo[1,2-*a*]pyridine Derivatives as Potential *Mycobacterium tuberculosis* PafA Inhibitors


**Haya Saad Alsubaie**

Submitted in the requirements for the degree of Doctor of Philosophy

Biosciences Institute

Newcastle University

May 2025

## Abstract

Tuberculosis (TB) continues to be a significant global health challenge, with the rise of multidrug-resistant (MDR-TB) and extensively drug-resistant (XDR-TB) strains increasing the demand for new therapeutic agents with novel mechanisms of action. Proteasome accessory factor A (PafA) is of particular interest due to its role in the virulence of *Mycobacterium tuberculosis* (*Mtb*) and its poor sequence conservation in humans. This study focuses on the design, synthesis, and biological evaluation of novel imidazo[1,2-*a*]pyridine analogues as antitubercular agents. Specifically, three-series of imidazo[1,2-*a*]pyridine-substituted amino acid hydrazides **44**, comprising a total of 120 novel compounds, are synthesised and evaluated for their activity against both drug-resistant and drug-susceptible *Mtb* strains utilising the Resazurin Microtiter Assay (REMA). A comprehensive structure–activity relationship study is conducted, focusing on the imidazo[1,2-*a*]pyridine scaffold and its three distinct components: the amino acid moiety (R), the hydrazine component ($R_1$), and the phenyl ring attached to the scaffold ($R_2$). Key SAR findings indicate that an increased amino acid side chain size and the incorporation of small halogens at the *meta* position of the phenylhydrazine enhance biological activity. To further elucidate these results, the most active compounds are subjected to *in silico* molecular docking studies to predict their binding interactions with PafA. These findings contribute to ongoing efforts to develop novel and effective antitubercular agents, ultimately advancing therapeutic strategies against TB.


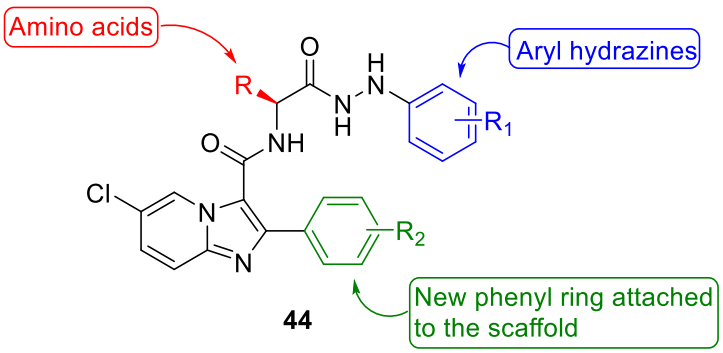


**44**

# Acknowledgements

First and foremost, all praise and gratitude belong to Allah, the Most Merciful, the Most Compassionate. He is the source of strength in moments of weakness, the light in times of darkness, and the ultimate guide through every challenge.

Then, I would like to thank my supervisor Dr. Jon Sellars for giving me the opportunity to pursue this PhD and for his guidance throughout. I also appreciate his valuable feedback on this thesis. My gratitude also extends to Dr. Brown for conducting the biological evaluation of my compounds.

My deepest thanks also go to Dr. Paul for assistance with x- ray crystallography, Dr. C. Wills and Dr. C. Dixon for their assistance in NMR spectroscopy, and Dr. Alex Charlton for his help with mass spectrometry.

Words cannot fully express my gratitude to my amazing family, whose love and support have been my greatest strength. To my father Saad, who instilled confidence in me, and my mother Fatimah, whose prayers have guided every step I take, I hope this achievement makes you proud. To my kind and caring brothers and sisters, your encouragement has meant more than you know. And to my grandchildren, especially Dodi, whose laughter fills our hearts with joy.

A special and heartfelt thanks to my husband, Rajeh, the person who has stood beside me through every moment of this journey. Through struggles and challenges, you have been my rock, lifting me when I felt weak and reminding me of my capabilities when I doubted myself. I could not have done this without you. And to my sunshine, the part of my soul my beloved son Saad, whose pictures fill my laptop wallpaper, desktop, and even printed on my coffee cup, you are my strength and my greatest inspiration. I am endlessly grateful for the light you bring into my life. This journey was never mine alone; it belongs to all of you.

To my friends and lab mates, I could not have asked for better companions in this journey. Special thanks to Dr. Fatimah and Noor, for being more than just colleagues you have been my sisters in this journey. We have laughed, cried, and supported each other through every challenge, and I know that this is just the beginning of a lifelong collaboration and friendship. I am also deeply thankful to Dr. Lina and Max for their kindness, help, and endless conversations that that filled the lab with joy and a sense of belonging.

A heartfelt thank you also to my dear friends in Newcastle, who made it feel like home. Bashair, Sahar, Ohoud, Nourah, Promise, Alaa, Elham and all the wonderful Bedson girls. Finally, to everyone who has been part of this journey, whether through a kind word, a moment of encouragement, or simply by being there thank you.

## Conference presentations

Royal Society of Chemistry Chemical Biology Community Meeting, September 11-12, **2023**, University of Leeds, “Synthesis and SAR Evaluation of Novel Imidazo[1,2-*a*]pyridine Derivatives as Potential *Mycobacterium tuberculosis* PafA Inhibitors” **(Poster Presentation)**

Health Innovation Meeting, supervised by the Saudi Attaché Embassy, Warwick University, Coventry, February 3, **2024 (Oral Presentation, Best Oral Presentation Award)**

BMCS 4th Synthesis in Drug Discovery and Development meeting 4-5th June 2024, “Synthesis and SAR Evaluation of Novel Imidazo[1,2-*a*]pyridine Derivatives as Potential *Mycobacterium tuberculosis* PafA Inhibitors” **(Flash Presentation)**

Dubai Pharmaceuticals and Technologies Conference and Exhibition (DUPHAT), January 10– 12, 2025, Dubai Trade centre **(Oral Presentation)**

**Table of abbreviations:**

| Abbreviation | Definition |
|---|---|
| AG | Arabinogalactan |
| ATP | Adenosine triphosphate synthase |
| BCG | Bacille Calmette-Guérin |
| BDQ | Bedaquiline |
| $CDCl_3$ | Deuterated chloroform |
| °C | Degrees Celsius |
| CNS | Central nervous system |
| dd | Doublet of doublets |
| d | Doublet |
| s | Singlet |
| t | Triplet |
| q | Quartet |
| DIPEA | *N,N*-diisopropylethylamine |
| DLM | Delamanid |
| DMSO | Dimethyl sulfoxide |
| DMSO-$d_6$ | Deuterated dimethyl sulfoxide |
| DNA | Deoxyribonucleic acid |
| EMB | Ethambutol |
| ESAT-6 | Early Secreted Antigenic Target 6 |
| $Et_2O$ | Diethyl ether |
| EtOAc | Ethyl acetate |
| EtOH | Ethanol |
| EX/EM | Excitation/emission wavelengths |
| FDA | Food and Drug Administration |
| FQs | Fluoroquinolones |
| HBTU | Hexafluorophosphate benzotriazole tetramethyluronium |
| HOBt | Hydroxybenzotriazole |
| HR-MS | High-resolution mass spectrometry |
| INH | Isoniazid |
| KAN | Kanamycin |
| KatG | Catalase-peroxidase enzyme |
| LAM | Lipoarabinomannan |
| LM | Lipomannan |
| LZD | Linezolid |
| mAGP | Mycolyl-arabinogalactan–peptidoglycan complex |

| Abbreviation | Definition |
|---|---|
| ManLAM | Mannosylated lipoarabinomannan |
| m.p. | Melting point |
| MeCN | Acetonitrile |
| MDR | Multidrug-resistant tuberculosis |
| MIC | Minimum inhibitory concentration |
| *Mtb* | *Mycobacterium tuberculosis* |
| $NaHCO_3$ | Sodium bicarbonate |
| $NH_4Cl$ | Ammonium chloride |
| NO | Nitric oxide |
| PAMP | Pathogen-associated molecular patterns |
| PA | Pyrazinoic acid |
| PAS | Para-aminosalicylic acid |
| Ph | Phenyl group |
| ppm | Parts per million |
| PTH | Prothionamide |
| PZA | Pyrazinamide |
| QcrB | Cytochrome bcc complex subunit |
| REMA | Resazurin Microtiter Assay |
| RIF | Rifampicin |
| RNA | Ribonucleic acid |
| rt | Room temperature |
| SAR | Structure–activity relationship |
| SZD | Sutezolid |
| PPS | The Pup-proteasome system |
| PafA | Proteasome Accessory Factor A |
| GS | Glutamine synthetase |
| TB | Tuberculosis |
| TDR-TB | Totally drug-resistant tuberculosis |
| THF | Tetrahydrofuran |
| TLRs | Toll-like receptors |
| TLC | Thin-layer chromatography |
| WHO | World Health Organization |
| XDR | Extensively drug-resistant |
| δ | Chemical shift |

# Originality Statement

I hereby declare that this submission is my own work and to the best of my knowledge, it contains no materials previously published or written by another person or substantial proportions of material which have been accepted for the award of any other degree or diploma at the University of Newcastle or any other educational institution, except where due acknowledgement is made in the thesis. Any contribution made to the research by others with whom I have worked at the University of Newcastle or elsewhere is explicitly acknowledged in the thesis. I also declare that the intellectual content of this thesis is the product of my own work, except to the extent that assistance from others in the project's design and conception or in style, presentation and linguistic expression is acknowledged.

Signed: Haya Saad Alsubaie
Date: 06/05/2025

## Table of Contents

# 1. Introduction

Tuberculosis (TB) is an infectious disease that is a primary cause of illness and death globally.[1] The effectiveness of current TB treatment regimens has been compromised by the limited availability of novel anti-tubercular medication and the emergence of TB resistance.[2] Consequently, significant efforts have been directed toward the synthesis of new anti-tubercular agents with novel mechanisms of action.

This thesis presents an investigation of novel compounds based on the imidazo[1,2-*a*]pyridine scaffold that potentially targets PafA, a promising anti-tubercular target. This chapter provides a background on the disease and current TB treatments, highlighting the challenges of drug resistance and introducing PafA as a new and promising TB target. Chapter 2 focuses on the synthesis of imidazo[1,2-*a*]pyridine derivatives as potential PafA inhibitors, while Chapter 3 presents the biological evaluation and structure-activity relationship (SAR) studies of the three series of imidazo[1,2-*a*]pyridine analogues utilising a REMA assay. Lastly, Chapter 4 explores the modification of the arylhydrazine moiety, replacing it with various heterocyclic analogues to evaluate their impact on anti-tubercular activity, then concludes the thesis by summarising the findings and discussing future directions for utilising the results of this work in the ongoing development of novel TB therapies.

## 1.1 Background

In 2024, TB has likely returned to its position as the main cause of death from a single infectious agent after 3 years in which it was replaced by coronavirus disease (COVID-19) and caused approximately twice as many deaths as HIV/AIDS.[1] According to the Global Tuberculosis Report 2024 from the World Health Organisation (WHO), approximately 10 million people were reported to have been diagnosed with TB in 2023, whilst the number of TB deaths was 1.25 million, a reduction from 1.4 million deaths in the worst years of the COVID-19 (2020 and 2021), returning the numbers closer to pre-pandemic levels in 2019.[1] Furthermore, around 55% of TB cases were found in men (approximately 6.0 million cases), whereas 33% were in women (estimated 3.6 million cases), and 12% among children (roughly 1.3 million cases).[1] Countries with the highest infection rates are India (26%), Indonesia (10%), China (6.8%), the

Philippines (6.8%), and Pakistan (6.3%), with the total number of cases in these countries accounted for 56% of global cases in 2023 (Figure 1).[1]

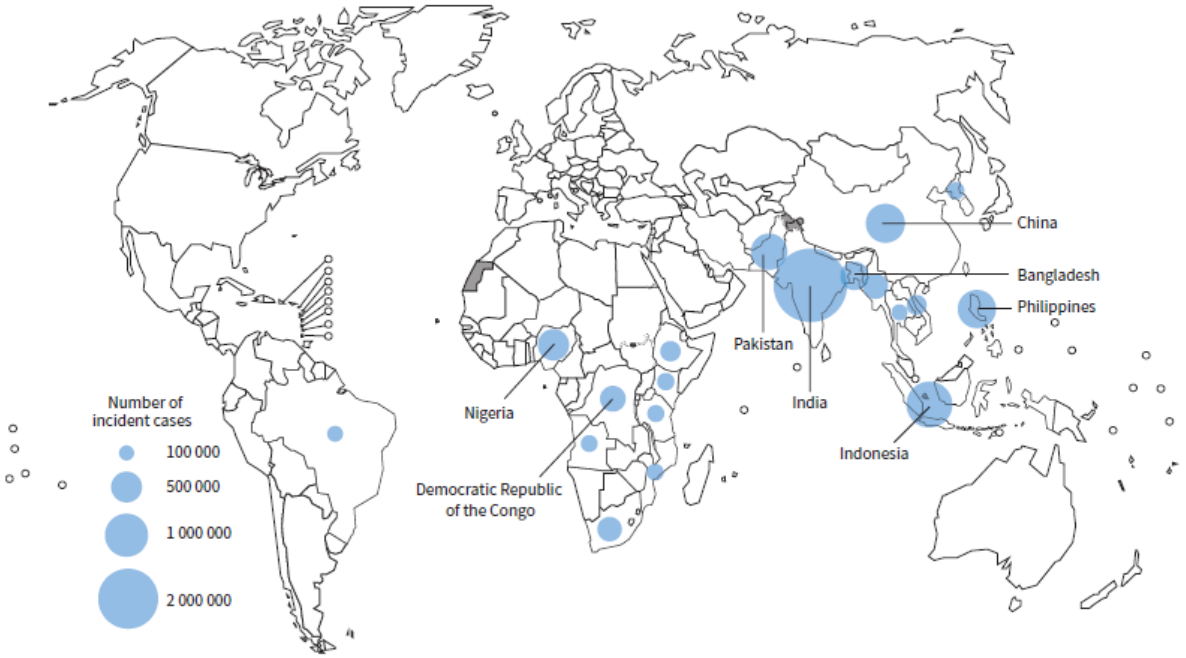


Figure 1. Estimated TB incidence cases around the world in 2023.

The End Tuberculosis Strategy, a WHO initiative, aims to reduce TB incidence by 90%, with the ultimate goal of eliminating TB as a global health concern by 2050.[1] However, the long treatment schedules (at least 6 months course) and unwanted side effects of current medications lead to poor patient compliance, resulting in the establishment of multidrug resistance (MDR-TB) strains.[3] This issue has recently been aggravated by the development of extensively drug-resistant (XDR) infections, which are defined as bacteria resistance to the two most potent first-line medications (isoniazid and rifampicin), as well as the second-line drugs fluoroquinolones and one of the injectables (amikacin, kanamycin, or capreomycin).[3] Globally, an estimated 175,923 individuals developed MDR-TB in 2023, and among newly diagnosed TB cases, approximately 3.2% were found to have MDR-TB.[1] The other issue is latent TB, which arises from the ability of *Mycobacterium tuberculosis* (*Mtb*) to enter a non-replicating state in which *Mtb* becomes phenotypically resistant to many of the current drugs. Consequently, there is an intense effort to identify and target the *Mtb* proteins that are essential for survival in the host. Recent studies have shown that *Mtb* relies on several enzymatic pathways to survive host stresses while entering a non-replicative state.[4] Among these is the Pup−proteasome system (PPS), which is important for both the virulence of *Mtb* and its ability to persist in the human host for prolonged periods.[4] This

last point is crucial because a quarter of the world's population is currently a carrier of *Mtb* in a dormant state.[1] As a result, targeting this system with new compounds that inhibit its activity may be able to eradicate active and latent *Mtb* from the host.

## 1.2 *Mycobacterium tuberculosis*

### 1.2.1 *Mtb* pathogenicity

TB is caused by the bacterium *Mycobacterium tuberculosis* (*Mtb)*, which ranks as one of the most lethal pathogens in the world and most commonly affects the lungs (pulmonary TB), but can also affect other organs, including the lymph nodes, spine, brain, liver and kidneys, resulting in extrapulmonary TB.[5] Generally, the prognosis of the disease after infection is determined by the ability of the host to remove the bacillus.[5] The disease begins when droplets from an infected person enter the respiratory tract of a healthy person.[5] Upon entry into the respiratory tract, *Mtb* is recognised by innate immune cells, including macrophages and dendritic cells, through pathogen-associated molecular patterns (PAMPs) that bind to toll-like receptors (TLRs) on these cells.[6,7] This recognition activates an immediate inflammatory response, which releases pro-inflammatory cytokines, such as IL-12 and nitric oxide.[6,7] Subsequently, alveolar macrophages ingest *Mtb* and after engulfment, a prolonged interaction between *Mtb* and the host cells leading to one of three outcomes: 5 – 10% of cases progress to active TB, while in most cases, infection is controlled, either through complete eradication of the bacteria leaving behind only immunologic memory of the interaction or the vast majority develop latent TB, where the bacterium persists inside the host and formation of a stable granuloma, the hallmark of TB disease (Figure 2).[7]

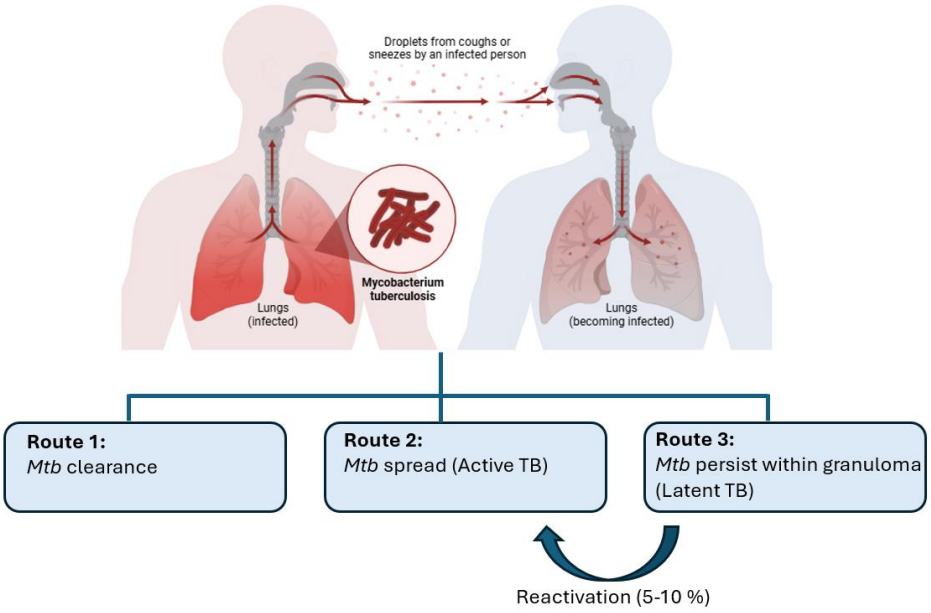


Figure 2: The three possible outcomes for *Mtb* infection

Persons with latent TB infection exhibit no symptoms, are not contagious, and cannot transmit TB to others.[8] Notwithstanding this, *Mtb* remains dormant for decades within the granuloma structure, and because of some medical conditions (e.g. HIV infection) or genetic factors, bacteria can reactivate.[5] Therefore, the interaction between *Mtb* and its host is extremely complex, with the outcome and progression of TB not only dependent on the virulence of the bacteria but also strongly linked to patient immunity.[9] In general, macrophages typically eliminate pathogens by forming a phagosome that fuses with a lysosome to form an acidic environment for pathogen degradation.[7,10] However, *Mtb* utilises different virulence factors that enable it to escape this process and survive within the granuloma. In particular, after being phagocytosed, *Mtb* uses the ESX-1 secretion system and its protein early secretory antigenic target-6 (ESAT-6) to escape this defence mechanism and prevent its fusion with lysosomes, allowing the bacteria to survive in the harsh environment within granulomas (Figure 3).[7,10]

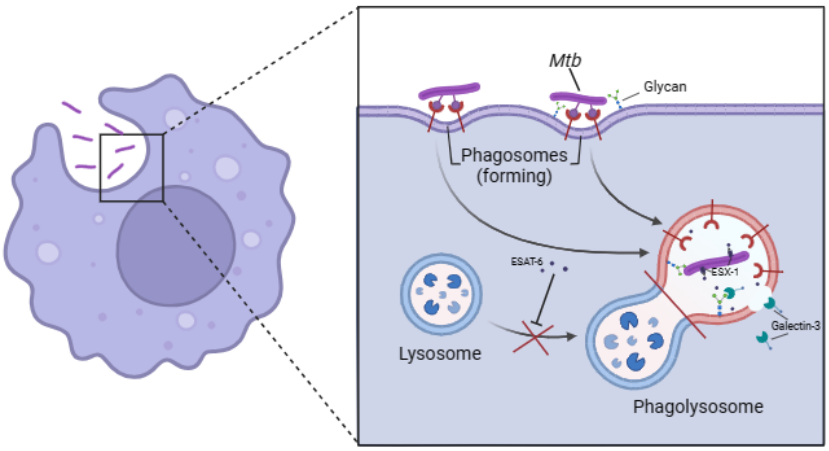


Figure 3. *Mtb* evades the immune system by preventing the fusion of lysosomes with phagosomes. Adapted from BioRinder.

During this period, the host prevents mycobacterial replication through different defences, including many stresses, and the ability of *Mtb* to cope with these external stresses, such as hypoxia, nutrient starvation, nitric oxide (NO), low pH, low iron and heat shock is critical for its survival.[11] This persistence is driven by a variety of molecules, including glycans, glycolipids, lipids and nucleic acids, many of which are crucial to the bacterial cell wall.[12] The unique structure and composition of the *Mtb* cell wall, a defining feature of its persistence and virulence, will be discussed in detail in the following section.

### *1.2.2 Mtb* cell wall

Bacteria are normally categorised depending on the bacterial cell wall structure into two types: Gram-positive bacteria and Gram-negative bacteria.[13] While Gram-positive bacteria contain multiple thick layers of peptidoglycan that function as a protective coating, the cell walls of Gram-negative bacteria are composed of a single and thin layer of peptidoglycan and a distinct outer membrane.[13] Interestingly, *Mtb* exhibits Gram-positive and Gram-negative characteristics by having a peptidoglycan layer nearly as thick as the Gram-positive bacteria and an outer waxy layer mimicking the outer membrane of the Gram-negative bacteria; therefore, it is classified as an acid-fast bacteria.[14] The cell envelope of *Mtb* is a thick, hydrophobic structure with very limited permeability and is one of the many challenges facing TB drug discovery.[15] It is comprised of three major structural components: the typical plasma membrane, the cell wall, and the outer membrane, also known as the mycomembrane.[16] Structurally, the mycomembrane consists of proteins, lipids, and glycolipids.[17] The outer layer

consists of mycolic acid linked to complex glycolipids, such as pentaacyl trehalose (PAT), phthiocerol dimycocerosates (PDIM), trehalose dimycolate (TDM) and sulfolipids. Moreover, the mycomembrane contains different lipids such as mannan, arabinomannan, and mannose-capped LAM (ManLAM), that are incorporated into the inner membrane and play a critical role in the development, survival, and virulence of *Mtb*.[12,17] In addition, mycolic acids are connected to the plasma membrane through the peptidoglycan layer, which covalently links these to the highly branched arabinogalactan polysaccharide to form mycolic acid-arabinogalactan-peptidoglycan complex (MAPc).[16] This complex is the feature of the *Mtb* cell wall and is critical for controlling the permeability and virulence of the pathogen.[16] Finally, the outer membrane, known as the capsule, is comprised of polysaccharides, with abundant α-glucan and also contains arabinomannan as well as trace amounts of proteins and lipids (Figure 4).[18] Taken together, the *Mtb* cell wall is a crucial barrier against most antibiotics and its specific components are important for *Mtb* survival inside the host.[15]

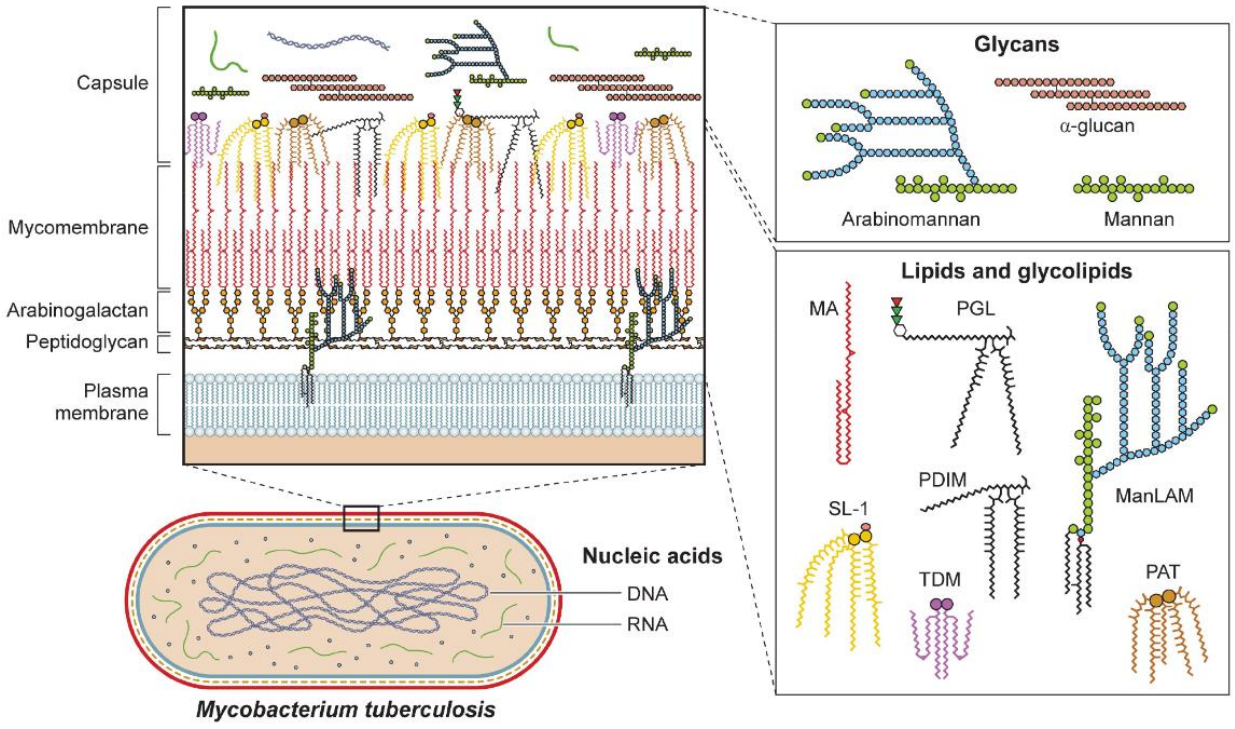


Figure 4. A schematic illustration of the cell wall structure of Mtb. MA: mycolic acid, PGL: phenolic glycolipid, ManLAM = mannose-capped LAM, SL-1: sulfolipid-1, TDM: trehalose dimycolate, PDIM: phthiocerol dimycocerosates, PAT: pentaacyl trehalose. Adapted from [12]

## 1.3 Current Anti-tubercular Compounds

Current approaches for combating TB include vaccination and a variety of drug regimens classified as first-line, second-line, and newer treatments.[19] Although the Bacillus Calmette–Guérin (BCG) vaccine is effective in avoiding severe types of TB in children, it offers only limited protection in adults.[20] First-line anti-TB medications are effective but need a prolonged treatment duration of at least six months which raises issues with adherence and the risk of TB resistance.[19] For those with TB resistance, second-line medications are usually expensive, more toxic, and less effective.[19] Recently, new anti-TB drugs such as bedaquiline, delamanid, and pretomanid have been introduced, showing promise against resistant TB strains.[21] However, the need for prolonged, combination regimens and the toxicity associated with many medications highlights the significant challenge in TB treatment, encouraging continuous research for safer, shorter and more effective treatments.[21] In the following subsections, different anti-TB treatment regimens will be explored, highlighting their key uses, limitations, and contributions to addressing the challenges of TB management.

### 1.3.1 Vaccination

As mentioned earlier, TB is one of the deadliest infectious diseases, and its prevention is increasingly challenged by the emergence of drug-resistant strains. Vaccination remains the most cost-effective and efficient method for decreasing the incidence of active TB at its source.[20] The only current vaccine, Bacille-Calmette-Guérin (BCG), is an attenuated strain of *Mycobacterium bovis* that has been in use since the 1920s; approximately 100 million infants receive BCG each year, making it the most used vaccine in the world with over four billion doses being administrated.[22] The high safety profile of the vaccine, measured as one major side effect from vaccine administration per one million doses administered to immunocompetent people, may also lead to continuing use in TB-endemic countries.[22] Importantly, BCG is effective in children, providing greater than 50% protection against lung disease and more than 80% protection against disseminated forms of TB.[23] However, it has shown variable and mostly poor protection against TB in adolescents and adults, requiring the urgent development of novel TB vaccines.[23] The development of new TB vaccines that are more effective and safer has been accelerated by advancements in the scientific understanding of the genetic system, the immune mechanisms against *Mtb*, and

proteomics.[24] The ideal vaccine strategy for TB should have three components: preventing primary infection and disease after exposure, preventing latent infection reactivation, and adding an immunotherapeutic adjuvant to conventional TB treatment to facilitate patient recovery.[25] Currently, there are many novel TB vaccines in the pipeline, including four in Phase I, eight in Phase II, and five in Phase III.[24] Despite advancements in the investigation of novel TB vaccines, there are still challenges, such as the lack of appropriate animal models for TB vaccine evaluation, the exclusion of pregnant women from current TB vaccine trials, the challenges associated with antigen epitope selection, and the poor sustainability of TB vaccine clinical trials.[26] However, the utilisation of new technologies has opened up novel directions for the study of TB vaccines, including the application of mRNA vaccines and deep learning in vaccine research.[24]

### 1.3.2 First-Line Drugs for TB

While vaccination is an important preventive strategy, it is insufficient to provide significant protection against TB, particularly due to its inadequate efficacy in adolescents and adults, as previously discussed. Therefore, the primary approach for treating TB today is using first-line anti-TB medications. The first-line anti-TB agents include a combination of four antibiotics: isoniazid (INH) **1**, rifampicin (RIF) **2**, ethambutol (EMB) **3** and pyrazinamide (PZA) **4** (Figure 5).[27]

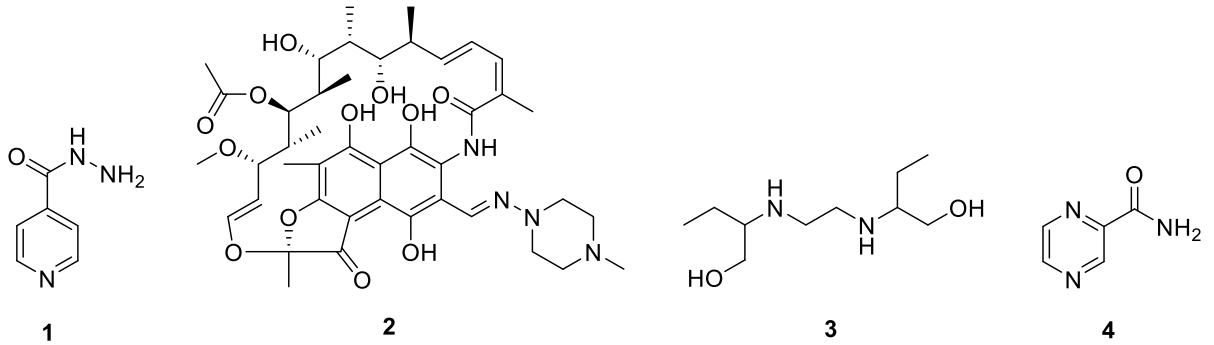


Figure 5. Front-line anti-TB agents.

This four-drug regimen should be administered for at least six months under directly observed therapy (DOT) to obtain high rates of treatment success.[28] The treatment protocol includes two different phases: the initial phase, which involves all four drugs administered for two months, followed by a continuation phase in which INH **1** and RIF **2** are given for another four months.[28]

### 1.3.2.1 Isoniazid (INH)

INH **1** has been the most effective first-line agent for more than 60 years.[29] It is a prodrug and is activated by the KatG enzyme (Catalase-peroxidase) producing the isonicotinic-acyl radical intermediate **5** which covalently couples with NADH to produce the nicotinoyl-NAD adduct **6** (Figure 6).

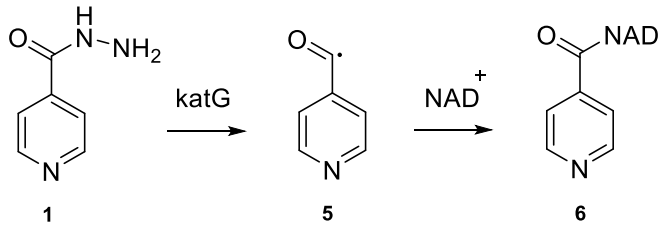


Figure 6. Activation of INH **1** to its active metabolite through KatG enzyme.

This INH–NADH adduct inhibits InhA (enoyl-acyl carrier protein reductase) which is involved in the synthesis of mycolic acids of the *Mtb* cell wall.[29] In addition, the active form of INH, the INH-NAD adduct **6** was demonstrated by X-ray crystallography to be coupled to InhA and to block its enzymatic activity.[29] These data support the identification of the drug target to which the drug INH binds and inhibits InhA, resulting in cell death.[29]

INH **1** is a bactericidal drug that kills actively growing mycobacteria with MIC of 0.02-0.2 µg/mL for drug-sensitive strains.[27] However, INH has been ineffective for more than 10 % of patients worldwide due to resistance.[30] Although a variety of different mutations in a variety of genes have been related to INH-resistance in *Mtb*, the most common cause is due to mutations in either *katG* (64%), or *inhA* (19%).[30]

Significant efforts have been made to identify INH **1** analogues as novel anti-TB agents. These analogues have been categorised according to their lipophilicity, structure, and structure-activity relationships (SAR), such as hydrazones, Schiff bases, and hydrazides which have exhibited significant anti-TB activity against both drug-susceptible and resistant *Mtb*. Notably, incorporating lipophilic fragments into the INH structure can increase the drug's ability to penetrate bacterial cells. Consequently, INH analogues with increased lipophilicity have gained significant interest as potential anti-TB agents.[27] The most well-known derivative has a pyrrole core, i.e., (LL-3858) **7** with MIC values of 0.06 – 0.5 µg/mL for drug-susceptible and MDR-TB strains and it is currently in clinical trials (Figure 7).[27]

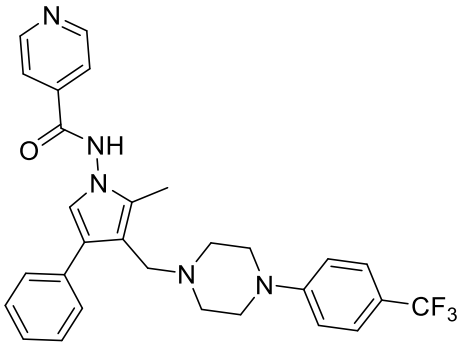

**7**

Figure 7. Chemical structure of LL-3858 **7** compound.

Different hydrazides and hydrazone analogues have gained significant interest in medicinal chemistry due to their extensive biological and pharmaceutical activity.[31,32] Among these, INH hydrazide-hydrazone analogues have been identified with a rational approach involves the modification of the hydrazide of INH with different functional groups that block acylation by *N*-acetyltransferase (NAT) while maintaining its potent anti-TB activity.[33] All tested analogues exhibited significant activity, with MIC ranging from 0.21 - 18.29 μM.[33] Notably, **8** and **9** were identified as the most potent analogues against the *Mtb* H37Rv strain, with MIC 0.28 μM and 0.65 μM, respectively (Figure 8).[33]

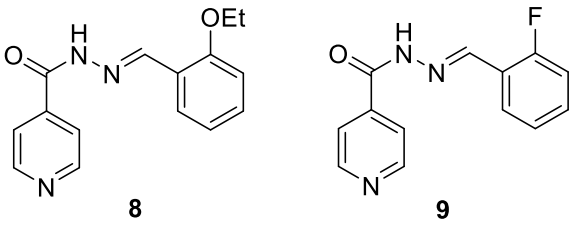

**8** **9**

Figure 8. Chemical structures of analogues **8** and **9** .

INH **1** is often well-tolerated but can be associated with various side effects, which can vary in severity depending on factors such as patient susceptibility and dosage.[34] Toxic effects from INH **1** can be reduced by administering pyridoxine (vitamin B6) alongside the treatment and close monitoring of the patient. In the absence of pyridoxine, peripheral neuritis is the most common side effect, affecting approximately 2% of patients who receive the standard dose of 5 mg/kg per day, and increasing to 10–20% at higher doses.[34] In general, the incidence of adverse reactions to INH **1** is estimated at 5.4%, with the most common being rash (2%), fever (1.2%), and jaundice (0.6%).[34]

#### 1.3.2.2 Rifampicin (RIF)

RIF **2** is currently the most important anti-TB medication, with a MIC of 0.1– 0.2 μg/ml, it is used in combination with isoniazid as a basis for anti-TB therapy to treat drug-susceptible TB.[27] It targets the RNA polymerase of *Mtb*, which is responsible for gene regulation and transcription.[21] Specifically, RIF interacts with the β subunit of RNA polymerase, disrupting the transcription process by interfering with protein synthesis, ultimately resulting in cellular death.[21] An important feature of RIF and other rifamycins is their ability to target non-replicating persisters (NRPs) and thereby treatment regimens that excluded RIF often last 12 to 18 months or longer and are often less effective.[35] Nevertheless, the emergence of RIF resistance has markedly compromised its effectiveness, offering a considerable challenge to TB treatment.[36] The RIF resistance mechanism is mostly promoted by mutations within the *rpoB* gene, which encodes the β-subunit of RNA polymerase.[36,37] Moreover, it has been reported that almost all RIF-resistant TB strains have established resistance to other medications, especially to INH, suggesting that RIF-resistance detection could be used as an alternative molecular marker for MDR.[38] Given the rise of RIF resistance and the significant role of this medication in TB therapy, significant efforts have been focused on the synthesis of RIF analogues.[39] Rifabutin **10**, rifapentine **11** and rifalazil (KRM-1648) **12** are the most important RIF analogues synthesised, targeting the resistant, while also increasing the antimicrobial activity and extending the half-life (Figure 9).[40]

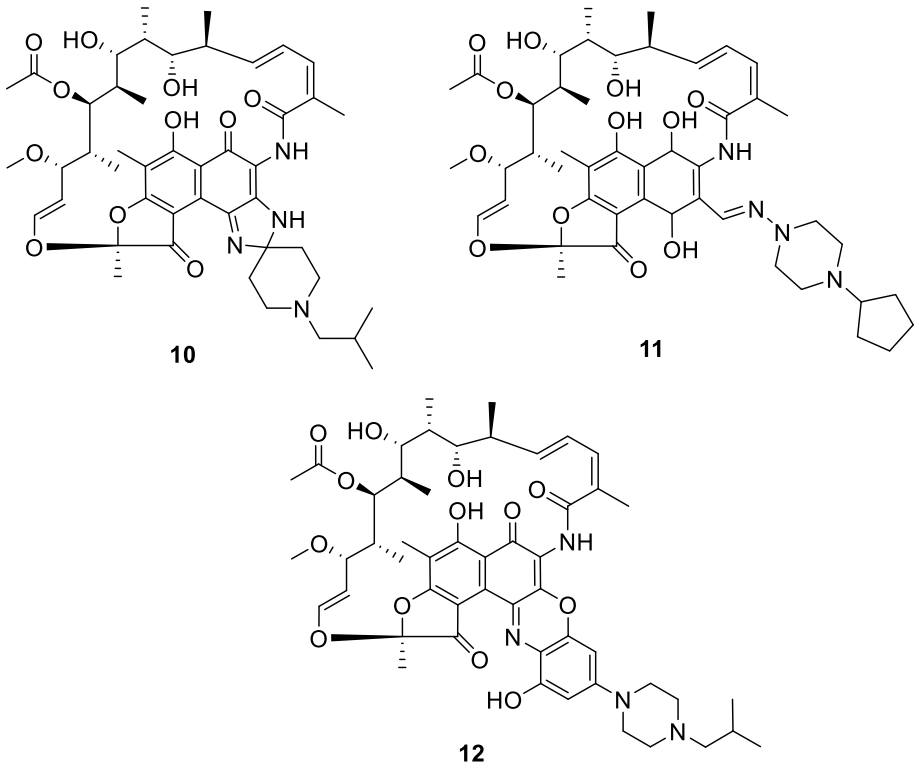


Figure 9. Chemical structures of rifabutin **10**, rifapentine **11** and KRM-1648 **12**.

In the late 1990s, rifapentine **11**, a more potent analogue of RIF, was approved as an alternative in response to the rising incidence of *Mtb* resistance, though it has since been linked to increased rates of TB relapse.[39,41] Moreover, another RIF analogue, KRM-1648 **12** is more effective against *Mtb* than RIF **2** and rifabutin **10**, and it passed phase 2 clinical trials.[40] However, the use of KRM-1648 **12** had to be stopped during the trials because of severe side effects.[27]

#### 1.3.2.3 Ethambutol (EMB)

EMB **3** or [(*S*,*S*)-ethambutol dihydrochloride] is a first-line drug used in combination with isoniazid, rifampicin and pyrazinamide in TB treatment.[30] It is a bacteriostatic agent and has an MIC of 0.5 µg/mL against growing drug-susceptible strains (Figure 10).[30]

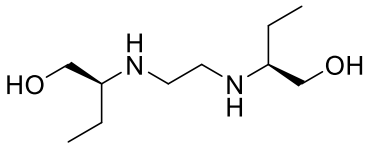


Figure 10. Chemical structure of EMB **3**.

The stereospecificity of EMB is connected to its activity as the (*S*,*S*)-isomer is 600 times more active than the (*R*,*R*)-isomer.[27] EMB blocks arabinogalactan biosynthesis

by inhibiting arabinosyltransferases (embB), particularly those in the *Mtb* cell wall.[42] Thereby, resistance to EMB is induced by mutation of the *embB* gene.[43] Furthermore, EMB can cause ocular damage and although this toxicity is reversible if treatment is discontinued, it is not recommended for use in young children.[42]

To produce second-generation EMBs with increased potency against *Mtb*, a research programme was initiated to modify the structure.[27] Using ethylenediamine and other commercially available amines, a library including 63,238 compounds was prepared and *N*-geranyl-*N*-(2-adamantyl)ethane-1,2-diamine (SQ109) **13** was the most active compound, showing a 14- to 35-fold increase in *in vitro* activity against both drug-resistant and drug-susceptible strains in comparison to EMB **3** (Figure 11).[15]

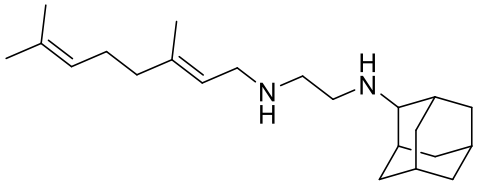


**13**

Figure 11. Chemical structure of SQ109 **13**.

Importantly, this compound is now in phase 2 of a clinical trial, and its mechanism of action differs significantly from that of EMB.[15] In a mouse model of TB, SQ109 **13** showed bactericidal activity by inhibiting mycolic acid synthesis and increased the efficacy of both INH and RIF to shorten the duration of TB treatment, thus presenting itself as a promising candidate for TB therapy.[15]

#### 1.3.2.4 Pyrazinamide (PZA)

Since the 1950s, PZA **4** has been an important first-line sterilizing medicine that performs a unique role in reducing anti-TB therapy from (9 - 12 months) to 6 months by killing latent *Mtb* (Figure 12).[44] It is a prodrug that is converted to pyrazinoic acid (POA) by the bacterial enzyme pyrazinamidase.[27]

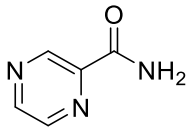


**4**

Figure 12. Chemical structure of PZA **4**.

PZA demonstrates potent antimicrobial effects; however, its administration is linked with adverse side effects, such as hepatotoxicity and liver damage, along with the development of resistance.[45] The majority of PZA-resistance is due to mutations in the

*pncA* gene, which encodes pyrazinamidase, where some resistant strains were discovered to have mutations in the drug target ribosomal protein S1 (*rpsA*).[46] Recently, the discovery that *panD* mutations are present in certain PZA-resistant strains even when neither *pncA* nor *rpsA* mutations are present may point to the existence of a third PZA resistance gene as well as a possible new target for PZA.[46,47] PanD is responsible for the production of β-alanine, a precursor for pantothenate and coenzyme A synthesis.[47] Therefore, it is likely POA, the bioactive component of PZA, binds to the aspartate decarboxylase PanD and induces its degradation by *Mtb*, thereby inhibiting the synthesis of both essential enzymes, pantothenate and Coenzyme A (Figure 13).[47]

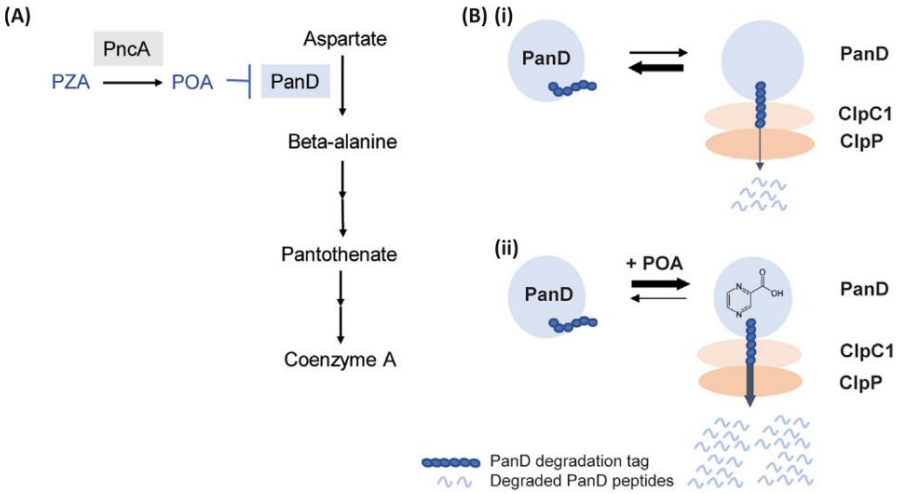


Figure 13. Proposed a novel Mechanism of Action of PZA.[46] (A)PZA converted to its active form POA by pyrazinamidase (PncA) which binds to aspartate decarboxylase PanD that catalyzed synthesis of the important cofactor Coenzyme A. (B) The level of PanD is regulated post-translationally by the caseinolytic protease complex ClpC1-ClpP, and the binding of POA to PanD increases the protein's degradation. (i) PanD (blue circle) has a C-terminal protease degradation tag and ClpC1 (light orange) recognises this tag and unfolds PanD in preparation for degradation by the ClpP protease (dark orange). (ii) The binding of POA to PanD results in conformational changes that enhance the exposure of the degradation tag and, therefore, the rate of PanD degradation by ClpC1-ClpP. Adapted from [47]

In conclusion, the front-line anti-TB agents remain the cornerstone of TB treatment, effectively targeting important biological processes in *Mtb*, as shown in the (Table 1) below, which outlines their mechanisms of action. The following section will explore second-line anti-TB agents, which are utilised when resistance to first-line therapies develops.

| Anti-TB agent | Bacterial target | Mechanism of action |
|---|---|---|
| INH **1** | Enoyl-acyl carrier protein reductase (InhA) | Bactericidal: It suppresses the formation of mycolic acid which is a key component of the *Mtb* cell membrane. |
| RIF **2** | RNA polymerase | Bactericidal: Cell Inhibition of the synthesis of RNA. |
| EMB **3** | Arabinosyltransferase | Bacteriostatic: It inhibits the synthesis of arabinogalactan and LAM, the components of the *Mtb* cell wall. |
| PZA **4** | Ribosomal protein S1 | Bactericidal: Cell Pyrazinoic acid (POA) disrupts membrane energy and inhibits membrane transport function at acidic pH. |

Table 1. A description of front-line drugs with their target and mechanism of action.

### 1.3.3 Second-Line Drugs for TB

As highlighted in the previous section, front-line drugs including INH **1**, RIF **2**, EMB **3** and PZA **4** are the cornerstone in the treatment of TB, giving a balance of efficacy and safety. Nevertheless, the rising incidence of drug-resistant strains has prompted the need for second-line medications. These medications are primarily used to treat MDR-TB and have limited sterilizing capabilities, significant side effects and higher prices.[48] They can be divided into families, namely the Aminoglycosides, Fluoroquinolones, Thioamides, Para Amino Salicylates (PAS) and Cycloserine, which will be discussed further in this section.

#### 1.3.3.1 Fluoroquinolones

Fluoroquinolones, one of the most recognised chemical classes in the second-line drug regimen for TB, include antibacterial agents such as moxifloxacin **14,** levofloxacin **15** and ofloxacin.[49] Ofloxacin is a second-generation fluoroquinolone, while levofloxacin is a third-generation and moxifloxacin a fourth-generation.[49] They have a bactericidal effect by targeting mycobacterial DNA gyrase, which inhibits bacterial DNA replicating.[50] Aside from having *in-vitro* efficacy against *Mtb*, fluoroquinolones also show good penetration into macrophages, which is a particularly crucial attribute given the capacity of *Mtb* to live and reproduce within host cells.[51] Initially, it was believed that fluoroquinolones might approach the sterilizing action of RIF; however, studies indicate that they appear to be less effective.[44] Moxifloxacin **14** and levofloxacin **15**, a

new class of fluoroquinolones, have shown greater activity against *Mtb* than ciprofloxacin and ofloxacin (Figure 14).[50] Furthermore, they are administered once daily, which improves treatment adherence.[50] However, fluoroquinolones can cause side effects including musculoskeletal disorders and QTc prolongation, so caution is important when combined with other QTc-prolonging medications, along with close electrocardiography (EKG) monitoring.[52]

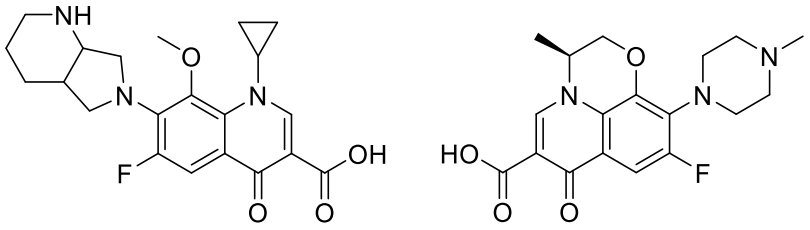


**14** **15**

Figure 14. Chemical structures of new generation of fluoroquinolones, moxifloxacin **14** and levofloxacin **15**.

Unless contraindicated, current guidelines recommend including a new generation of fluoroquinolone in all MDR TB regimens.[52] These recommendations are based on the findings of a recent individual patient data meta-analysis, which showed that the use of levofloxacin or moxifloxacin was strongly related to successful treatment results in patients with MDR-TB.[53]

#### 1.3.3.2 Aminoglycosides (AGs)

Streptomycin, discovered in 1943, was vital in the identification of the aminoglycoside (AG) class of antibiotics and has played an important role in TB treatment.[54] It was the first antibiotic used for TB and was part of the WHO's standard TB treatment regimen (Category II) until 2017.[54] The use of AGs in TB treatment has experienced fluctuations in popularity and efficacy over the years, influenced by factors such as rising resistance and development of alternative treatments.[54] Furthermore, AGs along with fluoroquinolones formed the backbone of any MDR-TB regimen, and AG resistance was part of the definition of XDR-TB until it was changed in October 2020.[55] Although AGs are not currently included in the recommended regimen for MDR-TB, they are still an effective alternative medication with a potent bactericidal effect that can be used in the treatment of patients with non-responsive MDR or XDR-TB.[50] Amikacin and kanamycin are common AGs, while capreomycin **16** is frequently misunderstood as another AG, but it is a cyclic polypeptide and due to their similar administration routes, toxicity profiles, and mechanism of action, they have traditionally been classified

together as second-line injectable compound (Figure 15).[50] AGs inhibit protein synthesis by targeting the 16S ribosomal RNA (rRNA) in the 30S ribosomal subunit, which leads to a conformational change in the rRNA, which prevents mRNA translation and translocation.[49] Furthermore, both AGs and capreomycin are linked to significant risks of nephrotoxicity and ototoxicity. Nephrotoxicity generally presents as an elevation in serum creatinine levels, which is an indicator of renal function.[44] Approximately 5–25% of individuals on AGs have this kidney impairment, though it is often mild or moderate, and reversible following withdrawal or dose adjustment.[56] Ototoxicity, on the other hand, can be more serious, usually involving irreversible hearing loss due to damage to the inner ear components, which is often related to the dosage duration but not dose size.[57]

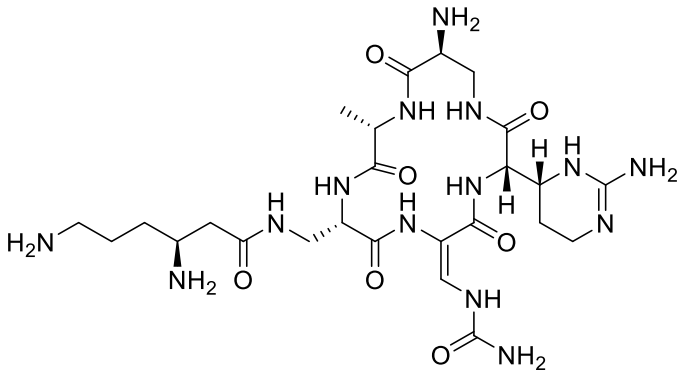

**16**

Figure 15. Chemical structure of capreomycin **16**.

### 1.3.3.3 Thionamides

Thionamides, such as ethionamide (ETH) **17** and prothionamide (PTA) **18**, are used as second-line therapies for MDR-TB (Figure 16).[54] Both have a similar chemical structure to INH and both are prodrugs that need activation by monooxygenase EthA.[58]

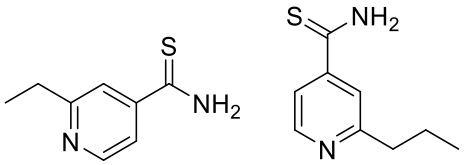

**17** **18**

Figure 16. Chemical structures of ETH **17** and PTA **18**.

Following activation, thionamides inhibit mycobacterial mycolic acid production by inhibiting the InhA enzyme.[58] Moreover, hypothyroidism is the most common side effect of ETA **17** occurring in up to 30 % of patients, but it is reversible following drug

withdrawal.[44] Nevertheless, they are not recommended by 2019 WHO guidelines unless more effective agents are unavailable.[59]

### 1.3.3.4 Cycloserine and Terizidone

Cycloserine **19** is a cyclic analogue of the amino acid D-alanine and is classified as a category B medication for use in prolonged MDR-TB regimens, while terizidone **20** is a structural analogue of cycloserine and they are considered interchangeable for the treatment of MDR-TB (Figure 17).[44] The bacteriostatic effect of cycloserine is related to its targeting of the alanine racemase and D-alanine ligase enzymes required for the synthesis of peptidoglycan, which is an important component of the bacterial cell wall.[60] The therapeutic index of cycloserine is low and it is known to induce neurological adverse effects such as seizure, suicidal ideation and depression, which have been observed to occur in around 6% of patients.[44] Pyridoxine 50 – 100 mg is recommended to counteract neuropathy, however, evidence of effectiveness is limited.[44]

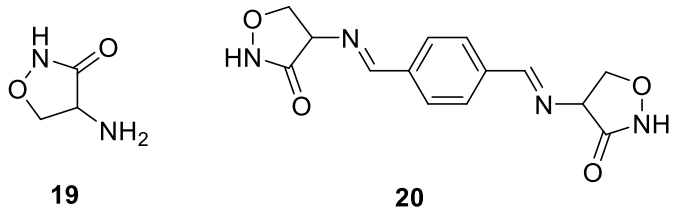


**19** **20**

Figure 17. Chemical structures of cycloserine **19** and terizidone **20**.

### 1.3.3.5 *Para*-aminosalicylic Acid

In 1943, Lehmann and colleagues suggested *para*-aminosalicylic acid (PAS) **21** as a treatment for TB, based on the finding that salicylic acid stimulates mycobacterial respiration, indicating that similar analogues may disrupt *Mtb* respiration (Figure 18).[61]

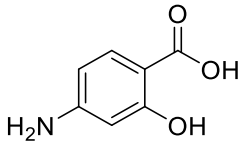


**21**

Figure 18. Chemical structure of para-aminosalicylic acid **21**.

As a result, the discovery of PAS and its combination with streptomycin in the early 1950s represented a breakthrough in TB therapy.[62] This combination, together with INH **1**, comprised the first effective TB regimen.[62] However, the approval of more effective and better-tolerated TB medications such as RIF **2**, EMB **3**, and PZA **4** relegated PAS to second-line treatment, while the rise of resistance has led to the

reintroduction of PAS for treating only XDR-TB cases.[63] PAS is an analogue to aminobenzoic acid and works by inhibiting the enzyme dihydropteroate synthase (DHPS), which disrupts folate synthesis in *Mtb*, leading to slowing bacterial growth.[64] It is a prodrug, activated by the dihydrofolate synthase enzyme encoded by the *folC* gene. A mutation in this gene causes resistance to PAS.[64] Moreover, PAS has fast clearance and moderate bioavailability, which requires high daily doses of up to 12 g per day.[65] The bioavailability of PAS is around 60% with most of the unabsorbed drug remaining in the gastrointestinal tract and contributing to gastrointestinal symptoms.[65] Additionally, other reported adverse effects are hypothyroidism and goitre, particularly when administered in conjunction with thioamides.[65]

## 1.3.4 New anti-TB drug candidates

Alongside the first- and second-line TB medications discussed in the previous sections, it is important to explore the more recently developed TB drugs, which are categorized as third-line treatment. The most recent anti-TB agents include bedaquiline, delamanid, and pretomanid, which were licenced as TB drugs in 2012, 2014, and 2019, respectively.[44] Furthermore, linezolid initially developed for Gram-positive bacterial infection, has been repurposed for TB therapy and was recently categorized by the WHO as a core regimen for MDR-TB.[66] In addition, Q203, a promising compound based on an imidazo[1,2-*a*]pyridine scaffold, is currently in phase 2 clinical trials, indicating ongoing efforts to enhance the arsenal against resistant TB.[67]

### 1.3.4.1 Diarylquinolines: Bedaquiline (BDQ)

BDQ **22** represents an important milestone in TB therapy since it was the first anti-TB agent in 40 years with a novel mechanism of action, receiving accelerated approval by the FDA.[43] It was identified using whole-cell phenotypic screening and showed outstanding bactericidal activity against both replicating and non-replicating *Mtb*, as well as a sterilizing activity in animal models.[44] BDQ targets ATP synthetase and its toxicological and pharmacological issues are related to its high lipophilicity, resulting in potential tissue accumulation and hepatotoxicity, mainly due to its prolonged duration of treatment (up to 4–6 months).[68]

A comprehensive optimisation of the diarylquinoline scaffold revealed important structural components and underscored the principal features important for activity (Figure 19).

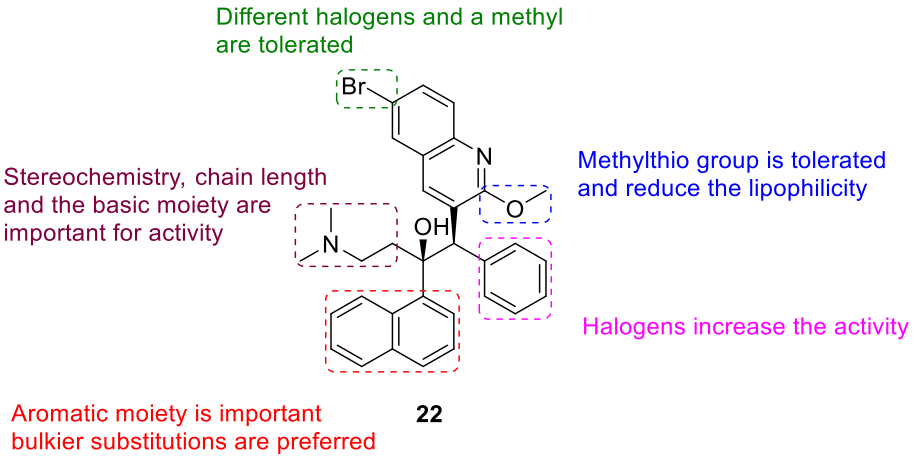


Figure 19. Chemical structure of BDQ **22** and SAR study of its analogues. [69]

Despite its promising therapeutic effect and the success of regimens utilising this drug, safety remains a concern, so its use is restricted to drug-resistant TB.[68] The most common side effects of BDQ include arthralgia, headache, vomiting, and nausea.[70] While the most concerning adverse effect is QTc prolongation, which strongly blocks the human ether-a-go-go-related gene (hERG) potassium channel and can result in severe cardiac events.[70] As a result, when introducing BDQ into the regimen, it is recommended to conduct ECGs after the first two weeks of treatment and subsequently at monthly intervals for monitoring QTc prolongation. Another concern involves BDQ's high lipophilicity (logP 7.25), this characteristic contributes to its long half-life elimination and can result in tissue accumulation with either daily dosing or high doses.[71] As a result of its pharmacokinetic properties, BDQ is administrated three times per week.[72] Consequently, this observation indicates that less lipophilic analogues of BDQ may be of interest in reducing the possibility of tissue accumulation and thus increasing suitability for once-daily dosing.

BDQ undergoes primary hepatic metabolism via cytochrome P450 isoenzyme CYP3A4, producing its *N*-monodesmethyl metabolite M2, which retains antimycobacterial activity but is around five times less potent against *Mtb* than the parent drug.[72] Given BDQ's reliance on CYP3A4 for metabolism, there is a significant potential for drug interactions when coadministered with agents that modulate CYP3A4 activity.[72] Co-administration with moderate to strong CYP3A4 inducers can lead to reduced systemic exposure to BDQ, potentially compromising its therapeutic efficacy.

Due to this safety issue and the necessity to enhance pharmacokinetic properties, researchers have developed analogues, for example, TBAJ-587 **23** and TBAJ-876 **24**, which are novel diarylquinolines where the naphthalene and aromatic are replaced by 3,5-dialkoxy-4-pyridyl (Figure 20). [21]

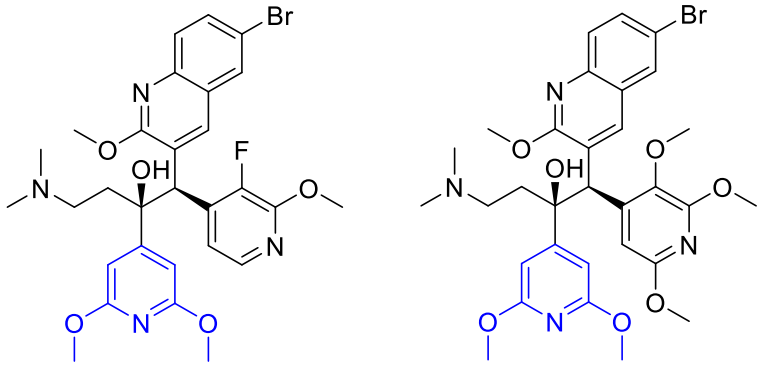


TBAJ-587
**23**

cLogP = 5.80
$MIC_{90}(H_{37}Rv)$ = 0.006 µg/ml
hERG $IC_{50}$ = 13 µM

TBAJ-876
**24**

cLogP = 5.15
$MIC_{90}(H_{37}Rv)$ = 0.004 µg/ml
hERG $IC_{50}$ = > 30 µM

Figure 20. Chemical structures of two pre-clinical candidates, TBAJ-587 **23** and TBAJ-876 **24.**

Both these compounds are less lipophilic and have lower MICs than BDQ against clinical isolates of *Mtb* virulent strain (H37Rv) and also lower potency against hERG. They are currently undergoing Phase 1 clinical trials to evaluate their potential as therapeutic candidates and preliminary findings indicate they have exhibited better safety and pharmacokinetic profiles than BDQ.[21]

### 1.3.4.2 Nitroimidazoles: Delamanid (DLM) and Pretomanid (PTM)

Two nitroimidazoles, PTM **25** and DLM **26**, are effective against *Mtb* and recommended by the WHO for treating MDR-TB.[44] DLM received FDA conditional approval in 2014, while in 2019 PTM received approval under the Limited Population Pathway for Antibacterial and Antifungal Drugs (Figure 21).[21]

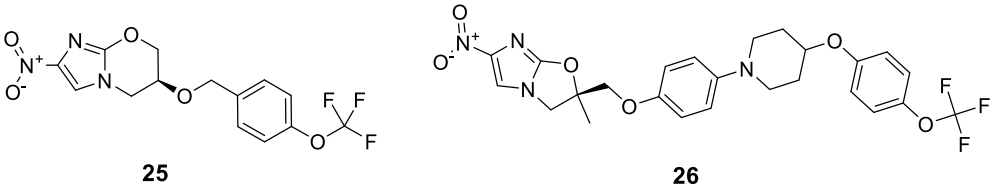


**25** **26**

Figure 21. Chemical structures of PTM **25** and DLM **26**.

They inhibit the formation of mycobacterial cell wall components methoxy- and keto-mycolic acids, both in anaerobic and hypoxic conditions.[44,73] Moreover, both nitroimidazoles are prodrugs that are activated via the mycobacterial F420-dependent reductase coenzyme system to create an active free radical.[44] The efficacy of DLM **26** was initially established in 2012 in a phase II clinical trial.[74] This study demonstrated that the incorporation of DLM **26** (100 mg twice daily) into a standard medication regimen resulted in a higher rate of sputum culture conversion after two months in patients with MDR-TB.[74] PTM **25,** on the other hand, obtained FDA approval in 2019 for the treatment of MDR-TB and XDR-TB.[52] This approval was based on the positive outcomes of the Nix-TB study, which demonstrated that a six-month therapy regimen containing bedaquiline, PTM **25**, and linezolid attained high success rates in patients with MDR-TB and XDR-TB.[75] Furthermore, despite the typical association of nitro groups with mutagenic characteristics, neither DLM nor PTM exhibited mutagenic properties in preclinical or clinical trials.[76] However, it is important to note that resistance to DLM has been recorded in many cases, linked to mutations in the gene that encodes the nitroreductase enzyme required for its activation.[77]

The second-generation nitroimidazole-oxazine derivative, TBA-354 **27**, represents an optimized analogue of PTM **25**, and significantly increased *in vitro* potency against both replicating and non-replicating *Mtb* strains, with a $MIC_{50}$ value of <0.015 µg/mL.[66] As a result, TBA-354 **27** has been accepted by the TB Alliance for further development, and it is currently undergoing Phase I clinical trials to evaluate its safety, pharmacokinetics, and potential as a new anti-TB agent (Figure 22).[66]

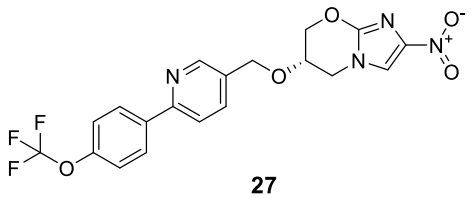


**27**

Figure 22. Chemical structure of the second generation candidate TBA-354 **27**.

### 1.3.4.3 Oxazolidinone

Linezolid (LZD) **28**, which was originally identified to combat infections from Gram-positive bacteria, has been repurposed for the treatment of drug-resistant TB and is currently classified as a category A drug by the WHO for the treatment of MDR-TB and XDR-TB (Figure 23).[78]

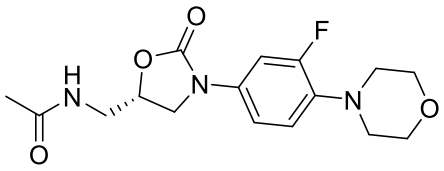

**28**

Figure 23. Chemical structure of LZD **28**.

Oxazolidinone antibiotics disrupt protein synthesis in *Mtb* by binding to the 30S and 50S ribosomal subunits, thereby blocking the translation process, which results in the bactericidal effect.[79] The binding of LZD to ribosomal RNA is not selective for *Mtb*, and its effect on mammalian mitochondria leads to the inhibition of mitochondrial protein synthesis, ultimately resulting in mitochondrial dysfunction.[66] Thereby, the efficacy of LZD is restricted due to its severe adverse effects including haematological toxicity, lactic acidosis and peripheral neuropathy.[66] Due to the severe side effects of LZD, different oxazolidinone analogues have been investigated against TB to identify a more tolerable yet equally or more effective alternative.[66] Consequently, several oxazolidinone compounds are now in clinical trials for TB treatment, including delpazolid **29**, sutezolid **30**, and TBI-223 **31** (Figure 24).[21]

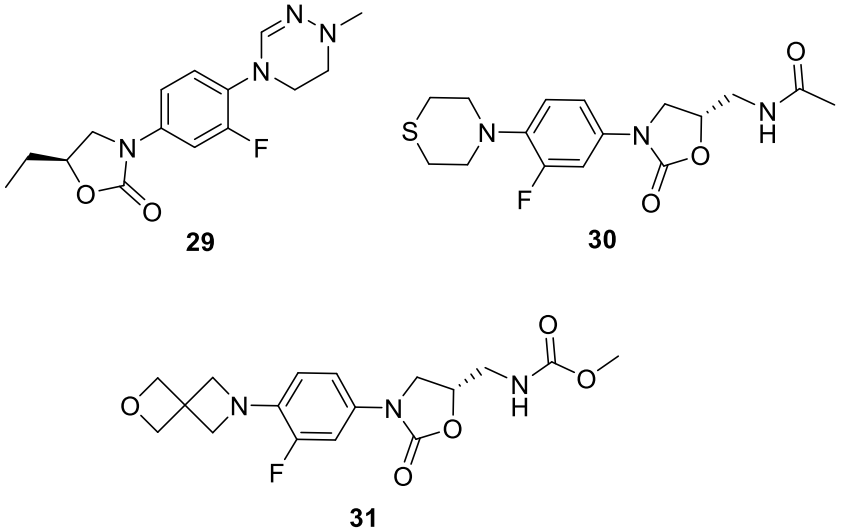

**29** **30** **31**

Figure 24. Chemical structures of delpazolid **29**, sutezolid **30**, and TBI-223 **31.**

Delpazolid **29**, a second-generation oxazolidinone analogue and sutezolid **30**, a thiomorpholinyl analogue of LZD, have both demonstrated promising activity in the management of MDR-TB.[80] Both drugs are currently in Phase 2 clinical trials and have successfully passed the evaluation of pharmacokinetics and safety in Phase I trials.[21] Sutezolid **30** is a thiomorpholine analogue of LZD **28** and exhibits a MIC range of ≤0.0625 to 0.5 mg/mL, which is three times lower than those of LZD **28**.[81] Furthermore,

**30** showed a higher mitochondrial protein synthesis $IC_{50}/MIC_{50}$ ratio than other oxazolidinones.[82] This combination of properties suggests its potential for better clinical outcomes, attributed to enhanced selectivity for targeting *Mtb* while minimizing toxicity.[82] Delpazolid **29** is a novel oxazolidinone synthesised with a cyclic amidrazone structure, which may allow for slow drug accumulation and effective excretion, which decreases long-term side effects. With a half-life ($t_{1/2}$) of 1.64 hours at an 800 mg oral dose, it is rapidly cleared from the body, reducing accumulation and toxicity during long-term TB treatment.[83] Another oxazolidinone is TBI-223 **31**, a novel compound in Phase 1 clinical trials.[84] Instead of the amide group and the morpholine ring structure in LZD **28**, it has a 2-oxa-6-azaspiro[3.3]heptane and a methyl carbamate moiety to enhance its pharmacokinetics and hydrophobicity.[84] It has been demonstrated to possess high oral bioavailability and a short half-life, no induction of Cytochrome (CYP) enzymes, and promising efficacy against *Mtb* in preclinical studies.[84]

#### 1.3.4.4 Q203 (Telacebec)

Imidazopyridines have been recognized as potent antitubercular scaffolds by different research groups.[85,86] Among these, the imidazo[1,2-*a*]pyridine amide (IPA) class shows remarkable selectivity toward *Mtb*.[87] The discovery of Q203 (Telacebec) **32**, the most advanced compound from the IPA class targeting QcrB, has initiated comprehensive lead optimization programs based on the IPA scaffold, which has resulted in the development of detailed SAR (Figure 25).[69,88]

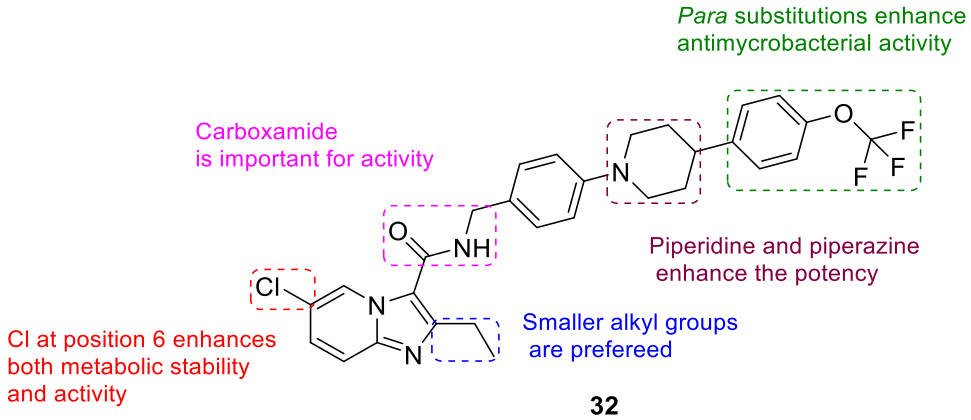


Figure 25. SAR study of Q203 **32**. Adapted from [69,89]

Pre-clinical studies demonstrated the high efficacy of Q203 as an anti-TB drug, while Phase 1 clinical trials indicated it is well-tolerated in healthy human participants.[67] In June 2019, Q203 successfully passed a Phase 2a Early Bactericidal Activity (EBA) clinical trial, showing its potential for use both alone or in combination.[67] Currently, it is

being assessed for its pharmacokinetic properties, safety and tolerability in ongoing clinical trials.[67,90] However, highly lipophilic hit compounds can cause toxicity by accumulation in fatty tissues, leading to prolonged exposure and side effects, especially in the kidneys and liver.[91] Given Q203 has a LogP of 7.64, a series of IPA derivatives with heteroatoms containing fused rings to mitigate the length of the side chain and logP values have been synthesised.[92] Among them, compound **33** showed significant antitubercular activity ($MIC_{80}$=0.009 μM) along with favourable metabolic stability with a reduced logP 6 value compared to Q203 (Figure 26).[92]

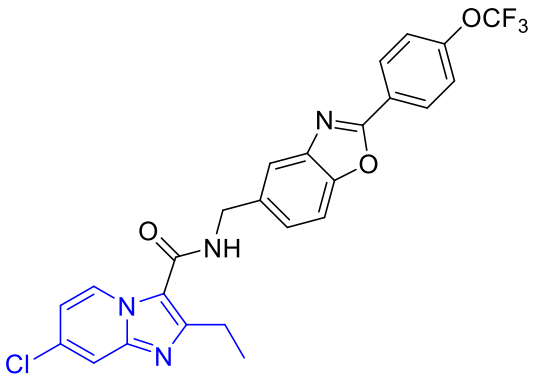


**33**

Figure 26. Chemical structure of compound **33**.

In a further study, with the similar objective of reducing the lipophilicity of Q203, Wang and colleagues developed a novel series of IPA derivatives.[91] These derivatives included basic heterocycles, primarily tetrahydroisoquinolines, formed by the fusion of benzene with pyrrolidine or piperidine rings. the optimized analogue **34** (Figure 27), which showed equipotent activity compared to Q203 ($MIC_{90}$ < 0.035 μM) against both drug-resistant and drug-susceptible *Mtb* strains, while having a reduced logP of 5.2.[91]

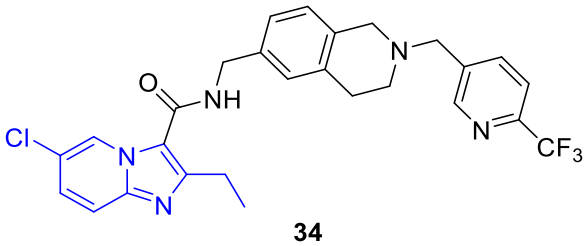


**34**

Figure 27. Chemical structure of compound **34**.

To conclude, the discovery of Q203 **32** has markedly advanced anti-TB drug development by inspiring different synthetic modification studies. These efforts have primarily emphasis on optimizing imidazo[1,2-*a*]pyridine amides, with particular

attention given to modifying the long side chain to decrease lipophilicity, thus improving drug-like properties.

As summarized in Figure 28, the history of TB treatment shows more than a century of important progress. After the discovery of *Mtb* by Robert Koch in 1882 and the introduction of the first TB vaccine in 1921, several key first-line medications including isoniazid, rifampicin, pyrazinamide and ethambutol were developed and became the foundation of standard TB therapy.[27] However, the emergence of TB drug resistant, which will be discussed in the next section, highlights the ongoing challenges in TB treatment and the need for continued research.

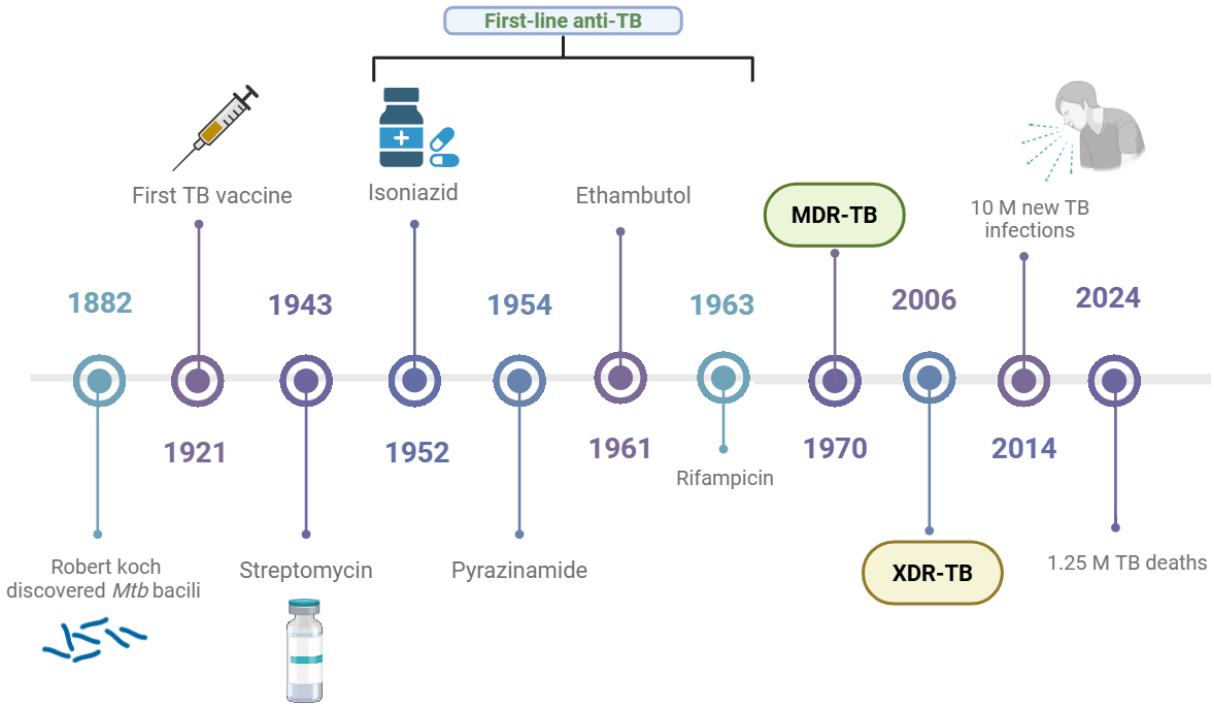


Figure 28. Timeline of major milestones in TB treatment.

## 1.4 Drug-resistant tuberculosis

Antimicrobial resistance (AMR) in bacterial species has emerged as a major global concern, significantly compromising existing treatment.[93,94] AMR is not only a significant complication in clinical settings but also ranks among the top ten worldwide public health challenges, demanding urgent attention and continuous research efforts.[93,94] One of the most concerning examples of AMR is drug-resistant TB, responsible for an estimated 13% of all AMR-related deaths worldwide, severely challenging TB control efforts.[95] Drug-resistant TB strains have rendered conventional treatments ineffective, resulting in extended illnesses, increased death rates, and the demand for more expensive and complex treatment options, hence making the fight against drug-resistant TB a crucial priority in the broader battle against AMR.[95] The emergence of drug resistant TB is affected by different factors, such as *Mtb* virulence, host-genetic factors, co-infection with HIV, and incomplete TB treatment.[55] Furthermore, ineffective medications or a low dose of anti-TB drugs used during therapy may give an additional advantage to the bacteria, allowing them to survive and choose resistant strains for future growth.[43] These factors promote the spread and emergence of drug resistant TB strains, complicating disease control efforts.[43]

Drug-resistant TB presents in various forms, each with specific therapeutic implications. RIF- resistant TB refers to TB resistance to only RIF, whereas MDR-TB indicates resistance to the most important front-line treatment INH and RIF, therefore resistance to these two drugs remains an important challenge for TB treatment.[96] However, the most severe type XDR-TB, exhibits resistance to both INH and RIF, any fluoroquinolone, and at least one of the three injectable second-line agents (kanamycin, amikacin, or capreomycin), which usually requires a treatment regimen containing of up to eight medications, with some involving daily injections for up to two years.[96] Despite this intensive and prolonged therapy, the prognosis for XDR-TB remains unfavourable, with survival and complete recovery rates of approximately 34%, highlighting the serious challenges to combating this resistant form of TB.[96]

The WHO recommends many MDR-TB treatment regimens, which are divided into short and long treatment regimens, with the short regimen recommended for 9 – 11 months, whereas the long regimen is recommended for 18 – 20 months (Table 2).[50,97,98]

| WHO class | Anti-TB agent | Effect |
|---|---|---|
| **A** (Include all three agents) | Bedaquiline | Bactericidal |
| | Levofloxacin/Moxifloxacin | Bactericidal |
| | Linezolid | Bacteriostatic |
| **B** (Add one or both agents) | Clofazimine | Bactericidal |
| | Cycloserine/ terizidone | Bacteriostatic |
| **C** (Add to complete the regimen and when agents from Groups **A** and **B** cannot be used) | Delamanid | Sterilizing and bactericidal |
| | Amikacin | Bactericidal |
| | Ethionamide/ prothionamide | Bacteriostatic |
| | Para aminosalicylic acid | Bacteriostatic |

Table 2. Summary of drugs for MDR-TB.

MDR-TB patients on longer regimens should get all Group **A** agents and at least one Group **B** agent to ensure therapy begins with at least four potentially efficacious TB drugs and continues with at least three agents after bedaquiline is discontinued.[78] If just one or two agents from Group **A** are included, both agents from Group **B** should be added.[78] If the regimen cannot be completed with agents from Groups **A** and **B** alone, then agents from Group **C** are introduced.[78] To further reduce the burden of resistance, the WHO consolidated guidelines for the treatment of drug-resistant TB, published in May 2022, introduce significant advancements in treatment protocols. These guidelines recommend all-oral, shorter regimens (6–9 or 9–12 months) including Group **A** agents and pretomanid.[99] The novel BPaLM and BPaL regimens, including bedaquiline, pretomanid, and linezolid, with or without moxifloxacin, showed some treatment success for MDR-TB and pre-XDR-TB while reducing the need for longer regimens.[99]

TB drug resistance is a multifaceted process influenced by several mechanisms at both genetic and phenotypic levels.[2] These mechanisms include intrinsic resistance, acquired resistance and phenotypic resistance.[100] Intrinsic resistance refers to the inherent properties of *Mtb* that naturally limit the effectiveness of many antibiotics.[100] The first line of defence is the unique and complex structure of the *Mtb* cell envelope, which is composed of a thick, waxy, lipid-rich outer layer (*cf.* Section 1.2.2).[100] The impermeability of this structure limits the penetration of many drugs, especially hydrophilic compounds, reducing their ability to reach intracellular targets. Furthermore, *Mtb* employs efflux pumps as part of its intrinsic defence.[101] These transmembrane proteins actively transport a wide range of antibiotics out of the bacterial cell, lowering intracellular drug concentrations.[101] The acquired drug resistance mechanism in *Mtb*

is primarily the result of chromosomal mutations.[2] This mutation confers resistance in *Mtb* via diverse mechanisms, including target alteration (such as resistance to RIF, PZA, linezolid and EMB), elimination of the prodrug activation necessity (such as resistance to front-line drugs INH, PZA and EMB), and a mutation increases a bacterial enzyme that inactivates the drug, leading to loss of drug activity (such as resistance to kanamycin and amikacin) (Figure 29).[2]

Resistance to front-line anti-TB agents has been associated with mutations in at least

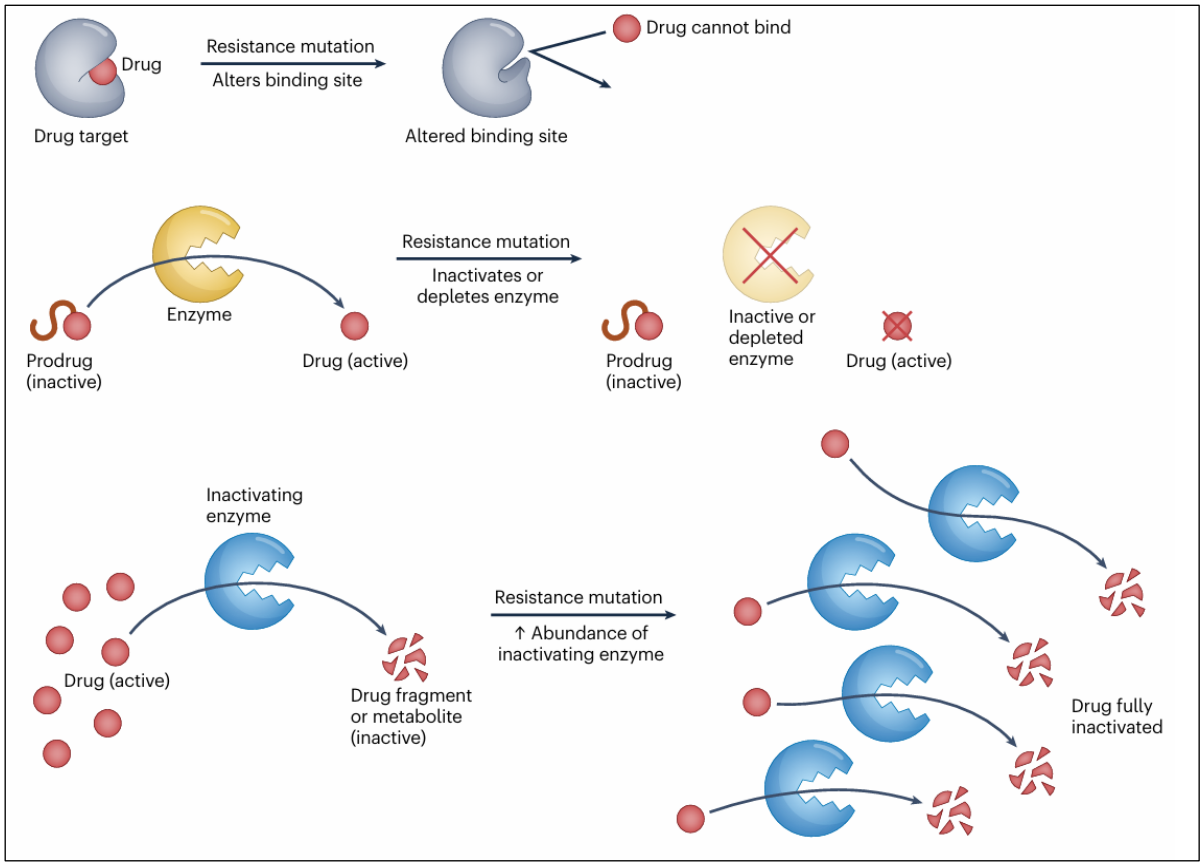


Figure 29. Common mechanisms of TB-drug resistance. Adapted from [2]

ten different genes.[100] For example, INH resistance-associated genes include *katG*, *inhA*, *ahpC* and *kasA*, whereas resistance to RIF is mainly linked to mutations in the *rpoB* gene. Some of the antibiotic target genes and associated resistance mechanisms are shown in Table 3.[100]

| Resistance mechanism | Antibiotics | Target gens |
|---|---|---|
| Drug target alteration | RIF | *rpoB* |
| | INH | *inhA* |
| | ETH | *embB* |
| | Ethionamide | *inhA* |
| | Fluoroquinolone | *gyrA/ gyrB* |
| | Streptomycin | *rrs* |
| Elimination of Prodrug Activation | INH | *katG* |
| | Pyrazinamide | *pncA* |
| | Ethionamide | *ethA* |
| | p-amino salicyclic acid | *folC* |

Table 3. Summary of antibiotic target genes and associated resistance mechanisms.

Phenotypic drug resistance, in contrast to genotypic drug resistance, is generally caused by inhibited cell division or decreased metabolic activity, rather than particular chromosomal mutations.[100] During latent infection, *Mtb* enters a dormant state, characterized by an important downregulation of its metabolic processes.[101] This metabolic dormancy increases the bacterium's resistance to antimicrobial drugs that are usually effective against replicating bacilli, therefore contributing to phenotypic drug resistance.[101] In latent TB, *Mtb* while residing within granulomas, encounters multiple stressors such as elevated temperature, pressure, low pH, nitrogen and oxygen stress.[101] These conditions lead to the misfolding and aggregation of certain *Mtb* proteins.[101] To survive these environmental challenges, *Mtb* requires mechanisms to eliminate or degrade these aggregated proteins, enabling the bacterium to adapt with external stresses, maintain cellular homeostasis, and ultimately enhance its survival in a nutrient-limited and hostile environment. One such crucial system is the pup-proteasome system, which will be discussed in the next section.

## 1.5 The Pup-proteasome system (PPS)

### 1.5.1 Background

Protein homeostasis is an essential component of cellular integrity, that is maintained by tightly regulated mechanisms at the translational, transcriptional, and post-translational levels.[102] Among these, post-translational modifications (PTMs) function as an important regulatory mechanism, enabling the diversification of proteins.[102] These modifications affect a wide range of protein behaviours and characteristics, including enzyme function and assembly, protein lifespan, protein-protein interactions, cell-cell interactions, receptor activation, protein folding and protein localization.[102,103] In particular, modifications that function as quality control systems by tagging proteins for degradation have been the focus of ongoing research.[104,105]

One of the PTM pathways responsible for protein degradation in eukaryotic systems is ubiquitination, which operates through the ubiquitin-proteasomal system (UPS).[106] The UPS is involved in several cellular processes, including the regulation of signalling cascades for cell growth, proliferation and differentiation. Ubiquitination is a three-step process that is ATP-dependent and highly regulated.[106] The process begins with the E1 enzyme that activates ubiquitin in an ATP-dependent manner, which is then transmitted to E2 ubiquitin-conjugating enzymes, and finally ligated to substrate lysine residues through E3 ubiquitin-ligase complexes (Figure 30).[106]

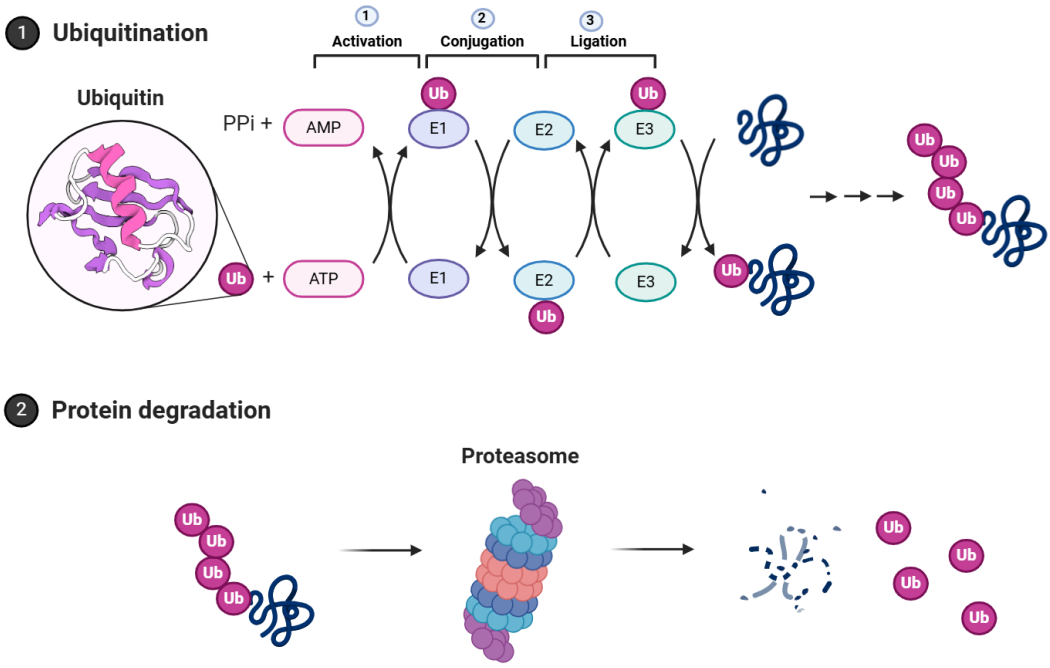


Figure 30. A schematic diagram of ubiquitin-proteasomal system. (Adapted with edits from BioRender)

There are two types of E1 enzymes and around 50 to 60 types of E2 enzymes, while more than 600 - 700 different E3 ligases have been identified.[107] The wide variety of E3 ligases is important for maintaining the specificity of ubiquitination among various cellular proteins.[107] During the ubiquitination process, this modification is frequently repeated many times, which leads to the formation of a polyubiquitin chain on the substrate.[107] This polyubiquitinated tail functions as a signal for identification by the 26S proteasome, tagging the protein for degradation (Figure 30).[107]

In contrast to this complex system, some prokaryotes employ a simpler system for modifying target proteins with small protein tags for degradation.[108] Specifically, in Actinobacteria such as *Mtb*, *Corynebacterium glutamicum*, and *Mycobacterium smegmatis*, a pup-proteasome system (PPS) is a post-translational protein-tagging system that identifies target proteins for degradation by a proteasome.[109] Moreover, within the PPS, the target protein is tagged for proteasomal degradation by a small, unstructured protein called prokaryotic ubiquitin-like protein (Pup), which, despite its functional similarity to eukaryotic ubiquitin, shares no sequence or structural homology with ubquitin.[110] Both proteins can exist as an inactive form that requires activation before use; upon activation, they are covalently linked to substrate lysine residues, functioning as signals before the degradation of the tagged protein by the 20S proteasome.[108]

A significant difference between these systems is that while ubiquitination requires a large cascade of enzymes to perform its functions, pupylation relies primarily on only two important enzymes.[111] Both of these enzymes are members of the γ-carboxylate amine ligase family: one activates the pro-form of Pup, while the other enzyme functions as the ligase, linking Pup to the substrates, a process that will be explained further in the subsequent sub-section.[111]

### 1.5.2 The pupylation cycle

The pupylation cycle comprises a highly regulated pathway for protein degradation in prokaryotes, including specific steps of deamination, ligation of pup to target proteins (pupylation), and ends with proteasomal degradation (Figure 31).[4]

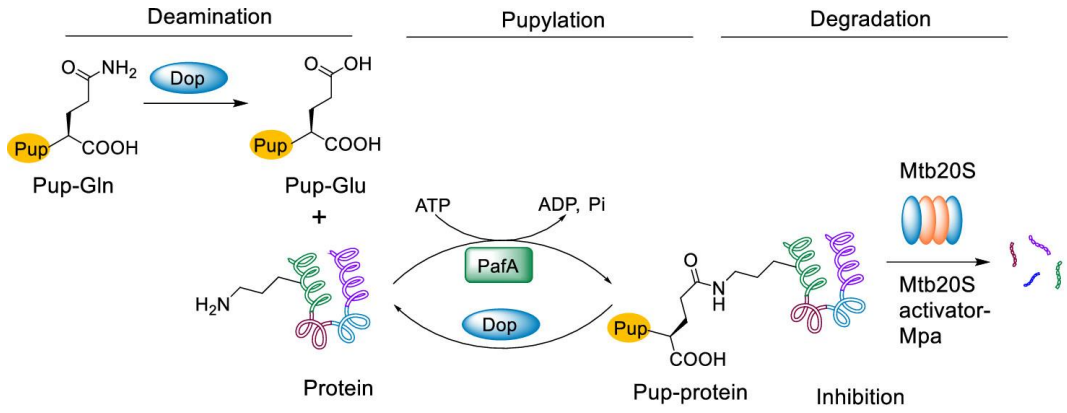


Figure 31. A schematic diagram of the pup-proteasomal system. Adapted from [4]

In several mycobacteria, including *Mtb*, Pup is initially expressed as C-terminal glutamine (PupQ), which is subsequently deaminated to glutamate (PupE) by the deamidase of Pup (Dop).[112] This reaction represents the first step of the pupylation cycle, facilitating the activation of Pup for subsequent protein tagging.[113] In the second step, the C-terminal glutamate is phosphorylated by Proteasome Accessory Factor A (PafA), followed by nucleophilic attack of a substrate lysine amino group to form an isopeptide bond between the C-terminal glutamate of PupE and a lysine ε-amino group of a protein substrate.[114] The pupylated protein is then recognised by mycobacterial proteasome ATPase (Mpa), which unfolds and delivers them into the *Mtb* proteasome for degradation.[110]

The PPS is essential for both *Mtb* persistence and virulence, regulating protein turnover, adapting to the hostile intracellular environment, and evading host immune defences.[115] Specifically, in terms of *Mtb* persistence, the pupylation pathway strengthens the pathogen's resistance to many stresses faced within host macrophages, such as nutritional deficiencies and abrupt changes in temperature or pH.[115,116] Moreover, it helps in resistance to many defensive mechanisms of macrophages including reactive oxygen species (ROS), and reactive nitrogen intermediates (RNI).[117] As shown in a study conducted by Darwin et al. (2003), an important link was identified between the PPS and resistance to reactive-nitrogen species (RNS) stress, before elucidating the pupylation pathway.[118] This investigation involved the induction of RNS stress by subjecting *Mtb* to sodium nitrite ($NaNO_2$) at an acidic pH of 5.5, resulting in a significant reduction in the survival rates of *Mtb* strains deficient in PPS components compared to wild-type strains.[118] A further study demonstrated that PPS protects *Mtb* from antimicrobial antifolates, including sulfonamides, by modulating folate reduction, thereby facilitating the bacteria's survival

amongst these treatments.[119] In addition to its central role in the persistence of *Mtb* in the host, PPS is necessary for the control of various metabolic pathways, including a copper homeostasis system required for complete *Mtb* virulence.[120,121]

Recent studies have highlighted PPS as a highly promising target for drug development, with an emphasis on combating *Mtb*. Efforts to identify novel anti-TB agents have notably focused on targeting the *Mtb* 20S proteasome, a key component in protein degradation.[122,123] In particular, a series of macrocycles were developed as *Mtb* 20S proteasome inhibitors, and a structure-guided study of their structure- activity relationship was performed to improve both potency and selectivity.[4] Among this series, compound **35** inhibited *Mtb*20S with $IC_{50}$ values of 7.4 nM (Figure 32).[4]

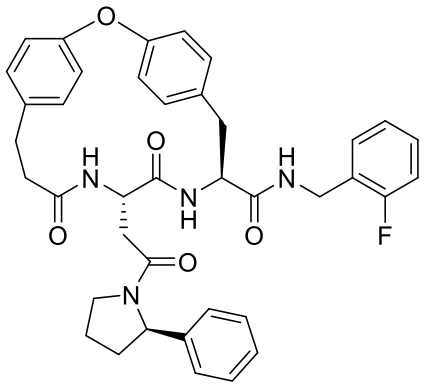

**35**

Figure 32. The structure of one of the series of macrocycle analogous to target 20S proteasome.

However, the 20S proteasome in *Mtb* is homologous to the eukaryotic core particle, indicating that drugs targeting this bacterial proteasome may also impact the human proteasome, leading to host side effects by interfering with critical proteolytic functions.[123] Consequently, alternative targets in this biochemical pathway would be of interest, one of which is PafA. Targeting PafA presents at least two advantages: its sequence lacks homology with ubiquitination transferases and other human proteins, hence minimizing the potential of off-target effects, and PafA is crucial to *Mtb* virulence and its persistence inside the host.[119,124]

### 1.5.3 Proteasome Accessory Factor A (PafA)

Unlike the ubiquitin-proteasome system, which uses hundreds of ubiquitin ligases, the pupylation pathway in *Mtb* is mediated by a single enzyme, PafA, that conjugates Pup to several protein substrates.[125] Aravind and colleagues conducted a detailed bioinformatic investigation shortly after discovering PafA was involved in pupylation,

which indicated it belongs to the superfamily of carboxylate amine/ammonia ligases.[115] This family includes glutamine synthetase (GS) which PafA has been shown to mimic with ATP-dependency and a similar two-steps mechanism (Scheme 1).[126]

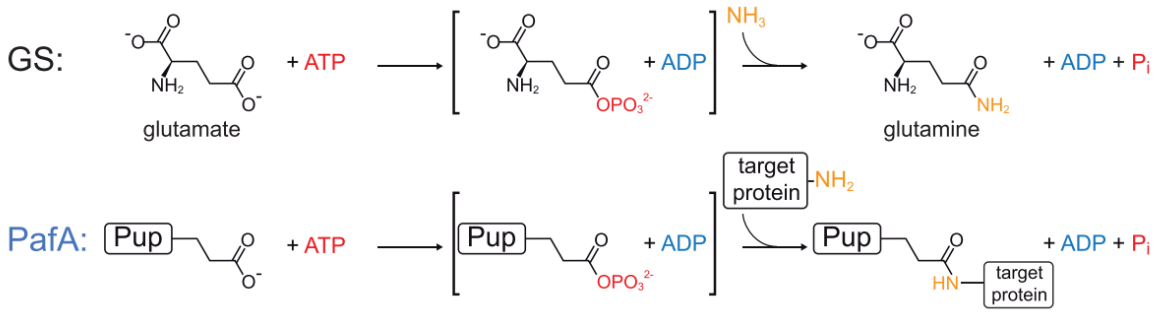


Scheme 1. Both GS (top) and PafA (bottom) use a two-step catalytic mechanism that involves the formation of an acyl phosphate intermediate in the first step followed by ligation of amine group of lysine residue in (PafA) or amine in (GS).

Recently research has focused on PafA as a therapeutic target, highlighting its crucial role as the sole Pup ligase in *Mtb* and its potential as a promising selective drug target.[125,127] The first PafA inhibitor was reported in a study conducted by Jigang *et al.*, which identified pan-protease inhibitor 4-(2-aminoethyl) benzenesulfonyl fluoride (AEBSF) **36** as a potent inhibitor for *Mtb* pafA.[128] AEBSF inhibits PafA by obstructing Pup attachment to target proteins and disrupting the pupylation process (Figure 33).[128]

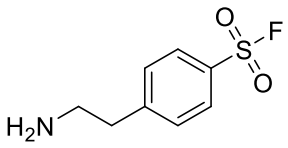

**36**

Figure 33. Chemical structure of AEBSF **36**.

Given the pupylation pathway is tightly regulated, it is hypothesised that both activating and inhibiting PafA might disturb bacterial protein homeostasis, thereby inhibiting *Mtb* growth. Based on this hypothesis, a recent paper reported that researchers targeted *Mtb*-PafA by screening 1,354 compounds, they identified two inhibitors ST1926 **37** and bithionol **38**, which hinder PafA activity via different mechanisms: ST1926 **37** binds to the Pup binding groove selectively, whereas bithionol **38** competes with ATP in the ATP-binding pocket.[125] Additionally, B-F2 (YM155) **39** was identified to activate pupylation in *Mtb*, presenting new avenues for anti-TB drug development targeting bacterial protein degradation (Figure 34).[125]

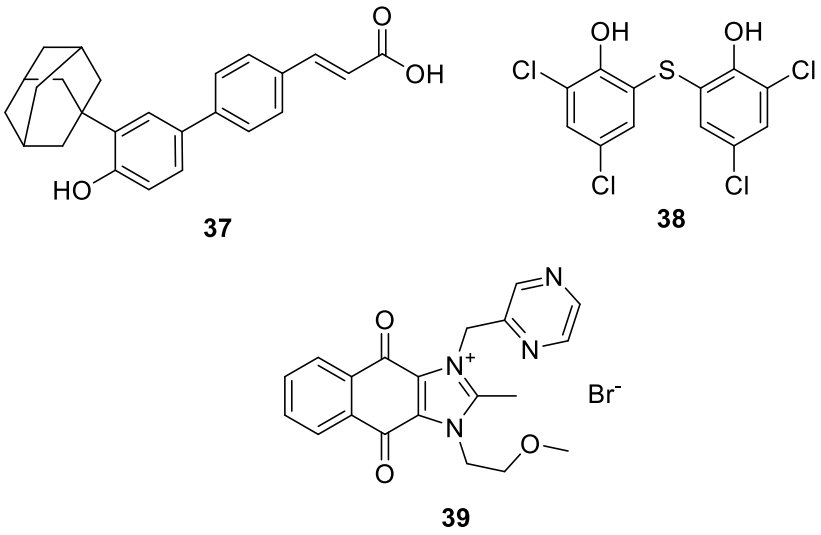


Figure 34. Chemical structures of ST1926 **37**, bithionol **38** and YM155 **39**.

#### 1.5.3.1 PafA potential binding site

The pupylation system and its essential enzymes, Dop and PafA, are structurally and mechanistically intriguing due to their distinct differences from ubiquitination in its simpler conjugation mechanism and unique structural components.[129] The Pup ligase PafA, which enables pupylation, is structurally distinct from eukaryotic ubiquitin ligases and, as previously stated retains the characteristic GS fold within its active site, along with the two-step catalytic mechanism of the GS superfamily.[130] Previous studies have reported the structural characterisation of the pupylation enzymes, revealing that PafA and Dop comprise two tightly interacting domains, as shown through extensive biochemical and mutational studies.[110,114,128] The enzyme's active site is located in the larger N-terminal domain, which is composed of the first 400 residues (Figure 35).[110]

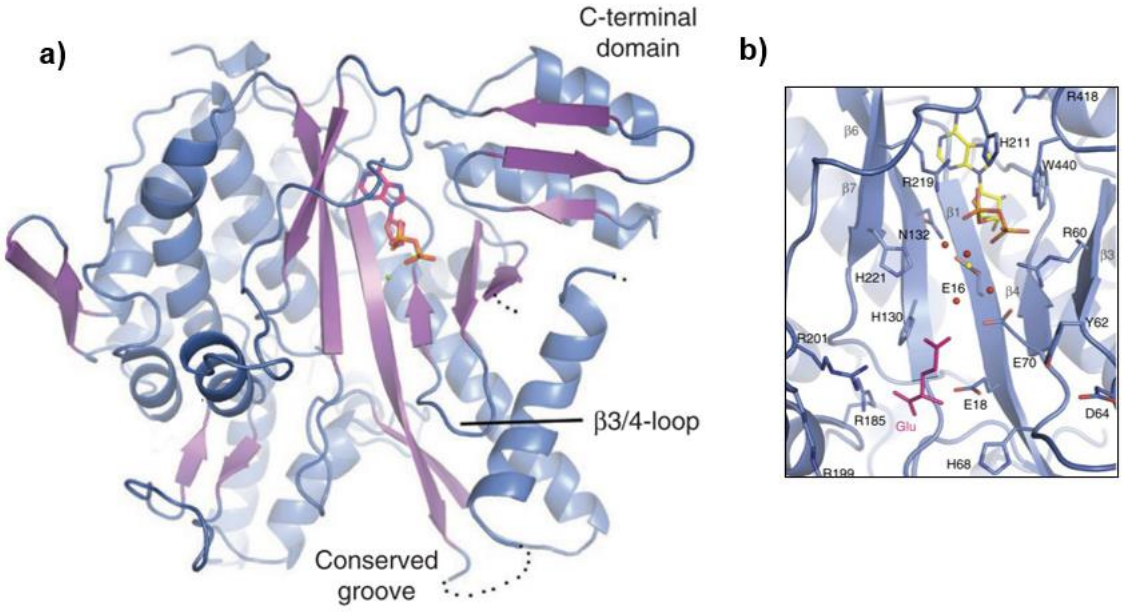


Figure 35. a) The crystal structures of PafA from *C. glutamicum* with ADP (PDB code: 4BJR), b) Zoomed view of the PafA active site. Important residues are shown in stick representation. A glutamate molecule (pink). Adapted from [110]

The active site itself is shallow and open, enabling interaction with a large variety of substrates while certain enzymes, such as glutamine synthetase, have an active site buried deep inside a huge oligomeric complex.[110] The N-terminal domain includes a twisted central β-sheet composed of six antiparallel β-strands, creating a concave surface known as the β-sheet cradle, which is crucial to PafA's catalytic mechanism and structurally this domain is similar to carboxylate-amine ligases.[110] However, both Dop and PafA feature a small C-terminal domain of approximately 70 residues, absent in other carboxylate-amine ligases, identifying it as unique to the Dop/PafA family.[110] This domain contains conserved residues (such as W440) around the nucleotide-binding pocket, which are essential for pupylation.[110] In particular, deletion of this C-terminal domain at locations 414 or 420 leads to a pupylation-deficient phenotype in *Mtb*, suggesting the C-terminal domain is critical for enzymatic activity.[110]

Despite the general homology of Dop and PafA, there is one feature that allows the two to be distinguished at the sequence level.[131] Dop has a length of 40-65 residues around its N-terminus known as the Dop loop, which is absent from PafA.[131] A specific role of this loop, on the other hand, is unclear and is currently being investigated.[131]

Overall, possible inhibitors specific to PafA could target unique features such as the Pup-binding groove or the nucleotide-binding pocket that includes the PafA/Dop-specific C-terminal domain.[110,114] Both binding sites are expected to be specific for

pupylation and the compounds that target them should not inhibit other γ-carboxylate amines/ammonia ligase family members.[110,114]

In another study, Regev et al. have established a conserved loop located at the edge of the PafA active site, which was determined to be important for substrate interactions.[132] By employing a combination of docking and mutational analysis, the researchers identified arginine 207 and adjacent residues in this loop, revealing that mutations in these residues impaired pupylation activity, highlighting the importance of these residues (Figure 36).[132]

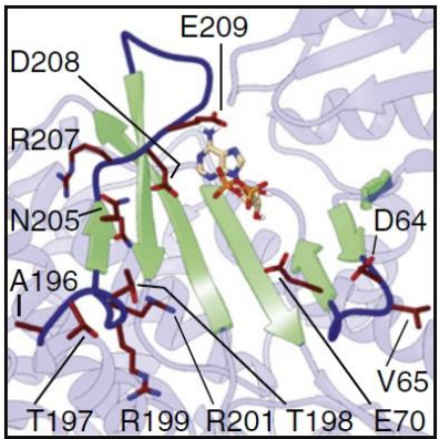


Figure 36. A crystal structure of *C.glutamicum* PafA (PDB code: 4BJR) showing the loop residues. Adapted from [132]

Additionally, another study identified the serine residue S119 on *Mtb* PafA as a key binding site for the inhibitor AEBSF **36**, which inhibits PafA activity.[128] A structural study indicated that S119 is positioned within a groove critical for Pup-binding despite its distance from the catalytic site.[128]

Taken together, previous biochemical and mutational studies have elucidated key structural features of PafA, highlighting its significance as a therapeutic target. These insights provide a vital framework for guiding the design and synthesis of novel PafA inhibitors in the fight against TB. While our focus is on developing inhibitors for PafA, reviewing GS inhibitors is valuable in light of the structural homology between GS and PafA, as it may provide significant insights into optimising inhibitor design.

## 1.6 Glutamine synthetase (GS)

Glutamine synthetase in *Mtb* (*Mt*GS) is a well-known therapeutic target due to its essential role in bacterial virulence and growth.[133] This enzyme, encoded by the *glnA1* gene, catalyzes the ATP-dependent transformation of ammonium and L-glutamate into L-glutamine, ADP, and phosphate.[134] Along with its primary role in nitrogen metabolism, *Mt*GS facilitates cell wall biosynthesis by synthesising a poly-L-glutamate-glutamine component specific to pathogenic mycobacteria.[134] A homologous variant of GS is present in eukaryotes, exhibiting a tissue-specific role in mammals.[133] For example, in neural tissue, GS is essential for regulating ammonia toxicity and transforming neurotoxic glutamate into glutamine, whereas in hepatic tissue, it plays a role in systemic ammonia detoxification.[133] Consequently, to prevent off-target effects on the mammalian enzyme, inhibitors developed for *Mt*GS must exhibit high specificity and selectivity for the bacteria.

### 1.6.1 Current GS inhibitors

Current GS inhibitors can be classified into two categories: the first targets the glutamate-binding site, and the second targets the nucleotide-binding site (ATP-competitive inhibitors).[135] The first group are typically low MW and highly polar amino acid analogues, and their SAR was discovered to be restricted; phosphinothricin (PPT) **40** was the most potent inhibitor of this class (Figure 37).

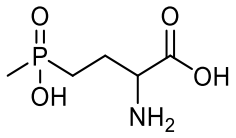


**40**

Figure 37. Chemical structure of PPT **40**.

These compounds target the glutamate-binding site, which is highly conserved in both eukaryotic and prokaryotic GS; hence, they lack selectivity.[134] In addition, they are polar and flexible with limited drug-like properties. This has led to more research into drug-like inhibitors for *Mt*GS.[134] In this context, ATP-competitive inhibitors are generally larger, more drug-like and more hydrophobic heterocyclics.[134] Notably, they target the nucleotide-binding site, which demonstrates low conservation between prokaryotic and eukaryotic GS, indicating it as a promising target for the development of selective inhibitors for the bacterial enzyme.[134]

### 1.6.1.1 Imidazo[1,2-*a*]pyridines as GS inhibitors

Imidazo[1,2-*a*]pyridine is a promising fused bicyclic heterocyclic ring that has been accepted as a drug scaffold due to its wide range of biological and pharmacological applications, including antitubercular, anticancer, antimicrobial, anticonvulsant, antiviral and antidiabetic.[136] Many imidazo-[1,2-*a*]pyridine derivatives are reported to have anti-TB activity.[135] The 3-aminoimidazo[1,2-*a*]pyridines have emerged as potential *Mt*GS inhibitors following an AstraZeneca high-throughput screening (HTS) campaign.[134] To explore the SAR of these inhibitors, two systematic approaches were used. The first focused on optimizing substituents on the pyridine and phenyl rings, enabling researchers to evaluate the impact of steric and electronic effects on binding affinity and inhibitory activity.[134] The second strategy included modifying the amine substituents to assess the impact of various functional groups on selectivity and potency against *Mt*GS.[134] In this study, a small library of 16 compounds was synthesised and evaluated for their *Mt*GS inhibitory activity.[135] Among all compounds, **41** was identified as a GS inhibitor with an $IC_{50}$ of 0.38 μM (Figure 38).[135]

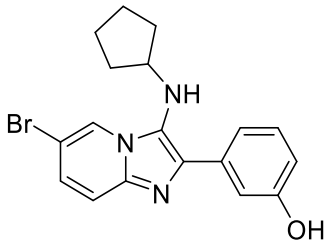


**41**

Figure 38. Chemical structure of analogue 3-aminomidazo[1,2-*a*]pyridine **41**.

## 1.7 Previous work in the group

In our previous work, a diverse library of approximately 100 compounds was developed as potential anti-tubercular agents, encompassing structural classes such as benzoxa-[2,1,3]-diazoles, thiocoumarins, purines, flavones, indolin-2-ones and quinolines.[137] To evaluate their antibacterial efficacy, resazurin microtiter assays (REMAs) were utilised at a fixed concentration of 128 μg/ml, targeting a broad range of drug-sensitive bacterial strains, including Gram-negative, Gram-positive, and mycotic species.[137] While certain compound classes exhibited significant inhibition of bacterial growth, others showed minimal or no activity, even at this high concentration.[137]

Subsequent analysis of the compound library revealed a class of compounds exhibiting selective activity against *mycobacteria*, featuring a benzoxa-[2,1,3]-diazole

pharmacophore.[137] An additional REMA assay was conducted to assess these benzo-[2,1,3]-diazole pharmacophore linked to the amino acid hydrazides component **42** where in both simple and branched amino acids, along with diverse modifications to phenyl hydrazine substituents, were investigated (Table 4).[137]

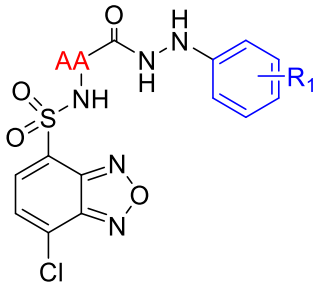

**42**

| Amino Acid (AA) | Hydrazine ($R_1$) | **Compound** | *M. tuberculosis* (μM) | Mammalian Cell Toxicity | *S. aureus (MRSA)* | *M. luteus* | *B. subtilis* | *B. cereus* | *E. faecalis* | *E. faecium* | *S. agalactiae* | *S. pyogenes* | *Y. enterocolitica* | *P. aeruginosa* | *S. marcescens* | *E. coli* |
|---|---|---|---|---|---|---|---|---|---|---|---|---|---|---|---|---|
| Gly | 4-Cl | **42a** | 19.2 | 43% | - | - | - | - | - | - | - | - | - | - | - | - |
| Gly | 4-$CF_3$ | **42b** | 12.0 | >90% | - | - | - | - | - | - | - | - | - | - | - | - |
| Gly | 4-F | **42c** | 20.0 | 60% | - | - | - | - | - | - | - | - | - | - | - | - |
| Gly | 3-Cl | **42d** | 19.2 | 22% | - | - | - | - | - | - | - | - | - | - | - | - |
| Gly | 2-Cl | **42e** | 19.2 | 29% | - | - | - | - | - | - | - | - | - | - | - | - |
| Ala | 4-$CF_3$ | **42f** | 17.2 | 60% | - | - | - | - | - | - | - | - | - | - | - | - |
| Phe | 4-$CF_3$ | **42g** | 59.2 | 85% | - | - | - | - | - | - | - | - | - | - | - | - |

Table 4. REMA assay result of selected benzoxa-[2,1,3]-diazole analogues where Glycin(Gly), Alanine(Ala) and phenylalanine(Phe) amino acids were utilised against Gram-positive, Gram-negative, and *mycolata* bacteria, as well as their mammalian cell toxicity. (- = No activity from the REMA assay at 128 μg/ml). Adapted from [137]

The findings demonstrated notable specificity and potency against *Mtb* compared to broad-spectrum Gram-negative and Gram-positive bacteria, highlighting the promise of benzo-[2,1,3]-diazole substituted amino acid hydrazides in targeted anti-mycobacterial therapy. The SAR investigation of these compounds revealed that benzo-[2,1,3]-diazole pharmacophore was essential for activity and the presence of

heavy halogen substitutions were favourable at *meta* position of the phenyl hydrazine part (Figure 39).[137]

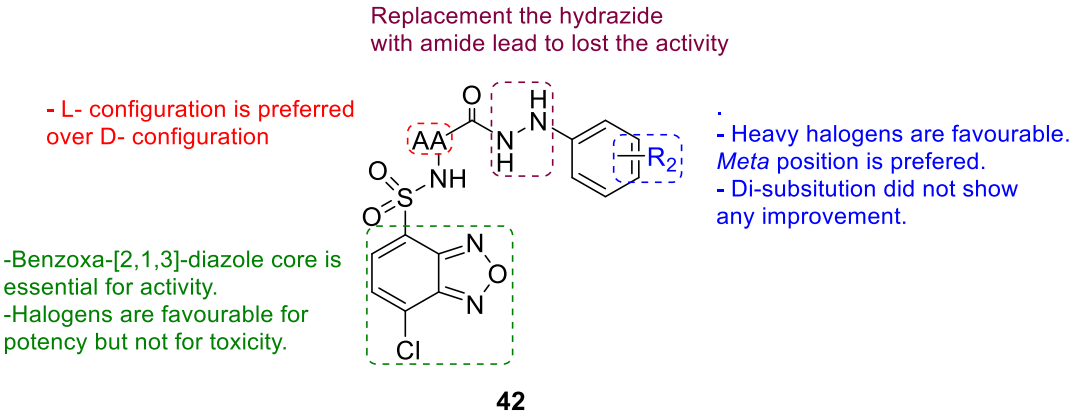


**42**

Figure 39. The previous SAR investigation of the benzoxa-[2,1,3]-diazole scaffold.

Although the results of benzoxa-[2,1,3]-diazole-substituted amino acid hydrazides were promising, concerns regarding their toxicity profile necessitated more research. To address this, the investigation was expanded using a scaffold-hopping approach, substituting the benzoxa-[2,1,3]-diazole core with well-known anti-TB pharmacophores.[138] One scaffold of particular interest was the imidazo[1,2-*a*]pyridine core, which forms the basis of Q203 **32**, a well-known drug currently undergoing phase 2 clinical trials that has demonstrated promising anti-TB activity. Nonetheless, as previously discussed in (*cf*. Section 1.3.4.4), the lipophilicity of Q203 **32** presents issues that affect its pharmacokinetic profile (Figure 25).

Given the initial findings of the benzoxa-[2,1,3]-diazole-substituted analogues, which showed promising antibacterial activity but were limited by toxicity concerns, we employed a scaffold-hopping approach to address these issues. By replacing the benzoxa-[2,1,3]-diazole core with the imidazo[1,2-*a*]pyridine scaffold, this approach aims to retain or enhance efficacy while mitigating toxicity observed in the initial findings.

Following this strategy, the imidazo[1,2-*a*]pyridine scaffold was incorporated with the amino acid hydrazide moiety resulting in derivatives exhibiting moderate anti-*Mtb* activity.[138] However, these compounds exhibited notable selectivity towards INH-resistant *Mtb* strain, with MIC results less than 10 µM for analogues containing the amino acids methionine (Met) and alanine (Ala) (Table 5).[138]

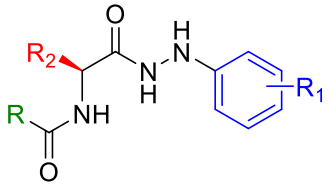

| R | $R_1$ | $R_2$ | MIC (μM) WT | Rif $^R$ | $INH^R$ |
|---|---|---|---|---|---|
| 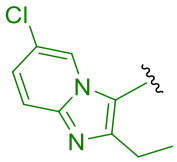 | 4-$CF_3$ | Ala | 35 | 35 | 35 |
| | | Met | - | - | 62 |
| | 3-Cl | Ala | 76 | 76 | 9 |
| | | Met | 33 | 33 | 8 |

Table 5. Previous data of imidazo[1,2-*a*]pyridine-3-carboxy scaffold. WT = Wild type *Mtb* strain; $Rif^R$ = Rifampicin resistant *Mtb* strain; $INH^R$ = Isoniazid resistant *Mtb* strain. Adapted from [138]

This finding emphasises the potential of these imidazo[1,2-*a*] pyridine-substituted amino acid hydrazides in combating drug resistant-TB, highlighting a scaffold that retains efficacy while selectively targeting resistant *Mtb*. Despite these promising findings, gaining a better understanding of the SAR and identifying possible targets of these compounds are crucial step toward clarifying the principles behind their selectivity for drug resistant-TB. Further details on the aims and scope of this project will be presented in the following section.

## 1.8 Aims of the present work

Building on the previous findings and considering the structural homology between PafA and GS discussed previously (*cf.* Section 1.5.3), GS inhibitors emerged as an area of interest, particularly compound **41**, due to its imidazo[1,2-*a*]pyridine scaffold, which attracted interest for its known anti-TB activity and the prior promising results with adaptations of this scaffold (Figure 40).

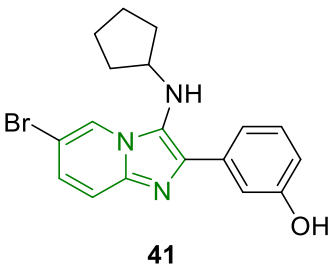

**41**

*Mt*GS $IC_{50}$ =3.3 μM

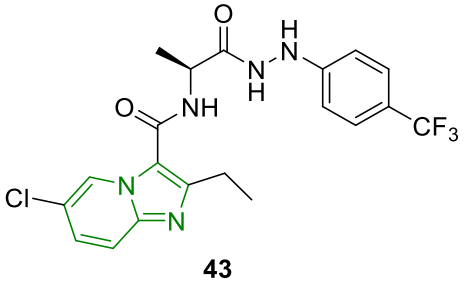

**43**

*Mtb* MIC= 35 μM

Figure 40. Example of ATP-competitive GS inhibitor **41**, and chemical structure of compound **43**, synthesised in our lab.

This project, therefore, aims to expand on previous findings by adapting compound **43**, previously synthesised by our group, and modifying the ethyl group with a phenyl ring to mirror the structure of compound **41**. Through this modification, a series of analogues based on the imidazo[1,2-*a*]pyridine scaffold will be investigated in a virtual screen at a specific PafA pocket to assess their potential as effective PafA inhibitors (Figure 41).

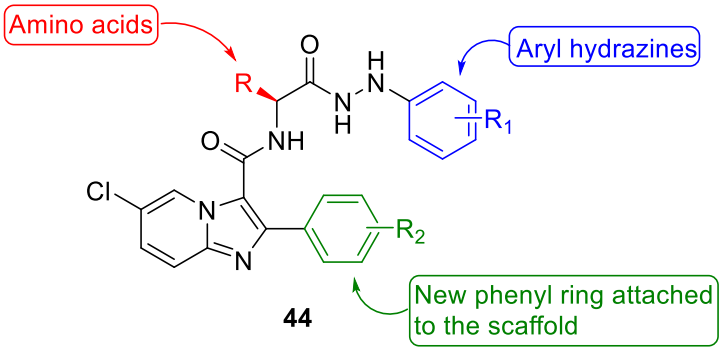


Figure 41. Chemical structure of final compound based on imidazo[1,2-*a*]pyridine scaffold, highlighting the key modifications.

Subsequently, different analogues of this scaffold will be synthesised, allowing a comprehensive structure-activity relationship study to evaluate anti-TB efficacy. This study will use REMA assay to assess compound activity, guiding the optimisation of the scaffold for increased anti-TB efficacy. All synthesised compounds will be screened against several *Mtb* strains, including both susceptible and resistant strains.

Based on the screening results, the most promising compounds will be chosen for further docking studies on the PafA binding pocket to understand key molecular interactions. Furthermore, the physicochemical properties and ADME profiles of the synthesised candidates will be predicted using ADMETlab 3.0 software. These parameters will then be compared to those of marketed anti-TB drugs to assess drug-likeness. This integrated an approach aims to identify potent antitubercular agents with enhanced drug-like properties and to assess their potential as PafA inhibitors for anti-TB treatment.

# 2. Synthesis of imidazo[1,2-*a*]pyridine analogues

## 2.1 Introduction and modelling study

As outlined in chapter one, TB continues to be the leading cause of death from a single infectious agent globally. This persistently high mortality rate is primarily driven by the significant challenges associated with TB therapy, particularly the emergence of drug-resistant TB. Hence, extensive global efforts are continuing to identify novel therapeutic approaches to tackle the challenges posed by TB. Prior research within the group has identified benzo-[2,1,3]-diazole-substituted amino acid hydrazides as selective inhibitors of *Mtb*, exhibiting specificity over broad-spectrum activity. Nonetheless, due to toxicity issues, alternative scaffolds are being explored to attain similar specificity with enhanced safety profiles. One promising scaffold explored in medicinal chemistry is imidazo[1,2-*a*]pyridine, a fused bicyclic heterocyclic framework largely regarded as a privileged scaffold due to its extensive range of applications across pharmacological and biological fields.[139,140] For example, alpidem **45**, a benzodiazepine receptor ligand, functions as an anxiolytic, whereas zolimidine **46**, is utilised for the treatment of gastro-oesophageal reflux disease and peptic ulcers.[141] The therapeutic importance of the imidazo[1,2-*a*]pyridine scaffold is also exemplified by zolpidem **47**, an FDA-approved medication for insomnia, emphasising the structural adaptability of this framework (Figure 42.).[141]

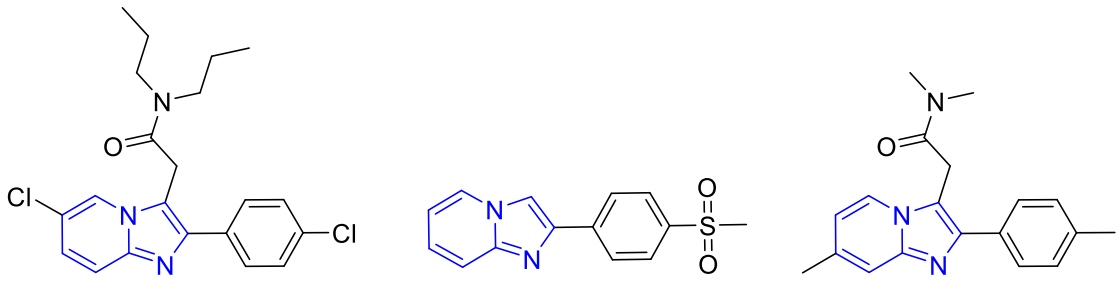


Figure 42. Three drugs based on the imidazo[1,2-*a*]pyridine scaffold, currently available on the market.

This framework inspired the researchers to repurpose zolpidem **47** for TB, resulting in encouraging activity ($MIC_{90}$ of 10 μM).[142] Consequently, through strategic structural modifications and the synthesis of a series of analogues, together with comprehensive SAR analysis, anagram 8 **48** was identified as the most potent analogue, showing an $MIC_{90}$ of 0.004 μM against *Mtb* without any toxicity, these series of compounds can be considered as the first generation imidazo[1,2-*a*]pyridine for TB therapy.[142] Moreover,

compound TB47 **49** was identified as a promising candidate and is currently going through preclinical safety evaluations (Figure 43).[143]

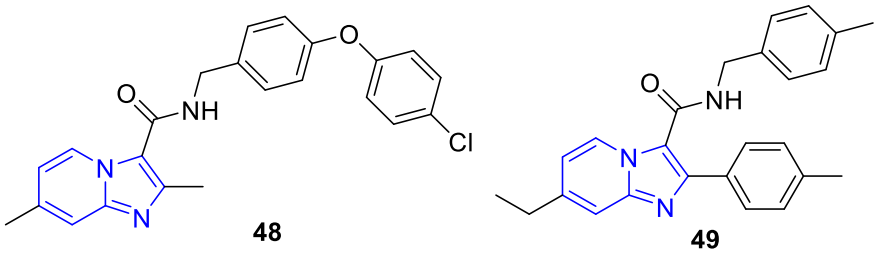


Figure 43. Promising anti-TB candidates based on imidazo[1,2-*a*]pyridine scaffold.

Besides this, the potential anti-TB candidate Q203 **32** has progressed to a phase 2 clinical trial (Figure 25).[87]

Considering the medicinal importance of the imidazo[1,2-*a*]pyridine scaffold and its promising results as an anti-TB agent, combined with the promising potential of PafA as a target for *Mtb* (*cf.* Section 1.5.3), these serve as the foundation for this research. Here, we intend to utilise virtual screening of compound **44** against PafA and evaluate the binding affinity and investigate its interactions with the target site (Figure 41).

**Molecular docking study:**

Molecular docking is a computational technique utilised to predict a ligand-receptor complex through two important steps: ligand sampling and scoring.[144] The sampling algorithm determines the optimal conformations of the ligand within the active site of a specific protein, evaluating potential binding interactions.[144] A scoring function is subsequently applied to score these conformations according to their predicted binding affinities.[144] In this research, docking studies were performed using GOLD 4.0, a software tool that employs a genetic algorithm to predict the binding of flexible ligands to protein binding sites.[145] This method determines the most favourable poses and conformations that best complement the active site of the protein.[145] The docked poses were then analysed utilising BIOVIA Discovery Studio Visualizer and PyMOL to evaluate molecular interactions, including hydrogen bonding and hydrophobic interactions.

An *in silico* investigation in this research was initiated utilising a simplified analogue (compound **44a**), the unsubstituted amino acid, hydrazine, and phenyl ring attached to the scaffold were evaluated to assess their potential binding interactions (Figure 44).

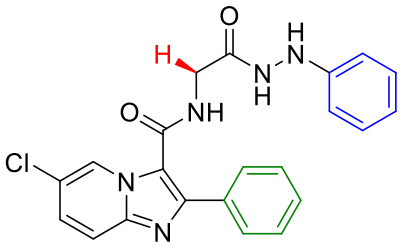


**44a**

Figure 44. Chemical structure of **44a**

The structure of *Mtb* PafA was obtained from the AlphaFold2 Protein Structure Database (ID: A5U4C3) and subsequently refined through the addition of hydrogen atoms. AlphaFold2 assigns a per-residue confidence score (pLDDT) ranging from 0 to 100, reflecting the reliability of structural predictions at each residue. The PafA model demonstrates high structural confidence, with pLDDT values exceeding 90 across most regions (Figure 45).

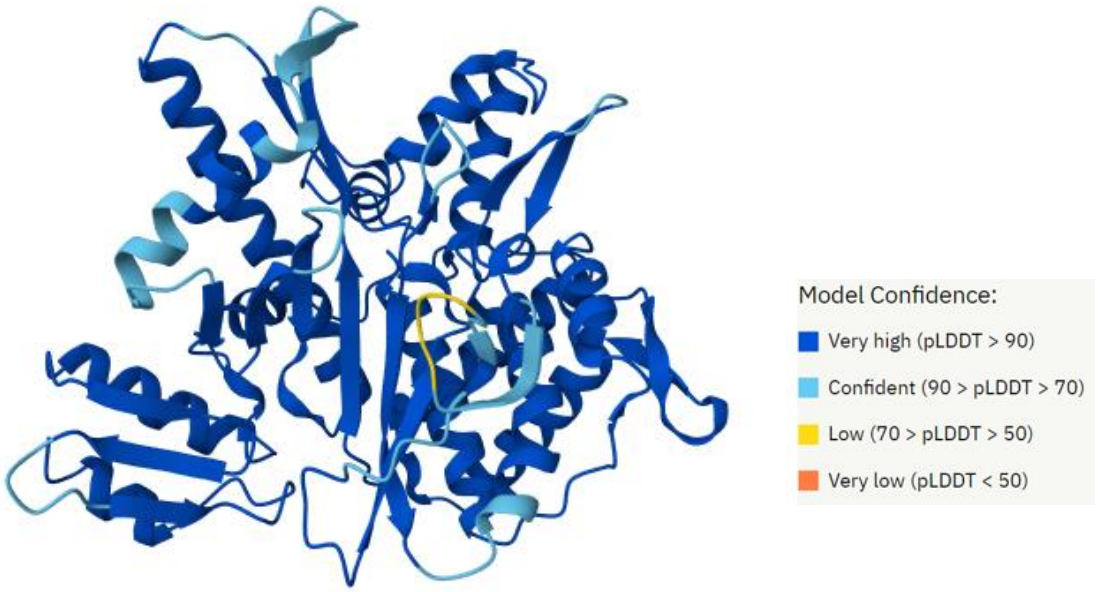


Figure 45. PafA model generated by AlphaFold2 (ID: A5U4C3) with confidence values indicating prediction reliability.

The binding site for this study was determined using previously published literature, as discussed in (*cf.* section 1.5.3.1). The ATP binding site was chosen as an important region, incorporating key residues significant for PafA activity. Specifically,

the binding site included residues from the C-terminal domain, such as Trp419, as well as Arg205, a critical residue within the flexible loop.[132] The significance of these residues for PafA activity has been confirmed by previous mutational studies.[110] Based on the docking analysis, compound **44a** was positioned within the ATP-binding pocket of PafA, using ATP as a reference ligand for comparison. The top-ranked docked poses of **44a** occupied the same region as the adenylyl ribose group of ATP (Figure 46).

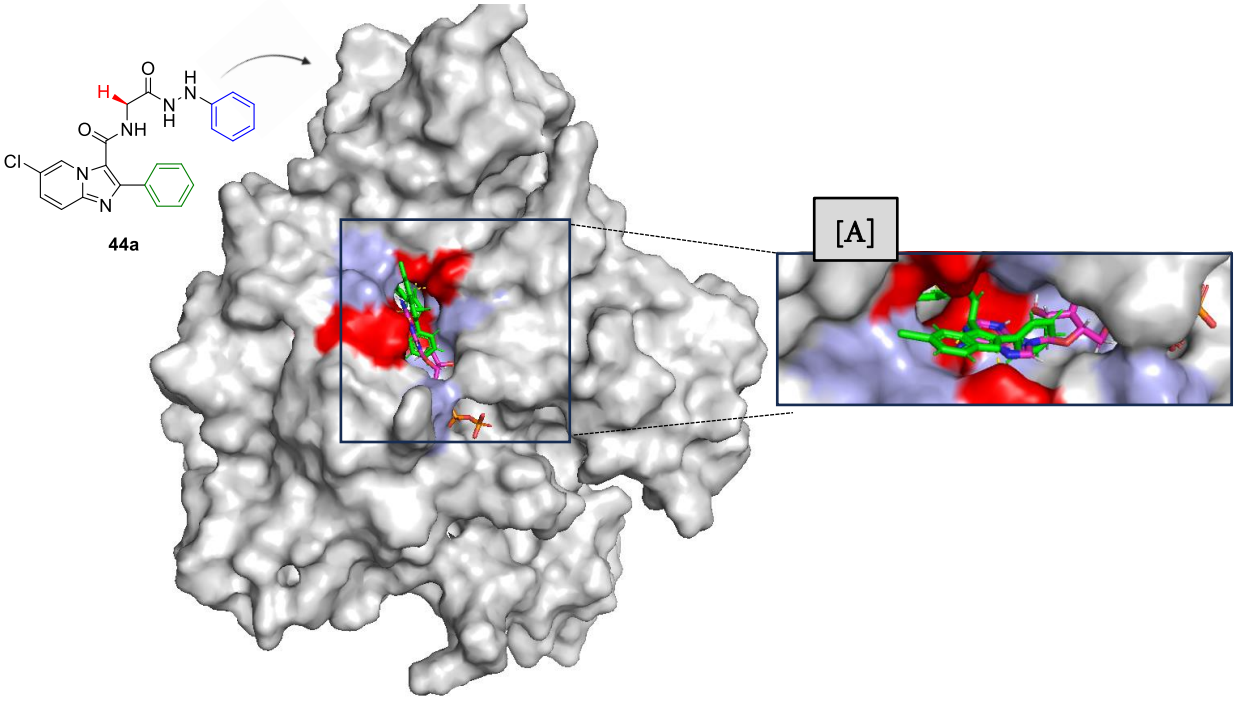


Figure 46. Docked **44a** (green) overlaid with ATP in the ATP binding pocket of PafA. (A) Zoomed view of **44a** compound interaction with PafA active site,

Further confirmation of this interaction was obtained through 3D and 2D visualizations, as depicted in Figure 47. Compound **44a** interacted with the ATP-binding pocket, forming multiple hydrogen bond interactions with important residues, including Trp419, Arg205 and Tyr55 (Figure 47).

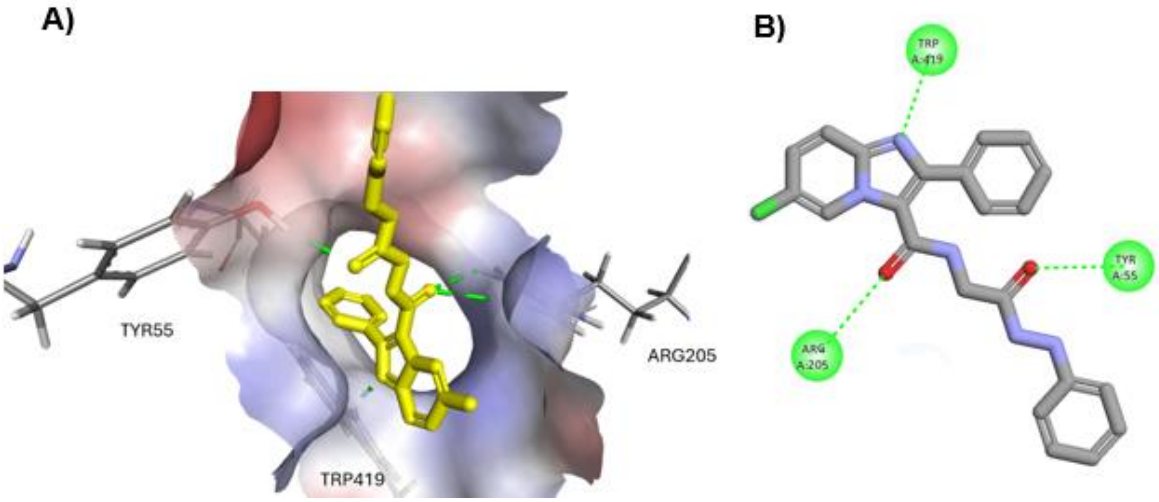


Figure 47. 3D visualisation of the interaction of **44a** compound in the ATP binding site. B) 2D diagram of the ligand-protein interaction.

To further investigate the potential of the compound and study the impact of structural modifications, the investigation was expanded to assess substitutions on the arylhydrazine moiety and its coupling with different amino acids. A total of 116 compounds were proposed, each consisting of arylhydrazines with different substitutions linked to amino acids such as glycine (Gly), alanine (Ala), Methionine (Met), phenylalanine (Phe), leucine (Leu) and Isoleucine (Ile). The modification of the arylhydrazine encompassed electron-donating groups (such as $OCH_3$, $CH_3$) and electron-withdrawing groups (such as $CF_3$, $OCF_3$) positioned at different locations around the aromatic ring, in addition to halogens like Cl and Br. Each compound was virtually docked, producing 10 poses per compound, resulting in a total of 1160 poses. Comparative analysis with **44a** demonstrated that incorporating substitutions on the arylhydrazine part markedly improved binding affinity scores and enhanced the number of hydrogen-bonding interactions with the residues at the ATP binding pocket, the comparative analysis of compound **44a** with the top 11 docked analogues is presented in Table 6.

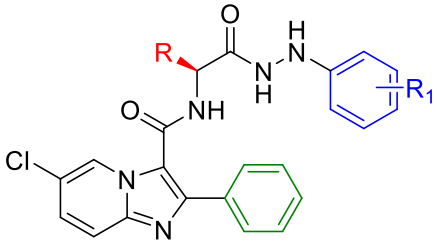

**44**

| R | $R_1$ | Docking Score | H-Bonding | R | $R_1$ | Docking Score | H-Bonding |
|---|---|---|---|---|---|---|---|
| Gly | H | 67.4 | Trp419,Arg205,Tyr55 | Ala | 2-$CF_3$ | 74.3 | Arg205,Trp419,Tyr55 |
| Gly | 3-$OCF_3$ | 97.7 | Glu9,Arg205,Arg53 | Ala | 3-$CF_3$ | 74.1 | Arg205,Trp419,Tyr55 |
| Gly | 4-$OCH_3$ | 97.6 | Arg205,Trp419 | Gly | 2-Br | 74.1 | Arg205,Trp419 |
| Gly | 3-$OCF_3$ | 82.6 | Arg205,Trp419 | Gly | 4-$CF_3$ | 73.7 | Arg205,Trp419 |
| Gly | 3-$CF_3$ | 77.9 | Arg205,Trp419,Tyr55 | Gly | 2-Cl | 73.3 | Arg205,Trp419 |
| Gly | 2-$OCF_3$ | 74.8 | Arg205,Trp419,Tyr55 | Gly | 2-$CF_3$ | 73.1 | Arg205,Trp419 |

Table 6. Comparison of the docking scores and hydrogen-bonding interactions for the compound **44a** and its modified analogues.

The glycine analogue with a 3-$CF_3$ substituent on the arylhydrazine moiety showed the best docking score of 97.7 (Figure 48). It formed five hydrogen bonds with important residues as well as a hydrophobic interaction with Trp419 a key residue at the ATP-binding site. These results highlight the enhanced interaction potential conferred by the modified aryl hydrazide derivatives, hence confirming the feasibility of structural optimization within this framework.

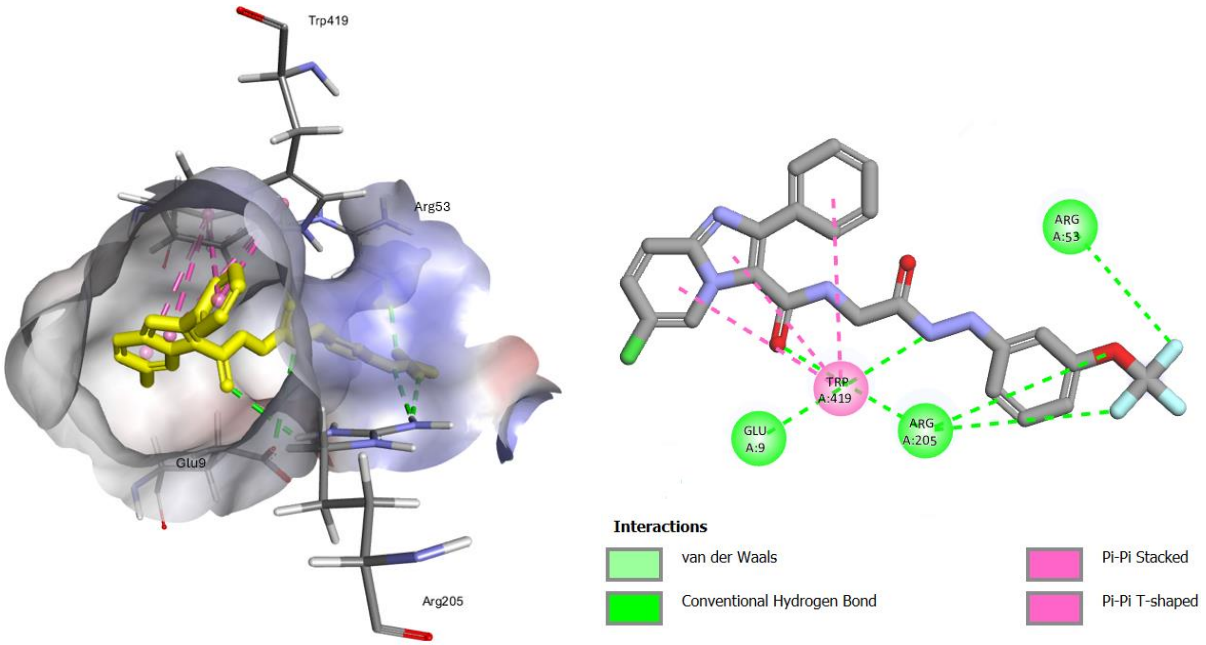


Figure 48. A) 3D interaction of 3-$CF_3$ analogue (the best-docked compound) in the PafA active site. B) 2D diagram of the ligand-protein interaction.

The *in silico* study detailed in this section highlights the potential of this compound as a promising candidate for targeting *Mtb* by binding to the PafA active site. Molecular docking and binding affinity analysis indicate a favourable interaction profile; nonetheless, experimental confirmation is essential to fully clarify its biological activity. Therefore, the synthesis and subsequent *in-vitro* assessment of these compounds are important to validate these agents. The following section will detail the synthesis of the final compounds, establishing a foundation for subsequent structure-activity relationship study, which will be thoroughly discussed in chapter 3.

## 2.2 Synthesis of the imidazo[1,2-*a*]pyridine amino acid hydrazides

Given the recognised significance of imidazo[1,2-*a*]pyridines as an anti-tubercular agent, along with the promising findings from the previous investigations within the group (*cf.* section 1.5.3), the *in-silico* results further support the hypothesis that these molecules could serve as ATP-competitive inhibitors by binding to the ATP pocket of PafA, an important enzyme in *Mtb*. This possible interaction could interfere with important degradation pathways in *Mtb*, making these compounds promising candidates for anti-TB therapy. Subsequently, a comprehensive structure-activity relationship investigation was initiated to determine the structural features important for the biological activity of the targeted compounds.

In the beginning, the retrosynthetic analysis of target compound **44** was undertaken with an initial disconnection at the amide bond, resulting two components: 6-chloro-2-phenylimidazo[1,2-*a*]pyridine-3-carboxylic acid **50** and amino acid hydrazide **51**. Another disconnection of the amino acid hydrazide **51** at the hydrazide bond produced aryl hydrazine **53** and *N*-protected amino acid **52** (Figure 49).

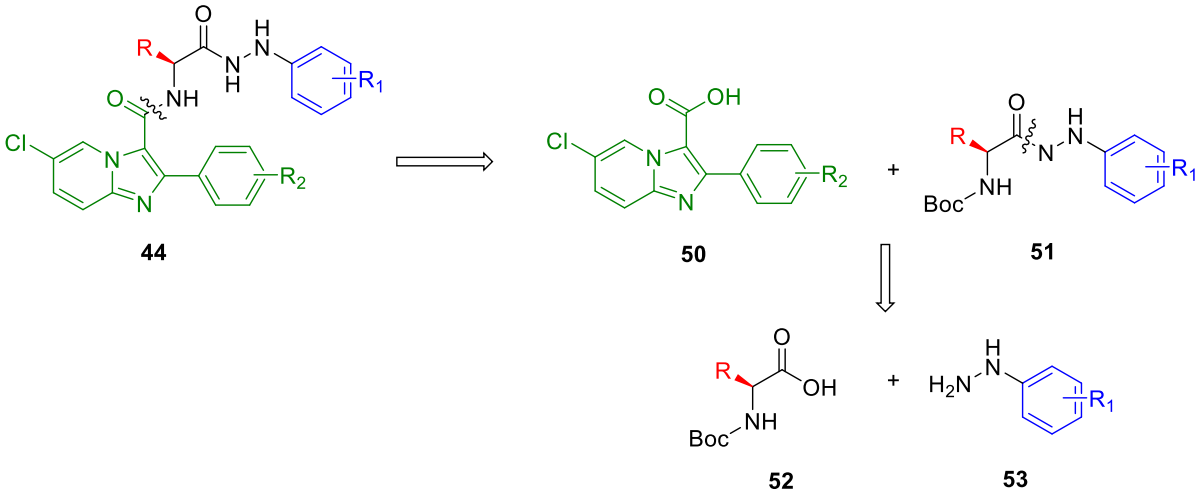


Figure 49. Retrosynthetic analysis of target compound 44, into its precursors.

While both arylhydrazine **53** and the *N*-protected amino acid **52** are commercially available, imidazo[1,2-*a*]pyridine-3-carboxylic acid **50** is not readily accessible and thus must be synthesised. Therefore, the initial step in the synthesis of the target compound **44** involves preparing this carboxylic acid. Accordingly, the retrosynthetic pathway begins with compound **50**, which results from the hydrolysis of the ester intermediate **54**. Subsequent cleavage steps lead to the formation of 2-amino-5-chloropyridine **55** and ethyl 2-bromop-3-oxo-3-phenylproponate **56**, an intermediate synthesised from commercially available ethyl 3-oxo-3-phenylpropanoate **57** (**Error! Reference source not found.**).

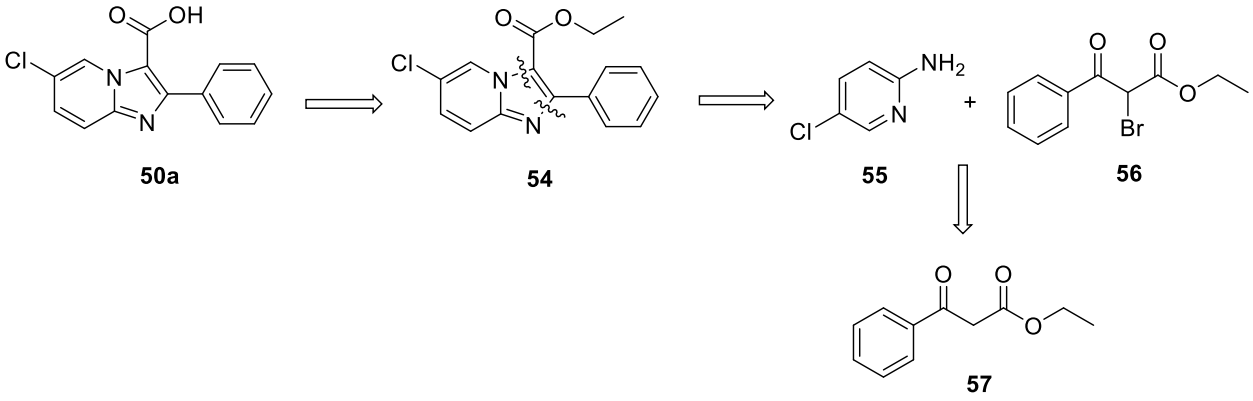


Figure 50. Retrosynthetic analysis of target compound ~~44~~, into its precursors.

### 2.2.1 Synthesis of the imidazo[1,2-*a*]pyridine-3-carboxylic acid precursor

To begin the synthesis, preparation of 6-chloro-2-phenylimidazo[1,2-*a*]pyridine-3-carboxylic acid is needed for the amide coupling. A literature review identified a procedure for synthesising this carboxylic acid **50** with an acceptable yield (Scheme 2).[146]

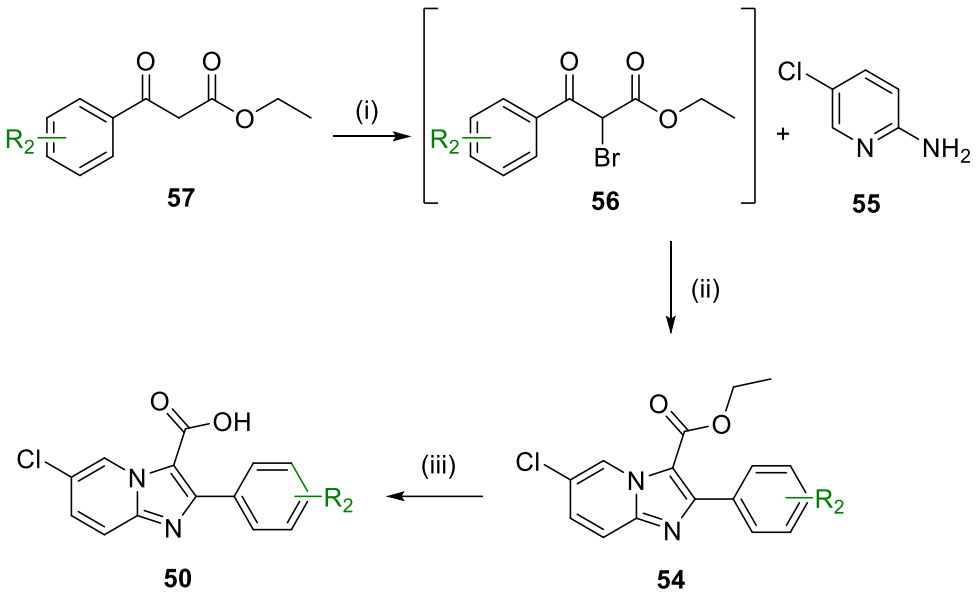


Scheme 2. Synthetic route of imidazo[1,2-*a*]pyridine-3-carboxylic acid. Reagents and conditions: (i) NBS, $NH_4OAc$, $Et_2O$. (ii) **55**, EtOH, 80 °C overnight. (iii) $LiOH.H_2O$, EtOH, rt, overnight.

The synthesis starts with the bromination of 1,3-dicarbonyl species **57** using *N*-bromosuccinimide (NBS) as a convenient brominating agent, resulting in an intermediate that subsequently condenses with 2-aminopyridine **55** in ethanol, leading to the production of the ester **54** which was isolated and purified utilising column chromatography with a hexane/ethyl acetate (2:1) solvent system. The structure of the ester was confirmed using several spectroscopic techniques, including $^1$H NMR, IR, and high-resolution mass spectrometry (HRMS). Furthermore, its structure was confirmed by growing crystals suitable for X-ray diffraction via slow evaporation from acetone (Figure 51).

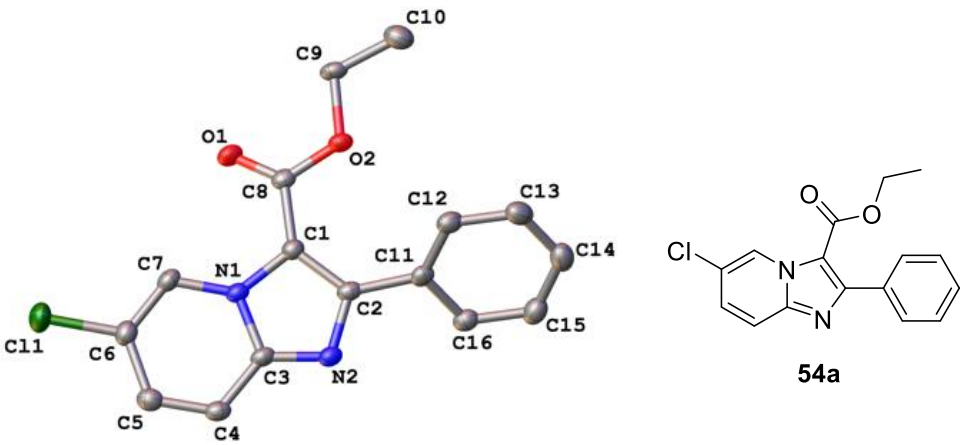


Figure 51. Single crystal X-ray structure of imidazo[1,2-*a*]pyridine ester **54a**.

Following the successful confirmation of ester production, the focus turned to the conversion of the ester into a carboxylic acid via hydrolysis. The hydrolysis reaction was conducted using aqueous lithium hydroxide, in accordance with a previous study, with the procedure modified by extending the reaction time from 4 hours to overnight.[147] Upon completion, $^1$H NMR analysis confirmed the full conversion of the ester to the desired carboxylic acid, with the disappearance of the characteristic ester signals which include a triplet for the methyl group ($CH_3$) at 1.25 ppm and a quartet for the methylene group ($CH_2$) at 4.3 ppm. Instead, a broad signal appeared at 13.5 ppm, corresponding to the hydroxyl (OH) group of the carboxylic acid, therefore confirming the successful conversion (Figure 52).

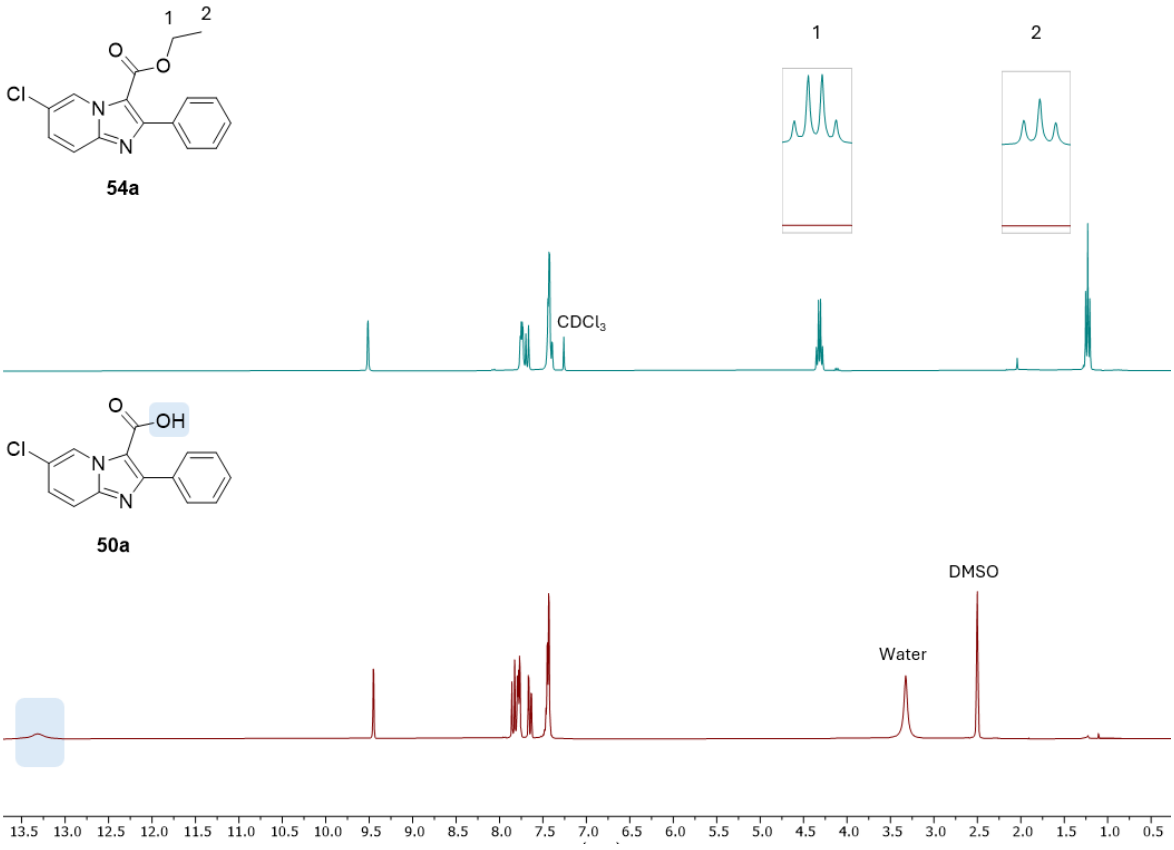


Figure 52. $^1$H NMR spectra confirmed the complete conversion of ester **54a** into carboxylic acid **50a**. The disappearance of 2 signals at 1.25 ppm and 4.3 ppm correspond to $CH_3$ and $CH_2$, respectively. Additionally, a new broad signal corresponding to the OH of a carboxylic acid appeared.

The structure of the carboxylic acid **50a** was further established using X-ray crystal structure analysis, with single crystals obtained from acetone by slow evaporation (Figure 53).

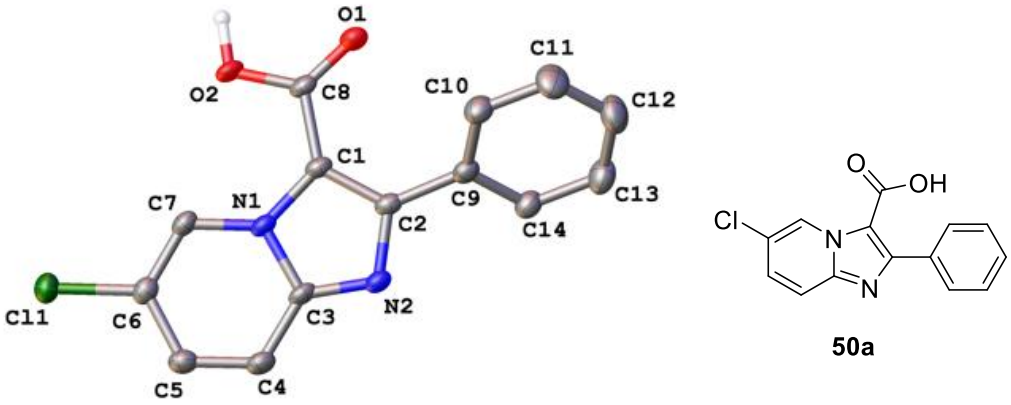


Figure 53. Single crystal X-ray structure of imidazo[1,2-*a*]pyridine carboxylic acid **50a**.

Following confirmation of the procedure, a range of imidazo[1,2-*a*]pyridine carboxylic acids were synthesised to facilitate a SAR investigation. These analogues sought to introduce different substituents on the phenyl ring attached to the imidazo[1,2-*a*]pyridine scaffold. Each analogue was synthesised according to the established protocol outlined previously, and good yields were obtained, comparable to those reported in the previous study (Figure 54).[146]

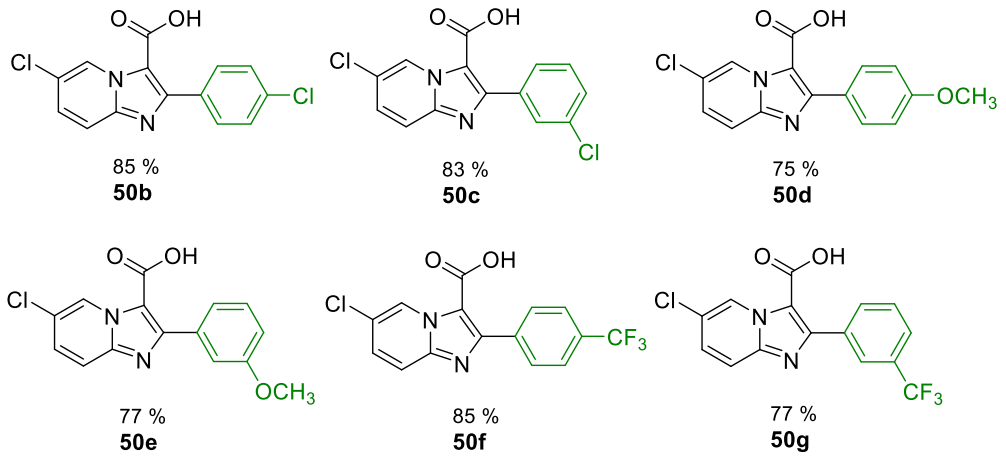


Figure 54. List of carboxylic acids successfully synthesised during this research.

With the successful synthesis of imidazo[1,2-*a*]pyridine carboxylic acids **50a – 50g**, the next step focused on obtaining the complementary hydrazide fragment. Hydrazides are versatile intermediates widely recognised for their significance in pharmacologically active compounds.[148] They have been used in drug design aimed

at addressing major health issues, such as infectious diseases, cancer and inflammation.[149] This versatility is demonstrated by their use in TB treatment, with INH **1** being a cornerstone of anti-TB treatment.[149] Furthermore, hydrazides are utilised in several medical applications, for example, isocarboxazid **58** and iproniazid **59** as antidepressants, which highlights their extensive therapeutic potential across diverse disease areas (Figure 55).[149]

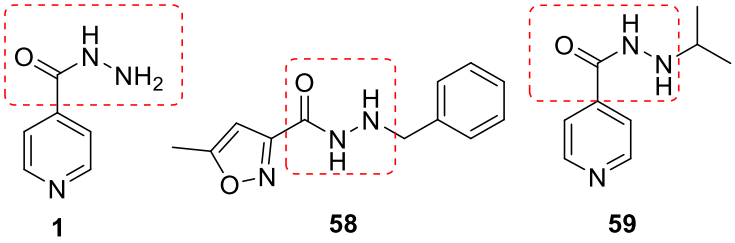


Figure 55. Chemical structures of notable hydrazide-based drugs, INH **1**, isocarboxazid **58** and iproniazid **59**.

Amino acid hydrazide derivatives have also drawn attention in drug development, with the early research within the group indicating that some derivatives exhibit important antimicrobial activity, specifically as antitubercular agents.[137] In light of these results and the established potential of hydrazides as anti-microbial agents, the following section explores the amide bond, an important structural motif extensively found in biological systems and many medications, as a key step in the hydrazide synthesis process.

**Amide bond:**

The amide bond, characterised by the link between a nitrogen atom (N) and a carbonyl group (C=O), is an essential structural component in both natural and synthetic compounds.[150] Its importance is highlighted by its presence in proteins, where it comprises the backbone through peptide bonds linking amino acids.[150] Amide bonds extend beyond biological systems, being present in a vast array of compounds, including numerous pharmaceuticals.[151] For example, atorvastatin **60** inhibits cholesterol synthesis and contains an amide bond. Similarly, lisinopril **61**, an angiotensin-converting enzyme inhibitor, and diltiazem **62**, a calcium channel blocker utilised in the treatment of hypertension and angina, both have amide bonds that enhance their therapeutic activity (Figure 56).[151]

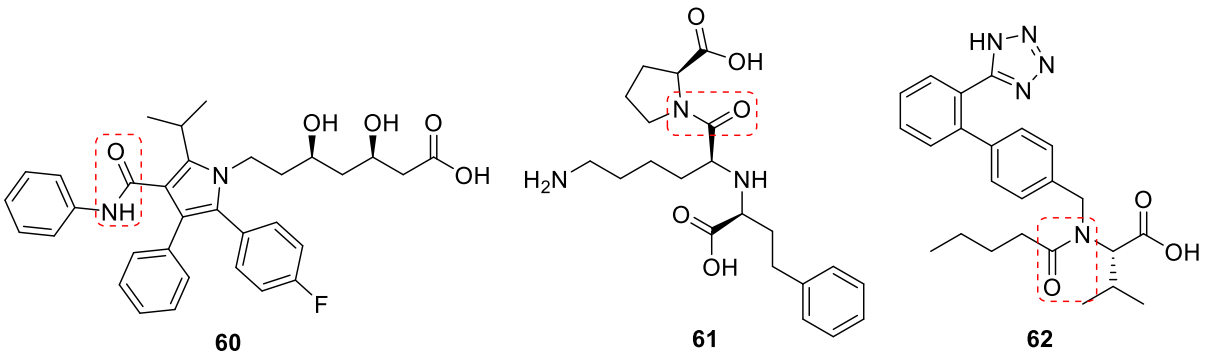


Figure 56. Chemical structures of marketed drugs containing amide group, atorvastatin **60**, lisinopril **61** and diltiazem **62**.

Furthermore, amide bonds show remarkable stability, mainly attributed to resonance delocalization between the carbonyl group and the lone pair of electrons on the nitrogen.[152] This resonance imparts partial double-bond character to the C–N bond, leading to restricted rotation around the bond axis and consequently, amide bonds are less susceptible to hydrolysis compared to other acyl derivatives, such as esters.[152] In contrast, esters lack this resonance stabilization between the oxygen and the carbonyl group, rendering the C–O bond more labile. Consequently, esters are more readily hydrolysed, particularly in biological systems where esterases the enzymes responsible for ester hydrolysis are far more abundant and catalytically efficient than amidases, which hydrolyse amide bonds. [152] This enzymatic preference further enhances the metabolic stability of amides relative to esters. [152] This stability is important for maintaining the structural integrity of proteins and peptides in biological systems.[152] This stability not only maintains biological structures but also makes amide bonds a significant target in synthetic chemistry. The next section focuses on the formation of amide bonds, a critical step in the synthesis of amino acid substituted hydrazide intermediates.

### 2.2.2 Synthesis of amino acid hydrazide intermediates.

To achieve the synthesis of amino acid hydrazide derivatives **51**, a procedure from prior work within the research group was utilised that includes coupling different arylhydrazines **53** with amino acids **52**.[137,138] Initially, the amino group of the amino acid need to be protected to prevent reaction at the carboxylic acid end, which could otherwise lead to self-condensation or unwanted side reactions. The *tert*-butyloxycarbonyl (Boc) group is commonly utilised for this purpose.[153] The Boc group is especially preferred because of its stability against bases; also, it can be easily

removed with acid in good yields.[153] In the hydrazide synthesis, we employed commercially available Boc-protected amino acids. The coupling reaction was undertaken with HBTU (2-(1*H*-benzotriazol-1-yl)-1,1,3,3- tetramethyluronium hexafluorophosphate), an extensively used coupling reagent in peptide synthesis, known for its effectiveness and low racemization.[154] HBTU activates the carboxyl group of the *N*-Boc- amino acid, providing an active ester intermediate that easily reacts with nucleophiles (Scheme 3).

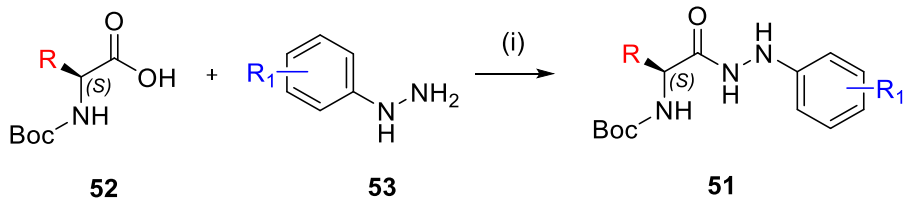


Scheme 3. Reagents and conditions: i) DIPEA, HBTU, THF, 6 h, rt, (58%-91%).

The reaction was able to produce amino acid hydrazides **51** in good yields in most cases (59 % - 94 %) and excellent purity, avoiding the necessity for further purification steps. The success of this reaction is mainly attributed to the byproduct, tetramethylurea (TMU), which is highly soluble in water and poorly soluble in less polar organic solvents such as diethyl ether, which we utilised in the work-up. This enables the ready removal of TMU by simple aqueous extraction (Figure 57).

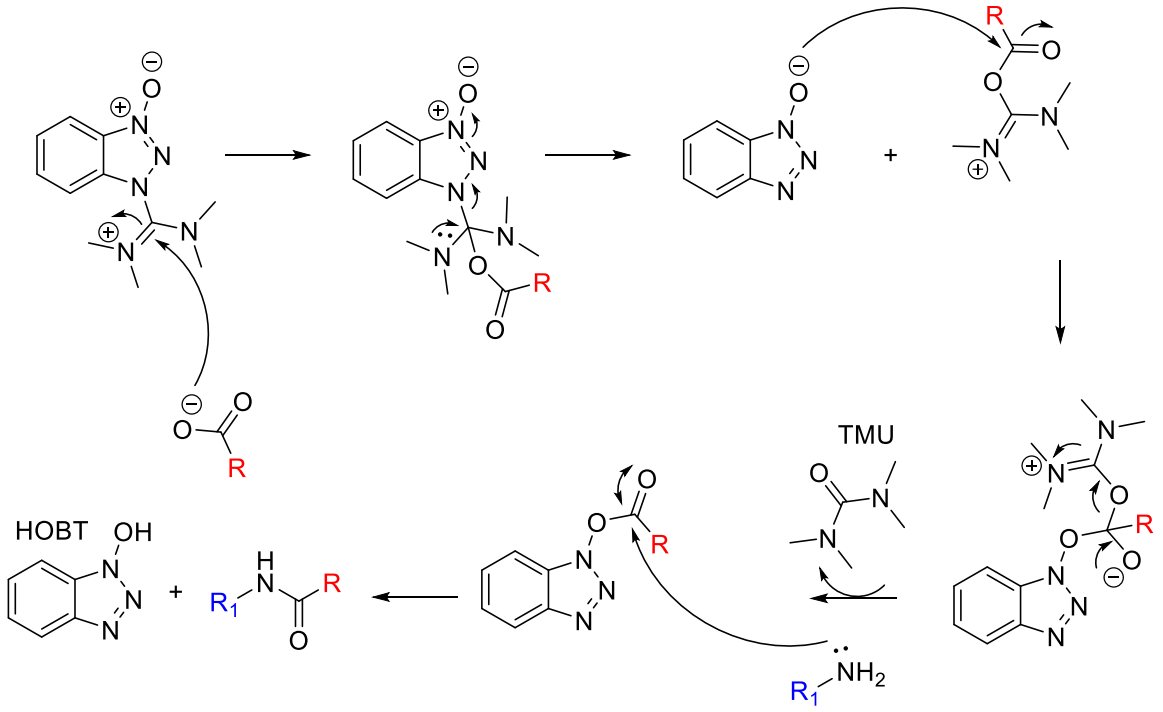


Figure 57. Amide coupling utilises HBTU to activate a carboxylic acid, facilitating an amine attack to form an amide bond, with water-soluble byproduct TMU.

In the aim of initiate SAR investigation, a total of 54 amino acid hydrazide derivatives were synthesised by introducing specific alterations in two important structural parts. The first part involved altering the amino acid side chain to evaluate the impact of different amino acids on activity. Several amino acids were utilised involving simple amino acids like glycine and alanine, branched-chain amino acids such as leucine, sulfur-containing amino acids like methionine, and aromatic amino acids such as phenylalanine and homophenylalanine (Hph). These modifications enabled the comprehensive assessment of size, and types of functional groups within the amino acid side chain, including hydrophobic, sulfur-containing, or aromatic groups, and their contributions to the overall anti-microbial activity. The second part focused on the phenylhydrazine moiety, where several substituents were introduced at different positions around the aromatic ring. Guided by prior research, which identified *meta* and *para* positions as optimal for activity, several substituents were included in the phenylhydrazine part to assess their steric and electronic effects.[137] These included a simple proton (H), which was used to evaluate the unsubstituted phenylhydrazine and serve as a reference for comparison, halogens such as Cl and Br, which were introduced to examine the impact of halogens with differing electronic effects and sizes, in addition to trifluoromethyl ($CF_3$) an electron-withdrawing group and trifluoromethoxy ($OCF_3$), which combines electron-withdrawing properties with additional steric bulk. These substitutions were included to facilitate the identification of substitution patterns that enhance biological activity and to produce intermediates that are necessary for the synthesis of final compounds. Details of these amino acid substituted hydrazide intermediates are provided in Table 7.

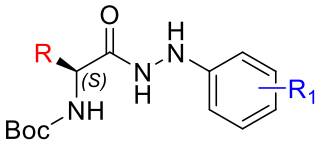

**51**

| R | $R_1$ | Entry | Yield (%) | R | $R_1$ | Entry | Yield (%) |
|---|---|---|---|---|---|---|---|
| Gly | H | **51Aa** | 73 | Gly | 3-Cl | **51Ab** | 68 |
| Gly | 4-Cl | **51Ac** | 83 | Gly | 3-Br | **51Ad** | 84 |
| Gly | 4-Br | **51Ae** | 69 | Gly | 3-$CF_3$ | **51Af** | 83 |
| Gly | 4-$CF_3$ | **51Ag** | 66 | Gly | 3-$OCF_3$ | **51Ah** | 70 |
| Gly | 4-$OCF_3$ | **51Ai** | 62 | Ala | H | **51Aj** | 75 |
| Ala | 3-Cl | **51Ak** | 65 | Ala | 4-Cl | **51Al** | 69 |
| Ala | 3-Br | **51Am** | 89 | Ala | 4-Br | **51An** | 59 |
| Ala | 3-$CF_3$ | **51Ao** | 70 | Ala | 4-$CF_3$ | **51Ap** | 73 |
| Ala | 3-$OCF_3$ | **51Aq** | 71 | Ala | 4-$OCF_3$ | **51Ar** | 71 |
| Leu | H | **51As** | 82 | Leu | 3-Cl | **51At** | 71 |
| Leu | 4-Cl | **51Au** | 69 | Leu | 3-Br | **51Av** | 89 |
| Leu | 4-Br | **51Aw** | 83 | Leu | 3-$CF_3$ | **51Ax** | 61 |
| Leu | 4-$CF_3$ | **51Ay** | 59 | Leu | 3-$OCF_3$ | **51Az** | 76 |
| Leu | 4-$OCF_3$ | **51Ba** | 66 | Met | H | **51Bb** | 77 |
| Met | 3-Cl | **51Bc** | 88 | Met | 4-Cl | **51Bd** | 94 |
| Met | 3-Br | **51Be** | 79 | Met | 4-Br | **51Bf** | 69 |
| Met | 3-$CF_3$ | **51Bg** | 74 | Met | 4-$CF_3$ | **51Bh** | 88 |
| Met | 3-$OCF_3$ | **51Bi** | 62 | Met | 4-$OCF_3$ | **51Bj** | 72 |
| Phe | H | **51Bk** | 90 | Phe | 3-Cl | **51Bl** | 58 |
| Phe | 4-Cl | **51Bm** | 72 | Phe | 3-Br | **51Bn** | 88 |
| Phe | 4-Br | **51Bo** | 86 | Phe | 3-$CF_3$ | **51Bp** | 77 |
| Phe | 4-$CF_3$ | **51Bq** | 75 | Phe | 3-$OCF_3$ | **51Br** | 70 |
| Phe | 4-$OCF_3$ | **51Bs** | 70 | Hph | H | **51Bt** | 87 |
| Hph | 3-Cl | **51Bu** | 82 | Hph | 4-Cl | **51Bv** | 84 |
| Hph | 3-Br | **51Bw** | 88 | Hph | 4-Br | **51Bx** | 86 |
| Hph | 3-$CF_3$ | **51By** | 91 | Hph | 4-$CF_3$ | **51Bz** | 73 |

Table 7. *N*-Boc substituted hydrazide intermediates containing Gly, Ala, Leu, Met, Phe and Hph amino acids with their yield percentage.

Synthesis of the hydrazide intermediates was confirmed using $^1$H NMR, for example, the spectrum for 3-$OCF_3$ glycine hydrazide **51Ah** displayed the characteristic doublet signal at (3.84 – 3.76 ppm), attributed to the $CH_2$ group present in all glycine hydrazide. A singlet at 1.45 ppm was assigned to the Boc protecting group, while the arylhydrazine fragment was identified by two doublet of doublets at 6.7–6.6 ppm and 7.1 ppm, consistent with aromatic proton coupling, and a singlet at 6.5 ppm corresponding to the remaining proton on the aromatic ring (Figure 58).

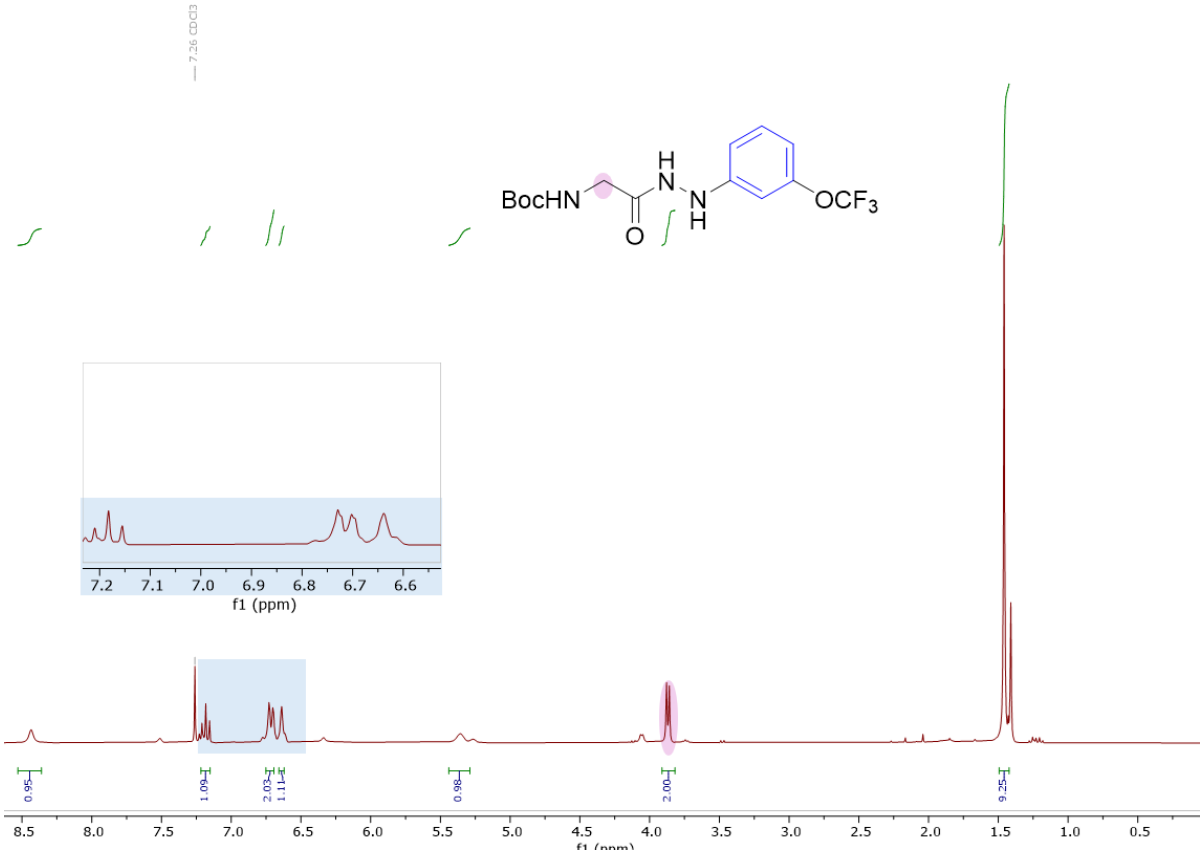


Figure 58. $^{1}$H NMR spectrum of compound **51Ah** exhibits the characteristic signals of the glycine hydrazide intermediate. The region highlighted in pink corresponds to the $CH_2$ group of glycine hydrazide, while the blue-highlighted region shows an expanded view of the phenyl hydrazine aromatic signals.

For aromatic amino acid hydrazides, such as phenylalanine, the spectrum displays, alongside the phenyl hydrazine peaks, signals from the aromatic ring of phenylalanine appearing in the deshielded region (Figure 59). Furthermore, the chiral proton appears at 4.4 ppm, while the $CH_2$ group of phenylalanine identified as a doublet in the alkyl region at 3.0 ppm, and the Boc group is observes as a singlet at 1.4 ppm.

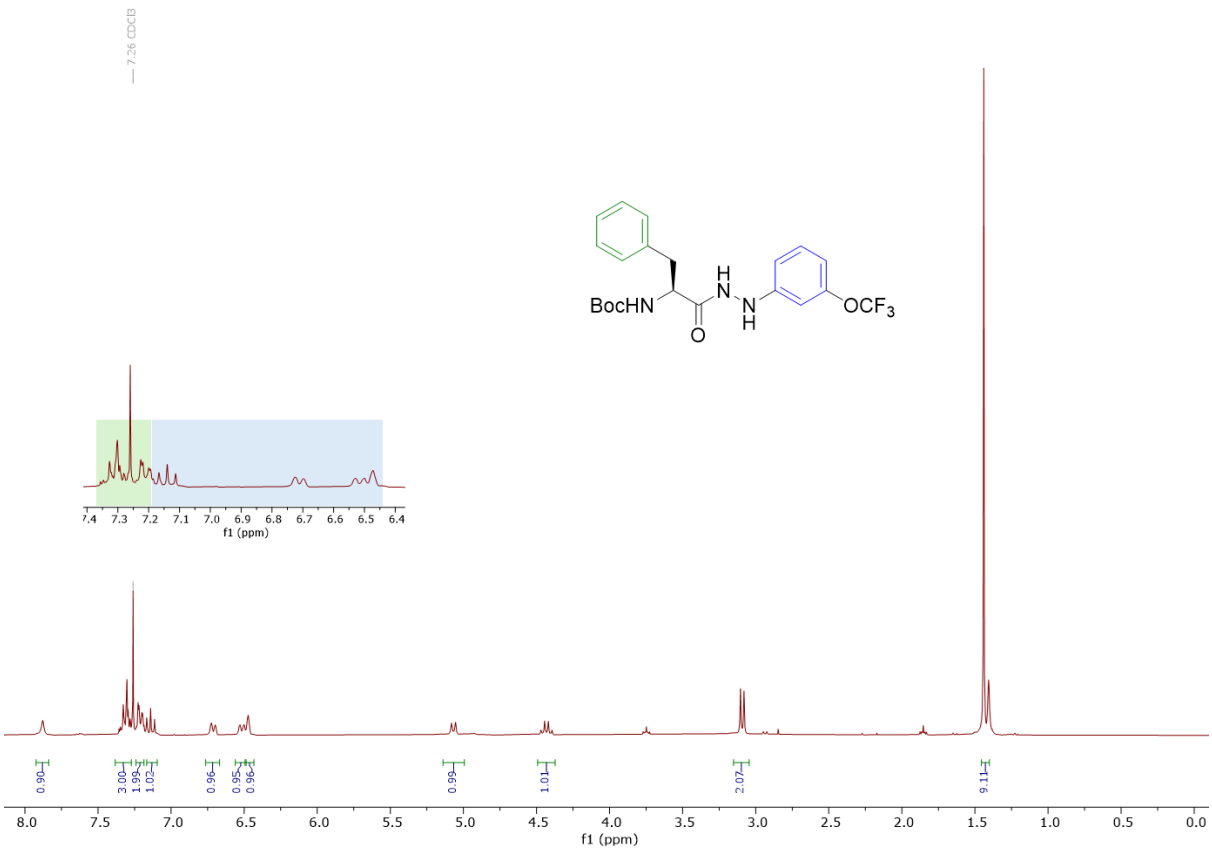


Figure 59. $^{1}$H NMR spectrum shows an expanded view of the aromatic region of phenylalanine hydrazide intermediate. The blue-highlighted signals indicate the phenyl hydrazine peaks, while the green-highlighted region corresponds to the aromatic ring of phenylalanine.

Following the successful synthesis of hydrazide intermediates, the subsequent step includes their coupling with precursor carboxylic acids as described (*cf.* Section 2.2.1) to yield imidazo[1,2-*a*]pyridine-substituted amino acid hydrazides as targeted compounds, prepared for screening against *Mtb* as potential anti-TB agents.

### 2.2.3 Final step: synthesis of targeted imidazo[1,2-*a*]pyridine compounds.

After the successful synthesis of the *N*-Boc amino acid hydrazide intermediates, attention turned to the deprotection of the Boc group as the first step for the final coupling reaction. The Boc group can be effectively removed utilising 4M HCl in dioxane, which has been shown to be an effective reagent for Boc deprotection.[137,155] The mechanism includes protonation of the carbonyl oxygen, which promotes the cleavage of the *tert*-butyl group, forming a stable *tert*-butyl cation and a protonated carbamic acid intermediate that subsequently decomposes to release carbon dioxide and produce the desired amine hydrochloride salt **63** (Figure 60).

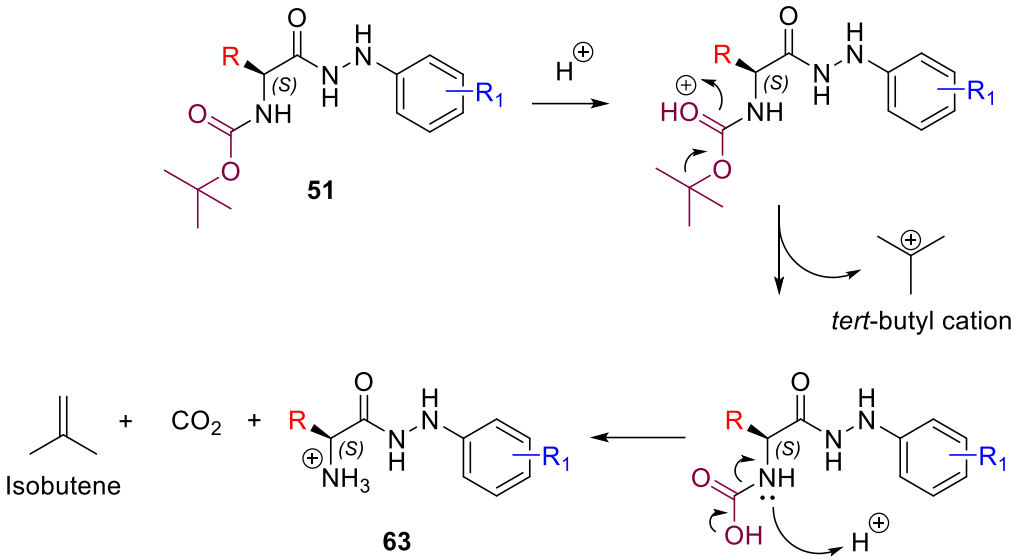


Figure 60. *N*- Boc deprotection mechanism using 4M HCl in dioxane.

Following deprotection, the intermediate hydrochloride salt was isolated by dissolving it in ethanol, followed by precipitation utilising diethyl ether as an antisolvent. This step effectively removed impurities, as the cleavage of the Boc protecting group generates volatile by-products such as isobutene and carbon dioxide, resulting in a highly pure *N*-terminal hydrazide without the need for further purification. Subsequently, this precipitation is coupled with the corresponding carboxylic acid using a coupling reagent. For this step, HBTU was selected due to its demonstrated efficacy in previous studies conducted by the research group.[137,138] The reaction aimed to couple *N*-Boc protected 3-bromophenylalanine with 6-chloro-2-phenylimidazo[1,2-*a*]pyridine-3-carboxylic acid, employing tetrahydrofuran (THF) as the solvent and *N*,*N*-diisopropylethylamine (DIPEA) as the base (Scheme 4).

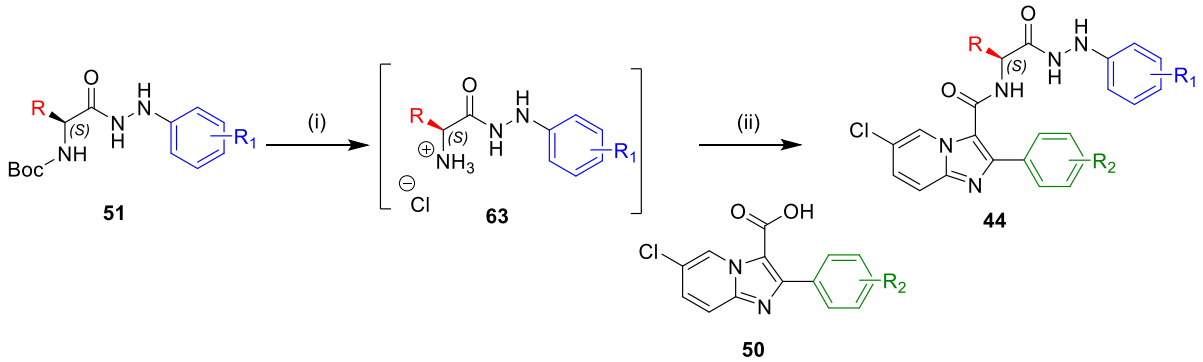


Scheme 4. Synthesis of final compounds from *N*-Boc protected amino acid hydrazides **51**; Reagents and conditions: i) 4M HCl in dioxane, 90 min, r.t. (ii) **50** , HBTU, DIPEA, THF, overnight, rt.

The reaction was stirred overnight, yielding a crude yellow powder, and subsequent purification by trituration with diethyl ether afforded the target compound in high purity but relatively low yield (25%), with the $^{1}$H NMR of compound **44Bq** shown in Figure 61.

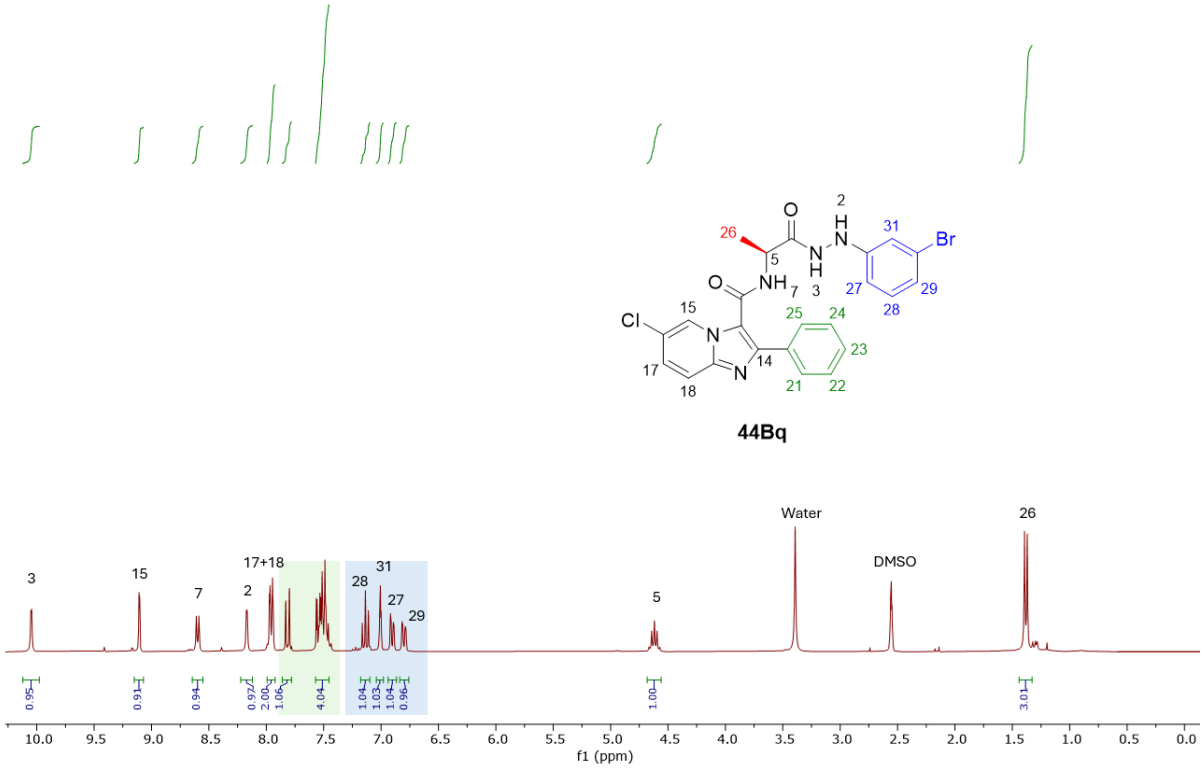


Figure 61. $^{1}$H NMR exhibits the characteristic signals of compound **44Bq**. The blue-highlighted signals indicate the phenyl hydrazine peaks, while the green-highlighted region corresponds to the aromatic ring attached to scaffold.

To address the low yield and ensure a sufficient amount for all necessary analyses, column chromatography was utilised as the purification technique in the subsequent series of final compounds. This adjustment resulted in an improvement in yield while maintaining the high purity of the final products. The synthetic procedure employed to produce the series of final compounds enabled the generation of a comprehensive library of imidazo[1,2-*a*]pyridine analogues.

With the reaction conditions established, attention shifted to the synthesis of a scaffold-diversified imidazo[1,2-*a*]pyridine library. This synthetic effort aimed to investigate the structure-activity relationship by modifying three key positions: (1) the amino acid component (R), (2) the phenylhydrazine moiety ($R_1$), and (3) the phenyl ring attached to the imidazo[1,2-*a*]pyridine framework ($R_2$) (Figure 62).

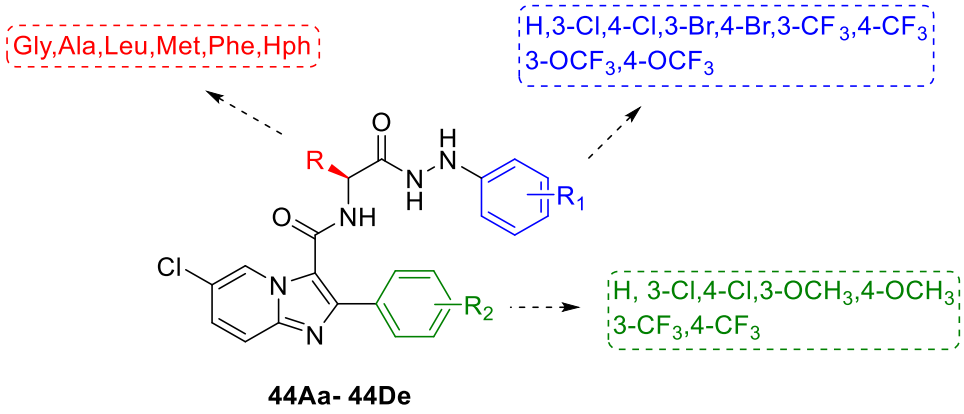


Figure 62. General structure of synthesised imidazo[1,2-*a*]pyridine compound, highlighting the key modification.

A library of compounds was successfully synthesised, and their structures were confirmed using a range of spectroscopic techniques. These included 1D and 2D NMR spectroscopy ($^1$H NMR, $^{13}$C NMR, COSY, HMBC, and HSQC), infrared (IR) spectroscopy, and high-resolution mass spectrometry with general analytical methods described in (*cf.* Section 6.1). The structures of some analogues were further confirmed via crystallographic analysis. For instance, the crystal structure of **44Bt**, including *L*-alanine, was elucidated via slow evaporation of a concentrated DMSO solution, followed by single-crystal X-ray diffraction (Figure 63). This analysis offered confirmation of its molecular structure. Furthermore, the absolute stereochemistry was determined with a Flack parameter of -0.013(5), indicating that the coupling process maintains the chiral centre without causing racemisation.

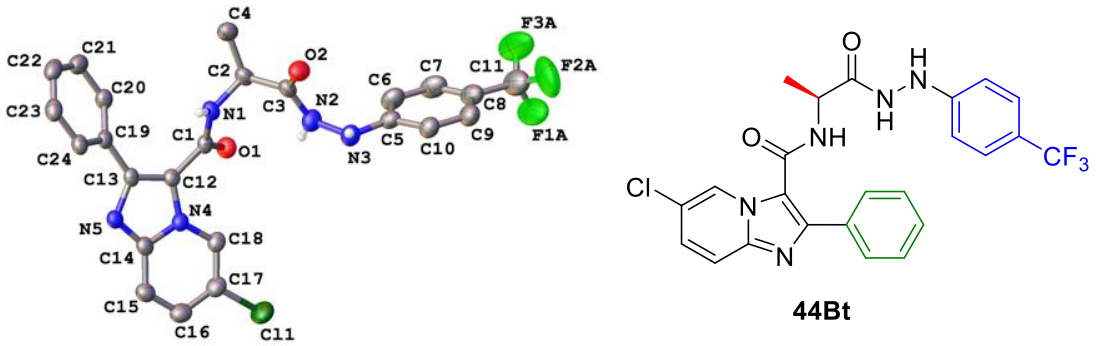


Figure 63. Single crystal X-ray structure of imidazo[1,2-*a*]pyridine carboxylic acid **44Bt**.

The research began with the synthesis of imidazo[1,2-a]pyridine analogues, retaining both phenylhydrazine and the phenyl ring linked to the scaffold, while incorporating various amino acids that includes Gly, Ala, Leu, Met, Phe and Hph (Figure 64). These functioned as reference analogues for comparison with other compounds.

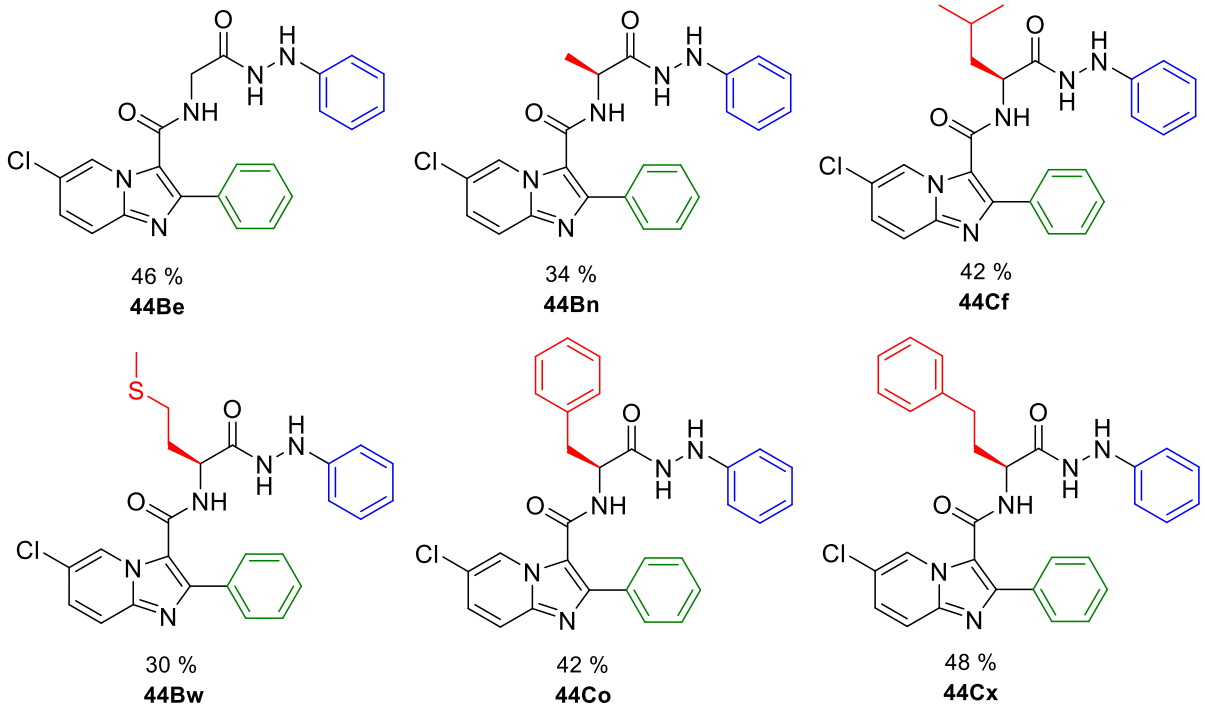


Figure 64. Chemical structure of imidazo[1,2-*a*]pyridine analogues containing unsubstituted phenylhydrazine combined with different amino acids.

**First- series of Imidazo[1,2-*a*]pyridine:**

In the initial phase of this research, modifications were made to both the amino acid moiety and the phenyl ring at the $R_2$ position, while maintaining the phenylhydrazine component as a constant structural element (Figure 65).

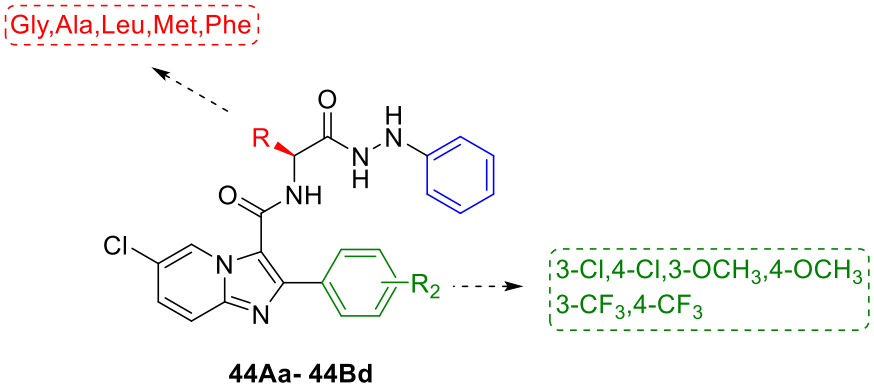


Figure 65. General structure of the first series of imidazo[1,2-*a*]pyridine analogues, highlighting the key modification at the amino acid (R) and the ($R_2$) position of phenyl ring.

In drug design, modifying the phenyl ring with different substituents is one of the strategies for optimizing the pharmacological properties of a compound.[156] These modifications can significantly change the electronic, solubility and steric properties of the molecule, which directly affect its interaction with biological targets, binding affinity, and overall activity.[156] Electron-withdrawing or electron-donating groups can alter the electronic density of the phenyl ring to improve interactions such as hydrogen bonding, while steric alterations from bulky substituents may enhance selectivity by influencing binding pocket compatibility, and variations in solubility via polar or hydrophobic groups can affect membrane permeability, bioavailability, and metabolic stability.[156] Thus, strategic modifications of the phenyl ring are a fundamental to SAR investigations, facilitating the development of more drug-like, selective, and potent candidates for therapeutic use.[157] As such, a total of 30 analogues were successfully synthesised to assess the effect of phenyl ring modifications ($R_2$) in combination with different amino acid components, as outlined in Table 8.

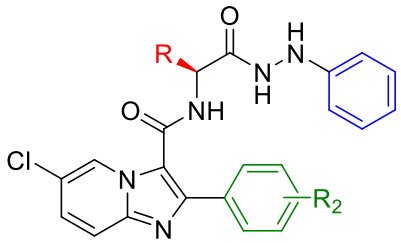

**44Aa- 44Bd**

| Compound | R | $R_2$ | Yield (%) | Entry | R | $R_2$ | Yield (%) |
|---|---|---|---|---|---|---|---|
| **44Aa** | Gly | 3-Cl | 34 | **44Ab** | Gly | 4-Cl | 50 |
| **44Ac** | Gly | 3-$CF_3$ | 48 | **44Ad** | Gly | 4-$CF_3$ | 54 |
| **44Ae** | Gly | 3-$OCH_3$ | 50 | **44Af** | Gly | 4-$OCH_3$ | 47 |
| **44Ag** | Ala | 3-Cl | 40 | **44Ah** | Ala | 4-Cl | 30 |
| **44Ai** | Ala | 3-$CF_3$ | 36 | **44Aj** | Ala | 4-$CF_3$ | 37 |
| **44Ak** | Ala | 3-$OCH_3$ | 54 | **44Al** | Ala | 4-$OCH_3$ | 43 |
| **44Am** | Met | 3-Cl | 32 | **44An** | Met | 4-Cl | 45 |
| **44Ao** | Met | 3-$CF_3$ | 33 | **44Ap** | Met | 4-$CF_3$ | 40 |
| **44Aq** | Met | 3-$OCH_3$ | 36 | **44Ar** | Met | 4-$OCH_3$ | 45 |
| **44As** | Leu | 3-Cl | 50 | **44At** | Leu | 4-Cl | 45 |
| **44Au** | Leu | 3-$CF_3$ | 40 | **44Av** | Leu | 4-$CF_3$ | 40 |
| **44Aw** | Leu | 3-$OCH_3$ | 49 | **44Ax** | Leu | 4-$OCH_3$ | 53 |
| **44Ay** | Phe | 3-Cl | 46 | **44Az** | Phe | 4-Cl | 50 |
| **44Ba** | Phe | 3-$CF_3$ | 41 | **44Bb** | Phe | 4-$CF_3$ | 45 |
| **44Bc** | Phe | 3-$OCH_3$ | 46 | **44Bd** | Phe | 4-$OCH_3$ | 40 |

Table 8. The synthesised imidazo[1,2-*a*]pyridine analogues, listing their structural alterations at the amino acid (R) and ($R_2$) positions along with their yield percentage.

**Second- series of Imidazo[1,2-*a*]pyridine:**

Following this, the next stage of the study focused on extensively exploring phenylhydrazine moiety by introducing different substitutions at this position while also incorporating various amino acid residues. To ensure a focused assessment, the phenyl ring at the $R_2$ position was maintained as a simple proton (Figure 66).

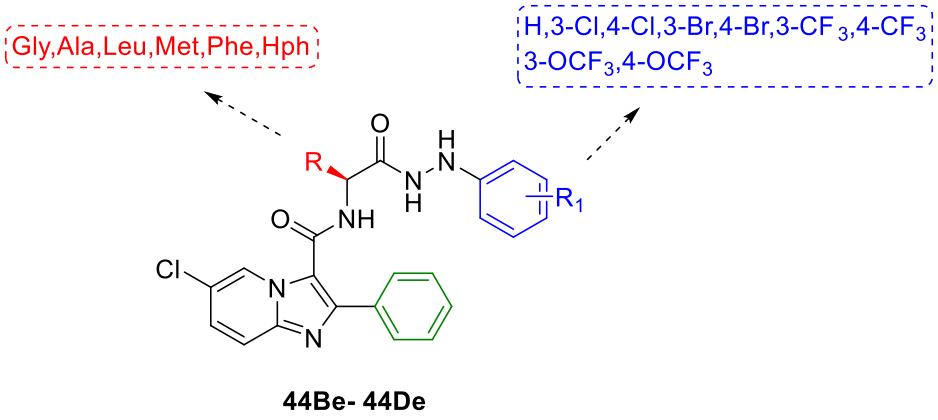


Figure 66. General structure of the second series of imidazo[1,2-*a*]pyridine derivatives, underscoring the key alteration at the amino acid (R) and the ($R_1$) position of arylhydrazine.

As part of this investigation, a halogen was introduced into the phenylhydrazine part, an important and common modification in drug design. Halogenated compounds are essential in medicinal chemistry, contributing significantly to the development of effective therapeutics for many diseases.[158] The incorporation of halogens in pharmaceutical compounds is driven by their ability to increase pharmacological properties via halogen bond formation, hence enabling various interactions with biological targets.[158] These interactions can markedly affect ADME properties, enhancing drug binding affinity, membrane permeability, and lipophilicity.[159] In particular, halogens are important components of different antibiotic classes and antimicrobial scaffolds, with around 25% of approved drugs and 40% of actively evaluated lead compounds containing halogens.[159] Among halogens, chlorine is particularly noteworthy for its ability to improve membrane permeability by enhancing the lipophilicity of compounds, thereby facilitating deeper penetration into the hydrophobic regions of target proteins.[160] Previous works, including ongoing research within the group, have shown that the incorporation of a chlorine atom at the *meta* or *para* position of the phenylhydrazine moiety confers promising antitubercular activity.[137] As such, several chlorinated analogues have been successfully synthesised with different amino acid moieties, enabling further investigation of their SAR (Figure 67).

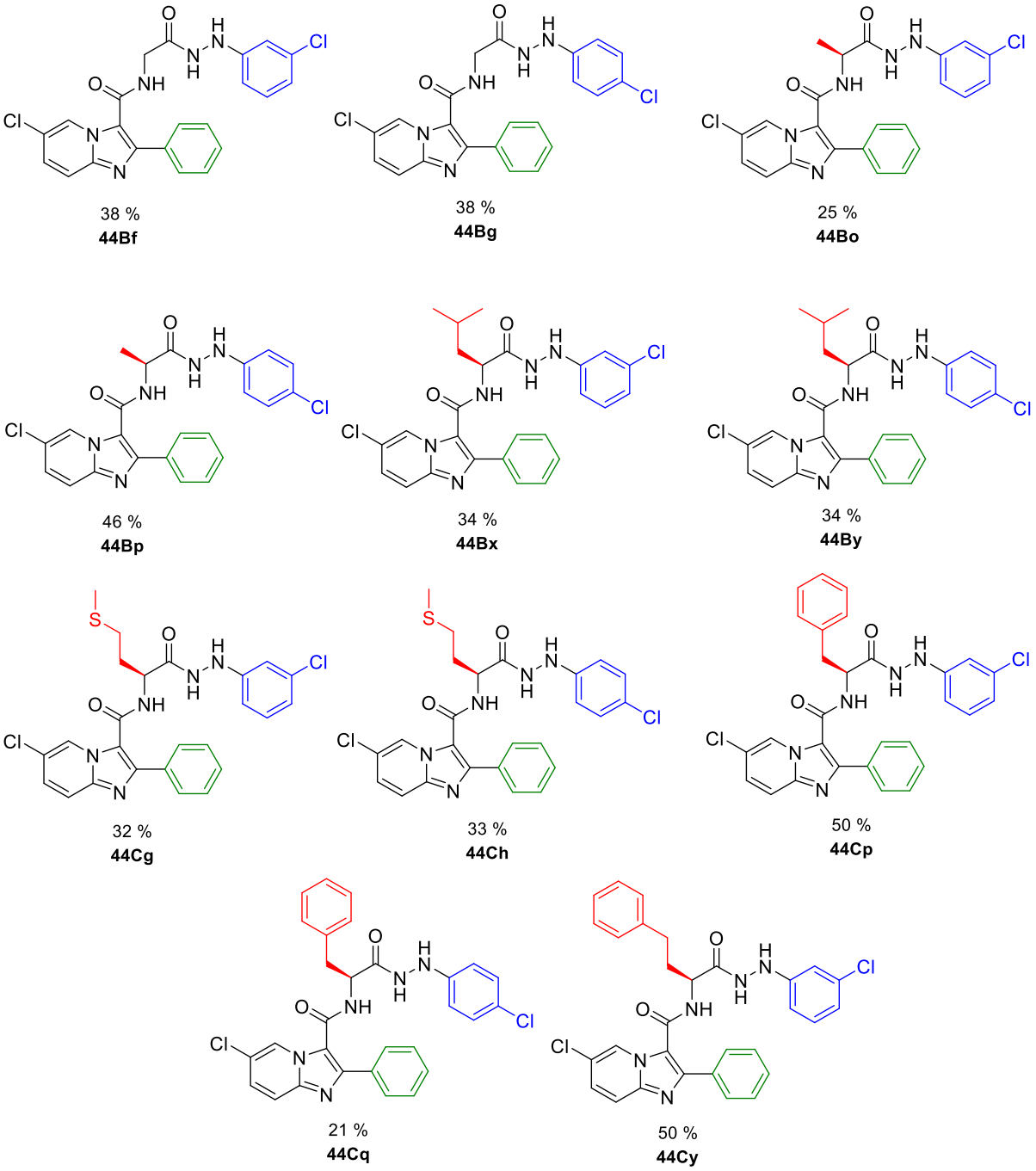


Figure 67. The chemical structure of final compounds, containing chlorine on arylhydrazine moiety.

Another halogen chosen for investigation was bromine, which varies in size and electronic properties from chlorine, allowing for the study of the comparative impacts between chlorinated and brominated analogues (Figure 68). While the use of heavier halogens such as bromine frequently promotes concerns regarding toxicity and safety, however, the successful development and clinical utilisation of bedaquiline as an anti-TB agent highlight the potential of brominated compounds in TB therapy.[161]

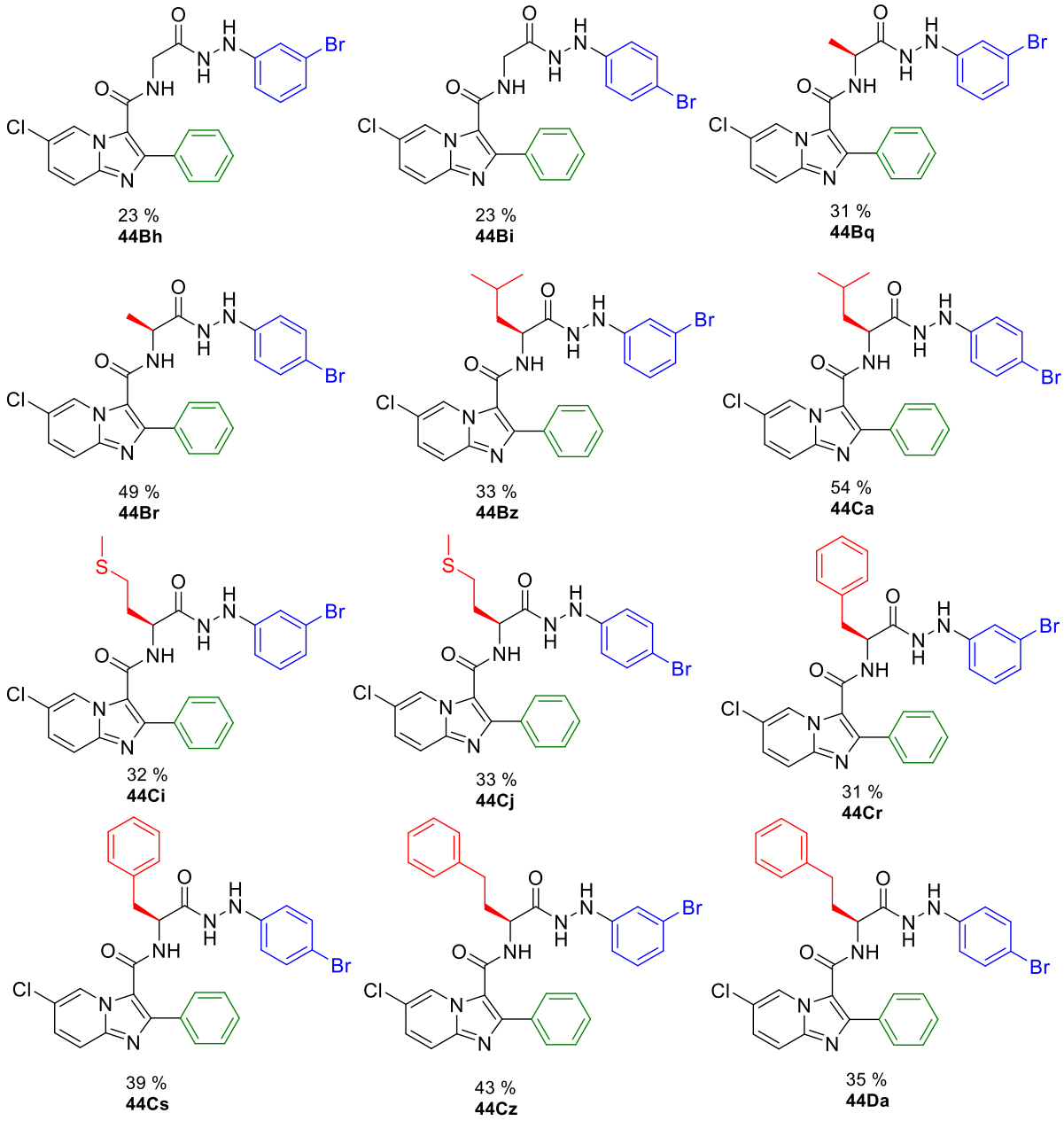


Figure 68. Chemical structure of brominated imidazo[1,2-*a*]pyridine analogues.

Another avenue of investigation focused on fluorinated compounds, particularly incorporating the $CF_3$ group, a modification widely recognized for its significant impact on the pharmacological properties of bioactive compounds.[162] The $CF_3$ group is a significant modification in medicinal chemistry, the presence of the trifluoromethyl group in biologically active compounds generally enhances lipophilicity and stability as well as imparting its high electronegativity.[163] An example of its efficacy in TB treatment is the fluoroquinolone class of antibiotics, which integrates fluorine to achieve potent antitubercular activity.[63] Importantly, in previous studies conducted within the research

group, the incorporation of trifluoromethyl moieties into the phenylhydrazine part has been shown to exhibit promising antitubercular activity (Figure 69).[137]

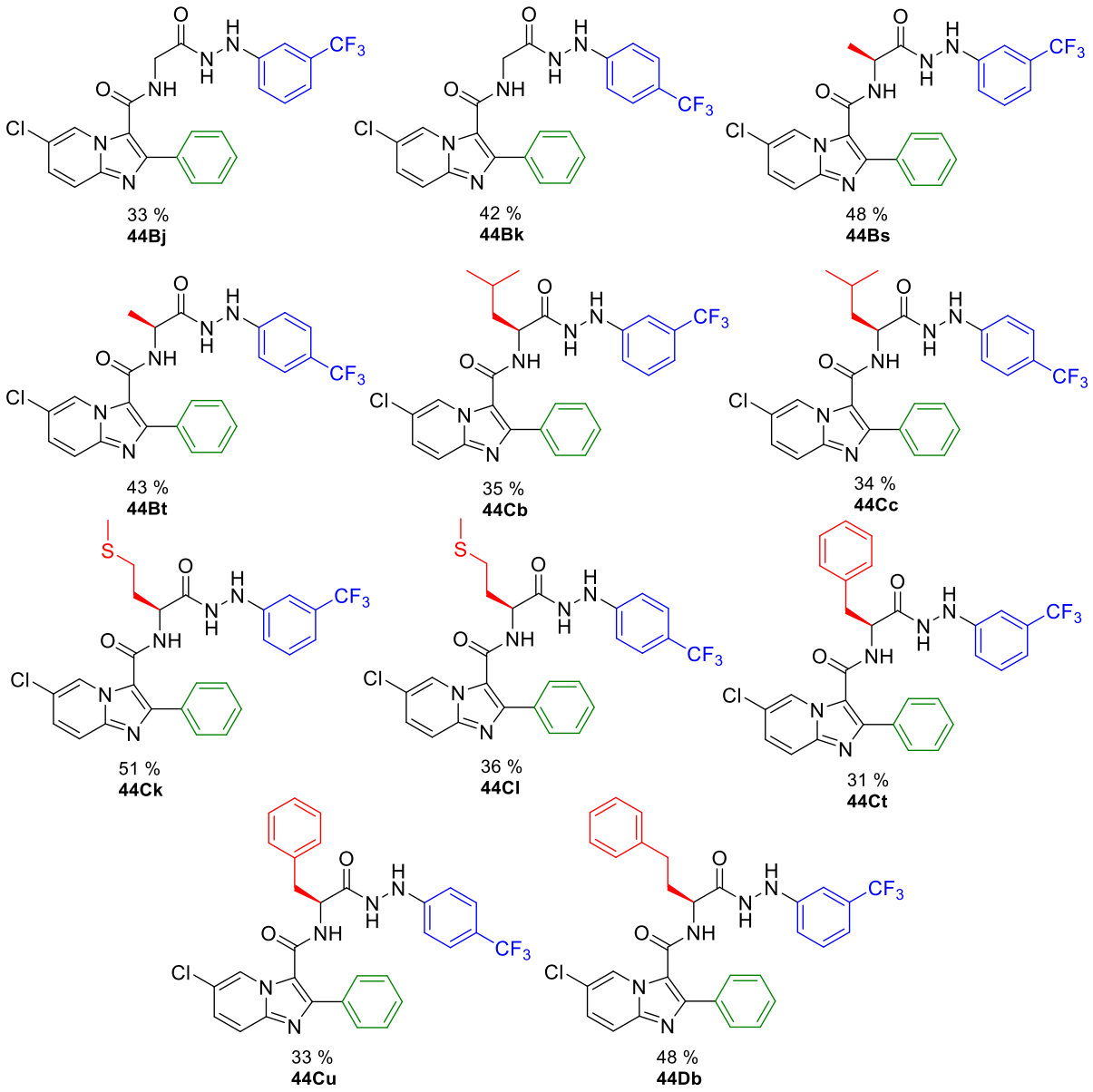


Figure 69. The substituted imidazo[1,2-*a*]pyridine hydrazides, with trifluoromethyl group on arylhydrazine.

For the fluorinated analogues such as compound **44Cc**, additional confirmation was provided by $^{19}$F NMR spectroscopy, which showed a single signal at 56.4 ppm, further supporting the structural integrity (Figure 70).

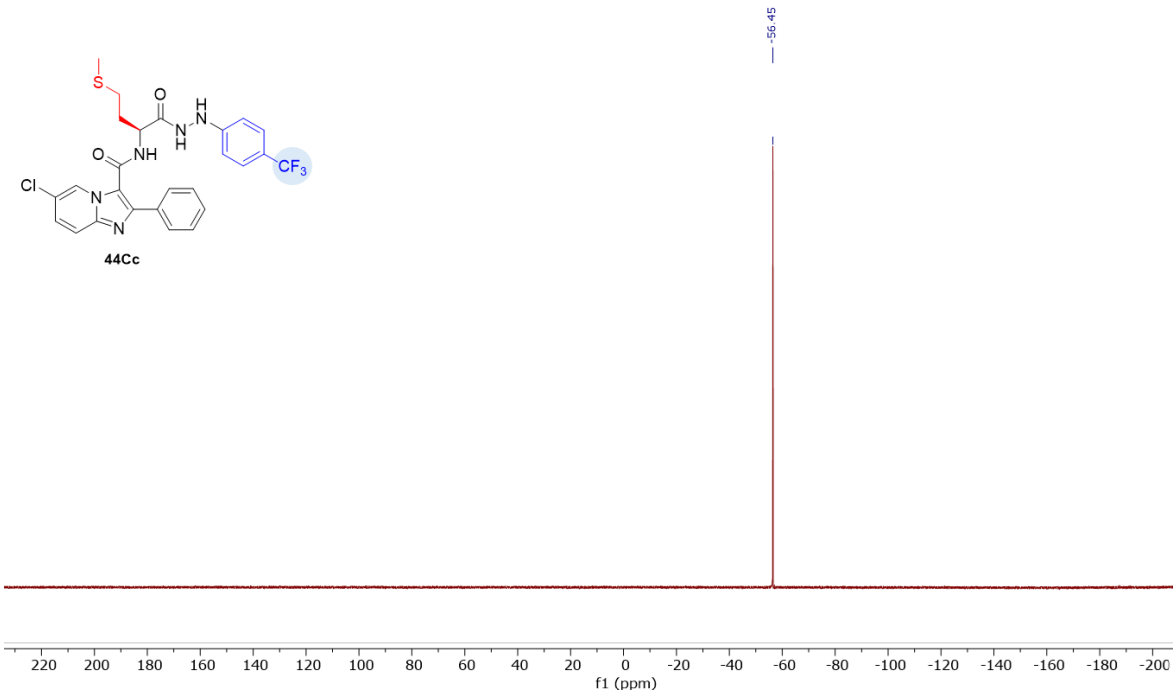


Figure 70. $^{19}$F NMR spectrum showing a single peak at 56 ppm, corresponding to the $CF_3$ group on the phenylhydrazine moiety.

Moreover, the trifluoromethoxy group, another fluorinated substituent, is gaining significance in both clinical research and medicinal chemistry and it can be seen in newly antituberculosis drugs such as delamanid, pretomanid and Q203.[164] Encouraged by this, substituted imidazo[1,2-*a*]pyridine hydrazides bearing a trifluoromethoxy group on the phenylhydrazine part were synthesised utilising the standard procedure, to assess their antitubercular activity (Figure 71).

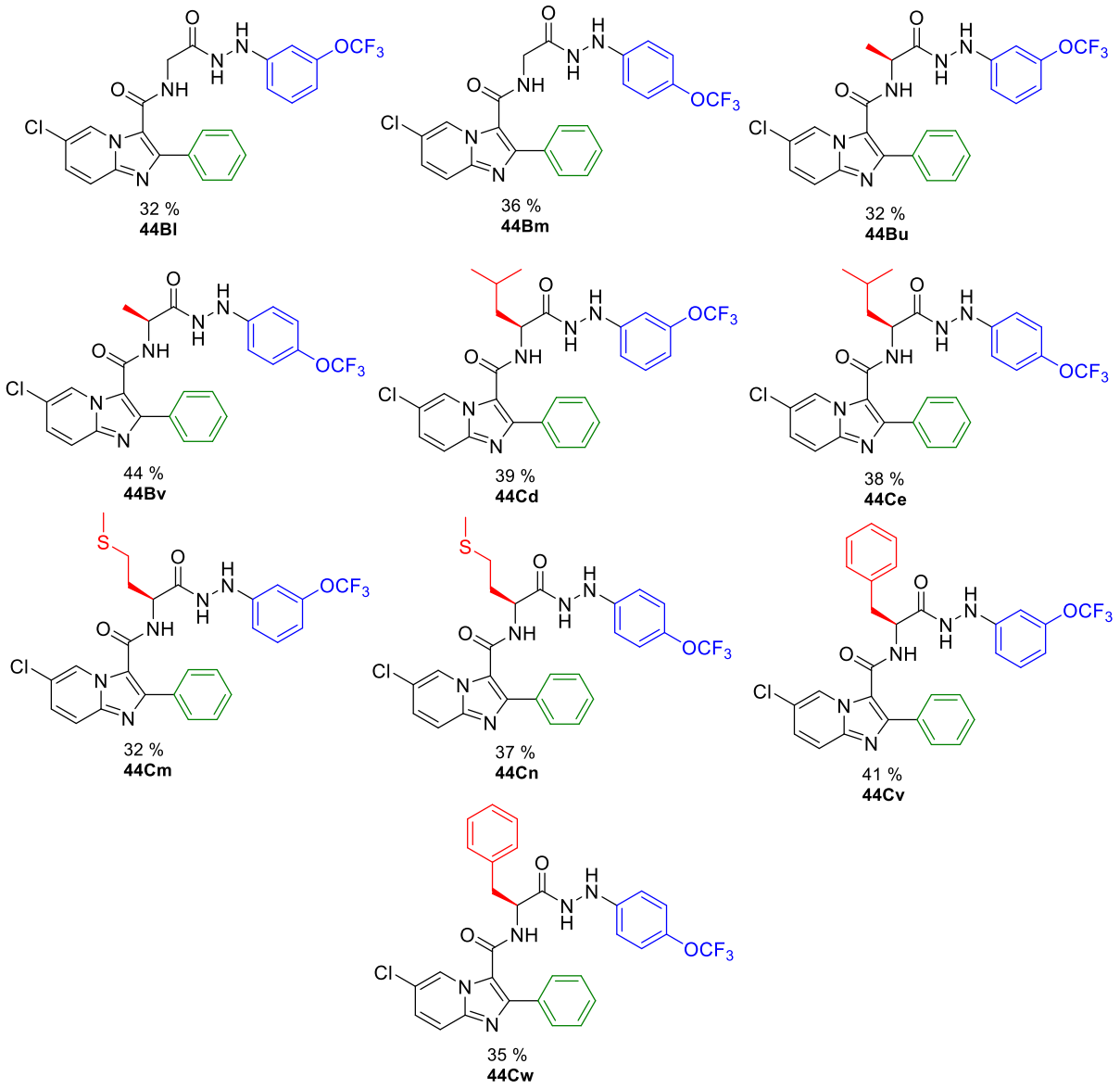


Figure 71. The chemical structure of final compounds, containing trifluoromethoxy on arylhydrazine moiety.

**Third- series of Imidazo[1,2-*a*]pyridine:**

In this phase, the amino acid component retained as phenylalanine, while structural modification was introduced at both the $R_1$ and $R_2$ positions (Figure 72).

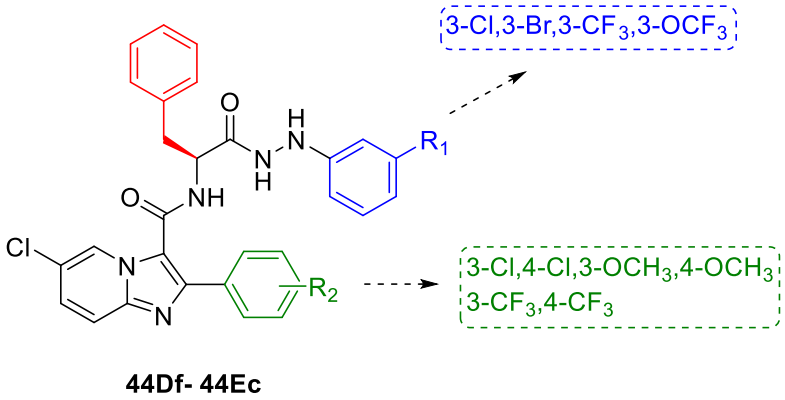


**44Df- 44Ec**

Figure 72. General structure of the third-series of compounds, highlighting the key modification.

The primary goal of this series was to determine whether modification of the phenyl ring at $R_2$, by incorporating key substituents such as chlorine, trifluoromethyl, and methoxy, could further enhance the antitubercular activity of these analogues. These alterations were designed to evaluate the impact of electronic properties of these substituents on antitubercular activity, clarifying their role in modulating biological activity and optimising the pharmacological profile of the imidazo[1,2-*a*]pyridine framework. Consequently, a series of different phenylalanine analogues from the third-series was successfully synthesised and subjected to *Mtb* screening (Figure 73).

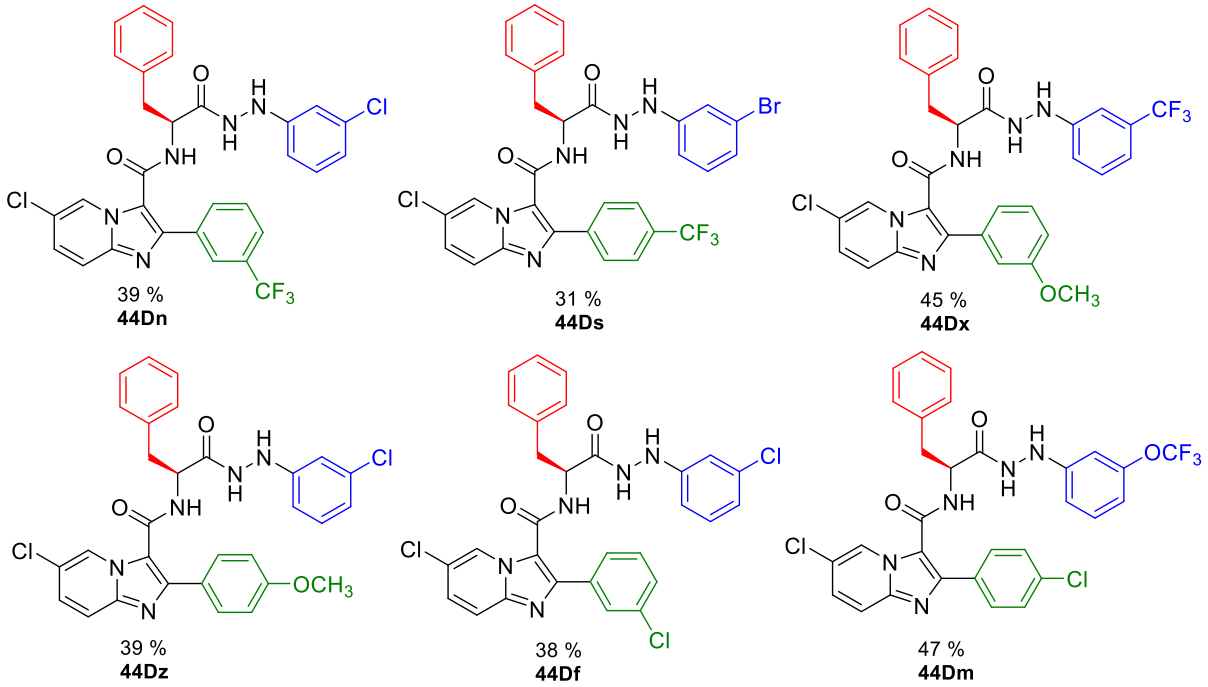


Figure 73. The chemical structure of selected compounds from the third series of imidazo[1,2-*a*]pyridine derivatives.

In summary, a diverse library of novel imidazo[1,2-*a*]pyridine-substituted amino acid hydrazides were successfully synthesised, containing three distinct areas of structural variations: the phenylhydrazine, amino acid fragment, and the phenyl ring attached to the imidazo[1,2-*a*]pyridine scaffold. Screening these novel compounds against different *Mtb* strains enabled an opportunity for a comprehensive SAR analysis. The detailed findings of the synthesised compounds, including their biological activity against *Mtb* and molecular docking studies targeting the specific PafA binding pocket, along with *in silico* ADME profile predictions, will be thoroughly discussed in the next chapter.

## 3. Structure-activity-relationship studies of of imidazo[1,2-*a*]pyridine analogues

In the previous chapter, synthesis of imidazo[1,2-*a*]pyridine analogues was discussed emphasising the successful development of three series of compounds, incorporating three distinct components; the amino acid (R), arylhydrazine ($R_1$) and attached to the aryl scaffold ($R_2$) (Figure 74). These compounds were designed with structural variations to create a diverse library for further assessment. This chapter builds on this work by exploring their biological activity and potential as anti-TB agents.

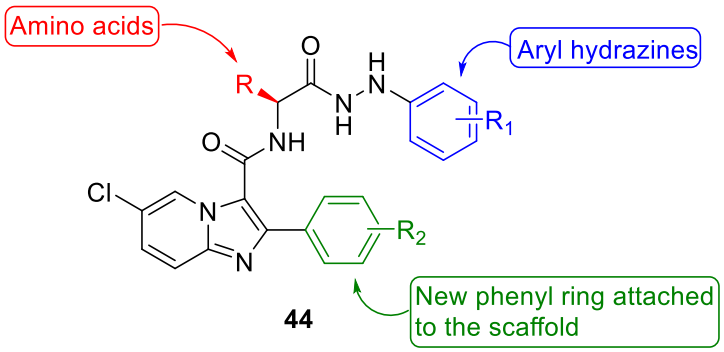


Figure 74. Chemical structure of final compound based on imidazo[1,2-*a*]pyridine scaffold, highlighting the key modification.

To assess their activity, all synthesised compounds were screened against various *Mtb* strains utilising the Resazurin Microtiter Assay (REMA). The findings of this screening allowed for a detailed structure-activity relationship analysis to determine the structural features that affect anti-TB activity. This analysis is essential for understanding how to redesign the compounds and improve their activity.

The most active compounds from the *Mtb* screening were subsequently analysed through molecular docking against the ATP-binding site of the potential target PafA. This docking study aimed to elucidate how the compounds bind to the potential target and identify the important interactions. Furthermore, the ADME profiles of all synthesised compounds were predicted utilising ADMETlab 3 software and compared with marketed anti-TB agents to assess their drug-likeness and potential suitability for further development.

### 3.1 Whole-cell *Mtb* screening

Whole-cell screening is a widely utilised technique to identify compounds having bactericidal activity against *Mtb*.[165,166] This method has historically been highly effective in screening thousands of compounds from various chemical libraries, resulting in the identification of promising anti-TB candidates that have advanced to preclinical and clinical evaluation.[167] For example, bedaquiline, an FDA-approved medication, was identified through whole-cell screening of a diverse library of 70,000 compounds.[165] This method also led to the discovery of pretomanid and delamanid.[165] A widely employed approach in whole-cell screening is the colorimetric redox indicator technique.[167] This method is based on the ability of live bacterial cells to metabolically reduce redox-sensitive dyes, resulting in a measurable colour change.[167] In this research, REMA was utilised to evaluate the viability of *Mtb* in the presence of test compounds. The WHO endorses the REMA assay as a direct, quick, and cost-effective method for determining the Minimum Inhibitory Concentrations (MICs) of bioactive compounds.[168] Resazurin **64** (7-hydroxy-3-oxo-3H-phenoxazine-10-oxides), is a cell-permeable redox active dye, functioning as the indicator in this experiment. In its oxidised form, resazurin appears as a deep blue-purple dye, however, upon entering *Mtb* cells it is metabolically reduced by intracellular dehydrogenases to resorufin **65**, which is pink.[169] This change indicates the existence of living bacterial cells, as it demonstrates active metabolic processes (Figure 75).

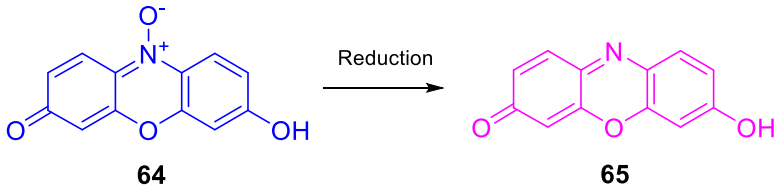


**64** **65**

Figure 75. Irreversible reduction of resazurin **64** (blue-purple) to resorufin **65** (pink) indicates the presence of live bacteria.

The REMA assay, which relies on the redox potential of resazurin **64** for both visual detection of colour changes and spectrophotometric measurement, was utilized in this research to evaluate the activity of the tested compounds. The experiments were conducted in 96-well plates, with each plate containing four replicates for each compound concentration, evaluating two compounds per plate. To prepare the assay, the *Mtb* strain was cultured in Middlebrook 7H9GC medium and subsequently added to the 96-well plates along with serially diluted concentrations of the test compounds. The starting concentration of each compound, set at 64 µg/mL, was added to column

1 of the plate. A two-fold serial dilution was conducted throughout the plate to achieve a range of concentrations. The plates were incubated at 37 °C for five days to allow bacterial growth. After incubation, resazurin was introduced to each well as a redox indicator to evaluate metabolic activity. The plates were subsequently incubated for another 48 hours, after which they were analysed for colour changes. The control wells were initially assessed to verify the validity of the experiment and to ensure the plates were free from contamination. The negative control, containing only media without bacteria, will maintain the original blue-purple colour of resazurin, signifying the absence of bacterial growth. On the other hand, the positive control, which had *Mtb* without any test compounds, will turn pink, indicating active bacterial growth (Figure 76).

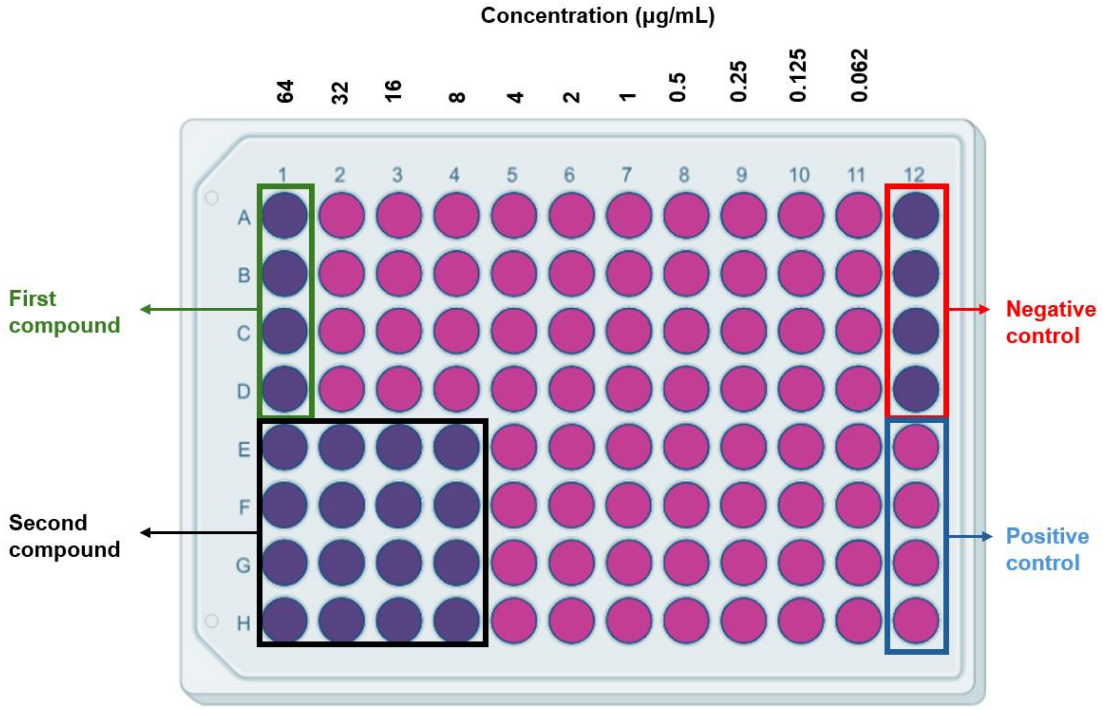


Figure 76. A 96-well plate utilised in the REMA assay determining MIC values. Compound 1 has an MIC of 64 µg/mL, whereas Compound 2 has an MIC of 8 µg/mL. Negative controls (no bacteria) remained purple, and positive controls (bacteria only) turned pink.

The MIC used in this experiment is defined as the lowest concentration of a compound that prevents colour change of resazurin (blue) and thereby inhibiting bacterial growth. Moreover, to validate the experimental methodology and ensure the accuracy of the results, control MIC measurements were conducted using known anti-TB medications, such as rifampicin, isoniazid, and ethambutol. The MIC values acquired for these standard drugs were compared with those reported in the literature, to validate the reliability of the assay.

### 3.2 The SAR exploration of imidazo[1,2-*a*]pyridine substituted amino acid hydrazides

Building upon the successful synthesis of imidazo[1,2-*a*]pyridine substituted amino acid hydrazides outlined in the previous chapter, a SAR investigation was conducted to study their potential as anti-tubercular agents. The biological evaluation of these novel compounds was conducted utilising the REMA assay, as described in the previous section. This assay determined their MICs against the wild-type (WT) *Mtb* strain alongside mono- and multidrug-resistant (MDR) strains. In this research, the key structural modification is illustrated in (Figure 77).

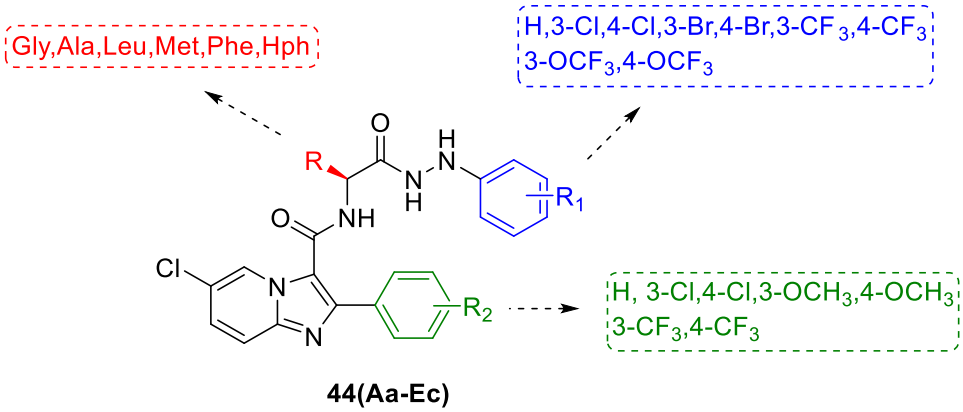


Figure 77. General scaffold representing the compounds synthesised in this study, highlighting the key modifications.

A library of imidazo[1,2-*a*]pyridine analogues were successfully synthesised, containing a variety of amino acids (R) with different sizes and physicochemical properties. These contained simple amino acids, like Gly and Ala, as well as bulkier aromatic amino acids, such as phenylalanine and homophenylalanine. The arylhydrazine part ($R_1$) was also subjected to structural alterations with the introduction of different substitutions, including halogens (Cl and Br) and fluorinated groups such as $CF_3$ and $OCF_3$, while $R_2$ was modified with different substitutions to study the impact of phenyl ring modification on the biological activity.

Initially, the investigation focused on assessing the impact of amino acid side chain variations on the anti-tubercular activity of the analogues. Consequently, both the arylhydrazine moiety and the phenyl ring at $R_2$ position were fixed with proton to mitigate their impact on activity. These analogues functioned as reference compounds for comparison in subsequent SAR studies across three series (Figure 78).

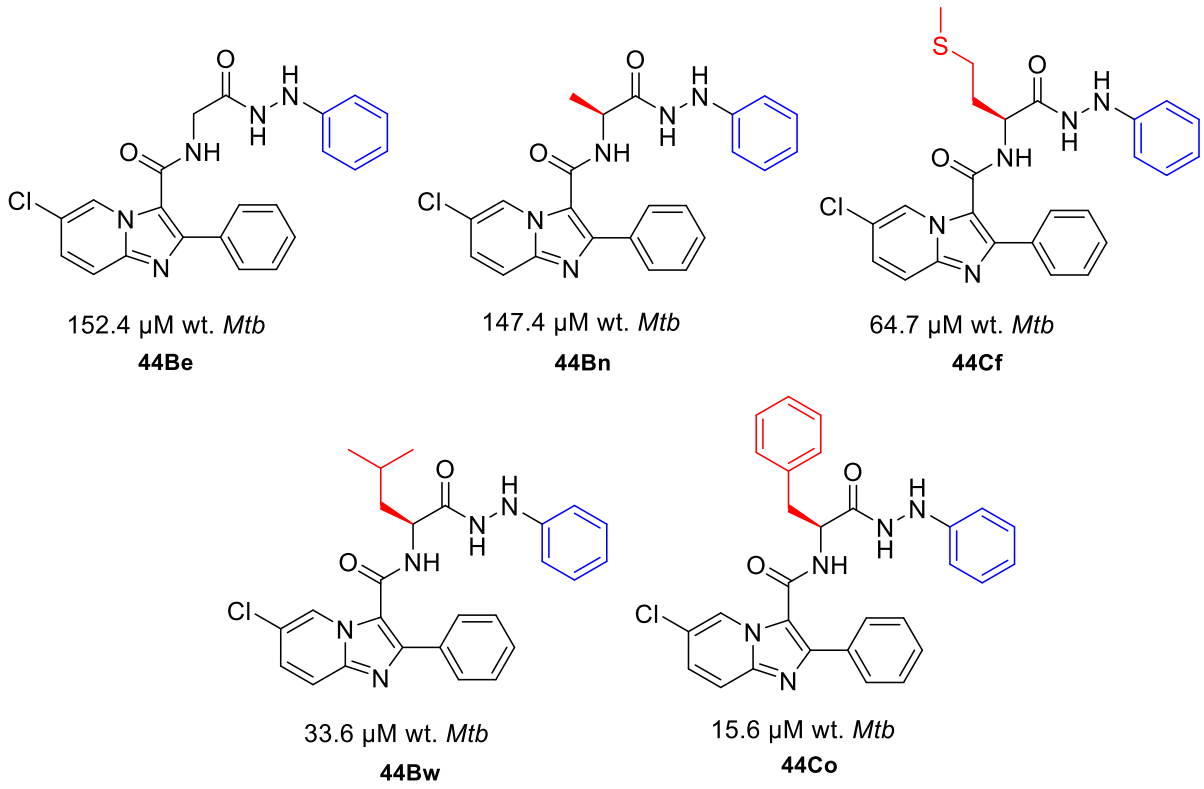


Figure 78. MIC values against wild-type *Mtb* of analogues with different amino acids.

The biological analysis demonstrated the significance of the amino acid side chain size in anti-tubercular activity. Compounds with no side chain, such as **44Be**, or containing small amino acid side chain, as observed with **44Bn**, exhibited minimal inhibitory activity. While continued increases in the side chain resulted in improved potency, with **44Cf** showing moderate activity and **44Bw** exhibiting further enhancement. The highest activity was noted with *L*-phenylalanine **44Co**, having an aromatic side chain, producing an MIC of 15 µM. These differences in activity are likely attributed to variations in lipophilicity, with larger, more hydrophobic side chains enhancing the logP and improving the membrane permeability of the compound.

### 3.2.1 First-series of imidazo[1,2-*a*]pyridine analogues

As the first stage of this study, the focus was on examining the impact of introducing different substitutions in the new phenyl ring ($R_2$) across various amino acid scaffolds. To maintain consistency in the phenylhydrazine moiety ($R_1$), arylhydrazine with a simple proton was retained, allowing a focused analysis of the relationship between $R_2$ substitutions and various amino acids (R). The selected amino acids include glycine, alanine, methionine, leucine and phenylalanine (**Error! Reference source not found.**).

Substituents at $R_2$ were chosen based on their distinct electronic properties to investigate their possible impact on biological activity. For instance, chlorine, a commonly used halogen in medicinal chemistry, increases lipophilicity while its moderate electronegativity and size enable favourable steric interactions and maintain electronic balance within the compound.[170] Moreover, $CF_3$ a strong electron-withdrawing group, confers unique physicochemical properties such as increased lipophilicity, while its inductive effects increasing hydrogen bonding interactions with the target binding site.[163] Conversely, the methoxy group ($OCH_3$), is an important functional group in medicinal chemistry because its ability to modulate electronic properties, increase binding interactions by engaging both lipophilic and hydrophilic regions.[171] These variations in substituents intend to explore whether incorporating different substitutions at the $R_2$ position could influence the activity of the imidazo[1,2-*a*]pyridine analogues across different amino acids. To this end, 30 compounds were successfully synthesised and screened against different *Mtb* strains (Table 9).

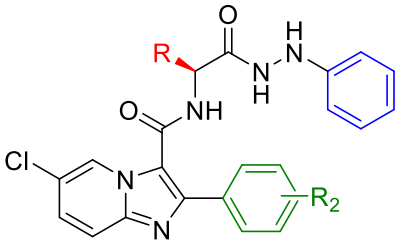

**44(Aa-Bd)**

| Compound | R | $R_2$ | clogP | WT (μM) | $INH^R$ (μM) | $RIF^R$ (μM) | $RIF/INH^R$ (μM) 8250 | $RIF/INH^R$ (μM) 8258 |
|---|---|---|---|---|---|---|---|---|
| **44Aa** | Gly | 3-Cl | 3.34 | - | - | - | - | - |
| **44Ab** | | 4-Cl | 3.34 | - | - | - | - | - |
| **44Ac** | | 3-$CF_3$ | 3.70 | - | - | - | - | - |
| **44Ad** | | 4-$CF_3$ | 3.70 | 65.6 | 32.8 | 65.6 | 65.6 | 32.8 |
| **44Ae** | | 3-$OCH_3$ | 2.65 | - | - | - | - | - |
| **44Af** | | 4-$OCH_3$ | 2.65 | - | - | - | - | - |
| **44Ag** | Ala | 3-Cl | 3.83 | - | - | - | - | - |
| **44Ah** | | 4-Cl | 3.83 | - | - | - | - | - |
| **44Ai** | | 3-$CF_3$ | 4.19 | - | - | - | - | - |
| **44Aj** | | 4-$CF_3$ | 4.19 | - | - | - | - | - |
| **44Ak** | | 3-$OCH_3$ | 3.15 | - | - | - | - | - |
| **44Al** | | 4-$OCH_3$ | 3.15 | - | - | - | - | - |
| **44Am** | Met | 3-Cl | 4.16 | - | - | - | - | - |
| **44An** | | 4-Cl | 4.16 | - | - | - | - | - |
| **44Ao** | | 3-$CF_3$ | 4.53 | - | - | - | - | - |
| **44Ap** | | 4-$CF_3$ | 4.53 | - | - | - | - | - |
| **44Aq** | | 3-$OCH_3$ | 3.48 | - | - | - | - | - |
| **44Ar** | | 4-$OCH_3$ | 3.48 | - | - | - | - | - |
| **44As** | Leu | 3-Cl | 5.06 | - | - | - | - | - |
| **44At** | | 4-Cl | 5.06 | - | - | - | - | - |
| **44Au** | | 3-$CF_3$ | 5.43 | - | - | - | - | - |
| **44Av** | | 4-$CF_3$ | 5.43 | - | - | - | - | - |
| **44Aw** | | 3-$OCH_3$ | 4.38 | - | - | - | - | - |
| **44Ax** | | 4-$OCH_3$ | 4.38 | - | - | - | - | - |
| **44Ay** | Phe | 3-Cl | 5.50 | 117.6 | 117.6 | - | 117.6 | 117.6 |
| **44Az** | | 4-Cl | 5.50 | - | - | - | - | - |
| **44Ba** | | 3-$CF_3$ | 5.87 | - | - | - | - | - |
| **44Bb** | | 4-$CF_3$ | 5.87 | - | - | - | - | - |
| **44Bc** | | 3-$OCH_3$ | 4.82 | - | 118.5 | - | 118.5 | 118.5 |
| **44Bd** | | 4-$OCH_3$ | 4.82 | - | - | - | - | - |

Table 9. The MIC results of the antimycobacterial testing of the imidazo[1,2-*a*]pyridine **44Aa-44Bd** against various *Mtb* strains; data represent mean $MIC_{90}$ values (μg/mL) where a (-) indicates no activity at the assay maximum concentration of 64 μg/ml. WT = Wild type *Mtb* strain; $Rif^R$ = Rifampicin resistant *Mtb* strain; $INH^R$ = Isoniazid resistant *Mtb* strain.

The data presented in Table 9 clearly indicate that introducing Cl, $CF_3$, or $OCH_3$ substituents into the *meta* and *para* positions of the $R_2$ moiety did not improve the antimycobacterial activity across different amino acids analogues. In the case of the leucine analogue, the incorporation of these substitutions led to a complete loss of activity, while the unsubstituted leucine analogue **44Bw** exhibited moderate activity against the WT strain and demonstrated promising activity against INH-resistant *Mtb* strain (Figure 79).

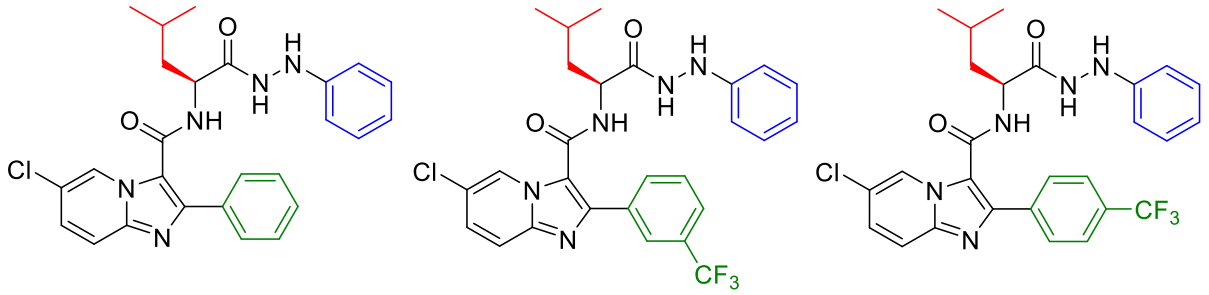


Figure 79. Incorporating different $R_2$ substitutions into the leucine analogue resulted in a loss of the activity against both WT and resistant strains.

The only compound from this series that exhibited inhibitory activity was compound **44Ad** which demonstrated moderate activity against INH-resistant *Mtb* strain. Significantly, when compared to the unsubstituted glycine analogue **44Be**, the incorporation of a 4-$CF_3$ group in the $R_2$ position led to a 4-fold enhancement in potency against INH-resistant strain (Figure 80).

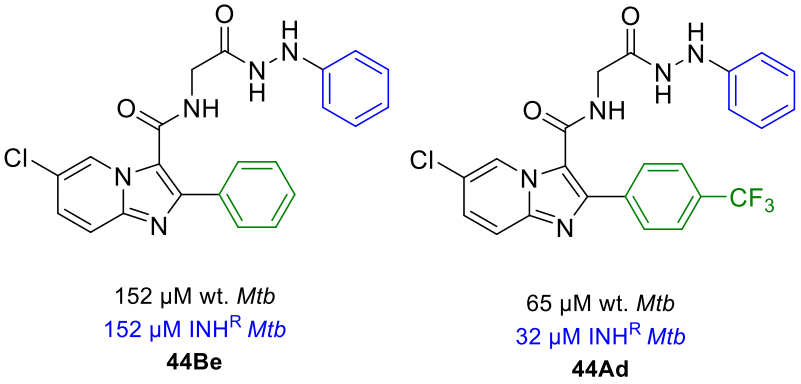


Figure 80. Introducing 4-$CF_3$ in the $R_2$ position resulted in increase the activity against INH resistant strain.

### 3.2.2 Second-series of imidazo[1,2-*a*]pyridine analogues

The next phase of the investigation was centred on incorporating different substitutions in the arylhydrazine moiety with various amino acids while keeping $R_2$ constant as a proton (Figure 66). The initial investigation focused on modifying the phenylhydrazine moiety, with the amino acid component include glycine, alanine and leucine (Table 10).

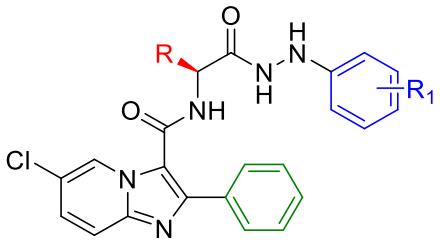


| Compound | R | $R_1$ | clogP | WT (µM) | $INH^R$ (µM) | $RIF^R$ (µM) | $RIF/INH^R$ (µM) 8250 |
|---|---|---|---|---|---|---|---|
| **44Be** | Gly | H | 2.78 | 152.43 | 152.43 | 152.43 | 152.43 |
| **44Bf** | | 3-Cl | 3.34 | 140.8 | 140.8 | 140.8 | 140.8 |
| **44Bg** | | 4-Cl | 3.34 | 140.8 | 140.8 | 140.8 | 140.8 |
| **44Bh** | | 3-Br | 3.61 | 128.3 | 128.3 | 128.3 | 128.3 |
| **44Bi** | | 4-Br | 3.61 | 128.3 | 128.3 | 128.3 | 128.3 |
| **44Bj** | | 3-$CF_3$ | 3.70 | 131.18 | 131.18 | 131.18 | 131.18 |
| **44Bk** | | 4-$CF_3$ | 3.70 | 131.18 | 131.18 | 131.18 | 131.18 |
| **44Bl** | | 3-$OCF_3$ | 4.31 | 63.50 | 63.50 | 127.01 | 63.50 |
| **44Bm** | | 4-$OCF_3$ | 4.31 | 63.504 | 63.50 | 127.01 | 63.50 |
| **44Bn** | Ala | H | 3.27 | 147.49 | 147.49 | 147.49 | 73.74 |
| **44Bo** | | 3-Cl | 3.83 | 136.65 | 68.33 | 136.65 | 136.65 |
| **44Bp** | | 4-Cl | 3.83 | 136.65 | 136.65 | 136.65 | 136.65 |
| **44Bq** | | 3-Br | 4.10 | 62.40 | 62.40 | 62.40 | 62.40 |
| **44Br** | | 4-Br | 4.10 | 124.81 | 124.81 | 124.81 | 124.81 |
| **44Bs** | | 3-$CF_3$ | 4.19 | 127.52 | 127.52 | 127.52 | 127.52 |
| **44Bt** | | 4-$CF_3$ | 4.19 | 63.76 | 63.76 | 127.52 | 63.76 |
| **44Bu** | | 3-$OCF_3$ | 4.80 | 30.89 | 15.44 | 30.89 | 30.89 |
| **44Bv** | | 4-$OCF_3$ | 4.80 | 61.78 | 61.78 | 61.78 | 61.78 |
| **44Bw** | Leu | H | 4.51 | 33.61 | 16.80 | 134.45 | 33.61 |
| **44Bx** | | 3-Cl | 5.06 | 125.39 | 125.39 | 125.39 | 125.39 |
| **44By** | | 4-Cl | 5.06 | 62.69 | 62.69 | 125.39 | 62.69 |
| **44Bz** | | 3-Br | 5.33 | 115.34 | 115.34 | - | 57.67 |
| **44Ca** | | 4-Br | 5.33 | 57.67 | 115.34 | - | 57.67 |
| **44Cb** | | 3-$CF_3$ | 5.43 | - | 29.41 | - | 29.41 |
| **44Cc** | | 4-$CF_3$ | 5.43 | - | 117.65 | - | 117.65 |
| **44Cd** | | 3-$OCF_3$ | 6.03 | - | 57.14 | - | 28.57 |
| **44Ce** | | 4-$OCF_3$ | 6.03 | 28.57 | 28.57 | - | 28.57 |

Table 10. The MIC results of the antimycobacterial susceptibility testing of the imidazo[1,2-*a*]pyridine **44Aa**-**44Ba** against different Mtb strains; data represent mean $MIC_{90}$ values (µg/mL) where a (-) indicates no activity at the assay maximum concentration of 64 µg/ml. WT = Wild type *Mtb* strain; $Rif^R$ = Rifampicin resistant *Mtb* strain; $INH^R$ = Isoniazid resistant *Mtb* strain.

Disappointingly, neither glycine (**44Be – 44Bm**) nor alanine (**44Bn – 44Bv**) derivatives showed any improvement in activity compared to their unsubstituted forms, confirming that the simplicity of these amino acids limits their potential for enhanced anti-tubercular efficacy. Notably, the 3-$OCF_3$ alanine derivative **44Bu** emerged as a significant exception, exhibiting a 4-fold increase in activity compared to the unsubstituted analogue **44Bn**. Moreover, this compound showed promising potency against the INH resistant strains of *Mtb*, with an MIC value of 15.4 μM (Figure 81).

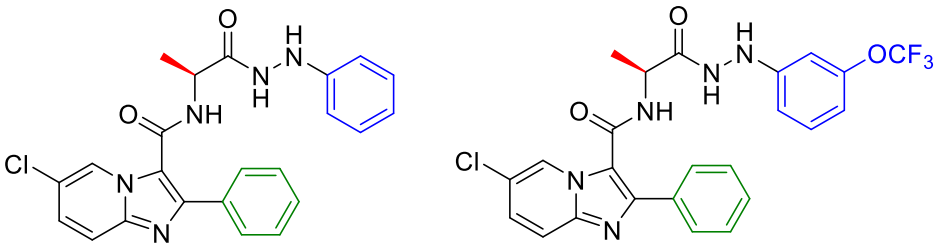


147.4 μM wt. *Mtb*
147.4 μM $INH^R$ *Mtb*
**44Bn**

30.8 μM wt. *Mtb*
15.4 μM $INH^R$ *Mtb*
**44Bu**

Figure 81. An improvement in MIC result of alanine analogue against both WT and INH resistant strains after introducing of 3-$OCF_3$ in the arylhydrazine.

Notwithstanding this, when leucine derivatives were investigated (**44Bw – 44Ce**) the opposite effect was observed. While the unsubstituted leucine compound **44Bw** exhibited moderate activity, the remaining analogues failed to exhibit significant inhibitory effects, yielding overall disappointing results. However, an exception was 4-$OCF_3$ leucine **44Ce** which demonstrated modest activity with an MIC of 29 μM. Also, despite the limited activity against the WT strain, 3-$CF_3$ leucine **44Cb** showed remarkable selectivity against the $INH^R$ strain, exhibiting a 4-fold enhancement in activity relative to the WT strain.

Whilst a reversal of activity was not observed, attention turned to the more active analogues to understand what role a substituent would play in their activity. Consequently, the methionine and phenylalanine analogues were similarly modified with substituents on the arylhydrazine (Table 11).

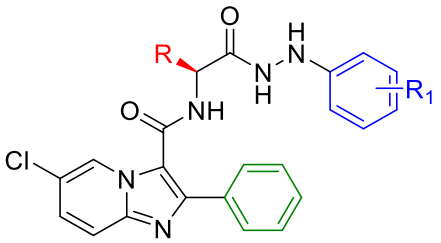

| Compound | R | $R_1$ | clogP | WT (μM) | $INH^R$ (μM) | $RIF/INH^R$ (μM) 8250 | $RIF/INH^R$ (μM) 8258 |
|---|---|---|---|---|---|---|---|
| **44Cf** | Met | H | 3.50 | 64.77 | 129.55 | 129.55 | 64.77 |
| **44Cg** | | 3-Cl | 4.06 | 60.55 | 60.55 | 30.27 | 121.10 |
| **44Ch** | | 4-Cl | 4.06 | 30.27 | 30.27 | 30.27 | 30.27 |
| **44Ci** | | 3-Br | 4.33 | 27.92 | 27.92 | 27.92 | 55.85 |
| **44Cj** | | 4-Br | 4.33 | 55.85 | 27.92 | 27.92 | 27.92 |
| **44Ck** | | 3-$CF_3$ | 4.42 | 56.93 | 28.46 | 56.93 | 28.46 |
| **44Cl** | | 4-$CF_3$ | 4.42 | 28.46 | 28.46 | 28.46 | 28.46 |
| **44Cm** | | 3-$OCF_3$ | 5.03 | - | - | - | 110.72 |
| **44Cn** | | 4-$OCF_3$ | 5.03 | 27.68 | 27.68 | 27.68 | 55.85 |
| **44Co** | Phe | H | 4.95 | 15.68 | 125.49 | 62.74 | 31.37 |
| **44Cp** | | 3-Cl | 5.50 | 3.67 | 58.77 | 7.34 | 7.34 |
| **44Cq** | | 4-Cl | 5.50 | 117.55 | - | - | 117.55 |
| **44Cr** | | 3-Br | 5.78 | 13.58 | 13.58 | 13.58 | 13.58 |
| **44Cs** | | 4-Br | 5.78 | 54.33 | 54.33 | 54.331 | 27.16 |
| **44Ct** | | 3-$CF_3$ | 5.87 | 6.92 | 55.36 | 13.84 | 13.84 |
| **44Cu** | | 4-$CF_3$ | 5.87 | 110.72 | 110.72 | - | 27.68 |
| **44Cv** | | 3-$OCF_3$ | 6.47 | 13.46 | 26.93 | 13.46 | 13.46 |
| **44Cw** | | 4- $OCF_3$ | 6.47 | 107.75 | 107.75 | - | 107.75 |

Table 11. The MIC results of the antimycobacterial susceptibility testing of the imidazo[1,2-*a*]pyridine **44Cf-44Cw** against different *Mtb* strains; data represent mean $MIC_{90}$ values (μg/mL) where a (-) indicates no activity at the assay maximum concentration of 64 μg/ml. WT = Wild type *Mtb* strain; $Rif^R$ = Rifampicin resistant *Mtb* strain; $INH^R$ = Isoniazid resistant *Mtb* strain.

This methionine series (**44Cf – 44Cn**) exhibited a general trend of moderate activity among the majority of the compounds, suggesting potential for anti-tubercular efficacy (Figure 82). Nonetheless, an anomaly was noted with the 3-$OCF_3$ methionine analogue **44Cm**, which failed to show any inhibitory activity against all tested strains.

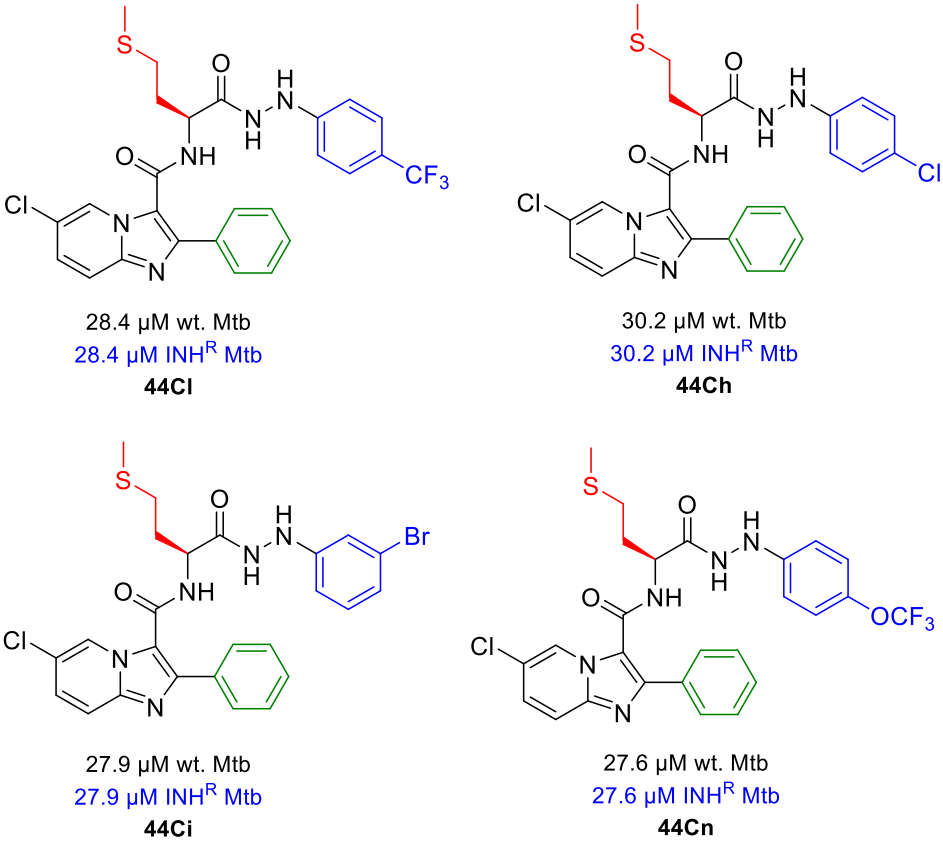


Figure 82. Methionine analogues showing a modest activity against WT and INH$^R$ strain.

The phenylalanine analogues (**44Co – 44Cw**) were the most interesting with two compounds **44Cp** and **44Ct** showing excellent activity < 10 µM against WT *Mtb*. As previously outlined, the unsubstituted phenylalanine compound **44Co** demonstrated a promising MIC value of 15 µM, highlighting its potential for further optimisation. Interestingly, the incorporation of a 3-Cl substituent to the arylhydrazine moiety **44Cp** led to an excellent enhancement in activity, yielding a 4-fold increase in potency compared to **44Co**, with an excellent MIC value of 3.6 µM (Figure 83).

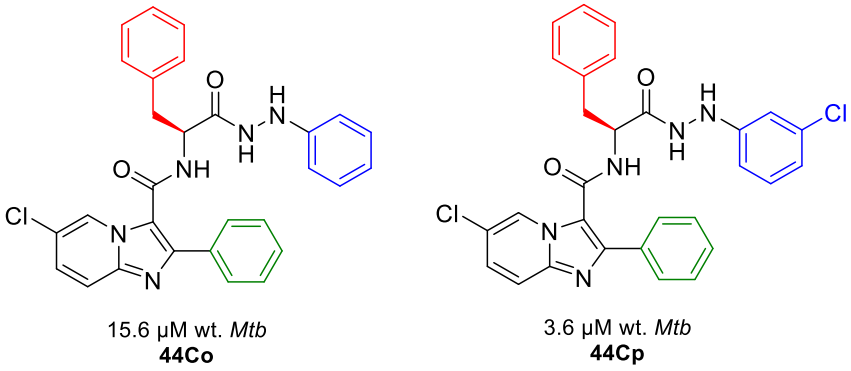


Figure 83. The positive impact of the introduction of 3-Cl in arylhydrazine of the phenylalanine analogue.

Building upon the promising activity observed with the 3-Cl substituted phenylalanine analogue, further modifications were undertaken to explore the influence of the nature of the substituent on anti-tubercular activity. To this end, the Cl substituent was replaced with a $CF_3$ group, a functional group extensively used in drug discovery due to its favourable physicochemical properties, including its small size, high electronegativity, and increased lipophilicity.[162,163] Consequently, the 3-$CF_3$ phenylalanine analogue **44Ct** was successfully synthesised and evaluated for its biological activity. While the introduction of the $CF_3$ group resulted in increased potency relative to the unsubstituted phenylalanine analogue **44Co**, it was observed to be less active than the 3-Cl derivative **44Cp**. Notwithstanding this slight reduction in activity, both the 3-Cl and 3-$CF_3$ analogues demonstrated comparable efficacy to ethambutol **3**, a frontline anti-TB agent, and ethionamide **14** (Figure 84)**.**

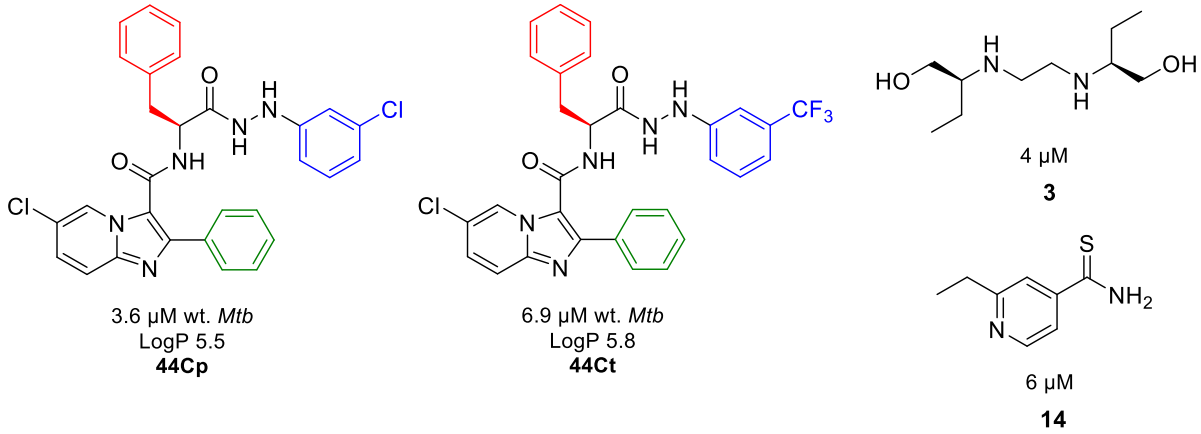


Figure 84. The MIC results of phenylalanine analogues compared to the marketed anti-TB treatment.

Following these encouraging results, further investigation of fluorinated derivatives was pursued. Among fluorinated substituents, $OCF_3$ was chosen for its recognised significance in TB drug discovery. Nonetheless, the incorporation of the $OCF_3$ group did not improve the activity relative to the unsubstituted analogue **44Co**. In fact, the activity of the 3-$OCF_3$-substituted analogue **44Cv** decreased by 2-fold and 4-fold compared to the 3-$CF_3$ and 3-Cl derivatives, respectively (Figure 85).

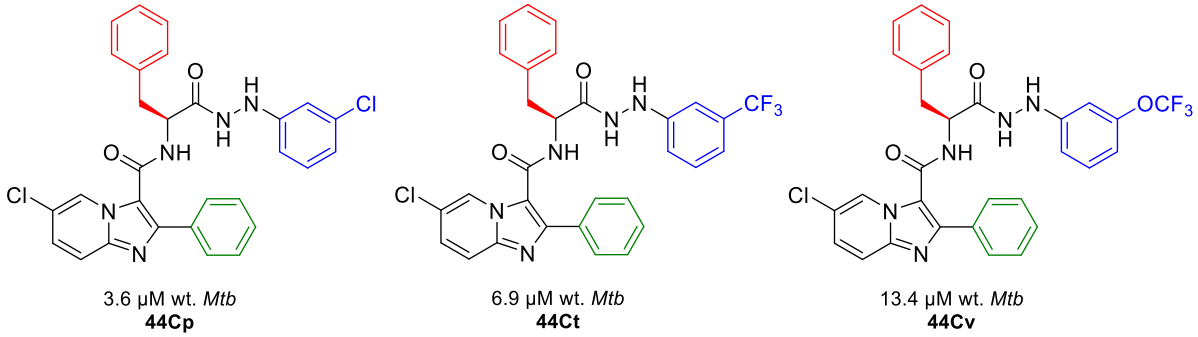


Figure 85. The decrease of anti-microbial activity of compound **44Cv** relative to **44Ct** and **44Cp** Phe analogue.

The lack of activity improvement observed with the introduction of the 3-$OCF_3$ group to the arylhydrazine moiety of the phenylalanine analogue may be attributed to steric hindrance, as $OCF_3$ is a relatively bulky substituent compared to Cl and $CF_3$. To investigate and confirm the potential impact of steric effects on activity, another bulky substituent, 3-Br, was introduced. Screening of the 3-bromo-substituted phenylalanine analogue **44Cr** yielded results similar to those of the 3-$OCF_3$ derivative **44Cv** (Figure 86). This may suggest that the hydrazine part of the compound fits into a relatively narrow pocket in the target, which makes it an unfavourably bulky group for this position.

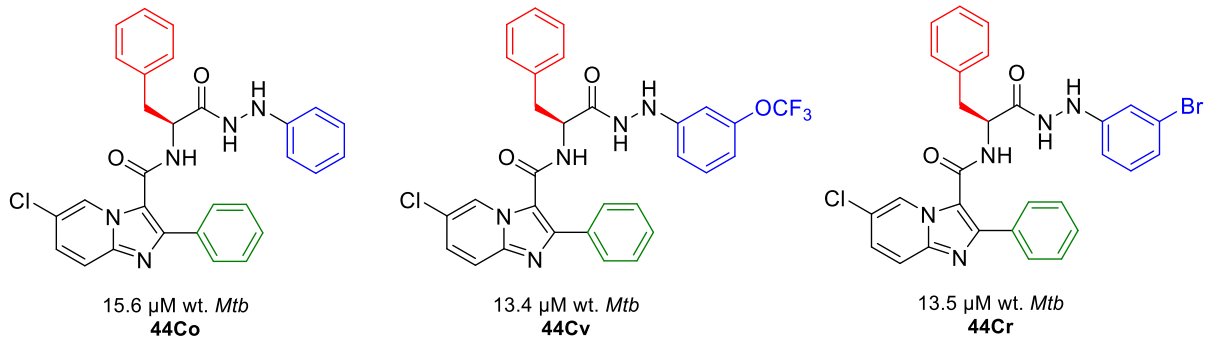


Figure 86. No improvement in activity was observed with the introducing of the 3-$OCF_3$ and 3-Br groups to the arylhydrazine part of the phenylalanine analogue.

With halogen substitutions thoroughly examined, the subsequent step was the introduction of a nitrile (-CN) group into the phenylhydrazine part to assess its impact on biological activity. The nitrile group is an often used substituent in drug design due to its polarity and low molecular weight, that affect molecular interactions and physiochemical properties.[172] As a result, the nitrile group is commonly used as a key structural feature in drug candidates to improve biological activity and therapeutic potential.[172] However, the incorporation of the nitrile group to the arylhydrazine of phenylalanine analogues led to a complete loss of activity (Figure 87).

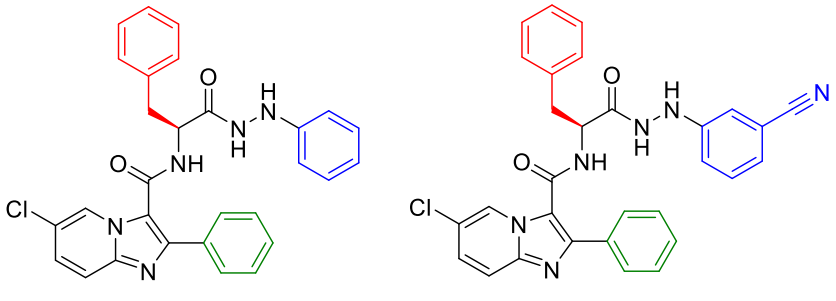


Figure 87. The introduction of 3-CN to arylhydrazine leads to the loss of activity.

Building on the insights gained regarding the impact of substituent nature on the biological activity, the subsequent exploration focused on examining the positional impacts of substituents within the arylhydrazine component. Since the *meta* position had demonstrated promising results for most phenylalanine analogues, this study aimed to understand whether substituents at the *para* position could enhance the biological activity. Surprisingly, changing the substituent position from the *meta* to *para* position led to a loss of activity, regardless of the nature of the substituent incorporated (Figure 88). This result highlights the important role of substituent positioning in determining the anti-tubercular activity of these analogues and indicates that the *para* position may not provide favourable interactions within the target binding site.

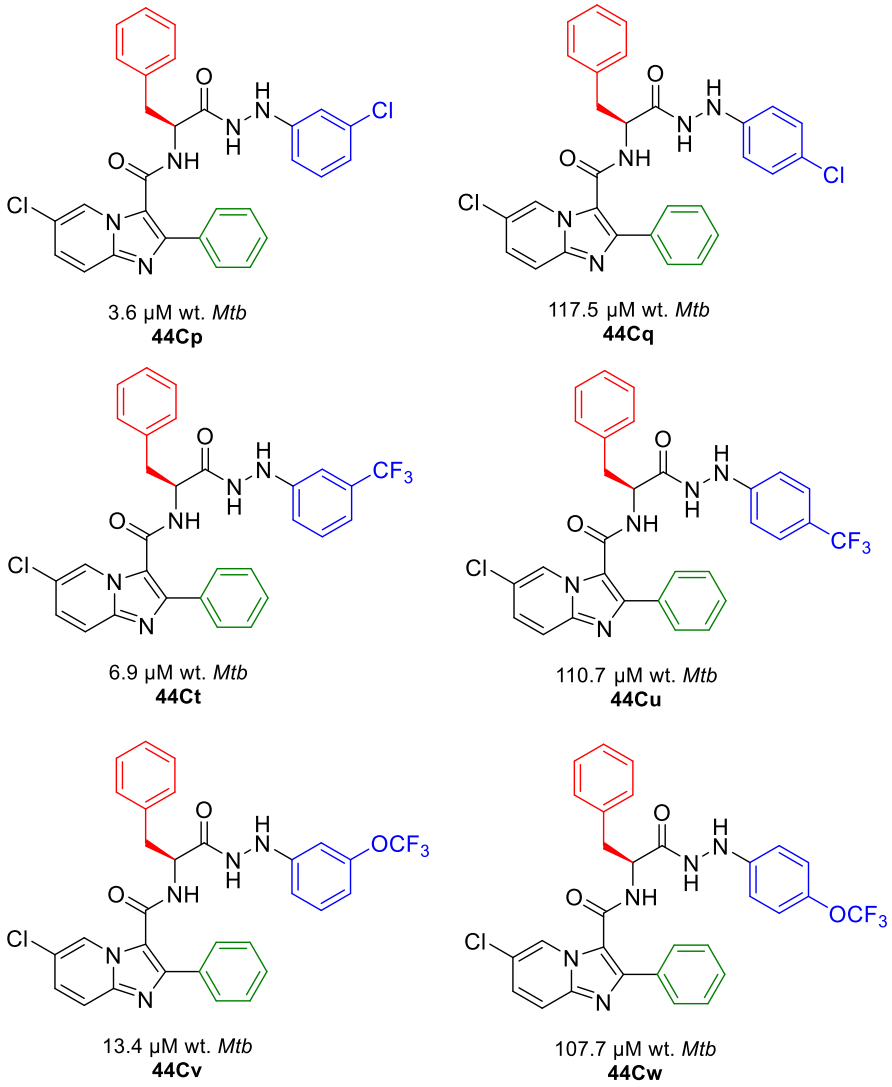


Figure 88. Changing the position of the substituent in the arylhydrazine moiety of phenylalanine analogues resulted in a loss of activity.

Beyond modifications to the arylhydrazine component, the encouraging results noted with phenylalanine derivatives warranted further exploration of the structural distance between the phenyl ring of phenylalanine and the chiral carbon. To study the impact of alkyl chain length on antimicrobial activity, a series of homophenylalanine derivatives were synthesised. These analogues were assessed alongside their phenylalanine derivatives, demonstrating that chain extension resulted in diminished activity relative to the phenylalanine analogues (Figure 89).

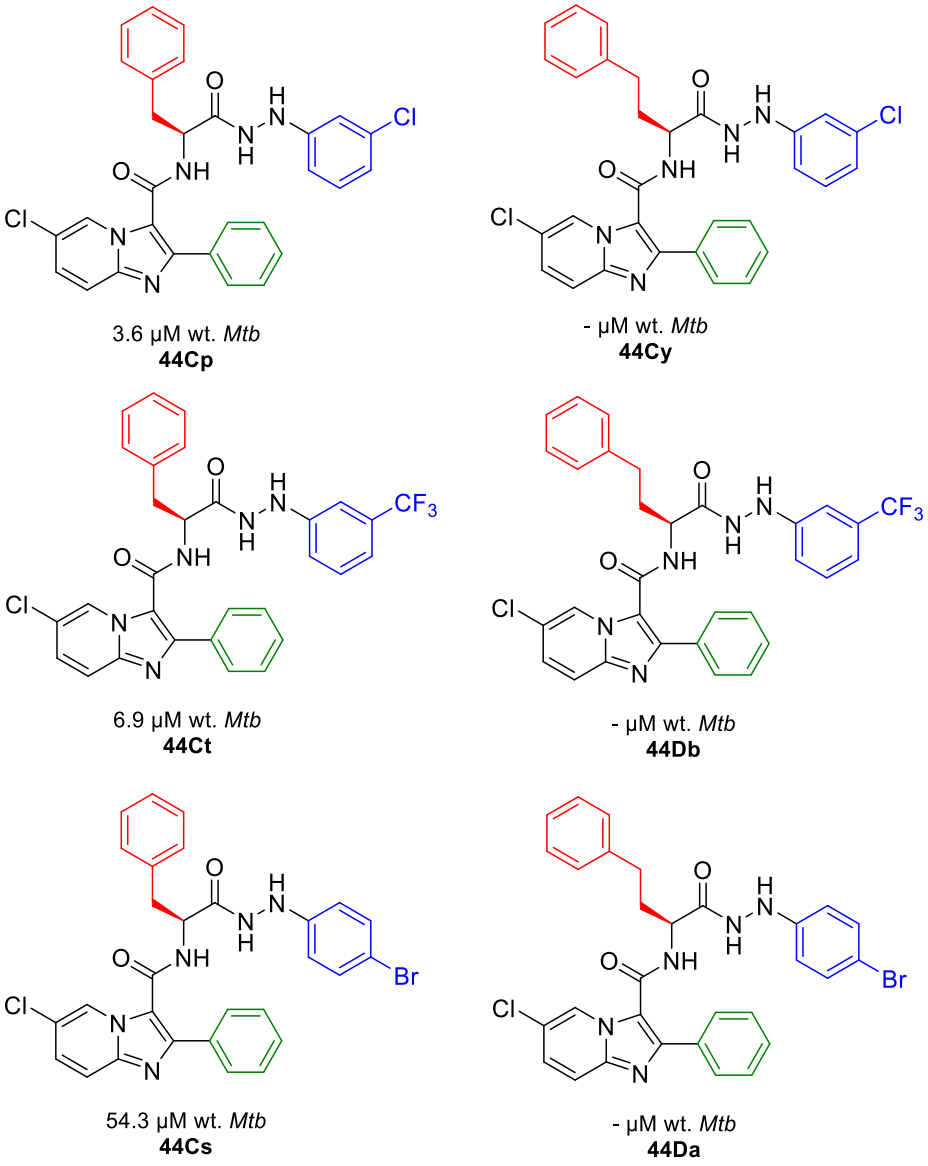


Figure 89. The negative impact of homophenylalanine analogues, compared to phenylalanine analogues, on MIC results against the susceptible *Mtb*.

Overall, the 53 compounds in this series provided valuable insights into the SAR of these compound analogues, highlighting the important contributions of both the amino acid and arylhydrazine moieties in antimicrobial activity. These findings guided the design of the third series with a more focused approach. Phenylalanine was retained in the amino acid part, given its contribution to activity, while substitutions in the arylhydrazine part were restricted to the *meta*-position as this position exhibited enhanced activity in the second series. In the subsequent section, the third series of compounds will explore whether the optimization of the $R_2$ position could enhance the antimicrobial efficacy of phenylalanine even further.

### 3.2.3 **Third-series of imidazo[1,2-*a*]pyridine analogues**

This section focuses on the biological evaluation of the third-series of imidazo[1,2-*a*]pyridine analogues with the main goal of this investigation being to study the impact of introducing different electronic substitutions in the phenyl ring ($R_2$) attached to the core scaffold on the antimicrobial activity.

The decision for developing the third series of compounds was guided by the promising findings demonstrated by phenylalanine analogues in the second series, as highlighted in the previous section. Thus, the design approach for this series has concentrated on maintaining phenylalanine in the amino acid component, aiming to build on its notable potential and demonstrated biological activity. For the arylhydrazine part ($R_1$), the most active compounds in the second series featured a substitution at the *meta* position. Consequently, in this series, the *meta*-substitution pattern was maintained. For the new phenyl ring attached to the core scaffold ($R_2$), the focus shifted to introduce different substituents with different electronic effects to further investigate their effects on activity (Figure 72).

A total of 30 derivatives were successfully synthesised from this series, with modifications introduced at both the $R_1$ and $R_2$, and screened against several strains of *Mtb* to determine their biological activity (Table 12).

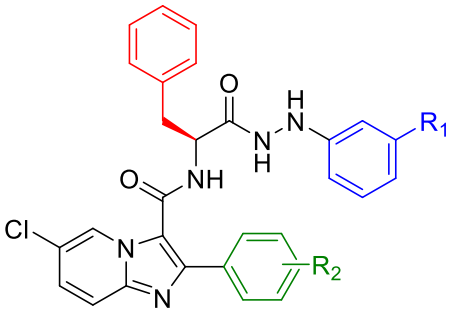


**44Df- 44Ec**

| Compound | $R_1$ | $R_2$ | clogP | WT (μM) | $INH^R$ (μM) | $RIF^R$ (μM) | $RIF/INH^R$ (μM) 8250 | $RIF/INH^R$ (μM) 8258 |
|---|---|---|---|---|---|---|---|---|
| **44Df** | 3-Cl | 3-Cl | 6.06 | 110.6 | 27.6 | 110.6 | 110.6 | 27.6 |
| **44Dg** | 3-Br | | 6.33 | - | 102.7 | - | 102.7 | 102.7 |
| **44Dh** | 3-$CF_3$ | | 6.43 | - | 104.5 | - | 104.5 | 52.3 |
| **44Di** | 3-$OCF_3$ | | 7.03 | - | - | - | - | - |
| **44Dj** | 3-Cl | 4-Cl | 6.06 | 55.2 | - | 33.6 | - | - |
| **44Dk** | 3-Br | | 6.33 | 16.4 | 25.6 | 16.0 | 52.6 | 28.5 |
| **44Dl** | 3-$CF_3$ | | 6.43 | 25.5 | 71.1 | 15.5 | 34.2 | 34.2 |
| **44Dm** | 3-$OCF_3$ | | 7.03 | 29.8 | 16.3 | 71.1 | - | 70.2 |
| **44Dn** | 3-Cl | 3-$CF_3$ | 6.43 | - | - | - | - | - |
| **44Do** | 3-Br | | 6.70 | - | 97.4 | - | - | 97.4 |
| **44Dp** | 3-$CF_3$ | | 6.79 | - | 117.6 | - | 117.6 | 58.8 |
| **44Dq** | 3-$OCF_3$ | | 7.39 | - | 96.7 | - | - | 96.7 |
| **44Dr** | 3-Cl | 4-$CF_3$ | 6.43 | 52.3 | 13.1 | 52.3 | 26.1 | 13.1 |
| **44Ds** | 3-Br | | 6.70 | 24.4 | 12.2 | 24.4 | 12.2 | 12.2 |
| **44Dt** | 3-$CF_3$ | | 6.79 | - | 99.1 | - | - | - |
| **44Du** | 3-$OCF_3$ | | 7.39 | - | - | - | - | - |
| **44Dv** | 3-Cl | 3-$OCH_3$ | 5.38 | - | 55.7 | - | 111.4 | 55.7 |
| **44Dw** | 3-Br | | 5.65 | - | 51.7 | - | 103.4 | 51.7 |
| **44Dx** | 3-$CF_3$ | | 5.74 | - | 52.6 | - | 105.3 | 105.3 |
| **44Dy** | 3-$OCF_3$ | | 6.35 | - | 102.6 | - | 102.6 | 102.6 |
| **44Dz** | 3-Cl | 4-$OCH_3$ | 5.38 | - | - | 46.6 | - | - |
| **44Ea** | 3-Br | | 5.65 | 117.55 | - | - | - | 117.55 |
| **44Eb** | 3-$CF_3$ | | 5.74 | 105.3 | 52.6 | 105.3 | 105.3 | 52.6 |
| **44Ec** | 3-$OCF_3$ | | 6.35 | - | - | 36.7 | 60.8 | - |

Table 12. The MIC results of the antimycobacterial susceptibility testing of the imidazo[1,2-*a*]pyridine **44Df-44Ec** against different *Mtb* strains; data represent mean $MIC_{90}$ values (μg/mL) where a (-) indicates no activity at the assay maximum concentration of 64 μg/ml. WT = Wild type *Mtb* strain; $Rif^R$ = Rifampicin resistant *Mtb* strain; $INH^R$ = Isoniazid resistant *Mtb* strain.

Firstly, introduction of a 3-Cl substituent at the $R_2$ position resulted in a loss of activity compared to the unsubstituted analogue, regardless of the nature of substitution in the arylhydrazine component (Figure 90).

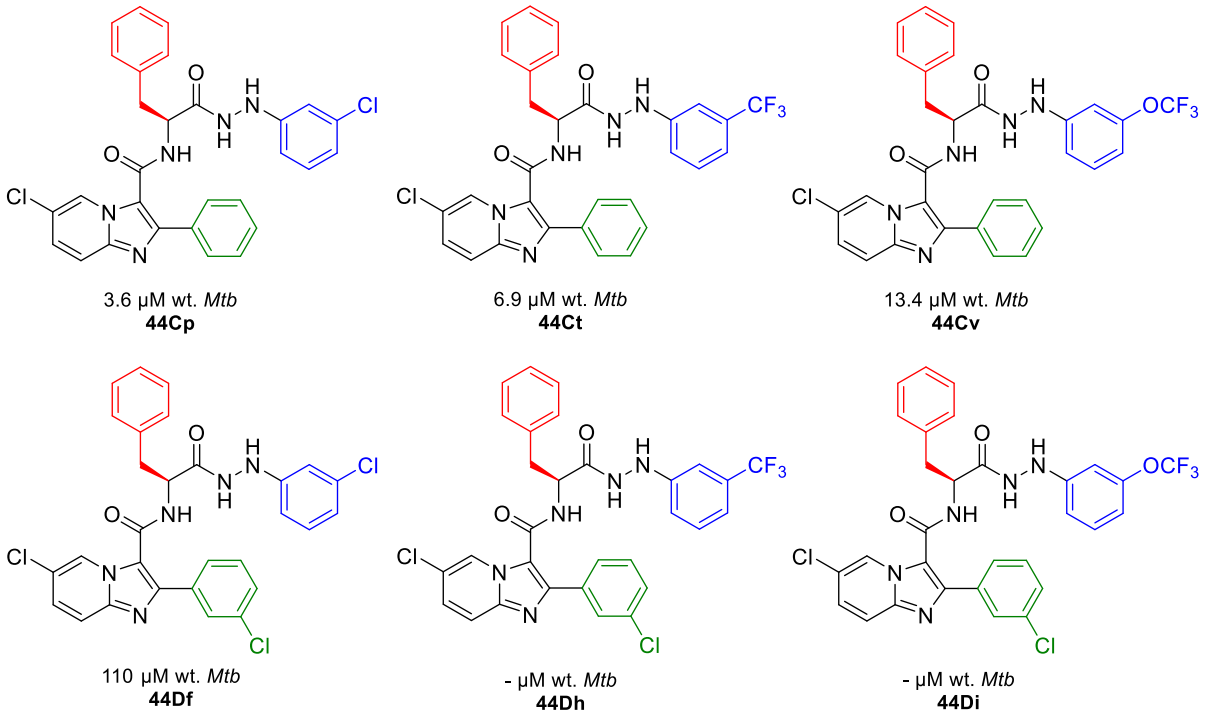


Figure 90. The negative impact of introducing 3-Cl in the phenyl ring attached to the scaffold on the activity, where (-) indicates the lack of inhibition at the assay maximum concentration of 64 µg/ml.

In contrast, introducing a 4-Cl substituent at $R_2$ generally led to diminished activity against the WT strain in most compounds. Nevertheless, the 4-Cl modification showed notable activity against resistant *Mtb* strains. For instance, compounds **44Dl**, **44Dk**, and **44Dj** exhibited significant activity against RIF-resistant strains, with MIC values of 15, 16, and 33 µM, respectively. Notably, compound **44Dm** differed from the others by showing promising activity against INH-resistant strain, achieving an MIC value of 16 µM. In general, it was noted that incorporating substitutions in the arylhydrazine part is important for activity, as the unsubstituted compound **44Az** failed to show any inhibition. Conversely, introducing different substituents at the *meta* position of arylhydrazine, while maintaining the 4-Cl group in $R_2$, resulted in moderate activity against the WT strain and promising activity against resistant strains (Figure 91).

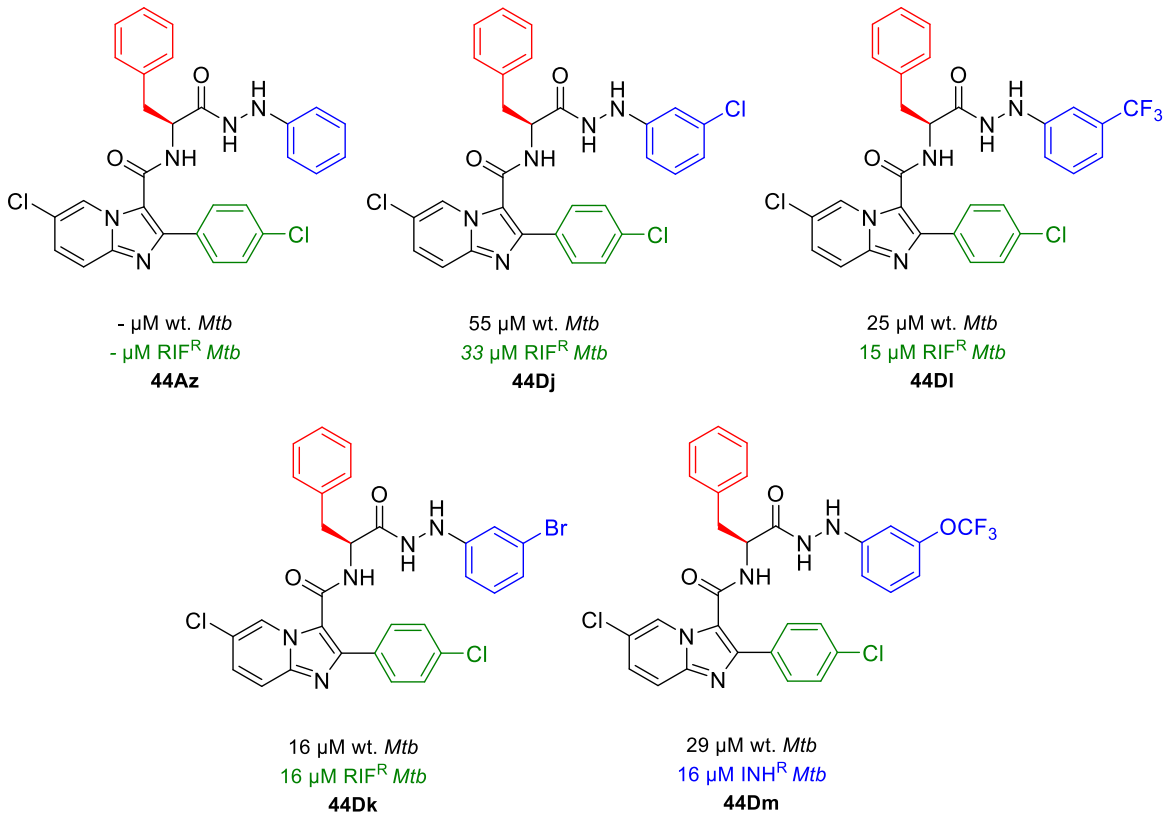


Figure 91. Introducing 4-Cl to the Phe analogues resulted in promising activity against *Mtb* resistant strains.

Further investigation focused on incorporation of $CF_3$, a strong electron-withdrawing group, into the phenyl ring attached to the scaffold ($R_2$). The introduction of 3-$CF_3$ at $R_2$ resulted in a complete loss of activity across all tested strains. Nonetheless, shifting the $CF_3$ group from the *meta* to the *para* position demonstrated differential selectivity towards *Mtb* resistant strains. From this series, 3-chlorophenyl phenylalanine hydrazide **44Dr** and 3-bromophenyl phenylalanine hydrazide **44Ds** exhibited enhanced activity against the INH-resistant strain. Compound **44Dr** demonstrated a 4-fold selectivity against INH-resistant strain over the WT strain, while **44Ds**, despite showing moderate activity against both WT and RIF-resistant strains, displayed promising potency against INH-resistant strain with an MIC value of 12 μM (Figure 92).

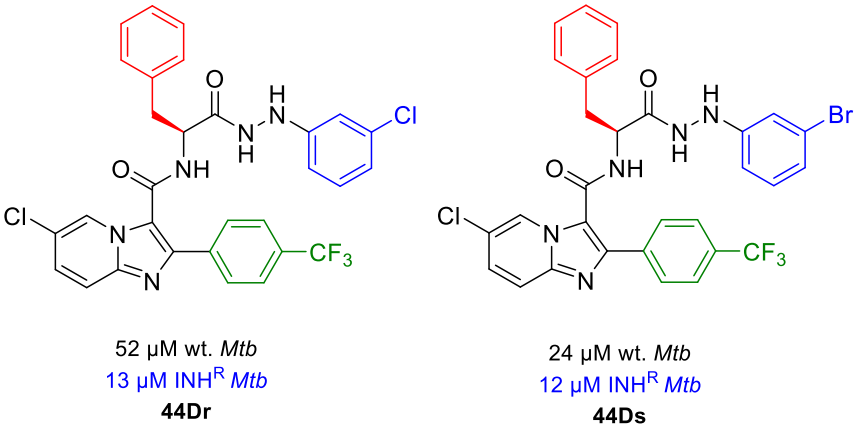


Figure 92. Introducing 4-$CF_3$ in the phenyl ring attached to the scaffold of Phe analogues yielded promising results against INH-resistant strain.

Interestingly, the modification of the arylhydrazine with 3-$CF_3$ or 3-$OCF_3$ substitutions resulted in a loss of activity, further highlighting the sensitivity of the activity profile to both substitution position and pattern. The next phase of the investigation focused on introducing electron-donating groups into the phenyl ring attached to the scaffold ($R_2$) to compare their impact with the previously studied electron-withdrawing groups. It was observed that the incorporation of a methoxy group to the phenyl ring led to loss of activity in the phenylalanine analogues, regardless of whether the substitution was at the *meta* or *para* position (Figure 93).

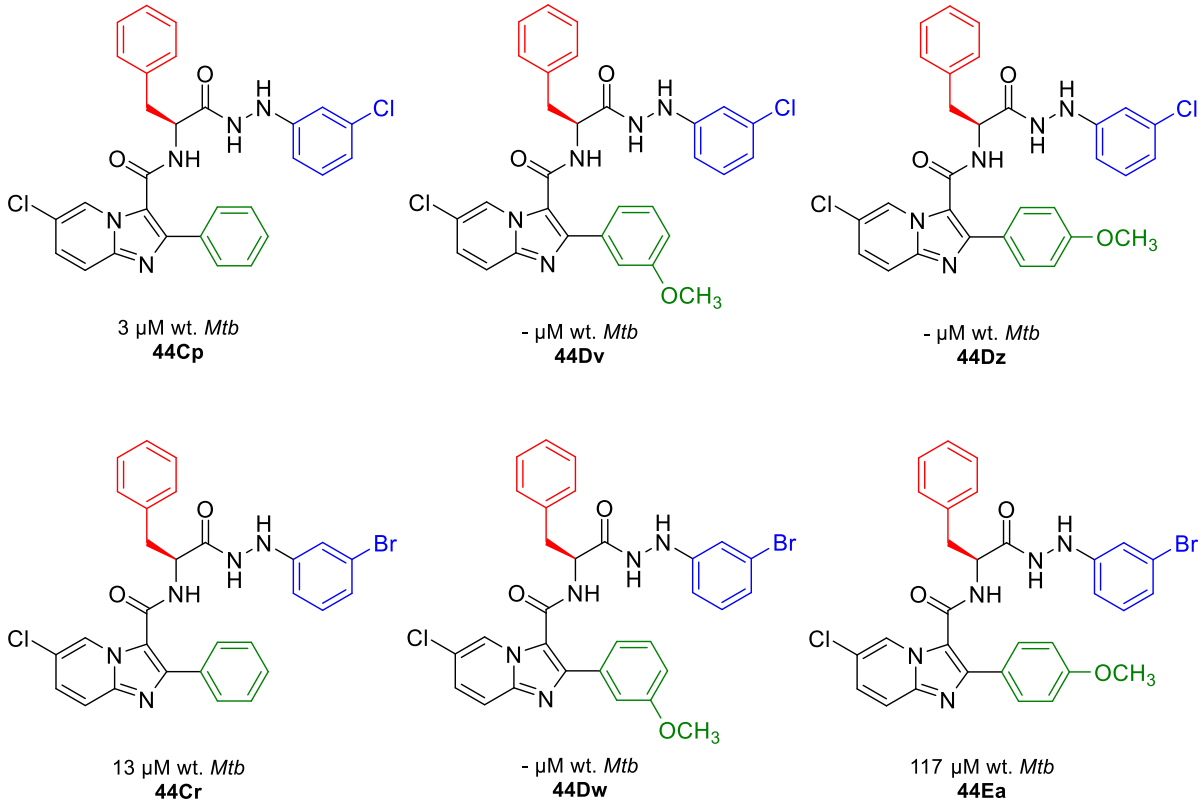


Figure 93. Introducing methoxy group to the phenyl ring attached to the scaffold leading to loss of antimycobacterial activity, irrespective of whether the substitution was at the *meta* or *para* position.

The only notable result from this series was the selectivity of 3-trifluoromethoxy phenylalanine hydrazide **44Ec** against RIF-resistant *Mtb* strain, with an MIC value of 36 µM, while showing no inhibition against the WT strain or INH-resistant *Mtb* strains. Considering the overall results of the third series of imidazo[1,2-*a*]pyridine analogues, it was noted that while introducing different substitutions in the phenyl ring attached to the scaffold ($R_2$) generally resulted in a reduction in antimycobacterial activity against the WT strain, these compounds exhibited inhibitory effects against resistant *Mtb* strains. This outcome underscores their potential as candidates for the development of therapies targeting drug-resistant *Mtb*.

In summary, the structure-activity relationship study of the three series of imidazo[1,2-*a*]pyridine analogues underscored the significant impact of the amino acid (R) moiety, the arylhydrazine part ($R_1$), and the substitutions incorporated at the ($R_2$) position on the biological activity. The amino acid (R) was significant in modulating activity, with phenylalanine analogues exhibiting the best activity, while other amino acids demonstrated varied results. The arylhydrazine moiety ($R_1$) was equally important, as specific substitution patterns played a significant role in either decreasing or improving activity. The incorporation of substitutions in the phenyl ring ($R_2$) offered further insights

into the role of electronic factor influencing activity, particularly against drug-resistant *Mtb* strains. With these insights, the subsequent section will shift focus to a docking study, employing the most active compounds to understand their molecular interactions with potential target PafA.

### 3.3 Molecular docking:

Building on the SAR analysis and MIC results, this section further investigates molecular docking aimed at exploring the interaction of the most active imidazo[1,2-*a*]pyridine derivatives with a potential target *Mtb* PafA. This computational method provides insights into the binding modes and key molecular interactions that may contribute to the reported biological activity.

This study employed GOLD 4.0 software to conduct docking models and analyse the binding interactions of chosen compounds with *Mtb* PafA. The docking process started with preparing the protein target, utilising a homology model produced by AlphaFold as previously described in (*cf.* Section 2.1). The ATP-binding site of PafA was selected as the docking site, and the binding pocket was identified within an 8 Å radius encompassing the key residues reported in prior studies as details in (*cf.* Section 1.5.3.1). The most active compounds from the three series of imidazo[1,2-*a*]pyridine derivatives were chosen for docking studies to investigate their interactions with the ATP-binding site of PafA, and visualisation of the docking results was conducted utilising BIOVIA Discovery Studio and PyMOL, highlighting both 3D and 2D representations. These visualisations provided detailed insights into the spatial orientation of the compounds within the binding pocket, highlighting key interactions including hydrogen bonds and hydrophobic interactions.

The most active ligand identified from the structure-activity relationship study was the 3-chlorophenyl phenylalanine analogue **44Cp** with an MIC value of 3 μM. This compound was docked into the ATP-binding site of PafA. The best pose of compound **44Cp** establishing key interactions with critical residues involved in ATP recognition. Specifically, the compound is predicted to form three hydrogen bonds with Trp419, Arg205, and Tyr55, residues that are essential for enzyme activity.[110,132] Beyond these hydrogen bonds, hydrophobic interactions were also observed between the aromatic moiety of the imidazo[1,2-*a*]pyridine scaffold in the compound and the nonpolar side chain of His197, further contributing to the stability of the predicted binding mode (Figure 94).

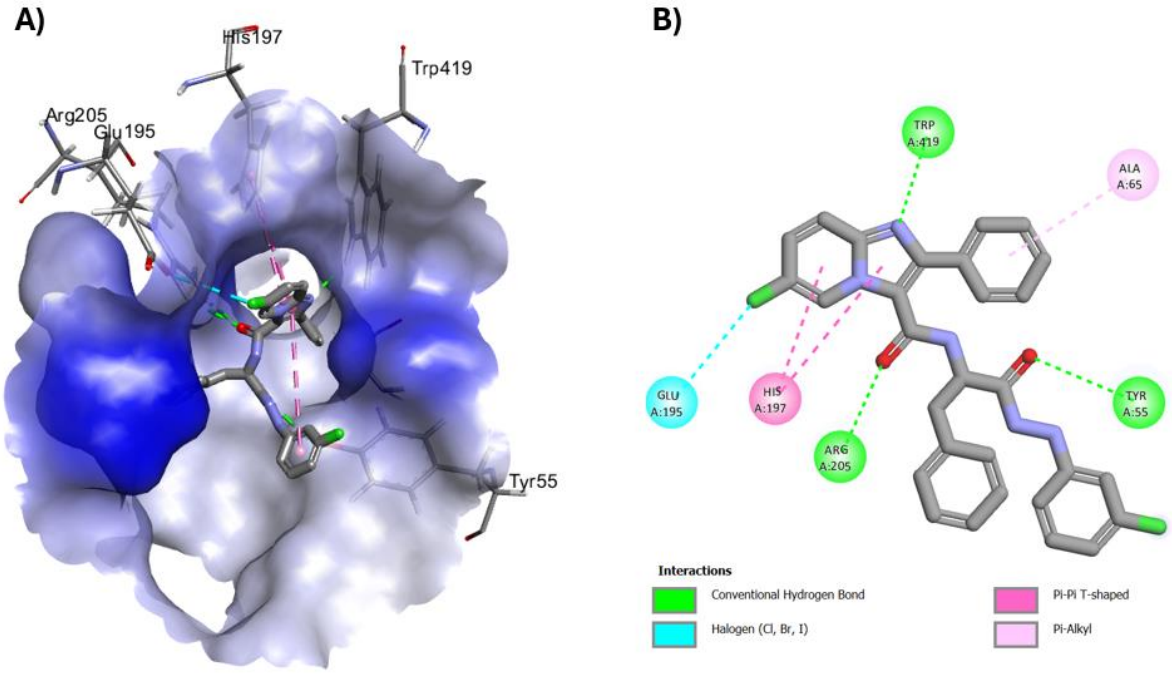


Figure 94. A) 3D visualization of Compound **44Cp** docked into the ATP-binding site of PafA, showing its interactions with key residues in the active site. B) 2D visualization of Compound **44Cp** within the ATP-binding site, displaying hydrogen bonds and hydrophobic interactions.

Similarly, 3-trifluoromethyl phenylalanine analogue **44Ct**, exhibiting a notable MIC value of 6 µM against *Mtb*, was docked into the ATP-binding region of PafA to assess its binding interactions (Figure 95).

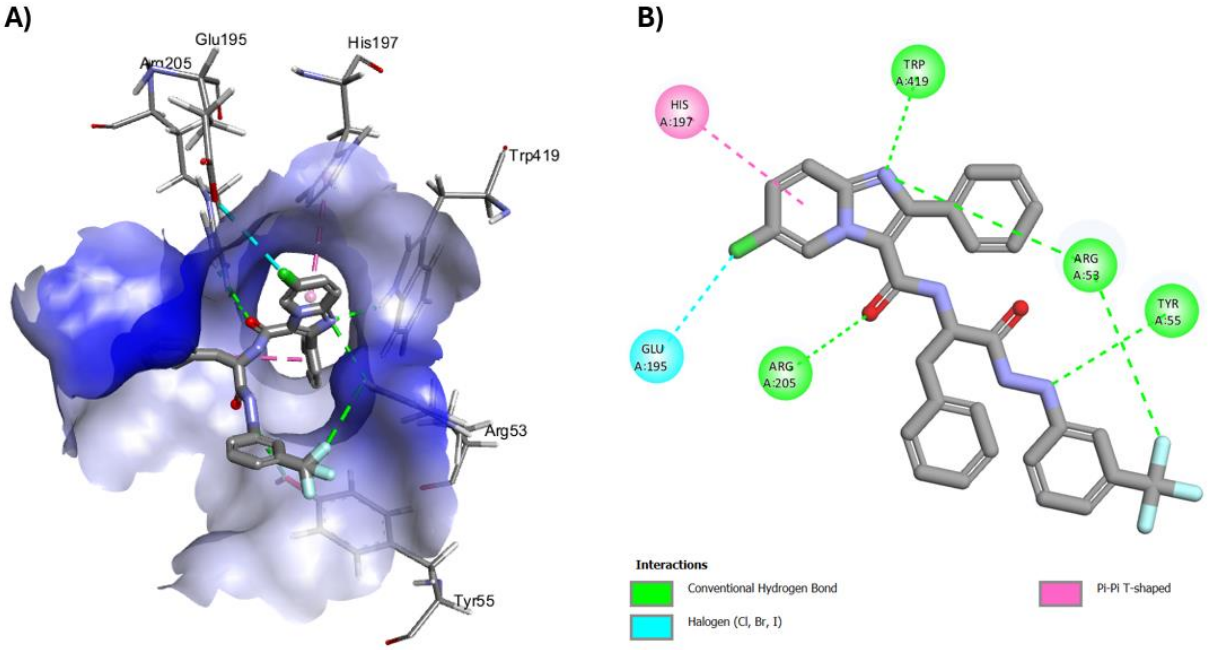


Figure 95. **A)** 3D view of Compound **44Ct** in the active site, illustrating hydrogen interactions with residues Trp419, Arg205, Tyr55, and Arg53. **B)** 2D view of ligand-target interaction.

The docking results indicated that compound **44Cp** shared a binding orientation similar to compound **44Ct**, positioning favourably within the active site. Hydrogen bonding interactions were identified with key residues, including Trp419, Arg205, Arg53, and Tyr55, which play a significant role in ligand binding within the ATP-binding pocket.

From the first series, it was noted that steric hindrance appears to be an important feature of the arylhydrazine moiety, since replacing 3-Cl with 3-Br led to a fourfold decrease in activity. 3-Br phenylalanine analogue **44Cr** was subjected to *in silico* docking study to further rationalise this experimental finding. Docking results revealed that the best pose of 3-Br compound **44Cr** exhibited a different orientation compared to 3-Cl, resulting in the loss of hydrophobic interaction with His419 (Figure 96).

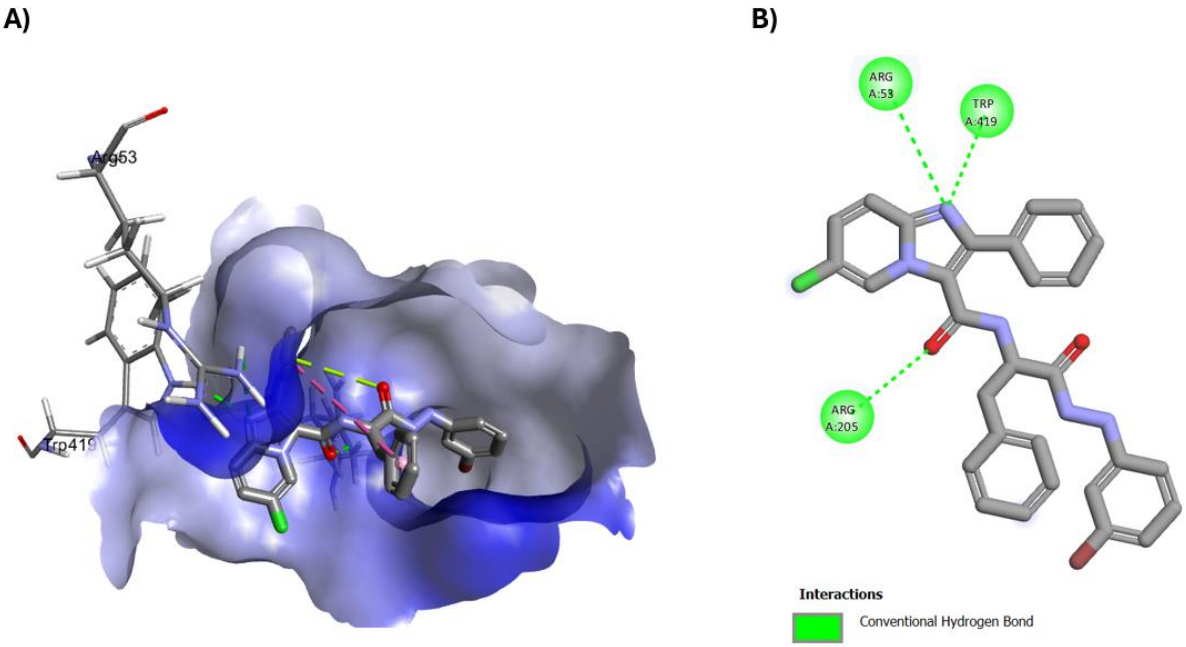


Figure 96. A) 3D visualization of **44Cr** within the ATP-binding pocket. B) 2D diagram depicting the ligand- protein interaction.

Another observation from the first series of compounds was the notable difference in activity caused by the positional change of the chlorine substituent on the phenyl ring from the *meta* position (Compound **44Cp**, 3-Cl) to the *para* position (Compound **44Cq**, 4-Cl). While structurally similar, Compound **44Cq** demonstrated a complete loss of activity. To investigate this, the 4-Cl analogue was docked into the ATP binding site of PafA utilising the same docking protocol, and its best pose was analysed (Figure 97).

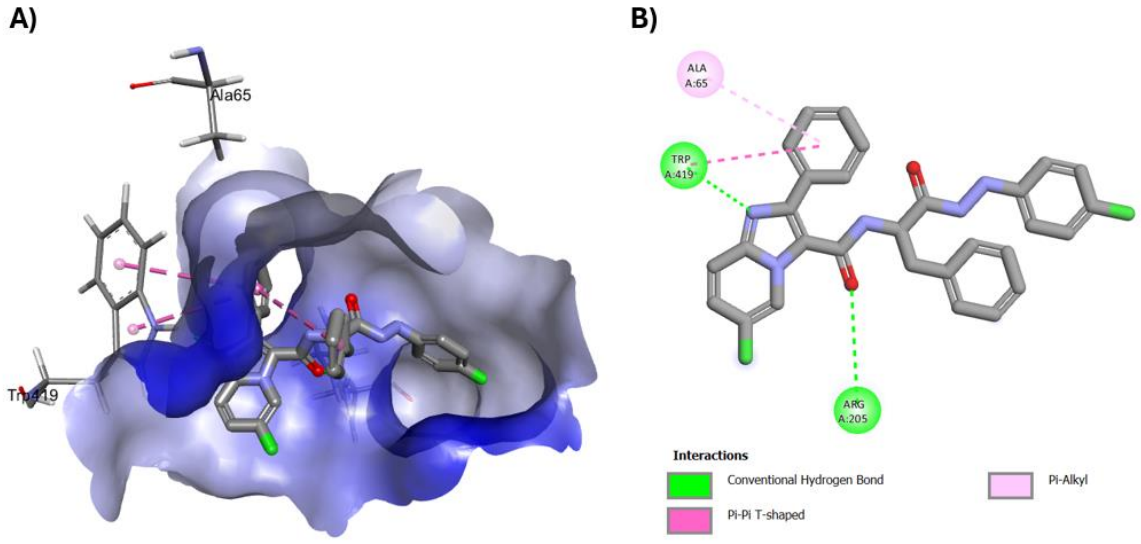


Figure 97. A) 3D visualization of **44Cq** within the PafA pocket. B) 2D diagram shows the important interactions.

The findings indicated that the best pose of compound **44Cq** exhibited a different binding orientation within the active site. This altered orientation disrupted important interactions, resulting in the loss of hydrogen bonding with Tyr55 and hydrophobic interaction with His197. Key docking and biological data for the selected compounds used in this study are summarised in Table 13.

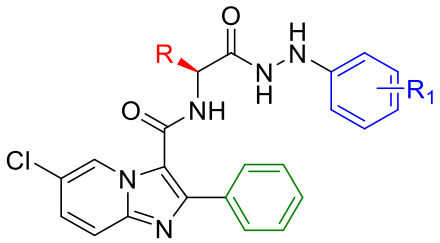


| Compound | R | $R_1$ | MIC (μM) | Docking score | H-Bonding |
|---|---|---|---|---|---|
| **44Cp** | Phe | 3-Cl | 3 | 63 | Trp419, Arg205, and Tyr55 |
| **44Ct** | | 3-$CF_3$ | 6 | 67 | Trp419, Arg205, and Arg53 |
| **44Cr** | | 3-Br | 13 | 58 | Trp419, Arg205, and Tyr55 |
| **44Cq** | | 4-Cl | 117 | 53 | Trp419, Arg205 |

Table 13. Selected compounds used in the molecular docking study with their corresponding docking scores against PafA and MIC values against *Mtb* H37Rv (wild-type) and key hydrogen-bonding interactions..

Overall, the results from this study indicate that the active compounds within this series demonstrate important interactions with key residues in the ATP-binding site, underscoring their potential as viable inhibitors. Moreover, as computational modelling has evolved into an essential part of drug discovery, its focus has expanded from predicting the ligand-target interaction to assessing ADME and physiochemical properties, a shift that will be investigated further in the next section.

### 3.4 *In silico* ADME and physiochemical properties:

The failure of drug candidates from inadequate absorption, distribution, metabolism, and excretion (ADME) characteristics continues to be a significant issue in drug discovery, leading to considerable delays, elevated costs, and high attrition rates in early stage research.[173] Recognizing this challenge, there has been a transition towards the early evaluation of ADME properties, utilising computational methods to detect and discard poorly optimised candidates to decrease late-stage failures. Researchers utilise predictive ADME modelling to optimise the selection of lead compounds with favourable physiochemical parameters, thus enhancing the efficiency

of drug development and increasing the chance of clinical success.[174] In this study, ADMETlab 3 platform, a tool for ADMET assessment of compounds using a comprehensively collected database was utilised to predict the pharmacokinetic and physicochemical characteristics of three series of imidazo[1,2-*a*]pyridine analogues.[175] The predicted data were analysed and compared with established physiochemical parameters of current anti-TB treatment, particularly the FDA approved oral medications isoniazid and bedaquiline, along with Q203, a promising anti-TB candidate currently in Phase 2 clinical trial. The predicted ADME and drug-likeness properties of the newly synthesised compounds were analysed to evaluate their pharmacokinetics and drug-likeness, providing a comparative assessment of imidazo[1,2-*a*]pyridine analogues against marketed anti-TB agents. The selected compounds are listed in Table 14, along with the complete dataset for all series of compounds included in the Appendix.

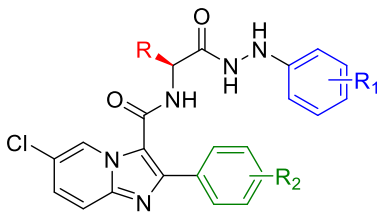

**44**

| Entry | R | $R_1$ | $R_2$ | Mwt | nRot | LogP | HBD | HBA | nLV | TPSA | LogS | HIA (%) | BBB |
|---|---|---|---|---|---|---|---|---|---|---|---|---|---|
| **INH** | - | - | - | 137.0 | 2 | -0.6 | 3 | 4 | 0 | 68.0 | -0.02 | High | no |
| **BDQ** | - | - | - | 554.1 | 8 | 7.5 | 1 | 4 | 2 | 45.5 | -5.1 | High | yes |
| **Q203** | - | - | - | 556.1 | 9 | 7.6 | 1 | 6 | 2 | 58.8 | -6.9 | High | yes |
| **First-series of compounds** | | | | | | | | | | | | | |
| **44Aa** | Gly | H | 3-Cl | 453.0 | 8 | 3.34 | 3 | 7 | 0 | 87.5 | -4.7 | High | yes |
| **44Ab** | | H | 4-Cl | 453.0 | 8 | 3.34 | 3 | 7 | 0 | 87.5 | -4.7 | High | yes |
| **44Ac** | | H | 3-CF3 | 487.1 | 9 | 3.70 | 3 | 7 | 0 | 87.5 | -4.8 | High | yes |
| **44Ad** | | H | 4-CF3 | 487.1 | 9 | 3.70 | 3 | 7 | 0 | 87.5 | -4.8 | High | yes |
| **44Ae** | | H | 3-$OCH_3$ | 449.1 | 9 | 2.65 | 3 | 8 | 0 | 96.7 | -4.7 | High | no |
| **44Af** | | H | 4-$OCH_3$ | 449.1 | 9 | 2.65 | 3 | 8 | 0 | 96.7 | -4.7 | High | no |
| **44Ag** | Ala | H | 3-Cl | 467.0 | 8 | 3.83 | 3 | 7 | 0 | 87.5 | -4.6 | High | yes |
| **44Ah** | | H | 4-Cl | 467.0 | 8 | 3.83 | 3 | 7 | 0 | 87.5 | -4.6 | High | yes |
| **44Ai** | | H | 3-$CF_3$ | 501.1 | 9 | 4.19 | 3 | 7 | 0 | 87.5 | -5.1 | High | yes |
| **44Aj** | | H | 4-$CF_3$ | 501.1 | 9 | 4.19 | 3 | 7 | 0 | 87.5 | -5.1 | High | yes |
| **44Ak** | | H | 3-$OCH_3$ | 463.1 | 9 | 3.15 | 3 | 8 | 0 | 96.7 | -4.8 | High | no |

| | | | | | | | | | | | | | |
|---|---|---|---|---|---|---|---|---|---|---|---|---|---|
| **44Al** | | H | 4-$OCH_3$ | 463.1 | 9 | 3.15 | 3 | 8 | 0 | 96.7 | -4.8 | High | no |
| **Second-series of compounds** | | | | | | | | | | | | | |
| **44Be** | Gly | H | H | 419.1 | 8 | 2.78 | 3 | 7 | 0 | 87.5 | -4.0 | High | yes |
| **44Bf** | | 3-Cl | H | 453.0 | 8 | 3.34 | 3 | 7 | 0 | 87.5 | -4.6 | High | yes |
| **44Bg** | | 4-Cl | H | 453.0 | 8 | 3.34 | 3 | 7 | 0 | 87.5 | -4.6 | High | yes |
| **44Bh** | | 3-Br | H | 497.0 | 8 | 3.61 | 3 | 7 | 0 | 87.5 | -4.7 | High | yes |
| **44Bi** | | 4-Br | H | 497.0 | 8 | 3.61 | 3 | 7 | 0 | 87.5 | -4.7 | High | yes |
| **44Bj** | | 3-$CF_3$ | H | 487.1 | 9 | 3.70 | 3 | 7 | 0 | 87.5 | -4.8 | High | yes |
| **44Bk** | | 4-$CF_3$ | H | 487.1 | 9 | 3.70 | 3 | 7 | 0 | 87.5 | -4.8 | High | yes |
| **44Bl** | | 3-$OCF_3$ | H | 503.1 | 10 | 4.31 | 3 | 8 | 0 | 96.7 | -5.2 | High | no |
| **44Bm** | | 4-$OCF_3$ | H | 503.1 | 10 | 4.31 | 3 | 8 | 0 | 96.7 | -5.2 | High | no |
| **44Bn** | Ala | H | H | 433.1 | 8 | 3.27 | 3 | 7 | 0 | 87.5 | -4.1 | High | yes |
| **44Bo** | | 3-Cl | H | 467.0 | 8 | 3.83 | 3 | 7 | 0 | 87.5 | -4.5 | High | yes |
| **44Bp** | | 4-Cl | H | 467.0 | 8 | 3.83 | 3 | 7 | 0 | 87.5 | -4.5 | High | yes |
| **44Bq** | | 3-Br | H | 511.0 | 8 | 4.10 | 3 | 7 | 1 | 87.5 | -4.6 | High | yes |
| **44Br** | | 4-Br | H | 511.0 | 8 | 4.10 | 3 | 7 | 1 | 87.5 | -4.6 | High | yes |
| **44Bs** | | 3-$CF_3$ | H | 501.1 | 9 | 4.19 | 3 | 7 | 0 | 87.5 | -4.9 | High | yes |
| **44Bt** | | 4-$CF_3$ | H | 501.1 | 9 | 4.19 | 3 | 7 | 0 | 87.5 | -4.9 | High | yes |
| **44Bu** | | 3-$OCF_3$ | H | 517.1 | 10 | 4.80 | 3 | 8 | 1 | 96.7 | -5.3 | High | no |
| **44Bv** | | 4-$OCF_3$ | H | 517.1 | 10 | 4.80 | 3 | 8 | 1 | 96.7 | -5.3 | High | no |
| **44Co** | Phe | H | H | 509.1 | 10 | 4.95 | 3 | 7 | 0 | 87.5 | -4.3 | High | no |
| **44Cp** | | 3-Cl | H | 543.1 | 10 | 5.50 | 3 | 7 | 2 | 87.5 | -5.1 | High | no |
| **44Cq** | | 4-Cl | H | 543.1 | 10 | 5.50 | 3 | 7 | 2 | 87.5 | -5.1 | High | no |
| **44Cr** | | 3-Br | H | 587.0 | 10 | 5.78 | 3 | 7 | 2 | 87.5 | -5.2 | High | no |
| **44Cs** | | 4-Br | H | 587.0 | 10 | 5.78 | 3 | 7 | 2 | 87.5 | -5.2 | High | no |
| **44Ct** | | 3-$CF_3$ | H | 577.1 | 11 | 5.87 | 3 | 7 | 2 | 87.5 | -5.6 | High | no |
| **44Cu** | | 4-$CF_3$ | H | 577.1 | 11 | 5.87 | 3 | 7 | 2 | 87.5 | -5.6 | High | no |
| **44Cv** | | 3-$OCF_3$ | H | 593.1 | 12 | 6.47 | 3 | 8 | 2 | 96.7 | -5.9 | High | no |
| **44Cw** | | 4-$OCF_3$ | H | 593.1 | 12 | 6.47 | 3 | 8 | 2 | 96.7 | -5.9 | High | no |
| **Third-series of compounds** | | | | | | | | | | | | | |
| **44Df** | | H | 3-Cl | 557.1 | 11 | 5.50 | 3 | 7 | 2 | 87.5 | -5.4 | High | no |
| **44Dg** | | 3-Cl | | 591.1 | 11 | 6.06 | 3 | 7 | 2 | 87.5 | -5.7 | High | no |
| **44Dh** | | 3-Br | | 635.0 | 11 | 6.33 | 3 | 7 | 2 | 87.5 | -5.8 | High | no |
| **44Di** | | 3-$CF_3$ | | 625.1 | 12 | 6.43 | 3 | 7 | 2 | 87.5 | -6.2 | High | no |
| **44Dj** | | 3-$OCF_3$ | | 641.1 | 13 | 7.03 | 3 | 8 | 2 | 96.7 | -6.5 | High | no |
| **44Dk** | | H | 4-Cl | 557.1 | 11 | 5.50 | 3 | 7 | 2 | 87.5 | -5.4 | High | no |
| **44Dl** | | 3-Cl | | 591.1 | 11 | 6.06 | 3 | 7 | 2 | 87.5 | -5.7 | High | no |
| **44Dm** | | 3-Br | | 635.0 | 11 | 6.33 | 3 | 7 | 2 | 87.5 | -5.8 | High | no |

| | | | | | | | | | | | | | |
|---|---|---|---|---|---|---|---|---|---|---|---|---|---|
| **44Df** | Phe | 3-$CF_3$ | 3-$OCH_3$ | 625.1 | 12 | 6.43 | 3 | 7 | 2 | 87.5 | -6.2 | High | no |
| **44Dg** | | 3-$OCF_3$ | | 641.1 | 13 | 7.03 | 3 | 8 | 2 | 96.7 | -6.5 | High | no |
| **44Dv** | | H | | 539.1 | 11 | 4.82 | 3 | 8 | 1 | 96.7 | -5.0 | High | no |
| **44Dw** | | 3-Cl | | 573.1 | 11 | 5.38 | 3 | 8 | 2 | 96.7 | -5.4 | High | no |
| **44Dx** | | 3-Br | | 617.0 | 11 | 5.65 | 3 | 8 | 2 | 96.7 | -5.5 | High | no |
| **44Dy** | | 3-$CF_3$ | | 607.1 | 12 | 5.74 | 3 | 8 | 2 | 96.7 | -5.6 | High | no |
| **44Dz** | | 3-$OCF_3$ | | 623.1 | 13 | 6.35 | 3 | 9 | 2 | 105.9 | -6.0 | High | no |
| **44Ea** | | H | 4-$OCH_3$ | 539.1 | 11 | 4.82 | 3 | 8 | 1 | 96.7 | -5.0 | High | no |
| **44Eb** | | 3-Cl | | 573.1 | 11 | 5.38 | 3 | 8 | 2 | 96.7 | -5.4 | High | no |
| **44Ec** | | 3-Br | | 617.0 | 11 | 5.65 | 3 | 8 | 2 | 96.7 | -5.5 | High | no |
| **44Dv** | | 3-$CF_3$ | | 607.1 | 12 | 5.74 | 3 | 8 | 2 | 96.7 | -5.6 | High | no |
| **44Dw** | | 3-$OCF_3$ | | 623.1 | 13 | 6.35 | 3 | 9 | 2 | 105.9 | -6.0 | High | no |

Table 14. ADME and physiochemical parameters of selected imidazo[1,2-*a*]pyridine analogues. *Mwt* molecular weight, *nRot* number of rotatable bond, *HBD* hydrogen bond donors, *HBA* hydrogen bond acceptors, *nLV* number of Lipiniski violation, *TPSA* Topological Polar Surface Area, *LogS* aqueous solubility, *HIA%* human intestinal absorption, *BBB* blood-brain barrier.

For a compound to be considered a promising drug candidate, it prefers to exhibit specific physicochemical parameters that determine its interactions within biological systems. Lipinski's Rule of Five (RO5) is a widely established guideline, associated with around 90% of orally administered medications that have progressed to Phase II clinical trials.[176] This rule is characterised by four essential physicochemical properties: molecular weight (≤ 500 Da), partition coefficient (log P ≤ 5), hydrogen bond donors (≤ 5) and hydrogen bond acceptors (≤ 10). The generated data demonstrates that most of the imidazo[1,2-*a*]pyridine analogues comply with Lipinski's RO5, suggesting their potential for oral medication development (Table 14). Nonetheless, multiple Phe analogues such as **44Cp – 44Cw** exceed the molecular weight and logP thresholds of 500 Da and 5. Despite these deviations, their physicochemical properties remain within an acceptable range comparable to current oral anti-TB medications. Moreover, alongside Lipinski's RO5, details different key physicochemical parameters were evaluated, such as Topological Polar Surface Area (TPSA), aqueous solubility (LogS), human intestinal absorption (HIA%) and blood-brain barrier (BBB) permeability.

Generally, TPSA affects membrane permeability and oral absorption, with values below 140 Å² associated with better absorption. All synthesised compounds fall within this range, suggesting they are likely to be absorbed efficiently. LogS is another important factor influencing drug absorption, as low solubility can restrict bioavailability. The predicted LogS values for the synthesised compounds range from (-0.40 to -0.65),

indicating moderate solubility. HIA% provides an estimate of how much of the drug is absorbed through the gastrointestinal tract. Compounds with HIA values above 30% are considered to have high absorption. The newly synthesised compounds show HIA values more than 30%, suggesting good absorption. BBB permeability is important in anti-TB drug discovery, especially for targeting CNS infections. Certain compounds are predicted to cross the BBB, while this could be advantageous for CNS-TB, it also increases the potential for CNS-related adverse effects, which would require further investigation.

Following the ADME evaluation of all compounds, the physicochemical characteristics of the most active analogue, compound **44Cp** (MIC = 3 μM), was further analysed utilising a radar chart (Figure 98). This visualization compares the compound's characteristics (yellow line) with defined lower (green region) and upper (blue region) thresholds. This visualization underscores the compound's alignment with essential drug-likeness parameters. However, minor deviations are noted, with logP and logD showing marginally elevated values, while logS is slightly below than the optimal range.

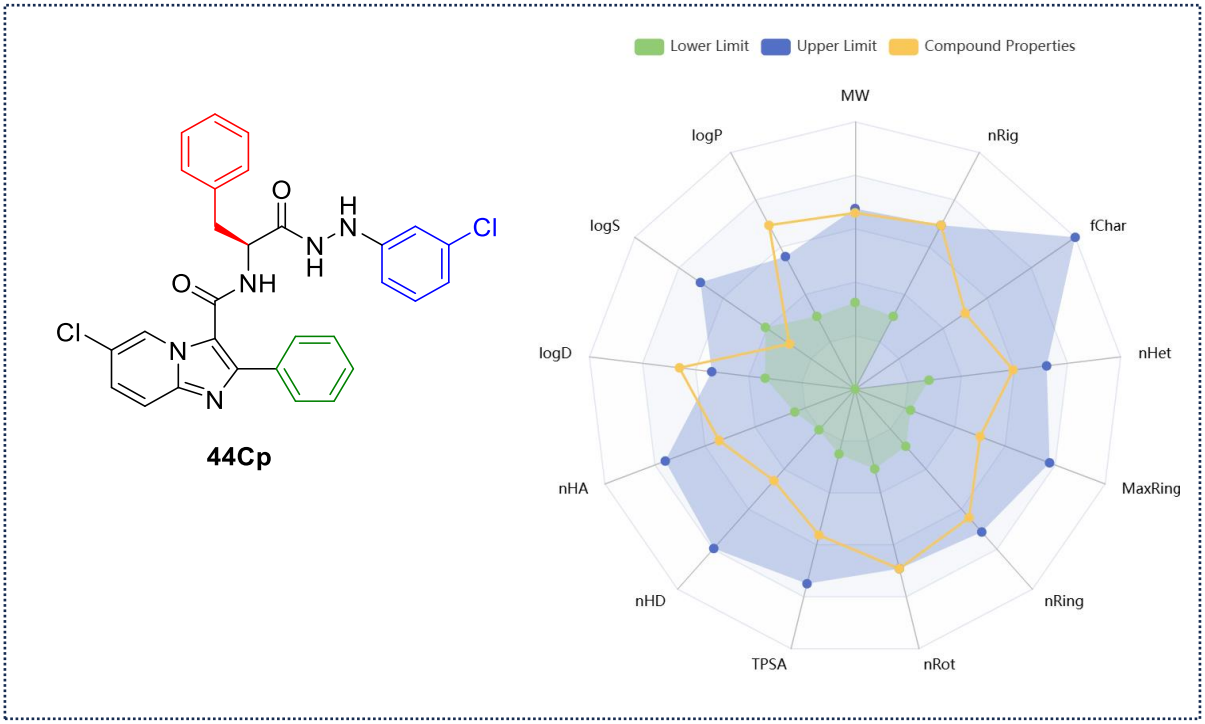


Figure 98. The radar chart demonstrates that Compound **44Cp** aligns well with the acceptable chemical space, with most of its physicochemical properties falling within the predefined limits. (*logD* Distribution Coefficient, *nRing* Number of Rings, MaxRing Ring Size, *nHet* Number of Heteroatoms, *fChar* Formal Charge, *nRig* Number of Rigid Bonds).

Collectively, the newly synthesised analogues fall within the established range of orally marketed anti-TB drugs, supporting their potential as drug-like candidates for further development.

In summary, we investigated the structure–activity relationship of imidazo[1,2-*a*]pyridine analogues, by modification of three distinct structural components, resulting in a diverse library of compounds. *in silico* molecular docking elucidated the binding interactions of the most active derivatives with the potential target pafA, indicating their ability to interact with key residues within the ATP-binding site. At the end of this chapter, *in silico* ADME analysis was discussed, demonstrating that these analogues possess favourable physicochemical properties, suggesting they are drug-like molecules within the acceptable range for oral anti-TB drugs.

To further optimize this scaffold, the subsequent chapter will investigate the strategic replacement of the arylhydrazine moiety with heterocyclic alternatives. This approach aims to optimise target interactions and improve pharmacokinetic properties, enabling a deeper understanding of the structure–activity relationship and the potential for improved anti-TB efficacy.

# 4. Synthesis and SAR studies of heterocyclic analogues of imidazo[1,2-*a*]pyridine

## 4.1 Introduction:

The imidazo[1,2-*a*]pyridine scaffold has drawn significant interest in drug development due to its versatility in medicinal chemistry, especially in the discovery of antimicrobial and anti-tubercular agents.[142,177] In the previous chapter, 108 analogues of this core structure were investigated, altering three key components: the amino acid (R), arylhydrazine substitution ($R_1$), and phenyl ring attached to the scaffold ($R_2$). These modifications offered significant insights into the impact of electronic and steric factors on antimycobacterial activity, contributing to a broader understanding of how structural variations influence biological function. Among the structural variations explored in the preceding chapter, phenylalanine emerged as the most active amino acid substitution, while compounds bearing an unsubstituted phenyl ring at the $R_2$ position demonstrated the highest activity. Based on these findings, the next stage of this study focuses on retaining the phenylalanine moiety and the unsubstituted phenyl ring at $R_2$, while replacing the arylhydrazine group with heterocyclic alternatives, which represent one of the most popular bioisosteric strategies in medicinal chemistry (Figure 99).[178]

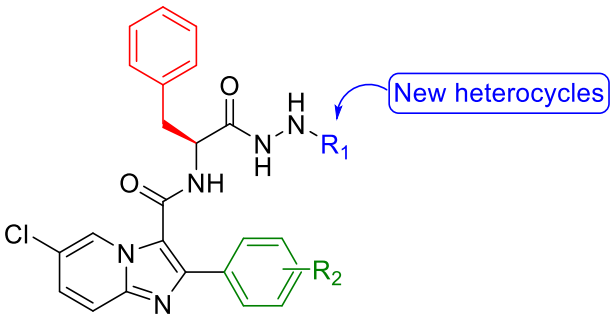


**44**

Figure 99. A structural representation of the final compound **44** featuring an imidazo[1,2-*a*]pyridine scaffold, where the arylhydrazine moiety is replaced with different heterocycles ($R_1$), while the ($R_2$) position remains as a proton.

Heterocycles provide many benefits compared to simple aromatic systems, functioning as a useful tool for modulating pharmacological activity and key physicochemical properties such as solubility, lipophilicity, polarity, and hydrogen bonding capacity.[179] Statistical analyses reveals that more than 85% of biologically active compounds include a heterocyclic core, highlighting their significance in drug design and

development.[178] Among these, nitrogen-containing heterocycles are particularly prevalent, comprising 59% of all U.S. FDA-approved small-molecule medications, hence establishing their role as one of the most extensively utilised scaffolds in pharmaceutical research. Furthermore, heterocyclic compounds are recognised for their significance in antimicrobial therapy, particularly as antitubercular agents, and their incorporation is expected to enhance the structure–activity relationship.[180] Building on these findings and aligning with our ongoing efforts to develop novel and potent antitubercular agents, this chapter presents the synthesis and biological evaluation of imidazo[1,2-*a*]pyridine analogues featuring various *N*-heterocyclic substitutions.

## 4.2 Synthesis of imidazo[1,2-*a*]pyridine amino acid hydrazides featuring *N*-heterocyclic substitutions

To explore the impact of heterocyclic bioisosteres on the antimycobacterial activity of imidazo[1,2-*a*]pyridine analogues, a series of compounds were designed by replacing the arylhydrazine component with various *N*-heterocyclic groups. Consequently, different commercially available *N*-heterocyclic hydrazines were utilised and coupled with *N*-Boc-phenylalanine, leading to the formation of an *N*-heterocyclic phenylalanine hydrazide framework. This was subsequently coupled with the imidazo[1,2-*a*]pyridine scaffold to yield a new series of imidazo[1,2-*a*]pyridine amino acid hydrazide analogues. These compounds were then tested against different strains of *Mtb*, including both drug-susceptible and drug-resistant strains, enabling a structure-activity relationship analysis to determine their antimycobacterial potential.

Initially, a retrosynthetic analysis of molecule **44** was conducted, with the initial disconnection targeting the amide bond in compound **44**, resulting in the formation of carboxylic acid **50** and phenylalanine hydrazide **51**. Moreover, the breaking of the hydrazide bond in phenylalanine hydrazide **51** produced *N*-protected amino acid **52** and heterocyclic hydrazine **53** (Figure 100).

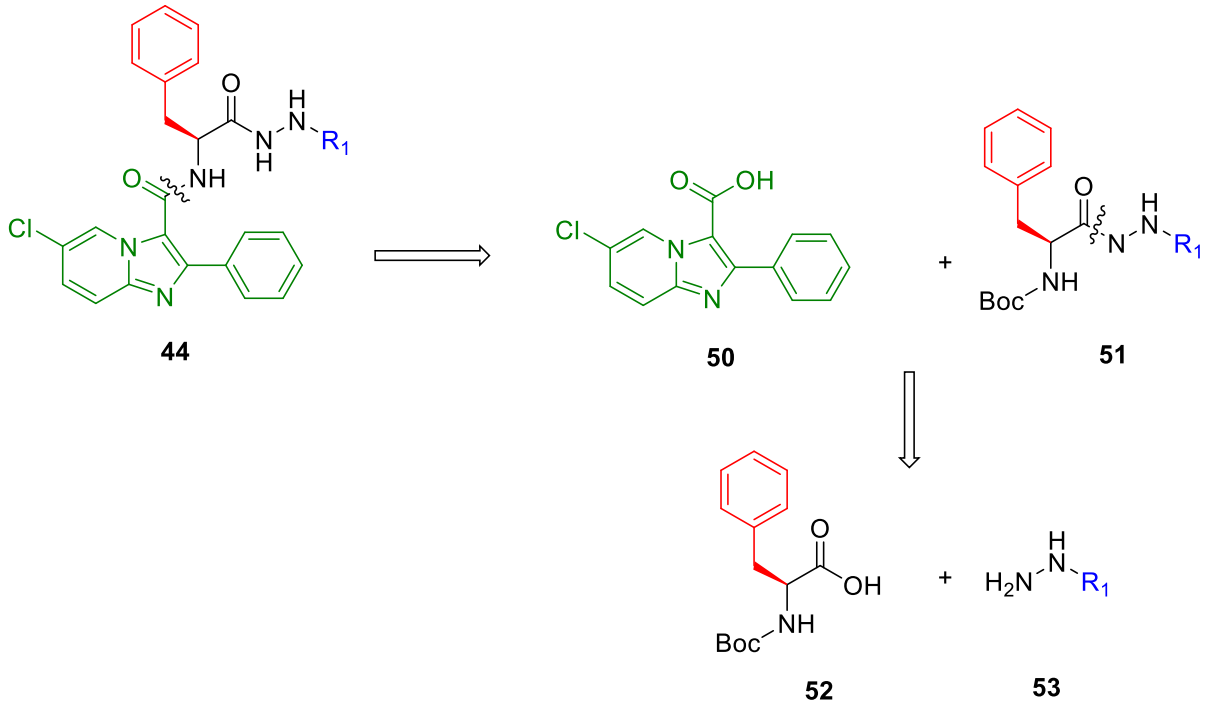


Figure 100. The target compound **44** was analysed through retrosynthetic deconstruction into its precursor components.

The synthesis of the target compounds begins with a peptide coupling reaction between *N*-protected phenylalanine **52** and a diverse heterocyclic hydrazines **53**, resulting in the formation of hydrazide intermediates **51** which after successful coupling undergo Boc deprotection to produce the free amine, enabling for subsequent condensation with carboxylic acid **50** which finally yields the target compound **44**. As the synthetic route for carboxylic acid **50** has been previously outlined (*cf.* section 2.2.1), the subsequent section will focus on the synthesis of the *N*-heterocyclic phenylalanine hydrazide framework.

### 4.2.1 Synthesis of *N*-heterocyclic phenylalanine hydrazide intermediates.

As outlined in chapter 2 (*cf.* section 2.2.2), the synthesis of the *N*-amino acid hydrazide backbone was carried out using a standard peptide coupling protocol previously established within the group.[137] This reaction employed conventional peptide coupling reagents, facilitating the conjugation of *N*-Boc-phenylalanine **52** with various heterocyclic hydrazines **53** to yield the protected amino acid hydrazide intermediate **51** (Scheme 5).

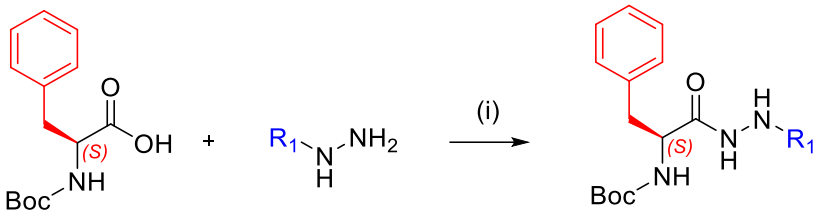


**52** **53** **51**

Scheme 5. Reagents and conditions: i) DIPEA, HBTU, acetonitrile, 6 h, rt.

The peptide coupling reaction successfully produced a series of amino acid hydrazides **51** featuring various *N*-heterocycles, including pyridine, pyrazine and pyrimidine. To further explore the influence of nitrogen positioning within these heterocyclic frameworks, several pyridine and pyrimidine analogues with various nitrogen placements were successfully synthesised. This variation enables evaluation of how nitrogen positioning within the heterocyclic ring affects the antimicrobial activity. Furthermore, two thiazole-based analogues were synthesised as five-membered heterocyclic derivatives to further expand the structure–activity relationship investigation (Table 15).

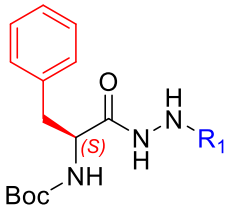


**51**

| Entry | $R_1$ | Yield (%) | Entry | $R_1$ | Yield (%) |
|---|---|---|---|---|---|
| **51Cd** | 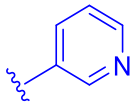 | 30 | **51Cj** | 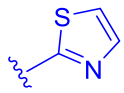 | 71 |
| **51Ce** | 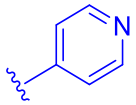 | 30 | **51Ck** | 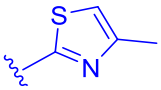 | 37 |
| **51Cf** | 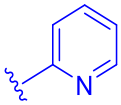 | 78 | **51Cl** | 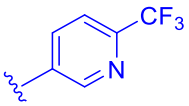 | 86 |
| **51Cg** | 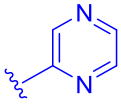 | 60 | **51Cm** | 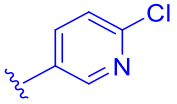 | 85 |
| **51Ch** | 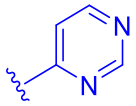 | 80 | **51Cn** | 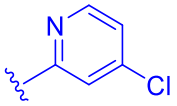 | 78 |

| | | | | | |
|---|---|---|---|---|---|
| **51Ci** | 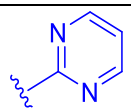 | 48 | **51Co** | 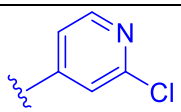 | 78 |

Table 15. *N*-Boc-protected hydrazide intermediates featuring heterocycles at the ($R_1$) position with their yield percentage.

The synthesis of novel heterocyclic hydrazide intermediates was confirmed via spectroscopic analysis, including 2D NMR, IR and HR-MS. For example, the $^1$H NMR spectrum of pyridine-hydrazide intermediate **51Cf** displayed characteristic signals corresponding to the aromatic protons of the phenylalanine moiety, alongside distinct signals from the pyridine ring, which appeared as four separate proton resonances: two doublets and two triplets. Additionally, the chiral proton was observed at 4.2 ppm, while the Boc protecting group appeared as a singlet at 1.3 ppm, further confirming the structural integrity of the synthesised intermediates (Figure 101).

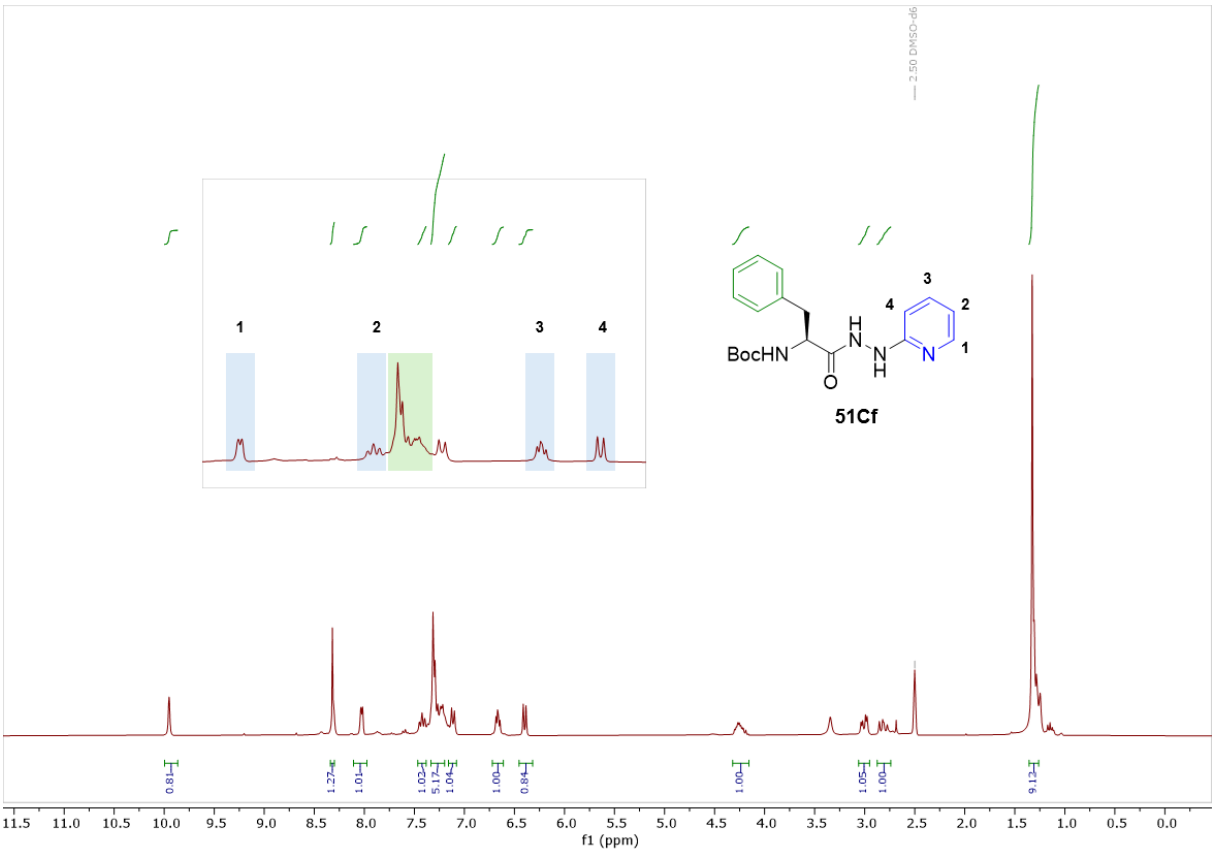


Figure 101. $^{1}$H NMR exhibits the characteristic signals of the pyridine hydrazide intermediate. The blue-highlighted signals indicate the pyridine peaks, while the green-highlighted region corresponds to the aromatic ring of phenylalanine.

Furthermore, the crystal structure of **51Cf** was elucidated through single-crystal X-ray diffraction following slow evaporation of a DCM solution, providing further confirmation of its molecular structure (Figure 102).

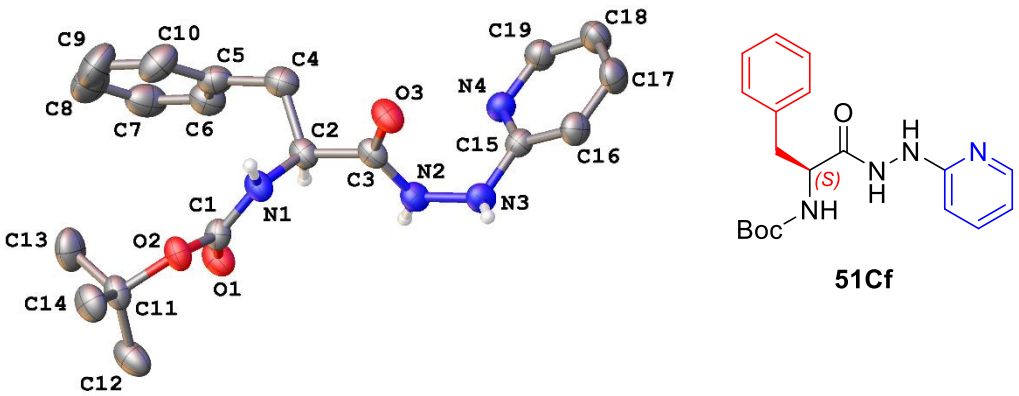


Figure 102. Single crystal X-ray structure of *N*- Boc phenylalanine pyridine intermediate.

Meanwhile, the $^{1}$H NMR spectrum of phenylalanine pyrimidine-hydrazide **51Ci** exhibited signals for the pyrimidine ring protons as two distinct peaks, with one triplet at 6.7 ppm and one doublet at 8.3 ppm. The aromatic protons of the phenylalanine

moiety appeared in the deshielded region, while the chiral proton was observed at 4.2 ppm (Figure 103).

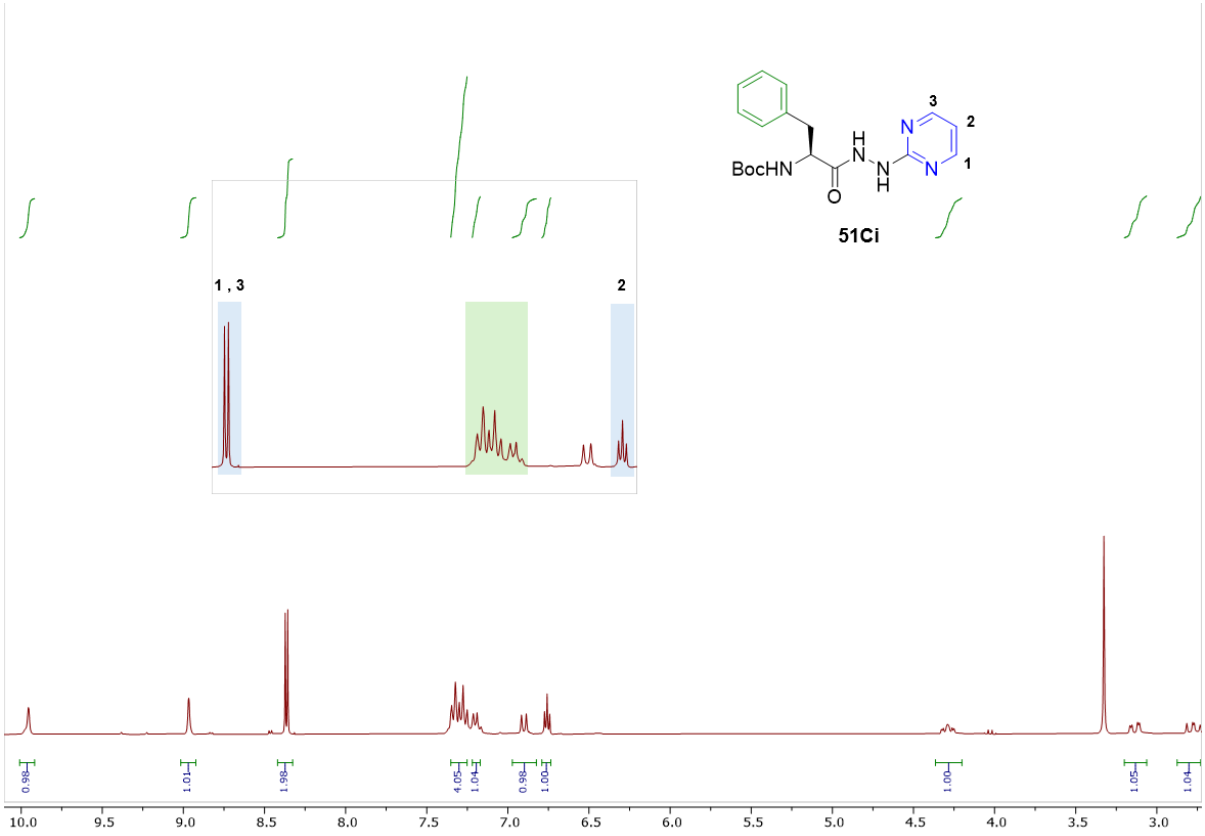


Figure 103. $^{1}$H NMR displays the characteristic signals of the pyrimidine hydrazide intermediate. The blue-highlighted signals indicate the pyrimidine peaks, whereas the green-highlighted region corresponds to the aromatic ring of phenylalanine.

### 4.2.2 Conversion of intermediate hydrazides into final compounds

Following the successful coupling reaction of the Boc-protected phenylalanine with heterocyclic hydrazines, the subsequent step includes the deprotection of Boc-phenylalanine hydrazide intermediates utilising 4M HCl in dioxane. As previously mentioned, this procedure resulted in the effective production of the amine-HCl salt, obtaining high conversion yields through precipitation with a mixture of ethanol and diethyl ether as an antisolvent. After that, the imidazo[1,2-*a*]pyridine scaffold was introduced by a final peptide coupling reaction, yielding the heterocycle-substituted imidazo[1,2-*a*]pyridine analogues **44Ed – 44Eo** (Scheme 6)**.**

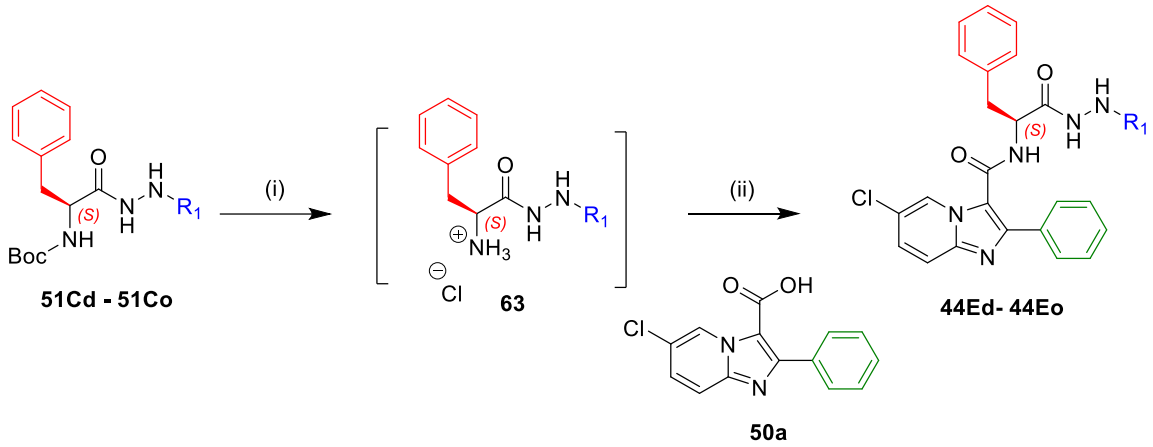


Scheme 6. Synthesis of final compounds **44** from *N*-Boc protected phenylalanine hydrazides **51**; Reagents and conditions: i) 4M HCl in dioxane, 90 min, r.t. (ii) **50a** , HBTU, DIPEA, acetonitrile, overnight, rt.

The reaction was stirred overnight, producing a crude product, which was subsequently purified using column chromatography, yielding the target compounds (Table 16).

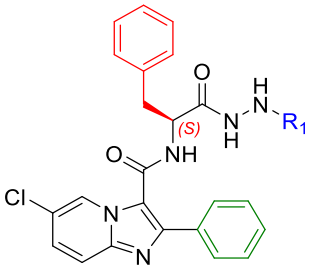

**44**

| Entry | $R_1$ | Yield (%) | Entry | $R_1$ | Yield (%) |
|---|---|---|---|---|---|
| **44Ed** | 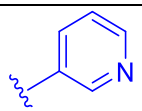 | 41 | **44Ej** | 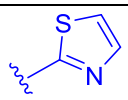 | 37 |
| **44Ee** | 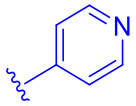 | 35 | **44Ek** | 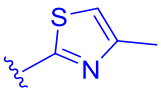 | 44 |
| **44Ef** | 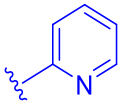 | 41 | **44El** | 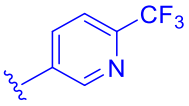 | 43 |
| **44Eg** | 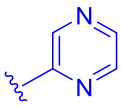 | 41 | **44Em** | 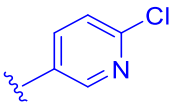 | 42 |
| **44Eh** | 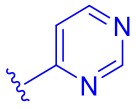 | 38 | **44En** | 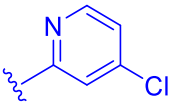 | 46 |

| | | | | | |
|---|---|---|---|---|---|
| **44Ei** | 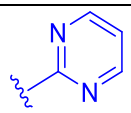 | 40 | **44Eo** | 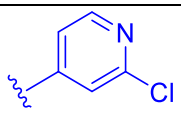 | 47 |

Table 16. Imidazo[1,2-*a*]pyridine analogues featuring heterocycles at the ($R_1$) position with their yield percentage.

The structures of the heterocycle-substituted phenylalanine hydrazide compounds **44Ed– 44Eo** were confirmed through $^{1}$H NMR, $^{13}$C NMR, 2D NMR, IR, and high-resolution mass spectrometry. An example of the $^{1}$H NMR spectrum of the pyridine analogue **44Ef** is illustrated in Figure 104.

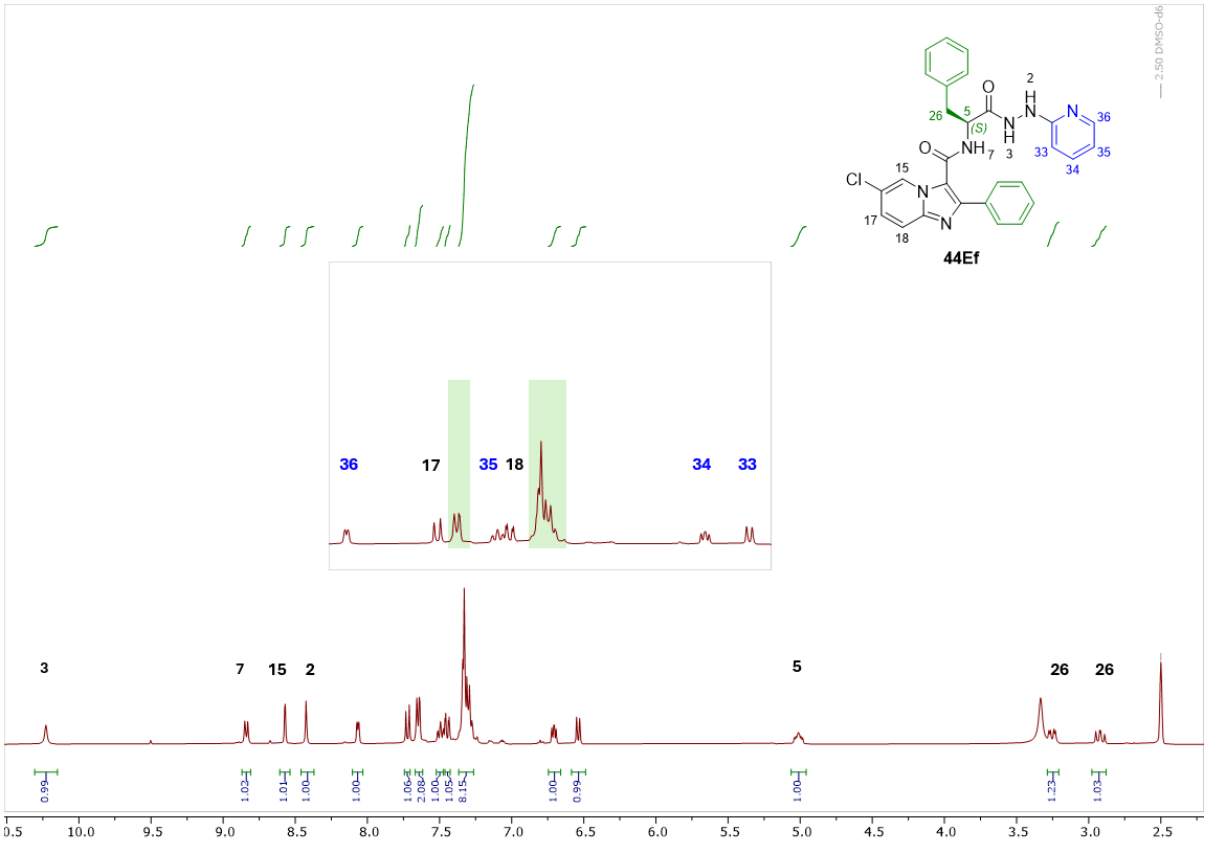


Figure 104. $^{1}$H NMR displays the characteristic signals of the imidazo[1,2-*a*]pyridine analogue featuring pyridine **44Ef**. The green-highlighted region corresponds to both the aromatic ring of phenylalanine and the aromatic ring attached to the scaffold.

The structural identification of compound **44Ef** was further confirmed by single-crystal X-ray diffraction obtained from crystals grown via slow evaporation of a concentrated DMSO solution over an extended period, therefore validating its molecular structure and stereochemistry (Figure 105).

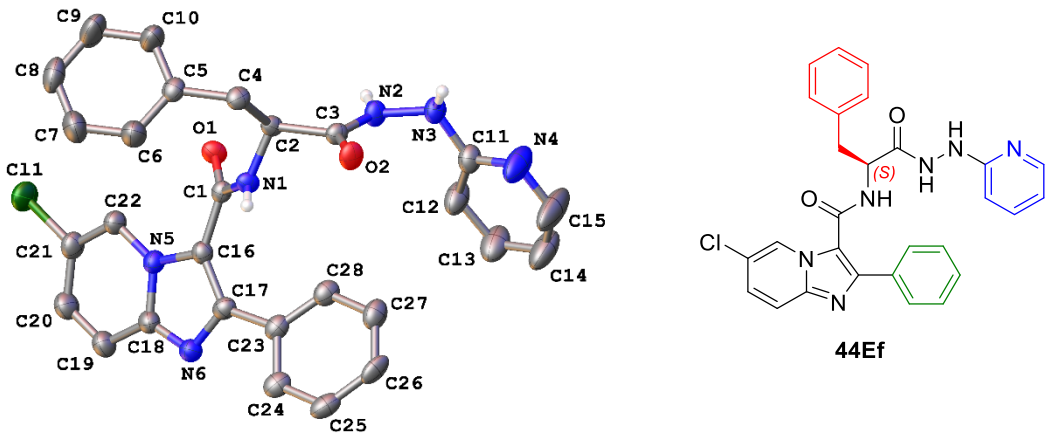


Figure 105. Single crystal X-ray structure of pyridine analogue of imidazo[1,2-*a*]pyridine **44Ef**.

The successful synthesis of heterocycle-substituted imidazo[1,2-*a*]pyridine analogues affords a further set of compounds for biological evaluation. With these analogues in hand, the subsequent section explores their structure–activity relationship study, evaluating their potential as anti-tubercular agents.

### 4.3 The SAR study of imidazo[1,2-*a*]pyridine substituted heterocyclic hydrazides

In the previous chapter, a comprehensive SAR study of imidazo[1,2-*a*]pyridine analogues explored the role of three key components: an amino acid (R), an arylhydrazine ($R_1$), and a phenyl ring ($R_2$), yielding promising anti-tubercular activity against *Mtb*. This chapter, however, explores the replacement of the arylhydrazine moiety with heterocyclic bioisosteres, aiming to enhance biological activity and refine pharmacokinetic properties (Figure 106).

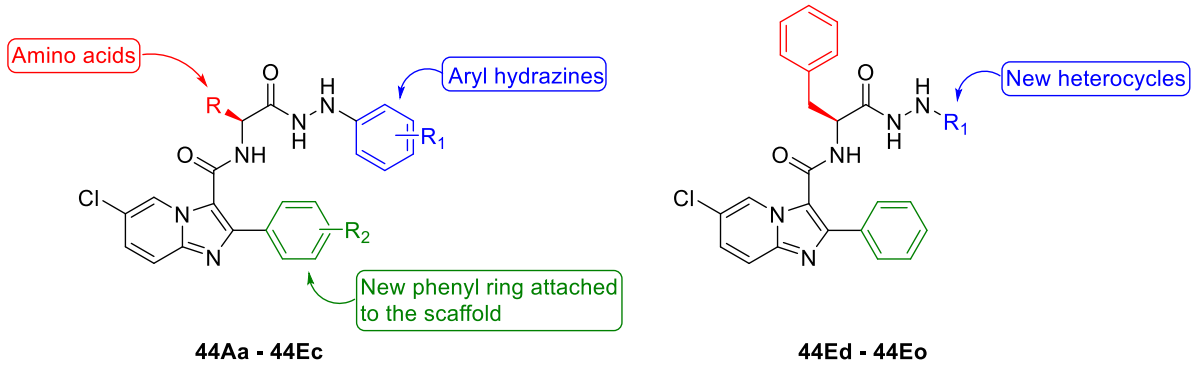


Figure 106. Antitubercular based on imidazo[1,2-*a*]pyridine scaffold. Compounds **44Aa – 44Ec** were designed through three structural modifications, while **44Ed – 44Eo** analogues resulted from substituting arylhydrazine with various *N*-heterocycles.

Building upon the successful synthesis of imidazo[1,2-*a*]pyridine-substituted heterocyclic hydrazides, attention turned to their SAR evaluation as anti-tubercular agents. The antimycobacterial assessment of these novel compounds was conducted utilising the REMA assay (*cf.* section 3.1) to determine their MICs against *Mtb*, including the wild-type strain and both mono- and multidrug-resistant strains (Table 17).

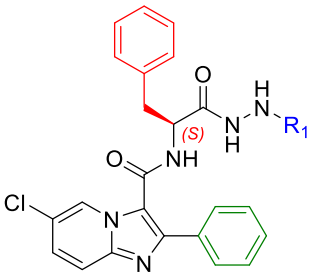

**44**

| Entry | $R_1$ | clogP | WT (μM) | $INH^R$ (μM) | $RIF^R$ (μM) | RIF/$INH^R$ (μM) 8250 | RIF/$INH^R$ (μM) 8256 |
|---|---|---|---|---|---|---|---|
| **44Ed** | 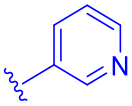 | 3.61 | - | - | - | - | - |
| **44Ee** | 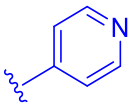 | 3.61 | - | - | - | - | - |
| **44Ef** | 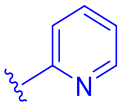 | 4.33 | - | - | - | - | - |
| **44Eg** | 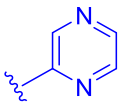 | 2.99 | - | - | - | - | - |
| **44Eh** | 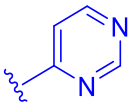 | 3.73 | - | - | - | - | - |
| **44Ei** | 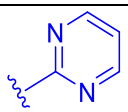 | 3.52 | - | - | - | - | - |
| **44Ej** | 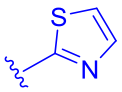 | 4.67 | - | - | - | - | - |
| **44Ek** | 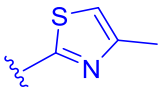 | 5.37 | - | - | - | - | - |
| **44El** | 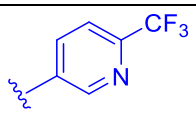 | 4.95 | - | - | - | - | - |
| **44Em** | 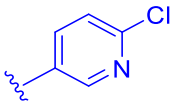 | 4.51 | - | - | - | - | - |
| **44En** | 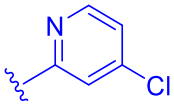 | 4.88 | 86.9 | 39.9 | 108 | 28.7 | 35.6 |
| **44Eo** | 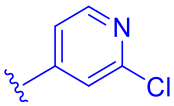 | 4.51 | 60.9 | 63.5 | 67.1 | 50.4 | 66.3 |
| **44Ep** | 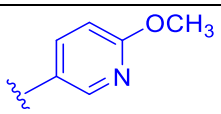 | 4.20 | - | - | - | - | - |

Table 17. The MIC results of the antimycobacterial susceptibility testing of the imidazo[1,2-*a*]pyridine **44Ed - 44Ep** against different *Mtb* strains; where a (-) indicates no activity at the assay maximum concentration of 64 μg/ml.

To start this study, pyridine was selected as a replacement for the arylhydrazine moiety, owing to its versatility as a privileged pharmacophore in drug discovery.[181] The distinctive structural and electronic properties of pyridine enhance its diverse biological activities, leading to its extensive application across different therapeutic areas such as antitubercular drugs (isoniazid **1**), antimalarials (enpiroline **66**), antiulcer therapy (omeprazole **67**), and neuroprotective medications (tacrine **68**) (Figure 107).[181]

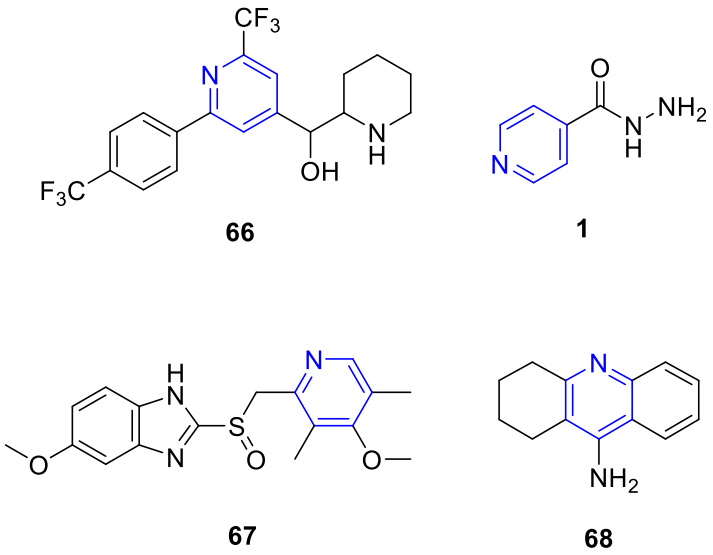


Figure 107. Examples of FDA-approved drugs featuring pyridine.

Beyond its extensive pharmacological applications, pyridine plays an important role in molecular recognition through engaging in various interactions with biological targets. Unlike benzene, which primarily participates in π–π stacking interactions, pyridine also contains a nitrogen atom that contributes to hydrogen bonding, hence improves the binding specificity and overall pharmacodynamic properties.[181] From a pharmacokinetic perspective, introduction of pyridine has demonstrated an improvement in solubility, metabolic stability, and drug-likeness, rendering it a favoured bioisosteric replacement for simple aromatic ring. Recognising the importance of pyridine in medicinal chemistry, a series of pyridine-substituted compounds was designed by substituting the arylhydrazine part in imidazo[1,2-*a*]pyridine derivatives **44Ed - 44Ef**. These analogues were subsequently synthesised and screened for their activity against different *Mtb* strains. However, substituting the phenyl ring with pyridine led to a loss of activity, regardless of the nitrogen positioning within the pyridine ring (Figure 108).

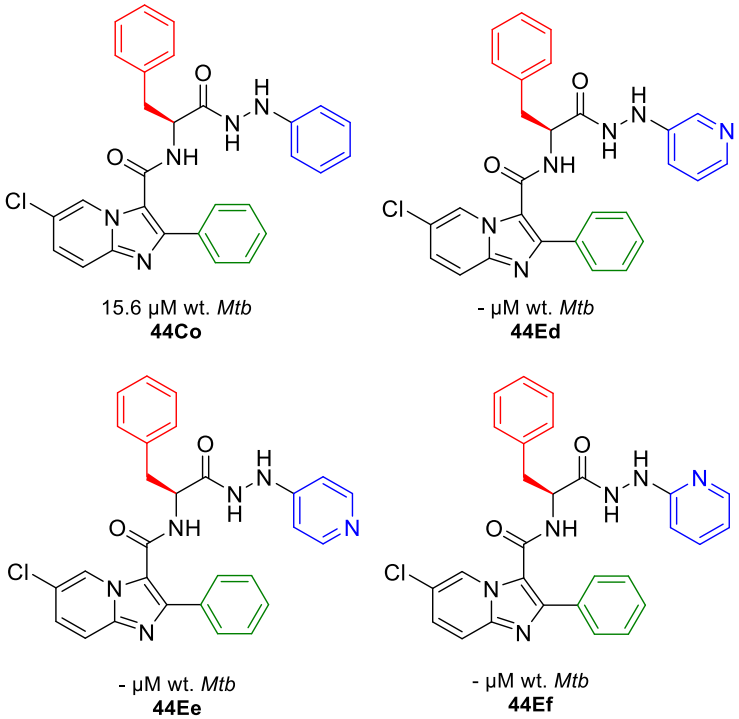


Figure 108. The negative impact of replacing arylhydrazine with different pyridine rings on antimicrobial activity.

To investigate whether electronic and steric modifications could restore activity, Cl, $CF_3$, and $OCH_3$ substituents were introduced at select positions within the pyridine ring, yielding compounds **44Em**, **44El**, and **44Ep**. However, these modifications did not lead to any improvement in potency.

To investigate the impact of substitution position on activity, additional chloro-substituted compounds were synthesised with diverse chlorine positions around the pyridine ring, with the only notable observation that compound **44En** exhibited moderate activity against the INH-resistant strain (Figure 109).

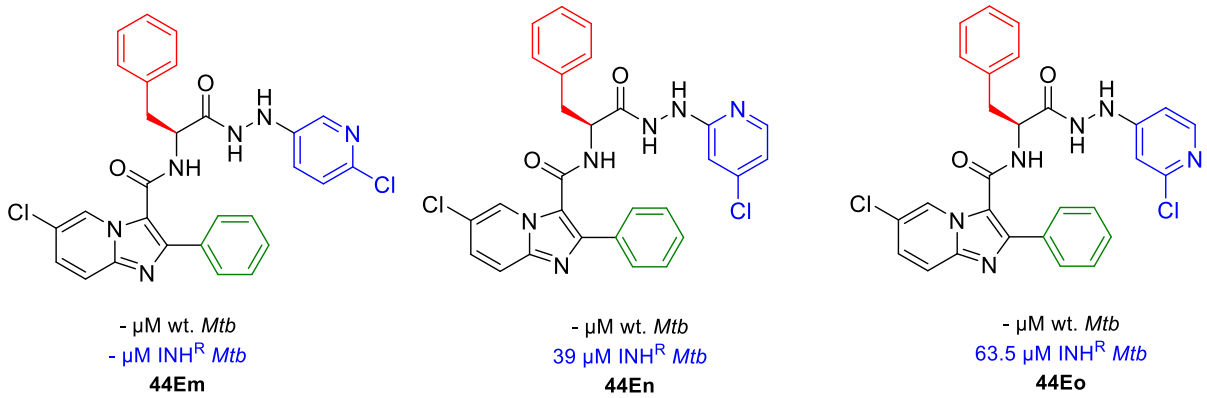


Figure 109. No antitubercular activity was observed upon incorporating chlorine at different positions around the pyridine ring.

Given the limited antimycobacterial activity observed with synthesised pyridine analogues, focus has shifted to another *N*-heterocycle, pyrimidine, as a potential

alternative. Due to its additional nitrogen atom, pyrimidine introduces improved hydrogen bonding and enhanced electronic properties, potentially resulting in better pharmacokinetic profiles, optimised drug-target interactions and enhanced therapeutic potential.[182] With its extensive application in medicinal chemistry, pyrimidine remains to play an important role in modern drug development (Figure 110).[182]

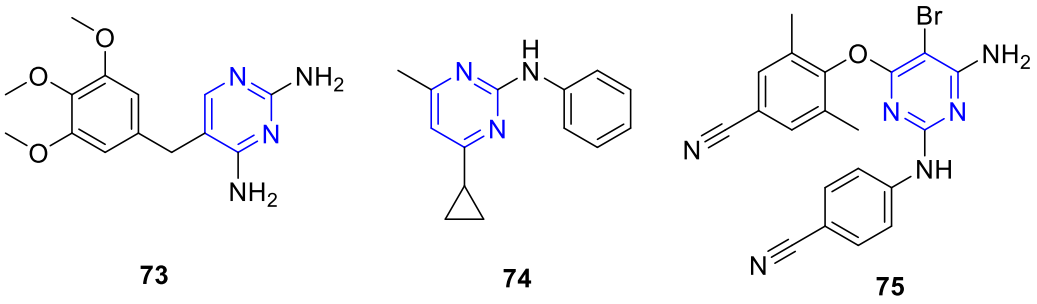


Figure 110. Examples of FDA-approved drugs featuring pyrimidine, trimethoprim (antibacterial) **73**, cyprodinil (antifungal) **74**, etravirine (antiviral) **75**.

Nonetheless, both pyrimidine analogues **44Eh** and **44Ei** failed to show any antimicrobial activity against *Mtb*. To improve bioactivity, a pyrazine analogue **44Eg** was subsequently synthesised, utilising the electronic effects and modified physicochemical properties conferred by the rearrangement of nitrogen atoms within the heterocyclic ring. Pyrazine-based scaffolds are of particular interest in anti-TB drug discovery, as seen with pyrazinamide, a first-line TB therapy. Regardless of this modification, the pyrazine analogue **44Eg** also failed to exhibit any notable antimycobacterial activity (Figure 111).

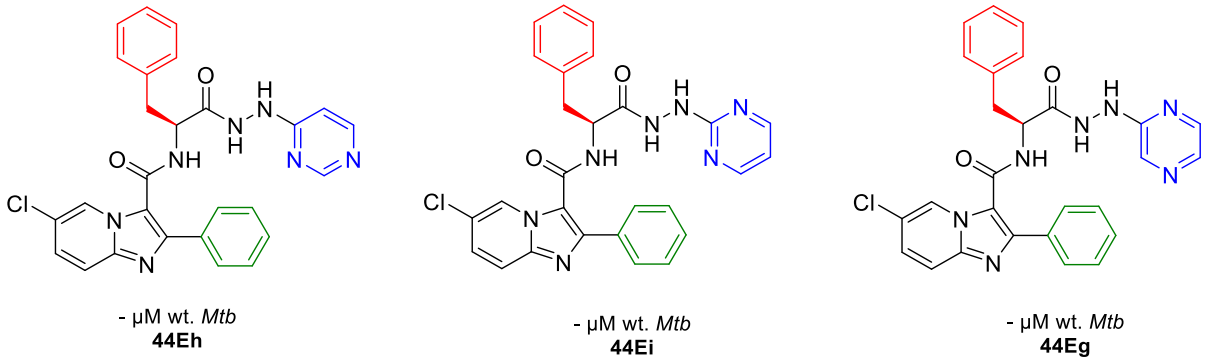


Figure 111. No *Mtb* inhibitory was observed in the pyrimidine analogues **44Em** and **44Ei** or the pyrazine analogue **44Eg**.

This indicates that simply altering the nitrogen positioning within the core scaffold does not sufficiently improve target engagement or biological activity. In light of these findings, a further avenue of investigation includes exploring five-membered heterocyclic rings. Thiazole, a privileged scaffold in drug discovery, is found in more than 18 FDA-approved drugs, underscoring its biological significance.[183] Notable

examples include cefiderocol **76**, the first FDA-approved siderophore antibiotic (2019), and alpelisib **77** approved in the same year for breast cancer therapy, while cobicistat **78** approved in 2018, prolongs the half-life of specific antiviral medications in HIV treatment (Figure 112). [183]

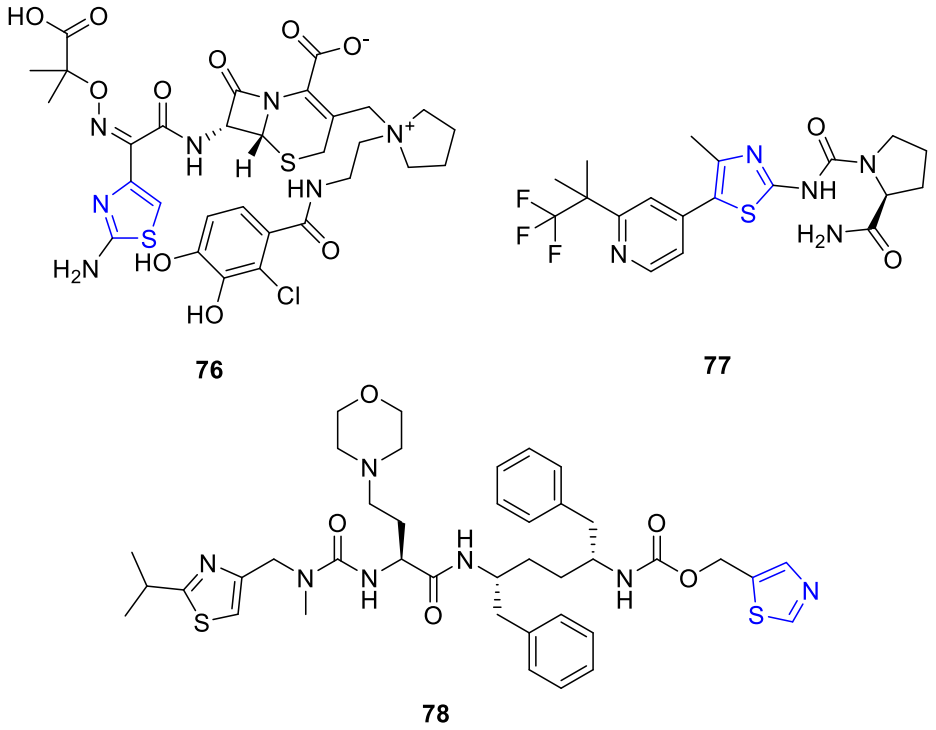


Figure 112. The FDA-approved drugs featuring thiazole.

Notably, the significance of thiazoles, particularly in antimicrobial agents, is evident in cephalosporins, where the introduction of a thiazole ring in the side chain of several of the cephalosporins improves their structure-activity relationship.[184] Moreover, the impact of thiazole extends beyond conventional antibacterial agents, as current research investigates its potential in antitubercular drug discovery.[183–185] However, the thiazole derivatives **44Ej** and **44Ek** synthesised in this research did not show any activity against all *Mtb* tested strains (Figure 113).

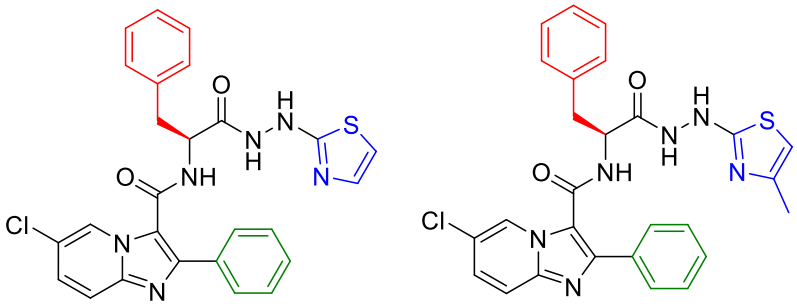


Figure 113. Lack of inhibitory activity in thiazole derivatives.

Overall, while the use of heterocycles in this SAR study failed to maintain efficacy, it remains well-established that heterocycles with their diverse structural frameworks, electronic properties, and improved physicochemical properties, provide a significant foundation for the optimization of drug candidates.[179] The subsequent section will investigate how replacing arylhydrazine with heterocyclic systems affects ADME characteristics and physicochemical properties, elucidating its wider impact on drug design.

### 4.4 *In silico* ADME and physiochemical properties:

Heterocycles work as important bioisosteres in drug design, not only enabling a strategic method to enhancing pharmacological activity but also significantly impacting physicochemical properties. Their incorporation enables the optimisation of potency, selectivity, and pharmacokinetic characteristics, while modifications in polarity, lipophilicity and solubility further optimise physicochemical properties.[178] Notably, their presence usually results in reduced clogP values compared to carbon analogues while also influencing molecular polarity, as indicated by parameters like Topological Polar Surface Area (TPSA).[179] Furthermore, their ability to participate in hydrogen bonding further improves aqueous solubility (LogS).[179] In this study, *in silico* ADME predictions were utilised via ADMETLab to evaluate the effect of aromatic ring bioisosteric replacement with different *N*-heterocycles on the physicochemical parameters of newly synthesised compounds. Comparing the heterocyclic compound data with currently marketed oral anti-TB medications including isoniazid, bedaquiline and Q203 facilitates the assessment whether this alteration led to drug-like molecules according to key ADME parameters (Table 18).

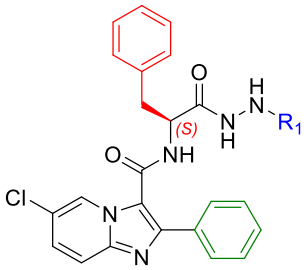

**44**

| Entry | $R_1$ | Mwt | nRot | logP | HBD | HBA | nLV | TPSA | LogS | HIA (%) | BBB |
|---|---|---|---|---|---|---|---|---|---|---|---|
| INH | - | 137.0 | 2 | -0.6 | 3 | 4 | 0 | 68.0 | -0.02 | High | no |
| BDQ | - | 554.1 | 8 | 7.5 | 1 | 4 | 2 | 45.5 | -5.1 | High | yes |
| Q203 | - | 556.1 | 9 | 7.6 | 1 | 6 | 2 | 58.8 | -6.9 | High | yes |
| Heterocyclic analogues | | | | | | | | | | | |
| 44Ed | 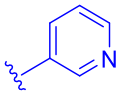 | 510.1 | 10 | 3.61 | 3 | 8 | 1 | 100.4 | -4.3 | High | No |
| 44Ee | 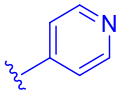 | 510.1 | 10 | 3.61 | 3 | 8 | 1 | 100.4 | -4.3 | High | No |
| 44Ef | 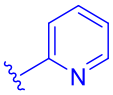 | 510.1 | 10 | 4.33 | 3 | 8 | 1 | 100.4 | -4.3 | High | No |
| 44Eg | 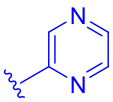 | 511.1 | 10 | 2.99 | 3 | 9 | 1 | 113.1 | -3.8 | High | No |
| 44Eh | 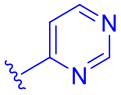 | 511.1 | 10 | 3.73 | 3 | 9 | 1 | 113.1 | -4.1 | High | No |
| 44Ei | 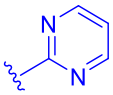 | 511.1 | 10 | 3.52 | 3 | 9 | 1 | 113.1 | -4.1 | High | No |
| 44Ej | 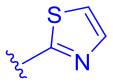 | 516.1 | 10 | 4.67 | 3 | 8 | 1 | 100.4 | -4.5 | High | No |
| 44Ek | 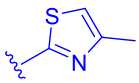 | 530.1 | 10 | 5.37 | 3 | 8 | 2 | 100.4 | -4.7 | High | No |
| 44El | 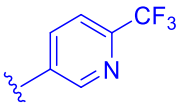 | 578.1 | 11 | 4.95 | 3 | 8 | 1 | 100.4 | -5.2 | High | No |
| 44Em | 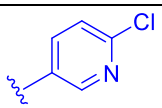 | 544.1 | 10 | 4.51 | 3 | 8 | 1 | 100.4 | -5.0 | High | No |

| | | | | | | | | | | | |
|---|---|---|---|---|---|---|---|---|---|---|---|
| **44En** | 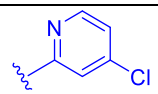 | 544.1 | 10 | 4.88 | 3 | 8 | 1 | 100.4 | -4.9 | High | No |
| **44Eo** | 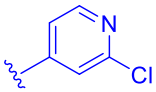 | 544.1 | 10 | 4.51 | 3 | 8 | 1 | 100.4 | -4.9 | High | No |
| **44Ep** | 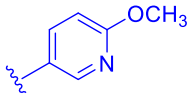 | 540.1 | 11 | 4.20 | 3 | 9 | 1 | 109.6 | -4.7 | High | No |

Table 18. ADME and physiochemical parameters of imidazo[1,2-*a*]pyridine substituted heterocycles. *Mwt* molecular weight, *nRot* number of rotatable bond, *HBD* hydrogen bond donors, *HBA* hydrogen bond acceptors, *nLV* number of Lipiniski violation, *TPSA* Topological Polar Surface Area, *LogS* aqueous solubility, *HIA%* human intestinal absorption, *BBB* blood-brain barrier.

The data demonstrates that all synthesised compounds **44Ed – 44Ep** comply with Lipinski's Rule of Five, including MW, HBD, HBA and clogP, exhibiting no more than two violations, hence indicating their potential for oral administration (Table 18). Other key ADME parameters, such as nRot, LogS, TPSA fall within the acceptable range further supporting drug-like properties. Moreover, HIA% indicates efficient absorbance, while BBB permeability predictions suggest these compounds are not accessible to CNS, decreasing the probability of CNS-related adverse effects. These findings together suggest the potential drug-likeness of the newly synthesised compounds. Having discussed the synthesis, biological evaluation and ADME prediction of imidazo[1,2-*a*]pyridine analogues featuring various *N*-heterocycles, the subsequent chapter will conclude this thesis by summarising key findings and outlining potential directions for future research.

# 5. Conclusion and future work

## 5.1 Thesis conclusion

Tuberculosis remains a significant global health challenge, exacerbated by the emergence of multidrug-resistant and extensively drug-resistant *Mtb* strains. The rising failure of conventional therapy necessitates the urgent need for new therapeutic agents with novel mechanisms of action. Previous research has demonstrated that incorporating an amino acid hydrazide framework into the imidazo[1,2-*a*]pyridine scaffold yielded analogues with moderate anti-*Mtb* activity while maintaining high selectivity against resistant- *Mtb* strains. Building on this, the imidazo[1,2-*a*]pyridine-based compound was modified and subjected to virtual screening to assess its potential as a PafA inhibitor. Binding analysis showed significant interactions with the PafA active site, suggesting its potential for further development. Consequently, as part of the structure-activity relationship analysis, 120 analogues were designed and synthesised and as detailed in chapter 2, their synthesis followed two-synthetic steps: initially, Boc-protected amino acids were coupled with various arylhydrazines to produce substituted-aryl hydrazides, followed by Boc deprotection and subsequent coupling with the corresponding carboxylic acid to yield the final imidazo[1,2-*a*]pyridine-substituted amino acid hydrazides. Accordingly, chapter 3 explored the structure-activity relationship of these compounds by investigating the effects of structural alterations at three positions: amino acid (R), arylhydrazine ($R_1$), and the phenyl ring attached to the scaffold ($R_2$). Phenylalanine analogues showed the highest activity, with small halogens at the *meta* position on the arylhydrazine moiety being important for activity. Notably, two compounds **44Cp** and **44Ct** demonstrated more efficacy than current anti-TB ethambutol and ethionamide. Moreover, $R_2$ modifications generally led to a decrease in activity against the WT strain; however, some of the Phe analogues maintained inhibitory activity against resistant *Mtb* strains, underscoring their potential as candidates for drug-resistant TB therapy. In chapter 4, although heterocycles are well-known for their role in drug optimization, the structure-activity relationship analysis revealed that substituting arylhydrazines with heterocyclic bioisosteres failed to retain efficacy (Figure 114).

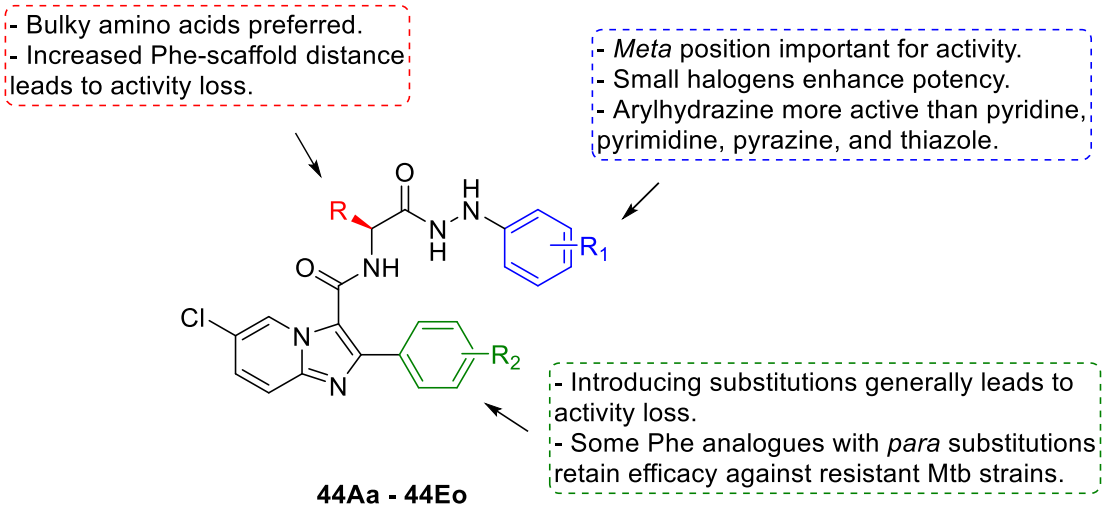


Figure 114. The structural modification of the imidazo[1,2-*a*]pyridine architecture.

The ultimate conclusion drawn from this work is that the imidazo[1,2-*a*]pyridine scaffold, with its three distinct components and comprehensive SAR analysis, shows strong potential in enhancing antimycobacterial activity. This study provides novel drug-like molecules with promising activity and identifies key structural features, establishing a foundation for future drug-target identification studies. Overall, these findings contribute to continuing efforts to develop novel and effective treatments for tuberculosis, with the ultimate goal of combating this global health issue.

## 5.2 Future work

- **PafA inhibition/binding:**

Since the synthesised compounds show activity against the whole-cell *Mtb*, indicating they may target an essential biological system within the bacterium. Computational studies predict that these compounds interact with the PafA active site via key molecular interactions, suggesting potential inhibition. However, experimental validation is necessary to confirm this hypothesis. An *in vitro* PafA assay utilising PafA-catalyzed PanB pupylation, a well-established method for assessing PafA pupylation activity, could be employed to measure the pupylation process and determine whether the compounds interfere with PafA activity.[125,127,132] If the compounds disrupt pupylation, it may suggest their role in impairing protein degradation through the pupylation-proteasome pathway. Additionally, binding studies using thermal shift assay could also be used as a method to detect changes in protein stability upon compound binding, providing further evidence for direct interaction with PafA.[132]

- **Glutamine synthetase inhibition assay:**

To assess the selectivity of the synthesised compounds, it is important to evaluate their potential off-target effects on glutamine synthetase, a key ATP-dependent enzyme in *Mtb*. A standard glutamine synthetase inhibition assay, typically based on a colorimetric or fluorescence method can be used to detect enzymatic inhibition.[133] Comparing the level of inhibition observed in glutamine synthetase assays with that seen in PafA assays will help determine whether the compounds selectively target PafA or act on multiple ATP-dependent enzymes.

- ***In vitro* cytotoxicity evaluation:**

The cytotoxicity of the synthesised compounds could be assessed utilising mammalian macrophage cell lines to evaluate their potential toxicity on immune cells, as demonstrated in previous studies.[138] This test will provide information about the safety profile of the compounds, evaluating their selectivity and potential for inducing cellular damage. The results will be crucial for elucidating the therapeutic window of these compounds and will guide their subsequent development as safe and effective antitubercular agents.

- **Assessing activity against other bacterial species:**

To determine the specificity of these compounds for *Mtb*, it is suggested to evaluate their activity against non-mycobacterial species including a range of Gram-positive and Gram-negative bacteria.[138] This will determine whether the compounds demonstrate broad-spectrum antibacterial activity or are selective for mycobacteria. This test is important for understanding the potential off-target effects and ensuring that the compounds are optimised for tuberculosis treatment without causing adverse effects on other bacteria.

# 6. Experimental section

## 6.1 General Experimental Information

Unless otherwise noted, all reactions were carried out in glassware that had been dried in an oven overnight (above 75 °C) or under a high vacuum utilising a heat gun in a nitrogen atmosphere. All solvents and reagents used as supplied direct from the chemical supplier unless stated otherwise. When mixing solvents, the ratios correspond to the volumes employed.

All reactions were monitored using analytical thin-layer chromatography (TLC) performed on aluminum-backed silica gel 60 Å F254 plates and visualized under UV light at 254 nm. All flash chromatography was executed using 12 g silica gel 40-63μ 60Å columns. All $^{1}H$, $^{13}C$, and $^{19}F$ NMR spectra were recorded in deuterated solvents $CDCl_3$ or DMSO-$d_6$ on a Bruker Advance III HD 700 MHz, Jeol Lambda 500 MHz, Jeol ECS-400 MHz or Bruker Advance III 300 MHz NMR spectrometer instruments. Spectra analysis reported as the following: chemical shifts δ (ppm) are reported with the number of equivalent protons, multiplicity, coupling constant J (Hz), and signal assignment. All chemical shift values are given in parts per million (ppm) relative to the internal standard tetramethylsilane (δH = 0.00 ppm), with coupling constants rounded to the nearest 1 Hz. Analysis and assignment of spectra supported by COSY, HSQC and HMBC experiments. Internal reference used dependant on solvent present using residual protic peaks of $CHCl_3$ to be $\delta_H$ = 7.26 or DMSO as $\delta_H$ = 2.50. Similarly, with $^{13}C$ NMR the internal reference was taken as the central resonance of $CDCl_3$ with $\delta_C$ = 77.0 ppm or DMSO with a value of $\delta_C$ = 39.5 ppm.

Melting points were measured utilising Stuart SMP3 melting point apparatus. Infrared spectra (IR) were obtained on either a Varian Scimitar 800 FT-IR spectrometer or a Perkin Elmer Spectrum Two FT-IR spectrometer. A Thermo LTQ mass spectrometer (ES) was employed at Newcastle University to acquire high-resolution mass spectra.

## 6.2 General Procedures

### 6.2.1 Synthesis of Imidazo[1,2-a]pyridine-3-carboxylate – General Procedure

Under a nitrogen atmosphere, ethyl 2-bromo-3-oxo-3-phenylpropanoate **56** (1 equiv.) was dissolved in EtOH followed by adding 2-amino-5-chloropyridine **55** (1 equiv.) and the reaction mixture was stirred overnight at reflux temperature. After cooling, the organic solvent was evaporated and the resulting white-yellowish residue was dissolved in EtOAc and washed with distilled water (10 ml x 3). The organic layer was dried over $MgSO_4$, then filtered under vacuum, followed by solvent evaporation and drying under reduced pressure to yield the desired product **54**. [137]

**Ethyl 6-chloro-2-phenylimidazo[1,2-*a*]pyridine-3-carboxylate 54a**

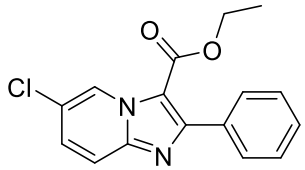


Using the standard procedure provided, ethyl 2-bromo-3-oxo-3-phenylpropanoate **56a** (2.0 g, 7.37 mmol) and 2-amino-5-chloropyridine **55** (0.94 g, 7.37 mmol) were transformed using column chromatography (*n*-hexane/EtOAc [4:1]) to the title compound as a white powder (0.85 g, 38 %); $R_f$ 0.20 (n-hexane/EtOAc [4:1]); m.p. 191 - 194 °C; $\nu_{max}$ 2980 (C-H), 1674 (C=O), 1517, 1490, 1443, 1418, 1377, 1339, 1211,1165, 1088, 951, 823, 688 $cm^{-1}$; $\delta_H$ (300 MHz, $CDCl_3$) 9.52 (1H, s, Ar-*H*), 7.78 – 7.72 (2H, m, Ar-*H*), 7.67 (1H, d, *J* 9, Ar-*H*), 7.46 – 7.37 (4H, m, Ar-*H*), 4.37 – 4.26 (2H, q, *J* 7, $OCH_2CH_3$), 1.26 – 1.18 (3H, t, *J* 7, $OCH_2CH_3$); $\delta_C$ (75 MHz, $CDCl_3$) 160.9 ($C$=$OOCH_2CH_3$), 153.9 *(ipso*-Ar-*C*), 145.3 (*ipso*-Ar-*C)*, 133.9 (*ipso*-Ar-*C)*, 130.1 (Ar-*C)*, 129.2 (Ar-*C)*, 128.9 (Ar-*C)*, 127.6 (Ar-*C)*, 126.3 (Ar-*C)*, 122.4 (*ipso*-Ar-*C)*, 117.7 (Ar-*C)*, 60.7 ($OCH_2CH_3$*)*, 13.9 ($OCH_2CH_3$*)*; *m/z* ($ES^+$) 301 ($[^{35}Cl]MH^+$), 303 ($[^{37}Cl]MH^+$); HRMS ($ES^+$) Found $[^{35}Cl]MH^+$, 301.0736 ($C_{16}H_{14}{}^{35}ClN_2O_2$ requires 301.0738).

**Ethyl 6-chloro-2-(4-chlorophenyl)imidazo[1,2-*a*]pyridine-3-carboxylate 54b**

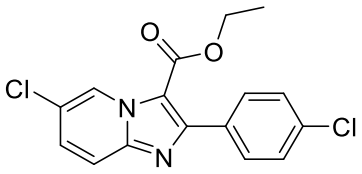

Using the standard procedure provided, ethyl 2-bromo-3-(4-chlorophenyl)-3-oxopropanoate **56b** (1.6 g, 5.40 mmol) and 2-amino-5-chloropyridine **55** (0.69 g, 5.40 mmol) were transformed using column chromatography (*n*-hexane/EtOAc [4:1]) to the title compound as a white powder (0.55 g, 30 %); $R_f$ 0.22 (*n*-hexane/EtOAc [4:1]); m.p. 193 - 195 °C; $\nu_{max}$ 2979 (C-H), 1682 (C=O), 1519, 1492, 1392, 1376, 1337, 1282, 1211, 1163, 1089, 1033, 828, 645 $cm^{-1}$; $\delta_H$ (300 MHz, $CDCl_3$) 9.48 (1H, s, Ar-*H*), 7.73 – 7.68 (2H, d, *J* 8, Ar-*H*), 7.66 (1H, dd, *J* 9, 2, Ar-*H*), 7.43 – 7.38 (3H, m, Ar-*H*), 4.38 – 4.28 (2H, q, *J* 6, OC*H*$_2$CH$_3$), 1.29 – 1.24 (3H, t, *J* 6, OCH$_2$C*H*$_3$); $\delta_C$ (75 MHz, $CDCl_3$) 160.6 (*C*=OOCH$_2$CH$_3$), 152.6 *(ipso*-Ar-*C*), 145.3 (*ipso*-Ar-*C)*, 135.0 (*ipso*-Ar-*C)*, 132.4 (*ipso*-Ar-*C)*, 131.5 (Ar-*C)*, 129.4 (Ar-*C)*, 127.9 (Ar-*C)*, 126.4 (Ar-*C)*, 126.4 (Ar-*C)*, 122.6 (Ar-*C)*, 117.7 (Ar-*C)*, 112.4 *(ipso*-Ar-*C*), 60.9 (O*C*H$_2$CH$_3$*)*, 14.2 (OCH$_2$*C*H$_3$*)*; *m/z* ($ES^+$) 335 ([$^{35,35}$Cl]$MH^+$), 337 ([$^{35,37}$Cl]$MH^+$), 339 ([$^{37,37}$Cl]$MH^+$); HRMS ($ES^+$) Found [$^{35,35}$Cl]$MH^+$, 335.0346 ($C_{16}H_{13}{}^{35,35}Cl_2N_2O_2$ requires 335.0349).

**Ethyl 6-chloro-2-(3-chlorophenyl)imidazo[1,2-*a*]pyridine-3-carboxylate 54c**

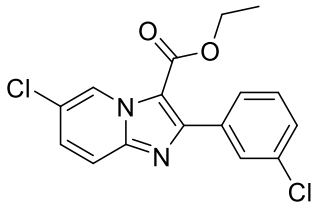


Using the standard procedure provided, ethyl 2-bromo-3-(3-chlorophenyl)-3-oxopropanoate **56c** (1.35 g, 4.41 mmol) and 2-amino-5-chloropyridine **55** (0.56 g, 4.41 mmol) were transformed using column chromatography (*n*-hexane/EtOAc [4:1]) to the title compound as a white powder (0.45 g, 30 %); $R_f$ 0.20 (*n*-hexane /EtOAc [4:1]); m.p. 195 - 197 °C; $\nu_{max}$ 2981 (C=H), 1680 (C=O), 1600, 1494, 1467, 1399, 1379, 1340, 1287, 1251, 1217,1169, 1089, 1040, 827, 688 $cm^{-1}$;$\delta_H$ (300 MHz, $CDCl_3$) 9.50 (1H, s, Ar-*H*), 7.75 (1H, s, Ar-*H*), 7.68 – 7.61 (2H, m, Ar-*H*), 7.43 – 7.34 (3H, m, Ar-*H*), 4.36 – 4.28 (2H, q, *J* 6, OC*H*$_2$CH$_3$), 1.29 – 1.22 (3H, t, *J* 6, OCH$_2$C*H*$_3$); $\delta_C$ (75 MHz, $CDCl_3$) 160.6 (*C*=OOCH$_2$CH$_3$), 152.2 *(ipso*-Ar-*C*), 145.4 (*ipso*-Ar-*C)*, 135.6 (*ipso*-Ar-*C)*, 133.4 (*ipso*-Ar-*C)*, 130.4 (Ar-*C)*, 129.9 (Ar-*C)*, 129.5 (Ar-*C)*, 128.9 (Ar-*C)*, 128.3 (Ar-*C)*, 126.3 (Ar-*C)*, 122.7 *(ipso*-Ar-*C*), 117.8 (Ar-*C)*, 112.5 *(ipso*-Ar-*C*), 61.0 (O*C*H$_2$CH$_3$*)*, 13.9 (OCH$_2$*C*H$_3$*)*; *m/z* ($ES^+$) 335 ([$^{35,35}$Cl]$MH^+$), 337 ([$^{35,37}$Cl]$MH^+$), 339 ([$^{37,37}$Cl]$MH^+$); HRMS ($ES^+$) Found [$^{35,35}$Cl]$MH^+$, 335.0346 ($C_{16}H_{13}{}^{35,35}Cl_2N_2O_2$ requires 335.0349).

**Ethyl 6-chloro-2-(4-methoxyphenyl)imidazo[1,2-*a*]pyridine-3-carboxylate 54d**

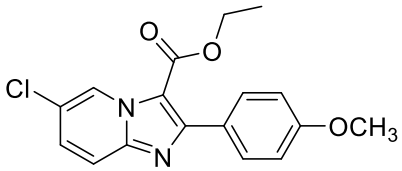

Using the standard procedure provided, ethyl 2-bromo-3-(4-methoxyphenyl)-3-oxopropanoate **56d** (1.60 g, 5.3 mmol) and 2-amino-5-chloropyridine **55** (0.68 g, 5.3 mmol) were transformed using column chromatography (*n*-hexane/EtOAc [4:1]) to the title compound as a white powder (0.58 g, 33 %); $R_f$ 0.17 (*n*-hexane/EtOAc [4:1]); m.p. 197 - 200 °C; $\nu_{max}$ 2980 (C-H), 1699 (C=O), 1545, 1488, 1374, 1336, 1287, 1262, 1210,1145, 1093, 791, 694 $cm^{-1}$; $\delta_H$ (300 MHz, $CDCl_3$) 9.49 (1H, s, Ar-*H*), 7.75 – 7.70 (2H, d, *J* 9, Ar-*H*), 7.64 (1H, d, *J* 9, Ar-*H*), 7.38 (1H, dd, *J* 9, 2, Ar-*H*), 6.98 – 6.93 (2H, d, *J* 9, Ar-*H*), 4.37 – 4.30 (2H, q, *J* 6, OC*H*$_2$CH$_3$), 3.86 (3H, s, Ar-OC*H*$_3$), 1.30 – 1.24 (3H, t, *J* 6, OCH$_2$C*H*$_3$); $\delta_C$ (75 MHz, $CDCl_3$) 160.3 (*C*=OOCH$_2$CH$_3$), 153.8 *(ipso*-Ar-*C*), 145.3 (*ipso*-Ar-*C)*, 131.6 (Ar-*C)*, 129.1 (Ar-*C)*, 126.4 (Ar-*C)*, 126.2 (Ar-*C)*, 122.1 (Ar-*C)*, 117.5 (Ar-*C)*, 113.1 (Ar-*C)*, 112.0 *(ipso*-Ar-*C*), 60.7 (O*C*H$_2$CH$_3$*)*, 55.3 (O*C*H$_3$), 14.0 (OCH$_2$*C*H$_3$*)*; *m/z* (ES$^+$) 331 ([$^{35}$Cl]MH$^+$), 333 ([$^{37}$Cl]MH$^+$); HRMS (ES$^+$) Found [$^{35}$Cl]MH$^+$, 331.0842 ($C_{17}H_{16}{}^{35}ClN_2O_3$ requires 331.0844).

**Ethyl 6-chloro-2-(3-methoxyphenyl)imidazo[1,2-*a*]pyridine-3-carboxylate 54e**

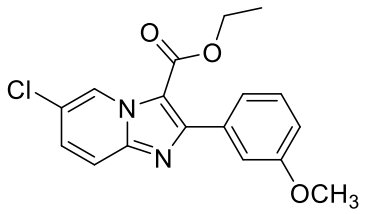

Using the standard procedure provided, ethyl 2-bromo-3-(3-chlorophenyl)-3-oxopropanoate **56e** (1.51 g, 5.01 mmol) and 2-amino-5-chloropyridine **55** (0.64 g, 5.01 mmol) were transformed using column chromatography (*n*-hexane/EtOAc [4:1]) to the title compound as a white powder (0.49 g, 30 %); $R_f$ 0.25 (*n*-hexane /EtOAc [4:1]); m.p. 195 - 198 °C; $\nu_{max}$ 2981 (C=H), 1673 (C=O), 1579, 1491, 1430, 1395, 1378, 1339, 1275, 1214, 1214, 1140, 1093, 1036, 866, 822, 699 $cm^{-1}$;$\delta_H$ (300 MHz, $CDCl_3$) 9.50 (1H, s, Ar-*H*), 7.67 (1H, dd, *J* 9, 1, Ar-*H*), 7.40 (1H, dd, *J* 9, 2, Ar-*H*), 7.34 – 7.28 (3H, m, Ar-*H*), 6.98 (1H, s, Ar-*H*), 4.35 – 4.28 (2H, q, *J* 6, OC*H*$_2$CH$_3$), 3.85 (3H, s, Ar-OC*H*$_3$), 1.26 – 1.20 (3H, t, *J* 6, OCH$_2$C*H*$_3$); $\delta_C$ (75 MHz, $CDCl_3$) 160.9 (*C*=OOCH$_2$CH$_3$), 159.0 *(ipso*-Ar-*C*), 153.7 (*ipso*-Ar-*C)*, 145.2 (*ipso*-Ar-*C)*, 135.1 (*ipso*-Ar-*C)*, 129.8 (Ar-*C)*,

128.6 (Ar-*C)*, 126.3 (Ar-*C)*, 122.7 *(ipso*-Ar-*C*), 117.7 (Ar-*C)*, 115.4 (Ar-*C)*, 114.8 (Ar-*C)*, 112.4 *(ipso*-Ar-*C*), 60.7 (O*C*$H_2CH_3$*)*, 55.3 (O*C*$H_3$), 13.9 (O$CH_2$*C*$H_3$*)*; ***m/z*** (ES$^+$) 331 ([$^{35}$Cl]$MH^+$), 333 ([$^{37}$Cl]$MH^+$); HRMS (ES$^+$) Found [$^{35}$Cl]$MH^+$, 331.0841 ($C_{17}H_{16}{}^{35}ClN_2O_3$ requires 331.0844).

**Ethyl 6-chloro-2-(4-(trifluoromethyl)phenyl)imidazo[1,2-*a*]pyridine-3-carboxylate 54f**

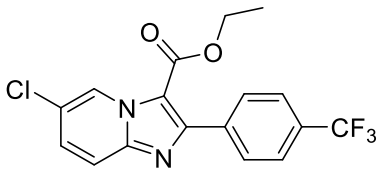


Using the standard procedure provided, ethyl 2-bromo-3-(4-(trifluoromethyl)phenyl)-3-oxopropanoate **56f** (2.0 g, 5.89 mmol) and 2-amino-5-chloropyridine **55** (0.75 g, 5.89 mmol) were transformed using column chromatography (*n*-hexane/EtOAc [4:1]) to the title compound as a white powder (0.64 g, 29 %); $R_f$ 0.30 (*n*-hexane/EtOAc [4:1]); m.p. 200 - 205 °C; $\nu_{max}$ 2981 (C-H), 1677 (C=O), 1576, 1481, 1400, 1379, 1323, 1210, 1161, 1109, 1014, 856, 692 cm$^{-1}$; $\delta_H$ (300 MHz, $CDCl_3$) 9.50 (1H, s, Ar-*H*), 7.90 – 7.85 (2H, d, *J* 8, Ar-*H*), 7.72 – 7.67 (3H, m, Ar-*H*), 7.44 (1H, dd, *J* 9, 2, Ar-*H*), 4.36 – 4.29 (2H, q, *J* 6, OC*H*$_2$CH$_3$), 1.25 – 1.20 (3H, t, *J* 6, $OCH_2CH_3$); $\delta_C$ (75 MHz, $CDCl_3$) 160.5 (*C*=O$OCH_2CH_3$), 152.2 *(ipso*-Ar-*C*), 145.4 (*ipso*-Ar-*C)*, 137.6 (*ipso*-Ar-*C)*, 131.0 (*ipso*-Ar-*C)*, 130.5 (Ar-*C)*, 129.6 (Ar-*C)*, 126.4 (Ar-*H)*, 124.5 (Ar-*C)*, 122.8 *(ipso*-Ar-*C*), 117.8 (Ar-*C)*, 112.7 *(ipso*-Ar-*C*), 61.0 (O*C*$H_2CH_3$*)*, 13.9 (O$CH_2$*C*$H_3$*)*; $\delta_F$ (282 MHz, $CDCl_3$) -62.6 (C*F*$_3$); ***m/z*** (ES$^+$) 369 ([$^{35}$Cl]$MH^+$), 371 ([$^{37}$Cl]$MH^+$); HRMS (ES$^+$) Found [$^{35}$Cl]$MH^+$, 369.0609 ($C_{17}H_{13}{}^{35}ClF_3N_2O_2$ requires 369.0612).

**Methyl 6-chloro-2-(3-(trifluoromethyl)phenyl)imidazo[1,2-*a*]pyridine-3-carboxylate 54g**

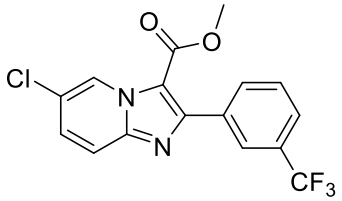


Using the standard procedure provided, methyl 2-bromo-3-(3-(trifluoromethyl)phenyl)-3-oxopropanoate **56g** (2.0 g, 6.15 mmol) and 2-amino-5-chloropyridine **55** (0.79 g, 6.15 mmol) were transformed using column chromatography (*n*-hexane/EtOAc [4:1]) to the

title compound as a white powder (0.57 g, 26 %); $R_f$ 0.35 (*n*-hexane/EtOAc [4:1]); m.p. 198 - 203 °C $\delta_C$; $\nu_{max}$ 2981 (C-H), 1683 (C=O), 1600, 1494, 1469, 1381, 1341, 1320, 1260, 1215, 1168, 1091, 691 $cm^{-1}$; $\delta_H$ (300 MHz, $CDCl_3$) 9.51 (1H, s, Ar-*H*), 8.05 (1H, s, Ar-*H*), 7.96 (1H, d, *J* 7, Ar-*H*), 7.73 – 7.67 (2H, dd, *J* 9, 1, Ar-*H*), 7.57 (1H, t, *J* 7, Ar-*H*), 7.44 (1H, dd, *J* 9, 2, Ar-*H*), 3.83 (3H, s, $OCH_3$); $\delta_C$ (75 MHz, $CDCl_3$) 160.8 ($C$=$OOCH_2CH_3$), 152.2 *(ipso*-Ar-*C*), 145.5 (*ipso*-Ar-*C)*, 134.6 (*ipso*-Ar-*C)*, 133.3 (Ar-*C)*, 130.4 *(ipso*-Ar-*C*), 129.7 (Ar-*C)*, 128.7 (Ar-*C)*, 127.3 (Ar-*C)*, 126.4 (Ar-*C)*, 125.9 (Ar-*C)*, 125.5 (Ar-*C)*, 122.9 *(ipso*-Ar-*C*), 117.8 (Ar-*C)*, 112.4 *(ipso*-Ar-*C*), 51.5 ($OCH_3$); $\delta_F$ (282 MHz, $CDCl_3$) -62.2 ($CF_3$); *m/z* ($ES^+$) 355 ($[^{35}Cl]MH^+$), 357 ($[^{37}Cl]MH^+$); HRMS ($ES^+$) Found $[^{35}Cl]MH^+$, 355.0451 ($C_{16}H_{11}{}^{35}ClF_3N_2O_2$ requires 355.0456).

### 6.2.2 Synthesis of Imidazo[1,2-*a*]pyridine-3-carboxylic acid – General Procedure

Under a nitrogen atmosphere, the aqueous solution of lithium hydroxide (4 equiv.) was added to ethyl 6-chloro-2-phenylimidazo[1,2-*a*]pyridine-3-carboxylate **54** (1 equiv.) in EtOH. The reaction mixture was stirred overnight at room temperature, the organic solvent evaporated, and 1N HCl was added to the aqueous solution until precipitation formed. The precipitation was then collected using vacuum filtration, washed with water, and dried to offer the desired compound **50**.[137]

**6-Chloro-2-phenylimidazo[1,2-*a*]pyridine-3-carboxylic acid 50a**

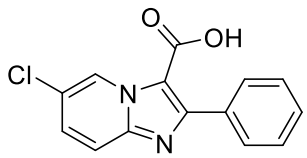


Following the standard general procedure, the aqueous solution of lithium hydroxide (1M) and ethyl 6-chloro-2-phenylimidazo[1,2-*a*]pyridine-3-carboxylate (1.2 g, 3.9 mmol) were transformed following acidified with 1N HCl into the title compound which was isolated as a white powder (0.95 g, 87 %); $R_f$ 0.40 (DCM/EtOAc [2:1]); m.p. 200 - 203 °C; $\nu_{max}$ 3386 (O-H), 1699 (C=O), 1545, 1488, 1374, 1336, 1287, 1262, 1210, 1145, 1093, 791, 694 $cm^{-1}$; $\delta_H$ (300 MHz, DMSO-$d_6$) 13.32 (1H, bs, COO*H*), 9.45 (1H, s, Ar-*H*), 7.84 (1H, *J* 9, d, Ar-*H*), 7.80 – 7.75 (2H, m, Ar-*H*), 7.65 (1H, dd, *J* 9, 2, Ar-*H*), 7.46

– 7.40 (3H, m, Ar-*H*); $\delta_C$ (75 MHz, DMSO-$d_6$) 162.1 (*C*OOH), 152.9 *(ipso*-Ar-*C*), 145.1 (*ipso*-Ar-*C)*, 134.3 (*ipso*-Ar-*C)*, 130.5 (Ar-*C)*, 129.4 (Ar-*C)*, 129.1 (Ar-*C)*, 128.0 (Ar-*C)*, 126.4 (Ar-*C)*, 121.5 (*ipso*-Ar-*C)*, 118.4 (Ar-*C)*; ***m/z*** ($ES^+$) 273 ($[^{35}Cl]MH^+$), 275 ($[^{37}Cl]MH^+$); HRMS ($ES^+$) Found $[^{35}Cl]MH^+$, 273.0443 ($C_{14}H_9{}^{35}ClN_2O_2$ requires 273.0431).

**6-chloro-2-(4-chlorophenyl)imidazo[1,2-*a*]pyridine-3-carboxylic acid 50b**

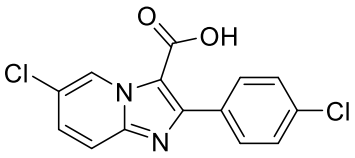


Following the standard general procedure, the aqueous solution of lithium hydroxide (1 M) and ethyl 6-chloro-2-(4-chlorophenyl)imidazo[1,2-*a*]pyridine-3-carboxylate (0.17 g, 0.52 mmol) were transformed following acidified with 1N HCl into the title compound as a white powder (0.13 g, 85 %); $R_f$ 0.35 (DCM/EtOAc [2:1]); m.p. 202 - 205 °C; $\nu_{max}$ 3397 (O-H), 1675 (C=O), 1601, 1496, 1324, 1282, 1212, 1147, 1096, 1038, 966, 827 $cm^{-1}$; $\delta_H$ (300 MHz, DMSO-$d_6$) 9.45 (1H, s, Ar-*H*), 7.86 – 7.76 (3H, d, *J* 8, Ar-*H*), 7.64 (1H, d, *J* 8, Ar-*H*), 7.53 – 7.46 (2H, d, *J* 8, Ar-*H*); $\delta_C$ (75 MHz, DMSO-$d_6$) 161.8 (*C*OOH), 150.1 *(ipso*-Ar-*C*), 145.3 (*ipso*-Ar-*C)*, 136.8 *(ipso*-Ar-*C*), 131.7 *(ipso*-Ar-*C*), 130.9 (Ar-*C)*, 129.6 (Ar-*C)*, 129.2 (Ar-*C)*, 126.1 (Ar-*C)*, 121.8 (*ipso*-Ar-*C)*, 118.4 (Ar-*C)*; ***m/z*** ($ES^+$) 307 ($[^{35,35}Cl]MH^+$), 309 ($[^{35,37}Cl]MH^+$), 311 ($[^{37,37}Cl]MH^+$); HRMS ($ES^+$) Found $[^{35,35}Cl]MH^+$, 307.0034 ($C_{14}H_9{}^{35,35}Cl_2N_2O_2$ requires 307.0036).

**6-chloro-2-(3-chlorophenyl)imidazo[1,2-*a*]pyridine-3-carboxylic acid 50c**

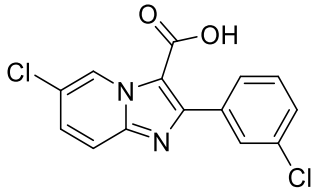


Following the standard general procedure, the aqueous solution of lithium hydroxide (1 M) and ethyl 6-chloro-2-(3-chlorophenyl)imidazo[1,2-*a*]pyridine-3-carboxylate (2.23 g, 6.63 mmol) were transformed following acidified with 1N HCl into the title compound as a white powder (1.82 g, 89 %); $R_f$ 0.35 (DCM/EtOAc [2:1]); m.p. 205 - 207 °C; $\nu_{max}$ 3353 (O-H), 1668 (C=O), 1600, 1534, 1491, 1433, 1366, 1318, 1251, 1215, 1155, 1092, 1035, 988, 855, 773 $cm^{-1}$; $\delta_H$ (300 MHz, DMSO-$d_6$) 9.43 (1H, s, Ar-*H*), 7.88 – 7.80 (2H,

m, Ar-*H*), 7.75 (1H, s, Ar-*H*), 7.67 (1H, d, *J* 9, Ar-*H*), 7.52 – 7.45 (2H, m, Ar-*H*); $\delta_C$ (75 MHz, DMSO-$d_6$) 161.8 (*C*OOH), 151.1 *(ipso*-Ar-*C*), 145.1 (*ipso*-Ar-*C)*, 136.4 *(ipso*-Ar-*C*), 132.7 *(ipso*-Ar-*C*), 130.1 (Ar-*C)*, 129.6 (Ar-*C)*, 129.2 (Ar-*C)*, 126.4 (Ar-*C)*, 121.8 (*ipso*-Ar-*C)*, 118.5 (Ar-*C)*; *m/z* ($ES^+$) 307 ($[^{35,35}Cl]MH^+$), 309 ($[^{35,37}Cl]MH^+$), 311 ($[^{37,37}Cl]MH^+$); HRMS ($ES^+$) Found $[^{35,35}Cl]MH^+$, 307.0034 ($C_{14}H_9{}^{35,35}Cl_2N_2O_2$ requires 307.0036).

**6-chloro-2-(4-methoxyphenyl)imidazo[1,2-*a*]pyridine-3-carboxylic acid 50d**

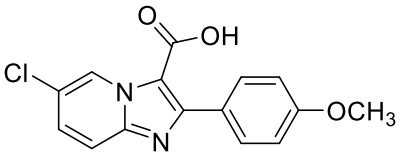


Following the standard general procedure, the aqueous solution of lithium hydroxide (1 M) and ethyl 6-chloro-2-(4-methoxyphenyl)imidazo[1,2-*a*]pyridine-3-carboxylate (3.02 mmol) were transformed following acidified with 1N HCl into the title compound as a white powder (0.78 g, 85 %); $R_f$ 0.42 (DCM/EtOAc [2:1]); m.p. 220 - 223 °C; $\nu_{max}$ 3240 (O-H), 2972 (C-H), 1667 (C=O), 1596, 1497, 1366, 1252, 1162, 1045, 988, 836, 776 $cm^{-1}$; $\delta_H$ (300 MHz, DMSO-$d_6$) 13.27 (1H, bs, COO*H*), 9.42 (1H, s, Ar-*H*), 7.83 – 7.71 (3H, m, Ar-*H*), 7.62 (1H, dd, *J* 9, 1, Ar-*H*), 7.03 – 6.94 (2H, d, *J* 9, Ar-*H*), 3.81 (3H, s, OC*H*$_3$); $\delta_C$ (75 MHz, DMSO-$d_6$) 162.2 (*C*OOH), 160.2 *(ipso*-Ar-*C*), 152.8 *(ipso*-Ar-*C*), 145.0 (*ipso*-Ar-*C)*, 132.0 (Ar-*C)*, 129.3 (Ar-*C)*, 126.4 (Ar-*H)*, 121.3 (*ipso*-Ar-*C)*, 118.1 (Ar-*C)*, 113.5 (Ar-*C)*, 55.6 (O*C*H$_3$); *m/z* ($ES^+$) 303 ($[^{35}Cl]MH^+$), 305 ($[^{37}Cl]MH^+$); HRMS ($ES^+$) Found $[^{35}Cl]MH^+$, 303.0542 ($C_{15}H_{12}{}^{35}ClN_2O_3$ requires 303.0531).

**6-chloro-2-(3-methoxyphenyl)imidazo[1,2-*a*]pyridine-3-carboxylic acid 50e**

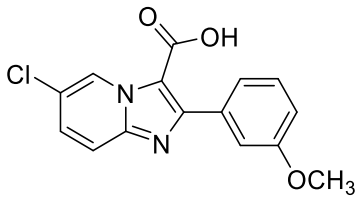


Following the standard general procedure, the aqueous solution of lithium hydroxide (1 M) and ethyl 6-chloro-2-(3-methoxyphenyl)imidazo[1,2-*a*]pyridine-3-carboxylate (1.7 g, 5.14 mmol) were transformed following acidified with 1N HCl into the title compound as a white powder (1.20 g, 77 %); $R_f$ 0.45 (DCM/EtOAc [2:1]); m.p. 220 - 225 °C; $\nu_{max}$ 3240 (O-H), 2981 (C-H), 1673 (C=O), 1579, 1491, 1430, 1395, 1378, 1339,

1275, 1214, 1036, 866, 822, 771, 724, 699 $cm^{-1}$; $\delta_H$ (300 MHz, DMSO-$d_6$) 9.43 (1H, s, Ar-*H*), 7.83 (1H, d, *J* 9, Ar-*H*), 7.64 (1H, dd, *J* 9, 1, Ar-*H*), 7.43 – 7.28 (3H, m, Ar-*H*), 6.99 (1H, m, Ar-*H*), 3.78 (3H, s, OC*H*$_3$); $\delta_C$ (75 MHz, DMSO-$d_6$) 162.1 (*C*OOH), 158.9 *(ipso*-Ar-*C*), 152.6 *(ipso*-Ar-*C*), 145.0 (*ipso*-Ar-*C)*, 135.5 *(ipso*-Ar-*C*), 129.4 (Ar-*C)*, 129.1 (Ar-*C)*, 126.4 (Ar-*C)*, 122.9 (Ar-*C)*, 121.6 (*ipso*-Ar-*C)*, 118.4 (Ar-*C)*, 116.0 (Ar-*C*), 114.8 (Ar-*C)*, 113.1 *(ipso*-Ar-*C*), 55.5 (O*C*H$_3$); ***m/z*** (ES$^+$) 303 ([$^{35}$Cl]MH$^+$), 305 ([$^{37}$Cl]MH$^+$); HRMS (ES$^+$) Found [$^{35}$Cl]MH$^+$, 303.0535 ($C_{15}H_{12}{}^{35}ClN_2O_3$ requires 303.0531).

**6-chloro-2-(4-trifluoromethylphenyl)imidazo[1,2-*a*]pyridine-3-carboxylic acid 50f**

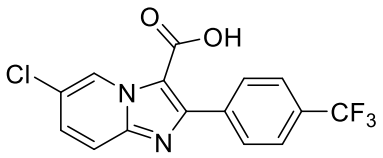


Following the standard general procedure, the aqueous solution of lithium hydroxide (1 M) and ethyl 6-chloro-2-(4-trifluoromethylphenyl)imidazo[1,2-*a*]pyridine-3-carboxylate (2.0 g, 5.42 mmol) were transformed following acidified with 1N HCl into the title compound as a white powder (1.60 g, 87 %); $R_f$ 0.30 (DCM/EtOAc [2:1]); m.p. 200 - 205 °C; $\nu_{max}$ 3322 (O-H), 1695 (C=O), 1585, 1473, 1413, 1366, 1326, 1245, 1218, 1167, 1102, 1066, 1017, 944, 842, 746 $cm^{-1}$; $\delta_H$ (300 MHz, DMSO-$d_6$) 9.45 (1H, s, Ar-*H*), 8.02 – 7.98 (2H, d, *J* 7, Ar-*H*), 7.88 (1H, dd, *J* 9, 1, Ar-*H*), 7.84 – 7.79 (2H, d, *J* 7, Ar-*H*), 7.68 (1H, dd, *J* 9, 2, Ar-*H*); $\delta_C$ (75 MHz, DMSO-$d_6$) 161.8 (*C*OOH), 151.1 *(ipso*-Ar-*C*), 145.1 (*ipso*-Ar-*C)*, 138.4 *(ipso*-Ar-*C*), 131.3 (Ar-*C)*, 129.6 (Ar-*C)*, 129.0 (Ar-*C)*, 126.4 (Ar-*C)*, 124.9 (Ar-*C)*, 121.9 (*ipso*-Ar-*C)*, 118.5 (Ar-*C)*, 113.6 *(ipso*-Ar-*C*); $\delta_F$ (282 MHz, DMSO-d6) -60.6 (C*F*$_3$); ***m/z*** (ES$^+$) 341 ([$^{35}$Cl]MH$^+$), 343 ([$^{37}$Cl]MH$^+$); HRMS (ES$^+$) Found [$^{35}$Cl]MH$^+$, 341.0312 ($C_{15}H_9{}^{35}ClF_3N_2O_2$ requires 341.0299).

**6-chloro-2-(3-(trifluoromethyl)phenyl)imidazo[1,2-*a*]pyridine-3-carboxylic acid 50g**

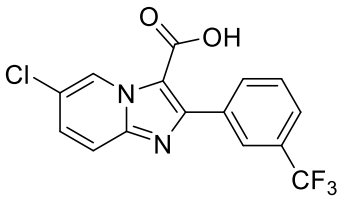

Following the standard general procedure, the aqueous solution of lithium hydroxide (1 M) and ethyl 6-chloro-2-(3-(trifluoromethyl)phenyl)imidazo[1,2-*a*]pyridine-3-carboxylate (1.19 g, 3.23 mmol) were transformed following acidified with 1N HCl into the title compound as a white powder (0.92 g, 83 %); $R_f$ 0.35 (DCM/EtOAc [2:1]); m.p. 200 - 205 °C; $\nu_{max}$ 3400 (O-H), 1652 (C=O), 1613, 1497, 1318, 1199, 1177, 1080, 965, 800, 774 $cm^{-1}$; $\delta_H$ (300 MHz, DMSO-$d_6$) 9.42 (1H, s, Ar-*H*), 8.15 – 8.06 (2H, m, Ar-*H*), 7.84 (1H, d, *J* 9, Ar-*H*), 7.78 (1H, d, *J* 7, Ar-*H*), 7.69 (1H, d, *J* 7, Ar-*H*), 7.64 (1H, dd, *J* 9, 1, Ar-*H*); $\delta_C$ (75 MHz, DMSO-$d_6$) 161.8 (*C*OOH), 150.9 *(ipso*-Ar-*C*), 145.1 (*ipso*-Ar-*C)*, 135.3 *(ipso*-Ar-*C*), 134.5 (Ar-*C)*, 129.6 (Ar-*C)*, 129.5 (Ar-*C)*, 129.1 (Ar-*C)*, 128.7 (Ar-*C)*, 127.0 (Ar-*C)*, 126.4 (Ar-*H)*, 125.7 (Ar-*C)*, 121.8 (*ipso*-Ar-*C)*, 118.5 (Ar-*C)*, 113.5 *(ipso*-Ar-*C*); $\delta_F$ (282 MHz, DMSO-d6) -61.3 (C*F*$_3$); ***m/z*** ($ES^+$) 341 ($[^{35}Cl]MH^+$), 343 ($[^{37}Cl]MH^+$); HRMS ($ES^+$) Found $[^{35}Cl]MH^+$, 341.0297 ($C_{15}H_9{}^{35}ClF_3N_2O_2$ requires 341.0299).

### 6.2.3 Synthesis of *N*-protected Hydrazides – General Procedure

Under a nitrogen atmosphere, substituted arylhydrazine **53** (1 equiv.) dissolved in THF and treated with *N*-protected amino acid **52** (1.2 equiv.) and DIPEA (1.5 equiv.), followed by the addition of HBTU (1.2 equiv.) and stirred for 6 hours at room temperature. Reaction mixed with diethyl ether (10 ml) and distilled water (5 ml) and after separating the two phases, the organic layer was washed again with distilled water (5 ml x 3 ml), sat. aq. $NaHCO_3$ (5 ml), sat. aq. $NH_4Cl$ (5 ml) and brine (10 ml). The organic layer was further dried over MgSO4, filtered, evaporated, and dried under vacuum to obtain the required *N*-Boc hydrazides **51 (Aa – Cc)**. All the hydrazides in this study have been previously synthesised.[137,186]

***tert*-Butyl (2-oxo-2-(2-phenylhydrazineyl)ethyl)carbamate 51Aa**

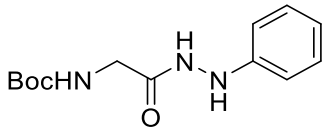


Using the standard procedure provided, *N*-Boc-Glycine (0.30 g, 1.7 mmol) and phenylhydrazine hydrochloride (0.22 g, 2.0 mmol) were transformed into the title compound as a yellow solid (0.34 g, 77 %); $\delta_H$ (300 MHz, $CDCl_3$) 8.05 (1H, s, CON*H*NH), 7.21 - 7.23 (2H, d, *J* 7, Ar-*H*), 6.92 (1H, t, *J* 7, Ar-*H*), 6.87 - 6.85 (2H, d, *J*

7, Ar-*H*), 5.18 (1H, bs, BocN*H*), 3.95 – 3.85 (2H, d, *J* 6, NHC$H_2$), 1.51 (9H, s, (C$H_3$)$_3$COC(O)NH).

***tert*-Butyl (2-(2-(3-chlorophenyl)hydrazinyl)-2-oxoethyl)carbamate 51Ab**

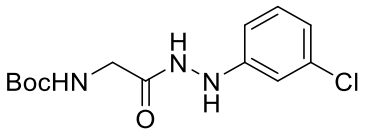


Using the standard procedure provided, *N*-Boc-Glycine (0.40 g, 2.2 mmol) and 3-chlorophenylhydrazine hydrochloride (0.49 g, 2.7 mmol) were transformed into the title compound as an orange solid (0.50 g, 73 %); $\delta_H$ (300 MHz, $CDCl_3$) 8.37 (1H, s, CON*H*NH), 7.03 (1H, t, *J* 7, Ar-*H*), 6.78 (1H, dd, *J* 7, 2, Ar-*H*), 6.72 (1H, s, Ar-*H*), 6.62 (1H, d, *J* 7, Ar-*H*), 5.27 (1H, bs, BocN*H*), 3.94 – 3.85 (2H, d, *J* 6, NHC$H_2$), 1.41 (9H, s, (C$H_3$)$_3$COC(O)NH).

***tert*-Butyl (2-oxo-2-(2-(4-chlorophenyl)hydrazineyl)ethyl)carbamate 51Ac**

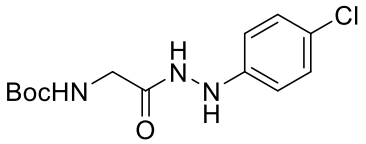


Using the standard procedure provided, *N*-Boc-Glycine (0.40 g, 2.3 mmol) and 4-chlorophenylhydrazine hydrochloride (0.39 g, 2.8 mmol) were transformed into the title compound as an orange solid (0.57 g, 83 %); $\delta_H$ (300 MHz, $CDCl_3$) 8.21 (1H, s, CON*H*NH), 7.10 - 7.08 (2H, d, *J* 9, Ar-*H*), 6.70 - 6.68 (2H, d, *J* 9, Ar-*H*), 5.19 (1H, bs, BocN*H*), 3.81 – 3.74 (2H, d, *J* 6, NHC$H_2$), 1.41 (9H, s, (C$H_3$)$_3$COC(O)NH).

***tert*-Butyl (2-(2-(3-bromophenyl)hydrazinyl)-2-oxoethyl)carbamate 51Ad**

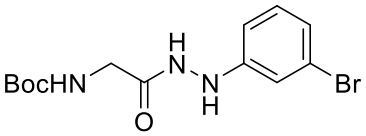


Following the standard general procedure, *N*-Boc-Glycine (0.20 g, 1.1 mmol) and 3-bromophenylhydrazine hydrochloride (0.25 g, 1.3 mmol) were transformed into the title compound as a brown solid (0.31 g, 79 %); $\delta_H$ (300 MHz, $CDCl_3$) 8.04 (1H, s, CON*H*NH), 7.26 (1H, t, *J* 7, Ar-*H*), 7.01 (1H, dd, *J* 7, 1, Ar-*H*), 6.70 (1H, s, Ar-*H*), 6.51 (1H, d, *J* 7, Ar-*H*), 5.30 (1H, bs, BocN*H*), 3.92 – 3.88 (2H, d, *J* 6, NHC$H_2$), 1.48 (9H, s, (C$H_3$)$_3$COC(O)NH).

***tert*-Butyl (2-oxo-2-(2-(4-bromophenyl)hydrazineyl)ethyl) carbamate 51Ae**

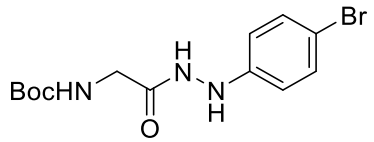


Using the standard procedure provided, *N*-Boc-Glycine (0.20 g, 1.2 mmol) and 4-bromophenyl hydrazine hydrochloride (0.26 g, 1.4 mmol) were transformed into the title compound as a brown solid (0.27 g, 69 %); $\delta_H$ (300 MHz, $CDCl_3$) 8.41 (1H, s, CON*H*NH), 7.27 – 7.25 (2H, d, *J* 9, Ar-*H*), 6.67 – 6.65 (2H, d, *J* 9, Ar-*H*), 5.41 (1H, bs, BocN*H*), 3.86 (2H, d, *J* 6, NHC$H_2$), 1.45 (9H, s, (C$H_3$)$_3$COC(O)NH).

***tert*-Butyl (2-oxo-2-(2-(3-(trifluoromethyl)phenyl)hydrazineyl)ethyl) carbamate 51Af**

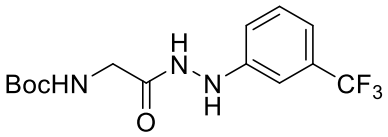


Using the standard procedure provided, *N*-Boc-Glycine (0.20 g, 1.1 mmol) and 3-trifluoromethylphenyl hydrazine hydrochloride (0.24 g, 1.4 mmol) were transformed into the title compound as a yellow solid (0.32 g, 85 %); $\delta_H$ (300 MHz, $CDCl_3$) 8.11 (1H, s, CON*H*NH), 7.35 (1H, t, *J* 7, Ar-*H*), 7.17 (1H, dd, *J* 7, 1, Ar-*H*), 7.08 (1H, s, Ar-*H*), 7.02 (1H, d, *J* 7, Ar-*H*), 6.17 (1H, bs, BocN*H*), 3.89 - 3.92 (2H, d, *J* 6, NHC$H_2$), 1.42 (9H, s, (C$H_3$)$_3$COC(O)NH).

***tert*-Butyl (2-oxo-2-(2-(4-(trifluoromethyl)phenyl)hydrazineyl)ethyl) carbamate 51Ag**

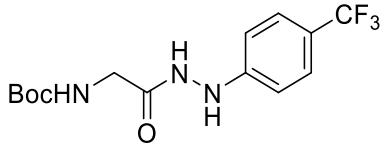


Using the standard procedure provided, *N*-Boc-Glycine (0.50 g, 2.8 mmol) and 4-trifluoromethylphenyl hydrazine hydrochloride (0.60 g, 3.4 mmol) were transformed into the title compound as an orange solid (0.62 g, 66 %); $\delta_H$ (300 MHz, $CDCl_3$) 8.10 (1H, s, CON*H*NH), 7.40 – 7.38 (2H, d, *J* 9, Ar-*H*), 6.79 – 6.77 (2H, d, *J* 9, Ar-*H*), 6.19 (1H, s, CONHN*H*), 5.11 (1H, bs, BocN*H*), 3.92 – 3.84 (2H, d, *J* 6, NHC$H_2$), 1.35 (9H, s, (C$H_3$)$_3$COC(O)NH).

***tert*-butyl (2-oxo-2-(2-(3-(trifluoromethoxy)phenyl)hydrazineyl)ethyl)carbamate 51Ah**

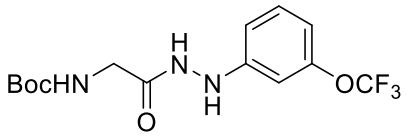


Using the standard procedure provided, *N*-Boc-Glycine (0.30 g, 1.7 mmol) and 3-trifluoromethoxyphenylhydrazine hydrochloride (0.39 g, 2.0 mmol) were transformed into the title compound as a yellow powder (0.41 g, 70 %); $R_f$ 0.51 (DCM/EtOAc [4:1]); m.p. 155 – 158 °C; $\nu_{max}$ 3357 (N-H), 3263 (N-H), 2958 (C-H), 1650 (C=O), 1614, 1512, 1473, 1367, 1243, 1166, 1051, 814 $cm^{-1}$; $\delta_H$ (300 MHz, $CDCl_3$) 8.13 (1H, bs, CON*H*NH), 7.14 (1H, dd, *J* 8, 8, Ar-*H*), 6.71 – 6.64 (2H, dd, *J* 8, 1, Ar-*H*), 6.57 (1H, s, Ar-*H*), 5.15 (1H, bs, BocN*H*), 3.84 – 3.76 (2H, d, *J* 6, NHC$H_2$), 1.45 (9H, s, (C$H_3$)$_3$COC(O)NH); $\delta_C$ (75 MHz, $CDCl_3$) 170.0 (*C*=ONHNH), 156.4 *(C*=ONH), 149.3 (Ar-O*C*$F_3$*)*, 143.5 (*ipso*-Ar-*C)*, 130.3 (Ar-*C)*, 113.0 (Ar-*C)*, 111.7 (Ar-*C)*, 106.0 (*ipso*-Ar-*C)*, 81.0 ((CH$_3$)$_3$*C*O), 43.3 (BocNH*C*H$_2$), 28.1 (*C*H$_3$)$_3$CO); $\delta_F$ (300 MHz, $CDCl_3$) -57.7 (OC*F*$_3$); *m/z* ($ES^+$) 348 ($MH^+$); HRMS ($ES^+$) Found $MH^+$, 348.1180 ($C_{14}H_{19}F_3N_3O_4$ requires 348.1171).

***tert*-butyl (2-oxo-2-(2-(4-(trifluoromethoxy)phenyl)hydrazineyl)ethyl)carbamate 51Ai**

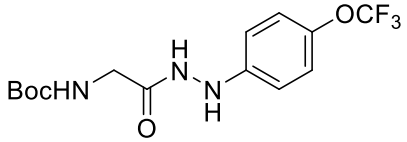


Using the standard procedure provided, *N*-Boc-Glycine (0.30 g, 1.7 mmol) and 4-trifluoromethoxyphenyl hydrazine hydrochloride (0.39 g, 2.0 mmol) were transformed into the title compound as a yellow powder (0.36 g, 62 %); $R_f$ 0.50 (DCM/EtOAc [4:1]); m.p. 159 – 162 °C; $\nu_{max}$ 3366 (N-H), 3250 (N-H), 2983(C-H), 1650 (C=O), 1613, 1592, 1526, 1505, 1439, 1269, 1221, 1150, 1052, 848, 509 $cm^{-1}$; $\delta_H$ (300 MHz, $CDCl_3$) 8.20 (1H, s, CON*H*NH), 7.03 – 6.95 (2H, d, *J* 8, Ar-*H*), 6.77 – 6.71 (2H, d, *J* 8, Ar-*H*), 5.18 (1H, bs, BocN*H*), 3.85 – 3.76 (2H, d, *J* 6, NHC$H_2$), 1.45 (9H, s, (C$H_3$)$_3$COC(O)NH); $\delta_C$ (75 MHz, $CDCl_3$) 169.7 (*C*=ONHNH), 156.4 *(C*=ONH), 146.2 (Ar-O*C*$F_3$*)*, 143.5 (*ipso*-Ar-*C)*, 122.2 (Ar-*C)*, 114.2 (Ar-*C)*, 109.0 (*ipso*-Ar-*C)*, 81.0 ((CH$_3$)$_3$*C*O), 43.3 (BocNH*C*H$_2$), 28.2 (*C*H$_3$)$_3$CO); $\delta_F$ (300 MHz, $CDCl_3$) -58.3 (OC*F*$_3$); *m/z* ($ES^+$) 348 ($MH^+$); HRMS ($ES^+$) Found $MH^+$, 348.1180 ($C_{14}H_{19}F_3N_3O_4$ requires 348.1171).

***tert*-Butyl (S)-(2-oxo-2-(2-phenylhydrazineyl)ethyl)carbamate 51Aj**

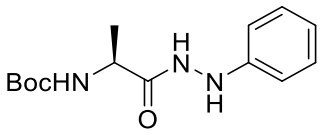


Using the standard procedure provided, *N*-Boc-*L*-Alanine (0.30 g, 1.6 mmol) and phenylhydrazine hydrochloride (0.20 g, 1.9 mmol) were transformed into the title compound as a yellow solid (0.40 g, 90 %); $\delta_H$ (300 MHz, $CDCl_3$) 8.01 (1H, s, CON*H*NH), 7.15 - 7.13 (2H, t, *J* 7, Ar-C*H*), 6.82 (1H, t, *J* 7, Ar-C*H*), 6.77 - 6.75 (2H, d, *J* 7, Ar-C*H*), 4.86 (1H, bs, BocN*H*) , 4.18 (1H, m, NHC*H*$CH_3$), 1.41 (9H, s, C(C*H*$_3$)$_3$), 1.37 – 1.33 (3H, d, *J* 7, NHCHC*H*$_3$).

***tert*-Butyl (S)-(1-oxo-1-(2-(3-chlorophenyl)hydrazineyl)propan-2-yl)carbamate 51Ak**

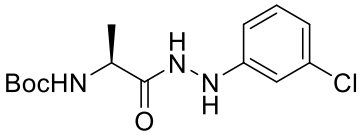


Using the standard procedure provided, *N*-Boc-*L*-Alanine (0.30 g, 1.5 mmol) and 3-bromophenylhydrazine hydrochloride (0.27 g, 1.9 mmol) were transformed into the title compound as an orange powder (0.31 g, 65 %); $\delta_H$ (300 MHz, $CDCl_3$) 8.25 (1H, s, CON*H*NH), 7.00 (1H, dd, *J* 7, 7, Ar-*H*), 7.08 (1H, dd, *J* 7, 1, Ar-*H*), 6.91 (1H, s, Ar-*H*), 6.70 (1H, d, *J* 7, Ar-*H*), 4.95 (1H, bs, BocN*H*), 4.21 (1H, m, NHC*H*$CH_3$), 1.50 (9H, s, (C*H*$_3$)$_3$COC(O)NH), 1.48 - 1.42 (3H, d, *J* 7, NHCHC*H*$_3$).

***tert*-Butyl (S)-(1-oxo-1-(2-(4-chlorophenyl)hydrazineyl)propan-2-yl)carbamate 51Al**

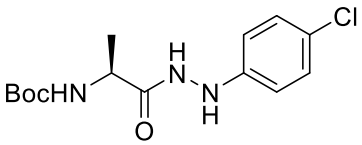


Using the standard procedure provided, *N*-Boc-*L*-Alanine (0.30 g, 1.5 mmol) and 4-chlorophenyl hydrazine hydrochloride (0.27 g, 1.9 mmol) were transformed into the title compound as an orange solid (0.42 g, 84 %); $\delta_H$ (300 MHz, $CDCl_3$) 8.11 (1H, s, CON*H*NH), 7.19 – 7.17 (2H, d, *J* 9, Ar-*H*), 6.79 – 6.77 (2H, d, *J* 9, Ar-*H*), 4.90 (1H, bs, BocN*H*), 4.24 (1H, m, NHC*H*$CH_3$), 1.50 (9H, s, (C*H*$_3$)$_3$COC(O)NH), 1.48 – 1.42 (3H, d, *J* 7, NHCHC*H*$_3$).

***tert*-Butyl (S)-(1-oxo-1-(2-(3-bromophenyl)hydrazineyl)propan-2-yl)carbamate 51Am**

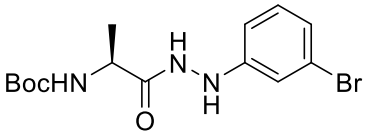


Using the standard procedure provided, *N*-Boc-*L*-Alanine (0.30 g, 1.5 mmol) and 3-bromophenylhydrazine hydrochloride (0.35 g, 1.9 mmol) were transformed into the title compound as a yellow powder (0.50 g, 89 %); $\delta_H$ (300 MHz, $CDCl_3$) 8.23 (1H, s, CON*H*NH), 7.08 (1H, dd, *J* 7, 7, Ar-*H*), 7.02 (1H, dd, *J* 7, 1, Ar-*H*), 6.98 (1H, s, Ar-*H*), 6.76 (1H, d, *J* 7, Ar-*H*), 4.98 (1H, bs, BocN*H*), 4.26 (1H, m, NHC*H*$CH_3$), 1.51 (9H, s, ($CH_3$)$_3$COC(O)NH), 1.45 - 1.40 (3H, d, *J* 7, NHCHC*H*$_3$).

***tert*-Butyl (S)-(1-oxo-1-(2-(4-bromophenyl)hydrazineyl)propan-2-yl)carbamate 51An**

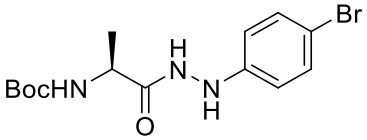


Using the standard procedure provided, *N*-Boc-*L*-Alanine (0.30 g, 1.6 mmol) and 4-bromophenylhydrazine hydrochloride (0.36 g, 1.9 mmol) were transformed into the title compound as an orange solid (0.33 g, 59 %); $\delta_H$ (300 MHz, $CDCl_3$) 8.01 (1H, s, CON*H*NH), 7.26 - 7.24 (2H, d, *J* 9, Ar-*H*), 6.67 - 6.65 (2H, d, *J* 9, Ar-*H*), 4.81 (1H, bs, BocN*H*), 4.16 (1H, m, NHC*H*$CH_3$), 1.41 (9H, s, ($CH_3$)$_3$COC(O)NH), 1.35 – 1.31 (3H, d, *J* 7, NHCHC*H*$_3$).

***tert*-Butyl (S)-(1-oxo-1-(2-(3-(trifluoromethyl)phenyl)hydrazineyl)propan-2-yl)carbamate 51Ao**

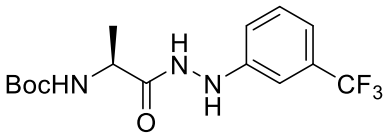


Using the standard procedure provided, *N*-Boc-*L*-Alanine (0.30 g, 1.6 mmol) and 3-trifluoromethylphenyl hydrazine hydrochloride (0.34 g, 1.9 mmol) were transformed into the title compound as a brown solid (0.38 g, 70 %); $\delta_H$ (300 MHz, $CDCl_3$) 8.22 (1H, s, CON*H*NH), 7.25 (1H, dd, *J* 7, 7, Ar-*H*), 7.05 (1H, dd, *J* 7, 1, Ar-*H*), 6.96 (1H, s, Ar-

*H*), 6.92 (1H, d, *J* 7, 2, Ar-*H*), 6.18 (1H, s, CONHN*H*), 4.93 (1H, bs, BocN*H*), 4.20 (1H, m, NHC*H*$CH_3$), 1.39 (9H, s, C(C$H_3$)$_3$), 1.38 – 1.33 (3H, d, *J* 7, NHCHC$H_3$).

**_tert_-Butyl (S)-(1-oxo-1-(2-(4-(trifluoromethyl)phenyl)hydrazineyl)propan-2-yl)carbamate 51Ap**

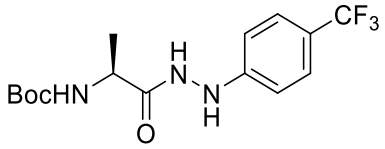


Using the standard procedure provided, *N*-Boc-*L*-Alanine (0.30 g, 1.6 mmol) and 4-trifluoromethylphenyl hydrazine hydrochloride (0.34 g, 1.9 mmol) were transformed into the title compound as an orange solid (0.40 g, 73 %); $\delta_H$ (300 MHz, $CDCl_3$) 8.4 (1H, s, CON*H*NH), 7.48 - 7.46 (2H, d, *J* 9, Ar-*H*), 6.89 - 6.87 (2H, d, *J* 9, Ar-*H*), 5.03 (1H, bs, BocN*H*), 4.29 (1H, m, NHC*H*$CH_3$), 1.50 (9H, s, C(C$H_3$)$_3$), 1.45 – 1.42 (3H, d, *J* 7, NHCHC$H_3$).

**_tert_-butyl (S)-(1-oxo-1-(2-(3-(trifluoromethoxy)phenyl)hydrazineyl)propan-2-yl)carbamate 51Aq**

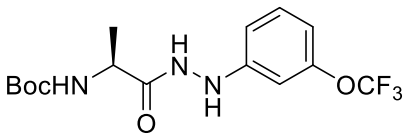


Using the standard procedure provided, *N*-Boc-*L*-Alanine (0.30 g, 1.5 mmol) and 3-trifluoromethoxyphenyl hydrazine hydrochloride (0.36 g, 1.9 mmol) were transformed into the title compound as an yellow powder (0.41 g, 71 %); $R_f$ 0.62 (DCM/EtOAc [4:1]); m.p. 165 – 167 °C; $\nu_{max}$ 3659 (N-H), 3308 (N-H), 2980(C-H), 1681 (C=O), 1614, 1525, 1382, 1325, 1259, 1212, 1153, 1075, 951, 848, 764 $cm^{-1}$; $\delta_H$ (300 MHz, $CDCl_3$) 8.37 (1H, s, CON*H*NH), 7.21 (1H, dd, *J* 8, 8, Ar-*H*), 6.78 – 6.71 (2H, dd, *J* 8, 1, Ar-*H*), 6.65 (1H, s, Ar-*H*), 5.03 (1H, bs, BocN*H*), 4.28 (1H, m, BocNHC*H*), 1.49 (9H, s, (C$H_3$)$_3$COC(O)NH); $\delta_C$ (75 MHz, $CDCl_3$) 172.2 (*C*=ONHNH), 150.3 *(*Ar-O*C*$F_3$), 149.5 (*ipso*-Ar-*C)*, 130.3 (Ar-*C)*, 112.8 (*ipso*-Ar-*C)*, 111.7 (Ar-*C)*, 105.9 (Ar-*C)*, 81.0 ((CH$_3$)$_3$*C*O), 49.0 (BocNH*C*HCH$_3$), 28.3 (*C*H$_3$)$_3$CO), 17.1 (BocNHCH*C*H$_3$); $\delta_F$ (282 MHz, $CDCl_3$) -57.8 (OC*F*$_3$); *m/z* (ES$^+$) 362 (MH$^+$); HRMS (ES$^+$) Found MH$^+$, 362.1338 ($C_{15}H_{21}F_3N_3O_4$ requires 362.1328).

***tert*-butyl (S)-(1-oxo-1-(2-(4-(trifluoromethoxy)phenyl)hydrazineyl)propan-2-yl)carbamate 51Ar**

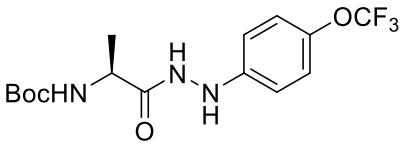

Using the standard procedure provided, *N*-Boc-*L*-Alanine (0.30 g, 1.5 mmol) and 4-trifluoromethoxyphenyl hydrazine hydrochloride (0.36 g, 1.9 mmol) were transformed into the title compound as an orange powder (0.40 g, 71 %); $R_f$ 0.58 (DCM/EtOAc [4:1]); m.p. 160 – 165 °C; $\nu_{max}$ 3305 (N-H), 2981 (C-H), 1614 (C=O), 1525, 1505, 1392, 1370, 1325, 1251, 1211, 1151, 1095, 1076, 997, 848, 763, 632 $cm^{-1}$; $\delta_H$ (300 MHz, $CDCl_3$) 8.28 (1H, s, CON*H*NH), 7.12 – 7.02 (2H, d, *J* 8, Ar-*H*), 6.87 – 6.76 (2H, d, *J* 8, Ar-*H*), 4.97 (1H, bs, BocN*H*), 4.24 (1H, m, BocNHC*H*), 1.49 (9H, s, $(CH_3)_3COC(O)NH$); $\delta_C$ (75 MHz, $CDCl_3$) 172.8 (*C*=ONHNH), 146.6 *(*Ar-O*C*$F_3$), 143.3 (*ipso*-Ar-*C)*, 122.1 (Ar-*C)*, 114.2 (Ar-*C)*, 81.0 ($(CH_3)_3CO$), 48.8 (BocNH*C*HCH$_3$), 28.3 ($CH_3)_3CO$), 17.2 (BocNHCH*C*H$_3$); $\delta_F$ (282 MHz, $CDCl_3$) -58.7 (OC*F*$_3$); ***m/z*** ($ES^+$) 362 ($MH^+$); HRMS ($ES^+$) Found $MH^+$, 362.1338 ($C_{15}H_{21}F_3N_3O_4$ requires 362.1328).

***tert*-Butyl (S)-(4-methyl-1-oxo-1-(2-phenylhydrazineyl)pentan-2-yl)carbamate 51As**

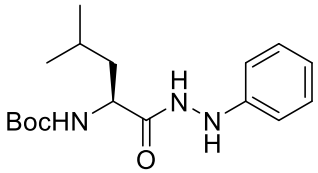

Using the standard procedure provided, *N*-Boc-*L*-Leucine (0.40 g, 1.7 mmol) and phenylhydrazine hydrochloride (0.22 g, 2.0 mmol) were transformed into the title compound as an orange solid (0.42 g, 76 %); $\delta_H$ (300 MHz, $CDCl_3$) 8.09 (1H, bs, CON*H*NH), 7-16 - 7.14 (2H, d, *J* 7, Ar-*H*), 6.82 (1H, t, *J* 7, Ar-*H*), 6.76 - 6.74 (2H, d, *J* 7, Ar-*H*), 4.87 (1H, bd, *J* 8, BocN*H*), 4.12 (1H, m, BocNHC*H*), 1.65 – 1.62 (3H, m, C$H_2$C*H*$(CH_3)_2$), 1.40 (9H, s, $(CH_3)_3CO$), 0.99 – 0.90 (6H, d, *J* 6, $CH_2CH(CH_3)_2$).

***tert*-Butyl (S)-(1-(2-(3-chlorophenyl)hydrazineyl)-4-methyl-1-oxopentan-2-yl)carbamate 51At**

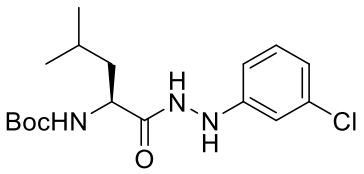


Using the standard procedure provided, *N*-Boc-*L*-Leucine (0.30 g, 1.3 mmol) and 3-chlorophenylhydrazine hydrochloride (0.22 g, 1.5 mmol) were transformed into the title compound as a yellow solid (0.32 g, 70 %); $\delta_H$ (300 MHz, $CDCl_3$) 8.15 (1H, s, CON*H*NH), 7.04 (1H, dd, *J* 7, 7, Ar-C*H*), 6.78 (1H, dd, *J* 7, 1, Ar-C*H*), 6.73 (1H, s, Ar-C*H*), 6.62 (1H, d, *J* 7, Ar-C*H*), 4.85 (1H, bs, BocN*H*), 4.11 (1H, m, BocNHC*H*), 1.68 – 1.63 (3H, m, $CH_2CH(CH_3)_2$), 1.41 (9H, s, $(CH_3)_3CO$), 0.99 – 0.85 (6H, d, *J* 6, $CH_2CH(CH_3)_2$).

**_tert_-Butyl (S)-(1-(2-(4-chlorophenyl)hydrazineyl)-4-methyl-1-oxopentan-2-yl)carbamate 51Au**

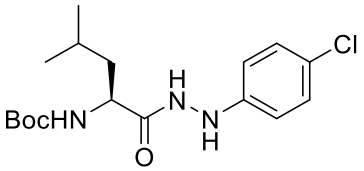


Using the standard procedure provided, *N*-Boc-*L*-Leucine (0.30 g, 1.3 mmol) and 4-chlorophenylhydrazine hydrochloride (0.22 g, 1.6 mmol) were transformed into the title compound as a yellow solid (0.32 g, 69 %); $\delta_H$ (300 MHz, $CDCl_3$) 8.11 (1H, s, CON*H*NH), 7.11 - 7.09 (2H, d, *J* 9, Ar-*H*), 6.70 - 6.68 (2H, d, *J* 9, Ar-*H*), 4.81 (1H, bs, BocN*H*), 4.09 (1H, m, BocNHC*H*), 1.67 – 1.62 (3H, m, $CH_2CH(CH_3)_2$, 1.38 (9H, s, $(CH_3)_3CO$), 0.95 – 0.88 (6H, d, *J* 6, $CH_2CH(CH_3)_2$).

**_tert_-Butyl (S)-(1-(2-(3-bromophenyl)hydrazineyl)-4-methyl-1-oxopentan-2-yl)carbamate 51Av**

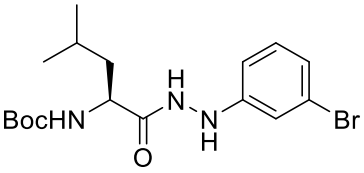


Using the standard procedure provided, *N*-Boc-*L*-Leucine (0.30 g, 1.3 mmol) and 3-bromophenylhydrazine hydrochloride (0.29 g, 1.6 mmol) were transformed into the title compound as a yellow solid (0.46 g, 89 %); $\delta_H$ (300 MHz, $CDCl_3$) 8.06 (1H, s, CON*H*NH), 6.98 (1H, dd, *J* 7, 7, Ar-C*H*), 6.95 (1H, dd, *J* 7, 1, Ar-C*H*), 6.89 (1H, s, Ar-

C*H*), 6.67 (1H, dd, *J* 7, 2, Ar-C*H*), 4.80 (1H, bs, BocN*H*), 4.10 (1H, m, BocNHC*H*), 1.68 – 1.62 (3H, m, C$H_2$C*H*($CH_3$)$_2$), 1.40 (9H, s, (C$H_3$)$_3$CO), 0.99 – 0.85 (6H, d, *J* 6, $CH_2$CH(C$H_3$)$_2$).

***tert*-Butyl (S)-(1-(2-(4-bromophenyl)hydrazineyl)-4-methyl-1-oxopentan-2-yl)carbamate 51Aw**

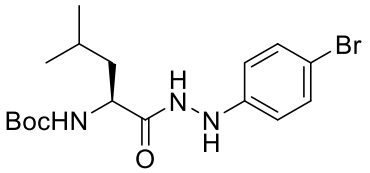


Using the standard procedure provided, *N*-Boc-*L*-Leucine (0.30 g, 1.3 mmol) and 4-bromophenylhydrazine hydrochloride (0.29 g, 1.6 mmol) were transformed into the title compound as an orange solid (0.43 g, 83 %); $\delta_H$ (300 MHz, $CDCl_3$) 8.23 (1H, s, CON*H*NH), 7.23 - 7.21 (2H, d, *J* 9, Ar-*H*), 6.64 - 6.62 (2H, d, *J* 9, Ar-*H*), 4.86 (1H, bs, BocN*H*), 4.10 (1H, m, BocNHC*H*), 1.65 – 1.60 (3H, m, C$H_2$C*H*($CH_3$)$_2$, 1.40 (9H, s, (C$H_3$)$_3$CO), 0.90 – 0.85 (6H, d, *J* 6, $CH_2$CH(C$H_3$)$_2$).

***tert*-Butyl (S)-(4-methyl-1-oxo-1-(2-(3(trifluoromethyl)phenyl)hydrazineyl)pentan-2-yl)carbamate 51Ax**

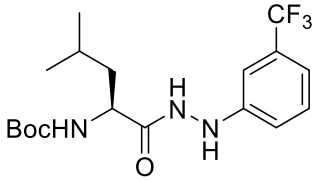


Using the standard procedure provided, *N*-Boc-*L*-Leucine (0.30 g, 1.3 mmol) and 3-trifluoromethylphenylhydrazine hydrochloride (0.27 g, 1.6 mmol) were transformed into the title compound as a yellow solid (0.40 g, 80 %); $\delta_H$ (300 MHz, $CDCl_3$) 8.22 (1H, s, CON*H*NH), 7.23 (1H, dd, *J* 7, 7, Ar-*H*), 7.06 (1H, dd, *J* 7, 1, Ar-*H*), 6.96 (1H, s, Ar-*H*), 6.90 (1H, d, *J* 7, Ar-*H*), 6.23 (1H, s, CONHN*H*), 4.85 (1H, bs, BocN*H*), 4.13 (1H, m, BocNHC*H*), 1.66 – 1.62 (3H, m, C$H_2$C*H*($CH_3$)$_2$), 1.40 (9H, s, (C$H_3$)$_3$CO), 0.90 – 0.85 (6H, d, *J* 6, $CH_2$CH(C$H_3$)$_2$).

***tert*-Butyl (S)-(4-methyl-1-oxo-1-(2-(4(trifluoromethyl)phenyl)hydrazineyl)pentan-2-yl)carbamate 51Ay**

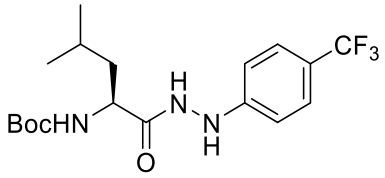

Using the standard procedure provided, *N*-Boc-*L*-Leucine (0.30 g, 1.3 mmol) and 4-trifluoromethylphenylhydrazine hydrochloride (0.27 g, 1.6 mmol) were transformed into the title compound as a yellow solid (0.39 g, 78 %); $\delta_H$ (300 MHz, $CDCl_3$) 8.25 (1H, s, CON*H*NH), 7.39 - 7.37 (2H, d, *J* 9, Ar-*H*), 6.79 - 6.77 (2H, d, *J* 9, Ar-*H*), 6.13 (1H, s, CONHN*H*), 4.88 (1H, bs, BocN*H*), 4.12 (1H, m, BocNHC*H*), 1.67 – 1.61 (3H, m, C$H_2$C*H*($CH_3$)$_2$), 1.42 (9H, s, (C$H_3$)$_3$CO), 0.95 – 0.88 (6H, d, *J* 6, $CH_2CH(CH_3)_2$).

**_tert_-butyl (S)-(4-methyl-1-oxo-1-(2-(3-(trifluoromethoxy)phenyl)hydrazineyl)pentan-2-yl)carbamate 51Az**

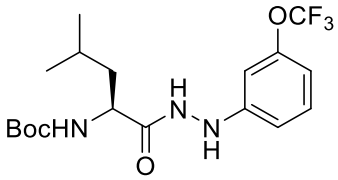

Using the standard procedure provided, *N*-Boc-*L*-Leucine (0.30 g, 1.29 mmol) and 3-trifluoromethoxyphenylhydrazine hydrochloride (0.29 g, 1.55 mmol) were transformed following work up with $Et_2O$ into the title compound which was isolated as a yellow powder (0.48 g, 93%); $R_f$ 0.50 (DCM/EtOAc [4:1]); m.p. 175 – 177 °C; $\nu_{max}$ 3304 (N-H), 2981 (C-H), 1662 (C=O), 1613, 1525, 1504, 1392, 1369, 1325, 1250, 1212, 1152, 1049, 848, 764, 632, 506 $cm^{-1}$; $\delta_H$ (300 MHz, $CDCl_3$) 8.33 (1H, bs, CON*H*NH), 7.20 (1H, dd, *J* 8, 8, Ar-*H*), 6.80 – 6.72 (2H, dd, *J* 8, 1, Ar-*H*), 6.66 (1H, s, Ar-*H*), 4.95 (1H, bs, BocN*H*CH), 4.20 (1H, m, BocNHC*H*), 1.79 – 1.57 (3H, m, C$H_2$CH($CH_3$)$_2$, $CH_2$C*H*($CH_3$)$_2$), 1.44 (9H, s, (C$H_3$)$_3$CO), 1.08 – 0.85 (6H, t, *J* 6, $CH_2CH(CH_3)_2$); $\delta_C$ (75 MHz, $CDCl_3$) 172.7 (*C*=ONHNH), 150.1 (*C*=ONH), 149.4 (Ar-O*C*$F_3$), 130.3 (Ar-*C*), 112.8 (Ar-*C*), 111.7 (*ipso*-Ar-*C*), 105.8 (Ar-*C*), 80.7 (($CH_3$)$_3$*C*O), 51.4 (BocNH*C*H), 40.4 (*C*$H_2$CH($CH_3$)$_2$), 28.3 ((*C*$H_3$)$_3$CO), 24.8 ($CH_2$*C*H($CH_3$)$_2$), 22.5 ($CH_2CH$(*C*$H_3$)$_2$), 21.8 ($CH_2CH$(*C*$H_3$)$_2$); $\delta_F$ (282 MHz, $CDCl_3$) -57.8 (OC*F*$_3$); ***m/z*** ($ES^+$) 404 ($MH^+$); HRMS ($ES^+$) Found $MH^+$, 404.1796 ($C_{18}H_{26}N_3O_4F_3$ requires 404.1797).

**_tert_-butyl (S)-(4-methyl-1-oxo-1-(2-(4-(trifluoromethoxy)phenyl)hydrazineyl)pentan-2-yl)carbamate 51Ba**

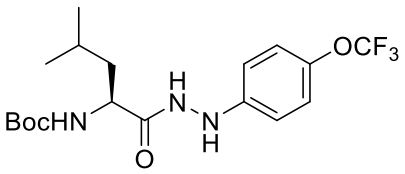

Using the standard procedure provided, *N*-Boc-*L*-Leucine (0.30 g, 1.29 mmol) and 4-trifluoromethoxyphenylhydrazine hydrochloride (0.29 g, 1.55 mmol) were transformed following work up with $Et_2O$ into the title compound which was isolated as a yellow powder (0.48 g, 93 %); $R_f$ 0.54 (DCM/EtOAc [4:1]); m.p. 168 – 170 °C;$\nu_{max}$ 3304 (N-H), 2981 (C-H), 1662 (C=O), 1613, 1525, 1504, 1392, 1369, 1325, 1250, 1212, 1152, 1049, 848, 764, 632, 506 $cm^{-1}$; $\delta_H$ (300 MHz, $CDCl_3$) 8.44 (1H, bs, CON*H*NH), 7.11 – 7.01 (2H, d, *J* 8, Ar-*H*), 6.85 – 6.76 (2H, d, *J* 8, Ar-*H*), 5.01 (1H, bs, BocN*H*CH), 4.22 (1H, m, BocNHC*H*), 1.76 – 1.58 (3H, m, C*H*$_2$CH(CH$_3$)$_2$, CH$_2$C*H*(CH$_3$)$_2$), 1.47 (9H, s, (C*H*$_3$)$_3$CO), 1.02 – 0.89 (6H, t, *J* 6, CH$_2$CH(C*H*$_3$)$_2$); $\delta_C$ (75 MHz, $CDCl_3$) 172.7 (*C*=ONHNH), 156.4 (*C*=ONH), 146.5 (Ar-O*C*F$_3$), 143.2 (*ipso*-Ar-*C*), 122.3 (Ar-*C*), 114.2 (Ar-*C*), 80.5 ((CH$_3$)$_3$*C*O), 51.4 (BocNH*C*H), 40.4 (*C*H$_2$CH(CH$_3$)$_2$), 28.5 ((*C*H$_3$)$_3$CO), 24.7 (CH$_2$*C*H(CH$_3$)$_2$), 22.5 (CH$_2$CH(*C*H$_3$)$_2$), 21.8 (CH$_2$CH(*C*H$_3$)$_2$); $\delta_F$ (282 MHz, $CDCl_3$) -58.3 (OC*F*$_3$); *m/z* ($ES^+$) 404 ($MH^+$); HRMS ($ES^+$) Found $MH^+$, 404.1796 ($C_{18}H_{26}N_3O_4F_3$ requires 404.1797).

**_tert_-butyl (S)-(4-(methylthio)-1-oxo-1-(2-phenylhydrazineyl)butan-2-yl)carbamate 51Bb**

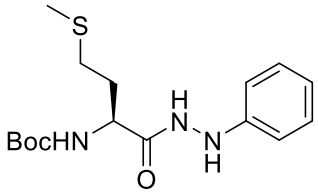

Using the standard procedure provided, *N*-Boc-*L*-Methionine (0.30 g, 1.2 mmol) and phenylhydrazine (0.15 ml, 1.4 mmol) were transformed following trituration with $Et_2O$ into the title compound which was isolated as a white solid (0.31 g, 77 %); $\delta_H$ (300 MHz, $CDCl_3$) 8.00 (1H, bs, CON*H*NH), 7.18 – 7.11 (2H, t, *J* 7, Ar-*H*), 6.85 (1H, t, *J* 7, Ar-*H*), 6.79 – 6.73 (2H, dd, *J* 8, *1,* Ar-*H*), 5.04 (1H, d, *J* 8, BocN*H*CH), 4.28 (1H, m, BocNHC*H*), 2.57 – 2.47 (2H, m, CHCH$_2$C*H*$_2$S), 2.04 (3H, s, CH$_2$CH$_2$SC*H*$_3$), 1.96 – 1.85 (2H, m, C*H*$_2$CH$_2$S), 1.49 (9H, s, (C*H*$_3$)$_3$CO).

***tert*-Butyl (S)-(1-(2-(3-chlorophenyl)hydrazineyl)-4-(methylthio)-1-oxobutan-2-yl)carbamate 51Bc**

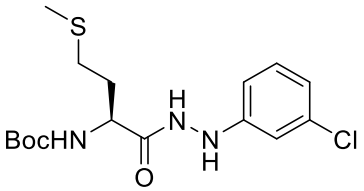


Using the standard procedure provided, *N*-Boc-*L*-Methionine (0.30 g, 1.2 mmol) and 3-chlorophenylhydrazine hydrochloride (0.20 g, 1.4 mmol) were transformed into the title compound which was isolated as a brown powder (0.39 g, 88%); $\delta_H$ (300 MHz, $CDCl_3$) 8.09 (1H, bs, CON*H*NH), 7.04 (1H, m, Ar-*H*), 6.79 (1H, d, *J* 7, Ar-*H*), 6.74 (1H, dd, *J* 2, 2, Ar-*H*), 6.63 (1H, dd, *J* 2, 1, Ar-*H*), 5.04 (1H, bs, BocN*H*CH), 4.28 (1H, m, BocNHC*H*), 2.63 – 2.56 (2H, m, $CH_2CH_2$S), 2.13 (3H, s, $CH_2CH_2SCH_3$), 2.03 – 1.90 (2H, m, $CH_2CH_2$S), 1.49 (9H, s, $(CH_3)_3CO$).

***tert*-Butyl (S)-(1-(2-(4-chlorophenyl)hydrazineyl)-4-(methylthio)-1-oxobutan-2-yl)carbamate 51Bd**

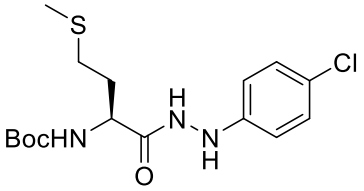


Using the standard procedure provided, *N*-Boc-*L*-Methionine (0.30 g, 1.2 mmol) and 4-chlorophenylhydrazine hydrochloride (0.20 g, 1.4 mmol) were transformed into the title compound which was isolated as an orange gum (0.42 g, 94%); $\delta_H$ (300 MHz, $CDCl_3$) 8.12 (1H, bs, CON*H*NH), 7.12 – 7.05 (2H, d, *J* 8, Ar-*H*), 6.71 – 6.64 (2H, d, *J* 8, Ar-*H*), 5.06 (1H, bs, BocN*H*CH), 4.26 (1H, m, BocNHC*H*), 2.55 – 2.46 (2H, m, $CH_2CH_2$S), 2.05 (3H, s, $CH_2CH_2SCH_3$), 1.96 – 1.85 (2H, m, $CH_2CH_2$S), 1.49 (9H, s, $(CH_3)_3CO$).

***tert*-Butyl (S)-(1-(2-(3-bromophenyl)hydrazineyl)-4-(methylthio)-1-oxobutan-2-yl)carbamate 51Be**

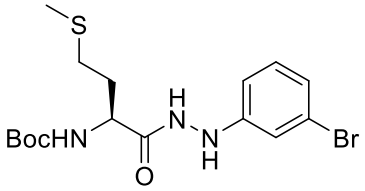


Using the standard procedure provided, *N*-Boc-*L*-Methionine (0.30 g, 1.2 mmol) and 3-chlorophenylhydrazine hydrochloride (0.27 g, 1.4 mmol) were transformed into the title compound which was isolated as a brown powder (0.42 g, 84 %); $\delta_H$ (300 MHz, $CDCl_3$) 8.23 (1H, bs, CON*H*NH), 7.05 (1H, d, *J* 7, Ar-*H*), 7.01 (1H, s, Ar-*H*), 6.97 (1H, dd, *J* 2, 2, Ar-*H*), 6.74 (1H, dd, *J* 7, 2, Ar-*H*), 5.04 (1H, bs, BocN*H*CH), 4.28 (1H, m, BocNHC*H*), 2.62 – 2.52 (2H, m, $CH_2CH_2$S), 2.11 (3H, s, $CH_2CH_2SCH_3$), 2.00 – 1.90 (2H, m, $CH_2CH_2$S), 1.49 (9H, s, $(CH_3)_3CO$).

**_tert_-Butyl (S)-(1-(2-(4-bromophenyl)hydrazineyl)-4-(methylthio)-1-oxobutan-2-yl)carbamate 51Bf**

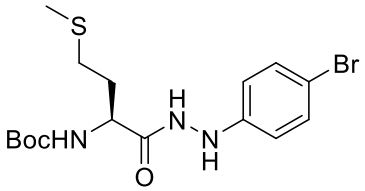


Using the standard procedure provided, *N*-Boc-*L*-Methionine (0.30 g, 1.2 mmol) and 4-bromophenylhydrazine hydrochloride (0.27 g, 1.4 mmol) were transformed into the title compound which was isolated as an brown solid (0.35 g, 70 %); $\delta_H$ (300 MHz, $CDCl_3$) 8.18 (1H, bs, CON*H*NH), 7.38 – 7.30 (2H, d, *J* 8, Ar-*H*), 6.77 – 6.69 (2H, d, *J* 8, Ar-*H*), 5.15 (1H, bs, BocN*H*CH), 4.35 (1H, m, BocNHC*H*), 2.63 – 2.56 (2H, m, $CH_2CH_2$S), 2.14 (3H, s, $CH_2CH_2SCH_3$), 2.03 – 1.90 (2H, m, $CH_2CH_2$S), 1.49 (9H, s, $(CH_3)_3CO$).

**_tert_-Butyl (S)-(1-(2-(3-trifluoromethylphenyl)hydrazineyl)-4-(methylthio)-1-oxobutan-2-yl)carbamate 51Bg**

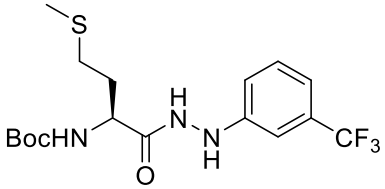

Using the standard procedure provided, *N*-Boc-*L*-Methionine (0.30 g, 1.2 mmol) and 3-trifluoromethylphenylhydrazine hydrochloride (0.25 g, 1.4 mmol) were transformed into the title compound which was isolated as an orange powder (0.43 g, 88%); $\delta_H$ (300 MHz, $CDCl_3$) 8.37 (1H, bs, CON*H*NH), 7.31 (1H, dd, *J* 8, *7,* Ar-*H*), 7.13 (1H, dd, *J* 8, 1, Ar-*H*), 7.04 (1H, s, Ar-*H*), 6.97 (1H, d, *J* 8, Ar-*H*), 5.17 (1H, bs, BocN*H*CH), 4.37 (1H, m, BocNHC*H*), 2.63 – 2.48 (2H, m, $CH_2CH_2S$), 2.10 (3H, s, $CH_2CH_2SCH_3$), 2.00 – 1.85 (2H, m, $CH_2CH_2S$), 1.47 (9H, s, $(CH_3)_3CO$).

**_tert_-Butyl (S)-(1-(2-(4-trifluoromethylphenyl)hydrazineyl)-4-(methylthio)-1-oxobutan-2-yl)carbamate 51Bh**

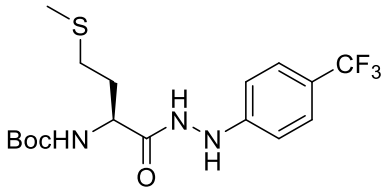


Using the standard procedure provided, *N*-Boc-*L*-Methionine (0.30 g, 1.2 mmol) and 4-trifluoromethylphenylhydrazine hydrochloride (0.25 g, 1.4 mmol) were transformed into the title compound which was isolated as an orange powder (0.43 g, 88%); $\delta_H$ (300 MHz, $CDCl_3$) 8.36 (1H, bs, CON*H*NH), 7.48 – 7.41 (2H, d, *J* 8, Ar-*H*), 6.90 – 6.79 (2H, d, *J* 8, Ar-*H*), 5.18 (1H, bs, BocN*H*CH), 4.37 (1H, m, BocNHC*H*), 2.64 – 2.48 (2H, m, $CH_2CH_2S$), 2.11 (3H, s, $CH_2CH_2SCH_3$), 2.02 – 1.87 (2H, m, $CH_2CH_2S$), 1.45 (9H, s, $(CH_3)_3CO$).

**_tert_-butyl (S)-(4-(methylthio)-1-oxo-1-(2-(3-(trifluoromethoxy)phenyl)hydrazineyl)butan-2-yl)carbamate 51Bi**

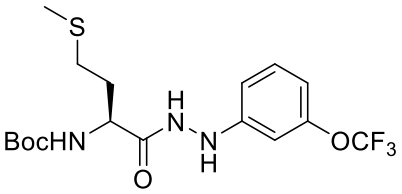


Using the standard procedure provided, *N*-Boc-*L*-Methionine (0.30 g, 1.20 mmol) and 3-trifluoromethoxyphenylhydrazine hydrochloride (0.27 g, 1.44 mmol) were transformed following work up with $Et_2O$ into the title compound which was isolated as a yellow solid (0.41 g, 82%); $R_f$ 0.58 (DCM/EtOAc [4:1]); m.p. 150 – 155 °C; $\nu_{max}$ 3252

(N-H), 2980 (C-H), 1645 (C=O), 1614, 1488, 1445, 1382, 1255, 1154, 1076, 1028, 955, 765, 687, 634 $cm^{-1}$; $\delta_H$ (300 MHz, $CDCl_3$) 8.40 (1H, bs, CON*H*NH), 7.11 (1H, dd, *J* 7, 7, Ar-*H*), 7.11 (1H, dd, *J* 7, 1, Ar-*H*), 6.69 – 6.60 (2H, dd, *J* 8, 2, Ar-*H*), 6.58 (1H, s, Ar-*H*), 5.16 (1H, bs, BocN*H*CH), 4.31 (1H, m, BocNHC*H*), 2.54 -2.43 (2H, t, *J* 7, $CH_2CH_2$S), 2.03 (3H, s, $CH_2CH_2SCH_3$), 1.94 – 1.73 (2H, m, $CH_2CH_2$S), 1.36 (9H, s, $(CH_3)_3CO$); $\delta_C$ (75 MHz, $CDCl_3$) 172.0 (*C*=ONHNH), 155.9 (*C*=ONH), 149.3 (Ar-O*C*$F_3$), 130.3 (Ar-*C*), 112.8 (Ar-*C*), 111.5 (Ar-*C*), 105.9 (Ar-*C*), 80.9 ($(CH_3)_3CO$), 51.9 (BocNH*C*H), 30.6 ($CH_2CH_2SCH_3$), 30.1 ($CH_2CH_2SCH_3$), 28.3 ($(CH_3)_3CO$), 15.2 ($CH_2CH_2SCH_3$); $\delta_F$ (282 MHz, $CDCl_3$) -57.8 ($CF_3$); *m/z* ($ES^+$) 422 ($MH^+$); HRMS ($ES^+$) Found $MH^+$, 422.1337 ($C_{17}H_{25}N_3O_4F_3S$ requires 422.1361).

**_tert_-butyl (S)-(4-(methylthio)-1-oxo-1-(2-(3-(trifluoromethoxy)phenyl)hydrazineyl)butan-2-yl)carbamate 51Bj**

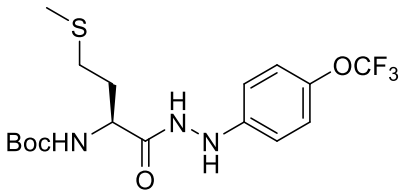


Using the standard procedure provided, *N*-Boc-*L*-Methionine (0.30 g, 1.20 mmol) and 4-trifluoromethoxyphenylhydrazine hydrochloride (0.27 g, 1.44 mmol) were transformed following work up with $Et_2O$ into the title compound which was isolated as a yellow solid (0.36 g, 72%); $R_f$ 0.62 (DCM/EtOAc [4:1]); m.p. 140 – 145 °C; $\nu_{max}$ 3252 (N-H), 2980 (C-H), 1661 (C=O), 1610, 1506, 1450, 1392, 1368, 1252, 1221, 1199, 1153, 1048, 1024, 996,861, 747, 698, 608 $cm^{-1}$; $\delta_H$ (300 MHz, $CDCl_3$) 8.42 (1H, bs, CON*H*NH), 7.07 – 6.90 (2H, d, *J* 9, Ar-*H*), 6.79 – 6.68 (2H, d, *J* 9, Ar-*H*), 5.20 (1H, bs, BocN*H*CH), 4.31 (1H, m, BocNHC*H*), 2.55 - 2.43 (2H, t, *J* 7, $CH_2CH_2$S), 2.03 (3H, s, $CH_2CH_2SCH_3$), 1.93 – 1.71 (2H, m, $CH_2CH_2$S), 1.35 (9H, s, $(CH_3)_3CO$); $\delta_C$ (75 MHz, $CDCl_3$) 172.2 (*C*=ONHNH), 155.9 (*C*=ONH), 146.1 (Ar-O*C*$F_3$), 143.5 (*ipso*-Ar-*C*),122.1 (Ar-*C*), 114.3 (Ar-*C*), 80.7 ($(CH_3)_3CO$), 51.2 (BocNH*C*H), 30.7 ($CH_2CH_2SCH_3$), 30.1 ($CH_2CH_2SCH_3$), 28.3 ($(CH_3)_3CO$), 15.2 ($CH_2CH_2SCH_3$); $\delta_F$ (282 MHz, $CDCl_3$) -58.3 ($CF_3$); *m/z* ($ES^+$) 422 ($MH^+$); HRMS ($ES^+$) Found $MH^+$, 422.1421 ($C_{17}H_{25}N_3O_4F_3S$ requires 422.1361).

***tert*-butyl (S)-(1-oxo-3-phenyl-1-(2-phenylhydrazineyl)propan-2-yl)carbamate 51Bk**

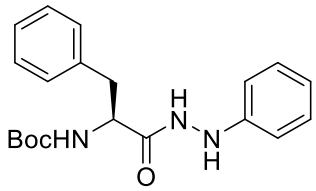


Using the standard procedure provided, *N*-Boc-*L*-Phenylalanine (0.30 g, 1.1 mmol) and phenylhydrazine hydrochloride (0.36 g, 1.3 mmol) were transformed into the title compound which was isolated as a yellow powder (0.37 g, 90%); $\delta_H$ (300 MHz, $CDCl_3$) 7.68 (1H, bs, CON*H*NH), 7.41 - 7.29 (3H, m, Ar-*H*), 7.27 – 7.21 (2H, dd*, J* 7, 2, Ar-*H*), 7.21 – 7.12 (2H, t*, J* 7, Ar-*H*), 6.89 (1H, t*, J* 7, Ar-*H*), 6.69 – 6.57 (2H, d*, J* 7, Ar-*H*), 5.01 (1H, bs, BocN*H*CH), 4.42 (1H, m, BocNHC*H*), 3.17 – 3.05 (2H, d, *J* 8, Ar-C$H_2$), 1.43 (9H, s, (C$H_3$)$_3$CO).

***tert*-butyl (S)-(1-(2-(3-chlorophenyl)hydrazineyl)-1-oxo-3-phenylpropan-2-yl)carbamate 51Bl**

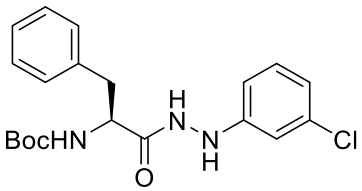


Using the standard procedure provided, *N*-Boc-*L*-Phenylalanine (0.90 g, 3.4 mmol) and 3-chlorophenylhydrazine hydrochloride (0.58 g, 4.0 mmol) were transformed into the title compound which was isolated as a yellow powder (0.39 g, 83%); $\delta_H$ (300 MHz, $CDCl_3$) 7.77 (1H, bs, CON*H*NH), 7.38 - 7.27 (3H, m, Ar-*H*), 7.24 – 7.21 (2H, m*,* Ar-*H*), 7.22 – 7.12 (2H, t, *J* 7, Ar-*H*), 6.89 (1H, t, *J* 7, Ar-*H*), 6.64 (1H, d, *J* 7, Ar-*H*), 5.02 (1H, bs, BocN*H*CH), 4.39 (1H, m, BocNHC*H*), 3.16 – 3.02 (2H, d, *J* 8, Ar-C$H_2$), 1.43 (9H, s, (C$H_3$)$_3$CO).

***tert*-butyl (S)-(1-(2-(4-chlorophenyl)hydrazineyl)-1-oxo-3-phenylpropan-2-yl)carbamate 51Bm**

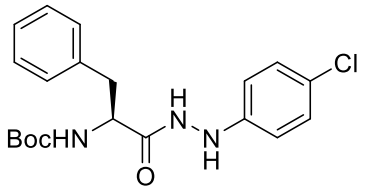


Using the standard procedure provided, *N*-Boc-*L*-Phenylalanine (0.30 g, 1.1 mmol) and 4-chlorophenylhydrazine hydrochloride (0.19 g,1.3 mmol) were transformed into the title compound which was isolated as an orange powder (0.31 g, 71 %); $\delta_H$ (300 MHz, $CDCl_3$) 7.66 (1H, bs, CON*H*NH), 7.36 - 7.29 (3H, m, Ar-*H*), 7.23 – 7.17 (2H, dd, *J* 7, 2, Ar-*H*), 7.13 – 7.05 (2H, d*, J* 8, Ar-*H*), 6.54 – 6.46 (2H, d*, J* 8, Ar-*H*), 5.00 (1H, bs, BocN*H*CH), 4.41 (1H, m, BocNHC*H*), 3.14 – 3.06 (2H, d, *J* 7, Ar-C$H_2$), 1.45 (9H, s, (C$H_3$)$_3$CO).

**_tert_-butyl (S)-(1-(2-(3-bromophenyl)hydrazineyl)-1-oxo-3-phenylpropan-2-yl)carbamate 51Bn**

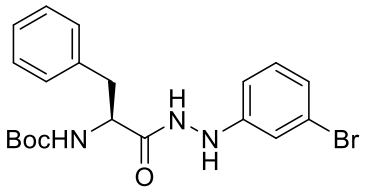


Using the standard procedure provided, *N*-Boc-*L*-Phenylalanine (0.90 g, 3.4 mmol) and 3-bromophenylhydrazine hydrochloride (0.76 g, 4.0 mmol) were transformed into the title compound which was isolated as a yellow powder (1.34 g, 88 %); $\delta_H$ (300 MHz, $CDCl_3$) 7.83 (1H, bs, CON*H*NH), 7.29 - 7.20 (3H, m, Ar-*H*), 7.15 – 7.08 (2H, m*,* Ar-*H*), 6.96 – 6.85 (2H, m*,* Ar-*H*), 6.75 (1H, s, Ar-*H*), 6.43 (1H, s, Ar-*H*), 5.03 (1H, bs, BocN*H*CH), 4.36 (1H, m, BocNHC*H*), 3.07 – 2.94 (2H, d, *J* 8, Ar-C$H_2$), 1.34 (9H, s, (C$H_3$)$_3$CO).

**_tert_-butyl (S)-(1-(2-(4-bromophenyl)hydrazineyl)-1-oxo-3-phenylpropan-2-yl)carbamate 51Bo**

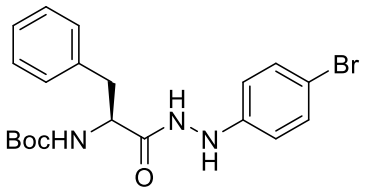

Using the standard procedure provided, *N*-Boc-*L*-Phenylalanine (0.30 g, 1.1 mmol) and 4-bromophenylhydrazine hydrochloride (0.25 g,1.3 mmol) were transformed into the title compound which was isolated as a yellow powder (0.42 g, 86 %); $\delta_H$ (300 MHz, $CDCl_3$) 7.67 (1H, bs, CON*H*NH), 7.35 - 7.21 (4H, m, Ar-*H*), 7.16 – 7.07 (2H, m, Ar-*H*), 6.48 – 6.27 (2H, d*, J* 7, Ar-*H*), 4.96 (1H, bs, BocN*H*CH), 4.32 (1H, m, BocNHC*H*), 3.08 – 2.97 (2H, d, *J* 7, Ar-C$H_2$), 1.33 (9H, s, (C$H_3$)$_3$CO).

***tert*-butyl (S)-(1-oxo-3-phenyl-1-(2-(3-(trifluoromethyl)phenyl)hydrazineyl)propan-2-yl)carbamate 51Bp**

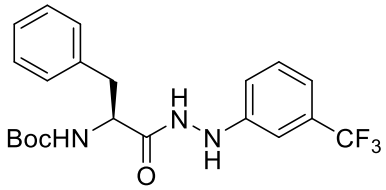


Using the standard procedure provided, *N*-Boc-*L*-Phenylalanine (0.30 g, 1.1 mmol) and 3-trifluoromethylphenylhydrazine hydrochloride (0.24 g, 1.3 mmol) were transformed into the title compound which was isolated as a yellow powder (0.37 g, 77 %); $\delta_H$ (300 MHz, $CDCl_3$) 7.82 (1H, bs, CON*H*NH), 7.34 - 7.27 (3H, m, Ar-*H*), 7.23 – 7.18 (2H, m*,* Ar-*H*), 7.08 – 6.95 (2H, d*, J* 7, Ar-*H*), 6.95 (1H, s, Ar-*H*), 6.74 (1H, d*, J* 7, Ar-*H*), 5.01 (1H, bs, BocN*H*CH), 4.43 (1H, m, BocNHC*H*), 3.15 – 3.05 (2H, d, *J* 8, Ar-C$H_2$), 1.43 (9H, s, (C$H_3$)$_3$CO).

***tert*-butyl (S)-(1-oxo-3-phenyl-1-(2-(4-(trifluoromethyl)phenyl)hydrazineyl)propan-2-yl)carbamate 51Bq**

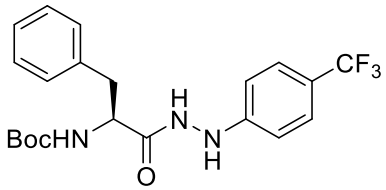


Using the standard procedure provided, *N*-Boc-*L*-Phenylalanine (0.30 g, 1.1 mmol) and 4-trifluoromethylphenylhydrazine hydrochloride (0.24 g, 1.3 mmol) were transformed into the title compound which was isolated as a yellow powder (0.26 g, 54 %); $\delta_H$ (300 MHz, $CDCl_3$) 7.81 (1H, bs, CON*H*NH), 7.46 - 7.28 (5H, m, Ar-*H*), 7.24 – 7.15 (2H, dd*, J* 7, 2, Ar-*H*), 6.65 – 6.53 (2H, d*, J* 7, Ar-*H*), 5.01 (1H, bs, BocN*H*CH), 4.41 (1H, m, BocNHC*H*), 3.17 – 3.02 (2H, d, *J* 8, Ar-C$H_2$), 1.43 (9H, s, (C$H_3$)$_3$CO).

***tert*-butyl (S)-(1-oxo-3-phenyl-1-(2-(3-(trifluoromethoxy)phenyl)hydrazineyl)propan-2-yl)carbamate 51Br**

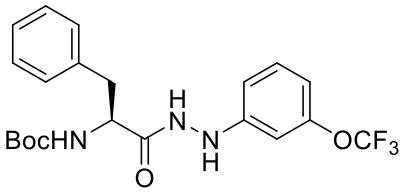


Using the standard procedure provided, *N*-Boc-*L*-Phenylalanine (0.30 g, 1.13 mmol) and 3-trifluoromethoxyphenylhydrazine hydrochloride (0.26 g, 1.35 mmol) were transformed following work up with $Et_2O$ into the title compound which was isolated as a yellow solid (0.35 g, 70 %); $R_f$ 0.56 (DCM/EtOAc [4:1]); m.p. 180 – 183 °C; $\nu_{max}$ 3255 (N-H), 2980 (C-H), 1660 (C=O), 1611, 1505, 1393, 1369, 1258, 1220, 1153, 1062, 1022, 995, 843, 754, 699 $cm^{-1}$; $\delta_H$ (300 MHz, $CDCl_3$) 7.78 (1H, bs, CON*H*NH), 7.36 – 7.29 (3H, m, Ar-*H*), 7.25 – 7.17 (2H, m, Ar-*H*), 7.05 - 6.97 (2H, d, *J* 7, Ar-*H*), 6.64 – 6.54 (2H, d, *J* 7, Ar-*H*), 5.04 (1H, bs, BocN*H*CH), 4.42 (1H, q, *J* 7, BocNHC*H*), 3.16 – 3.06 (2H, d, *J* 7, Ar-C$H_2$), 1.41 (9H, s, ($CH_3$)$_3$CO); $\delta_C$ (75 MHz, $CDCl_3$) 171.7 (*C*=ONHNH), 149.3 (Ar-O*C*$F_3$), 135.9 (*ipso*-Ar-*C*), 129.3 (*ipso*-Ar-*C*), 129.3 (Ar-*C*), 129.0 (Ar-*C*), 121.9 (Ar-*C*), 114.2 (Ar-*C*), 80.9 (($CH_3$)$_3$*C*O), 56.8 (BocNH*C*H), 37.6 (Ar-*C*$H_2$), 28.3 (($CH_3$)$_3$CO); $\delta_F$ (282 MHz, $CDCl_3$) -57.8 (OC*F*$_3$); ***m/z*** ($ES^+$) 438 ($MH^+$); HRMS ($ES^+$) Found $MH^+$, 438.1652 ($C_{21}H_{25}N_3O_4F_3$ requires 438.1641).

***tert*-butyl (S)-(1-oxo-3-phenyl-1-(2-(4-(trifluoromethoxy)phenyl)hydrazineyl)propan-2-yl)carbamate 51Bs**

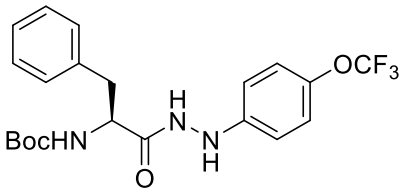


Using the standard procedure provided, *N*-Boc-*L*-Phenylalanine (0.30 g, 1.13 mmol) and 4-trifluoromethoxyphenylhydrazine hydrochloride (0.26 g, 1.35 mmol) were transformed following work up with $Et_2O$ into the title compound which was isolated as a yellow solid (0.35 g, 71 %); $R_f$ 0.52 (DCM/EtOAc [4:1]); m.p. 173 – 178 °C; $\nu_{max}$ 3333 (N-H), 2980 (C-H), 1615 (C=O), 1526, 1392, 1251, 1156, 1046, 992, 869, 762, 699 cm-

[1]; $\delta_H$ (300 MHz, $CDCl_3$) 7.81 (1H, bs, CON*H*NH), 7.27 – 7.20 (3H, m, Ar-*H*), 7.16 – 7.12 (2H, dd, *J* 7, 2, Ar-*H*), 7.06 (1H, t, *J* 7, Ar-*H*), 6.63 (1H, d, *J* 7, Ar-*H*), 6.44 (1H, d, *J* 7, Ar-*H*), 6.40 (1H, s, Ar-*H*), 4.99 (1H, bs, BocN*H*CH), 4.34 (1H, q, *J* 7, BocNHC*H*), 3.05 – 2.97 (2H, d, *J* 7, Ar-C$H_2$), 1.33 (9H, s, (C$H_3$)$_3$CO); $\delta_C$ (75 MHz, $CDCl_3$) 171.7 (*C*=ONHNH), 147.4 (Ar-O*C*$F_3$), 135.9 (*ipso*-Ar-*C*), 129.3 (*ipso*-Ar-*C*), 130.3 (Ar-*C*), 129.3 (Ar-*C*), 128.7 (Ar-*C*), 127.1 (Ar-*C*), 112.6 (Ar-*C*), 111.6 (Ar-*C*), 106.2 (Ar-*C*), 81.0 ((CH$_3$)$_3$*C*O), 54.5 (BocNH*C*H), 37.6 (Ar-*C*H$_2$), 28.2 ((*C*H$_3$)$_3$CO); $\delta_F$ (282 MHz, $CDCl_3$) -58.4 (C*F*$_3$); *m/z* ($ES^+$) 438 ($MH^+$); HRMS ($ES^+$) Found $MH^+$, 438.1597 ($C_{21}H_{25}N_3O_4F_3$ requires 438.1611).

**_tert_-butyl (S)-(1-oxo-4-phenyl-1-(2-phenylhydrazineyl)butan-2-yl)carbamate 51Bt**

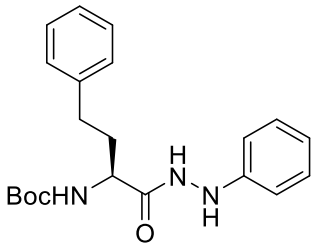


Using the standard procedure provided, *N*-Boc-*L*-homophenylalanine (0.30 g, 2.7 mmol) and phenylhydrazine hydrochloride (0.77 g, 2.7 mmol) were transformed into the title compound which was isolated as a yellow powder (0.89 g, 87 %); δH (300 MHz, $CDCl_3$) 8.17 (1H, s, CON*H*NH), 7.32 – 7.14 (7H, m, Ar-*H*), 6.88 (1H, t, *J* 7, Ar-*H*), 6.83 – 6.76 (2H, d, *J* 7, Ar-*H*), 6.08 (1H, s, CONHN*H*), 5.08 (1H, d, *J* 8, CON*H*CH), 4.16 (1H, m, CONHC*H*), 2.70 – 2.68 (2H, t, *J* 8, $CH_2CH_2$Phe), 2.19 (1H, m, C$H_2CH_2$Phe), 1.98 (1H, m, C$H_2CH_2$Phe), 1.46 (9H, s, (C$H_3$)$_3$CO).

**_tert_-butyl (S)-(1-(2-(3-chlorophenyl)hydrazineyl)-1-oxo-4-phenylbutan-2-yl)carbamate 51Bu**

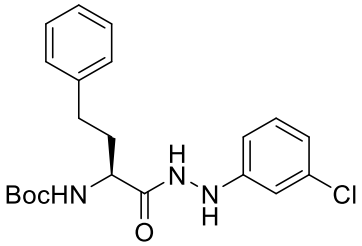


Using the standard procedure provided, *N*-Boc-*L*-homophenylalanine (0.15 g, 1.0 mmol) and 3-chlorophenylhydrazine hydrochloride (0.35 g, 1.2 mmol) were transformed into the

title compound which was isolated as a yellow powder (0.37 g, 87 %); δH (300 MHz, $CDCl_3$) 8.29 (1H, s, CON*H*NH), 7.31 – 7.26 (2H, m, Ar-*H*), 7.22 – 7.14 (3H, m, Ar-*H*), 7.05 (1H, dd, *J* 8, 8, Ar-*H*), 6.80 (1H, d, *J* 8, Ar-*H*), 6.79 (1H, s, Ar-*H*), 6.67 (1H, dd, *J* 8, 1, Ar-*H*), 5.07 (1H, d, *J* 8, CON*H*CH), 4.13 (1H, m, CONHC*H*), 2.73 – 2.67 (2H, t, *J* 8, $CH_2C\mathit{H}_2$-Phe), 2.15 (1H, m, $C\mathit{H}_2CH_2$Phe), 1.92 (1H, m, $C\mathit{H}_2CH_2$Phe), 1.40 (9H, s, $(C\mathit{H}_3)_3$CO).

***tert*-butyl (S)-(1-(2-(4-chlorophenyl)hydrazineyl)-1-oxo-4-phenylbutan-2-yl)carbamate 51Bv**

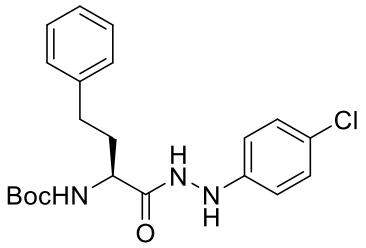


Using the standard procedure provided, *N*-Boc-*L*-homophenylalanine (0.20 g, 1.4 mmol) and 4-chlorophenylhydrazine hydrochloride (0.47 g, 1.6 mmol) were transformed into the title compound which was isolated as a yellow powder (0.48 g, 85 %); δH (300 MHz, $CDCl_3$) 8.11 (1H, s, CON*H*NH), 7.33 – 7.27 (2H, m, Ar-*H*), 7.22 – 7.12 (5H, m, Ar-*H*), 6.79 – 6.71 (2H, d, *J* 8, Ar-*H*), 6.79 (1H, s, Ar-*H*), 6.06 (1H, s, CONHN*H*, Ar-*H*), 5.00 (1H, d, *J* 8, CON*H*CH), 4.09 (1H, m, CONHC*H*), 2.73 – 2.65 (2H, t, *J* 8, $CH_2C\mathit{H}_2$-Phe), 2.18 (1H, m, $C\mathit{H}_2CH_2$Phe), 1.95 (1H, m, $C\mathit{H}_2CH_2$Phe), 1.46 (9H, s, $(C\mathit{H}_3)_3$CO).

***tert*-butyl (S)-(1-(2-(3-bromophenyl)hydrazineyl)-1-oxo-4-phenylbutan-2-yl)carbamate 51Bw**

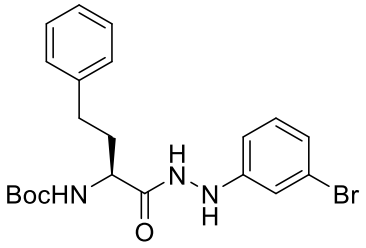


Using the standard procedure provided, *N*-Boc-*L*-homophenylalanine (0.19 g, 1.0 mmol) and 3-bromophenylhydrazine hydrochloride (0.35 g, 1.2 mmol) were transformed into the title compound which was isolated as a yellow powder (0.41 g, 87 %); δH (300 MHz, $CDCl_3$) 8.02 (1H, s, CON*H*NH), 7. 34 – 7.26 (2H, m, Ar-*H*), 7.24 – 7.14 (3H, m, Ar-*H*), 7.06 (1H, dd, *J* 8, 8, Ar-*H*), 6.80 (1H, dd, *J* 8, 1, Ar-*H*), 6.76 (1H, s, Ar-*H*), 6.64 (1H, dd, *J* 8, 1,

Ar-*H*), 5.07 (1H, d, *J* 8, CON*H*CH), 4.13 (1H, m, CONHC*H*), 2.71 – 2.63 (2H, t, *J* 8, $CH_2C\mathit{H}_2$-Phe), 2.15 (1H, m, $C\mathit{H}_2CH_2$Phe), 1.92 (1H, m, $C\mathit{H}_2CH_2$Phe), 1.40 (9H, s, $(C\mathit{H}_3)_3CO$).

**_tert_-butyl (S)-(1-(2-(4-bromophenyl)hydrazineyl)-1-oxo-4-phenylbutan-2-yl)carbamate 51Bx**

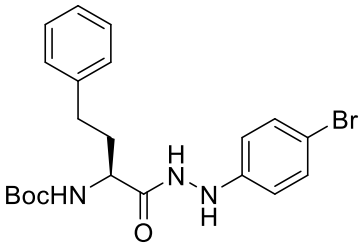


Using the standard procedure provided, *N*-Boc-*L*-homophenylalanine (0.15 g, 0.8 mmol) and 4-bromophenylhydrazine hydrochloride (0.26 g, 0.9 mmol) were transformed into the title compound which was isolated as a yellow powder (0.31 g, 86%); δH (300 MHz, $CDCl_3$) 8.18 (1H, s, CON*H*NH), 7.26 – 7.21 (2H, m, Ar-*H*), 7.16 – 7.03 (5H, m, Ar-*H*), 6.65 – 6.55 (2H, d, *J* 8, Ar-*H*), 6.04 (1H, s, CONHN*H*, Ar-*H*), 5.00 (1H, d, *J* 8, CON*H*CH), 4.03 (1H, m, CONHC*H*), 2.65 – 2.58 (2H, t, *J* 8, $CH_2C\mathit{H}_2$-Phe), 2.06 (1H, m, $C\mathit{H}_2CH_2$Phe), 1.87 (1H, m, $C\mathit{H}_2CH_2$Phe), 1.40 (9H, s, $(C\mathit{H}_3)_3CO$).

**_tert_-butyl (S)-(1-(2-(3-trifluoromethylphenyl)hydrazineyl)-1-oxo-4-phenylbutan-2-yl)carbamate 51By**

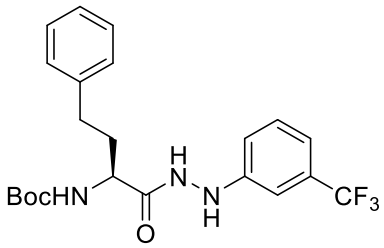


Using the standard procedure provided, *N*-Boc-*L*-homophenylalanine (0.20 g, 1.1 mmol) and 3-trifluoromethylphenylhydrazine hydrochloride (0.38 g, 1.3 mmol) were transformed into the title compound which was isolated as a yellow powder (0.42 g, 85 %); δH (300 MHz, $CDCl_3$) 8.37 (1H, s, CON*H*NH), 7.31 – 7.26 (3H, m, Ar-*H*), 7.21 (1H, d, *J* 7, Ar-*H*), 7.18 – 7.14 (2H, m, Ar-*H*), 7.11 (1H, d, *J* 7, Ar-*H*), 7.03 (1H, s, Ar-*H*), 6.94 (1H, d, *J* 7, Ar-*H*), 6.25 (1H, s, CONHN*H*), 5.07 (1H, d, *J* 8, CON*H*CH), 4.16 (1H, m, CONHC*H*), 2.72 –

2.62 (2H, t, *J* 8, $CH_2CH_2$-Phe), 2.17 (1H, m, $CH_2CH_2$Phe), 1.96 (1H, m, $CH_2CH_2$Phe), 1.43 (9H, s, $(CH_3)_3CO$).

***tert*-butyl (S)-(1-(2-(4-trifluoromethylphenyl)hydrazineyl)-1-oxo-4-phenylbutan-2-yl)carbamate 51Bz**

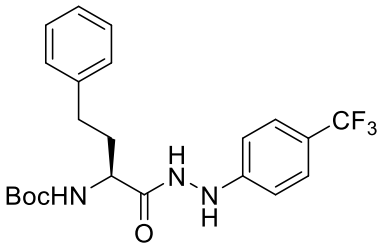


Using the standard procedure provided, *N*-Boc-*L*-homophenylalanine (0.20 g, 1.1 mmol) and 4-trifluoromethylphenylhydrazine hydrochloride (0.38 g, 1.3 mmol) were transformed into the title compound which was isolated as a yellow powder (0.36 g, 73 %); δH (300 MHz, $CDCl_3$) 8.02 (1H, s, CON*H*NH), 7.16 – 7.12 (2H, m, Ar-*H*), 7.10 – 7.00 (5H, m, Ar-*H*), 6.62 – 6.53 (2H, d, *J* 8, Ar-*H*), 6.00 (1H, s, CONHN*H*, Ar-*H*), 5.01 (1H, d, *J* 8, CON*H*CH), 4.00 (1H, m, CONHC*H*), 2.62 – 2.57 (2H, t, *J* 8, $CH_2CH_2$-Phe), 2.00 (1H, m, $CH_2CH_2$Phe), 1.84 (1H, m, $CH_2CH_2$Phe), 1.43 (9H, s, $(CH_3)_3CO$).

***tert*-butyl (S)-(1-(2-(2-chlorophenyl)hydrazineyl)-1-oxo-3-phenylpropan-2-yl)carbamate 51Ca**

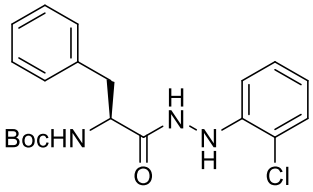


Using the standard procedure provided, *N*-Boc-*L*-Phenylalanine (0.66 g, 2.50 mmol) and 2-chlorophenylhydrazine hydrochloride (0.36 g, 2.50 mmol) were transformed into the title compound which was isolated as a yellow powder (0.50 g, 51%); $\delta_H$ (300 MHz, $CDCl_3$) 7.86 (1H, bs, CON*H*NH), 7.29 - 7.20 (3H, m, Ar-*H*), 7.15 – 7.05 (2H, m, Ar-*H*), 6.96 – 6.89 (2H, m, Ar-*H*), 6.72 (1H, s, Ar-*H*), 6.43 (1H, s, Ar-*H*), 5.01 (1H, bs, BocN*H*CH), 4.36 (1H, m, BocNHC*H*), 3.07 – 2.99 (2H, d, *J* 8, Ar-$CH_2$), 1.35 (9H, s, $(CH_3)_3CO$).

***tert*-butyl (S)-(1-(2-(3-cyanophenyl)hydrazineyl)-1-oxo-3-phenylpropan-2-yl)carbamate 51Cb**

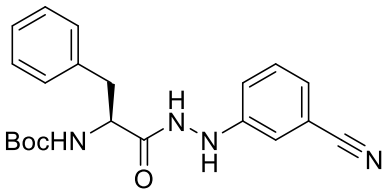


Using the standard procedure provided, *N*-Boc-*L*-Phenylalanine (0.66 g, 2.50 mmol) and 3-cyanophenylhydrazine hydrochloride (0.33 g, 2.50 mmol) were transformed following work up with $Et_2O$ into the title compound which was isolated as a beige solid (0.63 g, 67 %); $\delta_H$ (300 MHz, $CDCl_3$) 7.73 (1H, bs, CON*H*NH), 7.36 – 7.30 (3H, m, Ar-*H*), 7.25 – 7.20 (2H, m, Ar-*H*), 7.05 – 7.00 (2H, d, *J* 7, Ar-*H*), 6.64 – 6.58 (2H, d, *J* 7, Ar-*H*), 5.02 (1H, bs, BocN*H*CH), 4.40 (1H, q, *J* 7, BocNHC*H*), 3.16 – 3.00 (2H, d, *J* 7, Ar-C$H_2$), 1.45 (9H, s, (C$H_3$)$_3$CO).

***tert*-butyl (S)-(1-(2-(3-cyanophenyl)hydrazineyl)-1-oxo-3-phenylpropan-2-yl)carbamate 51Cc**

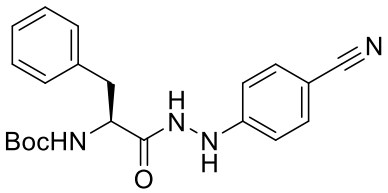


Using the standard procedure provided, *N*-Boc-*L*-Phenylalanine (0.66 g, 2.50 mmol) and 4-cyanophenylhydrazine hydrochloride (0.33 g, 2.50 mmol) were transformed following work up with $Et_2O$ into the title compound which was isolated as a white solid (0.43 g, 48 %); $\delta_H$ (300 MHz, $CDCl_3$) 7.67 (1H, bs, CON*H*NH), 7.35 - 7.30 (4H, m, Ar-*H*), 7.16 – 7.09 (2H, m, Ar-*H*), 6.45 – 6.29 (2H, d, *J* 7, Ar-*H*), 4.98 (1H, bs, BocN*H*CH), 4.31 (1H, m, BocNHC*H*), 3.08 – 2.99 (2H, d, *J* 7, Ar-C$H_2$), 1.38 (9H, s, (C$H_3$)$_3$CO).

### 6.2.4 Synthesis of *N*-protected Heterocyclic Hydrazides – General Procedure

Under a nitrogen atmosphere, heterocyclic hydrazine (1 equiv.) dissolved in acetonitrile and treated with *N*-protected amino acid **52** (1.2 equiv.) and DIPEA (1.5 equiv.) followed

by the addition of HBTU (1.2 equiv.) and stirred for 6 hours at room temperature. Reaction mixed with ethyl acetate (10 ml) and distilled water (5 ml). After separating the two phases, the organic layer was washed again with distilled water (5 ml x 3 ml), sat. aq. $NaHCO_3$ (5 ml), sat. aq. $NH_4Cl$ (5 ml) and brine (10 ml). The organic layer was then dried over $MgSO_4$, filtered, evaporated and dried in *vacuo* to obtain the required *N*-Boc hydrazides **51 (Cd – Co)**.

**_tert_-butyl (S)-(1-oxo-3-phenyl-1-(2-(pyridin-3-yl)hydrazineyl)propan-2-yl)carbamate 51Cd**

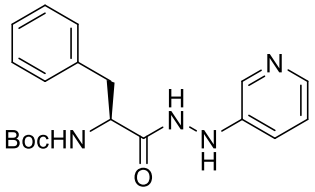


Using the standard procedure provided, *N*-Boc-*L*-Phenylalanine (0.58 g, 2.19 mmol) and 3-hydrazineylpyridine hydrochloride (0.20 g, 1.83 mmol) were transformed following work-up with EtOAc into the title compound which was isolated as a white powder (0.19 g, 30 %); $R_f$ 0.40 (DCM/EtOAc [1:2]); m.p. 183 – 188 °C; $\nu_{max}$ 3345 (N-H), 2980 (C-H), 1682 (C=O), 1517, 1494, 1455, 1445, 1391, 1366, 1326, 1249, 1164, 1022, 850, 762, 699 $cm^{-1}$; $\delta_H$ (300 MHz, DMSO-$d_6$) 9.90 (1H, bs, CON*H*NH), 8.00 (1H, d, *J* 7, CONHN*H*), 7.48 – 7.07 (8H, m, Ar-*H*), 6.97 (1H, m, Ar-*H*), 6.80 (1H, m, BocN*H*CH), 4.06 (1H, m, BocNHC*H*), 3.13 (1H, dd, *J* 13, 4, CONHCHC$H_2$), 2.74 (1H, dd, *J* 13, 10, CONHCHC$H_2$), 1.29 (9H, s, (C$H_3$)$_3$CO); $\delta_C$ (75 MHz, DMSO-$d_6$) 174.1 (*C*ONHNH), 155.6 (*ipso*-Ar-*C*), 145.6 (*ipso*-Ar-*C*), 138.8 (*ipso*-Ar-*C*), 129.7 (Ar-*C*), 129.6 (Ar-*C*), 128.6 (Ar-*C*), 128.4 (Ar-*C*), 126.6 (Ar-*C*), 78.3 ((CH$_3$)$_3$*C*O), 56.0 (BocNH*C*H), 38.0 (BocNHCH*C*H$_2$), 28.2 ((*C*H$_3$)$_3$CO); *m/z* (ES$^+$) 357 (MH$^+$); HRMS (ES$^+$) Found MH$^+$, 357.1921 ($C_{19}H_{25}N_4O_3$ requires 357.1921).

**_tert_-butyl (S)-(1-oxo-3-phenyl-1-(2-(pyridin-4-yl)hydrazineyl)propan-2-yl)carbamate 51Ce**

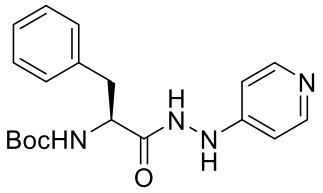


Using the standard procedure provided, *N*-Boc-*L*-Phenylalanine (0.58 g, 2.19 mmol) and 4-hydrazineylpyridine hydrochloride (0.20 g, 1.83 mmol) were transformed following work up with EtOAc into the title compound which was isolated as a white powder (0.19 g, 30 %); $R_f$ 0.40 (DCM/EtOAc [1:2]); m.p. 183 – 188 °C; $\nu_{max}$ 3343 (N-H), 2975 (C-H), 1672 (C=O), 1657, 1522, 1494, 1455, 1435, 1361, 1355, 1327, 1230, 1164, 1022, 870, 698 $cm^{-1}$; $\delta_H$ (300 MHz, DMSO-$d_6$) 8.59 – 8.43 (2H, d, *J* 6, Ar-*H*), 7.77 – 7.69 (2H, d, *J* 6, Ar-*H*), 7.35 – 7.16 (5H, m, Ar-*H*), 6.97 (1H, d, *J* 8, BocN*H*CH), 5.71 – 5.46 (2H, s, CON*H*N*H*), 5.26 (1H, t, *J* 8, BocNHC*H*), 3.14 (1H, dd, *J* 13, 4, CONHCHC$H_2$), 2.71 (1H, dd, *J* 13, 10, CONHCHC$H_2$), 1.31 (9H, s, $(CH_3)_3CO$); $\delta_C$ (75 MHz, DMSO-$d_6$) 175.7 (*C*=ONHNH), 156.0 (*ipso*-Ar-*C*), 150.8 (Ar-*C*), 150.3 (Ar-*C*), 139.2 (*ipso*-Ar-*C*), 129.5 (Ar-*C*), 128.5 (Ar-*C*), 126.7 (Ar-*C*), 115.4 (Ar-*C*), 78.4 ($(CH_3)_3CO$), 55.0 (BocNH*C*H), 36.4 (BocNHCH*C*$H_2$), 28.6 ($(CH_3)_3CO$); *m/z* ($ES^+$) 357 ($MH^+$); HRMS ($ES^+$) Found $MH^+$, 357.1922 ($C_{19}H_{25}N_4O_3$ requires 357.1921).

**_tert_-butyl (S)-(1-oxo-3-phenyl-1-(2-(pyridin-2-yl)hydrazineyl)propan-2-yl)carbamate 51Cf**

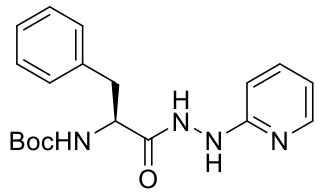


Using the standard procedure provided, *N*-Boc-*L*-Phenylalanine (0.58 g, 2.19 mmol) and 2-hydrazineylpyridine hydrochloride (0.20 g, 1.83 mmol) were transformed following work-up with EtOAc into the title compound which was isolated as a white powder (0.51 g, 78 %); $R_f$ 0.40 (DCM/EtOAc [1:2]); m.p. 183 – 188 °C; $\nu_{max}$ 3260 (N-H), 2979 (C-H), 1672 (C=O), 1598, 1495, 1386, 1251, 1164, 1078, 988, 837, 698 $cm^{-1}$; $\delta_H$ (300 MHz, DMSO-$d_6$) 9.95 (1H, s, CON*H*NH), 8.30 (1H, s, CONHN*H*), 8.01 (1H, d, *J* 2, Ar-*H*), 7.42 (1H, t, *J* 8, Ar-*H*), 7.35 – 7.19 (5H, m, Ar-*H*), 7.11 (1H, d, *J* 7, BocN*H*CH), 6.66 (1H, t, *J* 6, Ar-*H*), 6.39 (1H, d, *J* 8, Ar-*H*), 4.23 (1H, m, BocNHC*H*), 3.02 (1H, dd, *J* 13, 4, CONHCHC$H_2$), 2.79 (1H, dd, *J* 13, 10, CONHCHC$H_2$), 1.31 (9H,

s, (C*H*$_3$)$_3$CO); $\delta_C$ (75 MHz, DMSO-d$_6$) 172.1 (*C*ONHNH), 160.2 (*ipso*-Ar-*C*), 155.8 (*ipso*-Ar-*C*), 147.8 (*ipso*-Ar-*C*), 138.4 (*ipso*-Ar-*C*), 137.8 (*ipso*-Ar-*C*), 129.7 (Ar-*C*), 128.5 (Ar-*C*), 128.4, 126.7 (Ar-*C*), 114.8 (Ar-*C*), 106.6 (*ipso*-Ar-*C*), 79.6 (*ipso*-Ar-*C*), 78.5 ((CH$_3$)$_3$*C*O), 54.9 (BocNH*C*H), 37.7 (BocNHCH*C*H$_2$), 28.6 ((*C*H$_3$)$_3$CO); *m/z* (ES$^+$) 357 (MH$^+$); HRMS (ES$^+$) Found MH$^+$, 357.1922 ($C_{19}H_{25}N_4O_3$ requires 357.1921).

**_tert_-butyl (S)-(1-oxo-3-phenyl-1-(2-(pyrazin-2-yl)hydrazineyl)propan-2-yl)carbamate 51Cg**

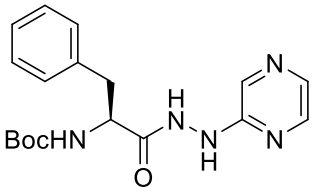


Using the standard procedure provided, *N*-Boc-*L*-Phenylalanine (1.15 g, 4.35 mmol) and 2-hydrazinopyrazine hydrochloride (0.40 g, 3.63 mmol) were transformed following work-up with EtOAc into the title compound which was isolated as a white powder (0.78 g, 60 %); $R_f$ 0.35 (DCM/EtOAc [1:3]); m.p. 190 – 192 °C; $\nu_{max}$ 3252 (N-H), 2978 (C-H), 1671 (C=O), 1597, 1495, 1388, 1367, 1250, 1164, 1048, 835, 741, 698 cm$^{-1}$; $\delta_H$ (300 MHz, DMSO-d$_6$) 10.10 (1H, s, CON*H*NH), 8.83 (1H, s, CONHN*H*), 8.04, 7.94 – 7.85 (2H, m, Ar-*H*), 7.36 – 7.25 (4H, m, Ar-*H*), 7.20 (1H, m, Ar-*H*), 7.13 (1H, d, *J* 7, Ar-*H*), 4.25 (1H, m, BocNHC*H*), 3.02 (1H, dd, *J* 13, 4, CONHCHC*H*$_2$), 2.82 (1H, dd, *J* 13, 10, CONHCHC*H*$_2$), 1.29 (9H, s, (C*H*$_3$)$_3$CO); $\delta_C$ (75 MHz, DMSO-d$_6$) 172.2 (*C*ONHNH), 155.9 (Ar-*C*), 142.0 (Ar-*C*), 138.4 (*ipso*-Ar-*C*), 134.7 (*ipso*-Ar-*C*), 131.1 (*ipso*-Ar-*C*), 129.7 (Ar-*C*), 129.6 (Ar-*C*), 128.6 (Ar-*C*), 128.4 (Ar-*C*), 126.8 (Ar-*C*), 78.6 ((CH$_3$)$_3$*C*O), 55.0 (BocNH*C*H), 37.5 (BocNHCH*C*H$_2$), 28.6 ((*C*H$_3$)$_3$CO); *m/z* (ES$^+$) 358 (MH$^+$); HRMS (ES$^+$) Found MH$^+$, 358.1873 ($C_{18}H_{24}N_5O_3$ requires 358.1874).

**_tert_-butyl (S)-(1-oxo-3-phenyl-1-(2-(pyrazin-2-yl)hydrazineyl)propan-2-yl)carbamate 51Ch**

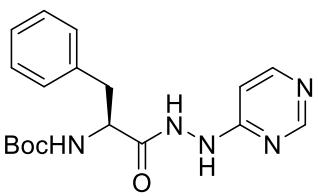

Using the standard procedure provided, *N*-Boc-*L*-Phenylalanine (0.72 g, 2.72 mmol) and 4-hydrazinopyrimidine hydrochloride (0.30 g, 2.72 mmol) were transformed following work-up with EtOAc into the title compound which was isolated as a white powder (0.78 g, 80 %); $R_f$ 0.35 (DCM/EtOAc [1:3]); m.p. 190 – 192 °C; $\nu_{max}$ 3252 (N-H), 2978 (C-H), 1671, 1597 (C=O), 1526, 1495, 1455, 1388, 1367, 1250, 1164, 1048, 835, 741, 698 $cm^{-1}$; $\delta_H$ (300 MHz, DMSO-$d_6$) 8.55 (1H, s, CON*H*NH), 8.17 (1H, d, *J* 6, Ar-*H*), 7.27 – 7.21 (2H, m, Ar-*H*), 7.18 – 7.09 (5H, m, Ar-*H*), 6.15 (1H, s, CONHN*H*), 4.99 (1H, d, *J* 7, BocN*H*CH), 4.34 (1H, m, BocNHC*H*), 3.11 – 2.97 (2H, d, *J* 7, CONHCHC$H_2$), 1.34 (9H, s, (C$H_3$)$_3$CO); $\delta_C$ (75 MHz, DMSO-$d_6$) 172.4 (*C*ONHNH), 157.0 (*ipso*-Ar-*C*), 144.0 (*ipso*-Ar-*C*), 138.1 (*ipso*-Ar-*C*), 134.6 (Ar-*C*), 131.9 (Ar-*C*), 129.8 (Ar-*C*), 129.6 (Ar-*C*), 128.9 (Ar-*C*), 128.8 (Ar-*C*), 126.9 (Ar-*C*), 78.2 ((CH$_3$)$_3$*C*O), 53.2 (BocNH*C*H), 38.5 (BocNHCH*C*H$_2$), 28.3 ((*C*H$_3$)$_3$CO); ***m/z*** (ES$^+$) 358 (MH$^+$); HRMS (ES$^+$) Found MH$^+$, 358.1869 ($C_{18}H_{24}N_5O_3$ requires 358.1874).

**_tert_-butyl (S)-(1-oxo-3-phenyl-1-(2-(pyrazin-2-yl)hydrazineyl)propan-2-yl)carbamate 51Ci**

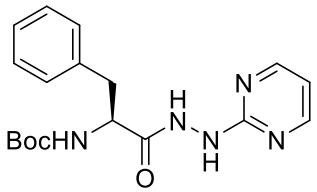


Using the standard procedure provided, *N*-Boc-*L*-Phenylalanine (0.66 g, 2.50 mmol) and 2-hydrazinopyrimidine hydrochloride (0.28 g, 2.50 mmol) were transformed following work-up with EtOAc into the title compound which was isolated as a white powder (0.43 g, 48 %); $R_f$ 0.35 (DCM/EtOAc [1:3]); m.p. 190 – 192 °C; $\nu_{max}$ 3262 (N-H), 2981 (C-H), 1675 (C=O), 1580, 1512, 1496, 1447, 1423, 1369, 1307, 1240, 1043, 1017, 843, 811, 758, 699, 566 $cm^{-1}$; $\delta_H$ (300 MHz, DMSO-$d_6$) 9.96 (1H, s, CON*H*NH), 8.97 (1H, s, CONHN*H*), 8.42 – 8.32 (2H, d, *J* 4, Ar-*H*), 7.36 – 7.20 (5H, m, Ar-*H*), 6.90 (1H, d, *J* 9, BocN*H*CH), 6.76 (1H, t, *J* 5, Ar-*H*), 4.28 (1H, m, BocNHC*H*), 3.15 (1H, dd, *J* 13, 4, CONHCHC$H_2$), 2.79 (1H, dd, *J* 13, 10, CONHCHC$H_2$), 1.27 (9H, s, (C$H_3$)$_3$CO); $\delta_C$ (75 MHz, DMSO-$d_6$) 172.4 (*C*ONHNH), 163.4 (*ipso*-Ar-*C*), 158.5 (*ipso*-Ar-*C*), 155.6 (*ipso*-Ar-*C*), 138.7 (*ipso*-Ar-*C*), 129.7 (Ar-*C*), 128.4 (Ar-*C*), 126.6 (Ar-*C*), 112.9 (Ar-*C*), 78.3 ((CH$_3$)$_3$*C*O), 54.7 (BocNH*C*H), 38.0 (BocNHCH*C*H$_2$), 28.6 ((*C*H$_3$)$_3$CO); ***m/z*** (ES$^+$) 358 (MH$^+$); HRMS (ES$^+$) Found MH$^+$, 358.1873 ($C_{18}H_{24}N_5O_3$ requires 358.1874).

***tert*-butyl (S)-(1-oxo-3-phenyl-1-(2-(thiazol-2-yl)hydrazineyl)propan-2-yl)carbamate 51Cj**

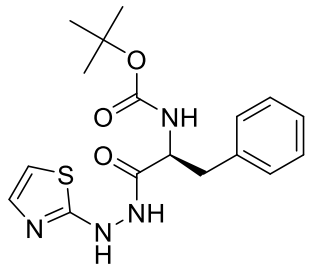

Using the standard procedure provided, *N*-Boc-*L*-Phenylalanine (0.57 g, 2.17 mmol) and 2-hydrazineylthiazole hydrochloride (0.25 g, 2.17 mmol) were transformed following work-up with EtOAc into the title compound which was isolated as a white powder (0.56 g, 71 %); $R_f$ 0.37 (DCM/EtOAc [1:3]); m.p. 170 – 174 °C; $\nu_{max}$ 3290 (N-H), 2981 (C-H), 1656 (C=O), 1537, 1512, 1494, 1444, 1390, 1365, 1325, 1249, 1163, 1045, 1045, 843, 754, 699, 629 $cm^{-1}$; $\delta_H$ (300 MHz, DMSO-$d_6$) 7.35 (1H, s, Ar-*H*), 7.28 – 7.17 (5H, m, Ar-*H*), 7.00 (1H, s, Ar-*H*), 6.78 (1H, d, *J* 9, BocN*H*CH), 4.07 (1H, m, BocNHC*H*), 2.94 (1H, dd, *J* 13, 4, CONHCHC$H_2$), 2.73 (1H, dd, *J* 13, 10, CONHCHC$H_2$), 1.27 (9H, s, (C$H_3$)$_3$CO); $\delta_C$ (75 MHz, DMSO-$d_6$) 174.1 (*C*ONHNH), 155.6 (*ipso*-Ar-*C*), 138.8 (*ipso*-Ar-*C*), 129.6 (Ar-*C*), 128.7 (Ar-*C*), 128.4 (Ar-*C*), 126.6 (Ar-*C*), 78.3 ((CH$_3$)$_3$*C*O), 56.0 (BocNH*C*H), 38.0 (BocNHCH*C*H$_2$), 28.6 ((*C*H$_3$)$_3$CO); ***m/z*** ($ES^+$) 363 ($MH^+$); HRMS ($ES^+$) Found $MH^+$, 363.1487 ($C_{17}H_{23}N_4O_3S$ requires 363.1485).

***tert*-butyl (S)-(1-oxo-3-phenyl-1-(2-(4-methylthiazol-2-yl)hydrazineyl)propan-2-yl)carbamate 51Ck**

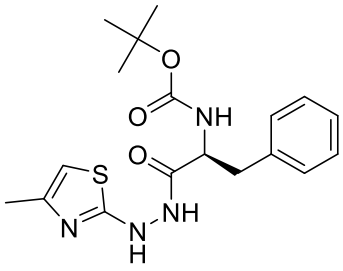

Using the standard procedure provided, *N*-Boc-*L*-Phenylalanine (0.25 g, 1.93 mmol) and 2-hydrazineyl-4-methylthiazole hydrochloride (0.56 g, 2.12 mmol) were transformed following work-up with EtOAc into the title compound which was isolated

as a white powder (0.16 g, 37 %); $R_f$ 0.37 (DCM/EtOAc [1:3]); m.p. 175 – 180 °C; $\nu_{max}$ 3295 (N-H), 2982 (C-H), 1666 (C=O), 1512, 1509, 1495, 1444, 1395, 1360, 1335, 1165, 1045, 1044, 843, 752, 698 $cm^{-1}$; $\delta_H$ (300 MHz, DMSO-$d_6$) 7.28 – 7.15 (6H, m, Ar-*H*), 6.77 (1H, d, *J* 9, BocN*H*CH), 6.61 (1H, s, SC*H*), 6.17 (1H, s, CONHN*H*), 4.07 (1H, m, BocNHC*H*), 3.16 (1H, dd, *J* 13, 4, CONHCHC$H_2$), 2.84 (1H, dd, *J* 13, 10, CONHCHC$H_2$), 2.26 (1H, s, NCC$H_3$), 1.33 (9H, s, (C$H_3$)$_3$CO); $\delta_C$ (75 MHz, DMSO-$d_6$) 179.1 (*C*ONHNH), 164.6 (*ipso*-Ar-*C*), 139.8 (*ipso*-Ar-*C*), 129.6 (Ar-*C*), 128.6 (Ar-*C*), 128.4 (Ar-*C*), 126.4 (Ar-*C*), 101.7, 78.1 ((CH$_3$)$_3$*C*O), 58.0 (BocNH*C*H), 38.6 (BocNHCH*C*H$_2$), 28.6 ((*C*H$_3$)$_3$CO) 13.5 (NC*C*H$_3$); *m/z* (ES$^+$) 377 (MH$^+$); HRMS (ES$^+$) Found MH$^+$, 377.1636 ($C_{18}H_{25}N_4O_3S$ requires 377.1642).

***tert*-butyl (S)-(1-oxo-3-phenyl-1-(2-(6-(trifluoromethyl)pyridin-3-yl)hydrazineyl)propan-2-yl)carbamate 51Cl**

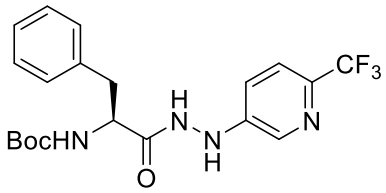


Using the standard procedure provided, *N*-Boc-*L*-Phenylalanine (0.33 g, 1.24 mmol) and 5-hydrazineyl-2-(trifluoromethyl)pyridine hydrochloride (0.20 g, 1.12 mmol) were transformed following work-up with EtOAc into the title compound which was isolated as a white powder (0.41 g, 86 %); $R_f$ 0.35 (DCM/EtOAc [1:2]); m.p. 175 – 178 °C; $\nu_{max}$ 3333 (N-H), 2980 (C-H), 1615 (C=O), 1526, 1392, 1251, 1156, 1046, 992, 869, 762, 699 $cm^{-1}$; $\delta_H$ (300 MHz, DMSO-$d_6$) 10.09 (1H, s, CON*H*NH), 8.69 (1H, s, CONHN*H*), 8.08 (1H, s, Ar-*H*), 7.50 (1H, d, *J* 8, Ar-*H*), 7.33 – 7.20 (5H, m, Ar-*H*), 6.91 (1H, dd, *J* 8, 2, Ar-*H*), 4.23 (1H, m, BocNHC*H*), 2.96 (1H, dd, *J* 13, 4, CONHCHC$H_2$), 2.84 (1H, dd, *J* 13, 10, CONHCHC$H_2$), 1.31 (9H, s, (C$H_3$)$_3$CO); $\delta_C$ (75 MHz, DMSO-$d_6$) 172.2 (*C*ONHNH), 158.5 (*ipso*-Ar-*C*), 155.9 (*ipso*-Ar-*C*), 138.2 (*ipso*-Ar-*C*), 135.1 (Ar-*C*), 129.7 (Ar-*C*), 128.6 (Ar-*C*), 126.9 (Ar-*C*), 118.2 (Ar-*C*), 78.7 ((CH$_3$)$_3$*C*O), 55.0 (BocNH*C*H), 37.3 (BocNHCH*C*H$_2$), 28.6 ((*C*H$_3$)$_3$CO); $\delta_F$ (282 MHz, DMSO-$d_6$) -64.7 (C*F*$_3$); *m/z* (ES$^+$) 425 (MH$^+$); HRMS (ES$^+$) Found MH$^+$, 425.1790 ($C_{20}H_{24}F_3N_4O_3$ requires 425.1795).

***tert*-butyl (S)-(1-(2-(6-chloropyridin-3-yl)hydrazineyl)-1-oxo-3-phenylpropan-2-yl)carbamate 51Cm**

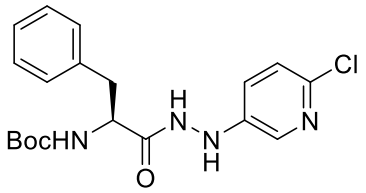


Using the standard procedure provided, *N*-Boc-*L*-Phenylalanine (0.50 g, 1.91 mmol) and 5-hydrazineyl-2-chloropyridine hydrochloride (0.25 g, 1.74 mmol) were transformed following work-up with EtOAc into the title compound which was isolated as a white powder (0.58 g, 85 %); $R_f$ 0.40 (DCM/EtOAc [1:3]); m.p. 178 – 180 °C; $\nu_{max}$ 3253 (N-H), 2980 (C-H), 1669 (C=O), 1598, 1519, 1494, 1386, 1251, 1227, 1156, 1078, 992, 835, 698 $cm^{-1}$; $\delta_H$ (300 MHz, DMSO-$d_6$) 9.97 (1H, s, CON*H*NH), 8.20 (1H, s, CONHN*H*), 7.75 (1H, d, *J* 3, Ar-*H*), 7.34 – 7.26 (3H, m, Ar-*H*), 7.24 (1H, m, BocN*H*CH), 7.20 (1H, m, Ar-*H*), 7.14 (1H, d, *J* 8, Ar-*H*), 6.89 (1H, dd, *J* 8, 2, Ar-*H*), 4.23 (1H, m, BocNHC*H*), 2.96 (1H, dd, *J* 13, 4, CONHCHC$H_2$), 2.84 (1H, dd, *J* 13, 10, CONHCHC$H_2$), 1.31 (9H, s, (C$H_3$)$_3$CO); $\delta_C$ (75 MHz, DMSO-$d_6$) 172.2 (*C*ONHNH), 155.8 (*ipso*-Ar-*C*), 145.2 (*ipso*-Ar-*C*), 138.2 (*ipso*-Ar-*C*), 134.4 (Ar-*C*), 129.7 (Ar-*C*), 128.6 (Ar-*C*), 126.8 (Ar-*C*), 124.1 (Ar-*C*), 123.0 (Ar-*C*), 78.6 ((CH$_3$)$_3$*C*O), 55.0 (BocNH*C*H), 37.6 (BocNHCH*C*H$_2$), 28.6 ((*C*H$_3$)$_3$CO); ***m/z*** (ES$^+$) 391 ([$^{35}$Cl]MH$^+$), 393 ([$^{37}$Cl]MH$^+$); HRMS (ES$^+$) Found [$^{35}$Cl]MH$^+$, 391.1529 ($C_{19}H_{24}{}^{35}ClN_4O_3$ requires 391.1531).

***tert*-butyl (S)-(1-(2-(4-chloropyridin-2-yl)hydrazineyl)-1-oxo-3-phenylpropan-2-yl)carbamate 51Cn**

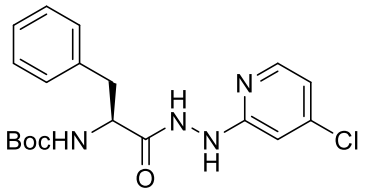


Using the standard procedure provided, *N*-Boc-*L*-Phenylalanine (0.50 g, 1.91 mmol) and 4-chloro-2-hydrazineylpyridine hydrochloride (0.25 g, 1.74 mmol) were transformed following work-up with EtOAc into the title compound which was isolated as a white powder (0.53 g, 78 %); $R_f$ 0.40 (DCM/EtOAc [1:3]); m.p. 178 – 180 °C; $\nu_{max}$ 3333 (N-H), 2980 (C-H), 1670 (C=O), 1596, 1526, 1492, 1379, 1339, 1249, 1218, 1165,

1042, 988, 835, 741, 688 $cm^{-1}$; $\delta_H$ (300 MHz, DMSO-$d_6$) 10.05 (1H, s, CON*H*NH), 8.87 (1H, s, CONHN*H*), 7.85 (1H, d, *J* 5, Ar-*H*), 7.34 – 7.19 (5H, m, Ar-*H*), 6.52 (1H, s, Ar-*H*), 6.43 (1H, d, *J* 5, Ar-*H*), 4.19 (1H, m, BocNHC*H*), 2.98 – 2.79 (2H, m, CONHCHC$H_2$), 1.33 (9H, s, (C$H_3$)$_3$CO); $\delta_C$ (75 MHz, DMSO-$d_6$) 172.1 (*C*ONHNH), 157.3 (*ipso*-Ar-*C*), 155.9 (*ipso*-Ar-*C*), 149.5 (*ipso*-Ar-*C*), 138.1 (*ipso*-Ar-*C*), 129.7 (Ar-*C*), 128.7 (Ar-*C*), 126.9 (Ar-*C*), 78.7 ((CH$_3$)$_3$*C*O), 55.0 (BocNH*C*H), 38.7 (BocNHCH*C*H$_2$), 28.6 ((*C*H$_3$)$_3$CO); ***m/z*** (ES$^+$) 391 ([$^{35}$Cl]MH$^+$), 393 ([$^{37}$Cl]MH$^+$); HRMS (ES$^+$) Found [$^{35}$Cl]MH$^+$, 391.1529 ($C_{19}H_{24}{}^{35}ClN_4O_3$ requires 391.1531).

### *tert*-butyl (S)-(1-(2-(2-chloropyridin-4-yl)hydrazineyl)-1-oxo-3-phenylpropan-2-yl)carbamate 51Co

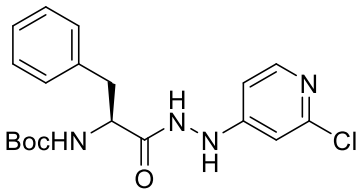


Using the standard procedure provided, *N*-Boc-*L*-Phenylalanine (0.50 g, 1.91 mmol) and 2-chloro-4-hydrazineylpyridine hydrochloride (0.25 g, 1.74 mmol) were transformed following work-up with EtOAc into the title compound which was isolated as a white powder (0.53 g, 78 %); $R_f$ 0.40 (DCM/EtOAc [1:3]); m.p. 178 – 180 °C; $\nu_{max}$ 3253 (N-H), 2979 (C-H), 1671 (C=O), 1598, 1494, 1386, 1322, 1252, 1229, 1165, 988, 836, 698 $cm^{-1}$; $\delta_H$ (300 MHz, DMSO-$d_6$) 10.05 (1H, s, CON*H*NH), 8.87 (1H, s, CONHN*H*), 7.85 (1H, d, *J* 5, Ar-*H*), 7.34 – 7.19 (5H, m, Ar-*H*), 6.52 (1H, s, Ar-*H*), 6.43 (1H, d, *J* 5, Ar-*H*), 4.19 (1H, m, BocNHC*H*), 2.98 – 2.79 (2H, m, CONHCHC$H_2$), 1.33 (9H, s, (C$H_3$)$_3$CO); $\delta_C$ (75 MHz, DMSO-$d_6$) 172.1 (*C*ONHNH), 157.3 (*ipso*-Ar-*C*), 155.9 (*ipso*-Ar-*C*), 149.5 (*ipso*-Ar-*C*), 138.1 (*ipso*-Ar-*C*), 129.7 (Ar-*C*), 128.7 (Ar-*C*), 126.9 (Ar-*C*), 78.7 ((CH$_3$)$_3$*C*O), 55.0 (BocNH*C*H), 38.7 (BocNHCH*C*H$_2$), 28.6 ((*C*H$_3$)$_3$CO); ***m/z*** (ES$^+$) 391 ([$^{35}$Cl]MH$^+$), 393 ([$^{37}$Cl]MH$^+$); HRMS (ES$^+$) Found [$^{35}$Cl]MH$^+$, 391.1530 ($C_{19}H_{24}{}^{35}ClN_4O_3$ requires 391.1531).

### *tert*-butyl (S)-(1-(2-(6-methoxypyridin-3-yl)hydrazineyl)-1-oxo-3-phenylpropan-2-yl)carbamate 51Cp

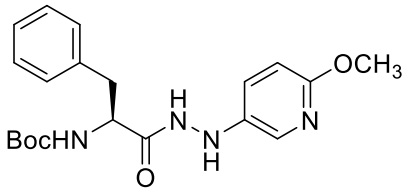


Using the standard procedure provided, *N*-Boc-*L*-Phenylalanine (0.41 g, 1.58 mmol) and 5-hydrazineyl-2-methoxypyridine hydrochloride (0.20 g, 1.43 mmol) were transformed following work-up with EtOAc into the title compound which was isolated as a white powder (0.44 g, 79 %); $R_f$ 0.35 (DCM/EtOAc [1:3]); m.p. 188 – 190 °C; $\nu_{max}$ 3254 (N-H), 2972 (C-H), 1671 (C=O), 1598, 1526, 1494, 1387, 1252, 1165, 1078, 988, 837, 741, 698 $cm^{-1}$; $\delta_H$ (300 MHz, DMSO-$d_6$) 9.85 (1H, s, CON*H*NH), 7.61 (1H, s, CONHN*H*), 7.58 (1H, m, Ar-*H*), 7.31 – 7.19 (5H, m, Ar-*H*), 7.12 (1H, s, BocN*H*CH), 6.98 (1H, dd, *J* 8, 2, Ar-*H*), 6.57 (1H, d, *J* 8, Ar-*H*), 4.20 (1H, m, BocNHC*H*), 3.74 (3H, s, Ar-OC*H*$_3$), 2.93 (1H, dd, *J* 13, 4, CONHCHC*H*$_2$), 2.80 (1H, dd, *J* 13, 10, CONHCHC*H*$_2$), 1.34 (9H, s, (C*H*$_3$)$_3$CO); $\delta_C$ (75 MHz, DMSO-$d_6$) 172.1 (*C*ONHNH), 157.9 (*ipso*-Ar-*C*), 155.8 (*ipso*-Ar-*C*), 140.6 (*ipso*-Ar-*C*), 138.3 (Ar-*C*), 130.1 (Ar-*C*), 129.7 (Ar-*C*), 128.8 (Ar-*C*), 128.6 (Ar-*C*), 126.8 (Ar-*C*), 125.5 (Ar-*C*), 110.3 (Ar-*C*), 78.5 ((CH$_3$)$_3$*C*O), 55.0 (BocNH*C*H), 53.3 (Ar-O*C*H$_3$), 37.6 (BocNHCH*C*H$_2$), 28.6 ((*C*H$_3$)$_3$CO); *m/z* (ES$^+$) 387 (MH$^+$); HRMS (ES$^+$) Found MH$^+$, 387.2024 ($C_{20}H_{27}N_4O_4$ requires 387.2027).

### 6.2.5 Synthesis of Imidazo[1,2-*a*]pyridine-3-carboxamides – General procedure

Under a nitrogen atmosphere *N*-Boc amino acid hydrazide **51** (1 equiv.) was added to 4 M HCl solution in dioxane (3 ml) and stirred at room temperature for 2 hours. The mixture was then evaporated, dried in *vacuo* and precipitated using EtOH and $Et_2O$. The precipitation was isolated and dissolved in THF before the addition of 6-chloro-2-phenylimidazo[1,2-*a*]pyridine-3-carboxylic acid **50** (1.10 equiv.), the mixture was stirred overnight with DIPEA (1.60 equiv.) and HBTU (1.10 equiv. ). The reaction was then quenched using EtOAc (10 ml) and distilled water (5 ml) and after separation of the two layers, the organic layer was washed again using distilled water (10 ml X 3) followed by adding sat. aq. $NaHCO_3$ (5 ml) and sat. aq. $NH_4Cl$ (5 ml) then adding brine (10 ml). The organic layer was dried over $MgSO_4$, then filtered under vacuum, followed

by solvent evaporation and drying under reduced pressure to yield the desired product **44 (Aa - Ec)**.

### 6.2.5.1 First- series of imidazo[1,2-*a*]pyridine-3-carboxamides

**6-chloro-2-(3-chlorophenyl)-N-(2-oxo-2-(2-phenylhydrazineyl)ethyl)imidazo[1,2-*a*]pyridine-3-carboxamide 44Aa**

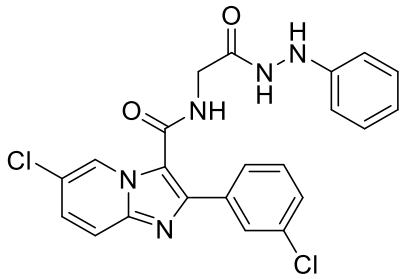

Using the standard procedure provided, *tert*-butyl (2-oxo-2-(2-phenylhydrazineyl)ethyl)carbamate **51Aa** (0.09 g, 0.33 mmol) was transformed following flash chromatography (DCM/EtOAc [1:2]) into the title compound as a white powder (52 mg, 34 %); $R_f$ 0.30 (DCM/EtOAc [1:2]); m.p. 200 - 204 °C; $\nu_{max}$ 3244 (N-H), 2981 (C-H), 1604 (C=O), 1492, 1381, 1251, 1154, 1075, 955, 792, 750 $cm^{-1}$; $\delta_H$ (300 MHz, DMSO-$d_6$) 9.86 (1H, d, *J* 2, CON*H*NH), 9.06 (1H, dd, *J* 2, 1, Ar-*H*), 8.92 (1H, t, *J* 5, CON*H*$CH_2$), 7.96 (1H, m, Ar-*H*), 7.89 (1H, m, Ar-*H*), 7.76 (1H, dd, *J* 9, 1, Ar-*H*), 7.50 (1H, dd, *J* 9, 2, Ar-*H*), 7.47 – 7.43 (2H, m, Ar-*H*), 7.18 – 7.08 (2H, t, *J* 7, Ar-*H*), 6.79 – 6.74 (2H, d, *J* 7, Ar-*H*), 6.70 (1H, t, *J* 7, Ar-*H*), 4.09 – 3.95 (2H, d, *J* 5, C*H*$_2$CO); δC (75 MHz, DMSO-$d_6$) 169.0 (*C*ONHNH), 161.1 (*C*ONHCH$_2$), 149.5 (*ipso*-Ar-*C)*, 143.8 (*ipso*-Ar-*C)*, 143.3 (*ipso*-Ar-*C)*, 135.5 (*ipso*-Ar-*C)*, 133.7 (*ipso*-Ar-*C)*, 130.9 (Ar-*C*), 129.1 (Ar-*C*), 128.8 (Ar-*C*), 128.1 (Ar-*C*), 127.4 (Ar-*C*), 125.2 (Ar-*C)*, 120.7 (*ipso*-Ar-*C)*, 118.9 (Ar-*C*), 118.2 (Ar-*C*), 117.5 (*ipso*-Ar-*C*), 112.6 (Ar-*C*), 41.7 (*C*H$_2$CO); *m/z* (ES$^+$) 454 ([$^{35,35}$Cl]MH$^+$), 456 ([$^{35,37}$Cl]MH$^+$), 458 ([$^{37,37}$Cl]MH$^+$); HRMS (ES$^+$) Found [$^{35,35}$Cl]MH$^+$, 454.0836 ($C_{22}H_{18}{}^{35,35}Cl_2N_5O_2$ requires 454.0832).

**6-chloro-2-(4-chlorophenyl)-N-(2-oxo-2-(2-phenylhydrazineyl)ethyl)imidazo[1,2-*a*]pyridine-3-carboxamid 44Ab**

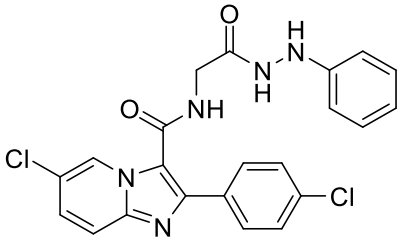

Using the standard procedure provided, *tert*-butyl (2-oxo-2-(2-phenylhydrazineyl)ethyl)carbamate **51Aa** (0.05 g, 0.20 mmol) was transformed following flash chromatography (DCM/EtOAc [1:2]) into the title compound as a white powder (47 mg, 50 %); $R_f$ 0.20 (DCM/EtOAc [1:2]); m.p. 205 - 208 °C; $\nu_{max}$ 3238 (N-H), 2981 (C-H), 1699 (C=O), 1629 (C=O), 1496, 1395, 1211, 1170, 1010, 956, 837, 800, 752, 691 $cm^{-1}$; $\delta_H$ (300 MHz, DMSO-$d_6$) 9.85 (1H, d, *J* 2, CON*H*NH), 9.05 (1H, s, Ar-*H*), 8.81 (1H, t, *J* 5, CON*H*$CH_2$), 7.97 - 7.90 (2H, d, *J* 8, Ar-*H*), 7.81 (1H, d, *J* 2, CONHN*H*), 7.74 (1H, d, *J* 10, Ar-*H*), 7.54 – 7.43 (3H, m, Ar-H), 7.17 - 7.09 (2H, t, *J* 8, Ar-*H*), 6.79 – 6.74 (2H, d, *J* 8, Ar-*H*), 6.70 (1H, t, *J* 8, Ar-*H*), 4.07 – 3.99 (2H, d, *J* 5, C*H*$_2$CO); δC (75 MHz, DMSO-$d_6$) 169.1 (*C*ONHNH), 161.2 (*C*ONHCH$_2$), 149.6 (*ipso*-Ar-*C)*, 144.5 (*ipso*-Ar-*C)*, 143.4 (*ipso*-Ar-*C)*, 133.7 (*ipso*-Ar-*C)*, 132.3 (*ipso*-Ar-*C)*, 130.5 (Ar-*C*), 129.5 (Ar-*C*), 129.1 (Ar-*C*), 128.1 (Ar-*C*), 125.2 (Ar-*C*), 120.5 (*ipso*-Ar-*C*), 118.9 (Ar-*C*), 118.1 (Ar-*C*), 117.1 (*ipso*-Ar-*C*), 112.6 (Ar-*C*), 41.7 (*C*H$_2$CO); ***m/z*** (ES$^+$) 454 ([$^{35,35}$Cl]MH$^+$), 456 ([$^{35,37}$Cl]MH$^+$), 458 ([$^{37,37}$Cl]MH$^+$); HRMS (ES$^+$) Found [$^{35,35}$Cl]MH$^+$, 454.0834 ($C_{22}H_{18}{}^{35,35}Cl_2N_5O_2$ requires 454.0832).

**6-chloro-N-(2-oxo-2-(2-phenylhydrazineyl)ethyl)-2-(3-(trifluoromethyl)phenyl)imidazo[1,2-*a*]pyridine-3-carboxamide 44Ac**

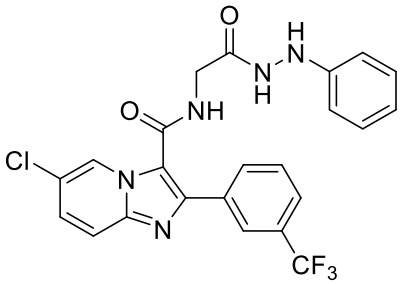

Using the standard procedure provided, *tert*-butyl (2-oxo-2-(2-phenylhydrazineyl)ethyl)carbamate **51Aa** (0.09 g, 0.33 mmol) was transformed following flash chromatography (DCM/EtOAc [1:2]) into the title compound as a white powder (80 mg, 48 %); $R_f$ 0.30 (DCM/EtOAc [1:2]); m.p. 210 - 215 °C; $\nu_{max}$ 3284 (N-H), 2981 (C-H), 1687 (C=O), 1605 (C=O), 1539, 1494, 1386, 1324, 1263, 1222, 1173,

1073, 815, 763, 691 $cm^{-1}$; $\delta_H$ (700 MHz, DMSO-$d_6$) 9.86 (1H, d, *J* 2, CON*H*NH), 9.05 (1H, dd, *J* 2, 1, Ar-*H*), 8.97 (1H, t, *J* 5, CON*H*$CH_2$), 8.27 - 8.20 (2H, m, Ar-H), 7.81 (1H, d, *J* 2, CONHN*H*), 7.79 (1H, dd, *J* 9, 1, Ar-*H*), 7.75 (1H, m, Ar-H), 7.65 (1H, t, *J* 8, Ar-H), 7.52 (1H, dd, *J* 9, 2, Ar-H), 7.16 - 7.09 (2H, t, *J* 7, Ar-H), 6.79 – 6.75 (2H, d, *J* 7, Ar-H), 6.70 (1H, t, *J* 7, Ar-*H*), 4.07 – 3.99 (2H, d, *J* 5, C*H*$_2$CO); δC (75 MHz, DMSO-$d_6$) 169.0 (*C*ONHNH), 161.1 (*C*ONHCH$_2$), 149.6 (*ipso*-Ar-*C)*, 143.8 (*ipso*-Ar-*C)*, 143.5 (*ipso*-Ar-*C)*, 134.5 (*ipso*-Ar-*C)*, 132.7 (Ar-*C)*, 130.2 (Ar-*C*), 129.1 (Ar-*C*), 128.3 (Ar-*C*), 125.5 (Ar-*C)*, 125.3 (Ar-*C)*, 120.7 (*ipso*-Ar-*C)*, 118.9 (Ar-*C*), 118.3 (Ar-*C*), 117.6 (*ipso*-Ar-*C*), 112.6 (Ar-*C*), 41.7 (*C*H$_2$CO); $\delta_F$ (282 MHz, DMSO-$d_6$) -61.2 (C*F*$_3$); *m/z* (ES$^+$) 488 ([$^{35}$Cl]MH$^+$), 490 ([$^{37}$Cl]MH$^+$); HRMS (ES$^+$) Found [$^{35}$Cl]MH$^+$, 488.1091 ($C_{23}H_{18}{}^{35}ClF_3N_5O_2$ requires 488.1096).

**6-chloro-N-(2-oxo-2-(2-phenylhydrazineyl)ethyl)-2-(4-(trifluoromethyl)phenyl)imidazo[1,2-*a*]pyridine-3-carboxamide 44Ad**

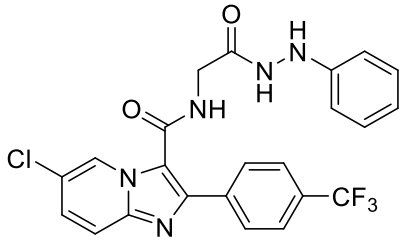


Using the standard procedure provided, *tert*-butyl (2-oxo-2-(2-phenylhydrazineyl)ethyl)carbamate **51Aa** (0.08 g, 0.32 mmol) was transformed following flash chromatography (DCM/EtOAc [1:2]) into the title compound as a white powder (85 mg, 54 %); $R_f$ 0.30 (DCM/EtOAc [1:2]); m.p. 212 - 215 °C; $\nu_{max}$ 3255 (N-H), 2980 (C-H), 1618 (C=O), 1536, 1494, 1384, 1251, 1175, 1077, 954, 812, 690 $cm^{-1}$; $\delta_H$ (300 MHz, DMSO-$d_6$) 9.89 (1H, d, *J* 2, CON*H*NH), 9.04 (1H, dd, *J* 2, 1, Ar-*H*), 8.97 (1H, t, *J* 5, CON*H*$CH_2$), 8.20 – 8.14 (2H, d, *J* 8, Ar-H), 7.83 (1H, d, *J* 2, CONHN*H*), 7.81 – 7.75 (3H, m, Ar-*H*), 7.52 (1H, dd, *J* 9, 2, Ar-*H*), 7.18 - 7.10 (2H, t, *J* 7, Ar-*H*), 6.80 – 6.76 (2H, d, *J* 7, Ar-H), 6.71 (1H, t, *J* 7, Ar-*H*), 4.10 – 3.99 (2H, d, *J* 6, C*H*$_2$C=O); δC (75 MHz, DMSO-$d_6$) 169.1 (*C*ONHNH), 161.1 (CONH*C*H$_2$), 149.6 (*ipso*-Ar-*C)*, 143.8 (*ipso*-Ar-*C)*, 143.4 (*ipso*-Ar-*C)*, 137.4 (*ipso*-Ar-*C)*, 129.4 (Ar-*C*), 129.1 (Ar-*C*), 128.8 (Ar-*C*), 128.3 (Ar-*C*), 125.8 (Ar-*C*), 125.2 (Ar-*C*), 120.7 (*ipso*-Ar-*C*), 118.9 (Ar-*C*), 118.3 (Ar-*C*), 117.9 (*ipso*-Ar-*C*), 112.6 (Ar-*C*), 41.7 (*C*H$_2$C=O); $\delta_F$ (282 MHz, DMSO-$d_6$) -61.1 (C*F*$_3$); *m/z* (ES$^+$) 488 ([$^{35}$Cl]MH$^+$), 490 ([$^{37}$Cl]MH$^+$); HRMS (ES$^+$) Found [$^{35}$Cl]MH$^+$, 488.1136 ($C_{23}H_{18}{}^{35}ClF_3N_5O_2$ requires 488.1096).

**6-chloro-2-(3-methoxyphenyl)-N-(2-oxo-2-(2-phenylhydrazineyl)ethyl)imidazo[1,2-*a*]pyridine-3-carboxamide 44Ae**

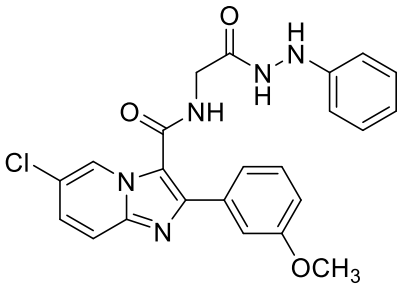

Using the standard procedure provided, *tert*-butyl (2-oxo-2-(2-phenylhydrazineyl)ethyl)carbamate **51Aa** (0.09 g, 0.33 mmol) was transformed following flash chromatography (DCM/EtOAc [1:2]) into the title compound as a white powder (77 mg, 50 %); $R_f$ 0.20 (DCM/EtOAc [1:2]); m.p. 210 - 212 °C; $\nu_{max}$ 3293 (N-H), 2981 (C-H), 1710 (C=O), 1605 (C=O), 1495, 1385, 1278, 1223, 1110, 811, 752, 692 $cm^{-1}$; $\delta_H$ (300 MHz, DMSO-$d_6$) 9.83 (1H, d, *J* 2, CON*H*NH), 9.10 (1H, dd, *J* 2, 1, Ar-*H*), 8.72 (1H, t, *J* 5, CON*H*$CH_2$), 7.81 (1H, d, *J* 2, CONHN*H*), 7.75 (1H, dd, *J* 9, 1, Ar-*H*), 7.50 – 7.45 (3H, m, Ar-*H*), 7.35 (1H, t, *J* 8, Ar-*H*), 7.17 - 7.08 (2H, t, *J* 7, Ar-H), 6.96 (1H, dd, *J* 8, 2, Ar-*H*), 6.79 – 6.74 (2H, t, *J* 7, Ar-*H*), 6.70 (1H, t, *J* 7, Ar-*H*), 4.07 – 3.97 (2H, d, *J* 5, C*H*$_2$CO), 3.79 (3H, s, Ar-OC*H*$_3$); δC (75 MHz, DMSO-$d_6$) 169.0 (*C*ONHNH), 161.4 (*C*ONHCH$_2$), 159.6 (*C*-OCH$_3$), 149.6 (*ipso*-Ar-*C*), 145.4 (*ipso*-Ar-*C*), 143.2 (*ipso*-Ar-*C*), 134.8 (*ipso*-Ar-*C*), 130.1 (Ar-*C*), 129.1 (Ar-*C*), 127.9 (Ar-*C*), 125.1 (Ar-*C*), 121.3 (Ar-*C*), 120.4 (*ipso*-Ar-*C*), 118.9 (Ar-*C*), 118.1 (Ar-*C*), 115.1 (Ar-*C*), 113.6 (Ar-*C*), 112.6 (Ar-*C*), 55.5 (Ar-O*C*H$_3$), 41.8 (*C*H$_2$CO); *m/z* (ES$^+$) 450 ([$^{35}$Cl]MH$^+$), 452 ([$^{37}$Cl]MH$^+$); HRMS (ES$^+$) Found [$^{35}$Cl]MH$^+$, 450.1688 ($C_{23}H_{21}{}^{35}ClN_5O_3$ requires 450.1327).

**6-chloro-2-(4-methoxyphenyl)-N-(2-oxo-2-(2-phenylhydrazineyl)ethyl)imidazo[1,2-*a*]pyridine-3-carboxamide 44Af**

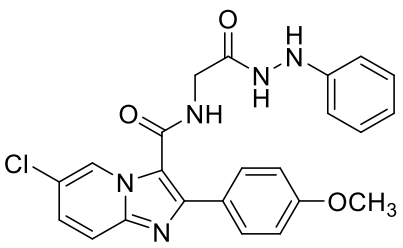

Using the standard procedure provided, *tert*-butyl (2-oxo-2-(2-phenylhydrazineyl)ethyl)carbamate **51Aa** (0.06 g, 0.24 mmol) was transformed following flash chromatography (DCM/EtOAc [1:2]) into the title compound as a white powder (52 mg, 47 %); $R_f$ 0.20 (DCM/EtOAc [1:2]); m.p. 212 - 217 °C; $\nu_{max}$ 3263 (N-H), 2981 (C-H), 1699 (C=O), 1621 (C=O), 1495, 1385, 1330, 1250, 1169, 1033, 954, 750, 646 $cm^{-1}$; $\delta_H$ (300 MHz, DMSO-$d_6$) 9.83 (1H, d, *J* 2, CON*H*NH), 9.07 (1H, dd, *J* 2, 1, Ar-*H*), 8.63 (1H, t, *J* 5, CON*H*$CH_2$), 7.91 - 7.84 (2H, d, *J* 8, Ar-*H*), 7.80 (1H, d, *J* 2, CONHN*H*), 7.71 (1H, dd, *J* 9, 1, Ar-*H*), 7.46 (1H, dd, *J* 9, 2, Ar-*H*), 7.18 - 7.07 (2H, t, *J* 7, Ar-*H*), 7.03 – 6.96 (2H, d, *J* 8, Ar-*H*), 6.81 – 6.74 (2H, t, *J* 7, Ar-*H*), 6.70 (1H, t, *J* 7, Ar-*H*), 4.07 – 3.97 (2H, d, *J* 5, C*H*$_2$C=O), 3.78 (3H, s, Ar-OC*H*$_3$); δC (75 MHz, DMSO-$d_6$) 169.1 (*C*ONHNH), 161.5 (*C*ONHCH$_2$), 160.0 (*C*-OCH$_3$*)*, 149.6 (*ipso*-Ar-*C)*, 145.9 (*ipso*-Ar-*C)*, 143.3 (*ipso*-Ar-*C)*, 136.5 (*ipso*-Ar-*C)*, 130.2 (Ar-*C*), 129.1 (Ar-*C*), 127.7 (Ar-*C*), 125.8 (Ar-*C*), 120.1 (*ipso*-Ar-*C*), 118.9 (Ar-*C*), 117.9 (Ar-*C*), 116.1 (*ipso*-Ar-*C*), 114.4 (Ar-*C*), 112.6 (Ar-*C*), 55.6 (Ar-O*C*H$_3$), 41.7 (*C*H$_2$CO); *m/z* (ES$^+$) 450 ([$^{35}$Cl]MH$^+$), 452 ([$^{37}$Cl]MH$^+$); HRMS (ES$^+$) Found [$^{35}$Cl]MH$^+$, 450.1322 ($C_{23}H_{21}{}^{35}ClN_5O_3$ requires 450.1327).

**(S)-6-chloro-2-(3-chlorophenyl)-N-(1-oxo-1-(2-phenylhydrazineyl)propan-2-yl)imidazo[1,2-*a*]pyridine-3-carboxamide 44Ag**

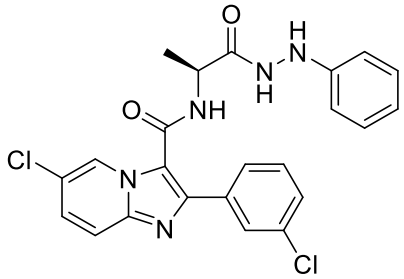

Using the standard procedure provided, *tert*-butyl (S)-(1-oxo-1-(2-phenylhydrazineyl)propan-2-yl)carbamate **51Aj** (0.09 g, 0.32 mmol) was transformed following flash chromatography (DCM/EtOAc [1:2]) into the title compound as a white powder (60 mg, 40 %); $R_f$ 0.30 (DCM/EtOAc [1:2]); m.p. 215 - 217 °C; $\nu_{max}$ 3241 (N-H), 2981 (C-H), 1690 (C=O), 1620, 1600, 1532, 1494, 1372, 1334, 1230, 1172, 1079, 955, 812, 791, 690 $cm^{-1}$; $\delta_H$ (300 MHz, DMSO-$d_6$) 9.93 (1H, d, *J* 2, CON*H*NH), 8.99 (1H, dd, *J* 2, 1, Ar-*H*), 8.85 (1H, d, *J* 7, CON*H*CH), 7.94 (1H, m, Ar-*H*), 7.87 (1H, m, Ar-*H*), 7.81 (1H, d, *J* 2, CONHN*H*), 7.76 (1H, dd, *J* 9, 1, Ar-*H*), 7.50 (1H, dd, *J* 9, 2, Ar-*H*), 7.48 – 7.43 (2H, m, Ar-*H*), 7.18 – 7.06 (2H, t, *J* 7, Ar-*H*), 6.80 – 6.73 (2H, d, *J* 7, Ar-*H*),

6.69 (1H, t, *J* 7, Ar-H), 4.60 (1H, m, C*H*$CH_3$), 1.43 – 1.28 (3H, d, *J* 6, CHC*H*$_3$); δC (75 MHz, DMSO-$d_6$) 172.4 (*C*ONHNH), 160.4 (*C*ONHCH), 149.6 (*ipso*-Ar-*C)*, 143.9 (*ipso*-Ar-*C)*, 143.3 (*ipso*-Ar-*C)*, 135.6 (*ipso*-Ar-*C)*, 133.6 (*ipso*-Ar-*C)*, 130.8 (Ar-*C)*, 129.1 (Ar-*C*), 128.8 (Ar-*C*), 128.2 (Ar-*C*), 127.4 (Ar-*C*), 125.2 (Ar-*C*), 120.6 (*ipso*-Ar-*C*), 118.9 (Ar-*C*), 118.2 (Ar-*C*), 117.4 (*ipso*-Ar-*C*), 112.6 (Ar-*C*), 48.4 (*C*H$CH_3$), 17.7 (CH*C*H$_3$); *m/z* ($ES^+$) 468 ([$^{35,35}$Cl]$MH^+$), 470 ([$^{35,37}$Cl]$MH^+$), 472 ([$^{37,37}$Cl]$MH^+$); HRMS ($ES^+$) Found [$^{35,35}$Cl]$MH^+$, 468.0988 ($C_{23}H_{20}{}^{35,35}Cl_2N_5O_2$ requires 468.0989).

**(S)-6-chloro-2-(4-chlorophenyl)-N-(1-oxo-1-(2-phenylhydrazineyl)propan-2-yl)imidazo[1,2-*a*]pyridine-3-carboxamide 44Ah**

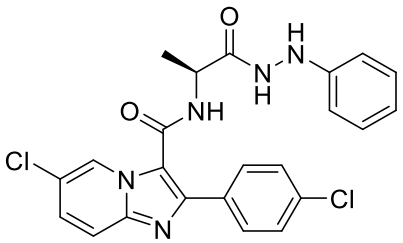

Using the standard procedure provided, *tert*-butyl (S)-(1-oxo-1-(2-phenylhydrazineyl)propan-2-yl)carbamate **51Aj** (0.09 g, 0.32 mmol) was transformed following flash chromatography (DCM/EtOAc [1:2]) into the title compound as a white powder (45 mg, 30 %); $R_f$ 0.33 (DCM/EtOAc [1:2]); m.p. 212 - 214 °C; $\nu_{max}$ 3289 (N-H), 2981 (C-H), 1693 (C=O), 1605, 1541, 1494, 1388, 1321, 1168, 1111, 1065, 952, 813, 756, 692 $cm^{-1}$; $\delta_H$ (300 MHz, DMSO-$d_6$) 9.93 (1H, s, CON*H*NH), 8.99 (1H, s, Ar-*H*), 8.81 (1H, d, *J* 7, CON*H*CH), 7.99 – 7.89 (2H, d, *J* 8, Ar-*H*), 7.74 (1H, d, *J* 9, Ar-*H*), 7.53 – 7.42 (3H, m, Ar-*H*), 7.18 – 7.06 (2H, t, *J* 7, Ar-*H*), 6.81 – 6.73 (2H, d, *J* 7, Ar-*H*), 6.68 (1H, t, *J* 7, Ar-*H*), 4.58 (1H, m, C*H*$CH_3$), 1.44 – 1.29 (3H, d, *J* 6, CHC*H*$_3$); δC (75 MHz, DMSO-$d_6$) 172.4 (*C*ONHNH), 160.6 (*C*ONHCH), 149.7 (*ipso*-Ar-*C)*, 144.3 (*ipso*-Ar-*C)*, 143.3 (*ipso*-Ar-*C)*, 133.6 (*ipso*-Ar-*C)*, 132.3 (*ipso*-Ar-*C)*, 130.4 (Ar-*C)*, 129.1 (Ar-*C*), 128.9 (Ar-*C*), 128.0 (Ar-*C*), 125.1 (Ar-*C*), 120.5 (*ipso*-Ar-*C*), 118.9 (Ar-*C*), 118.1 (Ar-*C*), 117.2 (*ipso*-Ar-*C*), 112.6 (Ar-*C*), 48.4 (*C*H$CH_3$), 17.8 (CH*C*H$_3$); *m/z* ($ES^+$) 468 ([$^{35,35}$Cl]$MH^+$), 470 ([$^{35,37}$Cl]$MH^+$), 472 ([$^{37,37}$Cl]$MH^+$); HRMS ($ES^+$) Found [$^{35,35}$Cl]$MH^+$, 468.0985 ($C_{23}H_{20}{}^{35,35}Cl_2N_5O_2$ requires 468.0989).

**(S)-6-chloro-N-(1-oxo-1-(2-phenylhydrazineyl)propan-2-yl)-2-(3-(trifluoromethyl)phenyl)imidazo[1,2-*a*]pyridine-3-carboxamide 44Ai**

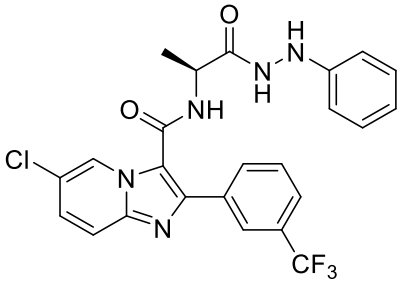

Using the standard procedure provided, *tert*-butyl (*S*)-(1-oxo-1-(2-phenylhydrazineyl)propan-2-yl)carbamate **51Aj** (0.09 g, 0.33 mmol) was transformed following flash chromatography (DCM/EtOAc [1:1]) into the title compound as a white powder (61 mg, 36 %); $R_f$ 0.33 (DCM/EtOAc [1:1]); m.p. 213 - 218 °C; $\nu_{max}$ 3247 (N-H), 1669 (C=O), 1615, 1535, 1494, 1377, 1323, 1227, 1164, 1118, 1073, 876, 806, 744, 691 $cm^{-1}$; $\delta_H$ (300 MHz, DMSO-$d_6$) 9.93 (1H, s, CON*H*NH), 8.99 (1H, s, Ar-*H*), 8.93 (1H, d, *J* 7, CON*H*CH), 8.27 – 8.16 (2H, m, Ar-*H*), 7.81 – 7.73 (2H, m, Ar-*H*), 7.66 (1H, t, *J* 7, Ar-*H*), 7.52 (1H, dd, *J* 9, 1, Ar-*H*), 7.19 – 7.06 (2H, t, *J* 7, Ar-*H*), 6.82 – 6.73 (2H, d, *J* 7, Ar-*H*), 6.70 (1H, t, *J* 7, Ar-*H*), 4.60 (1H, m, C*H*$CH_3$), 1.41 – 1.28 (3H, d, *J* 6, CHC*H*$_3$); δC (75 MHz, DMSO-$d_6$) 172.4 (*C*ONHNH), 160.5 (CONH*C*H), 149.6 (*ipso*-Ar-*C)*, 143.8 (*ipso*-Ar-*C)*, 143.4 (*ipso*-Ar-*C)*, 134.6 (*ipso*-Ar-*C)*, 132.7 (Ar-*C)*, 130.1 (Ar-*C)*, 129.1 (Ar-*C*), 128.3 (Ar-*C*), 125.5 (Ar-*C*), 125.2 (Ar-*C*), 124.9 (Ar-*C)*, 120.7 (*ipso*-Ar-*C*), 118.9 (Ar-*C*), 118.3 (Ar-*C*), 117.6 (*ipso*-Ar-*C*), 112.6 (Ar-*C*), 48.4 (*C*H$CH_3$), 17.6 (CH*C*$H_3$); $\delta_F$ (282 MHz, DMSO-$d_6$) -61.2 (C*F*$_3$); *m/z* ($ES^+$) 502 ([$^{35}$Cl]$MH^+$), 504 ([$^{37}$Cl]$MH^+$); HRMS ($ES^+$) Found [$^{35}$Cl]$MH^+$, 502.1248 ($C_{24}H_{20}{}^{35}ClF_3N_5O_2$ requires 502.1252).

**(S)-6-chloro-N-(1-oxo-1-(2-phenylhydrazineyl)propan-2-yl)-2-(4-(trifluoromethyl)phenyl)imidazo[1,2-*a*]pyridine-3-carboxamide 44Aj**

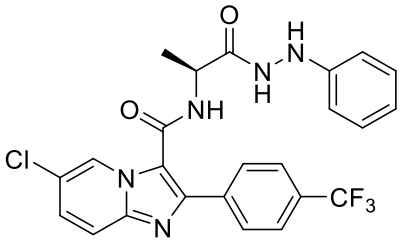

Using the standard procedure provided, *tert*-butyl (S)-(1-oxo-1-(2-phenylhydrazineyl)propan-2-yl)carbamate **51Aj** (0.10 g, 0.35 mmol) was transformed following flash chromatography (DCM/EtOAc [1:2]) into the title compound as a white powder (67 mg, 37 %); $R_f$ 0.30 (DCM/EtOAc [1:2]); m.p. 210 - 212 °C; $\nu_{max}$ 3289 (N-

H), 2981 (C-H), 1693 (C=O), 1605, 1541, 1494, 1388, 1321, 1168, 1111, 1065, 952, 813, 756, 692 $cm^{-1}$; $\delta_H$ (300 MHz, DMSO-$d_6$) 9.97 (1H, s, CON*H*NH), 9.05 – 8.89 (2H, m, Ar-*H*), 8.17 – 8.09 (2H, d, *J* 8, Ar-*H*), 7.85 (1H, s, CONHN*H*), 7.80 – 7.71 (3H, t, *J* 8, Ar-*H*), 7.50 (1H, dd, *J* 9, 2, Ar-*H*), 7.18 – 7.06 (2H, t, *J* 7, Ar-*H*), 6.82 – 6.74 (2H, d, *J* 7, Ar-*H*), 6.69 (1H, t, *J* 7, Ar-*H*), 4.63 (1H, m, C*H*$CH_3$), 1.43 – 1.30 (3H, d, *J* 6, CHC*H₃*); δC (75 MHz, DMSO-$d_6$) 172.5 (*C*ONHNH), 160.5 (CONH*C*H), 149.7 (*ipso*-Ar-*C)*, 143.6 (*ipso*-Ar-*C)*, 143.3 (*ipso*-Ar-*C)*, 137.5 (*ipso*-Ar-*C)*, 129.3 (Ar-*C*), 129.1 (Ar-*C*), 128.2 (Ar-*C*), 126.5 (Ar-*C*), 125.7 (Ar-*C*), 125.1 (Ar-*C*), 120.7 (*ipso*-Ar-*C*), 118.9 (Ar-*C*), 118.3 (Ar-*C*), 118.0 (*ipso*-Ar-*C*), 112.6 (Ar-*C*), 48.4 (*C*H$CH_3$), 17.7 (CH*C*$H_3$); $\delta_F$ (282 MHz, DMSO-$d_6$) -60.8 (C*F*$_3$); ***m/z*** ($ES^+$) 502 ([$^{35}$Cl]$MH^+$), 504 ([$^{37}$Cl]$MH^+$); HRMS ($ES^+$) Found [$^{35}$Cl]$MH^+$, 502.1250 ($C_{24}H_{20}{}^{35}ClF_3N_5O_2$ requires 502.1252).

**(S)-6-chloro-2-(3-methoxyphenyl)-N-(1-oxo-1-(2-phenylhydrazineyl)propan-2-yl)imidazo[1,2-*a*]pyridine-3-carboxamide 44Ak**

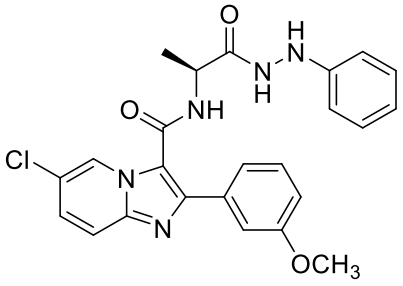


Using the standard procedure provided, *tert*-butyl (S)-(1-oxo-1-(2-phenylhydrazineyl)propan-2-yl)carbamate **51Aj** (0.09 g, 0.34 mmol) was transformed following flash chromatography (DCM/EtOAc [1:2]) into the title compound as a white powder (85 mg, 54 %); $R_f$ 0.35 (DCM/EtOAc [1:2]); m.p. 215 - 219 °C; $\nu_{max}$ 3263 (N-H), 2981 (C-H), 1690 (C=O), 1600, 1494, 1388, 1219, 1154, 1087, 954, 846, 790, 753, 683 $cm^{-1}$; $\delta_H$ (300 MHz, DMSO-$d_6$) 9.91 (1H, s, CON*H*NH), 9.05 (1H, s, Ar-*H*), 8.61 (1H, d, *J* 7, CON*H*CH), 7.75 (1H, d, *J* 9, Ar-*H*), 7.52 – 7.42 (3H, m, Ar-H), 7.35 (1H, t, *J* 8, Ar-*H*), 7.17 – 7.08 (2H, t, *J* 7, Ar-*H*), 6.97 (1H, d, *J* 8, Ar-*H*), 6.81 – 6.73 (2H, d, *J* 7, Ar-*H*), 6.68 (1H, t, *J* 7, Ar-*H*), 4.59 (1H, m, C*H*$CH_3$), 3.78 (3H, s, Ar-OC*H₃*), 1.43 – 1.24 (3H, d, *J* 6, CHC*H₃*); δC (75 MHz, DMSO-$d_6$) 172.4 (*C*ONHNH), 160.7 (CONH*C*H), 159.7 (Ar-*C*-$OCH_3$*)*, 149.6 (*ipso*-Ar-*C)*, 145.4 (*ipso*-Ar-*C)*, 143.2 (*ipso*-Ar-*C)*, 134.7 (*ipso*-Ar-*C)*, 130.1 (Ar-*C)*, 129.1 (Ar-*C*), 127.9 (Ar-*C*), 125.1 (Ar-*C*), 121.1 (Ar-*C*), 120.4 (*ipso*-Ar-*C*), 118.9 (Ar-*C*), 118.1 (Ar-*C*), 117.0 (*ipso*-Ar-*C*), 114.9 (Ar-*C*), 113.8 (Ar-*C*), 112.6 (Ar-*C*), 55.6 (Ar-O*C*$H_3$), 48.3 (*C*H$CH_3$), 17.9 (CH*C*$H_3$); ***m/z*** ($ES^+$)

464 ([$^{35}$Cl]MH$^+$), 466 ([$^{37}$Cl]MH$^+$); HRMS (ES$^+$) Found [$^{35}$Cl]MH$^+$, 464.1487 ($C_{24}H_{23}{}^{35}ClN_5O_3$ requires 464.1484).

**(S)-6-chloro-2-(4-methoxyphenyl)-N-(1-oxo-1-(2-phenylhydrazineyl)propan-2-yl)imidazo[1,2-*a*]pyridine-3-carboxamide 44Al**

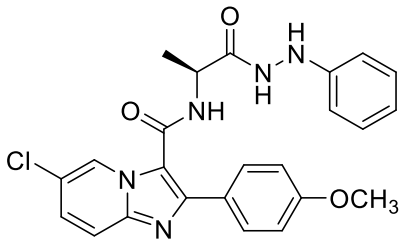

Using the standard procedure provided, *tert*-butyl (S)-(1-oxo-1-(2-phenylhydrazineyl)propan-2-yl)carbamate **51Aj** (0.09 g, 0.32 mmol) was transformed following flash chromatography (DCM/EtOAc [1:2]) into the title compound as a white powder (64 mg, 43 %); $R_f$ 0.35 (DCM/EtOAc [1:2]); m.p. 215 - 218 °C; $\nu_{max}$ 3302 (N-H), 2981 (C-H), 1686 (C=O), 1539, 1495, 1391, 1301, 1250, 1169, 951, 839, 695 cm$^{-1}$; $\delta_H$ (300 MHz, DMSO-d$_6$) 9.92 (1H, s, CON*H*NH), 9.03 (1H, s, Ar-*H*), 8.53 (1H, d, *J* 7, CON*H*CH), 7.94 – 7.77 (3H, d, *J* 8, Ar-*H*), 7.71 (1H, d, *J* 9, Ar-*H*), 7.47 (1H, d, *J* 9, Ar-*H*), 7.20 – 7.07 (2H, t, *J* 7, Ar-*H*), 7.04 – 6.95 (2H, d, *J* 8, Ar-*H*), 6.82 – 6.73 (2H, d, *J* 7, Ar-*H*), 6.69 (1H, t, *J* 7, Ar-*H*), 4.59 (1H, m, C*H*CH$_3$), 3.78 (3H, s, Ar-OC*H$_3$*), 1.44 – 1.29 (3H, d, *J* 6, CHC*H$_3$*); δC (75 MHz, DMSO-d$_6$) 172.4 (*C*ONHNH), 160.9 (*C*ONHCH), 160.1 (Ar-*C*-OCH$_3$*)*, 149.7 (*ipso*-Ar-*C)*, 145.9 (*ipso*-Ar-*C)*, 143.3 (*ipso*-Ar-*C)*, 130.2 (Ar-*C)*, 129.1 (Ar-*C*), 127.7 (Ar-*C*), 125.8 (*ipso*-Ar-*C*), 125.0 (Ar-*C*), 120.2 (*ipso*-Ar-*C*), 118.9 (Ar-*C*), 117.8 (Ar-*C*), 116.1 (*ipso*-Ar-*C*), 114.3 (Ar-*C*), 112.6 (Ar-*C*), 55.6 (Ar-O*C*H$_3$), 48.4 (*C*HCH$_3$), 17.9 (CH*C*H$_3$); *m/z* (ES$^+$) 464 ([$^{35}$Cl]MH$^+$), 466 ([$^{37}$Cl]MH$^+$); HRMS (ES$^+$) Found [$^{35}$Cl]MH$^+$, 464.1476 ($C_{24}H_{23}{}^{35}ClN_5O_3$ requires 464.1484).

**(S)-6-chloro-2-(3-chlorophenyl)-N-(4-(methylthio)-1-oxo-1-(2-phenylhydrazineyl)butan-2-yl)imidazo[1,2-*a*]pyridine-3-carboxamide 44Am**

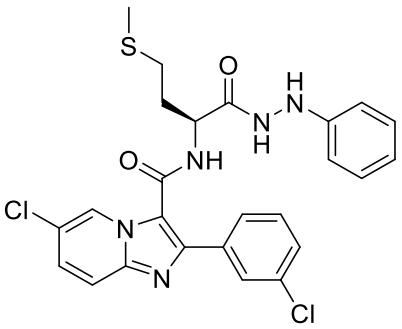

Using the standard procedure provided, *tert*-butyl (S)-(4-(methylthio)-1-oxo-1-(2-phenylhydrazineyl)butan-2-yl)carbamate **51Bb** (0.11 g, 0.32 mmol) was transformed following flash chromatography (DCM/EtOAc [1:2]) into the title compound as a white powder (55 mg, 32 %); $R_f$ 0.40 (DCM/EtOAc [1:2]); m.p. 210 - 212 °C; $\nu_{max}$ 3260 (N-H), 2981 (C-H), 1680 (C=O), 1622 (C=O), 1493, 1382, 1230, 1173, 1079, 953, 793, 691 $cm^{-1}$; $\delta_H$ (300 MHz, DMSO-$d_6$) 10.01 (1H, s, CON*H*NH), 8.93 (1H, s, Ar-*H*), 8.88 (1H, d, *J* 7, CON*H*CH), 7.91 (1H, s, Ar-*H*), 7.82 (1H, d, *J* 7, Ar-*H*), 7.77 (1H, d, *J* 9, Ar-*H*), 7.51 (1H, dd, *J* 9, 1, Ar-*H*), 7.48 – 7.40 (2H, m, Ar-*H*), 7.19 – 7.09 (2H, t, *J* 7, Ar-H), 6.81 – 6.74 (2H, d, *J* 7, Ar-*H*), 6.70 (1H, t, *J* 7, Ar-*H*), 4.64 (1H, m, CONHC*H*), 2.49 – 2.42 (2H, m, C*H*$_2$CH$_2$SCH$_3$), 2.10 – 1.84 (5H, m, CH$_2$C*H*$_2$S*CH*$_3$); δC (75 MHz, DMSO-$d_6$) 171.5 (*C*ONHNH), 161.1 (*C*ONHCH), 149.6 (*ipso*-Ar-*C)*, 144.1 (*ipso*-Ar-*C)*, 143.3 (*ipso*-Ar-*C)*, 135.7 (*ipso*-Ar-*C)*, 133.7 (*ipso*-Ar-*C)*, 130.8 (Ar-*C*), 129.1 (Ar-*C*), 128.8 (Ar-*C*), 128.3 (Ar-*C*), 127.4 (Ar-*C*), 124.9 (Ar-*C)*, 120.7 (*ipso*-Ar-*C)*, 119.0 (Ar-*C*), 118.3 (Ar-*C*), 117.4 (*ipso*-Ar-*C*), 112.6 (Ar-*C*), 52.2 (C=ONH*C*H), 31.1 (CH$_2$*C*H$_2$SCH$_3$), 30.1 (*C*H$_2$CH$_2$SCH$_3$), 14.9 (CH$_2$CH$_2$S*C*H$_3$); ***m/z*** (ES$^+$) 528 ([$^{35,35}$Cl]MH$^+$), 530 ([$^{35,37}$Cl]MH$^+$), 532 ([$^{37,37}$Cl]MH$^+$); HRMS (ES$^+$) Found [$^{35,35}$Cl]MH$^+$, 528.1016 ($C_{25}H_{24}{}^{35,35}Cl_2N_5O_2S$ requires 528.1022).

**(S)-6-chloro-2-(4-chlorophenyl)-N-(4-(methylthio)-1-oxo-1-(2-phenylhydrazineyl)butan-2-yl)imidazo[1,2-*a*]pyridine-3-carboxamide 44An**

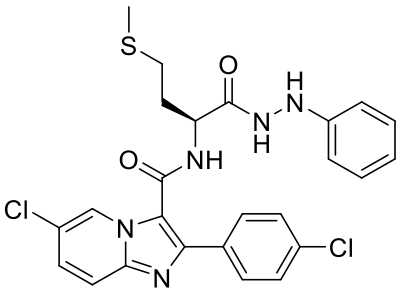

Using the standard procedure provided, *tert*-butyl (S)-(4-(methylthio)-1-oxo-1-(2-phenylhydrazineyl)butan-2-yl)carbamate **51Bb** (0.11 g, 0.32 mmol) was transformed following flash chromatography (DCM/EtOAc [3:1]) into the title compound as a white powder (77 mg, 45 %); $R_f$ 0.35 (DCM/EtOAc [3:1]); m.p. 213 - 218 °C; $\nu_{max}$ 3252 (N-H), 2981 (C-H), 1692 (C=O), 1622 (C=O), 1541, 1493, 1391, 1324, 1239, 1164, 1089, 955, 793, 692 $cm^{-1}$; $\delta_H$ (300 MHz, DMSO-$d_6$) 10.01 (1H, s, CON*H*NH), 8.89 (1H, dd, *J* 2, 1, Ar-*H*), 8.84 (1H, d, *J* 7, CON*H*CH), 7.90 – 7.85 (2H, d, *J* 8, Ar-*H*), 7.76 (1H, dd, *J* 9, 1, Ar-*H*), 7.50 (1H, dd, *J* 9, 2, Ar-*H*), 7.47 – 7.40 (2H, d, *J* 8, Ar-*H*), 7.18 – 7.09 (2H, t, *J* 7, Ar-*H*), 6.81 – 6.74 (2H, d, *J* 7, Ar-*H*), 6.70 (1H, t, *J* 7, Ar-*H*), 4.65 (1H, m, CONHC*H*), 2.49 – 2.41 (2H, m, C*H*$_2$CH$_2$SCH$_3$), 2.08 – 1.87 (5H, m, CH$_2$C*H*$_2$S*CH*$_3$); δC (75 MHz, DMSO-$d_6$) 171.5 (*C*ONHNH), 161.2 (*C*ONHCH), 149.7 (*ipso*-Ar-*C)*, 144.5 (*ipso*-Ar-*C)*, 143.3 (*ipso*-Ar-*C)*, 133.6 (*ipso*-Ar-*C)*, 132.4 (*ipso*-Ar-*C)*, 130.5 (Ar-*C*), 129.1 (Ar-*C*), 128.9 (Ar-*C*), 128.1 (Ar-*C*), 124.8 (Ar-*C)*, 120.6 (*ipso*-Ar-*C)*, 119.0 (Ar-*C*), 118.2 (Ar-*C*), 117.1 (*ipso*-Ar-*C*), 112.6 (Ar-*C*), 52.1 (CONH*C*H), 31.0 (CH$_2$*C*H$_2$SCH$_3$), 30.1 (*C*H$_2$CH$_2$SCH$_3$), 14.9 (CH$_2$CH$_2$S*C*H$_3$); *m/z* (ES$^+$) 528 ([$^{35,35}$Cl]MH$^+$), 530 ([$^{35,37}$Cl]MH$^+$), 532 ([$^{37,37}$Cl]MH$^+$); HRMS (ES$^+$) Found [$^{35,35}$Cl]MH$^+$, 528.1008 ($C_{25}H_{24}{}^{35,35}Cl_2N_5O_2S$ requires 528.1022).

**(S)-6-chloro-2-((3-trifluoromethyl)phenyl)-N-(4-(methylthio)-1-oxo-1-(2-phenylhydrazineyl)butan-2-yl)imidazo[1,2-*a*]pyridine-3-carboxamide 44Ao**

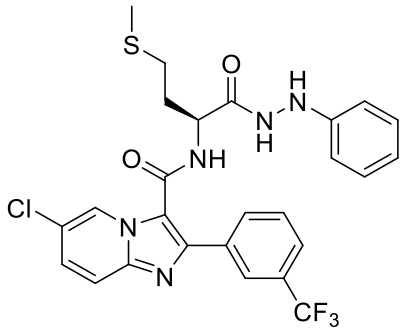


Using the standard procedure provided, *tert*-butyl (S)-(4-(methylthio)-1-oxo-1-(2-phenylhydrazineyl)butan-2-yl)carbamate **51Bb** (0.11 g, 0.32 mmol) was transformed following flash chromatography (DCM/EtOAc [3:1]) into the title compound as a white powder (60 mg, 33 %); $R_f$ 0.25 (DCM/EtOAc [3:1]); m.p. 213 - 218 °C; $\nu_{max}$ 3245 (N-H), 1667 (C=O), 1618 (C=O), 1536, 1493, 1322, 1232, 1159, 1118, 1072, 842, 689 $cm^{-1}$; $\delta_H$ (300 MHz, DMSO-$d_6$) 10.03 (1H, s, CON*H*NH), 8.98 (1H, d, *J* 7, CON*H*CH), 8.93 (1H, dd, *J* 2, 1, Ar-*H*), 8.23 (1H, s, Ar-*H*), 8.15 (1H, d, *J* 7, Ar-*H*), 7.84 (1H, bs,

CONHN*H*), 7.81 – 7.72 (2H, m, Ar-*H*), 7.63 (1H, t, *J* 7, Ar-*H*), 7.52 (1H, dd, *J* 9, 2, Ar-H), 7.19 – 7.08 (2H, t, *J* 7, Ar-*H*), 6.82 – 6.74 (2H, d, *J* 7, Ar-*H*), 6.70 (1H, t, *J* 7, Ar-*H*), 4.65 (1H, m, CONHC*H*), 2.49 -2.39 (2H, m, C*H*$_2$CH$_2$SCH$_3$), 2.07 – 1.85 (5H, m, CH$_2$C*H*$_2$S*CH*$_3$); δC (75 MHz, DMSO-d$_6$) 171.6 (*C*ONHNH), 161.1 (*C*ONHCH), 149.6 (*ipso*-Ar-*C)*, 143.9 (*ipso*-Ar-*C)*, 143.3 (*ipso*-Ar-*C)*, 134.6 (*ipso*-Ar-*C)*, 132.6 (Ar-*C)*, 130.0 (Ar-*C*), 129.1 (Ar-*C*), 128.3 (Ar-*C*), 125.0 (Ar-*C)*, 124.8 (Ar-*C)*, 120.8 (*ipso*-Ar-*C)*, 119.0 (Ar-*C*), 118.4 (Ar-*C*), 117.6 (*ipso*-Ar-*C*), 112.6 (Ar-*C*), 52.2 (CONH*C*H), 31.1 (CH$_2$*C*H$_2$SCH$_3$), 30.1 (*C*H$_2$CH$_2$SCH$_3$), 14.9 (CH$_2$CH$_2$S*C*H$_3$); δ$_F$ (282 MHz, DMSO-d$_6$) -61.2 (C*F*$_3$); ***m/z*** (ES$^+$) 562 ([$^{35}$Cl]MH$^+$), 564 ([$^{37}$Cl]MH$^+$); HRMS (ES$^+$) Found [$^{35}$Cl]MH$^+$, 562.1308 ($C_{26}H_{24}{}^{35}ClF_3N_5O_2S$ requires 562.1286).

**(S)-6-chloro-N-(4-(methylthio)-1-oxo-1-(2-phenylhydrazineyl)butan-2-yl)-2-(4-(trifluoromethyl)phenyl)imidazo[1,2-*a*]pyridine-3-carboxamide 44Ap**

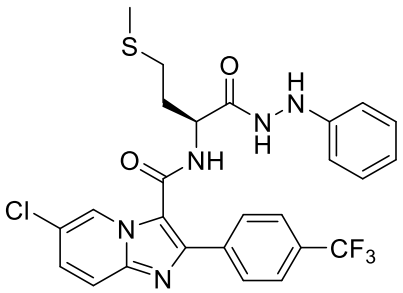


Using the standard procedure provided, *tert*-butyl (S)-(4-(methylthio)-1-oxo-1-(2-phenylhydrazineyl)butan-2-yl)carbamate **51Bb** (0.11 g, 0.32 mmol) was transformed following flash chromatography (DCM/EtOAc [3:1]) into the title compound as a white powder (72 mg, 40 %); R$_f$ 0.25 (DCM/EtOAc [3:1]); m.p. 210 - 214 °C; $\nu_{max}$ 3257 (N-H), 1620 (C=O), 1493, 1319, 1227, 1166, 1108, 1065, 1016, 850, 753, 691 cm$^{-1}$; δ$_H$ (300 MHz, DMSO-d$_6$) 10.04 (1H, s, CON*H*NH), 8.99 (1H, d, *J* 7, CON*H*CH), 8.88 (1H, dd, *J* 2, 1, Ar-*H*), 8.12 – 8.04 (2H, d, *J* 8, Ar-*H*), 7.79 (1H, dd, *J* 9, 1, Ar-*H*), 7.76 – 7.69 (2H, d, *J* 8, Ar-*H*), 7.52 (1H, dd, *J* 9, 2, Ar-*H*), 7.18 – 7.09 (2H, t, *J* 7, Ar-*H*), 6.83 – 6.75 (2H, d, *J* 7, Ar-*H*), 6.70 (1H, t, *J* 7, Ar-*H*), 4.66 (1H, m, CONHC*H*), 2.49 – 2.38 (2H, m, C*H*$_2$CH$_2$SCH$_3$), 2.09 – 1.86 (5H, m, CH$_2$C*H*$_2$S*CH*$_3$); δC (75 MHz, DMSO-d$_6$) 171.6 (*C*ONHNH), 161.1 (*C*ONHCH), 149.7 (*ipso*-Ar-*C)*, 143.9 (*ipso*-Ar-*C)*, 143.4 (*ipso*-Ar-*C)*, 129.4 (Ar-*C*), 129.1 (Ar-*C*), 128.3 (Ar-*C*), 125.7 (Ar-*C*), 124.9 (Ar-*C)*, 120.8 (*ipso*-Ar-*C)*, 118.9 (Ar-*C*), 118.4 (Ar-*C*), 117.9 (*ipso*-Ar-*C*), 112.6 (Ar-*C*), 52.2 (CONH*C*H), 31.1 (CH$_2$*C*H$_2$SCH$_3$), 30.1 (*C*H$_2$CH$_2$SCH$_3$), 14.9 (CH$_2$CH$_2$S*C*H$_3$); δ$_F$ (282 MHz, DMSO-

$d_6$) -61.2 (C*F*$_3$); *m/z* (ES$^+$) 562 ([$^{35}$Cl]MH$^+$), 564 ([$^{37}$Cl]MH$^+$); HRMS (ES$^+$) Found [$^{35}$Cl]MH$^+$, 562.1275 ($C_{26}H_{24}{}^{35}ClF_3N_5O_2S$ requires 562.1286).

**(S)-6-chloro-2-(3-methoxyphenyl)-N-(4-(methylthio)-1-oxo-1-(2-phenylhydrazineyl)butan-2-yl)imidazo[1,2-*a*]pyridine-3-carboxamide 44Aq**

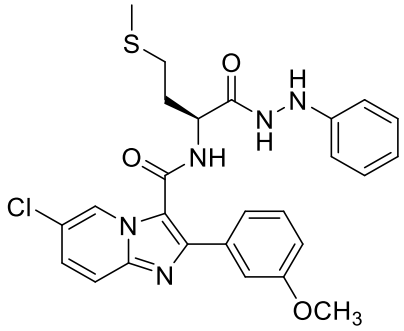

Using the standard procedure provided, *tert*-butyl (S)-(4-(methylthio)-1-oxo-1-(2-phenylhydrazineyl)butan-2-yl)carbamate **51Bb** (0.11 g, 0.34 mmol) was transformed following flash chromatography (DCM/EtOAc [3:1]) into the title compound as a white powder (65 mg, 36 %); $R_f$ 0.40 (DCM/EtOAc [3:1]); m.p. 223 - 228 °C; $\nu_{max}$ 3254 (N-H), 2919 (C-H), 1693 (C=O), 1602 (C=O), 1493, 1388, 1322, 1229, 1153, 1044, 846, 790, 692 cm$^{-1}$; $\delta_H$ (300 MHz, DMSO-$d_6$) 9.98 (1H, d, *J* 2, CON*H*NH), 8.97 (1H, dd, *J* 2, 1, Ar-*H*), 8.64 (1H, d, *J* 7, CON*H*CH), 7.82 (1H, d, *J* 2, CONHN*H*), 7.76 (1H, dd, *J* 9, 1, Ar-*H*), 7.49 (1H, dd, *J* 9, 2, Ar-*H*), 7.45 – 7.38 (2H, m, Ar-*H*), 7.33 (1H, t, *J* 8, Ar-*H*), 7.18 – 7.08 (2H, t, *J* 7, Ar-*H*), 6.99 (1H, m, Ar-*H*), 6.80 – 6.73 (2H, d, *J* 7, Ar-H), 6.70 (1H, t, *J* 7, Ar-*H*), 4.63 (1H, m, CONHC*H*), 3.78 (3H, s, Ar-OC*H*$_3$), 2.49 -2.39 (2H, m, C*H*$_2$CH$_2$SCH$_3$), 2.07 – 1.89 (5H, m, CH$_2$C*H*$_2$S*CH*$_3$); δC (75 MHz, DMSO-$d_6$) 171.5 (*C*ONHNH), 161.3 (CONH*C*H), 159.7 (Ar-*C*-OCH$_3$*)*, 149.6 (*ipso*-Ar-*C)*, 145.7 (*ipso*-Ar-*C)*, 143.3 (*ipso*-Ar-*C)*, 134.9 (*ipso*-Ar-*C)*, 130.0 (Ar-*C)*, 129.1 (Ar-*C*), 127.9 (Ar-*C*), 124.9 (Ar-*C*), 121.2 (Ar-*C*), 120.5 (*ipso*-Ar-*C*), 119.0 (Ar-*C*), 118.2 (Ar-*C*), 117.0 (*ipso*-Ar-*C*), 114.8 (Ar-*C*), 114.0 (Ar-*C*), 112.6 (Ar-*C*), 55.6 (Ar-O*C*H$_3$), 52.1 (CONH*C*H), 31.2 (CH$_2$*C*H$_2$SCH$_3$), 30.1 (*C*H$_2$CH$_2$SCH$_3$), 14.9 (CH$_2$CH$_2$S*C*H$_3$); *m/z* (ES$^+$) 524 ([$^{35}$Cl]MH$^+$), 526 ([$^{37}$Cl]MH$^+$); HRMS (ES$^+$) Found [$^{35}$Cl]MH$^+$, 524.1530 ($C_{26}H_{27}{}^{35}ClN_5O_3S$ requires 524.1518).

**(S)-6-chloro-2-(4-methoxyphenyl)-N-(4-(methylthio)-1-oxo-1-(2-phenylhydrazineyl)butan-2-yl)imidazo[1,2-*a*]pyridine-3-carboxamide 44Ar**

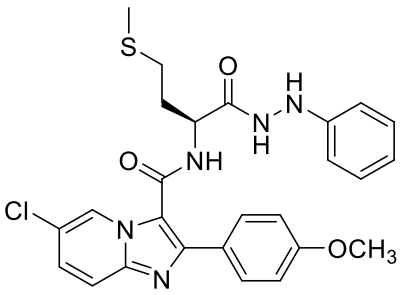

Using the standard procedure provided, *tert*-butyl (S)-(4-(methylthio)-1-oxo-1-(2-phenylhydrazineyl)butan-2-yl)carbamate **51Bb** (0.11 g, 0.32 mmol) was transformed following flash chromatography (DCM/EtOAc [3:1]) into the title compound as a white powder (77 mg, 45 %); $R_f$ 0.40 (DCM/EtOAc [3:1]); m.p. 225 - 228 °C; $\nu_{max}$ 3276 (N-H), 2981 (C-H), 1604 (C=O), 1537, 1493, 1386, 1323, 1249, 1168, 1028, 952, 836, 752, 692 $cm^{-1}$; $\delta_H$ (300 MHz, DMSO-$d_6$) 9.98 (1H, s, CON*H*NH), 8.94 (1H, s, Ar-*H*), 8.57 (1H, d, *J* 7, CON*H*CH), 7.85 (1H, bs, CONHN*H*), 7.82 – 7.75 (3H, d, *J* 8, Ar-*H*), 7.72 (1H, d, *J* 9, Ar-*H*), 7.47 (1H, dd, *J* 9, 2, Ar-*H*), 7.17 – 7.09 (2H, t, *J* 7, Ar-*H*), 7.00 – 6.94 (2H, d, *J* 8, Ar-*H*), 6.80 – 6.74 (2H, d, *J* 7, Ar-*H*), 6.70 (1H, t, *J* 7, Ar-*H*), 4.63 (1H, m, CONHC*H*), 3.79 (3H, s, Ar-OC*H*$_3$), 2.49 – 2.38 (2H, m, C*H*$_2$CH$_2$SCH$_3$), 2.09 – 1.85 (5H, m, CH$_2$C*H*$_2$S*CH*$_3$); δC (75 MHz, DMSO-$d_6$) 171.5 (*C*=ONHNH), 161.4 (*C*=ONHCH), 160.0 (Ar-*C*-OCH$_3$), 149.7 (*ipso*-Ar-*C)*, 146.1 (*ipso*-Ar-*C)*, 143.3 (*ipso*-Ar-*C)*, 130.3 (Ar-*C*), 129.1 (Ar-*C*), 127.7 (Ar-*C*), 125.9 (*ipso*-Ar-*C*), 124.8 (Ar-*C)*, 120.2 (*ipso*-Ar-*C)*, 118.9 (Ar-*C*), 117.9 (Ar-*C*), 116.1 (*ipso*-Ar-*C*), 114.3 (Ar-*C*), 112.6 (Ar-*C*), 55.6 (Ar-O*C*H$_3$), 52.0 (C=ONH*C*H), 31.1 (CH$_2$*C*H$_2$SCH$_3$), 30.1 (*C*H$_2$CH$_2$SCH$_3$), 14.9 (CH$_2$CH$_2$S*C*H$_3$); *m/z* (ES$^+$) 524 ([$^{35}$Cl]MH$^+$), 526 ([$^{37}$Cl]MH$^+$); HRMS (ES$^+$) Found [$^{35}$Cl]MH$^+$, 524.1539 ($C_{26}H_{27}{}^{35}ClN_5O_3S$ requires 524.1518).

**(S)-6-chloro-2-(3-chlorophenyl)-N-(4-methyl-1-oxo-1-(2-phenylhydrazineyl)pentan-2-yl)imidazo[1,2-*a*]pyridine-3-carboxamide 44As**

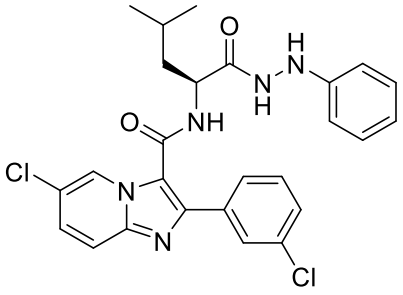

Using the standard procedure provided, *tert*-butyl (S)-(4-methyl-1-oxo-1-(2-phenylhydrazineyl)pentan-2-yl)carbamate **51Aj** (0.11 g, 0.35 mmol) was transformed

following flash chromatography (DCM/EtOAc [1:2]) into the title compound as a white powder (92 mg, 50 %); $R_f$ 0.40 (DCM/EtOAc [1:2]); m.p. 213 - 215 °C; $\nu_{max}$ 3271 (N-H), 2981 (C-H), 1678 (C=O), 1623, 1527, 1493, 1381, 1227, 1173, 1079, 952, 794, 750, 691 $cm^{-1}$; $\delta_H$ (300 MHz, DMSO-$d_6$) 10.01 (1H, s, CON*H*NH), 8.90 (1H, d, *J* 2, Ar-*H*), 8.85 (1H, d, *J* 7, CON*H*CH), 7.88 (1H, s, CONHN*H*), 7.83 (1H, m, Ar-*H*), 7.77 (1H, dd, *J* 9, 1, Ar-*H*), 7.50 (1H, dd, *J* 9, 2, Ar-*H*), 7.47 – 7.38 (2H, m, Ar-*H*), 7.19 – 7.07 (2H, t, *J* 7, Ar-*H*), 6.81 – 6.73 (2H, d, *J* 7, Ar-*H*), 6.69 (1H, t, *J* 7, Ar-*H*), 4.60 (1H, m, C*H*$CH_2CH(CH_3)_2$), 1.69 – 1.49 (3H, m, C*H*$_2CH(CH_3)_2$, $CH_2CH(CH_3)_2$), 1.02 – 0.93 (3H, d, *J* 6, $CH_2CH(CH_3)_2$), 0.93 – 0.85 (3H, d, *J* 6, $CH_2CH(CH_3)_2$); δC (75 MHz, DMSO-$d_6$) 172.3 (*C*ONHNH), 161.0 (*C*ONHCH), 149.6 (*ipso*-Ar-*C)*, 143.8 (*ipso*-Ar-*C)*, 143.2 (*ipso*-Ar-*C)*, 135.7 (*ipso*-Ar-*C*), 133.6 (*ipso*-Ar-*C)*, 130.8 (Ar-*C*), 129.1 (Ar-*C*), 128.8 (Ar-*C*), 128.1 (Ar-*C*), 127.2 (Ar-*C*), 124.8 (Ar-*C)*, 120.7 (*ipso*-Ar-*C)*, 118.9 (Ar-*C*), 118.3 (Ar-*C*), 117.5 (*ipso*-Ar-*C*), 112.6 (Ar-*C*), 51.2 (CONH*C*H), 40.54 (*C*$H_2CH(CH_3)_2$), 24.8 ($CH_2CH(CH_3)_2$), 23.4 ($CH_2CH(CH_3)_2$), 21.7 ($CH_2CH(CH_3)_2$); *m/z* ($ES^+$) 510 ([$^{35,35}$Cl]$MH^+$), 512 ([$^{35,37}$Cl]$MH^+$), 514 ([$^{37,37}$Cl]$MH^+$); HRMS ($ES^+$) Found [$^{35,35}$Cl]$MH^+$, 510.1462 ($C_{26}H_{26}{}^{35,35}Cl_2N_5O_2$ requires 510.1458).

**(S)-6-chloro-2-(4-chlorophenyl)-N-(4-methyl-1-oxo-1-(2-phenylhydrazineyl)pentan-2-yl)imidazo[1,2-*a*]pyridine-3-carboxamide 44At**

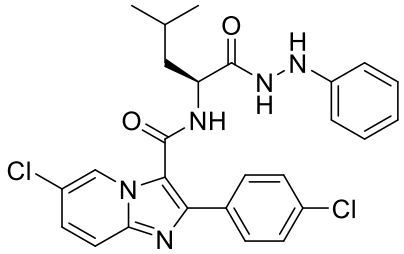


Using the standard procedure provided, *tert*-butyl (S)-(4-methyl-1-oxo-1-(2-phenylhydrazineyl)pentan-2-yl)carbamate **51As** (0.10 g, 0.31 mmol) was transformed following flash chromatography (DCM/EtOAc [1:2]) into the title compound as a white powder (72 mg, 45 %); $R_f$ 0.35 (DCM/EtOAc [1:2]); m.p. 211 - 215 °C; $\nu_{max}$ 3271 (N-H), 2981 (C-H), 1678 (C=O), 1623 (C=O), 1494, 1385, 1229, 1167, 1089, 844, 795, 692 $cm^{-1}$; $\delta_H$ (300 MHz, DMSO-$d_6$) 10.03 (1H, s, CON*H*NH), 8.88 (1H, dd, *J* 2, 1, Ar-*H*), 8.76 (1H, d, *J* 7, CON*H*CH), 7.89 – 7.84 (2H, d, *J* 8, Ar-H), 7.76 (1H, dd, *J* 9, 1, Ar-*H*), 7.49 (1H, dd, *J* 9, 2, Ar-*H*), 7.47 – 7.41 (2H, d, *J* 8, Ar-*H*), 7.20 – 7.09 (2H, t, *J* 7, Ar-H), 6.82 – 6.74 (2H, d, *J* 7, Ar-*H*), 6.69 (1H, t, *J* 7, Ar-*H*), 4.59 (1H, m,

C*H*$CH_2CH(CH_3)_2$), 1.65 – 1.43 (3H, m, C$H_2$$CH(CH_3)_2$, $CH_2$C*H*$(CH_3)_2$), 1.03 – 0.94 (3H, d, *J* 6, $CH_2CH(CH_3)_2$), 0.94 – 0.83 (3H, d, *J* 6, $CH_2CH(CH_3)_2$); δC (75 MHz, DMSO-$d_6$) 172.3 (*C*ONHNH), 161.0 (*C*ONHCH), 149.7 (*ipso*-Ar-*C)*, 144.4 (*ipso*-Ar-*C)*, 143.2 (*ipso*-Ar-*C)*, 133.6 (*ipso*-Ar-*C)*, 132.4 (*ipso*-Ar-*C)*, 130.3 (Ar-*C*), 129.1 (Ar-*C*), 128.9 (Ar-*C*), 128.0 (Ar-*C*), 124.7 (Ar-*C)*, 120.6 (*ipso*-Ar-*C*), 118.9 (Ar-*C*), 118.2 (Ar-*C*), 117.3 (*ipso*-Ar-*C*), 112.6 (Ar-*C*), 51.2 (CONH*C*H), 40.5 (*C*$H_2CH(CH_3)_2$), 24.8 ($CH_2$*C*$H(CH_3)_2$), 23.4 ($CH_2CH(CH_3)_2$), 21.7 ($CH_2CH(CH_3)_2$); *m/z* ($ES^+$) 510 ([$^{35,35}$Cl]$MH^+$), 512 ([$^{35,37}$Cl]$MH^+$), 514 ([$^{37,37}$Cl]$MH^+$); HRMS ($ES^+$) Found [$^{35,35}$Cl]$MH^+$, 510.1470 ($C_{26}H_{26}{}^{35,35}Cl_2N_5O_2$ requires 510.1458).

**(S)-6-chloro-N-(4-methyl-1-oxo-1-(2-phenylhydrazineyl)pentan-2-yl)-2-(3-(trifluoromethyl)phenyl)imidazo[1,2-*a*]pyridine-3-carboxamide 44Au**

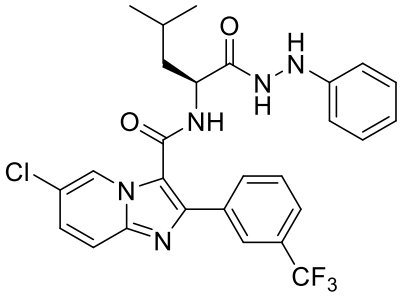


Using the standard procedure provided, *tert*-butyl (S)-(4-methyl-1-oxo-1-(2-phenylhydrazineyl)pentan-2-yl)carbamate **51Aj** (0.10 g, 0.34 mmol) was transformed following flash chromatography (DCM/EtOAc [3:1]) into the title compound as a white powder (74 mg, 40 %); $R_f$ 0.50 (DCM/EtOAc [3:1]); m.p. 220 - 225 °C; $\nu_{max}$ 3252 (N-H), 1664 (C=O), 1618, 1534, 1495, 1322, 1156, 1119, 1075, 802, 690 $cm^{-1}$; $\delta_H$ (300 MHz, DMSO-$d_6$) 10.05 (1H, d, *J* 2, CON*H*NH), 8.97 (1H, d, *J* 7, CON*H*CH), 8.93 (1H, dd, *J* 2, 1, Ar-*H*), 8.19 (1H, s, Ar-*H*), 8.15 (1H, d, *J* 8, Ar-H), 7.84 (1H, d, *J* 2, CONHN*H*), 7.82 – 7.72 (2H, m, Ar-*H*), 7.64 (1H, t, *J* 8, Ar-H), 7.51 (1H, dd, *J* 9, 2, Ar-H), 7.18 – 7.08 (2H, t, *J* 7, Ar-H), 6.83 – 6.74 (2H, d, *J* 7, Ar-H), 6.70 (1H, t, *J* 7, Ar-H), 4.63 (1H, m, C*H*$CH_2CH(CH_3)_2$), 1.67 – 1.45 (3H, m, C$H_2$$CH(CH_3)_2$, $CH_2$C*H*$(CH_3)_2$), 1.00 – 0.93 (3H, d, *J* 6, $CH_2CH(CH_3)_2$), 0.93 – 0.84 (3H, d, *J* 6, $CH_2CH(CH_3)_2$); δC (75 MHz, DMSO-$d_6$) 172.4 (*C*ONHNH), 160.9 (*C*ONHCH), 149.6 (*ipso*-Ar-*C)*, 143.6 (*ipso*-Ar-*C)*, 143.3 (*ipso*-Ar-*C)*, 134.6 (*ipso*-Ar-*C*), 132.4 (Ar-*C)*, 130.1 (Ar-*C*), 129.9 (Ar-*C*), 129.5 (Ar-*C)*, 129.1 (Ar-*C)*, 128.2 (Ar-*C)*, 124.8 (Ar-*C)*, 124.5 (Ar-*C)*, 120.8 (*ipso*-Ar-*C*), 118.9 (Ar-*C*), 118.4 (Ar-*C*), 117.7 (*ipso*-Ar-*C*), 112.6 (Ar-*C*), 51.2 (CONH*C*H), 40.5 (*C*$H_2CH(CH_3)_2$), 24.8 ($CH_2$*C*$H(CH_3)_2$), 23.3 ($CH_2CH(CH_3)_2$), 21.6 ($CH_2CH(CH_3)_2$); $\delta_F$ (282 MHz, DMSO-

$d_6$) -61.2 (C*F*$_3$); *m/z* (ES$^+$) 544 ([$^{35}$Cl]MH$^+$), 546 ([$^{37}$Cl]MH$^+$); HRMS (ES$^+$) Found [$^{35}$Cl]MH$^+$, 544.1735 ($C_{27}H_{26}{}^{35}ClF_3N_5O_2$ requires 544.1722).

**(S)-6-chloro-N-(4-methyl-1-oxo-1-(2-phenylhydrazineyl)pentan-2-yl)-2-(4-(trifluoromethyl)phenyl)imidazo[1,2-*a*]pyridine-3-carboxamide 44Av**

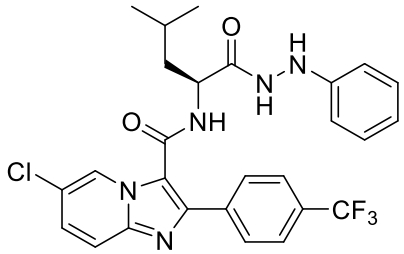

Using the standard procedure provided, *tert*-butyl (S)-(4-methyl-1-oxo-1-(2-phenylhydrazineyl)pentan-2-yl)carbamate **51Aj** (0.11 g, 0.34 mmol) was transformed following flash chromatography (DCM/EtOAc [1:2]) into the title compound as a white powder (75 mg, 40 %); $R_f$ 0.40 (DCM/EtOAc [1:2]); m.p. °C; $\nu_{max}$ 3249 (N-H), 2957 (C-H), 1678 (C=O), 1631, 1494, 1386, 1321, 1228, 1168, 1106, 1066, 1016, 846, 814, 752, 692 cm$^{-1}$; $\delta_H$ (300 MHz, DMSO-$d_6$) 10.04 (1H, s, CON*H*NH), 8.89 (1H, d, *J* 7, CON*H*CH), 8.87 (1H, dd, *J* 2, 1, Ar-*H*), 8.08 – 8.00 (2H, d, *J* 8, Ar-H), 7.85 (1H, bs, CONHN*H*), 7.80 (1H, dd, *J* 9, 1, Ar-*H*), 7.76 – 7.68 (2H, d, *J* 8, Ar-H), 7.52 (1H, dd, *J* 9, 2, Ar-*H*), 7.20 – 7.08 (2H, t, *J* 7, Ar-H), 6.83 – 6.75 (2H, d, *J* 7, Ar-H), 6.70 (1H, t, *J* 7, Ar-*H*), 4.58 (1H, m, C*H*CH$_2$CH(CH$_3$)$_2$), 3.80 (3H, s, Ar-OC*H*$_3$), 1.63 – 1.45 (3H, m, C*H*$_2$CH(CH$_3$)$_2$, CH$_2$C*H*(CH$_3$)$_2$), 0.99 – 0.91 (3H, d, *J* 6, CH$_2$CH(C*H*$_3$)$_2$), 0.91 – 0.83 (3H, d, *J* 6, CH$_2$CH(C*H*$_3$)$_2$); δC (75 MHz, DMSO-$d_6$) 172.2 (*C*ONHNH), 160.9 (*C*ONHCH), 149.7 (*ipso*-Ar-*C*), 143.9 (Ar-*C*F$_3$), 143.3 (*ipso*-Ar-*C*), 137.5 (*ipso*-Ar-*C*), 129.3 (Ar-*C*), 129.1 (Ar-*C*), 128.2 (Ar-*C*), 125.7 (Ar-*C*), 124.7 (Ar-*C*), 120.8 (*ipso*-Ar-*C*), 118.9 (Ar-*C*), 118.4 (Ar-*C*), 118.0 (Ar-*C*), 112.6 (Ar-*C*), 51.3 (C=ONH*C*H), 40.2 (*C*H$_2$CH(CH$_3$)$_2$), 24.7 (CH$_2$*C*H(CH$_3$)$_2$), 23.3 (CH$_2$CH(*C*H$_3$)$_2$), 21.7 (CH$_2$CH(*C*H$_3$)$_2$); $\delta_F$ (282 MHz, DMSO-$d_6$) -61.1 (C*F*$_3$); *m/z* (ES$^+$) 544 ([$^{35}$Cl]MH$^+$), 546 ([$^{37}$Cl]MH$^+$); HRMS (ES$^+$) Found [$^{35}$Cl]MH$^+$, 544.1739 ($C_{27}H_{26}{}^{35}ClF_3N_5O_2$ requires 544.1722).

**(S)-6-chloro-2-(3-methoxyphenyl)-N-(4-methyl-1-oxo-1-(2-phenylhydrazineyl)pentan-2-yl)imidazo[1,2-*a*]pyridine-3-carboxamide 44Aw**

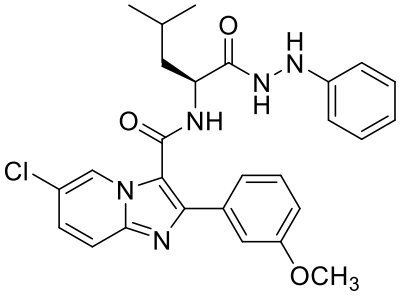

Using the standard procedure provided, *tert*-butyl (S)-(4-methyl-1-oxo-1-(2-phenylhydrazineyl)pentan-2-yl)carbamate **51Aj** (0.11 g, 0.34 mmol) was transformed following flash chromatography (DCM/EtOAc [3:1]) into the title compound as a white powder (85 mg, 49 %); $R_f$ 0.40 (DCM/EtOAc [3:1]); m.p. 223 - 225 °C; $\nu_{max}$ 3259 (N-H), 2964 (C-H), 1669 (C=O), 1621, 1532, 1493, 1377, 1329, 1225, 1152, 1046, 845, 751, 689 $cm^{-1}$; $\delta_H$ (300 MHz, DMSO-$d_6$) 10.00 (1H, s, CON*H*NH), 8.98 (1H, s, Ar-*H*), 8.54 (1H, d, *J* 7, CON*H*CH), 7.76 (1H, d, *J* 9, Ar-*H*), 7.49 (1H, dd, *J* 9, 1, Ar-*H*), 7.44 – 7.38 (2H, m, Ar-*H*), 7.33 (1H, t, *J* 8, Ar-*H*), 7.18 – 7.06 (2H, t, *J* 7, Ar-*H*), 6.98 (1H, d, *J* 8, Ar-*H*), 6.81 – 6.73 (2H, d, *J* 7, Ar-*H*), 6.68 (1H, t, *J* 7, Ar-*H*), 4.57 (1H, m, C*H*$CH_2CH(CH_3)_2$), 3.79 (3H, s, Ar-OC*H*$_3$), 1.67 – 1.43 (3H, m, C*H*$_2CH(CH_3)_2$, $CH_2CH(CH_3)_2$), 1.04 – 0.83 (3H, d, *J* 6, $CH_2CH(CH_3)_2$), 0.93 – 0.82 (3H, d, *J* 6, $CH_2CH(CH_3)_2$); δC (75 MHz, DMSO-$d_6$) 172.3 (*C*ONHNH), 161.1 (*C*ONHCH), 159.7 (*ipso*-Ar-*C)*, 149.7 (*ipso*-Ar-*C)*, 145.4 (*ipso*-Ar-*C)*, 143.1 (*ipso*-Ar-*C)*, 134.8 (*ipso*-Ar-*C*), 130.0 (Ar-*C*), 129.1 (Ar-*C*), 127.9 (Ar-*C*), 124.8 (Ar-*C)*, 121.0 (Ar-*C)*, 120.6 (*ipso*-Ar-*C*), 118.9 (Ar-*C*), 118.2 (Ar-*C*), 117.1 (*ipso*-Ar-*C*), 114.7 (Ar-*C*), 113.9 (Ar-*C*), 112.6 (Ar-*C*), 55.5 (Ar-O*C*$H_3$), 51.2 (CONH*C*H), 40.5 (*C*$H_2CH(CH_3)_2$), 24.7 ($CH_2$*C*$H(CH_3)_2$), 23.4 ($CH_2CH(CH_3)_2$), 21.6 ($CH_2CH(CH_3)_2$); ***m/z*** ($ES^+$) 506 ([$^{35}$Cl]$MH^+$), 508 ([$^{37}$Cl]$MH^+$); HRMS ($ES^+$) Found [$^{35}$Cl]$MH^+$, 506.1964 ($C_{27}H_{29}{}^{35}ClN_5O_3$ requires 506.1953).

**(S)-6-chloro-2-(4-methoxyphenyl)-N-(4-methyl-1-oxo-1-(2-phenylhydrazineyl)pentan-2-yl)imidazo[1,2-*a*]pyridine-3-carboxamide 44Ax**

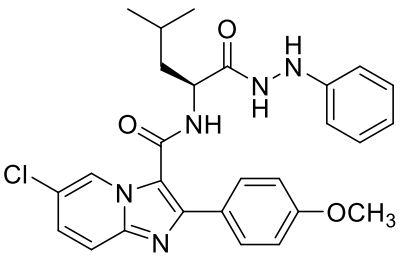

Using the standard procedure provided, *tert*-butyl (S)-(4-methyl-1-oxo-1-(2-phenylhydrazineyl)pentan-2-yl)carbamate **51Aj** (0.10 g, 0.31 mmol) was transformed following flash chromatography (DCM/EtOAc [1:2]) into the title compound as a white powder (84 mg, 53 %); $R_f$ 0.45 (DCM/EtOAc [1:2]); m.p. 225 - 229 °C; $\nu_{max}$ 3260 (N-H), 2981 (C-H), 1620 (C=O), 1494, 1385, 1250, 1167, 958, 836, 692 $cm^{-1}$; $\delta_H$ (300 MHz, DMSO-$d_6$) 9.98 (1H, s, CON*H*NH), 8.94 (1H, s, Ar-*H*), 8.44 (1H, d, *J* 7, CON*H*CH), 7.82 (1H, bs, CONHN*H*), 7.80 – 7.75 (2H, d, *J* 8, Ar-*H*), 7.72 (1H, d, *J* 9, Ar-*H*), 7.46 (1H, dd, *J* 9, 2, Ar-*H*), 7.19 – 7.08 (2H, t, *J* 7, Ar-*H*), 6.99 – 6.92 (2H, d, *J* 8, Ar-*H*), 6.80 – 6.73 (2H, d, *J* 7, Ar-*H*), 6.69 (1H, t, *J* 7, Ar-*H*), 4.56 (1H, m, C*H*$CH_2CH(CH_3)_2$), 3.80 (3H, s, Ar-OC$H_3$), 1.65 – 1.43 (3H, m, C$H_2CH(CH_3)_2$, $CH_2CH(CH_3)_2$), 1.01 – 0.93 (3H, d, *J* 6, $CH_2CH(CH_3)_2$), 0.93 – 0.82 (3H, d, *J* 6, $CH_2CH(CH_3)_2$); δC (75 MHz, DMSO-$d_6$) 172.3 (*C*ONHNH), 161.3 (*C*ONHCH), 160.0 (Ar-*C*-$OCH_3$), 149.7 (*ipso*-Ar-*C)*, 146.0 (*ipso*-Ar-*C)*, 143.3 (*ipso*-Ar-*C)*, 130.1 (Ar-*C*), 129.1 (Ar-*C*), 127.6 (Ar-*C*), 125.9 (Ar-*C*), 124.7 (Ar-*C)*, 120.3 (*ipso*-Ar-*C*), 118.9 (Ar-*C*), 118.0 (Ar-*C*), 116.2 (*ipso*-Ar-*C*), 114.3 (Ar-*C*), 112.6 (Ar-*C*), 55.6 ($CO*C*H_3$), 51.1 (CONH*C*H), 40.5 ($*C*H_2CH(CH_3)_2$), 24.7 ($CH_2*C*H(CH_3)_2$), 23.4 ($CH_2CH(*C*H_3)_2$), 21.7 ($CH_2CH(*C*H_3)_2$); *m/z* ($ES^+$) 506 ($[^{35}Cl]MH^+$), 508 ($[^{37}Cl]MH^+$); HRMS ($ES^+$) Found $[^{35}Cl]MH^+$, 506.1949 ($C_{27}H_{29}{}^{35}ClN_5O_3$ requires 506.1953).

**(S)-6-chloro-2-(3-chlorophenyl)-N-(1-oxo-3-phenyl-1-(2-phenylhydrazineyl)propan-2-yl)imidazo[1,2-*a*]pyridine-3-carboxamide 44Ay**

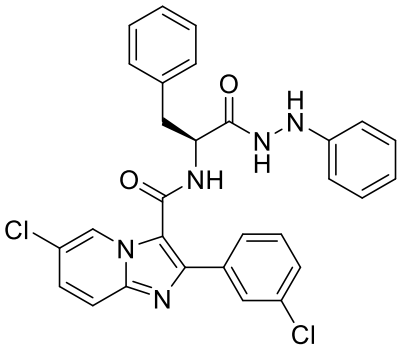


Using the standard procedure provided, *tert*-butyl (*S*)-(1-oxo-3-phenyl-1-(2-phenylhydrazineyl)propan-2-yl)carbamate **51Bk** (0.10 g, 0.28 mmol) was transformed following flash chromatography (DCM/EtOAc [3:1]) into the title compound as a white powder (70 mg, 46 %); $R_f$ 0.3 (DCM/EtOAc [3:1]); m.p. 222 - 225 °C; $\nu_{max}$ 3251 (N-H), 2980, 1667 (C=O), 1619 (C=O), 1535, 1494, 1385, 1251, 1229, 1175, 1077, 954, 797, 748, 696 $cm^{-1}$; $\delta_H$ (300 MHz, DMSO-$d_6$) 10.10 (1H, s, CON*H*NH), 9.04 (1H, d, *J* 7,

CON*H*CH), 8.58 (1H, dd, *J* 2, 1, Ar-*H*), 7.85 (1H, d, *J* 2, CONHN*H*), 7.73 (1H, dd, *J* 9, 1, Ar-*H*), 7.55 (1H, dt, *J* 8, 1, Ar-*H*), 7.47 (1H, dd, *J* 9, 2, Ar-*H*), 7.41 (1H, qd, *J* 8, 1, Ar-*H*), 7.35 – 7.28 (5H, m, Ar-*H*), 7.28 – 7.21 (2H, t, *J* 8, Ar-*H*), 7.15 – 7.06 (2H, t, *J* 8, Ar-*H*), 6.74 – 6.62 (3H, t, *J* 8, Ar-*H*), 4.99 (1H, m, CONHC*H*), 3.17 (1H, dd, *J* 13, 4, CONHCHC$H_2$) , 2.94 (1H, dd, *J* 13, 10, CONHCHC$H_2$); δC (75 MHz, DMSO-$d_6$) 171.2 (*C*ONHNH), 160.6 (*C*ONHCH), 149.4 (*ipso*-Ar-*C)*, 143.6 (*ipso*-Ar-*C)*, 143.1 (*ipso*-Ar-*C)*, 137.8 (*ipso*-Ar-*C)*, 135.4 (*ipso*-Ar-*C)*, 133.7 (*ipso*-Ar-*C)*, 130.8 (Ar-*C*), 129.5 (Ar-*C*), 128.8 (Ar-*C*), 128.1 (Ar-*C*), 127.9 (Ar-*C*), 127.0 (Ar-*C*), 124.7 (Ar-*C*), 120.6 (*ipso*-Ar-*C*), 119.0 (Ar-*C*), 118.2 (Ar-*C)*, 117.6 (*ipso*-Ar-*C)*, 112.6 (Ar-*C*), 53.7 (C=ONH*C*H), 37.7 (CONHCH*C*$H_2$); *m/z* (ES$^+$) 544 ([$^{35,35}$Cl]MH$^+$), 546 ([$^{35,37}$Cl]MH$^+$), 548 ([$^{37,37}$Cl]MH$^+$); HRMS (ES$^+$) Found [$^{35,35}$Cl]MH$^+$, 544.1306 ($C_{29}H_{24}{}^{35,35}Cl_2N_5O_2$ requires 544.1302).

**(S)-6-chloro-2-(4-chlorophenyl)-N-(1-oxo-3-phenyl-1-(2-phenylhydrazineyl)propan-2-yl)imidazo[1,2-*a*]pyridine-3-carboxamide 44Az**

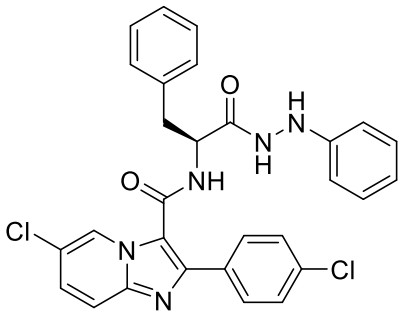


Using the standard procedure provided, *tert*-butyl (*S*)-(1-oxo-3-phenyl-1-(2-phenylhydrazineyl)propan-2-yl)carbamate **51Bk** (0.10 g, 0.34 mmol) was transformed following flash chromatography (DCM/EtOAc [3:1]) into the title compound as a white powder (77 mg, 50 %); $R_f$ 0.5 (DCM/EtOAc [3:1]); m.p. 225 - 228 °C; $\nu_{max}$ 3242 (N-H), 2981, 1616, 1532, 1494, 1387, 1229, 1166, 1088, 951, 835, 699 cm$^{-1}$; $\delta_H$ (300 MHz, DMSO-$d_6$) 10.12 (1H, s, CON*H*NH), 9.02 (1H, d, *J* 7, CON*H*CH), 8.50 (1H, s, Ar-*H*), 7.87 (1H, s, CONHN*H*), 7.73 (1H, d, *J* 9, Ar-*H*), 7.70 – 7.62 (2H, d, *J* 8, Ar-*H*), 7.46 (1H, dd, *J* 9, 2, Ar-*H*), 7.38 – 7.30 (5H, m, Ar-*H*), 7.29 – 7.21 (2H, d, *J* 8, Ar-*H*), 7.17 – 7.08 (2H, t, *J* 7, Ar-*H*), 6.79 – 6.61 (3H, m, Ar-*H*), 4.95 (1H, m, CONHC*H*), 3.18 (1H, dd, *J* 13, 4, CONHCHC$H_2$), 2.95 (1H, dd, *J* 13, 10, CONHCHC$H_2$); δC (75 MHz, DMSO-$d_6$) 171.2 (*C*ONHNH), 160.8 (CONH*C*H), 149.5 (*ipso*-Ar-*C)*, 144.1 (*ipso*-Ar-*C)*, 143.1 (*ipso*-Ar-*C)*, 137.9 (*ipso*-Ar-*C)*, 133.4 (*ipso*-Ar-*C)*, 132.1 (*ipso*-Ar-*C)*, 130.1(Ar-*C*), 129.6 (Ar-*C*), 129.1 (Ar-*C*), 128.8 (Ar-*C*), 127.9 (Ar-*C*), 127.0 (Ar-*C*), 124.6 (Ar-*C*), 120.5 (*ipso*-Ar-*C)*, 119.0 (Ar-*C*), 118.2 (Ar-*C*), 117.3 (*ipso*-Ar-*C*), 112.6 (Ar-*C*), 53.8

(CONH*C*H), 37.6 (CONHCH*C*$H_2$); *m/z* ($ES^+$) 544 ([$^{35,35}$Cl]$MH^+$), 546 ([$^{35,37}$Cl]$MH^+$), 548 ([$^{37,37}$Cl]$MH^+$); HRMS ($ES^+$) Found [$^{35,35}$Cl]$MH^+$, 544.1299 ($C_{29}H_{24}{}^{35,35}Cl_2N_5O_2$ requires 544.1302).

**(S)-6-chloro-N-(1-oxo-3-phenyl-1-(2-phenylhydrazineyl)propan-2-yl)-2-(3-(trifluoromethyl)phenyl)imidazo[1,2-*a*]pyridine-3-carboxamide 44Ba**

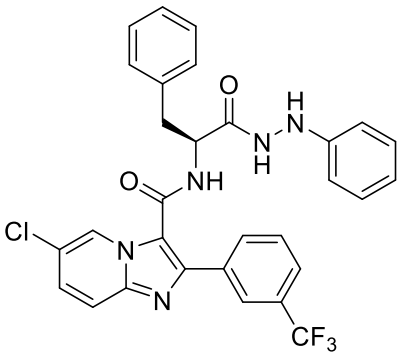


Using the standard procedure provided, *tert*-butyl (*S*)-(1-oxo-3-phenyl-1-(2-phenylhydrazineyl)propan-2-yl)carbamate **51Bk** (0.09 g, 0.25 mmol) was transformed using column chromatography (DCM/EtOAc [3:1]) into the title compound as a white powder (60 mg, 41 %); $R_f$ 0.3 (DCM/EtOAc [3:1]); m.p. 235 - 238 °C; $\nu_{max}$ 3268 (N-H), 2981, 1668 (C=O), 1615 (C=O), 1495, 1382, 1325, 1227, 1152, 1117, 1056, 792, 694 $cm^{-1}$; $\delta_H$ (300 MHz, DMSO-$d_6$) 10.11 (1H, s, CON*H*NH), 9.15 (1H, d, *J* 7, CON*H*CH), 8.58 (1H, s, Ar-*H*), 8.18 (1H, s, CONHN*H*), 7.87 – 7.82 (2H, m, Ar-*H*), 7.76 (1H, d, *J* 9, Ar-*H*), 7.72 (1H, d, *J* 8, Ar-*H*), 7.49 (1H, dd, *J* 9, 2, Ar-*H*), 7.43 (1H, t, *J* 8, Ar-*H*), 7.36 – 7.30 (5H, m, Ar-*H*), 7.15 – 7.09 (2H, t, *J* 8, Ar-*H*), 6.71 (1H, d, *J* 8, Ar-*H*), 6.70 – 6.67 (2H, d, *J* 8, Ar-*H*), 5.01 (1H, m, CONHC*H*), 3.19 (1H, dd, *J* 13, 4, CONHCHC*H*$_2$), 2.95 (1H, dd, *J* 13, 10, CONHCHC*H*$_2$); δC (75 MHz, DMSO-$d_6$) 171.1 (*C*ONHNH), 160.6 (C=ONH*C*H), 149.4 (*ipso*-Ar-*C)*, 143.5 (Ar-*C*$F_3$*)*, 143.2 (*ipso*-Ar-*C)*, 137.8 (*ipso*-Ar-*C)*, 134.3 (*ipso*-Ar-*C)*, 132.2 (Ar-*C*), 130.0 (Ar-*C*), 129.5 (Ar-*C*), 129.1 (Ar-*C*), 128.7 (Ar-*C*), 128.2 (Ar-*C*), 127.0 (Ar-*C*), 125.4 (Ar-*C*), 124.7 (Ar-*C*), 120.7 (*ipso*-Ar-*C)*, 119.0 (Ar-*C*), 118.3 (Ar-*C*), 117.8 (*ipso*-Ar-*C*), 112.6 (Ar-*C*), 53.7 (CONH*C*H), 37.6 (CONHCH*C*$H_2$); $\delta_F$ (282 MHz, DMSO-$d_6$) -61.3 (C*F*$_3$); *m/z* ($ES^+$) 578 ([$^{35}$Cl]$MH^+$), 580 ([$^{37}$Cl]$MH^+$); HRMS ($ES^+$) Found [$^{35}$Cl]$MH^+$, 578.1581 ($C_{30}H_{24}{}^{35}ClF_3N_5O_2$ requires 578.1565).

**(S)-6-chloro-N-(1-oxo-3-phenyl-1-(2-phenyl)hydrazineyl)propan-2-yl)-2-(4-(trifluoromethyl)phenyl)imidazo[1,2-*a*]pyridine-3-carboxamide 44Bb**

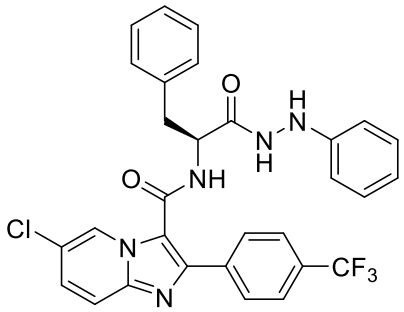


Using the standard procedure provided, *tert*-butyl (*S*)-(1-oxo-3-phenyl-1-(2-phenylhydrazineyl)propan-2-yl)carbamate **51Bk** (0.09 g, 0.28 mmol) was transformed using column chromatography (DCM/EtOAc [3:1]) into the title compound as a white powder (73 mg, 45 %); $R_f$ 0.4 (DCM/EtOAc [3:1]); m.p. 230 - 233 °C; $\nu_{max}$ 3252 (N-H), 2980, 1616 (C=O), 1535, 1493, 1385, 1251, 1165, 1077, 954, 834, 697 $cm^{-1}$; $\delta_H$ (300 MHz, DMSO-$d_6$) 10.15 (1H, s, CON*H*NH), 9.18 (1H, d, *J* 7, CON*H*CH), 8.44 (1H, s, Ar-*H*), 7.92 – 7.82 (3H, m, Ar-*H*), 7.76 (1H, d, *J* 9, Ar-*H*), 7.59 – 7.51 (2H, d, *J* 8, Ar-*H*), 7.48 (1H, dd, *J* 9, 2, Ar-*H*), 7.38 – 7.25 (5H, m, Ar-*H*), 7.17 – 7.07 (2H, t, *J* 8, Ar-*H*), 6.77 – 6.61 (3H, m, Ar-*H*), 5.00 (1H, m, CONHC*H*), 3.20 (1H, dd, *J* 13, 4, CONHCHC*H*$_2$), 2.96 (1H, dd, *J* 13, 10, CONHCHC*H*$_2$); δC (75 MHz, DMSO-$d_6$) 171.3 (*C*ONHNH), 160.7 (CONH*C*H), 149.5 (*ipso*-Ar-*C)*, 143.4 (Ar-*C*$F_3$*)*, 143.2 (*ipso*-Ar-*C)*, 137.9 (*ipso*-Ar-*C)*, 129.6 (Ar-*C*), 129.1 (Ar-*C*), 128.9 (Ar-*C*), 128.8 (Ar-*C*), 128.2 (Ar-*C*), 127.0 (Ar-*C*), 125.6 (Ar-*C*), 124.6 (Ar-*C*), 120.8 (*ipso*-Ar-*C)*, 118.9 (Ar-*C*), 118.4 (Ar-*C*), 112.6 (Ar-*C*), 53.8 (CONH*C*H), 37.6 (CONHCH*C*H$_2$); $\delta_F$ (282 MHz, DMSO-$d_6$) -61.1 (C*F*$_3$); *m/z* (ES$^+$) 578 ([$^{35}$Cl]MH$^+$), 580 ([$^{37}$Cl]MH$^+$); HRMS (ES$^+$) Found [$^{35}$Cl]MH$^+$, 578.1576 ($C_{30}H_{24}{}^{35}ClF_3N_5O_2$ requires 578.1565).

**(S)-6-chloro-2-(3-methoxyphenyl)-N-(1-oxo-3-phenyl-1-(2-phenylhydrazineyl)propan-2-yl)imidazo[1,2-*a*]pyridine-3-carboxamide 44Bc**

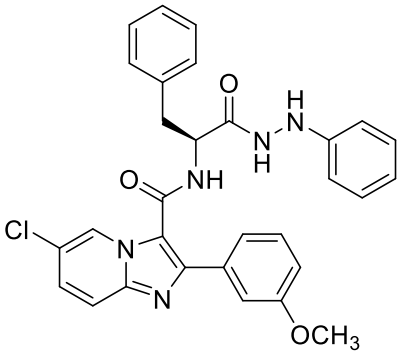

Using the standard procedure provided, *tert*-butyl (*S*)-(1-oxo-3-phenyl-1-(2-phenylhydrazineyl)propan-2-yl)carbamate **51Bk** (0.10 g, 0.29 mmol) was transformed using column chromatography (DCM/EtOAc [3:1]) into the title compound as a white powder (73 mg, 46 %); $R_f$ 0.3 (DCM/EtOAc [3:1]); m.p. 240 - 242 °C; $\nu_{max}$ 3265 (N-H), 2981, 1670 (C=O), 1615 (C=O), 1532, 1495, 1381, 1333, 1225, 1152, 1051, 844, 788, 748, 692 $cm^{-1}$; $\delta_H$ (300 MHz, DMSO-$d_6$) 10.09 (1H, d, *J* 2, CON*H*NH), 8.79 (1H, d, *J* 8, CON*H*CH), 8.64 (1H, dd, *J* 2, 1, Ar-*H*), 7.83 (1H, d, *J* 2, CONHN*H*), 7.73 (1H, dd, *J* 9, 1, Ar-*H*), 7.45 (1H, dd, *J* 9, 2, Ar-*H*), 7.36 (1H, m, Ar-*H*), 7.33 – 7.24 (5H, m, Ar-H), 7.22 – 7.17 (2H, m, Ar-*H*), 7.14 – 7.05 (2H, t, *J* 8, Ar-*H*), 6.92 (1H, m, Ar-*H*), 6.74 – 6.62 (3H, t, *J* 8, Ar-*H*), 4.94 (1H, m, CONHC*H*), 3.70 (3H, s, Ar-OC*H*$_3$), 3.13 (1H, dd, *J* 13, 4, CONHCHC*H*$_2$), 2.93 (1H, dd, *J* 13, 10, CONHCHC*H*$_2$); δC (75 MHz, DMSO-$d_6$) 171.2 (*C*ONHNH), 160.9 (*C*ONHCH), 159.7 (Ar-*C*-OCH$_3$*)*, 149.4 (*ipso*-Ar-*C)*, 145.3 (*ipso*-Ar-*C)*, 143.1 (*ipso*-Ar-*C)*, 137.8 (*ipso*-Ar-*C)*, 134.7 (*ipso*-Ar-*C)*, 130.0 (Ar-*C*), 129.5 (Ar-*C*), 128.8 (Ar-*C*), 127.8 (Ar-*C*), 127.0 (Ar-*C*), 124.7 (Ar-*C*), 120.8 (Ar-*C*), 120.4 (*ipso*-Ar-*C)*, 119.0 (Ar-*C*), 118.1 (Ar-*C*), 117.2 (*ipso*-Ar-*C)*, 115.1 (Ar-*C*), 113.3 (Ar-*C*), 112.6 (Ar-*C*), 55.3 (Ar-O*C*H$_3$), 53.8 (C=ONH*C*H), 37.8 (CONHCH*C*H$_2$); *m/z* (ES$^+$) 540 ([$^{35}$Cl]MH$^+$), 542 ([$^{37}$Cl]MH$^+$); HRMS (ES$^+$) Found [$^{35}$Cl]MH$^+$, 540.1821 ($C_{30}H_{27}{}^{35}ClN_5O_3$ requires 540.1797).

**(S)-6-chloro-N-(1-oxo-3-phenyl-1-(2-(3-(chlorophenyl)hydrazineyl)propan-2-yl)-2-(4-(trifluoromethoxy)phenyl)imidazo[1,2-*a*]pyridine-3-carboxamide 44Bd**

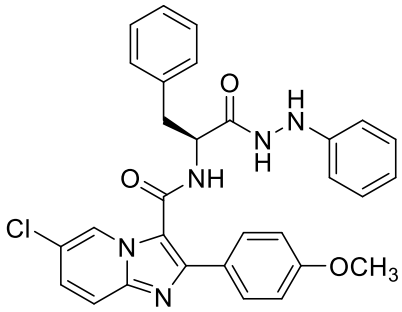

Using the standard procedure provided, *tert*-butyl (*S*)-(1-oxo-3-phenyl-1-(2-phenylhydrazineyl)propan-2-yl)carbamate **51Bk** (0.11 g, 0.30 mmol) was transformed using column chromatography (DCM/EtOAc [3:1]) into the title compound as a white powder (67 mg, 40 %); $R_f$ 0.4 (DCM/EtOAc [3:1]); m.p. 250 - 252 °C; $\nu_{max}$ 3242 (N-H), 1660, 1614 (C=O), 1533, 1494, 1389, 1250, 1224, 1166, 1036, 834, 696 $cm^{-1}$; $\delta_H$ (300 MHz, DMSO-$d_6$) 10.08 (1H, s, CON*H*NH), 8.73 (1H, d, *J* 7, CON*H*CH), 8.59 (1H, dd, *J* 2, 1, Ar-*H*), 7.70 (1H, d, *J* 9, Ar-*H*), 7.64 – 7.58 (2H, d, *J* 8, Ar-*H*), 7.43 (1H, dd, *J* 9, 2, Ar-*H*), 7.36 – 7.26 (5H, m, Ar-*H*), 7.15 – 7.06 (2H, t, *J* 8, Ar-H), 6.85 – 6.78 (2H, d, *J* 8, Ar-*H*), 6.74 – 6.64 (3H, m, Ar-*H*), 4.96 (1H, m, CONHC*H*), 3.77 (3H, s, Ar-OC*H*$_3$), 3.17 (1H, dd, *J* 13, 4, CONHCHC*H*$_2$), 2.95 (1H, dd, *J* 13, 4, CONHCHC*H*$_2$); δC (75 MHz, DMSO-$d_6$) 171.3 (*C*ONHNH), 161.0 (*C*ONHCH), 159.9 (Ar-*C*-OCH$_3$), 149.5 (*ipso*-Ar-*C*), 145.5 (*ipso*-Ar-*C*), 143.1 (*ipso*-Ar-*C*), 137.9 (*ipso*-Ar-*C*), 129.9 (Ar-*C*), 129.6 (Ar-*C*), 129.1 (Ar-*C*), 128.9 (Ar-*C*), 128.8 (Ar-*C*), 127.6 (Ar-*C*), 127.0 (Ar-*C*), 125.6 (Ar-*C*), 124.5 (Ar-*C*), 120.2 (*ipso*-Ar-*C*), 118.9 (Ar-*C*), 117.8 (Ar-*C*), 116.2 (*ipso*-Ar-*C*), 114.3 (Ar-*C*), 112.6 (Ar-*C*), 55.6 (Ar-O*C*H$_3$), 53.8 (CONH*C*H), 37.6 (CONHCH*C*H$_2$); *m/z* ($ES^+$) 540 ([$^{35}$Cl]$MH^+$), 542 ([$^{37}$Cl]$MH^+$); HRMS ($ES^+$) Found [$^{35}$Cl]$MH^+$, 540.1806 ($C_{30}H_{27}{}^{35}ClN_5O_3$ requires 540.1797).

### 6.2.5.2 Second- series of imidazo[1,2-*a*]pyridine-3-carboxamides

**6-chloro-N-(2-oxo-2-(2-phenylhydrazineyl)ethyl)-2-phenylimidazo[1,2-*a*]pyridine-3-carboxamide 44Be**

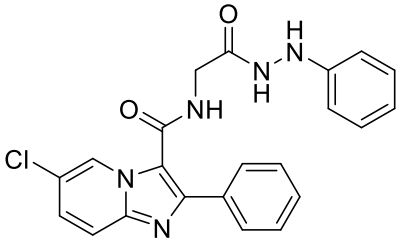

Using the standard procedure provided, *tert*-butyl (2-oxo-2-(2-phenylhydrazineyl)ethyl)carbamate **51Aa** (0.13 g, 0.49 mmol) was transformed using column chromatography (DCM/EtOAc [1:2]) into the title compound as a white powder (95 mg, 46 %); $R_f$ 0.30 (DCM/EtOAc [1:2]); m.p. 219 - 222 °C; $\nu_{max}$ 3422 (N-H), 3285 (N-H), 1685 (C=O), 1625 (C=O), 1535, 1491, 1382, 1323, 1220, 1172, 1074, 692, 502 $cm^{-1}$; $\delta_H$ (300 MHz, DMSO-$d_6$) 9.84 (1H, s, CON*H*NH), 9.07 (1H, s, Ar-*H*), 8.72 (1H, t, *J* 5, CON*H*$CH_2$), 7.96 – 7.90 (2H, dd, *J* 8, 1, Ar-*H*), 7.81 (1H, s, CONHN*H*), 7.74 (1H, dd, *J* 10, 1, Ar-*H*), 7.51 – 7.45 (2H, m, Ar-*H*), 7.44 – 7.39 (2H, m, Ar-*H*), 7.17 – 7.09 (2H, t, *J* 7, Ar-*H*), 6.80 – 6.75 (2H, d, *J* 7, Ar-*H*), 6.70 (1H, t, *J* 7, Ar-*H*) 4.09 – 3.99 (2H, d, *J* 6, C*H*$_2$C=O); $\delta_C$ (75 MHz, DMSO-$d_6$) 169.0 (*C*=ONHNH), 161.4 *(C*=ONHC$H_2$), 149.6 (*ipso*-Ar-*C)*, 145.7 (*ipso*-Ar-*C)*, 143.3 (*ipso*-Ar-*C)*, 133.4 (*ipso*-Ar-*C)*, 129.5 (Ar-*C)*, 129.1 (Ar-*C)*, 128.8 (Ar-*C)*, 128.6 (Ar-*C)*, 127.8 (Ar-*C)*, 125.1 (Ar-*C)*, 120.4 (*ipso*-Ar-*C)*, 118.9 (Ar-*C)*, 118.1 (Ar-*C)*, 116.9 (*ipso*-Ar-*C),* 112.6 (Ar-*C)*, 41.7 (*C*$H_2$C=O); ***m/z*** (ES$^+$) 420 ([$^{35}$Cl]MH$^+$), 422 ([$^{37}$Cl]MH$^+$); HRMS (ES$^+$) Found [$^{35}$Cl]MH$^+$, 420.1248 ($C_{22}H_{18}{}^{35}ClN_5O_2$ requires 420.1227).

**6-Chloro-N-(2-(2-(3-chlorophenyl)hydrazineyl)-2-oxoethyl)-2-phenylimidazo[1,2-*a*]pyridine-3-carboxamide, 51Bf**

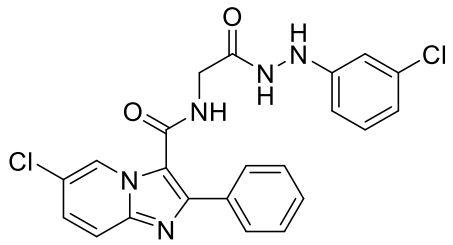


Using the standard procedure provided, *tert*-butyl (2-(2-(3-chlorophenyl)hydrazineyl)-2-oxoethyl)carbamate **28a** (0.14 g, 0.48 mmol) was transformed using column chromatography (DCM/EtOAc [1:2]) into the title compound as a white powder (70 mg, 38 %); $R_f$ 0.30 (DCM/EtOAc [1:2]); m.p. 192 - 195 °C; $\nu_{max}$ 3490 (N-H), 3297 (N-H), 1685 (C=O), 1641 (C=O), 1598, 1540, 1490, 1383, 1223, 1175, 1129, 1074, 541 $cm^{-1}$; $\delta_H$ (300 MHz, DMSO-$d_6$) 9.91 (1H, s, CON*H*NH), 9.07 (1H, s, Ar-*H*), 8.68 (1H, t, *J* 5, CON*H*$CH_2$), 8.10 (1H, s, CONHN*H*), 7.94 – 7.89 (2H, d, *J* 8, Ar-*H*), 7.75 (1H, d, *J* 10, Ar-*H*), 7.50 (1H, dd, *J* 10, 2, Ar-*H*), 7.45 – 7.37 (3H, m, Ar-*H*), 7.15 (1H, t, *J* 7, Ar-*H*), 6.79 (1H, s, Ar-*H*), 6.74 - 6.72 (2H, d, *J* 7, Ar-*H*) 4.04 – 4.00 (2H, d, *J* 6, C*H*$_2$CO); $\delta_C$ (75 MHz, DMSO-$d_6$) 169.2 (*C*ONHNH), 161.5 *(C*ONHC$H_2$), 151.2 (*ipso*-Ar-*C)*, 145.8 (*ipso*-Ar-*C)*, 143.4 (*ipso*-Ar-*C)*, 134.0 (*ipso*-Ar-*C)*, 133.4 (*ipso*-Ar-*C)*, 130.7 (Ar-*C)*,

129.1 (Ar-*C)*, 129.0 (Ar-*C)*, 128.8 (Ar-*C)*, 128.0 (Ar-*C)*, 125.1 (Ar-*C)*, 120.4 (*ipso*-Ar-*C)*, 118.2 (Ar-*C)*, 116.8 (*ipso*-Ar-*C),* 111.8 (Ar-*C)*, 111.3 (Ar-*C),* 41.8 (*C*$H_2$C=O); *m/z* ($ES^+$) 454 ([$^{35,35}$Cl]$MH^+$), 456 ([$^{35,37}$Cl]$MH^+$), 458 ([$^{37,37}$Cl]$MH^+$); HRMS ($ES^+$) Found [$^{35,35}$Cl]$MH^+$, 454.0847 ($C_{22}H_{18}{}^{35,35}Cl_2N_5O_2$ requires 454.0837).

**6-Chloro-N-(2-(2-(4-chlorophenyl)hydrazineyl)-2-oxoethyl)-2-phenylimidazo[1,2-*a*]pyridine-3-carboxamide 44Bg**

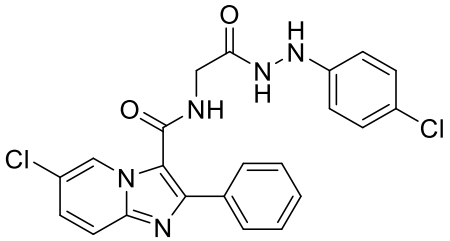


Using the standard procedure provided, *tert*-butyl (2-(2-(4-chlorophenyl)hydrazineyl)-2-oxoethyl)carbamate **51Ac** (0.09 g, 0.30 mmol) was transformed using column chromatography (DCM/EtOAc [1:2]) into the title compound as a pale pink powder (52 mg, 38 %); $R_f$ 0.30 (DCM/EtOAc [1:2]); m.p. 192 - 195 °C; $\nu_{max}$ 3490 (N-H), 3283 (N-H), 1687 (C=O), 1642 (C=O), 1598, 1539, 1490, 1383, 1222, 1173, 1130, 1075, 504 $cm^{-1}$; $\delta_H$ (300 MHz, DMSO-$d_6$) 9.90 (1H, d, *J* 2, CON*H*NH), 9.05 (1H, s, Ar-*H*), 8.72 (1H, t, *J* 5, CON*H*$CH_2$), 8.01 (1H, d, *J* 2, CONHN*H*), 7.95 - 7.90 (2H, d, *J* 8, Ar-*H*), 7.74 (1H, d, *J* 10, 1, Ar-*H*), 7.49 (1H, dd, *J* 10, 2, Ar-H), 7.46 - 7.39 (3H, m, Ar-H), 7.19 - 7.14 (2H, d, *J* 9, Ar-H), 6.80 – 6.75 (2H, d, *J* 9, Ar-*H*), 4.07 – 4.00 (2H, d, *J* 6, C*H*$_2$C=O); δC (75 MHz, DMSO-$d_6$) 169.1 (*C*ONHNH), 161.4 (*C*ONHCH$_2$), 148.5 (*ipso*-Ar-*C*), 145.7 (*ipso*-Ar-*C*), 143.4 (*ipso*-Ar-C), 133.4 (*ipso*-Ar-*C*), 129.0 (Ar-*C*), 128.6 (Ar-*C*), 127.9 (Ar-C), 125.1 (Ar-*C*), 122.2 (*ipso*-Ar-*C*), 120.4 (*ipso*-Ar-*C*), 118.1 (Ar-*C*), 116.8 (*ipso*-Ar-*C*), 114.1, (Ar-*C*), 41.7 (*C*$H_2$C=O); *m/z* ($ES^+$) 454 ([$^{35,35}$Cl]$MH^+$), 456 ([$^{35,37}$Cl]$MH^+$), 458 ([$^{37,37}$Cl]$MH^+$); HRMS ($ES^+$) Found [$^{35,35}$Cl]$MH^+$, 454.0585 ($C_{22}H_{18}{}^{35,35}Cl_2N_5O_2$ requires 454.0837).

**N-(2-(2-(3-bromophenyl)hydrazineyl)-2-oxoethyl)-6-chloro-2-phenylimidazo[1,2-*a*]pyridine-3-carboxamide 44Bh**

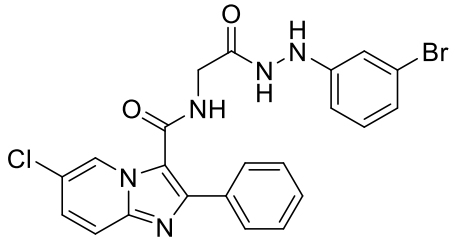

Using the standard procedure provided, *tert*-butyl (2-(2-(3-bromophenyl)hydrazineyl)-2-oxoethyl)carbamate **51Ad** (0.15 g, 0.44 mmol) was transformed using column chromatography (DCM/EtOAc [1:2]) into the title compound as a white powder (43 mg, 23 %); $R_f$ 0.29 (DCM/EtOAc [1:2]); m.p. 212 -216 °C; $\nu_{max}$ 3419 (N-H), 3301 (N-H), 1685 (C=O), 1624 (C=O), 1595, 1539, 1490, 1472, 1382, 1221, 1175, 841, 761, 703 $cm^{-1}$; $\delta_H$ (300 MHz, DMSO-d6) 9.92 (1H, s, CON*H*NH), 9.08 (1H, s, Ar-*H*), 8.69 (1H, t, *J* 5, CON*H*$CH_2$), 8.12 (1H, s, CONHN*H*), 7.95 - 7.91 (2H, d, *J* 8, Ar-*H*), 7.76 (1H, d, *J* 9, Ar-*H*), 7.49 (1H, dd, *J* 9, 2, Ar-*H*), 7.45 – 7.41 (3H, m, Ar-*H*), 7.09 (1H, t, *J* 7, Ar-*H*), 6.95 (1H, s, Ar-*H*), 6.86 (1H, d, *J* 7, Ar-*H*), 6.76 (1H, d, *J* 7, Ar-*H*), 4.06 – 4.00 (2H, d, *J* 6, C*H*$_2$CO); $\delta_C$ (75 MHz, DMSO-$d_6$) 169.1 (*C*ONHNH), 161.4 *(C*ONHC$H_2$), 151.3 (*C*-C=ONH*)*, 145.8 (*ipso*-Ar-*C)*, 143.4 (*ipso*-Ar-*C)*, 133.4 (Ar-*C)*, 131.0 (Ar-*C)*, 129.0 (Ar-*C)*, 128.8 (Ar-*C)*, 127.9 (*ipso*-Ar-*C)*, 125.2 (Ar-*C)*, 121.2 (*ipso*-Ar-*C)*, 120.4 (*ipso*-Ar-*C)*, 118.1 (Ar-*C),* 116.8 (*ipso*-Ar-*C)*, 114.7 (Ar-*C)*, 111.6 (Ar-*C),* 41.8 (*C*H2C=O); *m/z* ($ES^+$) 498 ([$^{35}$Cl, $^{79}$Br]$MH^+$), 500 ([$^{35}$Cl, $^{81}$Br]$MH^+$), 500 ([$^{37}$Cl, $^{79}$Br]$MH^+$), 502 ([$^{37}$Cl, $^{81}$Br]$MH^+$); HRMS ($ES^+$) Found ([$^{35}$Cl, $^{79}$Br]$MH^+$), 498.0323 ($C_{22}H_{18}{}^{35}Cl{}^{79}BrN_5O_2$ requires 498.0332).

**6-Chloro-N-(2-(2-(4-bromophenyl)hydrazineyl)-2-oxoethyl)-2-phenylimidazo[1,2-*a*]pyridine-3-carboxamide 44Bi**

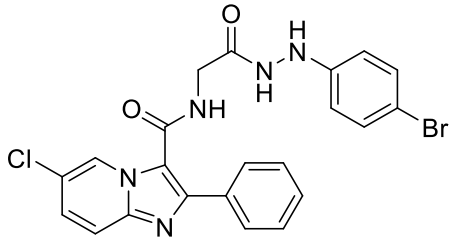

Using the standard procedure provided, *tert*-butyl (2-(2-(4-bromophenyl)hydrazineyl)-2-oxoethyl)carbamate **51Ae** (0.16 g, 0.48 mmol) was transformed using column chromatography (DCM/EtOAc [1:2]) into the title compound as a pale pink powder (30 mg, 15 %); $R_f$ 0.28 (DCM/EtOAc [1:2]); m.p. 215 - 220 °C; $\nu_{max}$ 3490 (N-H), 3267 (N-H), 1686 (C=O), 1640 (C=O), 1595, 1537, 1487, 1384, 1222, 1173 1072, 502 $cm^{-1}$; $\delta_H$

(300 MHz, DMSO-$d_6$) 9.91 (1H, bs, CON*H*NH), 9.04 (1H, s, Ar-*H*), 8.72 (1H, t, *J* 5, CON*H*$CH_2$), 8.01 (1H, s, CONHN*H*), 7.94 - 7.89 (2H, d, *J* 8, Ar-*H*), 7.74 (1H, d, *J* 10, Ar-*H*), 7.49 (1H, dd, *J* 10, 2, Ar-*H*), 7.45 - 7.40 (3H, m, Ar-*H*), 7.29 – 7.27 (2H, d, *J* 9, Ar-*H*), 6.74 – 6.70 (2H, d, *J* 9, Ar-*H*), 4.06 - 3.98 (2H, d, *J* 5, C*H*$_2$C=O); $\delta_C$ (75 MHz, DMSO-$d_6$) 169.1 (*C*ONHNH), 161.4 (*C*ONHCH$_2$), 148.9 (*ipso*-Ar-*C)*, 145.7 (*ipso*-Ar-*C)*, 143.4 (*ipso*-Ar-*C)*, 133.3 (Ar-*C)*, 131.7 (*ipso*-Ar-*C)*, 128.8 (Ar-*C)*, 127.9 (Ar-*C)*, 125.1 (Ar-*C)*, 120.4 (*ipso*-Ar-*C)*, 118.1 (Ar-*C)*, 116.8 (*ipso*-Ar-*C)*, 114.6 (Ar-*C)*, 109.7 (*ipso*-Ar-*C)*, 41.7 (*C*H$_2$C=O); *m/z* (ES$^+$) 498 ([$^{35}$Cl, $^{79}$Br]MH$^+$), 500 ([$^{35}$Cl, $^{81}$Br]MH$^+$), 500 ([$^{37}$Cl, $^{79}$Br]MH$^+$), 502 ([$^{37}$Cl, $^{81}$Br]MH$^+$); HRMS (ES$^+$) Found ([$^{35}$Cl,$^{79}$Br]MH$^+$), 498.0049 ($C_{22}H_{18}{}^{35}Cl{}^{79}BrN_5O_2$ requires 498.0332).

**6-Chloro-N-(2-oxo-2-(2-(3-(trifluoromethyl)phenyl)hydrazineyl)ethyl)-2-phenylimidazo[1,2-*a*]pyridine-3-carboxamide 44Bj**

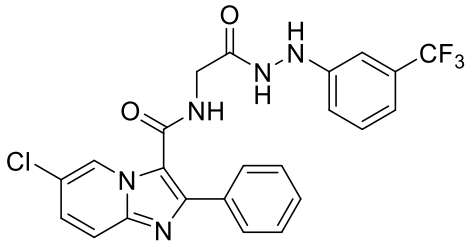


Using the standard procedure provided, *tert*-butyl (2-(2-(3-(trifluoromethyl)phenyl)hydrazineyl)-2-oxoethyl)carbamate **51Af** (0.10 g, 0.32 mmol) was transformed using column chromatography (DCM/EtOAc [1:2]) into the title compound as a white powder (51 mg, 33 %); $R_f$= 0.30 (DCM/EtOAc [1:2]); m.p. 229-235 °C; $\nu_{max}$ 3285 (N-H), 3239 (N-H), 1687 (C=O), 1619 (C=O), 1491, 1455, 1385, 1333, 1235, 1165, 1117, 1069, 954, 802, 751, 699 cm$^{-1}$; $\delta_H$ (300 MHz, DMSO-d6) 9.99 (1H, s, CON*H*NH), 9.05 (1H, s, Ar-*H*), 8.70 (1H, t, *J* 5, CON*H*$CH_2$), 8.27 (1H, s, CONHN*H*), 7.96 - 7.88 (2H, d, *J* 8, Ar-*H*), 7.76 (1H, d, *J* 9, Ar-*H*), 7.50 (1H, dd, *J* 9, 2, Ar-*H*), 7.47 - 7.44 (3H, m, Ar-*H*), 7.35 (1H, d, *J* 7, Ar-*H*), 7.09 – 6.98 (3H, m, Ar-*H*), 4.07 – 3.98 (2H, d, *J* 6, C*H*$_2$CO); $\delta_C$ (75 MHz, DMSO-$d_6$) 169.2 (*C*ONHNH), 161.5 *(C*ONHCH$_2$), 150.3 (*ipso*-Ar-*C)*, 145.8 (*ipso*-Ar-*C)*, 143.4 (*ipso*-Ar-*C)*, 133.4 (*ipso*-Ar-*C)*, 130.2 (Ar-*C)*, 129.06 (Ar-*C)*, 128.8 (Ar-*C)*, 127.9 (Ar-*C)*, 125.1 (Ar-*C)*, 120.4 (*ipso*-Ar-*C)*, 118.1 (Ar-*C),* 116.8 (*ipso*-Ar-*C)*, 116.2 (Ar-*C)*, 108.4 (Ar-*C),* 41.8 (*C*H$_2$C=O); $\delta_F$ (282 MHz, DMSO-d6) -61.2 (C*F*$_3$); *m/z* (ES$^+$) 488 ([$^{35}$Cl]MH$^+$), 490 ([$^{37}$Cl]MH$^+$); HRMS (ES$^+$) Found [$^{35}$Cl]MH$^+$, 488.0812 ($C_{23}H_{18}{}^{35}ClF_3N_5O_2$ requires 488.1101).

**6-Chloro-N-(2-oxo-2-(2-(4-(trifluoromethyl)phenyl)hydrazineyl)ethyl)-2-phenylimidazo[1,2-*a*]pyridine-3-carboxamide 44Bk**

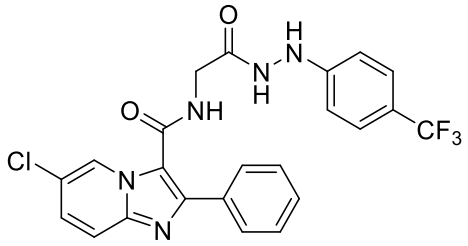

Using the standard procedure provided, *tert*-butyl (2-(2-(4-(trifluoromethyl)phenyl)hydrazineyl)-2-oxoethyl)carbamate **51Ag** (0.10 g, 0.32 mmol) was transformed using column chromatography (DCM/EtOAc [1:2]) into the title compound as a white powder (66 mg, 42 %); $R_f$ 0.29 (DCM/EtOAc [1:2]); m.p. 220 - 222 °C; $\nu_{max}$ 3414 (N-H), 3280 (N-H), 1687 (C=O), 1619 (C=O), 1539, 1490, 1384, 1327, 1223, 1067, 829, 761, 703 $cm^{-1}$; $\delta_H$ (300 MHz, DMSO-d6) 10.03 (1H, bs, CON*H*NH), 9.05 (1H, s, Ar-*H*), 8.76 (1H, t, *J* 5, CON*H*$CH_2$), 8.01 (1H, s, CONHN*H*), 7.95 - 7.91 (2H, d, *J* 8, Ar-*H*), 7.75 (1H, d, *J* 9, Ar-*H*), 7.50 (1H, dd, *J* 9, 2, Ar-*H*), 7.46 - 7.40 (5H, m, Ar-*H*), 6.91 – 6.85 (2H, d, *J* 9, Ar-*H*), 4.08 – 4.03 (2H, *J* 6, d, C$H_2$C=O); $\delta_C$ (75 MHz, DMSO-$d_6$) 169.2 (*C*ONHNH), 161.5 *(C*ONHCH), 152.2 (*ipso*-Ar-*C)*, 145.7 (*ipso*-Ar-*C)*, 143.4 (*ipso*-Ar-*C)*, 133.4 (*ipso*-Ar-*C)*, 128.9 (Ar-*C)*, 128.8 (Ar-*C)*, 127.8 (Ar-*C)*, 126.4 (Ar-*C)*, 125.1 (Ar-*C)*, 120.4 (*ipso*-Ar-*C)*, 118.1 (Ar-*C),* 116.9 (*ipso*-Ar-*C)*, 111.9 (Ar-*C),* 41.7 (*C*$H_2$C=O); $\delta_F$ (282 MHz, DMSO-d6) -61.2 (C*F*$_3$); *m/z* ($ES^+$) 488 ([$^{35}$Cl]$MH^+$), 490 ([$^{37}$Cl]$MH^+$); HRMS ($ES^+$) Found [$^{35}$Cl]$MH^+$, 488.1083 ($C_{23}H_{18}{}^{35}ClF_3N_5O_2$ requires 488.1101).

**6-chloro-N-(2-oxo-2-(2-(3-(trifluoromethoxy)phenyl)hydrazineyl)ethyl)-2-phenylimidazo[1,2-*a*]pyridine-3-carboxamide 44Bl**

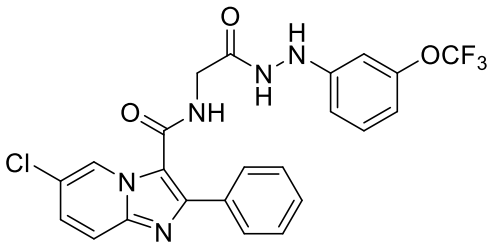

Using the standard procedure provided, *tert*-butyl (2-(2-(3-(trifluoromethoxy)phenyl)hydrazineyl)-2-oxoethyl)carbamate **51Ah** (0.09 g, 0.25 mmol) was transformed using column chromatography (DCM/EtOAc [1:1]) into the title compound as a white powder (42 mg, 32 %); $R_f$ 0.20 (DCM/EtOAc [1:1]); m.p. 217 –

224 °C; $\nu_{max}$ 3417 (N-H), 3282 (N-H), 1686 (C=O), 1641 (C=O), 1541, 1505, 1492, 1384, 1279, 1222, 1200, 1159, 968, 838, 760, 703, 505 $cm^{-1}$; $\delta_H$ (300 MHz, DMSO-d6) 9.95 (1H, s, CON*H*NH), 9.05 (1H, s, Ar-*H*), 8.70 (1H, t, *J* 5, CON*H*CH), 8.23 (1H, s, CONHN*H*), 7.95 - 7.89 (2H, dd, *J* 8, 1, Ar-*H*), 7.76 (1H, dd, *J* 9, 1, Ar-*H*), 7.49 (1H, dd, *J* 9, 2, Ar-*H*), 7.47 - 7.41 (3H, m, Ar-*H*), 7.24 (1H, t, *J* 8, Ar-*H*), 6.77 (1H, dd, *J* 8, 1, Ar-*H*), 6.70 (1H, s, Ar-*H*), 6.64 (1H, d, *J* 8, Ar-*H*), 4.07 – 3.96 (2H, d, *J* 6, C$H_2$C=O); $\delta_C$ (75 MHz, DMSO-$d_6$) 169.1 (*C*ONHNH), 161.5 *(C*ONHC$H_2$), 151.5 (*ipso*-Ar-*C)*, 149.8 (Ar-O*C*$F_3$), 143.3 (*ipso*-Ar-*C)*, 133.4 (*ipso*-Ar-*C)*, 130.5 (Ar-*C)*, 129.0 (Ar-*C)*, 128.9 (Ar-*C)*, 128.8 (Ar-*C)*, 127.9 (Ar-*C)*, 125.1 (Ar-*C)*, 120.4 (*ipso*-Ar-*C)*, 118.1 (Ar-*C),* 116.8 (*ipso*-Ar-*C)*, 111.3 (Ar-*C)*, 110.3 (Ar-*C)*, 104.5 (Ar-*C),* 41.7 (*C*$H_2$C=O); $\delta_F$ (282 MHz, DMSO-d6) -56.4 (OC*F*$_3$); *m/z* ($ES^+$) 502 ([$^{35}$Cl]$MH^+$), 504 ([$^{37}$Cl]$MH^+$); HRMS ($ES^+$) Found [$^{35}$Cl]$MH^+$, 502.0917 ($C_{23}H_{17}{}^{35}ClF_3N_5O_3$ requires 502.0894).

**6-Chloro-N-(2-oxo-2-(2-(4-(trifluoromethoxy)phenyl)hydrazineyl)ethyl)-2-phenylimidazo[1,2-*a*]pyridine-3-carboxamide 44Bm**

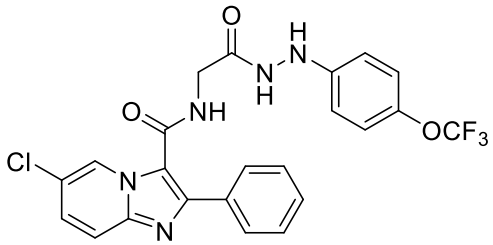

Using the standard procedure provided, *tert*-butyl (2-(2-(4-(trifluoromethoxy)phenyl)hydrazineyl)-2-oxoethyl)carbamate **51Ai** (0.14 g, 0.41 mmol) was transformed using column chromatography (DCM/EtOAc [1:1]) into the title compound as a white powder (74 mg, 36 %); $R_f$ 0.20 (DCM/EtOAc [1:1]); m.p. 210 – 215 °C; $\nu_{max}$ 3417 (N-H), 3282 (N-H), 1686 (C=O), 1641 (C=O), 1541, 1505, 1492, 1384, 1279, 1222, 1200, 1159, 968, 838, 760, 703, 505 $cm^{-1}$; $\delta_H$ (300 MHz, DMSO-d6) 9.94 (1H, s, CON*H*NH), 9.05 (1H, s, Ar-*H*), 8.73 (1H, t, *J* 5, CON*H*C$H_2$), 8.09 (1H, s, CONHN*H*), 7.96 - 7.88 (2H, d, *J* 8, Ar-*H*), 7.76 (1H, d, *J* 9, Ar-*H*), 7.49 (1H, dd, *J* 9, 2, Ar-*H*), 7.45 - 7.34 (3H, m, Ar-*H*), 7.18 – 7.07 (2H, d, *J* 9, Ar-*H*), 6.86 – 6.78 (2H, d, *J* 9, Ar-*H*), 4.08 – 4.00 (2H, d, *J* 6, C$H_2$CO); $\delta_C$ (75 MHz, DMSO-$d_6$) 169.1 (*C*ONHNH), 161.5 (*C*ONHC$H_2$), 161.4 (*ipso*-Ar-*C)*, 148.8 (Ar-O*C*$F_3$*)*, 145.7 (*ipso*-Ar-*C)*, 143.4 (*ipso*-Ar-*C)*, 133.4 (*ipso*-Ar-*C)*, 129.0 (Ar-*C)*, 128.9 (Ar-*C)*, 128.8 (Ar-*C)*, 127.8 (Ar-*C)*, 125.1 (Ar-*C)*, 122.2 (Ar-*C)*, 120.4 (*ipso*-Ar-*C)*, 118.1 (Ar-*C),* 116.8 (*ipso*-Ar-*C)*, 113.2 (Ar-*C)*, 41.7 (*C*$H_2$CO); $\delta_F$ (282 MHz, DMSO-d6) -57.2 (OC*F*$_3$); *m/z* ($ES^+$) 502 ([$^{35}$Cl]$MH^+$), 504

([$^{37}$Cl]MH$^+$); HRMS (ES$^+$) Found [$^{35}$Cl]MH$^+$, 502.0872 ($C_{23}H_{17}{}^{35}ClF_3N_5O_3$ requires 502.0894).

**(S)-6-Chloro-N-(1-oxo-1-(2-phenylhydrazineyl)propan-2-yl)-2-phenylimidazo[1,2-*a*]pyridine-3-carboxamide 44Bn**

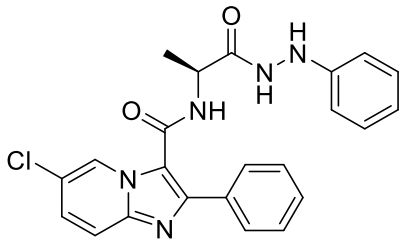

Using the standard procedure provided, *tert*-butyl (S)-(1-oxo-1-(2-phenylhydrazineyl)propan-2-yl)carbamate **51Aj** (0.12 g, 0.43 mmol) was transformed using column chromatography (*n*-Hexane/EtOAc [1:1]) into the title compound as a white powder (63 mg, 34 %); $R_f$ 0.40 (*n*-Hexane/EtOAc [1:1]); m.p. 201 - 203 °C; $\nu_{max}$ 3253 (N-H), 1646 (C=O), 1602 (C=O), 1520, 1493, 1444, 1383, 1222, 1168, 1090, 950, 843 751, 689 cm$^{-1}$; $\delta_H$ (300 MHz, DMSO-d$_6$) 9.92 (1H, s, CON*H*NH), 9.03 (1H, s, Ar-*H*), 8.61 (1H, d, *J* 6, CON*H*CH), 7.92 – 7.87 (2H, d, *J* 8, Ar-*H*), 7.76 (1H, d, *J* 9, Ar-*H*), 7.48 (1H, dd, *J* 9, 2, Ar-*H*), 7.46 – 7.40 (3H, m, Ar-*H*), 7.15 – 7.09 (2H, t, *J* 9, Ar-*H*), 6.79 – 6.74 (2H, d, *J* 9, Ar-*H*), 6.68 (1H, t, *J* 9, Ar-*H*), 4.61 (1H, m, C*H*CH$_3$), 1.38 – 1.32 (3H, d, *J* 6, CHC*H*$_3$); $\delta_C$ (75 MHz, DMSO-d$_6$) 172.4 (*C*=ONHNH), 160.7 *(C*=ONHCH), 149.6 (*ipso*-Ar-*C)*, 145.8 (*ipso*-Ar-*C)*, 143.3 (*ipso*-Ar-*C)*, 133.4 (*ipso*-Ar-*C)*, 129.0 (Ar-*C)*, 128.9 (Ar-*C)*, 128.8 (Ar-*C)*, 127.8 (Ar-*C)*, 125.1 (Ar-*C)*, 120.4 (*ipso*-Ar-*C),* 118.9 (Ar-*C)*, 118.1 (Ar-*C)*, 116.9 (*ipso*-Ar-*C)*, 112.6 (Ar-*C)*, 48.3 (*C*HCH$_3$), 17.9 (CH*C*H$_3$); *m/z* (ES$^+$) 434 ([$^{35}$Cl]MH$^+$), 436 ([$^{37}$Cl]MH$^+$); HRMS (ES$^+$) Found [$^{35}$Cl]MH$^+$, 434.1381 ($C_{23}H_{21}{}^{35}ClN_5O_2$ requires 434.1384).

**6-Chloro-N-(2-oxo-2-(2-(3-chlorophenyl)hydrazineyl)ethyl)-2-phenylimidazo[1,2-*a*]pyridine-3-carboxamide 44Bo**

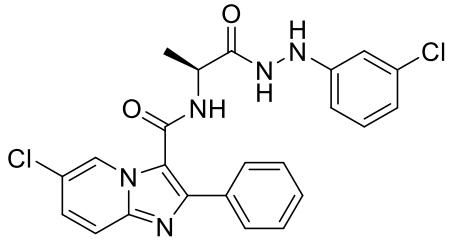

Using the standard procedure provided, *tert*-butyl (S)-(1-(2-(3-chloroophenyl)hydrazineyl)-1-oxopropan-2-yl)carbamate **44Ak** (0.11 g, 0.33 mmol) was transformed using column chromatography (DCM/EtOAc [1:2]) into the title compound as a pale pink powder (52 mg, 31 %); $R_f$ 0.30 (DCM/EtOAc [1:2]); m.p. 216 - 219 °C; $\nu_{max}$ 3265 (N-H), 1640 (C=O), 1631, 1531, 1490, 1372, 1320, 1216, 1170, 1125, 1082, 893, 522 $cm^{-1}$; $\delta_H$ (300 MHz, DMSO-d6) 10.07 (1H, d, *J* 2, CON*H*NH), 9.00 (1H, s, Ar-*H*), 8.64 (1H, d, *J* 6, CON*H*CH), 7.93 - 7.88 (2H, d, *J* 7, Ar-*H*), 7.76 (1H, d, *J* 9, Ar-*H*), 7.52 (1H, s, Ar-*H*), 7.49 (1H, dd, *J* 9, 2, Ar-*H*), 7.46 - 7.43 (2H, m, Ar-*H*), 7.40 (1H, t, *J* 7, Ar-*H*), 7.28 (1H, d, *J* 7, Ar-*H*), 7.13 (1H, t, *J* 7, Ar-*H*), 6.91 (1H, d, *J* 7, Ar-*H*), 6.74 (1H, t, *J* 7, Ar-*H*), 4.61 (1H, m, C*H*$CH_3$), 1.37 – 1.33 (3H, d, *J* 6, CHC*H*$_3$); $\delta_C$ (75 MHz, DMSO-$d_6$) 172.5 (*C*ONHNH), 160.8 (*C*ONHCH), 151.4 (*ipso*-Ar-*C)*, 146.0 (*ipso*-Ar-*C)*, 143.4 (*ipso*-Ar-*C)*, 134.1 (Ar-*C)*, 133.4 (Ar-*C)*, 131.0 (Ar-*C)*, 129.1 (Ar-*C)*, 128.9 (Ar-*C)*, 127.9 (Ar-*C)*, 125.1 (Ar-*C)*, 122.6 (*ipso*-Ar-*C)*, 121.2 (Ar-*C)*, 120.4 (*ipso*-Ar-*C),* 118.1 (Ar-*C)*, 114.8 (Ar-*C)*, 111.6 (Ar-*C),* 48.4 (*C*H$CH_3$), 17.6 (CH*C*$H_3$); *m/z* ($ES^+$) 468 ([$^{35,35}$Cl]$MH^+$), 470 ([$^{35,37}$Cl]$MH^+$), 472 ([$^{37,37}$Cl]$MH^+$); HRMS ($ES^+$) Found [$^{35,35}$Cl]$MH^+$, 468. 0998 ($C_{23}H_{20}{}^{35,35}Cl_2N_5O_2$ requires 468.0994).

**6-Chloro-N-(1-(2-(4-chlorophenyl)hydrazineyl)-1-oxopropan-2-yl)-2-phenylimidazo[1,2-*a*]pyridine-3-carboxamide 44Bp**

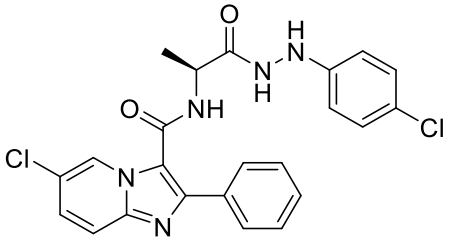

Using the standard procedure provided, tert-butyl (S)-(1-(2-(4-chlorophenyl)hydrazineyl)-1-oxopropan-2-yl)carbamate **51Al** (0.16 g, 0.51 mmol) was transformed using column chromatography (DCM/EtOAc [1:2]) into the title compound as a white powder (110 mg, 46 %); $R_f$ 0.25 (DCM/EtOAc [2:1]); m.p. 224 -227 °C; $\nu_{max}$ 3422 (N-H), 3252 (N-H), 1668 (C=O), 1644 (C=O), 1520, 1488, 1446, 1381, 1322, 1220, 1170, 1088, 818, 698 $cm^{-1}$; $\delta_H$ (300 MHz, DMSO-d6) 9.98 (1H, bs, CON*H*NH), 9.02 (1H, s, Ar-*H*), 8.63 (1H, d, *J* 6, CON*H*CH), 8.03 (1H, s, CONHN*H*), 7.92 - 7.88 (2H, d, *J* 8, Ar-*H*), 7.75 (1H, d, *J* 9, Ar-*H*), 7.49 (1H, dd, *J* 9, 2, Ar-*H*), 7.46 - 7.40 (3H, d*, J* 8, Ar-*H*), 7.20 – 7.15 (2H, *J* 7, d, Ar-*H*), 6.82 - 6.71 (2H, d, *J* 7, Ar-*H*), 4.59 (1H, m, C*H*$CH_3$), 1.38 – 1.32 (3H, d, *J* 6, CHC*H*$_3$); $\delta_C$ (75 MHz, DMSO-$d_6$) 172.5

(*C*ONHNH), 160.8 *(C*ONHCH), 148.6 (*ipso*-Ar-*C)*, 145.8 (*ipso*-Ar-*C)*, 143.3 (*ipso*-Ar-*C)*, 133.4 (*ipso*-Ar-*C)*, 129.0 (Ar-*C)*, 128.9 (Ar-*C)*, 127.8 (Ar-*C)*, 125.0 (Ar-*C)*, 122.2 (*ipso*-Ar-*C)*, 120.3 (*ipso*-Ar-*C)*, 118.1 (Ar-*C)*, 116.9 (*ipso*-Ar-*C)*, 114.1 (Ar-*C)*, 48.3 (*C*HCH$_3$), 17.7 (CH*C*H$_3$); *m/z* (ES$^+$) 468 ([$^{35,35}$Cl]MH$^+$), 470 ([$^{35,37}$Cl]MH$^+$), 472 ([$^{37,37}$Cl]MH$^+$); HRMS (ES$^+$) Found [$^{35,35}$Cl]MH$^+$, 468.1000 ($C_{23}H_{20}{}^{35,35}Cl_2N_5O_2$ requires 468.0994).

**6-Chloro-N-(2-oxo-2-(2-(3-bromophenyl)hydrazineyl)ethyl)-2-phenylimidazo[1,2-*a*]pyridine-3-carboxamide 44Bq**

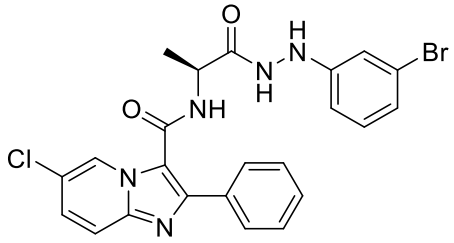


Using the standard procedure provided, *tert*-butyl (S)-(1-(2-(3-bromophenyl)hydrazineyl)-1-oxopropan-2-yl)carbamate **51Am** (0.11 g, 0.33 mmol) was transformed using column chromatography (DCM/EtOAc [1:2]) into the title compound as a pale pink powder (52 mg, 31 %); R$_f$ 0.30 (DCM/EtOAc [1:2]); m.p. 216 - 219 °C; $\nu_{max}$ 3263 (N-H), 1644 (C=O), 1671 (C=O), 1532, 1490, 1382, 1320, 1219, 1170, 1125, 1072, 893, 512 cm$^{-1}$; $\delta_H$ (300 MHz, DMSO-d6) 9.99 (1H, d, *J* 2, CON*H*NH), 9.06 (1H, s, Ar-*H*), 8.54 (1H, d, *J* 6, CON*H*CH), 8.12 (1H, d, *J* 2, CONHN*H*), 7.92 - 7.88 (2H, d, *J* 7, Ar-*H*), 7.75 (1H, d, *J* 9, Ar-*H*), 7.49 (1H, dd, *J* 9, 2, Ar-*H*), 7.48 - 7.45 (3H, m, Ar-*H*), 7.08 (1H, dd, *J* 7, 7, Ar-*H*), 6.95 (1H, s, Ar-*H*), 6.84 (1H, d, *J* 7, Ar-*H*), 6.74 (1H, d, *J* 7, Ar-*H*), 4.55 (1H, m, C*H*CH$_3$), 1.36 – 1.29 (3H, d, *J* 6, CHC*H$_3$*); $\delta_C$ (75 MHz, DMSO-d$_6$) 172.5 (*C*ONHNH), 160.8 (*C*ONHCH), 151.4 (*ipso*-Ar-*C)*, 146.0 (*ipso*-Ar-*C)*, 143.4 (*ipso*-Ar-*C)*, 134.1 (Ar-*C)*, 133.4 (Ar-*C)*, 131.0 (Ar-*C)*, 129.1 (Ar-*C)*, 128.9 (Ar-*C)*, 127.9 (Ar-*C)*, 125.1 (Ar-*C)*, 122.6 (*ipso*-Ar-*C)*, 121.2 (Ar-*C)*, 120.4 (*ipso*-Ar-*C),* 118.1 (Ar-*C)*, 114.8 (Ar-*C)*, 111.6 (Ar-*C),* 48.4 (*C*HCH$_3$), 17.6 (CH*C*H$_3$); *m/z* (ES$^+$) 512 ([$^{35}$Cl, $^{79}$Br]MH$^+$), 514 ([$^{35}$Cl, $^{81}$Br]MH$^+$), 514 ([$^{37}$Cl, $^{79}$Br]MH$^+$), 516 ([$^{37}$Cl, $^{81}$Br]MH$^+$); HRMS (ES$^+$) Found ([$^{35}$Cl, $^{79}$Br]MH$^+$), 512.0483 ($C_{23}H_{20}{}^{35}Cl^{79}BrN_5O_2$ requires 512.0489).

**N-(1-(2-(4-bromophenyl)hydrazineyl)-1-oxopropan-2-yl)-6-chloro-2-phenylimidazo[1,2-*a*]pyridine-3-carboxamide 44Br**

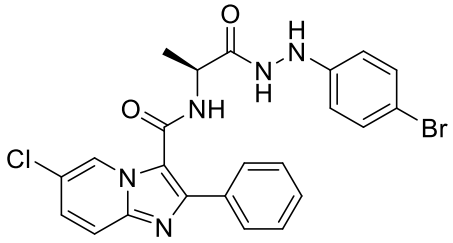

Using the standard procedure provided, *tert*-butyl (S)-(1-(2-(4-bromophenyl)hydrazineyl)-1-oxopropan-2-yl)carbamate **51An** (0.15 g, 0.41 mmol) was transformed using column chromatography (DCM/EtOAc [1:2]) into the title compound as a pale pink (105 mg, 49 %); $R_f$ 0.20 (DCM/EtOAc [2:1]); m.p. 201 - 206 °C; $\nu_{max}$ 3252 (N-H), 1671 (C=O), 1617 (C=O), 1520, 1487, 1384, 1323, 1223, 1171, 1105, 1065, 839,5 699, 557 $cm^{-1}$; $\delta_H$ (300 MHz, DMSO-d6) 10.00 (1H, s, CON*H*NH), 9.02 (1H, s, Ar-*H*), 8.62 (1H, d, *J* 6, CON*H*CH), 8.05 (1H, s, CONHN*H*), 7.93 – 7.88 (2H, d, *J* 8, Ar-*H*), 7.76 (1H, d, *J* 9, Ar-*H*), 7.48 (1H, dd, *J* 9, 2, Ar-*H*), 7.44 – 7.41 (3H, m, Ar-*H*), 7.31 – 7.27 (2H, *J* 7, d, Ar-*H*), 6.75 – 6.70 (2H, *J* 7, d, Ar-*H*), 4.59 (1H, t, *J* 6, C*H*$CH_3$), 1.36 – 1.33 (3H, d, *J* 6, CHC*H*$_3$); $\delta_C$ (75 MHz, DMSO-$d_6$) 172.5 (*C*ONHNH), 160.7 *(C*ONHCH), 149.0 (*ipso*-Ar-*C)*, 145.8 (*ipso*-Ar-*C)*, 143.3 (*ipso*-Ar-*C)*, 133.4 (*ipso*-Ar-*C)*, 131.7 (Ar-*C)*, 129.0 (Ar-*C)*, 128.9 (Ar-*C)*, 127.8 (Ar-*C)*, 125.1 (Ar-*C)*, 120.3 (*ipso*-Ar-*C),* 118.1 (Ar-*C)*, 116.8 (*ipso*-Ar-*C)*, 114.6 (Ar-*C)*, 109.7 (*ipso*-Ar-*C)*, 48.3 (*C*$HCH_3$), 17.7 (CH*C*$H_3$); *m/z* ($ES^+$) 512 ([$^{35}$Cl, $^{79}$Br]$MH^+$), 514 ([$^{35}$Cl, $^{81}$Br]$MH^+$), 514 ([$^{37}$Cl, $^{79}$Br]$MH^+$), 516 ([$^{37}$Cl, $^{81}$Br]$MH^+$); HRMS ($ES^+$) Found ([$^{35}$Cl, $^{79}$Br]$MH^+$), 512.0483 ($C_{23}H_{20}{}^{35}Cl{}^{79}BrN_5O_2$ requires 512.0489).

**6-chloro-N-(1-(2-(3-(trifluoromethyl)phenyl)hydrazineyl)-1-oxopropan-2-yl)-2-phenylimidazo[1,2-*a*]pyridine-3-carboxamide 44Bs**

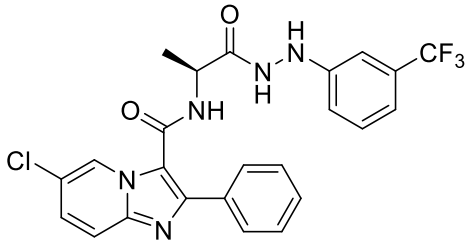

Using the standard procedure provided, *tert*-butyl (S)-(1-(2-(3-(trifluoromethyl)phenyl)hydrazineyl)-1-oxopropan-2-yl)carbamate **51Ao** (0.15 g, 0.43 mmol) was transformed using column chromatography (DCM/EtOAc [1:2]) into the title compound as a white powder (105 mg, 48%); $R_f$ 0.27 (DCM/EtOAc [1:2]); m.p. 211 - 215 °C; $\nu_{max}$ 3249 (N-H), 1682 (C=O), 1609 (C=O), 1532, 1489, 1445, 1379, 1336,

1229, 1164 1112, 1067, 695, 514 $cm^{-1}$; $\delta_H$ (300 MHz, DMSO-$d_6$) 10.09 (1H, s, CON*H*NH), 9.02 (1H, s, Ar-*H*), 8.57 (1H, d, *J* 6, CON*H*CH), 8.30 (1H, s, CONHN*H*), 7.94 – 7.88 (2H, d, *J* 8, Ar-*H*), 7.76 (1H, d, *J* 9, Ar-*H*), 7.49 (1H, dd, *J* 9, 2, Ar-*H*), 7.46 – 7.37 (3H, m, Ar-*H*), 7.35 (1H, d, *J* 7, Ar-*H*), 7.08 (1H, s, Ar-*H*), 7.06 – 6.98 (2H, t, *J* 7, Ar-*H*), 4.59 (1H, m, C*H*$CH_3$), 1.39 – 1.32 (3H, d, *J* 6, CHC*H*$_3$); $\delta_C$ (75 MHz, DMSO-$d_6$) 172.6 (*C*ONHNH), 160.8 *(C*ONHCH), 150.3 (*ipso*-Ar-*C)*, 146.0 (*ipso*-Ar-*C)*, 143.4 (*ipso*-Ar-*C)*, 133.4 (*ipso*-Ar-*C)*, 130.2 (Ar-*C)*, 128.9 (Ar-*C)*, 128.8 (Ar-*C),* 127.9 (Ar-*C)*, 125.1 (Ar-*C)*, 123.0 (*ipso*-Ar-*C)*, 120.4 (Ar-*C)*, 118.1 (Ar-*C)*, 116.7 (*ipso*-Ar-*C)*, 114.9 (Ar-*C)*, 108.4 (Ar-*C),* 48.5 (*C*H$CH_3$), 17.6 (CH*C*$H_3$); $\delta_F$ (282 MHz, DMSO-d6) -61.2 (C*F*$_3$); *m/z* (ES$^+$) 502 ([$^{35}$Cl]MH$^+$), 504 ([$^{37}$Cl]MH$^+$); HRMS (ES$^+$) Found [$^{35}$Cl]MH$^+$, 502.1269 ($C_{24}H_{20}{}^{35}ClF_3N_5O_2$ requires 502.1258).

**6-Chloro-N-(1-oxo-1-(2-(4-(trifluoromethyl)phenyl)hydrazineyl)propan-2-yl)-2-phenylimidazo[1,2-*a*]pyridine-3-carboxamide 44Bt**

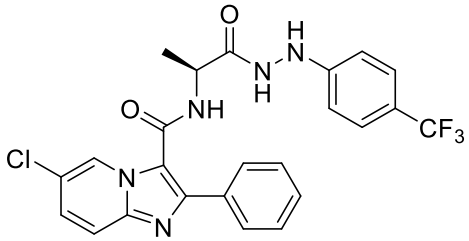


Using the standard procedure provided, *tert*-butyl (S)-(1-(2-(4-(trifluoromethyl) phenyl)hydrazineyl)-1-oxopropan-2-yl)carbamate **51Ap** (0.12 g, 0.36 mmol) was transformed using column chromatography (DCM/EtOAc [1:2]) into the title compound as a white powder (78 mg, 43 %); $R_f$ 0.20 (DCM/EtOAc [1:2]); m.p. 222 -226 °C; $\nu_{max}$ 3248 (N-H), 1681 (C=O), 1617 (C=O), 1522, 1491, 1387, 1324, 1230, 1158, 1105, 1065, 834, 700, 557 $cm^{-1}$; $\delta_H$ (300 MHz, DMSO-d6) 10.10 (1H, s, CON*H*NH), 9.00 (1H, s, Ar-*H*), 8.70 (1H, d, *J* 6, CON*H*CH), 8.48 (1H, s, CONHN*H*), 7.92 – 7.88 (2H, d, *J* 8, Ar-*H*), 7.76 (1H, d, *J* 9, Ar-*H*), 7.51 – 7.40 (6H, m, Ar-*H*), 6.88 – 6.82 (2H, d, *J* 7, Ar-*H*), 4.61 (1H, m, C*H*$CH_3$), 1.39 -1.33 (3H, d, *J* 6, CHC*H*$_3$); $\delta_C$ (75 MHz, DMSO-$d_6$) 172.6 (*C*ONHNH), 160.8 *(C*ONHCH), 152.8 (*ipso*-Ar-*C)*, 145.8 (*ipso*-Ar-*C)*, 143.3 (*ipso*-Ar-*C)*, 133.4 (*ipso*-Ar-*C)*, 129.0 (Ar-*C)*, 129.9 (Ar-*C)*, 128.9 (Ar-*C)*, 127.8 (Ar-*C)*, 126.5 (Ar-*C)*, 125.0 (Ar-*C)*, 120.3 (*ipso*-Ar-*C)*, 118.1 (Ar-*C)*, 116.8 (*ipso*-Ar-*C)*, 111.9 (Ar-*C)*, 48.4 (*C*H$CH_3$), 17.7 (CH*C*$H_3$); *m/z* (ES$^+$) 502 ([$^{35}$Cl]MH$^+$), 504 ([$^{37}$Cl]MH$^+$); HRMS (ES$^+$) Found [$^{35}$Cl]MH$^+$, 502.1269 ($C_{24}H_{20}{}^{35}ClF_3N_5O_2$ requires 502.1258).

**6-chloro-N-(1-oxo-1-(2-(3-(trifluoromethoxy)phenyl)hydrazineyl)propan-2-yl)-2-phenylimidazo[1,2-*a*]pyridine-3-carboxamide 44Bu**

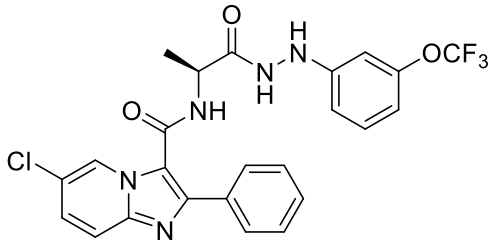

Using the standard procedure provided, *tert*-butyl (S)-(1-(2-(3-(trifluoromethoxy) phenyl)hydrazineyl)-1-oxopropan-2-yl)carbamate **51Aq** (0.08 g, 0.30 mmol) was transformed using column chromatography (DCM/EtOAc [3:1]) into the title compound as a white powder (50 mg, 32 %); $R_f$ 0.29 (DCM/EtOAc [3:1]); m.p. 215 - 220 °C; $\nu_{max}$ 3659 (N-H), 3247 (N-H), 1669 (C=O), 1644 (C=O), 1519, 1488, 1382, 1254, 1213, 1152, 1090, 949, 804, 764, 687, 634 $cm^{-1}$; $\delta_H$ (300 MHz, DMSO-d6) 10.03 (1H, s, CON*H*NH), 9.01 (1H, s, Ar-*H*), 8.59 (1H, d, *J* 6, CON*H*CH), 8.24 (1H, s, CONHN*H*), 7.95 - 7.87 (2H, d, *J* 7, Ar-*H*), 7.75 (1H, d, *J* 9, Ar-*H*), 7.50 (1H, dd, *J* 9, 2, Ar-*H*), 7.47 - 7.39 (3H, m, Ar-*H*), 7.24 (1H, t, *J* 8, Ar-*H*), 6.77 (1H, d, *J* 8, Ar-*H*), 6.69 (1H, s, Ar-*H*), 6.62 (1H, d, *J* 8, Ar-*H*), 4.57 (1H, m, C*H*$CH_3$), 1.38 – 1.27 (3H, d, *J* 6, CHC*H*$_3$); $\delta_C$ (75 MHz, DMSO-$d_6$) 172.6 (*C*ONHNH), 160.8 (*C*ONHCH), 151.7 (*ipso*-Ar-*C)*, 149.9 (Ar-O*C*$F_3$*)*, 143.4 (*ipso*-Ar-*C)*, 133.4 (*ipso*-Ar-*C)*, 130.7 (Ar-*C)*, 129.0 (Ar-*C)*, 128.8 (Ar-*C)*, 127.8 (Ar-*C)*, 125.0 (Ar-*C)*, 120.3 (*ipso*-Ar-*C)*, 118.1 (Ar-*C),* 116.8 (*ipso*-Ar-*C)*, 111.4 (Ar-*C)*, 110.4 (Ar-*C)*, 104.5 (Ar-*C),* 48.3 (*C*H$CH_3$), 17.6 (CH*C*$H_3$); $\delta_F$ (282 MHz, DMSO-$d_6$) -57.0 (OC*F*$_3$); ***m/z*** (ES$^+$) 518 ([$^{35}$Cl]MH$^+$), 520 ([$^{37}$Cl]MH$^+$); HRMS (ES$^+$) Found [$^{35}$Cl]MH$^+$, 518.1176 ($C_{24}H_{21}{}^{35}ClF_3N_5O_3$ requires 518.1207).

**6-chloro-N-(1-oxo-1-(2-(4-(trifluoromethoxy)phenyl)hydrazineyl)propan-2-yl)-2-phenylimidazo[1,2-*a*]pyridine-3-carboxamide 44Bv**

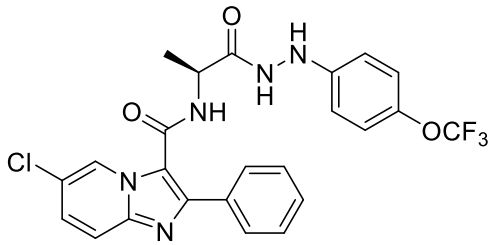

Using the standard procedure provided, *tert*-butyl (S)-(1-(2-(4-(trifluoromethoxy) phenyl)hydrazineyl)-1-oxopropan-2-yl)carbamate **51Ar** (0.10 g, 0.38 mmol) was transformed using column chromatography (DCM/EtOAc [3:1]) into the title compound

as a white powder (87 mg, 44 %); $R_f$ 0.34 (DCM/EtOAc [3:1]); m.p. 217 – 225 °C; $\nu_{max}$ 3279 (N-H), 1672 (C=O), 1622 (C=O), 1537, 1493, 1385, 1270, 1202, 1154, 1090, 949, 833, 797, 704, 519 $cm^{-1}$; $\delta_H$ (300 MHz, DMSO-d6) 10.00 (1H, s, CON*H*NH), 9.00 (1H, s, Ar-*H*), 8.65 (1H, d, *J* 6, CON*H*CH), 8.09 (1H, s, CONHN*H*), 7.95 - 7.86 (2H, d, *J* 7, Ar-*H*), 7.75 (1H, d, *J* 9, Ar-*H*), 7.49 (1H, dd, *J* 9, 2, Ar-*H*), 7.47 - 7.38 (3H, m, Ar-*H*), 7.18 – 7.08 (2H, d, *J* 8, Ar-*H*), 6.87 – 6.78 (2H, d, *J* 8, Ar-*H*), 4.59 (1H, m, C*H*$CH_3$), 1.42 – 1.30 (3H, d, *J* 6, CHC*H*$_3$); $\delta_C$ (75 MHz, DMSO-$d_6$) 172.5 (*C*=ONHNH), 160.9 *(C*=ONHCH), 149.0 (Ar-O*C*$F_3$), 145.7 (*ipso*-Ar-*C)*, 143.4 (*ipso*-Ar-*C)*, 133.4 (*ipso*-Ar-*C)*, 129.0 (Ar-*C)*, 128.9 (Ar-*C)*, 128.8 (Ar-*C)*, 127.8 (Ar-*C)*, 125.0 (Ar-*C)*, 122.3 (Ar-*C)*, 120.3 (*ipso*-Ar-*C)*, 118.1 (Ar-*C),* 116.9 (*ipso*-Ar-*C)*, 113.2 (Ar-*C)*, 48.4 (*C*$HCH_3$), 17.7 (CH*C*$H_3$); $\delta_F$ (282 MHz, DMSO-d6) -57.2 (OC*F*$_3$); *m/z* ($ES^+$) 518 ([$^{35}$Cl]$MH^+$), 520 ([$^{37}$Cl]$MH^+$); HRMS ($ES^+$) Found [$^{35}$Cl]$MH^+$, 518.1196 ($C_{24}H_{20}{}^{35}ClF_3N_5O_3$ requires 518.1201).

**6-Chloro-N-(1-(2-phenyl)hydrazineyl)-4-methyl-1-oxopentan-2-yl)-2-phenylimidazo[1,2-*a*]pyridine-3-carboxamide 44Bw**

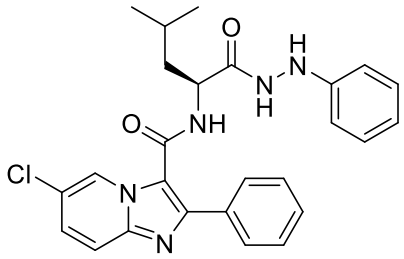


Using the standard procedure provided, *tert*-butyl (S)-(4-methyl-1-oxo-1-(2-phenylhydrazineyl)pentan-2-yl)carbamate **51As** (0.12 g, 0.37 mmol) was transformed using column chromatography (*n*-hexane/EtOAc [1:2]) into the title compound as a white powder (75 mg, 42 %); $R_f$ 0.3 (*n*-hexane/EtOAc [1:2]); m.p. 214 - 220 °C; $\nu_{max}$ 3270 (N-H), 1667 (C=O), 1617 (C=O), 1533, 1493, 1387, 1323, 1225, 1167, 1095, 843, 798, 778, 749, 690 $cm^{-1}$; $\delta_H$ (300 MHz, DMSO-$d_6$) 9.99 (1H, s, CON*H*NH), 8.93 (1H, s, Ar-*H*), 8.57 (1H, d, *J* 6, CON*H*CH), 7.88 – 7.83 (2H, m, Ar-*H*), 7.76 (1H, d, *J* 9, Ar-*H*), 7.49 (1H, dd, *J* 9, 2, Ar-*H*), 7.46 – 7.38 (3H, m, Ar-*H*), 7.18 – 7.09 (2H, t, *J* 7, Ar-*H*), 6.79 – 6.73 (2H, d, *J* 7, Ar-*H*), 6.70 (1H, t, *J* 7, Ar-*H*), 4.59 (1H, m, C*H*$CH_2CH(CH_3)_2$), 1.64 – 1.49 (3H, m, C*H*$_2$$CH(CH_3)_2$, $CH_2$C*H*$(CH_3)_2$), 0.99 – 0.93 (3H, d, *J* 6, $CH_2CH(CH_3)_2$), 0.92 – 0.88 (3H, d, *J* 6, $CH_2CH(CH_3)_2$); $\delta_C$ (75 MHz, DMSO-$d_6$) 172.2 (*C*=ONHNH), 161.1 *(C*=ONHCH), 149.6 (*ipso*-Ar-*C)*, 145.7 (*ipso*-Ar-*C)*, 143.3 (*ipso*-Ar-

*C)*, 133.5 (*ipso*-Ar-*C)*, 129.1 (Ar-*C)*, 128.9 (Ar-*C)*, 127.8 (Ar-*C)*, 124.7 (Ar-*C)*, 120.5 (*ipso*-Ar-*C)*, 118.9 (Ar-*C)*, 116.9 (*ipso*-Ar-*C),* 112.6 (Ar-*C),* 51.2 (C=ONH*C*H), 40.5 ($CH_2CH(CH_3)_2$), 24.7 ($CH_2CH(CH_3)_2$), 23.4 ($CH_2CH(CH_3)_2$), 21.6 ($CH_2CH(CH_3)_2$); ***m/z*** ($ES^+$) 476 ($[^{35}Cl]MH^+$), 478 ($[^{37}Cl]MH^+$); HRMS ($ES^+$) Found $[^{35}Cl]MH^+$, 476.1857 ($C_{26}H_{27}{}^{35}ClN_5O_2$ requires 476.1853).

**6-chloro-N-(1-(2-(3-chlorophenyl)hydrazineyl)-4-methyl-1-oxopentan-2-yl)-2-phenylimidazo[1,2-*a*]pyridine-3-carboxamide 44Bx**

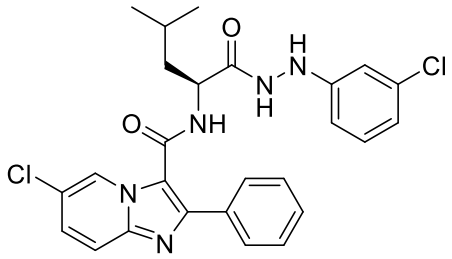

Using the standard procedure provided, *tert*-butyl (S)-(1-(2-(3-chlorophenyl)hydrazineyl)-4-methyl-1-oxopentan-2-yl)carbamate **51At** (0.17 g, 0.47 mmol) was transformed using column chromatography (DCM/EtOAc [3:1]) into the title compound as a white powder (84 mg, 34 %); $R_f$ 0.3 (DCM/EtOAc [3:1]); m.p. 223 - 228 °C; $\nu_{max}$ 3262 (N-H), 2960 (C=H), 1668 (C=O), 1618 (C=O), 1536, 1445, 1383, 1323, 1226, 1165, 1112, 799, 697 $cm^{-1}$; $\delta_H$ (300 MHz, DMSO-$d_6$) 10.07 (1H, s, CON*H*NH), 8.97 (1H, s, Ar-*H*), 8.47 (1H, d, *J* 6, CON*H*CH), 8.13 (1H, s, CONHN*H*), 7.88 – 7.81 (2H, m, Ar-*H*), 7.77 (1H, d, *J* 9, Ar-*H*), 7.50 (1H, dd, *J* 9, 2, Ar-*H*), 7.47 – 7.40 (3H, m, Ar-*H*), 7.14 (1H, t, *J* 7, Ar-*H*), 6.81 (1H, s, Ar-*H*), 6.74 – 6.64 (2H, dd, *J* 7, 2, Ar-*H*), 4.52 (1H, m, C*H*$CH_2CH(CH_3)_2$), 1.58 – 1.42 (3H, m, C*H*$_2$$CH(CH_3)_2$, $CH_2CH(CH_3)_2$), 0.97 – 0.92 (3H, d, *J* 6, $CH_2CH(CH_3)_2$), 0.90 – 0.84 (3H, d, *J* 6, $CH_2CH(CH_3)_2$); $\delta_C$ (75 MHz, DMSO-$d_6$) 172.4 (*C*ONHNH), 161.2 *(C*ONHCH), 151.2 (*ipso*-Ar-*C)*, 146.1 (*ipso*-Ar-*C)*, 143.4 (*ipso*-Ar-*C)*, 134.0 (Ar-*C)*, 133.6 (Ar-*C)*, 130.7 (Ar-*C)*, 129.0 (Ar-*C)*, 128.8 (Ar-*C)*, 127.9 (Ar-*C)*, 124.8 (Ar-*C)*, 120.5 (*ipso*-Ar-*C)*, 118.2 (Ar-*C)*, 116.7 (*ipso*-Ar-*C),* 111.9 (Ar-*C),* 111.2 (Ar-*C)*, 51.3 (CONH*C*H), 40.5 ($CH_2CH(CH_3)_2$), 24.7 ($CH_2CH(CH_3)_2$), 23.3 ($CH_2CH(CH_3)_2$), 21.7 ($CH_2CH(CH_3)_2$); ***m/z*** ($ES^+$) 510 ($[^{35,35}Cl]MH^+$), 512 ($[^{35,37}Cl]MH^+$), 514 ($[^{37,37}Cl]MH^+$); HRMS ($ES^+$) Found $[^{35,35}Cl]MH^+$, 510.1442 ($C_{26}H_{25}{}^{35,35}Cl_2N_5O_2$ requires 510.1464).

**6-chloro-N-(1-(2-(4-chlorophenyl)hydrazineyl)-4-methyl-1-oxopentan-2-yl)-2-phenylimidazo[1,2-*a*]pyridine-3-carboxamide 44By**

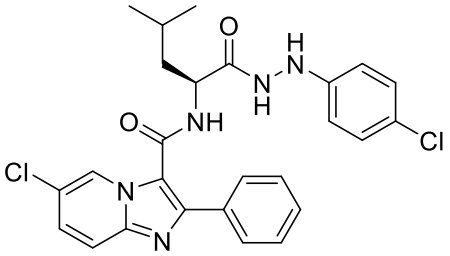

Using the standard procedure provided, *tert*-butyl (S)-(1-(2-(4-chlorophenyl)hydrazineyl)-4-methyl-1-oxopentan-2-yl)carbamate **51Au** (0.14 g, 0.41 mmol) was transformed using column chromatography (DCM/EtOAc [3:1]) into the title compound as a white powder (72 mg, 34 %); $R_f$ 0.30 (DCM/EtOAc [3:1]); m.p. 230 - 234 °C; $\nu_{max}$ 3256 (N-H), 2924, 1674 (C=O), 1616 (C=O), 1599, 1490, 1386, 1321, 1220, 1165, 1090, 951, 805, 703 $cm^{-1}$; $\delta_H$ (300 MHz, DMSO-$d_6$) 10.06 (1H, d, *J* 2, CON*H*NH), 8.91 (1H, s, Ar-*H*), 8.61 (1H, d, *J* 6, CON*H*CH), 8.02 (1H, d, *J* 2, CONHN*H*), 7.89 – 7.84 (2H, m, Ar-*H*), 7.77 (1H, d, *J* 9, Ar-*H*), 7.50 (1H, dd, *J* 9, 2, Ar-*H*), 7.44 – 7.39 (3H, m, Ar-*H*), 7.20 – 7.13 (2H, d, *J* 8, Ar-*H*), 6.81 – 6.73 (2H, d, *J* 8, Ar-*H*), 4.55 (1H, m, C*H*$CH_2CH(CH_3)_2$), 1.62 – 1.46 (3H, m, C*H*$_2$$CH(CH_3)_2$, $CH_2$C*H*$(CH_3)_2$), 0.99 – 0.93 (3H, d, *J* 6, $CH_2CH(CH_3)_2$), 0.92 – 0.85 (3H, d, *J* 6, $CH_2CH(CH_3)_2$); $\delta_C$ (75 MHz, DMSO-$d_6$) 172.4 (*C*=ONHNH), 161.3 (*C*=ONHCH), 148.7 (*ipso*-Ar-*C)*, 145.7 (*ipso*-Ar-*C)*, 143.2 (*ipso*-Ar-*C)*, 133.5 (*ipso*-Ar-*C)*, 128.9 (Ar-*C),* 127.8 (Ar-*C)*, 124.7 (Ar-*C)*, 122.2 (*ipso*-Ar-*C)*, 120.4 (*ipso*-Ar-*C)*, 118.2 (Ar-*C)*, 116.9 (*ipso*-Ar-*C),* 114.1 (Ar-*C)*, 51.2 (C=ONH*C*H), 40.5 (*C*$H_2CH(CH_3)_2$), 24.7 ($CH_2$*C*H$(CH_3)_2$), 23.4 ($CH_2CH($*C*$H_3)_2$), 21.6 ($CH_2CH($*C*$H_3)_2$); *m/z* ($ES^+$) 510 ([$^{35,35}$Cl]$MH^+$), 512 ([$^{35,37}$Cl]$MH^+$), 514 ([$^{37,37}$Cl]$MH^+$); HRMS ($ES^+$) Found [$^{35,35}$Cl]$MH^+$, 510.1465 ($C_{26}H_{26}{}^{35,35}Cl_2N_5O_2$ requires 510.1458).

**6-chloro-N-(1-(2-(3-bromophenyl)hydrazineyl)-4-methyl-1-oxopentan-2-yl)-2-phenylimidazo[1,2-*a*]pyridine-3-carboxamide 44Bz**

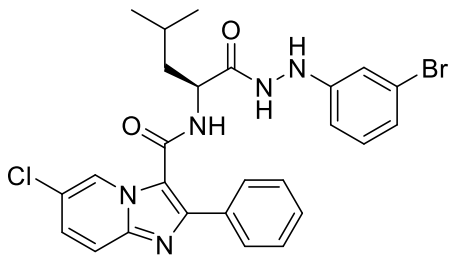

Using the standard procedure provided, *tert*-butyl (S)-(1-(2-(3-bromophenyl)hydrazineyl)-4-methyl-1-oxopentan-2-yl)carbamate **51Av** (0.18 g, 0.45 mmol) was transformed using column chromatography (DCM/EtOAc [3:1]) into the title compound as a white powder (82 mg, 33 %); $R_f$ 0.23 (DCM/EtOAc [3:1]); m.p. 228 - 232 °C; $\nu_{max}$ 3262 (N-H), 2960 (N-H), 1668 (C=O), 1618 (C=O), 1536, 1489, 1383, 1323, 1226, 1165, 1096, 1069, 844, 799, 697 $cm^{-1}$; $\delta_H$ (300 MHz, DMSO-$d_6$) 10.08 (1H, s, CON*H*NH), 8.97 (1H, s, Ar-*H*), 8.46 (1H, d, *J* 6, CON*H*CH), 8.31 (1H, s, CONHN*H*), 7.87 – 7.81 (2H, d, *J* 8, Ar-*H*), 7.77 (1H, d, *J* 9, Ar-*H*), 7.50 (1H, dd, *J* 9, 2, Ar-*H*), 7.46 – 7.37 (3H, m, Ar-*H*), 7.08 (1H, t, *J* 7, Ar-*H*), 6.96 (1H, s, Ar-*H*), 6.84 (1H, d, *J* 7, Ar-*H*), 6.74 (1H, d, *J* 7, Ar-*H*), 4.55 (1H, m, C*H*$CH_2CH(CH_3)_2$), 1.59 – 1.42 (3H, m, $CH_2CH(CH_3)_2$), 0.96 – 0.92 (3H, d, *J* 6, $CH_2CH(CH_3)_2$), 0.91 – 0.85 (3H, d, *J* 6, $CH_2CH(CH_3)_2$); $\delta_C$ (75 MHz, DMSO-$d_6$) 172.3 (*C*ONHNH), 161.1 *(C*ONHCH), 151.3 (*ipso*-Ar-*C)*, 145.9 (*ipso*-Ar-*C)*, 143.3 (*ipso*-Ar-*C)*, 133.4 (*ipso*-Ar-*C)*, 131.0 (Ar-*C)*, 128.9 (Ar-*C)*, 128.1 (Ar-*C)*, 124.8 (Ar-*C)*, 122.6 (*ipso*-Ar-*C)*, 121.2 (Ar-*C)*, 120.6 (*ipso*-Ar-*C)*, 118.1 (Ar-*C)*, 116.7 (*ipso*-Ar-*C),* 114.8 (Ar-*C)*, 111.6 (Ar-*C),* 51.3 (CONH*C*H), 24.7 ($CH_2CH(CH_3)_2$), 23.3 ($CH_2CH(CH_3)_2$), 21.7 ($CH_2CH(CH_3)_2$); ***m/z*** ($ES^+$) 554 ([$^{35}$Cl, $^{79}$Br]$MH^+$), 556 ([$^{35}$Cl, $^{81}$Br]$MH^+$), 556 ([$^{37}$Cl, $^{79}$Br]$MH^+$), 558 ([$^{37}$Cl, $^{81}$Br]$MH^+$); HRMS ($ES^+$) Found ([$^{35}$Cl, $^{79}$Br]$MH^+$), 554.0973 ($C_{26}H_{25}{}^{35}Cl{}^{79}BrN_5O_2$ requires 554.0958).

**6-Chloro-N-(1-(2-(4-bromophenyl)hydrazineyl)-4-methyl-1-oxopentan-2-yl)-2-phenylimidazo[1,2-*a*]pyridine-3-carboxamide 44Ca**

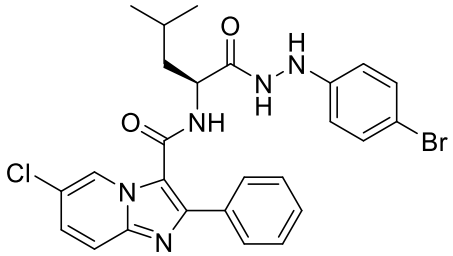


Using the standard procedure provided, *tert*-butyl (S)-(1-(2-(4-bromophenyl)hydrazineyl)-4-methyl-1-oxopentan-2-yl)carbamate **51Aw** (0.14 g, 0.37 mmol) was transformed using column chromatography (DCM/EtOAc [3:1]) into the title compound as a white powder (111 mg, 54 %); $R_f$ 0.3 (DCM/EtOAc [3:1]); m.p. 221 - 225 °C; $\nu_{max}$ 3263 (N-H), 2956 (N-H), 1668 (C=O), 1618 (C=O), 1536, 1489, 1382, 1344, 1226, 1166, 1112, 1059, 799, 697 $cm^{-1}$; $\delta_H$ (300 MHz, DMSO-$d_6$) 10.07 (1H, d, *J* 2, CON*H*NH), 8.90 (1H, s, Ar-*H*), 8.61 (1H, d, *J* 6, CON*H*CH), 8.04 (1H, d, *J* 2, CONHN*H*), 7.89 – 7.83 (2H, m, Ar-*H*), 7.76 (1H, d, *J*

9, Ar-*H*), 7.48 (1H, dd, *J* 9, 2, Ar-*H*), 7.46 – 7.40 (3H, m, Ar-*H*), 7.32 – 7.25 (2H, d, *J* 8, Ar-*H*), 6.69 – 6.67 (2H, d, *J* 8, Ar-*H*), 4.57 (1H, m, C*H*$CH_2CH(CH_3)_2$), 1.63 – 1.45 (3H, m, C*H*$_2CH(CH_3)_2$, $CH_2CH(CH_3)_2$), 0.99 – 0.92 (3H, d, *J* 6, $CH_2CH(CH_3)_2$), 0.90 – 0.83 (3H, d, *J* 6, $CH_2CH(CH_3)_2$); $\delta_C$ (75 MHz, DMSO-$d_6$) 172.3 (*C*ONHNH), 161.2 *(C*ONHCH), 149.1 (*ipso*-Ar-*C)*, 145.7 (*ipso*-Ar-*C)*, 143.3 (*ipso*-Ar-*C)*, 133.5 (*ipso*-Ar-*C)*, 131.7 (Ar-*C)*, 129.0 (Ar-*C)*, 128.8 (Ar-*C)*, 127.8 (Ar-*C)*, 124.7 (Ar-*C)*, 120.4 (*ipso*-Ar-*C)*, 118.2 (Ar-*C)*, 116.9 (*ipso*-Ar-*C),* 114.6 (Ar-*C),* 109.7 (*ipso*-Ar-*C)*, 51.2 (C=ONH*C*H), 40.5 (*C*$H_2CH(CH_3)_2$), 24.7 ($CH_2CH(CH_3)_2$), 23.4 ($CH_2CH(CH_3)_2$), 21.6 ($CH_2CH(CH_3)_2$); *m/z* ($ES^+$) 554 ([$^{35}$Cl, $^{79}$Br]$MH^+$), 556 ([$^{35}$Cl, $^{81}$Br]$MH^+$), 556 ([$^{37}$Cl, $^{79}$Br]$MH^+$), 558 ([$^{37}$Cl, $^{81}$Br]$MH^+$); HRMS ($ES^+$) Found ([$^{35}$Cl, $^{79}$Br]$MH^+$), 554.0973 ($C_{26}H_{25}{}^{35}Cl{}^{79}BrN_5O_2$ requires 554.0958).

**6-Chloro-N-(1-(2-(3-(trifluoromethyl)phenyl)hydrazineyl)-4-methyl-1-oxopentan-2-yl)-2-phenylimidazo[1,2-*a*]pyridine-3-carboxamide 44Cb**

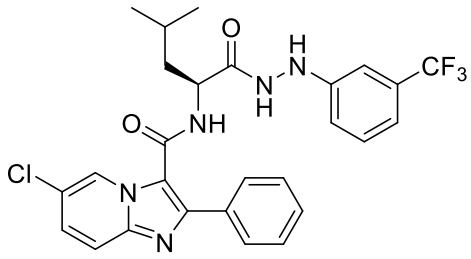

Using the standard procedure provided, *tert*-butyl (S)-(1-(2-(3-(trifluoromethyl)phenyl)hydrazineyl)-4-methyl-1-oxopentan-2-yl)carbamate **51Ax** (0.15 g, 0.38 mmol) was transformed using column chromatography (*n*-hexane /EtOAc [1:2]) into the title compound as a white powder (74 mg, 35 %); $R_f$ 0.25 (*n*-hexane/EtOAc [1:2]); m.p. 227 - 232 °C; $\nu_{max}$ 3260 (N-H), 2957 (N-H), 1673 (C=O), 1617 (C=O), 1536, 1493, 1383, 1338, 1225, 1164, 1112, 1068, 800, 697 $cm^{-1}$; $\delta_H$ (300 MHz, DMSO-d6) 10.16 (1H, bs, CON*H*NH), 8.90 (1H, s, Ar-*H*), 8.51 (1H, d, *J* 6, CON*H*CH), 8.30 (1H, s, CONHN*H*), 7.88 - 7.80 (2H, m, Ar-*H*), 7.76 (1H, d, *J* 9, Ar-*H*), 7.49 (1H, dd, *J* 9, 2, Ar-*H*), 7.45 – 7.40 (3H, m, Ar-*H*), 7.35 (1H, t, *J* 8, Ar-*H*), 7.08 – 6.93 (3H, m, Ar-*H*), 4.54 (1H, m, C*H*$CH_2CH(CH_3)_2$), 1.59 – 1.40 (3H, m, C*H*$_2CH(CH_3)_2$, $CH_2CH(CH_3)_2$), 0.99 – 0.91 (3H, d, *J* 6, $CH_2CH(CH_3)_2$), 0.90 – 0.81 (3H, d, *J* 6, $CH_2CH(CH_3)_2$); $\delta_C$ (75 MHz, DMSO-d6) 172.4 (*C*ONHNH), 161.2 *(C*ONHCH), 150.3 (*ipso*-Ar-*C)*, 146.0 (*ipso*-Ar-*C)*, 143.3 (*ipso*-Ar-*C)*, 133.5 (*ipso*-Ar-*C)*, 130.1 (Ar-*C)*, 128.8 (Ar-*C)*, 127.9 (Ar-*C)*, 124.7 (Ar-*C)*, 120.5 (*ipso*-Ar-*C)*, 118.2 (Ar-*C)*, 116.7 (*ipso*-Ar-*C*), 114.9 (Ar-*C),* 108.3 (Ar-*C)*, 51.3 (CONH*C*H), 40.5 (*C*$H_2CH(CH_3)_2$), 24.7 ($CH_2CH(CH_3)_2$), 23.3 ($CH_2CH(CH_3)_2$),

21.7 ($CH_2CH(CH_3)_2$); *m/z* ($ES^+$) 544 ($[^{35}Cl]MH^+$), 546 ($[^{37}Cl]MH^+$); HRMS ($ES^+$) Found $[^{35}Cl]MH^+$, 544.1704 ($C_{27}H_{26}{}^{35}ClF_3N_5O_2$ requires 544.1727).

**6-Chloro-N-(1-(2-(4-(trifluoromethyl)phenyl)hydrazineyl)-4-methyl-1-oxopentan-2-yl)-2-phenylimidazo[1,2-*a*]pyridine-3-carboxamide 44Cc**

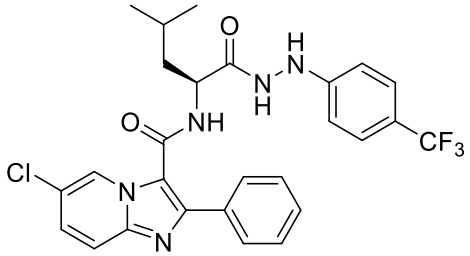

Using the standard procedure provided, *tert*-butyl (S)-(1-(2-(4-(trifluoromethyl)phenyl)hydrazineyl)-4-methyl-1-oxopentan-2-yl)carbamate **51Ay** (0.12 g, 0.32 mmol) was transformed using column chromatography (*n*-Hexane /EtOAc [1:1]) into the title compound as a white powder (60 mg, 34 %); $R_f$ 0.38 (*n*-Hexane/EtOAc [1:2]); m.p. 225 - 230 °C; $\nu_{max}$ 3260 (N-H), 1669 (C=O), 1617 (C=O), 1536, 1493, 1383, 1331, 1226, 1165, 1103, 1068, 829, 799, 763, 689 $cm^{-1}$; $\delta_H$ (300 MHz, DMSO-$d_6$) 10.18 (1H, s, CON*H*NH), 8.88 (1H, s, Ar-*H*), 8.66 (1H, d, *J* 6, CON*H*CH), 8.48 (1H, s, CONHN*H*), 7.90 – 7.83 (2H, d, *J* 8, Ar-*H*), 7.77 (1H, d, *J* 9, Ar-*H*), 7.50 (1H, dd, *J* 9, 2, Ar-*H*), 7.47 – 7.45 (2H, d, *J* 8, Ar-*H*), 7.43 – 7.40 (3H, m, Ar-*H*), 6.91 – 6.85 (2H, d, *J* 8, Ar-*H*), 4.57 (1H, m, C*H*$CH_2CH(CH_3)_2$), 1.66 – 1.47 (3H, m, $CHCH_2CH(CH_3)_2$, $CH_2CH(CH_3)_2$), 0.99 – 0.94 (3H, d, *J* 6, $CH_2CH(CH_3)_2$), 0.93 – 0.88 (3H, d, *J* 6, $CH_2CH(CH_3)_2$); $\delta_C$ (75 MHz, DMSO-$d_6$) 172.5 (*C*ONHNH), 161.3 *(C*ONHCH), 152.8 (*ipso*-Ar-*C)*, 145.8 (*ipso*-Ar-*C)*, 143.3 (*ipso*-Ar-*C)*, 133.5 (*ipso*-Ar-*C)*, 129.0 (Ar-*C)*, 128.7 (Ar-*C)*, 124.6 (Ar-*C)*, 120.4 (*ipso*-Ar-*C)*, 118.2 (Ar-*C)*, 116.9 (*ipso*-Ar-*C),* 111.9 (Ar-*C),* 51.3 (C=ONH*C*H), 40.5 ($CH_2CH(CH_3)_2$), 24.7 ($CH_2CH(CH_3)_2$), 23.4 ($CH_2CH(CH_3)_2$), 21.6 ($CH_2CH(CH_3)_2$); $\delta_F$ (282 MHz, DMSO-$d_6$) -61.3 ($CF_3$); *m/z* ($ES^+$) 544 ($[^{35}Cl]MH^+$), 546 ($[^{37}Cl]MH^+$); HRMS ($ES^+$) Found $[^{35}Cl]MH^+$, 544.1752 ($C_{27}H_{26}{}^{35}ClF_3N_5O_2$ requires 544.1727).

**6-chloro-N-(4-methyl-1-oxo-1-(2-(3-(trifluoromethoxy)phenyl)hydrazineyl)pentan-2-yl)-2-phenylimidazo[1,2-*a*]pyridine-3-carboxamide 44Cd**

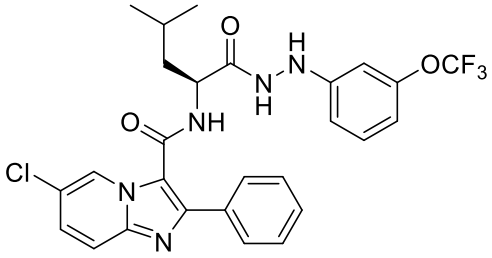

Using the standard procedure provided, *tert*-butyl (S)-(1-(2-(3-(trifluoromethoxy)phenyl)hydrazineyl)-4-methyl-1-oxopentan-2-yl)carbamate **51Az** (0.18 g, 0.44 mmol) was transformed using column chromatography (*n*-Hexane/EtOAc [1:1]) into the title compound as a white powder (97 mg, 39 %); $R_f$ 0.40 (*n*-Hexane/EtOAc [1:1]); m.p. 217 – 225 °C; $\nu_{max}$ 3659 (N-H), 3261 (N-H), 2980, 1671 (C=O), 1616 (C=O), 1537, 1493, 1383, 1263, 1154, 1079, 950, 844, 795, 688 $cm^{-1}$; $\delta_H$ (300 MHz, DMSO-d6) 10.14 (1H, s, CON*H*NH), 8.92 (1H, s, Ar-*H*), 8.52 (1H, d, *J* 6, CON*H*CH), 8.26 (1H, s, CONHN*H*), 7.90 - 7.82 (2H, m, Ar-*H*), 7.76 (1H, d, *J* 9, Ar-*H*), 7.50 (1H, dd, *J* 9, 2, Ar-*H*), 7.46 - 7.39 (3H, m, Ar-*H*), 7.24 (1H, t, *J* 8, Ar-*H*), 6.79 (1H, d, *J* 8, Ar-*H*), 6.71 (1H, s, Ar-*H*), 6.64 (1H, d, *J* 8, Ar-*H*), 4.57 (1H, m, C*H*$CH_2CH(CH_3)_2$), 1.65 – 1.43 (3H, m, C*H*$_2$$CH(CH_3)_2$, $CH_2$C*H*$(CH_3)_2$), 0.99 – 0.93 (3H, d, *J* 6, $CH_2CH(CH_3)_2$), 0.92 – 0.86 (3H, d, *J* 6, $CH_2CH(CH_3)_2$); $\delta_C$ (75 MHz, DMSO-$d_6$) 172.3 (*C*ONHNH), 161.3 *(C*ONHCH), 151.7 (*ipso*-Ar-*C)*, 149.9 (Ar-O*C*$F_3$*)*, 146.0 (*ipso*-Ar-*C)*, 143.4 (*ipso*-Ar-*C)*, 133.6 (*ipso*-Ar-*C)*, 130.6 (Ar-*C)*, 129.0 (Ar-*C)*, 128.8 (Ar-*C)*, 128.7 (Ar-*C)*, 127.8 (Ar-*C)*, 124.7 (Ar-*C)*, 120.5 (*ipso*-Ar-*C)*, 118.2 (Ar-*C),* 116.8 (*ipso*-Ar-*C)*, 111.4 (Ar-*C)*, 110.4 (Ar-*C)*, 104.4 (Ar-*C),* 51.2 (CONH*C*H), 24.6 ($CH_2$*C*$H(CH_3)_2$), 23.3 ($CH_2CH($*C*$H_3)_2$), 21.6 ($CH_2CH($*C*$H_3)_2$); $\delta_F$ (282 MHz, DMSO-$d_6$) -56.3 (OC*F*$_3$); ***m/z*** ($ES^+$) 560 ($[^{35}Cl]MH^+$), 562 ($[^{37}Cl]MH^+$); HRMS ($ES^+$) Found $[^{35}Cl]MH^+$, 560.1678 ($C_{27}H_{26}{}^{35}ClF_3N_5O_3$ requires 560.1676).

**6-chloro-N-(4-methyl-1-oxo-1-(2-(4-(trifluoromethoxy)phenyl)hydrazineyl)pentan-2-yl)-2-phenylimidazo[1,2-*a*]pyridine-3-carboxamide 44Ce**

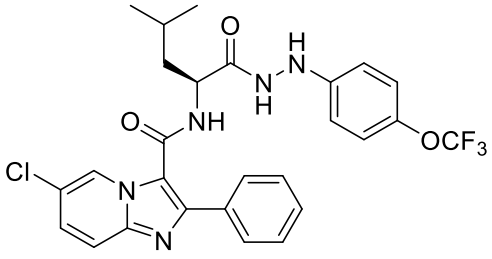

Using the standard procedure provided, *tert*-butyl (S)-(1-(2-(4-(trifluoromethoxy)phenyl)hydrazineyl)-4-methyl-1-oxopentan-2-yl)carbamate **51Ba** (0.14 g, 0.35 mmol) was transformed using column chromatography (*n*-Hexane/EtOAc [1:1]) into the title compound as a white powder (74 mg, 38 %); $R_f$ 0.35 (*n*-Hexane/EtOAc [1:1]); m.p. 220 – 225 °C; $\nu_{max}$ 3263 (N-H), 2980, 1668 (C=O), 1618 (C=O), 1537, 1507, 1493, 1383, 1257, 1225, 1155, 1078, 950, 830, 794, 687 $cm^{-1}$; $\delta_H$ (300 MHz, DMSO-d6) 10.08 (1H, s, CON*H*NH), 8.90 (1H, s, Ar-*H*), 8.61 (1H, d, *J* 6, CON*H*CH), 8.10 (1H, s, CONHN*H*), 7.90 - 7.82 (2H, m, Ar-*H*), 7.75 (1H, d, *J* 9, Ar-*H*), 7.49 (1H, dd, *J* 9, 2, Ar-*H*), 7.46 - 7.37 (3H, m, Ar-*H*), 7.20 – 7.10 (2H, d, *J* 9, Ar-*H*), 6.87 – 6.77 (2H, d, *J* 9, Ar-*H*), 4.57 (1H, m, C*H*$CH_2CH(CH_3)_2$), 1.65 – 1.45 (3H, m, C*H*$_2CH(CH_3)_2$, $CH_2CH(CH_3)_2$), 1.01 – 0.93 (3H, d, *J* 6, $CH_2CH(CH_3)_2$), 0.93 – 0.83 (3H, d, *J* 6, $CH_2CH(CH_3)_2$); $\delta_C$ (75 MHz, DMSO-$d_6$) 172.2 (*C*ONHNH), 161.3 *(C*ONHCH), 148.9 (Ar-O*C*$F_3$*)*, 145.8 (*ipso*-Ar-*C)*, 143.3 (*ipso*-Ar-*C)*, 133.5 (*ipso*-Ar-*C)*, 129.0 (Ar-*C)*, 128.9 (Ar-*C)*, 128.7 (Ar-*C)*, 127.8 (Ar-*C)*, 124.7 (Ar-*C)*, 122.3 (Ar-*C)*, 120.5 (*ipso*-Ar-*C)*, 118.2 (Ar-*C),* 116.9 (*ipso*-Ar-*C)*, 113.2 (Ar-*C)*, 51.2 (CONH*C*H), 24.7 ($CH_2CH(CH_3)_2$), 23.3 ($CH_2CH(CH_3)_2$), 21.5 ($CH_2CH(CH_3)_2$); $\delta_F$ (282 MHz, DMSO-d6) -57.2 (OC*F*$_3$); *m/z* ($ES^+$) 560 ([$^{35}$Cl]$MH^+$), 562 ([$^{37}$Cl]$MH^+$); HRMS ($ES^+$) Found [$^{35}$Cl]$MH^+$, 560.1678 ($C_{27}H_{26}{}^{35}ClF_3N_5O_3$ requires 560.1676).

**6-chloro-N-(4-(methylthio)-1-oxo-1-(2-phenylhydrazineyl)butan-2-yl)-2-phenylimidazo[1,2-*a*]pyridine-3-carboxamide 44Cf**

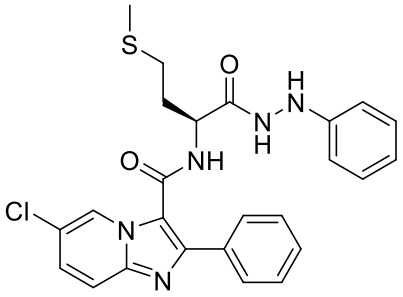

Using the standard procedure provided, *tert*-butyl (S)-(4-(methylthio)-1-oxo-1-(2-phenylhydrazineyl)butan-2-yl)carbamate **51Bb** (0.12 g, 0.35 mmol) was transformed using column chromatography (DCM /EtOAc [3:1]) into the title compound as a white powder (53 mg, 30 %); $R_f$ 0.2 (DCM/EtOAc [3:1]); m.p. 213 – 217 °C; $\nu_{max}$ 3264 (N-H), 2971, 1670 (C=O), 1619 (C=O), 1533, 1492, 1386, 1345, 1322, 1228, 1167, 1116, 950, 845, 800, 764, 697 $cm^{-1}$; $\delta_H$ (300 MHz, DMSO-$d_6$) 10.00 (1H, s, CON*H*NH), 8.95 (1H, s, Ar-*H*), 8.68 (1H, d, *J* 6, CON*H*CH), 7.92 – 7.84 (2H, m, Ar-*H*), 7.81 (1H, d, *J* 2,

CONHN*H*), 7.78 (1H, dd, *J* 9, 1, Ar-*H*), 7.50 (1H, dd, *J* 9, 2, Ar-*H*), 7.45 – 7.36 (3H, m, Ar-*H*), 7.18 – 7.08 (2H, t, *J* 7, Ar-*H*), 6.82 – 6.75 (2H, d, *J* 7, Ar-*H*), 6.70 (1H, t, *J* 7, Ar-*H*), 4.66 (1H, m, CONHC*H*), 2.48 – 2.38 (2H, m, C*H*$_2$CH$_2$SCH$_3$), 2.10 – 1.89 (5H, m, C*H*$_2$C*H*$_2$S*CH*$_3$); $\delta_C$ (75 MHz, DMSO-d$_6$) 171.4 (*C*ONHNH), 161.2 *(C*ONHCH), 149.5 145.6 (*ipso*-Ar-*C)*, 143.3 (*ipso*-Ar-*C)*, 133.5 (*ipso*-Ar-*C)*, 129.0 (Ar-*C)*, 128.6 (Ar-*C)*, 127.7 (Ar-*C)*, 126.4 (Ar-*C)*, 124.7 (Ar-*C)*, 120.4 (*ipso*-Ar-*C)*, 118.8 (Ar-*C)*, 118.1 (Ar-*C)*, 116.9 (*ipso*-Ar-*C),* 112.6 (Ar-*C),* 52.0 (CONH*C*H), 30.9 (CH$_2$*C*H$_2$SCH$_3$), 29.9 (*C*H$_2$CH$_2$SCH$_3$), 14.8 (CH$_2$CH$_2$S*C*H$_3$); ***m/z*** (ES$^+$) 494 ([$^{35}$Cl]MH$^+$), 496 ([$^{37}$Cl]MH$^+$); HRMS (ES$^+$) Found [$^{35}$Cl]MH$^+$, 494.1414 ($C_{25}H_{24}{}^{35}ClN_5O_2S$ requires 494.1418).

**6-chloro-N-(1-(2-(3-chlorophenyl)hydrazineyl)-4-(methylthio)-1-oxobutan-2-yl)-2-phenylimidazo[1,2-*a*]pyridine-3-carboxamide 44Cg**

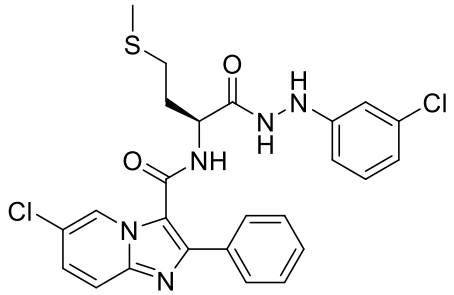

Using the standard procedure provided, *tert*-butyl (S)-(1-(2-(3-chlorophenyl)hydrazineyl)-4-(methylthio)-1-oxobutan-2-yl)carbamate **51Bc** (0.13 g, 0.34 mmol) was transformed using column chromatography (DCM /EtOAc [3:1]) into the title compound as a white powder (59 mg, 32 %); $R_f$ 0.23 (DCM/EtOAc [3:1]); m.p. 225 – 232 °C; $\nu_{max}$ 3255 (N-H), 2922, 1674 (C=O), 1616 (C=O), 1599, 1533, 1490, 1389, 1321, 1227, 1157, 1077, 1035, 897, 843, 805, 761, 705 cm$^{-1}$; $\delta_H$ (300 MHz, DMSO-d$_6$) 10.07 (1H, s, CON*H*NH), 8.96 (1H, s, Ar-*H*), 8.65 (1H, d, *J* 6, CON*H*CH), 7.88 – 7.82 (2H, d, *J* 7, Ar-*H*), 7.78 (1H, d, *J* 9, 1, Ar-*H*), 7.51 (1H, dd, *J* 9, 2, Ar-*H*), 7.46 – 7.40 (3H, m, Ar-*H*), 7.14 (1H, t, *J* 7, Ar-*H*), 6.82 (1H, s, Ar-*H*), 6.74 – 6.68 (2H, m, Ar-*H*), 4.61 (1H, m, CONHC*H*), 2.47 – 2.40 (2H, m, C*H*$_2$CH$_2$SCH$_3$), 2.00 – 1.88 (5H, m, C*H*$_2$C*H*$_2$S*CH*$_3$); $\delta_C$ (75 MHz, DMSO-d$_6$) 171.7 (*C*ONHNH), 161.3 *(C*ONHCH), 151.2 (*ipso*-Ar-*C)*, 146.1 (*ipso*-Ar-*C)*, 143.1 (*ipso*-Ar-*C)*, 133.4 (*ipso*-Ar-*C)*, 130.6 (Ar-*C)*, 128.9 (Ar-*C)*, 127.9 (Ar-*C)*, 124.9 (Ar-*C)*, 120.5 (*ipso*-Ar-*C)*, 118.3 (Ar-*C)*, 116.7 (*ipso*-Ar-*C),* 111.9 (Ar-*C)*, 111.3 (Ar-*C),* 52.1 (CONH*C*H), 30.8 (CH$_2$*C*H$_2$SCH$_3$), 30.0 (*C*H$_2$CH$_2$SCH$_3$), 14.8 (CH$_2$CH$_2$S*C*H$_3$); ***m/z*** (ES$^+$) 528 ([$^{35,35}$Cl]MH$^+$), 530 ([$^{35,37}$Cl]MH$^+$),

532 ([$^{37,37}$Cl]MH$^+$); HRMS (ES$^+$) Found [$^{35}$Cl]MH$^+$, 528.1032 ($C_{25}H_{24}{}^{35,35}Cl_2N_5O_2S$ requires 528.1028).

**6-chloro-N-(1-(2-(4-chlorophenyl)hydrazineyl)-4-(methylthio)-1-oxobutan-2-yl)-2-phenylimidazo[1,2-*a*]pyridine-3-carboxamide 44Ch**

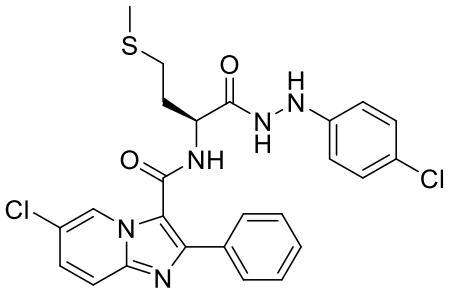

Using the standard procedure provided, *tert*-butyl (S)-(1-(2-(4-chlorophenyl)hydrazineyl)-4-(methylthio)-1-oxobutan-2-yl)carbamate **51Bd** (0.15 g, 0.40 mmol) was transformed using column chromatography (DCM /EtOAc [3:1]) into the title compound as a white powder (70 mg, 33 %); $R_f$ 0.27 (DCM/EtOAc [3:1]); m.p. 230 – 234 °C; $\nu_{max}$ 3267 (N-H), 1669 (C=O), 1618 (C=O), 1533, 1491, 1385, 1322, 1229, 1166, 1080, 797, 763, 699 cm$^{-1}$; $\delta_H$ (300 MHz, DMSO-d$_6$) 10.06 (1H, s, CON*H*NH), 8.90 (1H, s, Ar-*H*), 8.72 (1H, d, *J* 6, CON*H*CH), 8.02 (1H, s, CONHN*H*), 7.91 – 7.82 (2H, d, *J* 7, Ar-*H*), 7.76 (1H, d, *J* 9, Ar-*H*), 7.49 (1H, dd, *J* 9, 2, Ar-*H*), 7.48 – 7.40 (3H, m, Ar-*H*), 7.23 – 7.14 (2H, d, *J* 8, Ar-*H*), 6.86 – 6.74 (2H, d, *J* 8, Ar-*H*), 4.63 (1H, m, CONHC*H*), 2.48 – 2.35 (1H, m, C*H*$_2$CH$_2$SCH$_3$), 2.10 – 1.87 (5H, m, C*H*$_2$C*H*$_2$S*CH*$_3$); $\delta_C$ (75 MHz, DMSO-d$_6$) 171.7 (*C*ONHNH), 161.4 *(C*ONHCH), 148.7 (*ipso*-Ar-*C)*, 145.9 (*ipso*-Ar-*C)*, 143.4 (*ipso*-Ar-*C)*, 133.5 (Ar-*C)*, 128.9 (Ar-*C)*, 127.8 (Ar-*C)*, 124.8 (Ar-*C)*, 122.3 (*ipso*-Ar-*C)*, 120.4 (*ipso*-Ar-*C)*, 118.2 (Ar-*C)*, 116.8 (*ipso*-Ar-*C),* 114.1 (Ar-*C)*, 52.0 (CONH*C*H), 30.9 (CH$_2$*C*H$_2$SCH$_3$), 30.1 (*C*H$_2$CH$_2$SCH$_3$), 14.9 (CH$_2$CH$_2$S*C*H$_3$); *m/z* (ES$^+$) 528 ([$^{35,35}$Cl]MH$^+$), 530 ([$^{35,37}$Cl]MH$^+$), 532 ([$^{37,37}$Cl]MH$^+$); HRMS (ES$^+$) Found [$^{35}$Cl]MH$^+$, 528.1023 ($C_{25}H_{24}{}^{35,35}Cl_2N_5O_2S$ requires 528.1028).

**6-chloro-N-(1-(2-(3-bromophenyl)hydrazineyl)-4-(methylthio)-1-oxobutan-2-yl)-2-phenylimidazo[1,2-*a*]pyridine-3-carboxamide 44Ci**

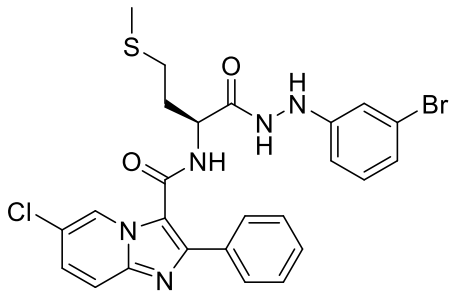

Using the standard procedure provided, *tert*-butyl (S)-(1-(2-(3-bromophenyl)hydrazineyl)-4-(methylthio)-1-oxobutan-2-yl)carbamate **51Be** (0.15 g, 0.36 mmol) was transformed using column chromatography (DCM /EtOAc [3:1]) into the title compound as a white powder (76 mg, 36 %); $R_f$ 0.2 (DCM/EtOAc [3:1]); m.p. 232 – 235 °C; $\nu_{max}$ 3257 (N-H), 1673 (C=O), 1616 (C=O), 1534, 1491, 1388, 1322, 1228, 1164, 1068, 1099, 843, 797, 760, 703 $cm^{-1}$; $\delta_H$ (300 MHz, DMSO-$d_6$) 10.07 (1H, s, CON*H*NH), 8.96 (1H, s, Ar-*H*), 8.62 (1H, d, *J* 6, CON*H*CH), 8.13 (1H, s, CONHN*H*), 7.91 – 7.84 (2H, d, *J* 8, Ar-*H*), 7.78 (1H, d, *J* 9, Ar-*H*), 7.51 (1H, dd, *J* 9, 2, Ar-*H*), 7.46 – 7.34 (3H, m, Ar-*H*), 7.09 (1H, t, *J* 7, Ar-*H*), 6.97 (1H, s, Ar-*H*), 6.86 (1H, d, *J* 7, Ar-*H*), 6.76 (1H, d, *J* 7, Ar-*H*), 4.61 (1H, m, CONHC*H*), 2.49 – 2.40 (2H, m, C*H*$_2$CH$_2$SCH$_3$), 2.08 – 1.88 (5H, m, C*H*$_2$C*H*$_2$S*CH*$_3$); $\delta_C$ (75 MHz, DMSO-$d_6$) 171.7 (*C*ONHNH), 161.4 *(C*ONHCH), 151.3 (*ipso*-Ar-*C)*, 146.2 (*ipso*-Ar-*C)*, 143.4 (*ipso*-Ar-*C)*, 133.6 (*ipso*-Ar-*C)*, 131.0 (Ar-*C)*, 128.9 (Ar-*C)*, 128.0 (Ar-*C)*, 124.9 (Ar-*C)*, 122.6 (*ipso*-Ar-*C)*, 121.2 (Ar-*C)*, 120.5 (*ipso*-Ar-*C)*, 118.2 (Ar-*C)*, 116.7 (*ipso*-Ar-*C),* 114.8 (Ar-*C)*, 111.6 (Ar-*C),* 52.1 (C=ONH*C*H), 31.9 (CH$_2$*C*H$_2$SCH$_3$), 30.0 (*C*H$_2$CH$_2$SCH$_3$), 14.9 (CH$_2$CH$_2$S*C*H$_3$); ***m/z*** (ES$^+$) 572 ([$^{35}$Cl, $^{79}$Br]MH$^+$), 574 ([$^{35}$Cl, $^{81}$Br]MH$^+$), 574 ([$^{37}$Cl, $^{79}$Br]MH$^+$), 576 ([$^{37}$Cl, $^{81}$Br]MH$^+$); HRMS (ES$^+$) Found ([$^{35}$Cl, $^{79}$Br]MH$^+$), 572.0522 ($C_{25}H_{24}{}^{35}Cl{}^{79}BrN_5O_2S$ requires 572.0522).

**6-chloro-N-(1-(2-(4-bromophenyl)hydrazineyl)-4-(methylthio)-1-oxobutan-2-yl)-2-phenylimidazo[1,2-*a*]pyridine-3-carboxamide 44Cj**

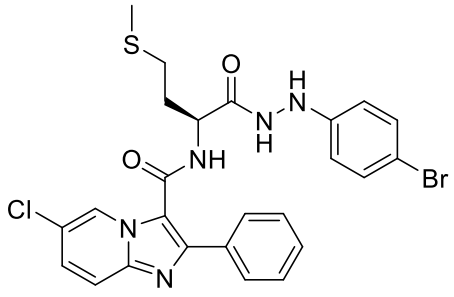

Using the standard procedure provided, *tert*-butyl (S)-(1-(2-(4-bromophenyl)hydrazineyl)-4-(methylthio)-1-oxobutan-2-yl)carbamate **51Bf** (0.13 g, 0.32 mmol) was transformed using column chromatography (DCM /EtOAc [3:1]) into the title compound as a white powder (64 mg, 35 %); $R_f$ 0.25 (DCM/EtOAc [3:1]); m.p. 235 – 238 °C; $\nu_{max}$ 3080 (N-H), 1677 (C=O), 1607 (C=O), 1478, 1449, 1366, 1301, 1271, 1206, 1104, 989, 843, 752, 700 $cm^{-1}$; $\delta_H$ (300 MHz, DMSO-$d_6$) 10.06 (1H, d, *J* 2, CON*H*NH), 8.91 (1H, s, Ar-*H*), 8.72 (1H, d, *J* 6, CON*H*CH), 8.04 (1H, d, *J* 2, CONHN*H*), 7.91 – 7.84 (2H, m, Ar-*H*), 7.75 (1H, d, *J* 9, Ar-*H*), 7.50 (1H, dd, *J* 9, 2, Ar-*H*), 7.45 – 7.38 (3H, m, Ar-*H*), 7.33 – 7.27 (2H, d, *J* 8, Ar-*H*), 6.80 – 6.69 (2H, d, *J* 8, Ar-*H*), 4.63 (1H, m, CONHC*H*), 2.49 – 2.38 (2H, m, C$H_2$$CH_2$$SCH_3$), 2.08 – 1.88 (5H, m, C$H_2$C$H_2$S$CH_3$); $\delta_C$ (75 MHz, DMSO-$d_6$) 171.6 (*C*=ONHNH), 161.4 *(C*=ONHCH), 149.0 (*ipso*-Ar-*C)*, 145.9 (*ipso*-Ar-*C)*, 143.3 (*ipso*-Ar-*C)*, 133.5 (*ipso*-Ar-*C)*, 131.7 (Ar-*C)*, 128.9 (Ar-*C)*, 128.8 (Ar-*C)*, 127.9 (Ar-*C)*, 124.8 (Ar-*C)*, 120.4 (*ipso*-Ar-*C)*, 118.2 (Ar-*C)*, 116.8 (*ipso*-Ar-*C),* 114.6 (Ar-*C)*, 109.7 (*ipso*-Ar-*C),* 52.0 (CONH*C*H), 30.9 ($CH_2$*C*$H_2SCH_3$), 30.1 (*C*$H_2CH_2SCH_3$), 14.9 ($CH_2CH_2$S*C*$H_3$); *m/z* ($ES^+$) 572 ([$^{35}$Cl, $^{79}$Br]$MH^+$), 574 ([$^{35}$Cl, $^{81}$Br]$MH^+$), 574 ([$^{37}$Cl, $^{79}$Br]$MH^+$), 576 ([$^{37}$Cl, $^{81}$Br]$MH^+$); HRMS ($ES^+$) Found ([$^{35}$Cl, $^{79}$Br]$MH^+$), 572.0502 ($C_{25}H_{24}{}^{35}Cl^{79}BrN_5O_2S$ requires 572.0522).

**6-chloro-N-(4-(methylthio)-1-oxo-1-(2-(3-(trifluoromethyl)phenyl)hydrazineyl) butan-2-yl)-2-phenylimidazo[1,2-*a*]pyridine-3-carboxamide 44Ck**

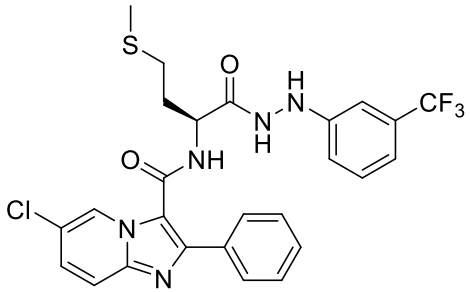


Using the standard procedure provided, *tert*-butyl (S)-(1-(2-(3-(trifluoromethyl)phenyl)hydrazineyl)-4-(methylthio)-1-oxobutan-2-yl)carbamate **51Bg** (0.13 g, 0.31 mmol) was transformed using column chromatography (DCM /EtOAc [1:1]) into the title compound as a white powder (91 mg, 51 %); $R_f$ 0.3 (DCM/EtOAc [1:1]); m.p. 228 – 232 °C; $\nu_{max}$ 3264 (N-H), 3051 (N-H), 1671 (C=O), 1619 (C=O), 1532, 1492, 1387, 1344, 1327, 1227, 1166, 1116, 1069, 996, 859, 845, 800, 764, 696 $cm^{-1}$; $\delta_H$ (300 MHz, DMSO-$d_6$) 10.16 (1H, bs, CON*H*NH), 8.91 (1H, s, Ar-*H*), 8.64 (1H, d, *J* 6, CON*H*CH), 8.31 (1H, s, CONHN*H*), 7.91 – 7.83 (2H, m, Ar-*H*), 7.77 (1H, d, *J* 9, 1,

Ar-*H*), 7.50 (1H, dd, *J* 9, 2, Ar-*H*), 7.47 – 7.40 (3H, m, Ar-*H*), 7.36 (1H, d, *J* 7, Ar-*H*), 7.08 (1H, s, Ar-*H*), 7.07 – 7.00 (2H, m, Ar-*H*), 4.63 (1H, m, CONHC*H*), 2.48 – 2.38 (2H, m, C*H*$_2$CH$_2$SCH$_3$), 2.10 – 1.86 (5H, m, CH$_2$C*H*$_2$S*CH*$_3$); $\delta_C$ (75 MHz, DMSO-d$_6$) 171.7 (*C*ONHNH), 161.4 *(C*ONHCH), 150.3 (*ipso*-Ar-*C)*, 146.2 (*ipso*-Ar-*C)*, 143.4 (*ipso*-Ar-*C)*, 133.6 (*ipso*-Ar-*C)*, 130.2 (Ar-*C)*, 128.9 (Ar-*C)*, 127.9 (Ar-*C)*, 124.8 (Ar-*C)*, 120.5 (*ipso*-Ar-*C)*, 118.2 (Ar-*C)*, 116.8 (*ipso*-Ar-*C),* 116.1 (Ar-*C)*, 108.4 (Ar-*C),* 52.1 (CONH*C*H), 31.1 (CH$_2$*C*H$_2$SCH$_3$), 30.0 (*C*H$_2$CH$_2$SCH$_3$), 14.8 (CH$_2$CH$_2$S*C*H$_3$); $\delta_F$ (282 MHz, DMSO-d$_6$) -61.3 (C*F*$_3$); *m/z* (ES$^+$) 562 ([$^{35}$Cl]MH$^+$), 564 ([$^{37}$Cl]MH$^+$); HRMS (ES$^+$) Found [$^{35}$Cl]MH$^+$, 562.1300 ($C_{26}H_{23}{}^{35}ClF_3N_5O_2S$ requires 562.1292).

**6-chloro-N-(4-(methylthio)-1-oxo-1-(2-(4-(trifluoromethyl)phenyl)hydrazineyl) butan-2-yl)-2-phenylimidazo[1,2-*a*]pyridine-3-carboxamide 44Cl**

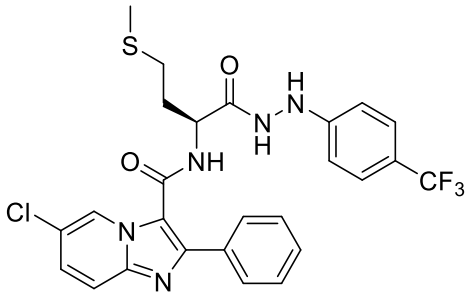


Using the standard procedure provided, *tert*-butyl (S)-(1-(2-(4-(trifluoromethyl)phenyl)hydrazineyl)-4-(methylthio)-1-oxobutan-2-yl)carbamate **51Bh** (0.13 g, 0.31 mmol) was transformed using column chromatography (DCM /EtOAc [3:1]) into the title compound as a white powder (64 mg, 36 %); $R_f$ 0.25 (DCM/EtOAc [3:1]); m.p. 236 – 240 °C; $\nu_{max}$ 3262 (N-H), 2917, 1672 (C=O), 1617 (C=O), 1537, 1492, 1329, 1281, 1230, 1162, 1098, 1067, 950, 829, 761, 686 cm$^{-1}$; $\delta_H$ (300 MHz, DMSO-d$_6$) 10.17 (1H, bs, CON*H*NH), 8.90 (1H, s, Ar-*H*), 8.76 (1H, d, *J* 6, CON*H*CH), 8.48 (1H, s, CONHN*H*), 7.92 – 7.84 (2H, m, Ar-*H*), 7.77 (1H, d, *J* 9, Ar-*H*), 7.50 (1H, dd, *J* 9, 2, Ar-*H*), 7.48 – 7.35 (5H, m, Ar-*H*), 7.33 – 7.27 (2H, d, *J* 8, Ar-*H*), 6.93 – 6.84 (2H, d, *J* 8, Ar-*H*), 4.64 (1H, m, CONHC*H*), 2.49 – 2.40 (2H, m, C*H*$_2$CH$_2$SCH$_3$), 2.07 – 1.90 (5H, m, CH$_2$C*H*$_2$S*CH*$_3$); $\delta_C$ (75 MHz, DMSO-d$_6$) 171.7 (*C*ONHNH), 161.5 *(C*ONHCH), 152.8 (*ipso*-Ar-*C*), 145.8 (*ipso*-Ar-*C)*, 143.3 (*ipso*-Ar-*C)*, 133.5 (*ipso*-Ar-*C)*, 128.6 (Ar-*C)*, 127.7 (Ar-*C)*, 126.3 (Ar-*C)*, 124.6 (Ar-*C)*, 120.2 (*ipso*-Ar-*C)*, 118.1 (Ar-*C)*, 116.7 (*ipso*-Ar-*C),* 111.9 (Ar-*C),* 52.0 (CONH*C*H), 30.6 (CH$_2$*C*H$_2$SCH$_3$), 29.9 (*C*H$_2$CH$_2$SCH$_3$), 14.8 (CH$_2$CH$_2$S*C*H$_3$); $\delta_F$ (282 MHz, DMSO-d$_6$) -56.4 (C*F*$_3$); *m/z* (ES$^+$)

562 ([$^{35}$Cl]MH$^+$), 564 ([$^{37}$Cl]MH$^+$); HRMS (ES$^+$) Found [$^{35}$Cl]MH$^+$, 562.1270 ($C_{26}H_{24}{}^{35}ClF_3N_5O_2S$ requires 562.1292).

**6-chloro-N-(4-(methylthio)-1-oxo-1-(2-(3-(trifluoromethoxy)phenyl)hydrazineyl)butan-2-yl)-2-phenylimidazo[1,2-*a*]pyridine-3-carboxamide 44Cm**

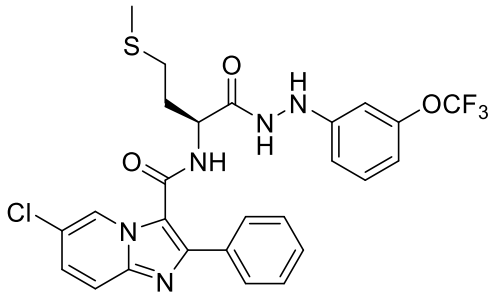

Using the standard procedure provided, *tert*-butyl (S)-(1-(2-(3-(trifluoromethoxy)phenyl)hydrazineyl)-4-(methylthio)-1-oxobutan-2-yl)carbamate **51Bi** (0.07 g, 0.26 mmol) was transformed using column chromatography (*n*-Hexane/EtOAc [1:1]) into the title compound as a white powder (48 mg, 32 %); $R_f$ 0.28 (*n*-Hexane/EtOAc [1:1]); m.p. 225 – 229 °C; $\nu_{max}$ 3658 (N-H), 3259 (N-H), 2980 (C-H), 1670 (C=O), 1620 (C=O), 1493, 1387, 1262, 1152, 1080, 952, 796, 764 cm$^{-1}$; $\delta_H$ (300 MHz, DMSO-d6) 10.10 (1H, s, CON*H*NH), 8.90 (1H, s, Ar-*H*), 8.66 (1H, d, *J* 6, CON*H*CH), 8.25 (1H, s, CONHN*H*), 7.91 - 7.82 (2H, m, Ar-*H*), 7.77 (1H, d, *J* 9, Ar-*H*), 7.50 (1H, dd, *J* 9, 2, Ar-*H*), 7.47 - 7.37 (3H, m, Ar-*H*), 7.23 (1H, t, *J* 7, Ar-*H*), 6.77 (1H, d, *J* 7, Ar-*H*), 6.70 (1H, s, Ar-*H*), 6.64 (1H, d, *J* 7, Ar-*H*), 4.62 (1H, m, CONHC*H*), 2.48 – 2.37 (2H, m, C*H*$_2$CH$_2$SCH$_3$), 2.07 – 1.84 (5H, m, C*H*$_2$C*H*$_2$S*CH*$_3$); $\delta_C$ (75 MHz, DMSO-d$_6$) 171.7 (*C*ONHNH), 161.4 *(C*ONHCH), 151.6 (*ipso*-Ar-*C)*, 149.9 (Ar-O*C*F$_3$*)*, 146.1 (*ipso*-Ar-*C)*, 143.4 (*ipso*-Ar-*C)*, 133.5 (*ipso*-Ar-*C)*, 130.7 (Ar-*C)*, 128.9 (Ar-*C)*, 127.9 (Ar-*C)*, 124.8 (Ar-*C)*, 120.4 (*ipso*-Ar-*C)*, 118.2 (Ar-*C),* 116.7 (*ipso*-Ar-*C)*, 111.4 (Ar-*C)*, 110.5 (Ar-*C)*, 104.4 (Ar-*C),* 52.1 (CONHC*H*), 31.1 (CH$_2$CH(*C*H$_3$)$_2$), 30.0 (CH$_2$*C*H(CH$_3$)$_2$), 14.8 (CH$_2$CH(*C*H$_3$)$_2$); $\delta_F$ (282 MHz, DMSO-d6) -56.4 (OC*F*$_3$); ***m/z*** (ES$^+$) 578 ([$^{35}$Cl]MH$^+$), 580 ([$^{37}$Cl]MH$^+$); HRMS (ES$^+$) Found [$^{35}$Cl]MH$^+$, 578.1246 ($C_{26}H_{24}{}^{35}ClF_3N_5O_3S$ requires 578.1240).

**6-chloro-N-(4-(methylthio)-1-oxo-1-(2-(4-(trifluoromethoxy)phenyl)hydrazineyl)butan-2-yl)-2-phenylimidazo[1,2-*a*]pyridine-3-carboxamide 44Cn**

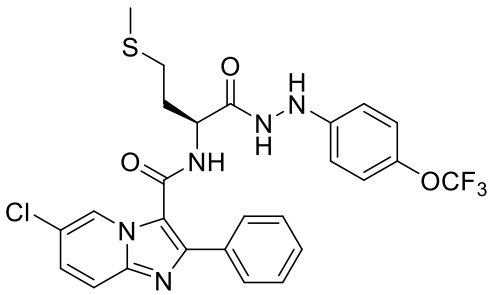

Using the standard procedure provided, *tert*-butyl (S)-(1-(2-(4-(trifluoromethoxy)phenyl)hydrazineyl)-4-(methylthio)-1-oxobutan-2-yl)carbamate **51Bj** (0.16 g, 0.37 mmol) was transformed using column chromatography (DCM/EtOAc [3:1]) into the title compound as a white powder (80 mg, 37 %); $R_f$ 0.23 (DCM/EtOAc [3:1]); m.p. 232 – 237 °C; $\nu_{max}$ 3253 (N-H), 2980, 1670 (C=O), 1614 (C=O), 1506, 1392, 1259, 1221, 1199, 1155, 952, 794, 762 $cm^{-1}$; $\delta_H$ (300 MHz, DMSO-d6) 10.08 (1H, s, CON*H*NH), 8.91 (1H, s, Ar-*H*), 8.71 (1H, d, *J* 6, CON*H*CH), 8.10 (1H, s, CONHN*H*), 7.92 - 7.83 (2H, m, Ar-*H*), 7.76 (1H, d, *J* 9, Ar-*H*), 7.50 (1H, dd, *J* 9, 2, Ar-*H*), 7.45 - 7.37 (3H, m, Ar-*H*), 7.17 – 7.09 (2H, d, *J* 8, Ar-*H*), 6.86 – 6.77 (2H, d, *J* 8, Ar-*H*), 4.62 (1H, m, CONHC*H*), 2.48 – 2.37 (2H, m, C*H*$_2$CH$_2$SCH$_3$), 2.07 – 1.89 (5H, m, C*H*$_2$C*H*$_2$S*CH*$_3$); $\delta_C$ (75 MHz, DMSO-d$_6$) 171.7 (*C*ONHNH), 161.4 *(C*ONHCH), 148.8 (Ar-O*C*F$_3$*)*, 145.9 (*ipso*-Ar-*C)*, 143.4 (*ipso*-Ar-*C)*, 133.5 (*ipso*-Ar-*C)*, 129.0 (Ar-*C)*, 128.9 (Ar-*C)*, 128.8 (Ar-*C)*, 127.9 (Ar-*C)*, 124.8 (Ar-*C)*, 122.3 (Ar-*C)*, 120.4 (*ipso*-Ar-*C)*, 118.2 (Ar-*C),* 116.8 (*ipso*-Ar-*C)*, 113.2 (Ar-*C)*, 52.1 (CONH*C*H), 30.9 (CH$_2$CH(*C*H$_3$)$_2$), 30.1 (CH$_2$*C*H(CH$_3$)$_2$), 14.9 (CH$_2$CH(*C*H$_3$)$_2$); $\delta_F$ (282 MHz, DMSO-d6) -57.2 (OC*F*$_3$); ***m/z*** (ES$^+$) 578 ([$^{35}$Cl]MH$^+$), 580 ([$^{37}$Cl]MH$^+$); HRMS (ES$^+$) Found [$^{35}$Cl]MH$^+$, 578.1246 ($C_{26}H_{24}{}^{35}ClF_3N_5O_3S$ requires 578.1240).

**6-chloro-N-(1-oxo-3-phenyl-1-(2-phenylhydrazineyl)propan-2-yl)-2-phenylimidazo[1,2-*a*]pyridine-3-carboxamide 44Co**

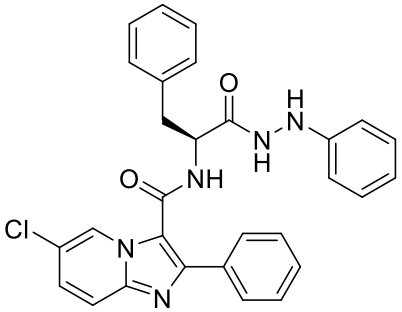

Using the standard procedure provided, *tert*-butyl (S)-(1-oxo-3-phenyl-1-(2-phenylhydrazineyl)propan-2-yl)carbamate **51Bk** (0.10 g, 0.28 mmol) was transformed

using column chromatography (DCM /EtOAc [3:1]) into the title compound as a white powder (60 mg, 42 %); $R_f$ 0.3 (DCM/EtOAc [3:1]); m.p. 275 – 282 °C; $\nu_{max}$ 3279 (N-H), 2980, 1665 (C=O), 1620 (C=O), 1532, 1493, 1384, 1322, 1265, 1220, 1167, 1080, 834, 799, 781, 745, 686, 639, 499 $cm^{-1}$; $\delta_H$ (300 MHz, DMSO-$d_6$) 10.09 (1H, s, CON*H*NH), 8.82 (1H, d, *J* 6, CON*H*CH), 8.61 (1H, s, Ar-*H*), 7.84 (1H, s, CONHN*H*), 7.73 (1H, d, *J* 9, Ar-*H*), 7.70 – 7.63 (2H, d, *J* 7, Ar-*H*), 7.46 (1H, dd, *J* 9, 1, Ar-*H*), 7.37 – 7.28 (10H, m, Ar-*H*), 7.17 – 7.07 (2H, t, *J* 7, Ar-*H*), 6.72 – 6.67 (2H, m, Ar-*H*), 4.98 (1H, m, CONHC*H*), 3.19 (1H, dd, *J* 13, 4, CONHCHC$H_2$), 2.97 (1H, m, CONHCHC$H_2$); $\delta_C$ (75 MHz, DMSO-$d_6$) 171.2 (*C*ONHNH), 160.8 *(C*ONHCH), 149.4 (*ipso*-Ar-*C)*, 145.4 (*ipso*-Ar-*C)*, 143.1 (*ipso*-Ar-*C)*, 137.8 (*ipso*-Ar-*C)*, 133.2 (*ipso*-Ar-*C)*, 129.6 (Ar-*C)*, 129.1 (Ar-*C)*, 128.9 (Ar-*C)*, 128.4 (Ar-*C)*, 127.7 (Ar-*C)*, 127.0 (Ar-*C)*, 124.6 (Ar-*C)*, 120.4 (*ipso*-Ar-*C)*, 118.9 (Ar-*C)*, 118.1 (Ar-*C)*, 117.0 (*ipso*-Ar-*C*), 112.6 (Ar-*C),* 53.6 (CONH*C*H), 37.7 (C=ONHCH*C*$H_2$); ***m/z*** ($ES^+$) 510 ([$^{35}$Cl]$MH^+$), 512 ([$^{37}$Cl]$MH^+$); HRMS ($ES^+$) Found [$^{35}$Cl]$MH^+$, 510.1719 ($C_{29}H_{25}{}^{35}ClN_5O_2$ requires 510.1697).

**(S)-6-chloro-N-(1-(2-(3-chlorophenyl)hydrazineyl)-1-oxo-3-phenylpropan-2-yl)-2-phenylimidazo[1,2-*a*]pyridine-3-carboxamide 44Cp**

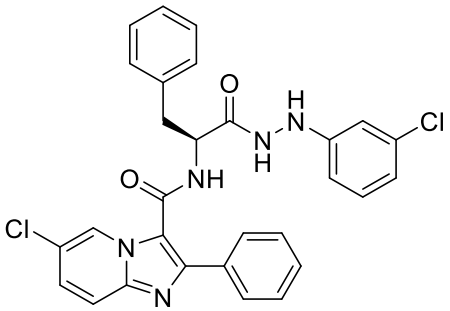


Using the standard procedure provided, *tert*-butyl (S)-(1-(2-(3-chlorophenyl)hydrazineyl)-1-oxo-3-phenylpropan-2-yl)carbamate **51BI** (0.13 g, 0.33 mmol) was transformed using column chromatography (DCM /EtOAc [1:1]) into the title compound as a white powder (90 mg, 50 %); $R_f$ 0.30 (DCM/EtOAc [1:1]); m.p. 288 – 295 °C; $\nu_{max}$ 3276 (N-H), 1669 (C=O), 1619 (C=O), 1598, 1537, 1493, 1384, 1322, 1230, 1167, 1080, 994, 835, 798, 762, 699, 678 $cm^{-1}$; $\delta_H$ (300 MHz, DMSO-$d_6$) 10.16 (1H, s, CON*H*NH), 8.72 (1H, d, *J* 6, CON*H*CH), 8.66 (1H, s, Ar-*H*), 8.16 (1H, s, CONHN*H*), 7.74 (1H, d, *J* 9, Ar-*H*), 7.70 – 7.65 (2H, d, *J* 7, Ar-*H*), 7.46 (1H, dd, *J* 9, 2, Ar-*H*), 7.38 – 7.22 (8H, m, Ar-*H*), 7.13 (1H, t, *J* 8, Ar-*H*), 6.77 (1H, s, Ar-*H*), 6.71 (1H, d, *J* 8, Ar-*H*), 6.63 (1H, d, *J* 8, Ar-*H*), 4.94 (1H, m, CONHC*H*), 3.17 (1H, dd, *J* 13, 4,

CONHCHC*H2*), 2.94 (1H, m, CONHCHC*H2*); $\delta_C$ (75 MHz, DMSO-$d_6$) 171.2 (*C*ONHNH), 160.9 *(C*ONHCH), 151.1 (*ipso*-Ar-*C)*, 145.7 (*ipso*-Ar-*C)*, 143.1 (*ipso*-Ar-*C)*, 137.5 (*ipso*-Ar-*C)*, 133.9 (*ipso*-Ar-*C)*, 130.8 (Ar-*C)*, 129.5 (Ar-*C)*, 128.9 (Ar-*C)*, 128.5 (Ar-*C)*, 127.8 (Ar-*C)*, 124.7 (Ar-*C)*, 120.4 (*ipso*-Ar-*C)*, 118.4 (Ar-*C)*, 118.1 (Ar-*C)*, 116.8 (*ipso*-Ar-*C),* 111.9 (Ar-*C)*, 111.2 (Ar-*C),* 53.8 (C=ONH*C*H), 37.3 (CONHCH*C*$H_2$); *m/z* ($ES^+$) 544 ([$^{35,35}$Cl]$MH^+$), 546 ([$^{35,37}$Cl]$MH^+$), 548 ([$^{37,37}$Cl]$MH^+$); HRMS ($ES^+$) Found [$^{35}$Cl]$MH^+$, 544.1320 ($C_{29}H_{23}{}^{35,35}Cl_2N_5O_2$ requires 544.1307).

**(S)-6-chloro-N-(1-(2-(4-chlorophenyl)hydrazineyl)-1-oxo-3-phenylpropan-2-yl)-2-phenylimidazo[1,2-*a*]pyridine-3-carboxamide 44Cq**

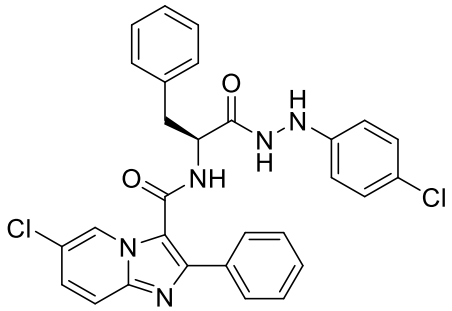


Using the standard procedure provided, *tert*-butyl (S)-(1-(2-(4-chlorophenyl)hydrazineyl)-1-oxo-3-phenylpropan-2-yl)carbamate **51Bm** (0.13 g, 0.35 mmol) was transformed using column chromatography (DCM /EtOAc [3:1]) into the title compound as a white powder (40 mg, 21 %); $R_f$ 0.40 (DCM/EtOAc [3:1]); m.p. 290 – 295 °C; $\nu_{max}$ 3253 (N-H), 1668 (C=O), 1620 (C=O), 1598, 1537, 1489, 1386, 1323, 1224, 1167, 1093, 834, 795, 779, 698, 559 $cm^{-1}$; $\delta_H$ (300 MHz, DMSO-$d_6$) 10.14 (1H, s, CON*H*NH), 8.81 (1H, d, *J* 6, CON*H*CH), 8.61 (1H, s, Ar-*H*), 8.05 (1H, s, CONHN*H*), 7.72 (1H, d, *J* 9, Ar-*H*), 7.70 – 7.61 (2H, d, *J* 7, Ar-*H*), 7.45 (1H, d, *J* 9, Ar-*H*), 7.36 – 7.22 (8H, m, Ar-*H*), 7.18 – 7.08 (2H, d, *J* 8, Ar-*H*), 6.73 – 6.60 (2H, d, *J* 8, Ar-*H*), 4.94 (1H, m, CONHC*H*), 3.17 (1H, dd, *J* 12, 4, CONHCHC*H2*), 2.95 (1H, m, CONHCHC*H2*); $\delta_C$ (75 MHz, DMSO-$d_6$) 171.3 (*C*ONHNH), 160.9 *(C*ONHCH), 148.4 (*ipso*-Ar-*C*), 145.5 (*ipso*-Ar-*C*), 143.2 (*ipso*-Ar-*C)*, 137.7 (*ipso*-Ar-*C)*, 133.3 (*ipso*-Ar-*C)*, 129.6 (Ar-*C)*, 128.9 (Ar-*C)*, 128.5 (Ar-*C)*, 127.7 (Ar-*C)*, 127.0 (Ar-*C)*, 124.6 (Ar-*C)*, 122.2 (*ipso*-Ar-*C)*, 120.4 (*ipso*-Ar-*C)*, 118.1 (Ar-*C)*, 117.0 (*ipso*-Ar-*C),* 114.1 (Ar-*C),* 53.7 (CONH*C*H), 37.6 (CONHCH*C*$H_2$); *m/z* ($ES^+$) 544 ([$^{35,35}$Cl]$MH^+$), 546 ([$^{35,37}$Cl]$MH^+$), 548 ([$^{37,37}$Cl]$MH^+$); HRMS ($ES^+$) Found [$^{35}$Cl]$MH^+$, 544.1317 ($C_{29}H_{24}{}^{35,35}Cl_2N_5O_2$ requires 544.1307).

**(S)-6-chloro-N-(1-(2-(3-bromophenyl)hydrazineyl)-1-oxo-3-phenylpropan-2-yl)-2-phenylimidazo[1,2-*a*]pyridine-3-carboxamide 44Cr**

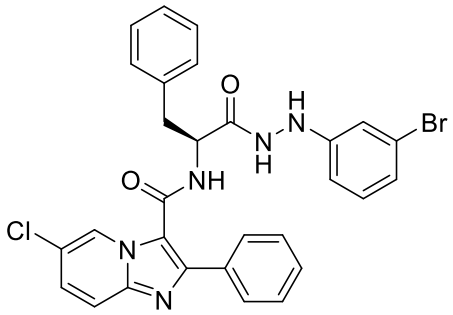


Using the standard procedure provided, *tert*-butyl (S)-(1-(2-(3-bromophenyl)hydrazineyl)-1-oxo-3-phenylpropan-2-yl)carbamate **51Bn** (0.07 g, 0.16 mmol) was transformed using column chromatography (DCM /EtOAc [1:1]) into the title compound as a white powder (29 mg, 31 %); $R_f$ 0.30 (DCM/EtOAc [1:1]); m.p. 295 – 297 °C; $\nu_{max}$ 3276 (N-H), 2980, 1620 (C=O), 1493, 1384, 1231, 1166, 1079, 697 $cm^{-1}$; $\delta_H$ (300 MHz, DMSO-$d_6$) 10.16 (1H, s, CON*H*NH), 8.72 (1H, d, *J* 6, CON*H*CH), 8.66 (1H, dd, *J* 2, 1, Ar-*H*), 8.14 (1H, s, CONHN*H*), 7.73 (1H, d, *J* 9, Ar-*H*), 7.70 – 7.62 (2H, dd, *J* 7, 1, Ar-*H*), 7.47 (1H, dd, *J* 9, 2, Ar-*H*), 7.37 – 7.24 (8H, m, Ar-*H*), 7.06 (1H, t, *J* 8, Ar-*H*), 6.93 (1H, s, Ar-*H*), 6.85 (1H, d, *J* 8, Ar-*H*), 6.66 (1H, dd, *J* 8, 1, Ar-*H*), 4.93 (1H, m, CONHC*H*), 3.15 (1H, dd, *J* 13, 4, CONHCHC$H_2$), 2.93 (1H, m, CONHCHC$H_2$); $\delta_C$ (75 MHz, DMSO-$d_6$) 171.3 (*C*ONHNH), 160.9 *(C*ONHCH), 151.2 (*ipso*-Ar-*C)*, 145.7 (*ipso*-Ar-*C)*, 143.2 (*ipso*-Ar-*C)*, 137.7 (*ipso*-Ar-*C)*, 133.3 (*ipso*-Ar-*C)*, 131.1 (Ar-*C)*, 129.5 (Ar-*C)*, 128.9 (Ar-*C)*, 128.8 (Ar-*C)*, 128.6 (Ar-*C)*, 127.8 (Ar-*C)*, 127.1 (Ar-*C)*, 124.7 (Ar-*C)*, 122.5 (*ipso*-Ar-*C)*, 121.3 (Ar-*C)*, 120.5 (*ipso*-Ar-*C)*, 118.1 (Ar-*C)*, 116.8 (*ipso*-Ar-*C),* 114.8 (Ar-*C)*, 111.5 (Ar-*C)*, 53.8 (CONH*C*H), 37.5 (CONHCH*C*$H_2$); ***m/z*** (ES$^+$) 588 ([$^{35}$Cl, $^{79}$Br]MH$^+$), 590 ([$^{35}$Cl, $^{81}$Br]MH$^+$), 590 ([$^{37}$Cl, $^{79}$Br]MH$^+$), 592 ([$^{37}$Cl, $^{81}$Br]MH$^+$); HRMS (ES$^+$) Found ([$^{35}$Cl, $^{79}$Br]MH$^+$), 588.0803 ($C_{29}H_{24}{}^{35}Cl{}^{79}BrN_5O_2$ requires 588.0796).

**(S)-6-chloro-N-(1-(2-(4-bromophenyl)hydrazineyl)-1-oxo-3-phenylpropan-2-yl)-2-phenylimidazo[1,2-*a*]pyridine-3-carboxamide 44Cs**

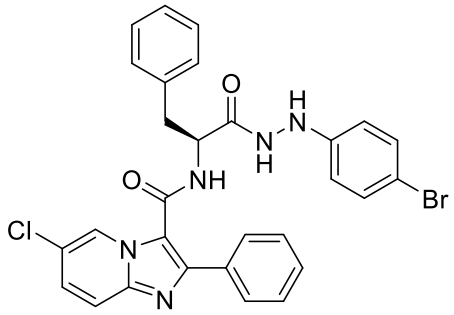

Using the standard procedure provided, *tert*-butyl (S)-(1-(2-(4-bromophenyl)hydrazineyl)-1-oxo-3-phenylpropan-2-yl)carbamate **51Bo** (0.08 g, 0.18 mmol) was transformed using column chromatography (DCM /EtOAc [3:1]) into the title compound as a white powder (42 mg, 39 %); $R_f$ 0.30 (DCM/EtOAc [3:1]); m.p. 293 – 298 °C; $\nu_{max}$ 3261 (N-H), 1671 (C=O), 1681 (C=O), 1533, 1492, 1324, 1229, 1163, 1098, 1067, 829, 797, 761, 698 $cm^{-1}$; $\delta_H$ (300 MHz, DMSO-$d_6$) 10.14 (1H, s, CON*H*NH), 8.83 (1H, d, *J* 6, CON*H*CH), 8.60 (1H, s, Ar-*H*), 8.06 (1H, s, CONHN*H*), 7.72 (1H, d, *J* 9, Ar-*H*), 7.69 – 7.62 (2H, dd, *J* 7, 1, Ar-*H*), 7.46 (1H, dd, *J* 9, 2, Ar-*H*), 7.40 – 7.28 (8H, m, Ar-*H*), 7.26 – 7.19 (2H, d, *J* 8, Ar-*H*), 6.68 – 6.56 (2H, d, *J* 8, Ar-*H*), 4.94 (1H, m, CONHC*H*), 3.14 (1H, dd, *J* 13, 4, CONHCHC*H*$_2$), 2.93 (1H, m, CONHCHC*H*$_2$); $\delta_C$ (75 MHz, DMSO-$d_6$) 171.3 (*C*ONHNH), 160.9 *(C*ONHCH), 148.9 (*ipso*-Ar-*C*), 145.5 (*ipso*-Ar-*C)*, 143.2 (*ipso*-Ar-*C)*, 137.7 (*ipso*-Ar-*C)*, 133.3 (*ipso*-Ar-*C)*, 131.7 (Ar-*C)*, 129.6 (Ar-*C)*, 128.9 (Ar-*C)*, 128.8 (Ar-*C)*, 128.5 (Ar-*C)*, 127.0 (Ar-*C)*, 124.6 (Ar-*C)*, 120.4 (*ipso*-Ar-*C)*, 118.1 (Ar-*C)*, 117.0 (*ipso*-Ar-*C),* 114.6 (Ar-*C)*, 109.7 (*ipso*-Ar-*C)*, 53.7 (CONH*C*H), 37.6 (CONHCH*C*H$_2$); *m/z* ($ES^+$) 588 ([$^{35}$Cl, $^{79}$Br]$MH^+$), 590 ([$^{35}$Cl, $^{81}$Br]$MH^+$), 590 ([$^{37}$Cl, $^{79}$Br]$MH^+$), 592 ([$^{37}$Cl, $^{81}$Br]$MH^+$); HRMS ($ES^+$) Found ([$^{35}$Cl, $^{79}$Br]$MH^+$), 588.0806 ($C_{29}H_{24}{}^{35}Cl{}^{79}BrN_5O_2$ requires 588.0802).

**6-chloro-N-(1-oxo-3-phenyl-1-(2-(3-(trifluoromethyl)phenyl)hydrazineyl)propan-2-yl)-2-phenylimidazo[1,2-*a*]pyridine-3-carboxamide 44Ct**

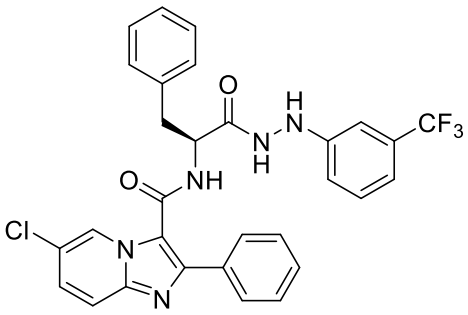

Using the standard procedure provided, *tert*-butyl (S)-(1-(2-(3-(trifluoromethyl)phenyl)hydrazineyl)-1-oxo-3-phenylpropan-2-yl)carbamate **51Bp** (0.10 g, 0.23 mmol) was transformed using column chromatography (DCM /EtOAc [3:1]) into the title compound as a white powder (42 mg, 31 %); $R_f$ 0.30 (DCM/EtOAc [3:1]); m.p. 288 – 295 °C; $\nu_{max}$ 3251 (N-H), 3045 (N-H), 1670 (C=O), 1621 (C=O), 1493, 1387, 1337, 1165, 1116, 1067, 860, 797, 695, 485 $cm^{-1}$; $\delta_H$ (300 MHz, DMSO-$d_6$) 10.24 (1H, s, CON*H*NH), 8.73 (1H, d, *J* 6, CON*H*CH), 8.63 (1H, s, Ar-*H*), 8.33 (1H, s, CONHN*H*), 7.74 (1H, d, *J* 9, Ar-*H*), 7.70 – 7.64 (2H, dd, *J* 7, 1, Ar-*H*), 7.47 (1H, dd, *J* 9, 2, Ar-*H*), 7.37 – 7.27 (9H, m, Ar-*H*), 7.07 (1H, s, Ar-*H*), 7.03 (1H, d, *J* 7, Ar-*H*), 6.92 (1H, d, *J* 7, Ar-*H*), 4.96 (1H, m, CONHC*H*), 3.18 (1H, dd, *J* 13, 4, CONHCHC$H_2$), 2.93 (1H, m, CONHCHC$H_2$); $\delta_C$ (75 MHz, DMSO-$d_6$) 171.4 (*C*ONHNH), 160.9 (*C*ONHCH), 150.1 (*ipso*-Ar-*C)*, 145.7 (*ipso*-Ar-*C)*, 143.2 (*ipso*-Ar-*C)*, 137.6 (*ipso*-Ar-*C)*, 133.3 (*ipso*-Ar-*C)*, 130.3 (Ar-*C)*, 129.5 (Ar-*C)*, 128.8 (Ar-*C)*, 128.5 (Ar-*C)*, 127.8 (Ar-*C)*, 127.1 (Ar-*C)*, 124.6 (Ar-*C)*, 120.4 (*ipso*-Ar-*C)*, 118.1 (Ar-*C)*, 116.8 (*ipso*-Ar-*C),* 116.0 (Ar-*C),* 115.0 (Ar-*C),* 108.9 (Ar-*C),* 53.8 (CONH*C*H), 37.5 (CONHCH*C*$H_2$); $\delta_F$ (282 MHz, DMSO-$d_6$) -61.3 (C*F*$_3$); *m/z* ($ES^+$) 578 ([$^{35}$Cl]$MH^+$), 580 ([$^{37}$Cl]$MH^+$); HRMS ($ES^+$) Found [$^{35}$Cl]$MH^+$, 578.1590 ($C_{30}H_{24}{}^{35}ClF_3N_5O_2$ requires 578.1570).

**6-chloro-N-(1-oxo-3-phenyl-1-(2-(4-(trifluoromethyl)phenyl)hydrazineyl)propan-2-yl)-2-phenylimidazo[1,2-*a*]pyridine-3-carboxamide 44Cu**

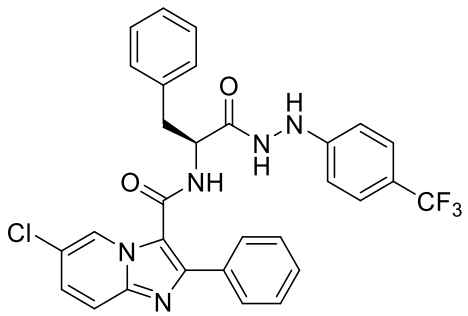


Using the standard procedure provided, *tert*-butyl (S)-(1-(2-(4-(trifluoromethyl)phenyl)hydrazineyl)-1-oxo-3-phenylpropan-2-yl)carbamate **51Bq** (0.10 g, 0.23 mmol) was transformed using column chromatography (DCM /EtOAc [3:1]) into the title compound as a white powder (45 mg, 33 %); $R_f$ 0.30 (DCM/EtOAc [3:1]); m.p. 292 – 295 °C; $\nu_{max}$ 3257 (N-H), 1670 (C=O), 1619 (C=O), 1524, 1493, 1387, 1328, 1164, 1101, 1067, 832, 797, 698, 508 $cm^{-1}$; $\delta_H$ (300 MHz, DMSO-$d_6$) 10.27 (1H, s, CON*H*NH), 8.86 (1H, d, *J* 6, CON*H*CH), 8.59 (1H, s, Ar-*H*), 8.51 (1H, s,

CONHN*H*), 7.76 – 7.63 (3H, m, Ar-*H*), 7.49 – 7.39 (3H, m, Ar-*H*), 7.38 – 7.26 (8H, m, Ar-*H*), 6.84 – 6.68 (2H, d, *J* 8, Ar-*H*), 4.97 (1H, m, CONHC*H*), 3.18 (1H, dd, *J* 13, 4, CONHCHC*H*$_2$), 2.98 (1H, m, CONHCHC*H*$_2$); $\delta_C$ (75 MHz, DMSO-d$_6$) 171.4 (*C*ONHNH), 161.0 *(C*ONHCH), 152.6 (*ipso*-Ar-*C)*, 145.6 (*ipso*-Ar-*C)*, 143.2 (*ipso*-Ar-*C)*, 137.7 (*ipso*-Ar-*C)*, 133.3 (*ipso*-Ar-*C)*, 129.6 (Ar-*C)*, 128.9 (Ar-*C)*, 128.8 (Ar-*C)*, 127.7 (Ar-*C)*, 126.5 (Ar-*C)*, 124.6 (Ar-*C)*, 120.4 (*ipso*-Ar-*C)*, 118.1 (Ar-*C)*, 116.9 (*ipso*-Ar-*C),* 111.9 (Ar-*C),* 53.8 (CONH*C*H), 37.5 (CONHCH*C*H$_2$); $\delta_F$ (282 MHz, DMSO-d$_6$) -59.1 (C*F*$_3$); ***m/z*** (ES$^+$) 578 ([$^{35}$Cl]MH$^+$), 580 ([$^{37}$Cl]MH$^+$); HRMS (ES$^+$) Found [$^{35}$Cl]MH$^+$, 578.1590 ($C_{30}H_{24}{}^{35}ClF_3N_5O_2$ requires 578.1570).

**6-chloro-N-(1-oxo-3-phenyl-1-(2-(3-(trifluoromethoxy)phenyl)hydrazineyl)propan-2-yl)-2-phenylimidazo[1,2-*a*]pyridine-3-carboxamide 44Cv**

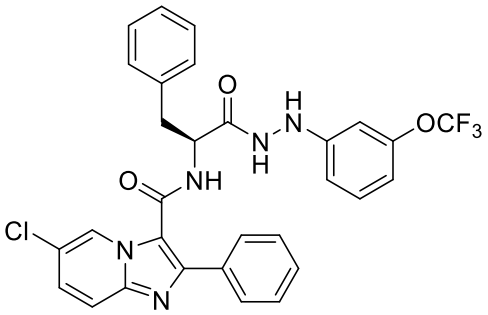


Using the standard procedure provided, *tert*-butyl (S)-(1-(2-(3-(trifluoromethoxy)phenyl)hydrazineyl)-1-oxo-3-phenylpropan-2-yl)carbamate **51Br** (0.10 g, 0.37 mmol) was transformed using column chromatography (DCM /EtOAc [3:1]) into the title compound as a white powder (92 mg, 41 %); $R_f$ 0.36 (DCM/EtOAc [3:1]); m.p. 300 – 307 °C; $\nu_{max}$ 3263 (N-H), 2980, 1669 (C=O), 1620 (C=O), 1493, 1384, 1257, 1154, 1079, 951, 795, 689 cm$^{-1}$; $\delta_H$ (300 MHz, DMSO-d$_6$) 10.22 (1H, bs, CON*H*NH), 8.75 (1H, d, *J* 6, CON*H*CH), 8.65 (1H, s, Ar-*H*), 8.28 (1H, s, CONHN*H*), 7.74 (1H, d, *J* 9, Ar-*H*), 7.71 – 7.63 (2H, d, *J* 7, Ar-*H*), 7.45 (1H, d, *J* 9, Ar-*H*), 7.37 – 7.25 (8H, m, Ar-*H*), 7.20 (1H, d, *J* 8, Ar-*H*), 6.75 – 6.50 (3H, m, Ar-*H*), 4.96 (1H, m, CONHC*H*), 3.17 (1H, dd, *J* 13, 4, CONHCHC*H*$_2$), 2.93 (1H, m, CONHCHC*H*$_2$); $\delta_C$ (75 MHz, DMSO-d$_6$) 171.3 (*C*ONHNH), 160.9 *(C*ONHCH), 151.4 (*ipso*-Ar-*C)*, 149.8 (Ar-O*C*F$_3$*)*, 145.7 (*ipso*-Ar-*C)*, 143.2 (*ipso*-Ar-*C)*, 137.7 (*ipso*-Ar-*C)*, 133.3 (*ipso*-Ar-*C)*, 130.8 (Ar-*C)*, 129.5 (Ar-*C)*, 128.9 (Ar-*C)*, 128.6 (Ar-*C)*, 127.8 (Ar-*C)*, 127.1 (*ipso*-Ar-*C)*, 124.7 (Ar-*C)*, 120.4 (*ipso*-Ar-*C)*, 118.1 (Ar-*C)*, 116.9 (*ipso*-Ar-*C),* 111.3 (Ar-*C),* 110.5 (Ar-*C)*, 104.5 (Ar-*C),* 53.8 (CONH*C*H), 37.5 (CONHCH*C*H$_2$); $\delta_F$ (282 MHz, DMSO-d$_6$)

-57.0 (OC*F*$_3$); *m/z* (ES$^+$) 594 ([$^{35}$Cl]MH$^+$), 596 ([$^{37}$Cl]MH$^+$); HRMS (ES$^+$) Found [$^{35}$Cl]MH$^+$, 594.1526 ($C_{30}H_{24}{}^{35}ClF_3N_5O_3$ requires 594.1520).

**6-chloro-N-(1-oxo-3-phenyl-1-(2-(4-(trifluoromethoxy)phenyl)hydrazineyl)propan-2-yl)-2-phenylimidazo[1,2-*a*]pyridine-3-carboxamide 44Cw**

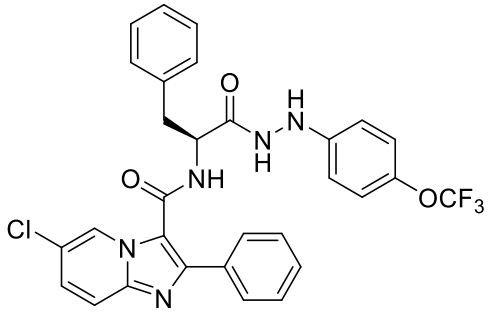

Using the standard procedure provided, *tert*-butyl (S)-(1-(2-(4-(trifluoromethoxy)phenyl)hydrazineyl)-1-oxo-3-phenylpropan-2-yl)carbamate **51Bs** (0.07 g, 0.27 mmol) was transformed using column chromatography (DCM /EtOAc [3:1]) into the title compound as a white powder (96 mg, 35 %); R$_f$ 0.28 (DCM/EtOAc [3:1]); m.p. 305 – 307 °C; $\nu_{max}$ 3253 (N-H), 2980, 1670 (C=O), 1614 (C=O), 1506, 1392, 1259, 1155, 1079, 952, 794, 689 cm$^{-1}$; $\delta_H$ (300 MHz, DMSO-d$_6$) 10.18 (1H, s, CON*H*NH), 8.86 (1H, d, *J* 6, CON*H*CH), 8.58 (1H, s, Ar-*H*), 8.13 (1H, s, CONHN*H*), 7.73 (1H, d, *J* 9, Ar-*H*), 7.70 – 7.67 (2H, d, *J* 7, Ar-*H*), 7.46 (1H, dd, *J* 9, 2, Ar-*H*), 7.36 – 7.27 (8H, m, Ar-*H*), 7.12 – 7.07 (2H, d, *J* 8, Ar-*H*), 6.73 – 6.68 (2H, d, *J* 8, Ar-*H*), 4.95 (1H, m, CONHC*H*), 3.15 (1H, dd, *J* 13, 4, CONHCHC*H*$_2$), 2.94 (1H, m, CONHCHC*H*$_2$); $\delta_C$ (75 MHz, DMSO-d$_6$) 171.3 (*C*ONHNH), 160.9 *(C*ONHCH), 148.7 (Ar-O*C*F$_3$*)*, 145.5 (*ipso*-Ar-*C)*, 143.2 (*ipso*-Ar-*C)*, 137.8 (*ipso*-Ar-*C)*, 133.3 (*ipso*-Ar-*C)*, 129.6 (Ar-*C)*, 128.9 (Ar-*C)*, 128.5 (Ar-*C)*, 127.7 (Ar-*C)*, 127.1 (Ar-*C)*, 124.6 (Ar-*C)*, 122.3 (Ar-*C)*, 120.4 (*ipso*-Ar-*C)*, 118.1 (Ar-*C)*, 117.0 (*ipso*-Ar-*C),* 113.2 (Ar-*C),* 53.7 (CONH*C*H), 37.6 (CONHCH*C*H$_2$); $\delta_F$ (282 MHz, DMSO-d$_6$) -56.4 (OC*F*$_3$); *m/z* (ES$^+$) 594 ([$^{35}$Cl]MH$^+$), 596 ([$^{37}$Cl]MH$^+$); HRMS (ES$^+$) Found [$^{35}$Cl]MH$^+$, 594.1523 ($C_{30}H_{24}{}^{35}ClF_3N_5O_3$ requires 594.1514).

**(S)-6-chloro-N-(1-oxo-4-phenyl-1-(2-phenylhydrazineyl)butan-2-yl)-2-phenylimidazo[1,2-*a*]pyridine-3-carboxamide 44Cx**

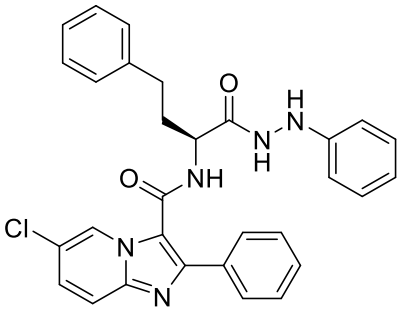

Using the standard procedure provided, *tert*-butyl (S)-(1-oxo-4-phenyl-1-(2-phenylhydrazineyl)butan-2-yl)carbamate **51Bt** (0.11 g, 0.29 mmol) was transformed using column chromatography (*n*-Hexane /EtOAc [3:1]) into the title compound as a white powder (75 mg, 48 %); $R_f$ 0.3 (*n*-Hexane /EtOAc [3:1]); m.p. 280 – 285 °C; $\nu_{max}$ 3260 (N-H), 3032 (N-H), 1667 (C=O), 1617 (C=O), 1536, 1493, 1388, 1323, 1250, 1229, 1166, 1084, 839, 797, 746, 688, 639, 495 $cm^{-1}$; $\delta_H$ (300 MHz, DMSO-$d_6$) 9.99 (1H, s, CON*H*NH), 9.03 (1H, s, Ar-*H*), 8.67 (1H, d, *J* 7, CON*H*CH), 7.93 – 7.88 (2H, d, *J* 7, Ar-*H*), 7.84 (1H, s, CONHN*H*), 7.77 (1H, d, *J* 9, Ar-*H*), 7.50 (1H, dd, *J* 9, 1, Ar-*H*), 7.46 – 7.39 (3H, m, Ar-*H*), 7.33 – 7.27 (2H, t, *J* 7, Ar-*H*), 7.22 – 7.16 (3H, m, Ar-*H*), 7.16 – 7.09 (2H, t, *J* 7, Ar-*H*), 6.80 – 6.73 (2H, d, *J* 7, Ar-*H*), 6.69 (1H, t, *J* 7, Ar-*H*), 4.56 (1H, m, CONHC*H*), 2.69 – 2.54 (2H, m, CONHCH(C*H*$_2$CH$_2$Ph)), 2.10 – 1.90 (2H, m, CONHCH(CH$_2$C*H*$_2$Ph)); $\delta_C$ (75 MHz, DMSO-$d_6$) 171.7 (*C*ONHNH), 161.2 (*C*ONHCH), 149.7 (*ipso*-Ar-*C)*, 145.9 (*ipso*-Ar-*C)*, 143.3 (*ipso*-Ar-*C)*, 141.5 (*ipso*-Ar-*C)*, 133.6 (*ipso*-Ar-*C)*, 129.1 (Ar-*C)*, 128.9 (Ar-*C)*, 128.7 (Ar-*C)*, 127.9 (Ar-*C)*, 126.4 (Ar-*C)*, 124.9 (Ar-*C)*, 120.5 (*ipso*-Ar-*C)*, 118.9 (Ar-*C)*, 118.2 (Ar-*C)*, 116.9 (*ipso*-Ar-*C*), 112.6 (Ar-*C),* 52.7 (CONH*C*H), 33.6 (CONHCH(CH$_2$*C*H$_2$Ph)), 32.0 (CONHCH(*C*H$_2$CH$_2$Ph)); *m/z* ($ES^+$) 524 ([$^{35}$Cl]$MH^+$), 526 ([$^{37}$Cl]$MH^+$); HRMS ($ES^+$) Found [$^{35}$Cl]$MH^+$, 524.1843 ($C_{30}H_{27}{}^{35}ClN_5O_2$ requires 524.1848).

**(S)-6-chloro-N-(1-(2-(3-chlorophenyl)hydrazineyl)-1-oxo-4-phenylbutan-2-yl)-2-phenylimidazo[1,2-*a*]pyridine-3-carboxamide 44Cy**

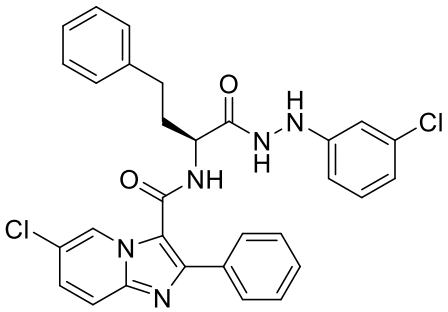

Using the standard procedure provided, *tert*-butyl (S)-(1-oxo-4-phenyl-1-(2-(3-chlorophenyl)hydrazineyl)butan-2-yl)carbamate **51Bu** (0.10 g, 0.24 mmol) was transformed using column chromatography (*n*-Hexane /EtOAc [3:1]) into the title compound as a white powder (60 mg, 43 %); $R_f$ 0.3 (*n*-Hexane /EtOAc [3:1]); m.p. 290 – 295 °C; $\nu_{max}$ 3261 (N-H), 1666 (C=O), 1619 (C=O), 1537, 1493, 1383, 1322, 1261, 1224, 1161, 1031, 820, 792, 758, 685, 635, 535 $cm^{-1}$; $\delta_H$ (300 MHz, DMSO-$d_6$) 10.06 (1H, s, CON*H*NH), 9.04 (1H, s, Ar-*H*), 8.61 (1H, d, *J* 7, CON*H*CH), 8.14 (1H, s, CONHN*H*), 7.93 – 7.86 (2H, d, *J* 7, Ar-*H*), 7.78 (1H, d, *J* 9, Ar-*H*), 7.50 (1H, dd, *J* 9, 1, Ar-*H*), 7.47 – 7.38 (3H, m, Ar-*H*), 7.34 – 7.26 (2H, t, *J* 7, Ar-*H*), 7.23 – 7.14 (3H, m, Ar-*H*), 7.07 (1H, t, *J* 7, Ar-*H*), 6.96 (1H, s, Ar-*H*), 6.84 (1H, d, *J* 7, Ar-*H*), 6.74 (1H, d, *J* 7, Ar-*H*), 4.51 (1H, m, CONHC*H*), 2.67 – 2.53 (2H, m, CONHCH(C$H_2$C$H_2$Ph)), 2.06 – 1.89 (2H, m, CONHCH(C$H_2$C$H_2$Ph)); $\delta_C$ (75 MHz, DMSO-$d_6$) 171.8 (*C*ONHNH), 161.3 (*C*ONHCH), 151.4 (*ipso*-Ar-*C)*, 146.2 (*ipso*-Ar-*C)*, 143.4 (*ipso*-Ar-*C)*, 141.4 (*ipso*-Ar-*C)*, 133.6 (*ipso*-Ar-*C)*, 131.1 (Ar-*C)*, 129.1 (Ar-*C)*, 128.9 (Ar-*C)*, 128.7 (Ar-*C)*, 126.4 (Ar-*C)*, 122.6 (Ar-*C)*, 121.2 (Ar-*C)*, 120.6 (*ipso*-Ar-*C)*, 118.2 (Ar-*C)*, 116.8 (*ipso*-Ar-*C*), 114.8 (Ar-*C),* 52.7 (CONH*C*H), 33.4 (CONHCH(C$H_2$*C*$H_2$Ph)), 32.0 (CONHCH(*C*$H_2$C$H_2$Ph)); *m/z* ($ES^+$) 558 ([$^{35,35}$Cl]$MH^+$), 560 ([$^{35,37}$Cl]$MH^+$), 562 ([$^{37,37}$Cl]$MH^+$); HRMS ($ES^+$) Found [$^{35}$Cl]$MH^+$, 558.1452 ($C_{30}H_{26}{}^{35,35}Cl_2N_5O_2$ requires 558.1458).

**(S)-6-chloro-N-(1-(2-(3-bromophenyl)hydrazineyl)-1-oxo-4-phenylbutan-2-yl)-2-phenylimidazo[1,2-*a*]pyridine-3-carboxamide 44Cz**

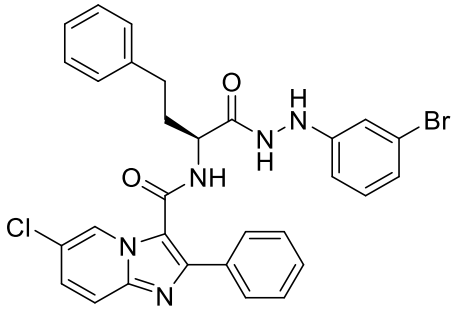


Using the standard procedure provided, *tert*-butyl (S)-(1-oxo-4-phenyl-1-(2-(3-bromophenyl)hydrazineyl)butan-2-yl)carbamate **51Bw** (0.10 g, 0.22 mmol) was transformed using column chromatography (*n*-Hexane /EtOAc [3:1]) into the title compound as a white powder (60 mg, 43 %); $R_f$ 0.3 (*n*-Hexane /EtOAc [3:1]); m.p. 295 – 298 °C; $\nu_{max}$ 3251 (N-H), 3028 (N-H), 1671 (C=O), 1618 (C=O), 1599, 1493, 1388, 1323, 1281, 1232, 1166, 1077, 990, 844, 800, 697, 495 $cm^{-1}$; $\delta_H$ (300 MHz, DMSO-$d_6$) 10.09 (1H, s, CON*H*NH), 9.04 (1H, s, Ar-*H*), 8.63 (1H, d, *J* 7, CON*H*CH), 8.15 (1H,

s, CONHN*H*), 7.95 – 7.85 (2H, d, *J* 7, Ar-*H*), 7.77 (1H, d, *J* 9, Ar-*H*), 7.50 (1H, dd, *J* 9, 1, Ar-*H*), 7.46 – 7.39 (2H, m, Ar-*H*), 7.34 – 7.25 (2H, t, *J* 7, Ar-*H*), 7.25 – 7.09 (5H, m, Ar-*H*), 6.81 (1H, s, Ar-*H*), 6.75 – 6.64 (2H, dd, *J* 7, 1, Ar-*H*), 4.51 (1H, m, CONHC*H*), 2.67 – 2.53 (2H, m, CONHCH(C*H*$_2$CH$_2$Ph)), 2.07 – 1.87 (2H, m, CONHCH(CH$_2$C*H*$_2$Ph)); $\delta_C$ (75 MHz, DMSO-d$_6$) 171.9 (*C*ONHNH), 161.3 (*C*ONHCH), 151.3 (*ipso*-Ar-*C)*, 146.2 (*ipso*-Ar-*C)*, 143.4 (*ipso*-Ar-*C)*, 141.4 (*ipso*-Ar-*C)*, 133.6 (*ipso*-Ar-*C)*, 130.7 (Ar-*C)*, 129.1 (Ar-*C)*, 128.9 (Ar-*C)*, 128.7 (Ar-*C)*, 126.4 (Ar-*C)*, 125.0 (Ar-*C)*, 120.6 (*ipso*-Ar-*C)*, 118.3 (Ar-*C)*, 118.2 (Ar-*C)*, 116.8 (*ipso*-Ar-*C*), 111.9 (Ar-*C),* 111.3 (Ar-*C)*, 52.8 (CONH*C*H), 33.4 (CONHCH(CH$_2$*C*H$_2$Ph)), 32.0 (CONHCH(*C*H$_2$CH$_2$Ph)); *m/z* (ES$^+$) 602 ([$^{35}$Cl, $^{79}$Br]MH$^+$), 604 ([$^{35}$Cl, $^{81}$Br]MH$^+$), 604 ([$^{37}$Cl, $^{79}$Br]MH$^+$), 606 ([$^{37}$Cl, $^{81}$Br]MH$^+$); HRMS (ES$^+$) Found ([$^{35}$Cl, $^{79}$Br]MH$^+$), 602.0950 ($C_{30}H_{26}{}^{35}Cl^{79}BrN_5O_2$ requires 602.0953).

**(S)-6-chloro-N-(1-(2-(4-bromophenyl)hydrazineyl)-1-oxo-4-phenylbutan-2-yl)-2-phenylimidazo[1,2-*a*]pyridine-3-carboxamide 44Da**

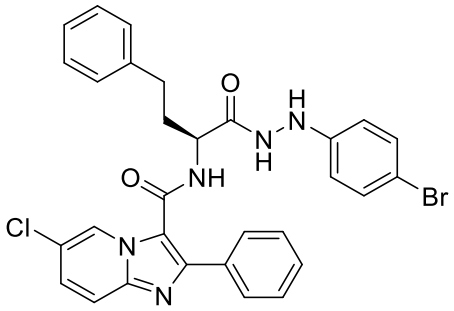


Using the standard procedure provided, *tert*-butyl (S)-(1-oxo-4-phenyl-1-(2-(4-bromophenyl)hydrazineyl)butan-2-yl)carbamate **51Bx** (0.07 g, 0.16 mmol) was transformed using column chromatography (*n*-Hexane /EtOAc [3:1]) into the title compound as a white powder (35 mg, 35 %); $R_f$ 0.3 (*n*-Hexane /EtOAc [3:1]); m.p. 290 – 297 °C; $\nu_{max}$ 3250 (N-H), 3023 (N-H), 1672 (C=O), 1620 (C=O), 1538, 1492, 1390, 1322, 1251, 1217, 1167, 1076, 802, 781, 697, 497 cm$^{-1}$; $\delta_H$ (300 MHz, DMSO-d$_6$) 10.10 (1H, s, CON*H*NH), 8.99 (1H, s, Ar-*H*), 8.72 (1H, d, *J* 7, CON*H*CH), 8.05 (1H, s, CONHN*H*), 7.95 – 7.85 (2H, d, *J* 7, Ar-*H*), 7.77 (1H, d, *J* 9, Ar-*H*), 7.50 (1H, dd, *J* 9, 2, Ar-*H*), 7.46 – 7.35 (3H, m, Ar-*H*), 7.31 – 7.12 (7H, m, Ar-*H*), 6.81 – 6.67 (2H, d, *J* 9, Ar-*H*), 4.53 (1H, m, CONHC*H*), 2.72 – 2.55 (2H, m, CONHCH(C*H*$_2$CH$_2$Ph)), 2.08 – 1.88 (2H, m, CONHCH(CH$_2$C*H*$_2$Ph)); $\delta_C$ (75 MHz, DMSO-d$_6$) 171.9 (*C*ONHNH), 161.3 (*C*ONHCH), 149.1 (*ipso*-Ar-*C)*, 145.9 (*ipso*-Ar-*C)*, 143.3 (*ipso*-Ar-*C)*, 141.4 (*ipso*-Ar-*C)*, 133.5 (*ipso*-Ar-*C)*, 131.7 (Ar-*C)*, 129.1 (Ar-*C)*, 128.9 (Ar-*C)*, 128.8 (Ar-*C)*, 127.9 (Ar-*C)*,

126.4 (Ar-*C)*, 124.9 (Ar-*C)*, 120.5 (*ipso*-Ar-*C)*, 118.2 (Ar-*C)*, 116.9 (*ipso*-Ar-*C*), 114.9 (Ar-*C),* 109.7 (Ar-*C)*, 52.7 (CONH*C*H), 33.4 (CONHCH($CH_2$*C*$H_2$Ph)), 32.0 (CONHCH(*C*$H_2$$CH_2$Ph)); ***m/z*** ($ES^+$) 602 ([$^{35}$Cl, $^{79}$Br]$MH^+$), 604 ([$^{35}$Cl, $^{81}$Br]$MH^+$), 604 ([$^{37}$Cl, $^{79}$Br]$MH^+$), 606 ([$^{37}$Cl, $^{81}$Br]$MH^+$); HRMS ($ES^+$) Found ([$^{35}$Cl, $^{79}$Br]$MH^+$), 602.0949 ($C_{30}H_{26}{}^{35}Cl{}^{79}BrN_5O_2$ requires 602.0953).

**(S)-6-chloro-N-(1-(2-((3-trifluoromethyl)phenyl)hydrazineyl)-1-oxo-4-phenylbutan-2-yl)-2-phenylimidazo[1,2-*a*]pyridine-3-carboxamide 44Db**

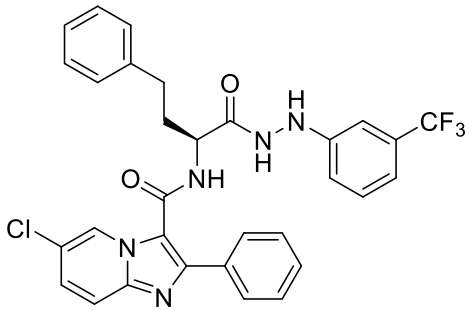

Using the standard procedure provided, *tert*-butyl (S)-(1-oxo-4-phenyl-1-(2-((3-trifluoromethyl)phenyl)hydrazineyl)butan-2-yl)carbamate **51By** (0.10 g, 0.22 mmol) was transformed using column chromatography (*n*-Hexane /EtOAc [3:1]) into the title compound as a white powder (65 mg, 48 %); $R_f$ 0.3 (*n*-Hexane /EtOAc [3:1]); m.p. 280 – 285 °C; $\nu_{max}$ 3253 (N-H), 3025 (N-H), 1672 (C=O), 1619 (C=O), 1535, 1492, 1387, 1342, 1256, 1229, 1166, 1086, 833, 796, 761, 698 $cm^{-1}$; $\delta_H$ (300 MHz, DMSO-$d_6$) 10.15 (1H, s, CON*H*NH), 8.99 (1H, s, Ar-*H*), 8.64 (1H, d, *J* 7, CON*H*CH), 8.32 (1H, s, CONHN*H*), 7.94 – 7.86 (2H, dd, *J* 7, 2, Ar-*H*), 7.77 (1H, dd, *J* 9, 1, Ar-*H*), 7.50 (1H, dd, *J* 9, 2, Ar-*H*), 7.46– 7.35 (3H, m, Ar-*H*), 7.34 – 7.26 (2H, m, Ar-*H*), 7.23 – 7.12 (4H, m, Ar-*H*), 7.07 (1H, s, Ar-*H*), 7.05 – 6.97 (2H, t, *J* 7, Ar-*H*), 4.52 (1H, m, CONHC*H*), 2.68 – 2.56 (2H, m, CONHCH(C*H*$_2$$CH_2$Ph)), 2.07 – 1.87 (2H, m, CONHCH($CH_2$C*H*$_2$Ph)); $\delta_C$ (75 MHz, DMSO-$d_6$) 171.9 (*C*ONHNH), 161.4 (*C*ONHCH), 150.3 (*ipso*-Ar-*C)*, 146.2 (*ipso*-Ar-*C)*, 143.4 (*ipso*-Ar-*C)*, 141.3 (*ipso*-Ar-*C)*, 133.6 (*ipso*-Ar-*C)*, 130.2 (Ar-*C)*, 129.1 (Ar-*C)*, 128.9 (Ar-*C)*, 128.7 (Ar-*C)*, 127.9 (Ar-*C)*, 126.4 (Ar-*C)*, 124.9 (Ar-*C)*, 120.5 (*ipso*-Ar-*C)*, 118.2 (Ar-*C)*, 116.8 (*ipso*-Ar-*C*), 116.2 (Ar-*C*), 115.2 (Ar-*C*)*,* 108.4 (Ar-*C*), 52.8 (C=ONH*C*H), 33.4 (CONHCH($CH_2$*C*$H_2$Ph)), 32.1 (CONHCH(*C*$H_2$$CH_2$Ph)); $\delta_F$ (282 MHz, DMSO-$d_6$) -61.3 (C*F*$_3$); ***m/z*** ($ES^+$) 592 ([$^{35}$Cl]$MH^+$), 594 ([$^{37}$Cl]$MH^+$); HRMS ($ES^+$) Found [$^{35}$Cl]$MH^+$, 592.1714 ($C_{31}H_{26}F_3{}^{35}ClN_5O_2$ requires 592.1722).

**(S)-6-chloro-N-(1-(2-(2-chlorophenyl)hydrazineyl)-1-oxo-3-phenylpropan-2-yl)-2-phenylimidazo[1,2-*a*]pyridine-3-carboxamide 44Dc**

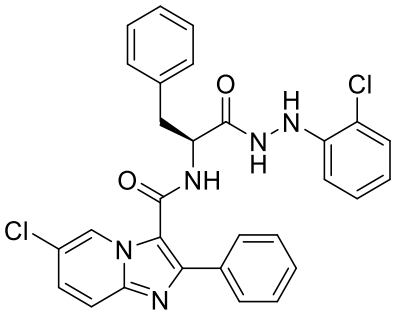

Using the standard procedure provided, *tert*-butyl (S)-(1-(2-(2-chlorophenyl)hydrazineyl)-1-oxo-3-phenylpropan-2-yl)carbamate **51Ca** (0.10 g, 0.37 mmol) was transformed using column chromatography (DCM /EtOAc [3:1]) into the title compound as a white powder (70 mg, 42 %); $R_f$ 0.30 (DCM/EtOAc [3:1]); m.p. 284 – 289 °C; $\nu_{max}$ 3283 (N-H), 1674 (C=O), 1618 (C=O), 1587, 1531, 1495, 1384, 1323, 1228, 1169, 805, 697 $cm^{-1}$; $\delta_H$ (300 MHz, DMSO-$d_6$) 10.27 (1H, s, CON*H*NH), 8.85 (1H, d, *J* 6, CON*H*CH), 8.55 (1H, dd, *J* 2, 1, Ar-*H*), 7.72 (1H, dd, *J* 9, 1, Ar-*H*), 7.70 – 7.63 (2H, m, Ar-*H*), 7.57 (1H, s, CONHN*H*), 7.45 (1H, dd, *J* 9, 2, Ar-*H*), 7.37 – 7.22 (9H, m, Ar-*H*), 7.11 (1H, m, Ar-*H*), 6.77 (1H, dd, *J* 7, 1, Ar-*H*), 6.72 (1H, m, Ar-*H*), 5.00 (1H, m, CONHC*H*), 3.20 (1H, dd, *J* 13, 4, CONHCHC$H_2$), 2.94 (1H, m, CONHCHC$H_2$); $\delta_C$ (75 MHz, DMSO-$d_6$) 171.3 (*C*ONHNH), 160.9 *(C*ONHCH), 145.6 (*ipso*-Ar-*C)*, 144.8 (*ipso*-Ar-*C)*, 143.2 (*ipso*-Ar-*C)*, 137.9 (*ipso*-Ar-*C)*, 133.3 (*ipso*-Ar-*C)*, 129.6 (Ar-*C)*, 128.9 (Ar-*C)*, 128.8 (Ar-*C)*, 128.5 (Ar-*C)*, 128.2 (Ar-*C)*, 127.7 (Ar-*C)*, 127.1 (Ar-*C)*, 124.6 (Ar-*C)*, 120.4 (*ipso*-Ar-*C)*, 119.9 (Ar-*C)*, 118.1 (Ar-*C)*, 117.6 (*ipso*-Ar-*C)*, 117.0 (*ipso*-Ar-*C),* 113.3 (Ar-*C),* 53.7 (CONH*C*H), 37.6 (C=ONHCH*C*$H_2$); ***m/z*** ($ES^+$) 544 ([$^{35,35}$Cl]$MH^+$), 546 ([$^{35,37}$Cl]$MH^+$), 548 ([$^{37,37}$Cl]$MH^+$); HRMS ($ES^+$) Found [$^{35}$Cl]$MH^+$, 544.1296 ($C_{29}H_{24}{}^{35,35}Cl_2N_5O_2$ requires 544.1302).

**(S)-6-chloro-N-(1-(2-(3-cyanophenyl)hydrazineyl)-1-oxo-3-phenylpropan-2-yl)-2-phenylimidazo[1,2-*a*]pyridine-3-carboxamide 44Dd**

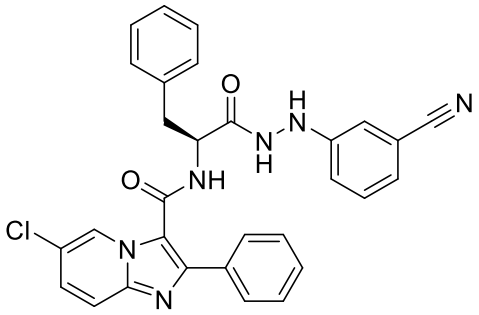

Using the standard procedure provided, *tert*-butyl (S)-(1-(2-(3-cyanophenyl)hydrazineyl)-1-oxo-3-phenylpropan-2-yl)carbamate **51Cb** (0.10 g, 0.37 mmol) was transformed using column chromatography (DCM /EtOAc [1:3]) into the title compound as a white powder (85 mg, 51 %); $R_f$ 0.50 (DCM/EtOAc [1:3]); m.p. 300 – 305 °C; $\nu_{max}$ 3243 (N-H), 2215 (C≡N), 1677 (C=O), 1619 (C=O), 1529, 1493, 1386, 1321, 1226, 1167, 1080, 746, 698, 486 $cm^{-1}$; $\delta_H$ (300 MHz, DMSO-$d_6$) 10.20 (1H, s, CON*H*NH), 8.80 (1H, d, *J* 7, CON*H*CH), 8.61 (1H, dd, *J* 2, 1, Ar-*H*), 8.36 (1H, s, CONHN*H*), 7.71 (1H, d, *J* 9, Ar-*H*), 7.71 – 7.65 (1H, d, *J* 8, Ar-*H*), 7.46 (1H, dd, *J* 9, 2, Ar-*H*), 7.37 – 7.23 (9H, m, Ar-*H*), 7.12 (1H, d, *J* 7, Ar-*H*), 7.00 – 6.92 (2H, m, Ar-*H*), 4.95 (1H, m, CONHC*H*), 3.16 (1H, dd, *J* 13, 4, CONHCHC$H_2$), 2.95 (1H, m, CONHCHC$H_2$); $\delta_C$ (75 MHz, DMSO-$d_6$) 171.4 (*C*ONHNH), 161.0 *(C*ONHCH), 150.1 (*ipso*-Ar-*C)*, 145.6 (*ipso*-Ar-*C)*, 143.2 (*ipso*-Ar-*C)*, 137.7 (*ipso*-Ar-*C)*, 133.3 (*ipso*-Ar-*C)*, 130.5 (Ar-*C)*, 129.6 (Ar-*C)*, 128.9 (Ar-*C)*, 128.8 (Ar-*C)*, 128.5 (Ar-*C)*, 127.8 (Ar-*C)*, 127.1 (Ar-*C)*, 124.6 (Ar-*C)*, 122.3 (Ar-*C*), 120.4 (*ipso*-Ar-*C)*, 119.6 (*ipso*-Ar-*C)*, 118.1 (Ar-*C)*, 117.3 (Ar-*C)*, 116.9 (*ipso*-Ar-*C)*, 114.7 (Ar-*C),* 112.0 (*ipso*-Ar-*C)*, 53.8 (CONH*C*H), 37.4 (CONHCH*C*$H_2$); ***m/z*** ($ES^+$) 535 ([$^{35}$Cl]$MH^+$), 537 ([$^{37}$Cl]$MH^+$); HRMS ($ES^+$) Found [$^{35}$Cl]$MH^+$, 535.1652 ($C_{30}H_{24}{}^{35}ClF_3N_6O_2$ requires 535.1644).

**(S)-6-chloro-N-(1-(2-(4-cyanophenyl)hydrazineyl)-1-oxo-3-phenylpropan-2-yl)-2-phenylimidazo[1,2-*a*]pyridine-3-carboxamide 44De**

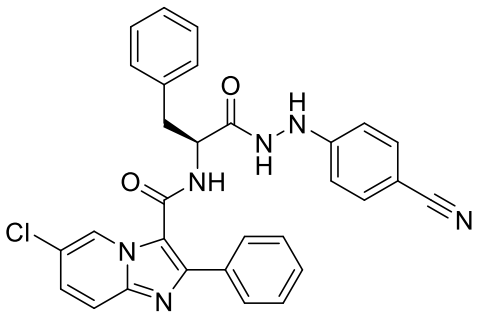

Using the standard procedure provided, *tert*-butyl (S)-(1-(2-(4-cyanophenyl)hydrazineyl)-1-oxo-3-phenylpropan-2-yl)carbamate **51Cc** (0.11 g, 0.30 mmol) was transformed using column chromatography (DCM /EtOAc [1:3]) into the title compound as a white powder (75 mg, 45 %); $R_f$ 0.50 (DCM/EtOAc [1:3]); m.p. 290 – 293 °C; $\nu_{max}$ 3272 (N-H), 2217 (C≡N), 1679 (C=O), 1623 (C=O), 1607, 1493, 1386, 1325, 1278, 1166, 1078, 751, 701, 517 $cm^{-1}$; $\delta_H$ (300 MHz, DMSO-$d_6$) 10.29 (1H, s, CON*H*NH), 8.87 (1H, d, *J* 7, CON*H*CH), 8.74 (1H, s, CONHN*H*), 8.59 (1H, dd, *J* 2, 1, Ar-*H*), 7.73 (1H, d, *J* 9, Ar-*H*), 7.71 – 7.66 (2H, d, *J* 7, Ar-*H*), 7.53 – 7.9 (2H, d, *J* 8, Ar-*H*), 7.46 (1H, dd, *J* 9, 2, Ar-*H*), 7.39 – 7.27 (8H, m, Ar-*H*), 6.73 – 6.66 (2H, d, *J* 8, Ar-*H*), 4.95 (1H, m, CONHC*H*), 3.17 (1H, dd, *J* 13, 4, CONHCHC$H_2$), 2.97 (1H, m, CONHCHC$H_2$); $\delta_C$ (75 MHz, DMSO-$d_6$) 171.3 (*C*ONHNH), 161.0 *(C*ONHCH), 153.1 (*ipso*-Ar-*C)*, 145.6 (*ipso*-Ar-*C)*, 143.2 (*ipso*-Ar-*C)*, 137.6 (*ipso*-Ar-*C)*, 133.8 (*ipso*-Ar-*C)*, 133.3 (Ar-*C)*, 129.6 (Ar-*C)*, 128.9 (Ar-*C)*, 128.8 (Ar-*C)*, 128.5 (Ar-*C)*, 127.8 (Ar-*C)*, 127.1 (Ar-*C)*, 124.6 (Ar-*C)*, 120.4 (*ipso*-Ar-*C)*, 118.2 (Ar-*C)*, 116.9 (*ipso*-Ar-*C)*, 112.2 (*ipso*-Ar-*C)*, 99.4 (*ipso*-Ar-*C)*, 53.8 (CONH*C*H), 37.5 (CONHCH*C*$H_2$); *m/z* ($ES^+$) 535 ([$^{35}$Cl]$MH^+$), 537 ([$^{37}$Cl]$MH^+$); HRMS ($ES^+$) Found [$^{35}$Cl]$MH^+$, 535.1639 ($C_{30}H_{24}{}^{35}ClN_6O_2$ requires 535.1644).

### 6.2.5.3 Third- Series of Imidazo[1,2-*a*]pyridine-3-carboxamides

**(S)-6-chloro-N-(1-(2-(3-chlorophenyl)hydrazineyl)-1-oxo-3-phenylpropan-2-yl)-2-(3-chlorophenyl)imidazo[1,2-*a*]pyridine-3-carboxamide 44Df**

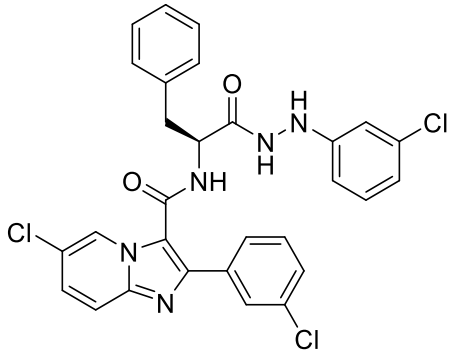


Using the standard procedure provided, (S)-(1-(2-(3-chlorophenyl)hydrazineyl)-1-oxo-3-phenylpropan-2-yl)carbamate **51BI** (0.09 g, 0.23 mmol) was transformed using column chromatography (DCM/EtOAc [3:1]) into the title compound as a white powder (52 mg, 38 %); $R_f$ 0.4 (DCM/EtOAc [3:1]); m.p. 225 - 227 °C; $\nu_{max}$ 3255 (N-H), 2980, 1619 (C=O), 1599, 1538, 1494, 1386, 1298, 1251, 1222, 1175, 1079, 869, 797, 719,

678 $cm^{-1}$; $\delta_H$ (300 MHz, DMSO-$d_6$) 10.17 (1H, d, *J* 2, CON*H*NH), 8.98 (1H, d, *J* 7, CON*H*CH), 8.60 (1H, d, *J* 2, Ar-*H*), 8.14 (1H, d, *J* 2, CONHN*H*), 7.85 (1H, s, Ar-*H*), 7.74 (1H, dd, *J* 9, 1, Ar-*H*), 7.56 (1H, dt, *J* 7, 1, Ar-*H*), 7.48 (1H, dd, *J* 9, 2, Ar-*H*), 7.42 (1H, qd, *J* 7, 1, Ar-*H*), 7.35 – 7.22 (6H, m, Ar-H), 7.12 (1H, t, *J* 8, Ar-H), 6.75 (1H, s, Ar-*H*), 6.71 (1H, d, *J* 8, Ar-H), 6.60 (1H, dd, *J* 8, 1, Ar-*H*), 4.94 (1H, m, CONHC*H*), 3.16 (1H, dd, *J* 13, 4, CONHCHC$H_2$), 2.94 (1H, m, CONHCHC$H_2$); δC (75 MHz, DMSO-$d_6$) 171.3 (*C*ONHNH), 160.7 (CONH*C*H), 151.1 (*ipso*-Ar-*C)*, 143.8 (*ipso*-Ar-*C)*, 143.2 (*ipso*-Ar-*C)*, 137.7 (*ipso*-Ar-*C)*, 133.9 (*ipso*-Ar-*C)*, 133.7 (*ipso*-Ar-*C)*, 130.8 (Ar-*C*), 129.5 (Ar-*C*), 128.8 (Ar-*C*), 128.0 (Ar-*C*), 127.1 (Ar-*C*), 124.7 (Ar-*C*), 120.7 (*ipso*-Ar-*C*), 118.4 (Ar-*C*), 118.3 (Ar-*C*), 117.4 (*ipso*-Ar-*C)*, 112.0 (Ar-*C*), 111.2 (Ar-*C*), 53.8 (C=ONH*C*H), 37.5 (CONHCH*C*$H_2$); *m/z* ($ES^+$) 578 ([$^{35,35,35}$Cl]$MH^+$), 580 ([$^{35,35,37}$Cl]$MH^+$), 582 ([$^{35,37,37}$Cl]$MH^+$), 584 ([$^{37,37,37}$Cl]$MH^+$); HRMS ($ES^+$) Found [$^{35,35,35}$Cl]$MH^+$, 578.0920 ($C_{29}H_{23}{}^{35,35,35}Cl_3F_3N_5O_2$ requires 578.0912).

**(S)-N-(1-(2-(3-bromophenyl)hydrazineyl)-1-oxo-3-phenylpropan-2-yl)-6-chloro-2-(3-chlorophenyl)imidazo[1,2-*a*]pyridine-3-carboxamide 44Dg**

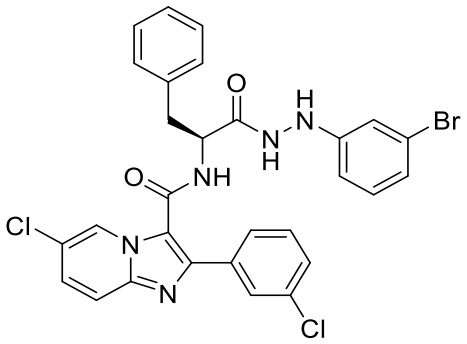


Using the standard procedure provided, (S)-(1-(2-(3-bromophenyl)hydrazineyl)-1-oxo-3-phenylpropan-2-yl)carbamate **51Bn** (0.11 g, 0.27 mmol) was transformed using column chromatography (DCM/EtOAc [3:1]) into the title compound as a white powder (55 mg, 32 %); $R_f$ 0.5 (DCM/EtOAc [3:1]); m.p. 235 - 238 °C; $\nu_{max}$ 3251 (N-H), 2980, 1614 (C=O), 1536, 1486, 1386, 1250, 1152, 1079, 1034, 954, 834, 698 $cm^{-1}$; $\delta_H$ (300 MHz, DMSO-$d_6$) 10.17 (1H, s, CON*H*NH), 8.98 (1H, d, *J* 7, CON*H*CH), 8.61 (1H, s, Ar-*H*), 8.14 (1H, s, CONHN*H*), 7.85 (1H, s, Ar-*H*), 7.75 (1H, dd, *J* 9, 1, Ar-*H*), 7.56 (1H, dt, *J* 7, 1, Ar-*H*), 7.48 (1H, dd, *J* 9, 2, Ar-*H*), 7.42 (1H, qd, *J* 7, 1, Ar-*H*), 7.36 – 7.21 (6H, m, Ar-H), 7.06 (1H, t, *J* 8, Ar-H), 6.92 (1H, s, Ar-*H*), 6.85 (1H, d, *J* 7, Ar-*H*), 6.65 (1H, dd, *J* 7, 2, Ar-*H*), 4.96 (1H, m, CONHC*H*), 3.16 (1H, dd, *J* 13, 4, CONHCHC$H_2$), 2.95 (1H, dd, *J* 13, 10, CONHCHC$H_2$); δC (75 MHz, DMSO-$d_6$) 171.3 (*C*ONHNH), 160.7

(CONH*C*H), 151.2 (*ipso*-Ar-*C)*, 143.8 (*ipso*-Ar-*C)*, 143.2 (*ipso*-Ar-*C)*, 137.7 (*ipso*-Ar-*C)*, 135.4 (*ipso*-Ar-*C)*, 133.7 (*ipso*-Ar-*C)*, 131.1 (Ar-*C*), 130.7 (Ar-*C*), 129.5 (Ar-*C*), 128.8 (Ar-*C*), 128.7 (Ar-*C*), 128.0 (Ar-*C*), 127.1 (Ar-*C*), 127.0 (Ar-*C*), 124.7 (Ar-*C*), 122.5 (Ar-*C*), 121.3 (Ar-*C*), 120.7 (*ipso*-Ar-*C*), 118.3 (Ar-*C*), 117.4 (*ipso*-Ar-*C)*, 114.9 (Ar-*C*), 111.5 (Ar-*C)*, 53.8 (C=ONH*C*H), 37.5 (CONHCH*C*$H_2$); *m/z* ($ES^+$) 622 ([$^{35,35}$Cl, $^{79}$Br]$MH^+$), 624 ([$^{35,35}$Cl, $^{81}$Br]$MH^+$), 626 ([$^{35,37}$Cl, $^{81}$Br]$MH^+$), 628 ([$^{37,37}$Cl, $^{81}$Br]$MH^+$); HRMS ($ES^+$) Found [$^{35,35}$Cl, $^{79}$Br]$MH^+$, 622.0391 ($C_{29}H_{23}{}^{35,35}Cl_2{}^{79}BrN_5O_2$ requires 622.0407).

**(S)-6-chloro-2-(3-chlorophenyl)-N-(1-oxo-3-phenyl-1-(2-(3-(trifluoromethyl)phenyl)hydrazineyl)propan-2-yl)imidazo[1,2-*a*]pyridine-3-carboxamide 44Dh**

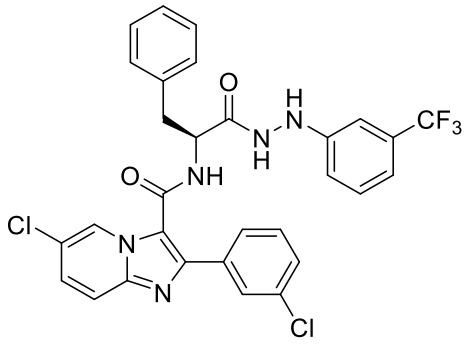


Using the standard procedure provided, (S)-(1-(2-((3-trifluoromethyl)phenyl)hydrazineyl)-1-oxo-3-phenylpropan-2-yl)carbamate **51Bp** (0.11 g, 0.27 mmol) was transformed using column chromatography (DCM/EtOAc [3:1]) into the title compound as a white powder (69 mg, 41 %); $R_f$ 0.4 (DCM/EtOAc [3:1]); m.p. 230 - 235 °C; $\nu_{max}$ 3256 (N-H), 2980, 1615 (C=O), 1486, 1386, 1250, 1153, 1078, 954, 834, 798, 696 $cm^{-1}$; $\delta_H$ (300 MHz, DMSO-$d_6$) 10.26 (1H, s, CON*H*NH), 8.99 (1H, d, *J* 7, CON*H*CH), 8.57 (1H, dd, *J* 2, 1, Ar-*H*), 7.84 (1H, s, Ar-*H*), 7.74 (1H, dd, *J* 9, 1, Ar-*H*), 7.56 (1H, dt, *J* 7, 1, Ar-*H*), 7.47 (1H, dd, *J* 9, 2, Ar-*H*), 7.41 (1H, qd, *J* 7, 1, Ar-*H*), 7.36 – 7.29 (5H, m, Ar-H), 7.29 – 7.20 (2H, t, *J* 7, Ar-H), 7.05 (1H, s, Ar-*H*), 7.01 (1H, d, *J* 7, Ar-H), 6.90 (1H, d, *J* 7, Ar-*H*), 4.96 (1H, m, CONHC*H*), 3.16 (1H, dd, *J* 13, 5, CONHCHC$H_2$), 2.95 (1H, dd, *J* 13, 10, CONHCHC$H_2$); δC (75 MHz, DMSO-$d_6$) 171.3 (*C*=ONHNH), 160.6 (*C*=ONHCH), 151.1 (*ipso*-Ar-*C)*, 143.8 (*ipso*-Ar-*C)*, 143.2 (*ipso*-Ar-*C)*, 137.7 (*ipso*-Ar-*C)*, 135.4 (*ipso*-Ar-*C)*, 133.7 (*ipso*-Ar-*C)*, 130.7 (Ar-*C*), 130.3 (Ar-*C*), 129.5 (Ar-*C*), 128.8 (Ar-*C*), 128.7 (Ar-*C*), 128.1 (Ar-*C*), 127.1 (Ar-*C*), 127.0 (Ar-*C*), 124.7 (Ar-*C*), 120.7 (*ipso*-Ar-*C*), 118.3 (Ar-*C*), 117.4 (*ipso*-Ar-*C)*, 116.1 (Ar-*C)*, 115.0

(Ar-*C*), 108.5 (Ar-*C)*, 53.8 (CONH*C*H), 37.5 (CONHCH*C*$H_2$); $\delta_F$ (282 MHz, DMSO-$d_6$) -61.2 (C*F*$_3$); *m/z* (ES$^+$) 612 ([$^{35,35}$Cl]MH$^+$), 614 ([$^{35,37}$Cl]MH$^+$), 616 ([$^{37,37}$Cl]MH$^+$); HRMS (ES$^+$) Found [$^{35,35}$Cl]MH$^+$, 612.1191 ($C_{30}H_{23}{}^{35,35}Cl_2F_3N_5O_2$ requires 612.1175).

**(S)-6-chloro-2-(3-chlorophenyl)-N-(1-oxo-3-phenyl-1-(2-(3-(trifluoromethoxy)phenyl)hydrazineyl)propan-2-yl)imidazo[1,2-*a*]pyridine-3-carboxamide 44Di**

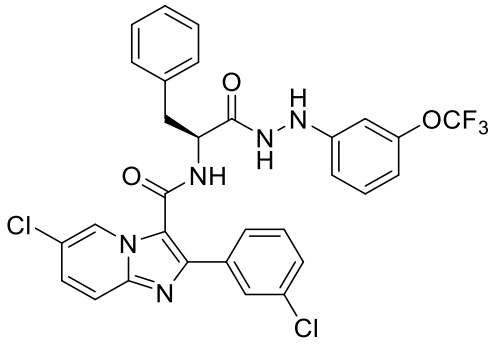


Using the standard procedure provided, (S)-(1-(2-((3-trifluoromethoxy)phenyl)hydrazineyl)-1-oxo-3-phenylpropan-2-yl)carbamate **51Br** (0.12 g, 0.27 mmol) was transformed using column chromatography (DCM/EtOAc [3:1]) into the title compound as a white powder (56 mg, 33 %); $R_f$ 0.5 (DCM/EtOAc [3:1]); m.p. 235 - 238 °C; $\nu_{max}$ 3248 (N-H), 2980, 1613 (C=O), 1492, 1386, 1251, 1152, 1078, 1035, 955, 793, 678 cm$^{-1}$; $\delta_H$ (300 MHz, DMSO-$d_6$) 10.21 (1H, s, CON*H*NH), 9.00 (1H, d, *J* 7, CON*H*CH), 8.58 (1H, dd, *J* 2, 1, Ar-*H*), 7.85 (1H, s, Ar-*H*), 7.74 (1H, dd, *J* 9, 1, Ar-*H*), 7.56 (1H, dt, *J* 7, 1, Ar-*H*), 7.48 (1H, dd, *J* 9, 2, Ar-*H*), 7.42 (1H, qd, *J* 7, 1, Ar-*H*), 7.36 – 7.27 (5H, m, Ar-H), 7.24 (1H, d, *J* 8, Ar-H), 7.19 (1H, d, *J* 8, Ar-H), 6.71 – 6.58 (3H, m, Ar-*H*), 4.95 (1H, m, CONHC*H*), 3.17 (1H, dd, *J* 13, 4, CONHCHC*H*$_2$), 2.94 (1H, dd, *J* 13, 10, CONHCHC*H*$_2$); δC (75 MHz, DMSO-$d_6$) 171.3 (*C*ONHNH), 160.7 (*C*ONHCH), 151.4 (*ipso*-Ar-*C)*, 149.7 (Ar-OCF$_3$), 143.7 (*ipso*-Ar-*C)*, 143.2 (*ipso*-Ar-*C)*, 137.6 (*ipso*-Ar-*C)*, 135.3 (*ipso*-Ar-*C)*, 133.7 (*ipso*-Ar-*C)*, 130.7 (Ar-*C*), 129.5 (Ar-*C*), 128.8 (Ar-*C*), 128.7 (Ar-*C*), 128.0 (Ar-*C*), 127.1 (Ar-*C*), 124.7 (Ar-*C*), 120.7 (*ipso*-Ar-*C*), 118.2 (Ar-*C*), 117.5 (*ipso*-Ar-*C)*, 111.3 (*ipso*-Ar-*C)*, 110.5 (Ar-*C*), 104.5 (Ar-*C*), 53.8 (CONH*C*H), 37.5 (CONHCH*C*$H_2$); $\delta_F$ (282 MHz, DMSO-$d_6$) -56.4 (OC*F*$_3$); *m/z* (ES$^+$) 628 ([$^{35,35}$Cl]MH$^+$), 630 ([$^{35,37}$Cl]MH$^+$), 632 ([$^{37,37}$Cl]MH$^+$); HRMS (ES$^+$) Found [$^{35,35}$Cl]MH$^+$, 628.1138 ($C_{30}H_{23}{}^{35,35}Cl_2F_3N_5O_3$ requires 628.1125).

**(S)-6-chloro-2-(4-chlorophenyl)-N-(1-(2-(3-chlorophenyl)hydrazineyl)-1-oxo-3-phenylpropan-2-yl)imidazo[1,2-*a*]pyridine-3-carboxamide 44Dj**

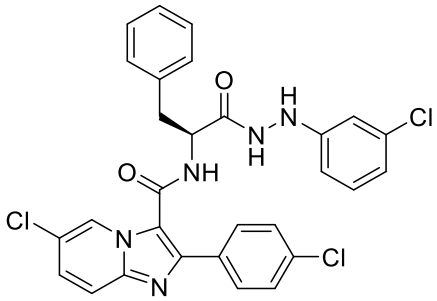

Using the standard procedure provided, (S)-(1-(2-(3-chlorophenyl)hydrazineyl)-1-oxo-3-phenylpropan-2-yl)carbamate **51BI** (0.10 g, 0.33 mmol) was transformed using column chromatography (DCM/EtOAc [3:1]) into the title compound as a white powder (49 mg, 30 %); $R_f$ 0.4 (DCM/EtOAc [3:1]); m.p. 230 - 234 °C; $\nu_{max}$ 3245 (N-H), 2981, 1621 (C=O), 1475, 1386, 1230, 1167, 1110, 833, 697 $cm^{-1}$; $\delta_H$ (300 MHz, DMSO-$d_6$) 10.18 (1H, d, *J* 2, CON*H*NH), 8.96 (1H, d, *J* 7, CON*H*CH), 8.53 (1H, d, *J* 2, Ar-*H*), 8.17 (1H, d, *J* 2, CONHN*H*), 7.73 (1H, dd, *J* 9, 1, Ar-*H*), 7.70 – 7.62 (2H, d, *J* 8, Ar-*H*), 7.47 (1H, dd, *J* 9, 2, Ar-*H*), 7.38 – 7.29 (5H, m, Ar-H), 7.29 – 7.22 (2H, d, *J* 8, Ar-*H*), 7.12 (1H, t, *J* 8, Ar-H), 6.77 (1H, s, Ar-*H*), 6.72 (1H, d, *J* 8, Ar-*H*), 6.64 (1H, d, *J* 8, Ar-*H*), 4.93 (1H, m, CONHC*H*), 3.16 (1H, dd, *J* 13, 4, CONHCHC$H_2$), 2.93 (1H, dd, *J* 13, 10, CONHCHC$H_2$); δC (75 MHz, DMSO-$d_6$) 171.4 (*C*ONHNH), 160.9 (*C*ONHCH), 151.1 (*ipso*-Ar-*C)*, 143.2 (*ipso*-Ar-*C)*, 137.8 (*ipso*-Ar-*C)*, 134.0 (*ipso*-Ar-*C)*, 132.1 (*ipso*-Ar-*C)*, 130.8 (Ar-*C*), 130.1 (Ar-*C*), 129.6 (Ar-*C*), 128.9 (Ar-*C*), 128.8 (Ar-*C*), 128.0 (Ar-*C*), 127.0 (Ar-*C*), 124.6 (Ar-*C*), 120.6 (*ipso*-Ar-*C*), 118.4 (Ar-*C*), 118.1 (Ar-*C*), 112.0 (Ar-*C*), 111.3 (Ar-*C*), 53.8 (CONH*C*H), 37.4 (CONHCH*C*$H_2$); *m/z* ($ES^+$) 578 ([$^{35,35,35}$Cl]$MH^+$), 580 ([$^{35,35,37}$Cl]$MH^+$), 582 ([$^{35,37,37}$Cl]$MH^+$), 584 ([$^{37,37,37}$Cl]$MH^+$); HRMS ($ES^+$) Found [$^{35,35,35}$Cl]$MH^+$, 578.0920 ($C_{29}H_{23}{}^{35,35,35}Cl_3N_5O_2$ requires 578.0912).

**(S)-N-(1-(2-(3-bromophenyl)hydrazineyl)-1-oxo-3-phenylpropan-2-yl)-6-chloro-2-(4-chlorophenyl)imidazo[1,2-*a*]pyridine-3-carboxamide 44Dk**

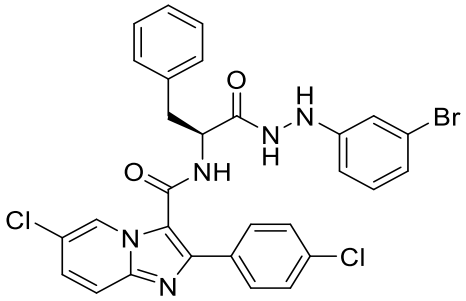

Using the standard procedure provided, (S)-(1-(2-(3-bromophenyl)hydrazineyl)-1-oxo-3-phenylpropan-2-yl)carbamate **51Bn** (0.12 g, 0.28 mmol) was transformed using column chromatography (DCM/EtOAc [3:1]) into the title compound as a white powder (81 mg, 46 %); $R_f$ 0.5 (DCM/EtOAc [3:1]); m.p. 235 - 238 °C; $\nu_{max}$ 3236 (N-H), 2981, 1664 (C=O), 1620 (C=O), 1593, 1474, 1386, 1323, 1229, 1166, 1110, 1091, 832, 698 $cm^{-1}$; $\delta_H$ (300 MHz, DMSO-$d_6$) 10.20 (1H, s, CON*H*NH), 8.97 (1H, d, *J* 8, CON*H*CH), 8.53 (1H, dd, *J* 2, 1, Ar-*H*), 8.16 (1H, bs, CONHN*H*), 7.74 (1H, dd, *J* 9, 1, Ar-*H*), 7.70 – 7.63 (2H, d, *J* 8, Ar-*H*), 7.47 (1H, dd, *J* 9, 2, Ar-*H*), 7.36 – 7.30 (5H, m, Ar-H), 7.30 – 7.25 (2H, d, *J* 8, Ar-*H*), 7.07 (1H, t, *J* 8, Ar-H), 6.94 (1H, s, Ar-*H*), 6.87 (1H, dd, *J* 8, 1, Ar-*H*), 6.68 (1H, dd, *J* 8, 1, Ar-*H*), 4.95 (1H, m, CONHC*H*), 3.17 (1H, dd, *J* 13, 4, CONHCHC$H_2$), 2.95 (1H, dd, *J* 13, 10, CONHCHC$H_2$); δC (75 MHz, DMSO-$d_6$) 171.3 (*C*=ONHNH), 160.8 (*C*=ONHCH), 151.2 (*ipso*-Ar-*C)*, 144.3 (*ipso*-Ar-*C)*, 143.2 (*ipso*-Ar-*C)*, 137.8 (*ipso*-Ar-*C)*, 133.5 (*ipso*-Ar-*C)*, 132.1 (*ipso*-Ar-*C)*, 131.1 (Ar-*C*), 130.1 (Ar-*C*), 129.6 (Ar-*C*), 128.8 (Ar-*C*), 128.0 (Ar-*C*), 127.1 (Ar-*C*), 124.6 (Ar-*C*), 122.6 (*ipso*-Ar-*C)*, 121.3 (Ar-*C*), 120.6 (*ipso*-Ar-*C*), 118.2 (Ar-*C*), 117.1 (*ipso*-Ar-*C*), 114.9 (Ar-*C*), 111.6 (Ar-*C*), 53.8 (C=ONH*C*H), 37.4 (C=ONHCH*C*$H_2$); *m/z* ($ES^+$) 622 ([$^{35,35}$Cl, $^{79}$Br]$MH^+$), 624 ([$^{35,35}$Cl, $^{81}$Br]$MH^+$), 626 ([$^{35,37}$Cl, $^{81}$Br]$MH^+$), 628 ([$^{37,37}$Cl, $^{81}$Br]$MH^+$); HRMS ($ES^+$) Found [$^{35,35}$Cl, $^{79}$Br]$MH^+$, 622.0408 ($C_{29}H_{23}{}^{35,35}Cl_2{}^{79}BrN_5O_2$ requires 622.0407).

**(S)-6-chloro-2-(4-chlorophenyl)-N-(1-oxo-3-phenyl-1-(2-(3-(trifluoromethyl)phenyl)hydrazineyl)propan-2-yl)imidazo[1,2-*a*]pyridine-3-carboxamide 44Dl**

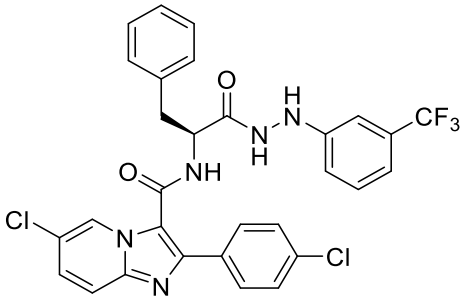

Using the standard procedure provided, (S)-(1-(2-((3-trifluoromethyl)phenyl)hydrazineyl)-1-oxo-3-phenylpropan-2-yl)carbamate **51Bp** (0.12 g, 0.38 mmol) was transformed using column chromatography (DCM/EtOAc [3:1]) into the title compound as a white powder (92 mg, 53 %); $R_f$ 0.4 (DCM/EtOAc [3:1]); m.p. 235 - 240 °C; $\nu_{max}$ 3263 (N-H), 2981, 1624 (C=O), 1614, 1532, 1493, 1384, 1231, 1172, 1072, 951, 694 $cm^{-1}$; $\delta_H$ (300 MHz, DMSO-$d_6$) 10.27 (1H, s, CON*H*NH), 8.97 (1H, d, *J* 8, CON*H*CH), 8.51 (1H, dd, *J* 2, 1, Ar-*H*), 8.31 (1H, s, CONHN*H*), 7.73 (1H, dd, *J* 9, 1, Ar-*H*), 7.69 – 7.61 (2H, d, *J* 8, Ar-*H*), 7.46 (1H, dd, *J* 9, 2, Ar-*H*), 7.34 – 7.29 (5H, m, Ar-*H*), 7.27 – 7.23 (2H, d, *J* 8, Ar-*H*), 7.07 (1H, s, Ar-*H*), 7.02 (1H, d, *J* 7, Ar-*H*), 6.93 (1H, d, *J* 7, Ar-*H*), 4.96 (1H, m, CONHC*H*), 3.17 (1H, dd, *J* 13, 4, CONHCHC$H_2$), 2.95 (1H, dd, *J* 13, 10, CONHCHC$H_2$); δC (75 MHz, DMSO-$d_6$) 171.4 (*C*ONHNH), 160.9 (*C*ONHCH), 150.2 (*ipso*-Ar-*C)*, 144.3 (*ipso*-Ar-*C)*, 143.2 (*ipso*-Ar-*C)*, 137.8 (*ipso*-Ar-*C)*, 133.5 (*ipso*-Ar-*C)*, 132.1 (*ipso*-Ar-*C)*, 130.3 (Ar-*C*), 130.1 (Ar-*C*), 129.6 (Ar-*C*), 128.8 (Ar-*C*), 128.0 (Ar-*C*), 127.0 (Ar-*C*), 124.6 (Ar-*C*), 120.6 (*ipso*-Ar-*C)*, 118.2 (Ar-*C*), 117.1 (*ipso*-Ar-*C*), 116.1 (Ar-*C*), 115.1 (Ar-*C*), 108.5 (Ar-*C*), 53.9 (CONH*C*H), 37.4 (CONHCH*C*$H_2$); $\delta_F$ (282 MHz, DMSO-$d_6$) -61.3 (C*F*$_3$); *m/z* ($ES^+$) 612 ([$^{35,35}$Cl]$MH^+$), 614 ([$^{35,37}$Cl]$MH^+$), 616 ([$^{37,37}$Cl]$MH^+$); HRMS ($ES^+$) Found [$^{35,35}$Cl]$MH^+$, 612.1180 ($C_{30}H_{23}{}^{35,35}Cl_2F_3N_5O_2$ requires 612.1175).

**(S)-6-chloro-2-(4-chlorophenyl)-N-(1-oxo-3-phenyl-1-(2-(3-(trifluoromethoxy)phenyl)hydrazineyl)propan-2-yl)imidazo[1,2-*a*]pyridine-3-carboxamide 44Dm**

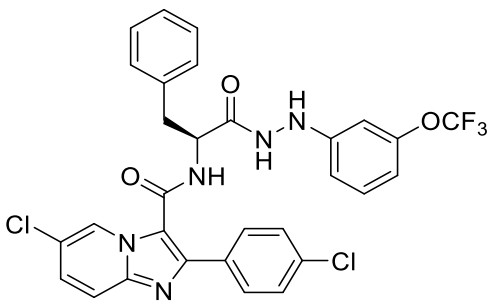

Using the standard procedure provided, (S)-(1-(2-((3-trifluoromethoxy)phenyl)hydrazineyl)-1-oxo-3-phenylpropan-2-yl)carbamate **51Br** (0.12 g, 0.27 mmol) was transformed using column chromatography (DCM/EtOAc [3:1]) into the title compound as a white powder (80 mg, 47 %); $R_f$ 0.5 (DCM/EtOAc [3:1]); m.p. 240 - 245 °C; $\nu_{max}$ 3252 (N-H), 2981, 1620 (C=O), 1531, 1493, 1386, 1254, 1151, 1090, 835, 796, 696 $cm^{-1}$; $\delta_H$ (300 MHz, DMSO-$d_6$) 10.25 (1H, s, CON*H*NH), 8.99 (1H, d, *J* 8, CON*H*CH), 8.52 (1H, dd, *J* 2, 1, Ar-*H*), 8.30 (1H, bs, CONHN*H*), 7.74 (1H, dd, *J* 9, 1, Ar-*H*), 7.70 – 7.64 (2H, d, *J* 8, Ar-*H*), 7.47 (1H, dd, *J* 9, 2, Ar-*H*), 7.38 – 7.31 (5H, m, Ar-H), 7.30 – 7.26 (2H, d, *J* 8, Ar-*H*), 7.22 (1H, d, *J* 8, Ar-H), 6.72 – 6.58 (3H, m, Ar-*H*), 4.96 (1H, m, CONHC*H*), 3.18 (1H, dd, *J* 13, 4, CONHCHC$H_2$), 2.95 (1H, dd, *J* 13, 10, CONHCHC$H_2$); δC (75 MHz, DMSO-$d_6$) 171.4 (*C*ONHNH), 160.9 (*C*ONHCH), 151.4 (*ipso*-Ar-*C)*, 149.8 (*ipso*-Ar-*C)*, 144.2 (*ipso*-Ar-*C)*, 143.2 (*ipso*-Ar-*C)*, 137.8 (*ipso*-Ar-*C)*, 133.5 (*ipso*-Ar-*C)*, 132.1 (*ipso*-Ar-*C)*, 130.8 (Ar-*C*), 130.1 (Ar-*C*), 129.6 (Ar-*C*), 128.9 (Ar-*C*), 128.8 (Ar-*C*), 128.0 (Ar-*C*), 127.0 (Ar-*C*), 124.6 (Ar-*C*), 120.6 (*ipso*-Ar-*C*), 118.2 (Ar-*C*), 117.2 (*ipso*-Ar-*C*), 111.3 (Ar-*C*), 110.5 (Ar-*C*), 104.5 (Ar-*C*), 53.9 (CONH*C*H), 37.4 (CONHCH*C*$H_2$); $\delta_F$ (282 MHz, DMSO-$d_6$) -56.4 (OC*F*$_3$); *m/z* ($ES^+$) 628 ([$^{35,35}$Cl]$MH^+$), 630 ([$^{35,37}$Cl]$MH^+$), 632 ([$^{37,37}$Cl]$MH^+$); HRMS ($ES^+$) Found [$^{35,35}$Cl]$MH^+$, 628.1126 ($C_{30}H_{23}{}^{35,35}Cl_2F_3N_5O_3$ requires 628.1125).

**(S)-6-chloro-N-(1-(2-(3-chlorophenyl)hydrazineyl)-1-oxo-3-phenylpropan-2-yl)-2-(3-(trifluoromethyl)phenyl)imidazo[1,2-*a*]pyridine-3-carboxamide 44Dn**

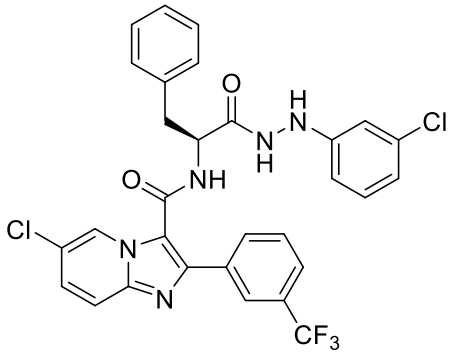


Using the standard procedure provided, (S)-(1-(2-(3-chlorophenyl)hydrazineyl)-1-oxo-3-phenylpropan-2-yl)carbamate **51Bl** (0.09 g, 0.23 mmol) was transformed using column chromatography (DCM/EtOAc [3:1]) into the title compound as a white powder (55 mg, 39 %); $R_f$ 0.3 (DCM/EtOAc [3:1]); m.p. 240 - 242 °C; $\nu_{max}$ 3266 (N-H), 2981,

1668 (C=O), 1615 (C=O), 1530, 1496, 1380, 1324, 1229, 1159, 1118, 1075, 810, 748, 700 $cm^{-1}$; $\delta_H$ (300 MHz, DMSO-$d_6$) 10.17 (1H, s, CON*H*NH), 9.09 (1H, d, *J* 7, CON*H*CH), 8.60 (1H, d, *J* 2, Ar-*H*), 8.18 (1H, s, Ar-*H*), 8.15 (1H, s, CONHN*H*), 7.86 (1H, d, *J* 8, Ar-*H*), 7.78 (1H, dd, *J* 9, 1, Ar-*H*), 7.72 (1H, d, *J* 8, Ar-*H*), 7.50 (1H, dd, *J* 9, 2, Ar-*H*), 7.43 (1H, t, *J* 8, Ar-*H*), 7.36 – 7.25 (5H, m, Ar-H), 7.11 (1H, t, *J* 7, Ar-H), 6.76 (1H, s, Ar-*H*), 6.72 (1H, d, *J* 7, Ar-H), 6.62 (1H, d, *J* 7, Ar-H), 4.96 (1H, m, CONHC*H*), 3.16 (1H, dd, *J* 13, 4, CONHCHC$H_2$), 2.94 (1H, dd, *J* 13, 10, CONHCHC$H_2$); δC (75 MHz, DMSO-$d_6$) 171.3 (*C*ONHNH), 160.7 (*C*ONHCH), 151.0 (*ipso*-Ar-*C)*, 143.7 (Ar-*C*$F_3$), 143.3 (*ipso*-Ar-*C)*, 137.7 (*ipso*-Ar-*C)*, 134.4 (*ipso*-Ar-*C)*, 133.9 (*ipso*-Ar-*C)*, 132.2 (Ar-*C*), 130.8 (Ar-*C*), 130.0 (Ar-*C*), 129.5 (Ar-*C*), 128.8 (Ar-*C*), 128.3 (Ar-*C*), 127.1 (Ar-*C*), 125.4 (Ar-*C*), 124.8 (Ar-*C*), 124.5 (Ar-*C*), 120.8 (*ipso*-Ar-*C*), 118.4 (Ar-*C*), 117.6 (*ipso*-Ar-*C*), 112.0 (Ar-*C*), 111.2 (Ar-*C*), 53.8 (CONH*C*H), 37.4 (CONHCH*C*$H_2$); $\delta_F$ (282 MHz, DMSO-$d_6$) -61.2 (C*F*$_3$); *m/z* ($ES^+$) 612 ([$^{35,35}$Cl]$MH^+$), 614 ([$^{35,37}$Cl]$MH^+$), 616 ([$^{37,37}$Cl]$MH^+$); HRMS ($ES^+$) Found [$^{35,35}$Cl]$MH^+$, 612.1193 ($C_{30}H_{23}{}^{35,35}Cl_2F_3N_5O_2$ requires 612.1175).

**(S)-N-(1-(2-(3-bromophenyl)hydrazineyl)-1-oxo-3-phenylpropan-2-yl)-6-chloro-2-(3-(trifluoromethyl)phenyl)imidazo[1,2-*a*]pyridine-3-carboxamide 44Do**

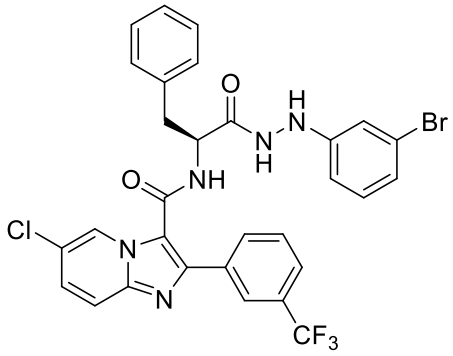


Using the standard procedure provided, (S)-(1-(2-(3-bromophenyl)hydrazineyl)-1-oxo-3-phenylpropan-2-yl)carbamate **51Bn** (0.09 g, 0.20 mmol) was transformed using column chromatography (DCM/EtOAc [3:1]) into the title compound as a white powder (50 mg, 37 %); $R_f$ 0.3 (DCM/EtOAc [3:1]); m.p. 245 - 248 °C; $\nu_{max}$ 3263 (N-H), 2981, 1669 (C=O), 1615 (C=O), 1532, 1495, 1382, 1333, 1228, 1162, 1114, 876, 746, 696 $cm^{-1}$; $\delta_H$ (300 MHz, DMSO-$d_6$) 10.19 (1H, s, CON*H*NH), 9.08 (1H, d, *J* 7, CON*H*CH), 8.60 (1H, s, Ar-*H*), 8.19 (1H, s, CONHN*H*), 8.15 (1H, s, Ar-*H*), 7.86 (1H, d, *J* 7, Ar-*H*), 7.78 (1H, d, *J* 9, Ar-*H*), 7.72 (1H, d, *J* 7, Ar-*H*), 7.50 (1H, dd, *J* 9, 2, Ar-*H*), 7.43 (1H, t,

*J* 7, Ar-*H*), 7.34 – 7.23 (5H, m, Ar-H), 7.06 (1H, t, *J* 8, Ar-H), 6.92 (1H, s, Ar-*H*), 6.86 (1H, d, *J* 8, Ar-H), 6.65 (1H, d, *J* 8, Ar-H), 4.96 (1H, m, CONHC*H*), 3.16 (1H, dd, *J* 14, 4, CONHCHC$H_2$), 2.92 (1H, dd, *J* 14, 10, CONHCHC$H_2$); δC (75 MHz, DMSO-$d_6$) 171.3 (*C*ONHNH), 160.7 (*C*ONHCH), 151.2 (*ipso*-Ar-*C)*, 143.3 (*ipso*-Ar-*C)*, 137.7 (*ipso*-Ar-*C)*, 134.4 (*ipso*-Ar-*C)*, 132.2 (Ar-*C*), 131.1, 130.0 (Ar-*C*), 129.5 (Ar-*C*), 128.8 (Ar-*C*), 128.3 (Ar-*C*), 127.1 (Ar-*C*), 124.8 (Ar-*C*), 122.5 (*ipso*-Ar-*C)*, 121.3 (Ar-*C*), 120.8 (*ipso*-Ar-*C*), 118.2 (Ar-*C*), 117.6 (*ipso*-Ar-*C*), 114.9 (Ar-*C*), 111.5 (Ar-*C*), 53.8 (CONHC*H*), 37.5 (CONHCH*C*$H_2$); $\delta_F$ (282 MHz, DMSO-$d_6$) -61.2 (C*F*$_3$); *m/z* ($ES^+$) 656 ([$^{35}$Cl, $^{79}$Br]$MH^+$), 658 ([$^{35}$Cl, $^{81}$Br]$MH^+$), 658 ([$^{37}$Cl, $^{79}$Br]$MH^+$), 660 ([$^{37}$Cl, $^{81}$Br]$MH^+$); HRMS ($ES^+$) Found ([$^{35}$Cl, $^{79}$Br]$MH^+$), 656.0681 ($C_{30}H_{23}{}^{35}Cl{}^{79}BrF_3N_5O_2$ requires 656.0670).

**(S)-6-chloro-N-(1-oxo-3-phenyl-1-(2-(3-(trifluoromethyl)phenyl)hydrazineyl)propan-2-yl)-2-(3-(trifluoromethyl)phenyl)imidazo[1,2-*a*]pyridine-3-carboxamide 44Dp**

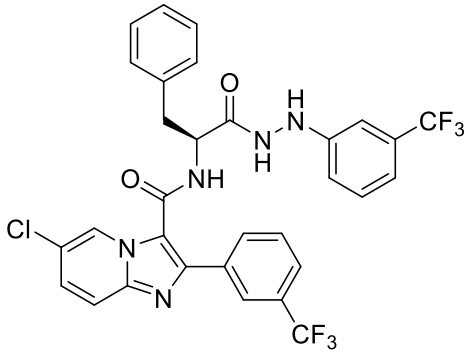

Using the standard procedure provided, (S)-(1-(2-(3-chlorophenyl)hydrazineyl)-1-oxo-3-phenylpropan-2-yl)carbamate **51Bp** (0.10 g, 0.23 mmol) was transformed using column chromatography (DCM/EtOAc [3:1]) into the title compound as a white powder (75 mg, 49 %); $R_f$ 0.3 (DCM/EtOAc [3:1]); m.p. 242 - 245 °C; $\nu_{max}$ 3271 (N-H), 2981, 1669 (C=O), 1620 (C=O), 1530, 1494, 1383, 1327, 1232, 1167, 1125, 956, 694 cm$^{-1}$; $\delta_H$ (300 MHz, DMSO-$d_6$) 10.27 (1H, d, *J* 2, CON*H*NH), 9.09 (1H, d, *J* 7, CON*H*CH), 8.57 (1H, d, *J* 2, Ar-*H*), 8.32 (1H, d, *J* 2, CONHN*H*), 8.19 (1H, s, Ar-*H*), 7.86 (1H, d, *J* 8, Ar-*H*), 7.78 (1H, dd, *J* 9, 1, Ar-*H*), 7.72 (1H, d, *J* 8, Ar-*H*), 7.50 (1H, dd, *J* 9, 2, Ar-*H*), 7.43 (1H, t, *J* 8, Ar-*H*), 7.36 – 7.30 (5H, m, Ar-H), 7.28 (1H, m, Ar-H), 7.06 (1H, s, Ar-*H*), 7.02 (1H, d, *J* 8, Ar-H), 6.90 (1H, d, *J* 8, Ar-H), 4.98 (1H, m, CONHC*H*), 3.17 (1H, dd, *J* 13, 4, CONHCHC$H_2$), 2.94 (1H, dd, *J* 13, 10,

CONHCHC$H_2$); δC (75 MHz, DMSO-$d_6$) 171.4 (*C*ONHNH), 160.7 (*C*ONHCH), 150.1 (*ipso*-Ar-*C)*, 143.7 (Ar-*C*$F_3$), 143.3 (*ipso*-Ar-*C)*, 137.7 (*ipso*-Ar-*C)*, 134.4 (*ipso*-Ar-*C)*, 132.2 (Ar-*C*), 130.3 (Ar-*C*), 130.0 (Ar-*C*), 129.9 (Ar-*C*), 129.5 (Ar-*C*), 128.8 (Ar-*C*), 128.2 (Ar-*C*), 127.1 (Ar-*C*), 125.3 (Ar-*C*), 124.7 (Ar-*C*), 120.8 (*ipso*-Ar-*C*), 118.3 (Ar-*C*), 117.6 (*ipso*-Ar-*C*), 116.1 (Ar-*C*), 115.0 (Ar-*C*), 108.5 (Ar-*C*), 53.9 (CONH*C*H), 37.4 (CONHCH*C*$H_2$); $\delta_F$ (282 MHz, DMSO-$d_6$) -61.2 (C*F*$_3$), -61.3 (C*F*$_3$); ***m/z*** (ES$^+$) 646 ([$^{35}$Cl]MH$^+$), 648 ([$^{37}$Cl]MH$^+$); HRMS (ES$^+$) Found [$^{35}$Cl]MH$^+$, 646.1452 ($C_{31}H_{23}{}^{35}ClF_6N_5O_2$ requires 646.1439).

**(S)-6-chloro-N-(1-oxo-3-phenyl-1-(2-(3-(trifluoromethoxy)phenyl)hydrazineyl)propan-2-yl)-2-(3-(trifluoromethyl)phenyl)imidazo[1,2-*a*]pyridine-3-carboxamide 44Dq**

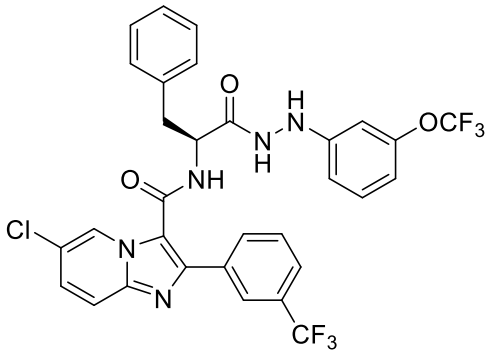


Using the standard procedure provided, (S)-(1-(2-(3-trifluoromethoxy phenyl)hydrazineyl)-1-oxo-3-phenylpropan-2-yl)carbamate **51Br** (0.09 g, 0.20 mmol) was transformed using column chromatography (DCM/EtOAc [3:1]) into the title compound as a white powder (55 mg, 41 %); $R_f$ 0.4 (DCM/EtOAc [3:1]); m.p. 255 - 257 °C; $\nu_{max}$ 3262 (N-H), 2981, 1615 (C=O), 1531, 1495, 1382, 1326, 1256, 1164, 957, 843, 698 cm$^{-1}$; $\delta_H$ (300 MHz, DMSO-$d_6$) 10.23 (1H, bs, CON*H*NH), 9.12 (1H, d, *J* 7, CON*H*CH), 8.58 (1H, s, Ar-*H*), 8.27 (1H, s, CONHN*H*), 8.19 (1H, s, Ar-*H*), 7.86 (1H, d, *J* 7, Ar-*H*), 7.77 (1H, d, *J* 9, Ar-*H*), 7.72 (1H, d, *J* 7, Ar-*H*), 7.50 (1H, dd, *J* 9, 2, Ar-*H*), 7.44 (1H, t, *J* 7, Ar-*H*), 7.36 – 7.25 (5H, m, Ar-H), 7.21 (1H, t, *J* 8, Ar-H), 6.72 – 6.56 (3H, m, Ar-*H*), 4.98 (1H, m, CONHC*H*), 3.15 (1H, dd, *J* 13, 4, CONHCHC*H*$_2$), 2.94 (1H, dd, *J* 13, 10, CONHCHC*H*$_2$); δC (75 MHz, DMSO-$d_6$) 171.4 (*C*ONHNH), 160.7 (*C*ONHCH), 151.4 (*ipso*-Ar-*C)*, 149.8 (Ar-*OC*$F_3$*)*, 143.6 (Ar-*C*$F_3$), 143.3 (*ipso*-Ar-*C)*, 137.6 (*ipso*-Ar-*C)*, 134.3 (*ipso*-Ar-*C)*, 132.2 (Ar-*C*), 130.8 (Ar-*C*), 130.0 (Ar-*C*), 129.5 (Ar-*C*), 128.8 (Ar-*C*), 128.2 (Ar-*C*), 127.1 (Ar-*C*), 125.3 (Ar-*C*), 124.7 (Ar-*C*), 120.7

(*ipso*-Ar-*C*), 118.3 (Ar-*C*), 117.6 (*ipso*-Ar-*C*), 111.3 (*ipso*-Ar-*C*), 110.5 (Ar-*C*), 104.5 (Ar-*C*), 53.8 (CONH*C*H), 37.5 (CONHCH*C*$H_2$); $\delta_F$ (282 MHz, DMSO-$d_6$) -56.4 (OC*F*$_3$), -61.2 (C*F*$_3$); *m/z* (ES$^+$) 662 ([$^{35}$Cl]MH$^+$), 664 ([$^{37}$Cl]MH$^+$); HRMS (ES$^+$) Found [$^{35}$Cl]MH$^+$, 662.1387 ($C_{31}H_{23}{}^{35}ClF_6N_5O_3$ requires 662.1388).

**(S)-6-chloro-N-(1-(2-(3-chlorophenyl)hydrazineyl)-1-oxo-3-phenylpropan-2-yl)-2-(4-(trifluoromethyl)phenyl)imidazo[1,2-*a*]pyridine-3-carboxamide 44Dr**

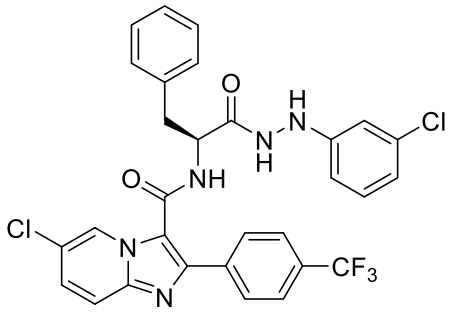


Using the standard procedure provided, (S)-(1-(2-(3-chlorophenyl)hydrazineyl)-1-oxo-3-phenylpropan-2-yl)carbamate **51BI** (0.09 g, 0.24 mmol) was transformed using column chromatography (DCM/EtOAc [3:1]) into the title compound as a white powder (73 mg, 49 %); $R_f$ 0.4 (DCM/EtOAc [3:1]); m.p. 235 - 238 °C; $\nu_{max}$ 3266 (N-H), 2980, 1668 (C=O), 1618 (C=O), 1530, 1493, 1383, 1327, 1252, 1227, 1160, 1110, 1069, 954, 699 cm$^{-1}$; $\delta_H$ (300 MHz, DMSO-$d_6$) 10.21 (1H, d, *J* 2, CON*H*NH), 9.15 (1H, d, *J* 7, CON*H*CH), 8.47 (1H, dd, *J* 2, 1, Ar-*H*), 8.18 (1H, d, *J* 2, CONHN*H*), 7.91 – 7.83 (2H, d, *J* 7, Ar-*H*), 7.76 (1H, dd, *J* 9, 1, Ar-*H*), 7.57 – 7.51 (2H, d, *J* 7, Ar-*H*), 7.48 (1H, dd, *J* 9, 2, Ar-*H*), 7.37 – 7.23 (5H, m, Ar-H), 7.13 (1H, t, *J* 8, Ar-H), 6.79 (1H, s, Ar-*H*), 6.72 (1H, dd, *J* 8, 2, Ar-*H*), 6.66 (1H, dd, *J* 8, 2, Ar-*H*), 4.96 (1H, m, CONHC*H*), 3.18 (1H, dd, *J* 13, 4, CONHCHC*H*$_2$), 2.94 (1H, dd, *J* 13, 10, CONHCHC*H*$_2$); δC (75 MHz, DMSO-$d_6$) 171.4 (*C*ONHNH), 160.7 (*C*ONHCH), 151.2 (*ipso*-Ar-*C)*, 143.6 (Ar-*C*F$_3$), 143.3 (*ipso*-Ar-*C)*, 137.8 (*ipso*-Ar-*C)*, 134.0 (*ipso*-Ar-*C)*, 130.7 (Ar-*C*), 129.6 (Ar-*C*), 128.9 (Ar-*C*), 128.8 (Ar-*C*), 128.2 (Ar-*C*), 127.0 (Ar-*C*), 125.6 (Ar-*C*), 124.6 (Ar-*C*), 120.8 (*ipso*-Ar-*C*), 118.4 (Ar-*C*), 112.0 (Ar-*C*), 111.2 (Ar-*C*), 53.9 (C=ONH*C*H), 37.3 (CONHCH*C*$H_2$); $\delta_F$ (282 MHz, DMSO-$d_6$) -61.2 (C*F*$_3$); *m/z* (ES$^+$) 612 ([$^{35,35}$Cl]MH$^+$), 614 ([$^{35,37}$Cl]MH$^+$), 616 ([$^{37,37}$Cl]MH$^+$); HRMS (ES$^+$) Found [$^{35,35}$Cl]MH$^+$, 612.1186 ($C_{30}H_{23}{}^{35,35}Cl_2F_3N_5O_2$ requires 612.1175).

**(S)-6-chloro-N-(1-(2-(3-bromophenyl)hydrazineyl)-1-oxo-3-phenylpropan-2-yl)-2-(4-(trifluoromethyl)phenyl)imidazo[1,2-*a*]pyridine-3-carboxamide 44Ds**

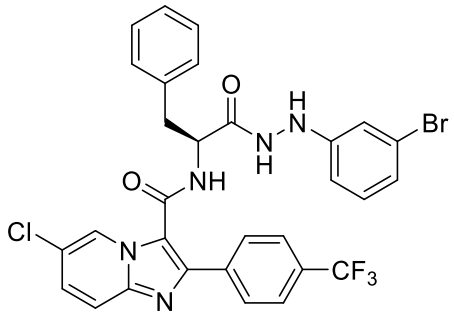


Using the standard procedure provided, (S)-(1-(2-(3-bromophenyl)hydrazineyl)-1-oxo-3-phenylpropan-2-yl)carbamate **51Bn** (0.12 g, 0.28 mmol) was transformed using column chromatography (DCM/EtOAc [3:1]) into the title compound as a white powder (58 mg, 31 %); $R_f$ 0.4 (DCM/EtOAc [3:1]); m.p. °C; $\nu_{max}$ 3247 (N-H), 2981, 1618 (C=O), 1530, 1493, 1386, 1323, 1249, 1168, 1110, 1069, 692 $cm^{-1}$; $\delta_H$ (300 MHz, DMSO-$d_6$) 10.23 (1H, d, *J* 2, CON*H*NH), 9.14 (1H, d, *J* 7, CON*H*CH), 8.47 (1H, s, Ar-*H*), 8.18 (1H, d, *J* 2, CONHN*H*), 7.94 – 7.82 (2H, d, *J* 8, Ar-*H*), 7.77 (1H, d, *J* 9, Ar-*H*), 7.59 – 7.52 (2H, d, *J* 8, Ar-*H*), 7.48 (1H, dd, *J* 9, 2, Ar-*H*), 7.36 – 7.24 (5H, m, Ar-H), 7.07 (1H, t, *J* 7, Ar-H), 6.95 (1H, s, Ar-*H*), 6.86 (1H, d, *J* 7, Ar-*H*), 6.71 (1H, d, *J* 7, Ar-*H*), 4.98 (1H, m, CONHC*H*), 3.17 (1H, dd, *J* 14, 4, CONHCHC$H_2$), 2.95 (1H, dd, *J* 14, 10, CONHCHC$H_2$); δC (75 MHz, DMSO-$d_6$) 171.4 (*C*=ONHNH), 160.8 (*C*=ONHCH), 151.3 (*ipso*-Ar-*C)*, 143.6 (Ar-*C*$F_3$), 143.3 (*ipso*-Ar-*C)*, 137.8 (*ipso*-Ar-*C)*, 131.1 (Ar-*C*), 129.5 (Ar-*C*), 128.9 (Ar-*C*), 128.8 (Ar-*C*), 128.2 (Ar-*C*), 127.0 (Ar-*C*), 125.6 (Ar-*C*), 124.6 (Ar-*C*), 121.3 (Ar-*C*), 120.8 (*ipso*-Ar-*C*), 118.4 (Ar-*C*), 118.0 (*ipso*-Ar-*C*), 114.9 (Ar-*C*), 111.6 (Ar-*C*), 53.9 (CONH*C*H), 37.4 (CONHCH*C*$H_2$); $\delta_F$ (282 MHz, DMSO-$d_6$) -61.1 (C*F*$_3$); *m/z* (ES$^+$) 656 ([$^{35}$Cl, $^{79}$Br]MH$^+$), 658 ([$^{35}$Cl, $^{81}$Br]MH$^+$), 658 ([$^{37}$Cl, $^{79}$Br]MH$^+$), 660 ([$^{37}$Cl, $^{81}$Br]MH$^+$); HRMS (ES$^+$) Found ([$^{35}$Cl, $^{79}$Br]MH$^+$), 656.0671 ($C_{30}H_{23}{}^{35}Cl{}^{79}BrF_3N_5O_2$ requires 656.0670).

**(S)-6-chloro-N-(1-oxo-3-phenyl-1-(2-(3-(trifluoromethyl)phenyl)hydrazineyl)propan-2-yl)-2-(4-(trifluoromethyl)phenyl)imidazo[1,2-*a*]pyridine-3-carboxamide 44Dt**

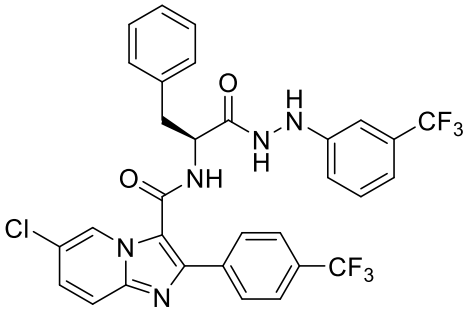

Using the standard procedure provided, (S)-(1-(2-(3-(trifluoromethyl)phenyl)hydrazineyl)-1-oxo-3-phenylpropan-2-yl)carbamate **51Bp** (0.11 g, 0.26 mmol) was transformed using column chromatography (DCM/EtOAc [3:1]) into the title compound as a white powder (60 mg, 36 %); $R_f$ 0.4 (DCM/EtOAc [3:1]); m.p. 230 - 233 °C; $\nu_{max}$ 3258 (N-H), 2980, 1669 (C=O), 1618 (C=O), 1533, 1493, 1383, 1338, 1251, 1163, 1119, 954, 844, 697 $cm^{-1}$; $\delta_H$ (300 MHz, DMSO-$d_6$) 10.30 (1H, d, *J* 2, CON*H*NH), 9.15 (1H, d, *J* 7, CON*H*CH), 8.43 (1H, dd, *J* 2, 1, Ar-*H*), 8.35 (1H, d, *J* 2, CONHN*H*), 7.91 – 7.82 (2H, d, *J* 8, Ar-*H*), 7.76 (1H, dd, *J* 9, 1, Ar-*H*), 7.54 – 7.44 (3H, m, Ar-*H*), 7.35 – 7.23 (6H, m, Ar-H), 7.08 (1H, s, Ar-H), 7.01 (1H, d, *J* 8, Ar-*H*), 6.96 (1H, d, *J* 8, Ar-*H*), 4.98 (1H, m, CONHC*H*), 3.18 (1H, dd, *J* 13, 4, CONHCHC$H_2$), 2.94 (1H, dd, *J* 13, 10, CONHCHC$H_2$); δC (75 MHz, DMSO-$d_6$) 171.5 (*C*ONHNH), 160.8 (*C*ONHCH), 150.2 (*ipso*-Ar-*C)*, 143.5 (Ar-*C*$F_3$), 143.2 (*ipso*-Ar-*C)*, 137.8 (*ipso*-Ar-*C)*, 130.3 (Ar-*C*), 129.5 (Ar-*C*), 128.9 (Ar-*C*), 128.8 (Ar-*C*), 128.2 (Ar-*C*), 127.0 (Ar-*C*), 125.6 (Ar-*C*), 124.5 (Ar-*C*), 120.8 (Ar-*C*), 118.4 (Ar-*C*), 118.0 (*ipso*-Ar-*C*), 116.1 (Ar-*C*), 115.2 (Ar-*C*), 108.4 (Ar-*C*), 53.9 (CONH*C*H), 37.4 (CONHCH*C*$H_2$); $\delta_F$ (282 MHz, DMSO-$d_6$) -61.1 (C*F*$_3$), -61.2 (C*F*$_3$); *m/z* ($ES^+$) 646 ([$^{35}$Cl]$MH^+$), 648 ([$^{37}$Cl]$MH^+$); HRMS ($ES^+$) Found [$^{35}$Cl]$MH^+$, 646.1448 ($C_{31}H_{23}{}^{35}ClF_6N_5O_2$ requires 646.1439).

**(S)-6-chloro-N-(1-oxo-3-phenyl-1-(2-(3-(trifluoromethoxy)phenyl)hydrazineyl)propan-2-yl)-2-(4-(trifluoromethyl)phenyl)imidazo[1,2-*a*]pyridine-3-carboxamide 44Du**

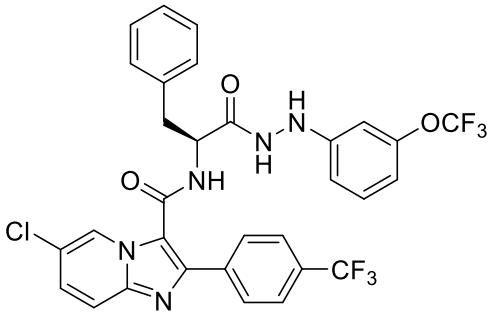

Using the standard procedure provided, (S)-(1-(2-(3-(trifluoromethoxy)phenyl)hydrazineyl)-1-oxo-3-phenylpropan-2-yl)carbamate **51Br** (0.12 g, 0.27 mmol) was transformed using column chromatography (DCM/EtOAc [3:1]) into the title compound as a white powder (65 mg, 36 %); $R_f$ 0.5 (DCM/EtOAc [3:1]); m.p. 250 - 253 °C; $\nu_{max}$ 3258 (N-H), 2980, 1670 (C=O), 1615 (C=O), 1531, 1493, 1383, 1325, 1254, 1222, 1154, 1119, 1067, 1016, 698 $cm^{-1}$; $\delta_H$ (300 MHz, DMSO-$d_6$) 10.26 (1H, s, CON*H*NH), 9.17 (1H, d, *J* 7, CON*H*CH), 8.44 (1H, dd, *J* 2, 1, Ar-*H*), 8.30 (1H, s, CONHN*H*), 7.92 – 7.86 (2H, d, *J* 8, Ar-*H*), 7.77 (1H, dd, *J* 9, 1, Ar-*H*), 7.60 – 7.52 (2H, d, *J* 8, Ar-*H*), 7.49 (1H, dd, *J* 9, 2, Ar-*H*), 7.39 – 7.26 (5H, m, Ar-H), 7.23 (1H, t, *J* 8, Ar-H), 6.72 (1H, dd, *J* 8, 2, Ar-*H*), 6.69 – 6.59 (2H, m, Ar-*H*), 4.97 (1H, m, CONHC*H*), 3.20 (1H, dd, *J* 13, 4, CONHCHC$H_2$), 2.95 (1H, dd, *J* 13, 10, CONHCHC$H_2$); δC (75 MHz, DMSO-$d_6$) 171.4 (*C*ONHNH), 160.8 (*C*ONHCH), 151.5 (*ipso*-Ar-*C)*, 149.8 (Ar-O*C*$F_3$), 143.5 (Ar-*C*$F_3$), 143.2 (*ipso*-Ar-*C)*, 137.8 (*ipso*-Ar-*C)*, 130.8 (Ar-*C*), 129.5 (Ar-*C*), 128.9 (Ar-*C*), 128.8 (Ar-*C*), 128.2 (Ar-*C*), 127.0 (Ar-*C*), 125.6 (Ar-*C*), 124.5 (Ar-*C*), 120.8 (*ipso*-Ar-*C*), 118.4 (Ar-*C*), 118.0 (*ipso*-Ar-*C*), 111.3 (Ar-*C*), 110.5 (Ar-*C*), 104.6 (Ar-*C*), 53.9 (C=ONH*C*H), 37.4 (CONHCH*C*$H_2$); $\delta_F$ (282 MHz, DMSO-$d_6$) -56.4 (OC*F*$_3$), -61.1 (C*F*$_3$); *m/z* ($ES^+$) 662 ([$^{35}$Cl]$MH^+$), 664 ([$^{37}$Cl]$MH^+$); HRMS ($ES^+$) Found [$^{35}$Cl]$MH^+$, 662.1579 ($C_{31}H_{23}{}^{35}ClF_6N_5O_3$ requires 662.1388).

**(S)-6-chloro-N-(1-(2-(3-chlorophenyl)hydrazineyl)-1-oxo-3-phenylpropan-2-yl)-2-(3-methoxyphenyl)imidazo[1,2-*a*]pyridine-3-carboxamide 44Dv**

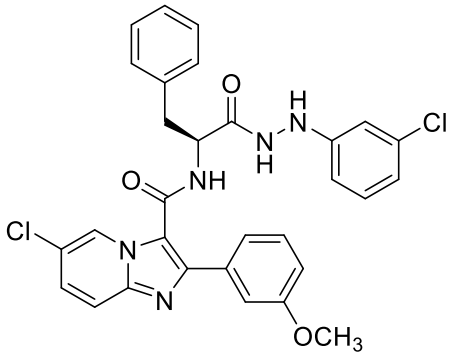

Using the standard procedure provided, tert-butyl (S)-(1-(2-(3-chlorophenyl)hydrazineyl)-1-oxo-3-phenylpropan-2-yl)carbamate **51BI** (0.11 g, 0.28 mmol) was transformed using column chromatography (DCM/EtOAc [3:1]) into the title compound as a white powder (66 mg, 41 %); $R_f$ 0.2 (DCM/EtOAc [3:1]); m.p. 245 - 248 °C; $\nu_{max}$ 3271 (N-H), 1670 (C=O), 1615 (C=O), 1538, 1494, 1380, 1278, 1232, 1150, 1048, 846, 728, 698 $cm^{-1}$; $\delta_H$ (300 MHz, DMSO-$d_6$) 10.15 (1H, s, CON*H*NH), 8.70 (1H, s, Ar-*H*), 8.66 (1H, d, *J* 7, CON*H*CH), 8.15 (1H, s, CONHN*H*), 7.73 (1H, d, *J* 9, Ar-*H*), 7.46 (1H, dd, *J* 9, 2, Ar-*H*), 7.36 – 7.18 (8H, m, Ar-H), 7.11 (1H, t, *J* 7, Ar-H), 6.95 (1H, m, Ar-*H*), 6.76 (1H, s, Ar-H), 6.71 (1H, d, *J* 7, Ar-*H*), 6.61 (1H, d, *J* 7, Ar-*H*), 4.90 (1H, m, CONHC*H*), 3.72 (3H, s, Ar-OC*H*$_3$), 3.13 (1H, dd, *J* 13, 4, CONHCHC*H*$_2$), 2.90 (1H, dd, *J* 13, 10, CONHCHC*H*$_2$); δC (75 MHz, DMSO-$d_6$) 171.3 (*C*ONHNH), 161.0 (*C*ONHCH), 159.7 (Ar-*C*-OCH$_3$*)*, 151.1 (*ipso*-Ar-*C)*, 145.6 (*ipso*-Ar-*C)*, 143.2 (*ipso*-Ar-*C*), 137.6 (*ipso*-Ar-*C)*, 134.7 (*ipso*-Ar-*C)*, 134.0 (*ipso*-Ar-*C)*, 130.8 (Ar-*C*), 130.1 (Ar-*C*), 129.5 (Ar-*C*), 128.8 (Ar-*C*), 127.9 (Ar-*C*), 127.1 (Ar-*C*), 124.7 (Ar-*C*), 120.9 (Ar-*C*), 120.5 (*ipso*-Ar-*C)*, 118.4 (Ar-*C*), 118.1 (Ar-*C*), 116.9 (*ipso*-Ar-*C)*, 115.2 (Ar-*C*), 113.4 (Ar-*C*), 112.0 (Ar-*C*), 111.2 (Ar-*C*), 55.5 (Ar-O*C*H$_3$), 53.9 (C=ONH*C*H), 37.6 (CONHCH*C*H$_2$); *m/z* (ES$^+$) 574 ([$^{35,35}$Cl]MH$^+$), 576 ([$^{35,37}$Cl]MH$^+$), 578 ([$^{37,37}$Cl]MH$^+$); HRMS (ES$^+$) Found [$^{35,35}$Cl]MH$^+$, 574.1353 ($C_{30}H_{26}{}^{35,35}Cl_2N_5O_3$ requires 574.1407).

**(S)-6-chloro-N-(1-(2-(3-bromophenyl)hydrazineyl)-1-oxo-3-phenylpropan-2-yl)-2-(3-methoxyphenyl)imidazo[1,2-*a*]pyridine-3-carboxamide 44Dw**

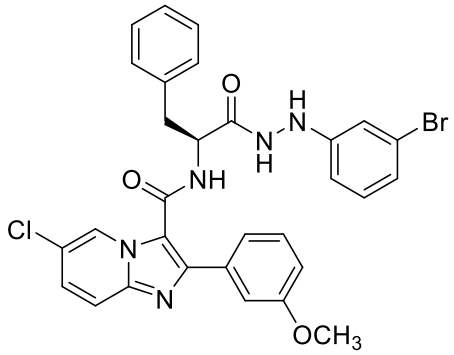

Using the standard procedure provided, (S)-(1-(2-(3-bromophenyl)hydrazineyl)-1-oxo-3-phenylpropan-2-yl)carbamate **51Bn** (0.13 g, 0.31 mmol) was transformed using column chromatography (DCM/EtOAc [3:1]) into the title compound as a white powder (96 mg, 50 %); $R_f$ 0.3 (DCM/EtOAc [3:1]); m.p. 253 - 258 °C; $\nu_{max}$ 3266 (N-H), 2980, 1669 (C=O), 1615 (C=O), 1537, 1494, 1381, 1251, 1231, 1150, 1077, 1049, 954, 800, 747, 697 $cm^{-1}$; $\delta_H$ (300 MHz, DMSO-$d_6$) 10.16 (1H, s, CON*H*NH), 8.70 (1H, s, Ar-*H*), 8.67 (1H, d, *J* 7, CON*H*CH), 8.16 (1H, s, CONHN*H*), 7.74 (1H, d, *J* 9, Ar-*H*), 7.46 (1H, dd, *J* 9, 2, Ar-*H*), 7.34 – 7.18 (8H, m, Ar-H), 7.05 (1H, t, *J* 7, Ar-H), 6.98 – 6.88 (2H, m, Ar-*H*), 6.85 (1H, d, *J* 7, Ar-*H*), 6.65 (1H, d, *J* 7, Ar-*H*), 4.90 (1H, m, CONHC*H*), 3.72 (3H, s, Ar-OC*H*$_3$), 3.13 (1H, dd, *J* 13, 4, CONHCHC*H*$_2$), 2.88 (1H, dd, *J* 13, 10, CONHCHC*H*$_2$); δC (75 MHz, DMSO-$d_6$) 171.3 (*C*ONHNH), 161.0 (*C*ONHCH), 159.7 (Ar-*C*-OCH$_3$*)*, 151.2 (*ipso*-Ar-*C)*, 145.6 (*ipso*-Ar-*C)*, 143.2 (*ipso*-Ar-*C)*, 137.6 (*ipso*-Ar-*C)*, 134.7 (*ipso*-Ar-*C)*, 131.1 (Ar-*C*), 130.1 (Ar-*C*), 129.5 (Ar-*C*), 128.8 (Ar-*C*), 127.9 (Ar-*C*), 124.8 (Ar-*C*), 122.5 (Ar-*C*), 121.3 (Ar-*C)*, 120.5 (*ipso*-Ar-*C)*, 118.1 (Ar-*C*), 116.9 (*ipso*-Ar-*C)*, 115.2 (Ar-*C*), 114.8 (Ar-*C*), 113.4 (Ar-*C*), 111.5 (Ar-*C*), 55.5 (Ar-O*C*H$_3$), 53.9 (CONH*C*H), 37.5 (CONHCH*C*H$_2$); *m/z* (ES$^+$) 618 ([$^{35}$Cl, $^{79}$Br]MH$^+$), 620 ([$^{35}$Cl, $^{81}$Br]MH$^+$), 620 ([$^{37}$Cl, $^{79}$Br]MH$^+$), 622 ([$^{37}$Cl, $^{81}$Br]MH$^+$); HRMS (ES$^+$) Found ([$^{35}$Cl, $^{79}$Br]MH$^+$), 618.0920 ($C_{30}H_{26}{}^{35}Cl^{79}BrN_5O_3$ requires 618.0902).

**(S)-6-chloro-N-(1-(2-(3-trifluoromethyl phenyl)hydrazineyl)-1-oxo-3-phenylpropan-2-yl)-2-(3-methoxyphenyl)imidazo[1,2-*a*]pyridine-3-carboxamide 44Dx**

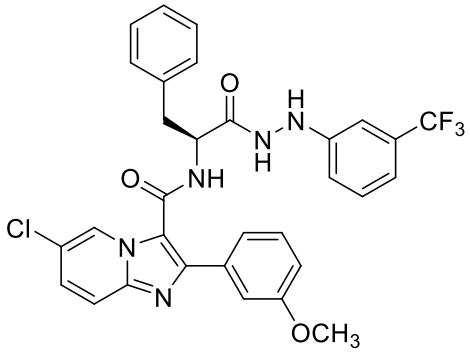

Using the standard procedure provided, (S)-(1-(2-(3-trifluoromethyl phenyl)hydrazineyl)-1-oxo-3-phenylpropan-2-yl)carbamate **51Bp** (0.12 g, 0.29 mmol) was transformed using column chromatography (DCM/EtOAc [3:1]) into the title compound as a white powder (80 mg, 45 %); $R_f$ 0.3 (DCM/EtOAc [3:1]); m.p. 250 - 252 °C; $\nu_{max}$ 3259 (N-H), 2981, 1616 (C=O), 1494, 1382, 1332, 1220, 1152, 1113, 696 $cm^{-1}$; $\delta_H$ (300 MHz, DMSO-$d_6$) 10.24 (1H, s, CON*H*NH), 8.67 (1H, s, Ar-*H*), 8.65 (1H, d, *J* 7, CON*H*CH), 8.32 (1H, s, CONHN*H*), 7.74 (1H, d, *J* 9, Ar-*H*), 7.47 (1H, dd, *J* 9, 2, Ar-*H*), 7.37 – 7.15 (9H, m, Ar-H), 7.07 (1H, s, Ar-*H*), 7.02 (1H, d, *J* 7, Ar-*H*), 6.79 – 6.84 (2H, m, Ar-*H*), 4.92 (1H, m, CONHC*H*), 3.71 (3H, s, Ar-OC*H*$_3$), 3.13 (1H, dd, *J* 13, 4, CONHCHC*H*$_2$), 2.91 (1H, dd, *J* 13, 10, CONHCHC*H*$_2$); δC (75 MHz, DMSO-$d_6$) 171.4 (*C*ONHNH), 161.0 (*C*ONHCH), 159.7 (Ar-*C*-OCH$_3$*)*, 150.1 (*ipso*-Ar-*C)*, 145.6 (*ipso*-Ar-*C)*, 143.2 (*ipso*-Ar-*C)*, 137.6 (*ipso*-Ar-*C)*, 134.7 (*ipso*-Ar-*C)*, 130.0 (Ar-*C*), 129.5 (Ar-*C*), 128.8 (Ar-*C*), 127.9 (Ar-*C*), 124.7 (Ar-*C*), 120.9 (Ar-*C*), 120.5 (*ipso*-Ar-*C)*, 118.1 (Ar-*C*), 116.9 (*ipso*-Ar-*C)*, 115.2 (Ar-*C*), 113.4 (Ar-*C*), 108.6 (Ar-*C*), 55.5 (Ar-O*C*H$_3$), 53.9 (CONH*C*H), 37.5 (CONHCH*C*H$_2$); $\delta_F$ (282 MHz, DMSO-$d_6$) -61.3 (C*F*$_3$); *m/z* ($ES^+$) 608 ([$^{35}$Cl]$MH^+$), 610 ([$^{37}$Cl]$MH^+$); HRMS ($ES^+$) Found [$^{35}$Cl]$MH^+$, 608.1686 ($C_{31}H_{26}{}^{35}ClF_3N_5O_3$ requires 608.1671).

**(S)-6-chloro-2-(3-methoxyphenyl)-N-(1-oxo-3-phenyl-1-(2-(3-(trifluoromethoxy)phenyl)hydrazineyl)propan-2-yl)imidazo[1,2-*a*]pyridine-3-carboxamide 44Dy**

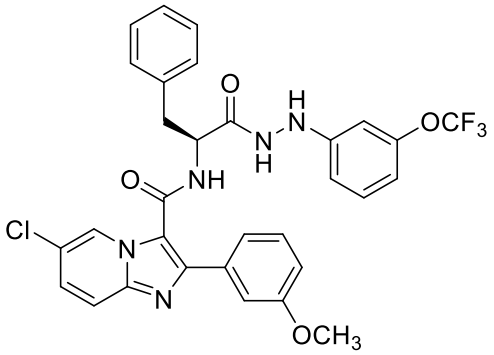

Using the standard procedure provided, (S)-(1-(2-(3-trifluoromethoxyphenyl)hydrazineyl)-1-oxo-3-phenylpropan-2-yl)carbamate **51Br** (0.14 g, 0.31 mmol) was transformed using column chromatography (DCM/EtOAc [3:1]) into the title compound as a white powder (92 mg, 46 %); $R_f$ 0.3 (DCM/EtOAc [3:1]); m.p. 258 - 260 °C; $\nu_{max}$ 3265 (N-H), 2981, 1615 (C=O), 1495, 1383, 1333, 1220, 1152, 697 $cm^{-1}$; $\delta_H$ (300 MHz, DMSO-$d_6$) 10.20 (1H, d, *J* 2, CON*H*NH), 8.70 (1H, d, *J* 7, CON*H*CH), 8.67 (1H, dd, *J* 2, 1, Ar-*H*), 8.26 (1H, d, *J* 2, CONHN*H*), 7.73 (1H, dd, *J* 9, 1, Ar-*H*), 7.46 (1H, dd, *J* 9, 2, Ar-*H*), 7.35 (1H, s, Ar-*H*), 7.31 – 7.17 (8H, m, Ar-H), 6.94 (1H, m, Ar-H), 6.69 – 6.60 (3H, m, Ar-*H*), 4.91 (1H, m, CONHC*H*), 3.73 (3H, s, Ar-OC*H*$_3$), 3.14 (1H, dd, *J* 13, 4, CONHCHC*H*$_2$), 2.93 (1H, dd, *J* 13, 10, CONHCHC*H*$_2$); δC (75 MHz, DMSO-$d_6$) 171.4 (*C*ONHNH), 161.0 (*C*ONHCH), 159.7 (Ar-*C*-OCH$_3$*)*, 151.4 (*ipso*-Ar-*C)*, 149.8 (Ar-O*C*F$_3$*)*, 145.5 (*ipso*-Ar-*C)*, 143.1 (*ipso*-Ar-*C)*, 137.6 (*ipso*-Ar-*C)*, 134.7 (*ipso*-Ar-*C)*, 130.8 (Ar-*C*), 130.0 (Ar-*C*), 129.5 (Ar-*C*), 128.8 (Ar-*C*), 127.9 (Ar-*C*), 127.1 (Ar-*C*), 124.7 (Ar-*C*), 120.9 (Ar-*C*), 120.5 (*ipso*-Ar-*C)*, 118.1 (Ar-*C*), 116.9 (*ipso*-Ar-*C)*, 115.1 (Ar-*C*), 113.4 (Ar-*C*), 111.3 (Ar-*C*), 110.5 (Ar-*C*), 104.5 (Ar-*C*), 55.5 (Ar-O*C*H$_3$), 53.9 (CONH*C*H), 37.6 (CONHCH*C*H$_2$); $\delta_F$ (282 MHz, DMSO-$d_6$) -56.4 (OC*F*$_3$); *m/z* (ES$^+$) 624 ([$^{35}$Cl]MH$^+$), 626 ([$^{37}$Cl]MH$^+$); HRMS (ES$^+$) Found [$^{35}$Cl]MH$^+$, 624.1371 ($C_{31}H_{26}{}^{35}ClF_3N_5O_4$ requires 624.1620).

**(S)-6-chloro-N-(1-oxo-3-phenyl-1-(2-(3-(chlorophenyl)hydrazineyl)propan-2-yl)-2-(4-(trifluoromethoxy)phenyl)imidazo[1,2-*a*]pyridine-3-carboxamide 44Dz**

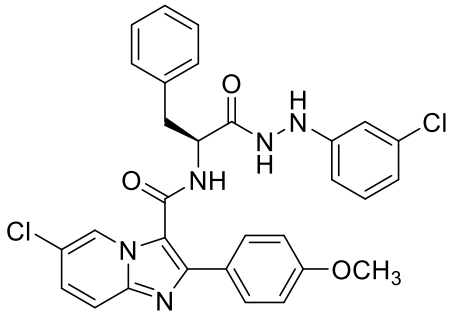

Using the standard procedure provided, (S)-(1-(2-(3-chlorophenyl)hydrazineyl)-1-oxo-3-phenylpropan-2-yl)carbamate **51BI** (0.11 g, 0.28 mmol) was transformed using column chromatography (DCM/EtOAc [3:1]) into the title compound as a white powder (63 mg, 39 %); $R_f$ 0.40 (DCM/EtOAc [3:1]); m.p. 243 - 248 °C; $\nu_{max}$ 3240 (N-H), 2980, 1614 (C=O), 1532, 1474, 1386, 1248, 1165, 1076, 1022, 950, 833, 697 $cm^{-1}$; $\delta_H$ (300 MHz, DMSO-$d_6$) 10.15 (1H, s, CON*H*NH), 8.70 – 8.58 (2H, m, Ar-*H*), 8.18 (1H, s, CONHN*H*), 7.71 (1H, dd, *J* 9, 1, Ar-*H*), 7.66 – 7.58 (2H, d, *J* 8, Ar-*H*), 7.45 (1H, dd, *J* 9, 2, Ar-*H*), 7.35 – 7.23 (5H, m, Ar-H), 7.13 (1H, t, *J* 7, Ar-*H*), 6.86 – 6.80 (2H, d, *J* 8, Ar-H), 6.78 (1H, t, *J* 2, Ar-*H*), 6.78 (1H, dd, *J* 7, 2, Ar-*H*), 6.63 (1H, dd, *J* 7, 2, Ar-*H*), 4.93 (1H, m, CONHC*H*), 3.15 (1H, dd, *J* 13, 4, CONHCHC$H_2$), 2.94 (1H, dd, *J* 13, 10, CONHCHC$H_2$); δC (75 MHz, DMSO-$d_6$) 171.3 (*C*ONHNH), 161.1 (*C*ONHCH), 159.9 (Ar-*C*-$OCH_3$*)*, 151.1 (*ipso*-Ar-*C)*, 145.9 (*ipso*-Ar-*C)*, 143.2 (*ipso*-Ar-*C)*, 137.7 (*ipso*-Ar-*C)*, 130.8 (Ar-*C*), 130.0 (Ar-*C*), 129.6 (Ar-*C*), 128.8 (Ar-*C*), 128.2 (Ar-*C*), 127.7 (Ar-*C*), 127.1 (Ar-*C*), 124.7 (Ar-*C*), 120.3 (*ipso*-Ar-*C)*, 118.4 (Ar-*C*), 117.9 (Ar-*C*), 116.0 (*ipso*-Ar-*C)*, 114.3 (Ar-*C*), 112.0 (Ar-*C*), 111.2 (Ar-*C*), 55.6 (Ar-O*C*$H_3$), 53.8 (CONH*C*H), 37.4 (CONHCH*C*$H_2$); *m/z* ($ES^+$) 574 ([$^{35,35}$Cl]$MH^+$), 576 ([$^{35,37}$Cl]$MH^+$), 578 ([$^{37,37}$Cl]$MH^+$); HRMS ($ES^+$) Found [$^{35,35}$Cl]$MH^+$, 574.1403 ($C_{30}H_{26}{}^{35,35}Cl_2N_5O_3$ requires 574.1407).

**(S)-N-(1-(2-(3-bromophenyl)hydrazineyl)-1-oxo-3-phenylpropan-2-yl)-6-chloro-2-(4-methoxyphenyl)imidazo[1,2-*a*]pyridine-3-carboxamide 44Ea**

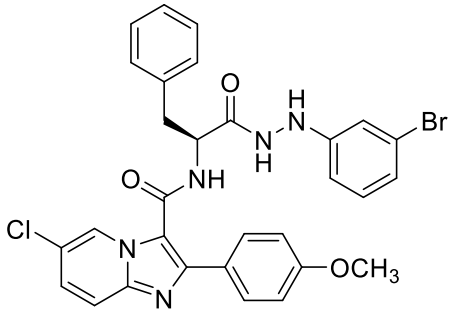

Using the standard procedure provided, (S)-(1-(2-(3-bromophenyl)hydrazineyl)-1-oxo-3-phenylpropan-2-yl)carbamate **51Bn** (0.12 g, 0.28 mmol) was transformed using column chromatography (DCM/EtOAc [3:1]) into the title compound as a white powder (71 mg, 41 %); $R_f$ 0.50 (DCM/EtOAc [3:1]); m.p. 260 - 268 °C; $\nu_{max}$ 3241 (N-H), 2980, 1659 (C=O), 1614 (C=O), 1532, 1473, 1386, 1248, 1166, 1072, 951, 833, 698 $cm^{-1}$; $\delta_H$ (300 MHz, DMSO-$d_6$) 10.14 (1H, d, *J* 2, CON*H*NH), 8.66 (1H, dd, *J* 2, 1, Ar-*H*), 8.60 (1H, d, *J* 7, CON*H*CH), 8.15 (1H, d, *J* 2, CONHN*H*), 7.70 (1H, dd, *J* 9, 1, Ar-*H*), 7.64 – 7.57 (2H, d, *J* 8, Ar-*H*), 7.44 (1H, dd, *J* 9, 2, Ar-*H*), 7.36 – 7.24 (5H, m, Ar-*H*), 7.06 (1H, t, *J* 8, Ar-*H*), 6.93 (1H, s, Ar-*H*), 6.87 (1H, s, Ar-*H*), 6.85 – 6.80 (2H, d, *J* 8, Ar-*H*), 6.67 (1H, dd, *J* 8, 2, Ar-*H*), 4.92 (1H, m, CONHC*H*), 3.76 (3H, s, OC$H_3$), 3.14 (1H, dd, *J* 13, 4, CONHCHC$H_2$), 2.92 (1H, dd, *J* 13, 10, CONHCHC$H_2$); δC (75 MHz, DMSO-$d_6$) 171.3 (*C*ONHNH), 161.1 (*C*ONHCH), 159.9 (Ar-*C*-$OCH_3$), 151.2 (*ipso*-Ar-*C)*, 145.9 (*ipso*-Ar-*C)*, 143.2 (*ipso*-Ar-*C)*, 137.7 (*ipso*-Ar-*C)*, 131.1 (Ar-*C*), 130.0 (Ar-*C*), 129.5 (Ar-*C*), 128.8 (Ar-*C*), 127.1 (Ar-*C*), 125.6 (*ipso*-Ar-*C*), 124.7 (Ar-*C*), 122.6 (*ipso*-Ar-*C)*, 121.3 (Ar-*C*), 120.2 (*ipso*-Ar-*C)*, 117.9 (Ar-*C*), 116.0 (*ipso*-Ar-*C*), 114.8 (Ar-*C*), 114.3 (Ar-*C*), 111.6 (Ar-*C*), 55.6 (O*C*$H_3$), 53.7 (CONH*C*H), 37.5 (CONHCH*C*$H_2$); *m/z* ($ES^+$) 618 ([$^{35}$Cl, $^{79}$Br]$MH^+$), 620 ([$^{35}$Cl, $^{81}$Br]$MH^+$), 620 ([$^{37}$Cl, $^{79}$Br]$MH^+$), 622 ([$^{37}$Cl, $^{81}$Br]$MH^+$); HRMS ($ES^+$) Found ([$^{35}$Cl, $^{79}$Br]$MH^+$), 618.0927 ($C_{30}H_{26}{}^{35}Cl^{79}BrN_5O_3$ requires 618.0902).

**(S)-6-chloro-2-(4-methoxyphenyl)-N-(1-oxo-3-phenyl-1-(2-(3-(trifluoromethyl)phenyl)hydrazineyl)propan-2-yl)imidazo[1,2-*a*]pyridine-3-carboxamide 44Eb**

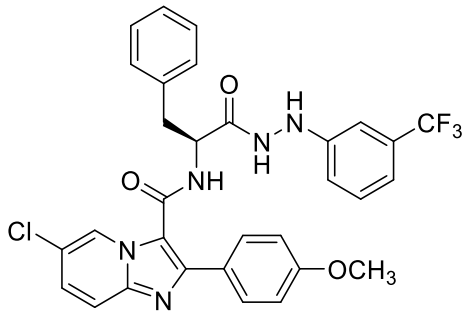


Using the standard procedure provided, (S)-(1-(2-((3-trifluoromethyl)phenyl)hydrazineyl)-1-oxo-3-phenylpropan-2-yl)carbamate **51Bp** (0.10 g, 0.34 mmol) was transformed using column chromatography (DCM/EtOAc [3:1]) into the title compound as a white powder (88 mg, 51 %); $R_f$ 0.50 (DCM/EtOAc [3:1]); m.p.

263 - 268 °C; $\nu_{max}$ 3244 (N-H), 2980, 1667 (C=O), 1615 (C=O), 1534, 1484, 1386, 1334, 1251, 1163, 1071, 1025, 950, 868, 696 $cm^{-1}$; $\delta_H$ (300 MHz, DMSO-$d_6$) 10.22 (1H, s, CON*H*NH), 8.74 – 8.52 (2H, m, Ar-*H*), 8.30 (1H, s, CONHN*H*), 7.69 (1H, dd, *J* 9, 1, Ar-*H*), 7.64 – 7.56 (2H, d, *J* 8, Ar-*H*), 7.43 (1H, dd, *J* 9, 2, Ar-*H*), 7.36 – 7.24 (6H, m, Ar-H), 7.06 (1H, s, Ar-H), 7.02 (1H, d, *J* 8, Ar-*H*), 6.92 (1H, d, *J* 8, Ar-*H*), 6.85 – 6.77 (2H, d, *J* 8, Ar-H), 4.93 (1H, m, CONHC*H*), 3.76 (3H, s, OC$H_3$), 3.16 (1H, dd, *J* 13, 4, CONHCHC$H_2$), 2.93 (1H, dd, *J* 13, 10, CONHCHC$H_2$); δC (75 MHz, DMSO-$d_6$) 171.4 (*C*ONHNH), 161.1 (*C*ONHCH), 159.9 (Ar-*C*-$OCH_3$), 150.2 (*ipso*-Ar-*C*), 143.2 (*ipso*-Ar-*C)*, 137.7 (*ipso*-Ar-*C)*, 130.0 (Ar-*C*), 129.5 (Ar-*C*), 128.8 (Ar-*C*), 127.1 (Ar-*C*), 125.6 (Ar-*C*), 124.6 (Ar-*C*), 120.2 (*ipso*-Ar-*C)*, 117.9 (Ar-*C*), 116.1 (Ar-*C*), 116.0 (*ipso*-Ar-*C)*, 114.3 (Ar-*C*), 108.6 (Ar-*C*), 55.5 (Ar-O*C*$H_3$), 53.8 (CONH*C*H), 37.8 (CONHCH*C*$H_2$); $\delta_F$ (282 MHz, DMSO-$d_6$) -61.3 (C*F*$_3$); *m/z* ($ES^+$) 608 ([$^{35}$Cl]$MH^+$), 610 ([$^{37}$Cl]$MH^+$); HRMS ($ES^+$) Found [$^{35}$Cl]$MH^+$, 608.1672 ($C_{31}H_{26}{}^{35}ClF_3N_5O_3$ requires 608.1671).

**(S)-6-chloro-2-(4-methoxyphenyl)-N-(1-oxo-3-phenyl-1-(2-(3-(trifluoromethoxy)phenyl)hydrazineyl)propan-2-yl)imidazo[1,2-*a*]pyridine-3-carboxamide 44Ec**

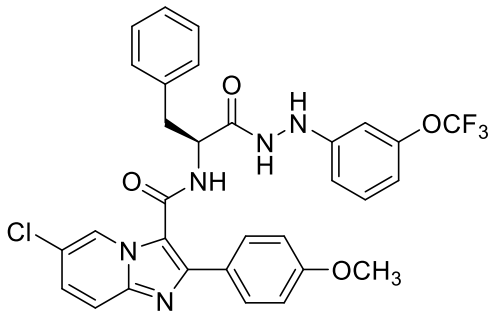


Using the standard procedure provided, (S)-(1-(2-((3-trifluoromethoxy)phenyl)hydrazineyl)-1-oxo-3-phenylpropan-2-yl)carbamate **51Br** (0.12 g, 0.27 mmol) was transformed using column chromatography (DCM/EtOAc [3:1]) into the title compound as a white powder (70 mg, 40 %); $R_f$ 0.52 (DCM/EtOAc [3:1]); m.p. 263 - 266 °C; $\nu_{max}$ 3251 (N-H), 2980, 1613 (C=O), 1533, 1485, 1386, 1249, 1151, 1080, 1034, 951, 833, 697 $cm^{-1}$; $\delta_H$ (300 MHz, DMSO-$d_6$) 10.19 (1H, s, CON*H*NH), 8.69 – 8.58 (2H, m, Ar-*H*), 8.26 (1H, s, CONHN*H*), 7.69 (1H, dd, *J* 9, 1, Ar-*H*), 7.64 – 7.58 (2H, d, *J* 8, Ar-*H*), 7.43 (1H, dd, *J* 9, 2, Ar-*H*), 7.36 – 7.26 (5H, m, Ar-H), 7.21 (1H, t, *J* 8, Ar-H), 6.88 – 6.77 (2H, d, *J* 8, Ar-*H*), 6.72 – 6.57 (3H, m, Ar-H), 4.93 (1H, m, CONHC*H*), 3.76 (1H, s, OC$H_3$), 3.14 (1H, dd, *J* 13, 4, CONHCHC$H_2$),

2.94 (1H, dd, *J* 13, 10, CONHCHC*H*$_2$); δC (75 MHz, DMSO-d$_6$) 171.4 (*C*ONHNH), 161.1 (CONH*C*H), 159.8 (Ar-*C*-OCH$_3$), 151.4 (*ipso*-Ar-*C*), 149.8 (O*C*F$_3$*)*, 145.8, 143.2 (*ipso*-Ar-*C)*, 137.7 (*ipso*-Ar-*C)*, 130.8 (Ar-*C*), 130.0 (Ar-*C*), 129.5 (Ar-*C*), 128.8 (Ar-*C*), 127.1 (Ar-*C*), 125.6 (Ar-*C*), 124.6 (Ar-*C*), 120.2 (*ipso*-Ar-*C)*, 117.9 (Ar-*C*), 116.0 (*ipso*-Ar-*C*), 114.3 (Ar-*C*), 111.3 (Ar-*C*), 110.5 (Ar-*C*), 104.5 (Ar-*C*), 55.5 (Ar-O*C*H$_3$), 53.7 (CONH*C*H), 37.5 (CONHCH*C*H$_2$); δ$_F$ (282 MHz, DMSO-d$_6$) -56.4 (OC*F*$_3$); *m/z* (ES$^+$) 624 ([$^{35}$Cl]MH$^+$), 626 ([$^{37}$Cl]MH$^+$); HRMS (ES$^+$) Found [$^{35}$Cl]MH$^+$, 624.1642 ($C_{31}H_{26}{}^{35}ClF_3N_5O_4$ requires 624.1620).

### 6.2.6 Synthesis of Imidazo[1,2-*a*]pyridine-3-carboxamide Heterocyclic analogues – General Procedure

Under a nitrogen atmosphere *N*-protected heterocyclic hydrazide **51 (Cd – Co)** (1 equiv.) was added to 4 M HCl solution in dioxane (3 ml) and stirred at room temperature for 2 hours. The mixture was then evaporated, dried in *vacuo* and precipitated using EtOH and Et$_2$O. The precipitation was isolated and dissolved in acetonitrile before the addition of 6-chloro-2-phenylimidazo[1,2-*a*]pyridine-3-carboxylic acid **50a** (1.10 equiv.), the mixture was stirred overnight with DIPEA (1.60 equiv.) and HBTU (1.10 equiv. ). The reaction was then quenched using EtOAc (10 ml) and distilled water (5 ml) and after separation of the two layers, the organic layer was washed again using distilled water (10 ml X 3) followed by adding sat. aq. NaHCO$_3$ (5 ml) and sat. aq. NH$_4$Cl (5 ml) then adding brine (10 ml). The organic layer was dried over MgSO$_4$, then filtered under vacuum, followed by solvent evaporation and drying under reduced pressure to yield the desired product **44 (Ed - Ep)**.

**(S)-6-chloro-N-(1-oxo-3-phenyl-1-(2-(pyridin-3-yl)hydrazineyl)propan-2-yl)-2-phenylimidazo[1,2-*a*]pyridine-3-carboxamide 44Ed**

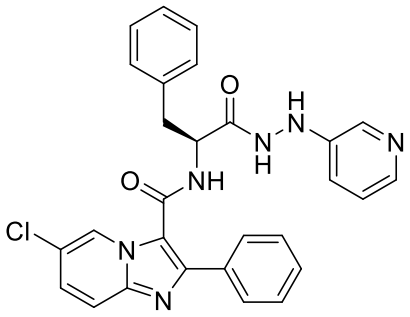

Using the standard procedure provided, *tert*-butyl (S)-(1-oxo-3-phenyl-1-(2-(pyridin-3-yl)hydrazineyl)propan-2-yl)carbamate **51Cd** (0.11 g, 0.30 mmol) was transformed following trituration with diethyl ether into the title compound as a white powder (65 mg, 41 %); $R_f$ 0.30 (DCM/EtOAc [1:1]); m.p. 230 - 235 °C; $\nu_{max}$ 3253 (N-H), 3030 (N-H), 1672 (C=O), 1618 (C=O), 1586, 1534, 1493, 1450, 1419, 1385, 1322, 1228, 1166, 1082, 742, 698 $cm^{-1}$; $\delta_H$ (300 MHz, DMSO-$d_6$) 8.69 (1H, s, Ar-*H*), 8.67 (1H, d, *J* 7, CON*H*CH), 7.74 – 7.68 (2H, d, *J* 9, Ar-*H*), 7.66 – 7.58 (2H, d, *J* 7, Ar-*H*), 7.44 (1H, dd, *J* 9, 2, Ar-*H*), 7.41 – 7.19 (11H, m, Ar-*H*), 4.84 (1H, m, CONHC*H*), 3.18 (1H, dd, *J* 13, 4, CONHCHC$H_2$), 2.80 (1H, dd, *J* 13, 10, CONHCHC$H_2$); $\delta_C$ (75 MHz, DMSO-$d_6$) 173.1 (*C*ONHNH), 160.7 (*C*ONHCH), 145.1 (*ipso*-Ar-*C)*, 143.0 (*ipso*-Ar-*C)*, 138.3 (*ipso*-Ar-*C)*, 133.3 (*ipso*-Ar-*C)*, 129.5 (Ar-*C)*, 128.9 (Ar-*C)*, 128.6 (Ar-*C)*, 128.4 (Ar-*C)*, 127.6 (Ar-*C)*, 126.8 (Ar-*C)*, 124.8 (Ar-*C)*, 120.3 (*ipso*-Ar-*C)*, 118.0 (Ar-*C)*, 117.3 (*ipso*-Ar-*C)*, 54.5 (CONH*C*H), 37.7 (CONHCH*C*$H_2$); *m/z* ($ES^+$) 511 ([$^{35}$Cl]$MH^+$), 513 ([$^{37}$Cl]$MH^+$); HRMS ($ES^+$) Found [$^{35}$Cl]$MH^+$, 511.1646 ($C_{28}H_{24}{}^{35}ClN_6O_2$ requires 511.1644).

**(S)-6-chloro-N-(1-oxo-3-phenyl-1-(2-(pyridin-4-yl)hydrazineyl)propan-2-yl)-2-phenylimidazo[1,2-*a*]pyridine-3-carboxamide 44Ee**

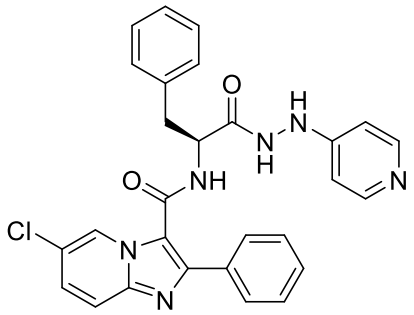


Using the standard procedure provided, *tert*-butyl (S)-(1-oxo-3-phenyl-1-(2-(pyridin-4-yl)hydrazineyl)propan-2-yl)carbamate **51Ce** (0.10 g, 0.28 mmol) was transformed using column chromatography (DCM /EtOAc [1:1]) into the title compound as a white powder (50 mg, 35 %); $R_f$ 0.30 (DCM/EtOAc [1:1]); m.p. 230 - 235 °C; $\nu_{max}$ 3253 (N-H), 3033 (N-H), 1676 (C=O), 1620 (C=O), 1588, 1525, 1487, 1450, 1384, 1321, 1268, 1218, 1166, 819, 698 $cm^{-1}$; $\delta_H$ (300 MHz, DMSO-$d_6$) 8.89 (1H, d, *J* 7, CON*H*CH), 8.58 (1H, d, *J* 6, Ar-*H*), 8.55 (1H, dd, *J* 2, 1, Ar-*H*), 7.81 – 7.76 (2H, d, *J* 6, Ar-*H*), 7.76 – 7.68 (3H, m, Ar-*H*), 7.45 (1H, dd, *J* 9, 2, Ar-*H*), 7.38 – 7.24 (8H, m, Ar-*H*), 5.93 (1H, m, CONHC*H*), 5.82 (2H, s, CON*H*N*H*), 3.41 (1H, dd, *J* 13, 4, CONHCHC$H_2$), 2.81 (1H, dd, *J* 13, 10, CONHCHC$H_2$); $\delta_C$ (75 MHz, DMSO-$d_6$) 174.6 (*C*ONHNH), 160.8

(*C*ONHCH), 150.7 (*ipso*-Ar-*C)*, 145.4 (*ipso*-Ar-*C)*, 143.1 (*ipso*-Ar-*C)*, 138.6 (*ipso*-Ar-*C)*, 133.3 (*ipso*-Ar-*C)*, 129.4 (Ar-*C)*, 128.9 (Ar-*C)*, 128.8 (Ar-*C)*, 128.6 (Ar-*C)*, 127.8 (Ar-*C)*, 127.6 (Ar-*C)*, 126.9 (Ar-*C)*, 124.6 (Ar-*C)*, 120.4 (*ipso*-Ar-*C)*, 118.1 (Ar-*C)*, 117.2 (*ipso*-Ar-*C)*, 115.6 (Ar-*C),* 54.1 (CONH*C*H), 36.4 (CONHCH*C*$H_2$); *m/z* ($ES^+$) 511 ($[^{35}Cl]MH^+$), 513 ($[^{37}Cl]MH^+$); HRMS ($ES^+$) Found $[^{35}Cl]MH^+$, 511.1643 ($C_{28}H_{24}{}^{35}ClN_6O_2$ requires 511.1644).

**(S)-6-chloro-N-(1-oxo-3-phenyl-1-(2-(pyridin-2-yl)hydrazineyl)propan-2-yl)-2-phenylimidazo[1,2-*a*]pyridine-3-carboxamide 44Ef**

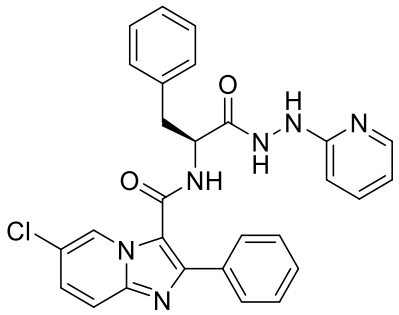

Using the standard procedure provided, *tert*-butyl (S)-(1-oxo-3-phenyl-1-(2-(pyridin-2-yl)hydrazineyl)propan-2-yl)carbamate **51Cf** (0.11 g, 0.30 mmol) was transformed following trituration with diethyl ether into the title compound as a white powder (64 mg, 41 %); $R_f$ 0.30 (DCM/EtOAc [1:1]); m.p. 230 - 235 °C; $\nu_{max}$ 3282 (N-H), 3028 (N-H), 1672 (C=O), 1620 (C=O), 1600, 1531, 1438, 1385, 1326, 1224, 1171, 1127, 810, 698 $cm^{-1}$; $\delta_H$ (300 MHz, DMSO-$d_6$) 10.23 (1H, s, CON*H*NH), 8.83 (1H, d, *J* 7, CON*H*CH), 8.57 (1H, s, Ar-*H*), 8.42 (1H, s, CONHN*H*), 8.06 (1H, d, *J* 5, Ar-*H*), 7.71 (1H, d, *J* 9, Ar-*H*), 7.66 – 7.61 (2H, d, *J* 7, Ar-*H*), 7.49 (1H, t, *J* 9, Ar-*H*), 7.44 (1H, dd, *J* 9, 2, Ar-*H*), 7.37 – 7.24 (8H, m, Ar-*H*), 6.70 (1H, t, *J* 5, Ar-*H*), 6.53 (1H, *J* 9, Ar-*H*), 5.00 (1H, m, CONHC*H*), 3.25 (1H, dd, *J* 13, 4, CONHCHC*H*$_2$), 2.92 (1H, *J* 13, 10, CONHCHC*H*$_2$); $\delta_C$ (75 MHz, DMSO-$d_6$) 171.3 (*C*ONHNH), 160.8 (*C*ONHCH), 160.1 (*ipso*-Ar-*C)*, 148.0 (Ar-*C)*, 145.4 (*ipso*-Ar-*C)*, 143.1 (*ipso*-Ar-*C)*, 137.9 (*ipso*-Ar-*C)*, 133.2 (*ipso*-Ar-*C)*, 129.6 (Ar-*C)*, 128.9 (Ar-*C)*, 128.8 (Ar-*C)*, 128.5 (Ar-*C)*, 127.7 (Ar-*C)*, 127.0 (Ar-*C)*, 124.6 (Ar-*C)*, 120.4 (*ipso*-Ar-*C)*, 118.1 (Ar-*C)*, 117.0 (*ipso*-Ar-*C)*, 114.9 (Ar-*C)*, 106.6 (Ar-*C)*, 53.6 (CONH*C*H), 37.7 (CONHCH*C*$H_2$); *m/z* ($ES^+$) 511 ($[^{35}Cl]MH^+$), 513 ($[^{37}Cl]MH^+$); HRMS ($ES^+$) Found $[^{35}Cl]MH^+$, 511.1633 ($C_{28}H_{24}{}^{35}ClN_6O_2$ requires 511.1644).

**(S)-6-chloro-N-(1-oxo-3-phenyl-1-(2-(pyrazin-2-yl)hydrazineyl)propan-2-yl)-2-phenylimidazo[1,2-*a*]pyridine-3-carboxamide 44Eg**

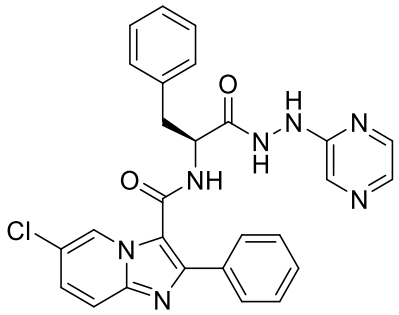

Using the standard procedure provided, *tert*-butyl (S)-(1-oxo-3-phenyl-1-(2-(pyrazine-2-yl)hydrazineyl)propan-2-yl)carbamate **51Cg** (0.11 g, 0.30 mmol) was transformed following trituration with $Et_2O$ into the title compound as a white powder (65 mg, 41 %); $R_f$ 0.35 (DCM/EtOAc [1:3]); m.p. 243 - 248 °C; $\nu_{max}$ 3272 (N-H), 1675 (C=O), 1620 (C=O), 1537, 1494, 1422, 1386, 1324, 1229, 1171, 808, 698 $cm^{-1}$; $\delta_H$ (300 MHz, DMSO-$d_6$) 10.37 (1H, s, CON*H*NH), 8.99 (1H, s, CONHN*H*), 8.85 (1H, d, *J* 7, CON*H*CH), 8.53 (1H, s, Ar-*H*), 8.07 (1H, s, Ar-*H*), 8.03 (1H, s, Ar-*H*), 7.93 (1H, d, *J* 2, Ar-*H*), 7.72 (1H, d, *J* 9, Ar-*H*), 7.68 – 7.60 (2H, d, *J* 7, Ar-*H*), 7.44 (1H, dd, *J* 9, 1, Ar-*H*), 7.36 – 7.24 (8H, m, Ar-*H*), 5.00 (1H, m, CONHC*H*), 3.22 (1H, dd, *J* 13, 4, CONHCHC$H_2$), 2.92 (1H, dd, *J* 13, 10, CONHCHC$H_2$); $\delta_C$ (75 MHz, DMSO-$d_6$) 171.4 (*C*ONHNH), 160.9 (*C*ONHCH*)*, 155.8 (*ipso*-Ar-*C)*, 145.5 (*ipso*-Ar-*C*), 143.1 (*ipso*-Ar-*C)*, 142.2 (Ar-*C)*, 137.9 (*ipso*-Ar-*C)*, 134.9 (Ar-*C)*, 133.2 (*ipso*-Ar-*C)*, 131.3 (Ar-*C)*, 129.6 (Ar-*C)*, 128.9 (Ar-*C)*, 128.8 (Ar-*C)*, 128.4 (Ar-*C)*, 127.7 (Ar-*C)*, 127.0 (Ar-*C)*, 124.6 (Ar-*C)*, 120.4 (*ipso*-Ar-*C)*, 118.1 (Ar-*C)*, 117.0 (*ipso*-Ar-*C)*, 53.6 (CONH*C*H), 37.6 (CONHCH*C*$H_2$); *m/z* ($ES^+$) 512 ([$^{35}$Cl]$MH^+$), 514 ([$^{37}$Cl]$MH^+$); HRMS ($ES^+$) Found [$^{35}$Cl]$MH^+$, 512.1594 ($C_{27}H_{23}{}^{35}ClN_7O_2$ requires 512.1596).

**(S)-6-chloro-N-(1-oxo-3-phenyl-1-(2-(pyrimidin-4-yl)hydrazineyl)propan-2-yl)-2-phenylimidazo[1,2-*a*]pyridine-3-carboxamide 44Eh**

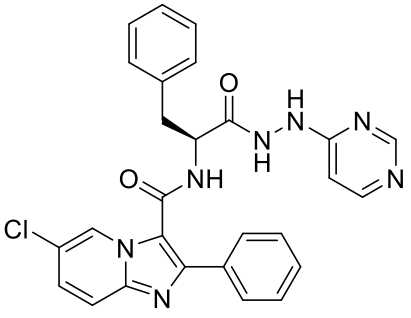

Using the standard procedure provided, *tert*-butyl (S)-(1-oxo-3-phenyl-1-(2-(pyrimidin-4-yl)hydrazineyl)propan-2-yl)carbamate **51Ch** (0.16 g, 0.44 mmol) was transformed using column chromatography (DCM /EtOAc [1:3]) into the title compound as a white powder (60 mg, 38 %); $R_f$ 0.35 (DCM/EtOAc [1:3]); m.p. 243 - 248 °C; $\nu_{max}$ 3251 (N-H), 3035 (N-H), 1674 (C=O), 1619 (C=O), 1593, 1534, 1493, 1386, 1322, 1229, 1167, 1128, 806, 698 $cm^{-1}$; $\delta_H$ (300 MHz, DMSO-$d_6$) 10.42 (1H, s, CON*H*NH), 9.36 (1H, s, CONHN*H*), 8.89 (1H, d, *J* 7, CON*H*CH), 8.53 (1H, dd, *J* 2, 1, Ar-*H*), 8.51 (1H, s, Ar-*H*), 8.19 (1H, d, *J* 6, Ar-*H*), 7.73 (1H, dd, *J* 9, 1, Ar-*H*), 7.69 – 7.62 (2H, dd, *J* 8, 1, Ar-*H*), 7.45 (1H, dd, *J* 9, 2, Ar-*H*), 7.37 – 7.24 (8H, m, Ar-*H*), 6.48 (1H, s, Ar-*H*), 4.98 (1H, m, CONHC*H*), 3.22 (1H, dd, *J* 13, 4, CONHCHC$H_2$), 2.94 (1H, m, CONHCHC$H_2$); $\delta_C$ (75 MHz, DMSO-$d_6$) 171.2 (*C*ONHNH), 161.0 (*C*ONHCH), 158.4 (*ipso*-Ar-*C)*, 145.5 (*ipso*-Ar-*C)*, 143.2 (*ipso*-Ar-*C)*, 137.8 (*ipso*-Ar-*C)*, 133.2 (*ipso*-Ar-*C)*, 129.6 (Ar-*C)*, 128.9 (Ar-*C)*, 128.8 (Ar-*C)*, 128.5 (Ar-*C)*, 127.7 (Ar-*C)*, 127.1 (Ar-*C)*, 124.6 (Ar-*C)*, 120.4 (*ipso*-Ar-*C)*, 118.1 (Ar-*C)*, 117.0 (*ipso*-Ar-*C)*, 53.6 (CONH*C*H), 37.5 (C=ONHCH*C*$H_2$); *m/z* ($ES^+$) 512 ([$^{35}$Cl]$MH^+$), 514 ([$^{37}$Cl]$MH^+$); HRMS ($ES^+$) Found [$^{35}$Cl]$MH^+$, 512.1602 ($C_{27}H_{23}{}^{35}ClN_7O_2$ requires 512.1596).

**(S)-6-chloro-N-(1-oxo-3-phenyl-1-(2-(pyrimidin-2-yl)hydrazineyl)propan-2-yl)-2-phenylimidazo[1,2-*a*]pyridine-3-carboxamide 44Ei**

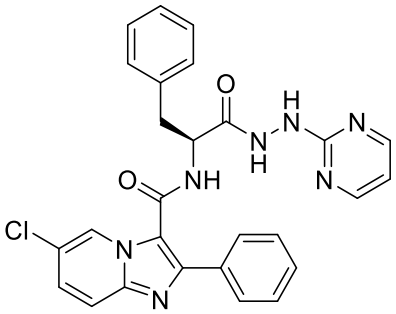


Using the standard procedure provided, *tert*-butyl (S)-(1-oxo-3-phenyl-1-(2-(pyrimidin-2-yl)hydrazineyl)propan-2-yl)carbamate **51Ci** (0.11 g, 0.30 mmol) was transformed using column chromatography (DCM /EtOAc [1:3]) into the title compound as a white powder (63 mg, 40 %); $R_f$ 0.30 (DCM/EtOAc [1:3]); m.p. 243 - 248 °C; $\nu_{max}$ 3280 (N-H), 1674 (C=O), 1618 (C=O), 1586, 1525, 1495, 1450, 1419, 1384, 1323, 1228, 1169, 805, 697 $cm^{-1}$; $\delta_H$ (300 MHz, DMSO-$d_6$) 10.25 (1H, s, CON*H*NH), 9.10 (1H, s, CONHN*H*), 8.82 (1H, d, *J* 8, CON*H*CH), 8.56 (1H, dd, *J* 2, 1, Ar-*H*), 8.43 – 8.33 (2H, d, *J* 4, Ar-*H*), 7.71 (1H, dd, *J* 9, 1, Ar-*H*), 7.64 – 7.55 (2H, dd, *J* 8, 2, Ar-*H*), 7.45 (1H,

dd, *J* 9, 2, Ar-*H*), 7.39 – 7.20 (8H, m, Ar-*H*), 6.80 (1H, t, *J* 4, Ar-*H*), 5.06 (1H, m, CONHC*H*), 3.33 (1H, dd, *J* 13, 4, CONHCHC$H_2$), 2.94 (1H, m, CONHCHC$H_2$); $\delta_C$ (75 MHz, DMSO-$d_6$) 171.2 (*C*ONHNH), 163.4 (*ipso*-Ar-*C)*, 160.5 (*C*ONHCH), 158.6 (*ipso*-Ar-*C)*, 145.2 (*ipso*-Ar-*C)*, 143.1 (*ipso*-Ar-*C)*, 138.1 (*ipso*-Ar-*C)*, 133.2 (*ipso*-Ar-*C)*, 129.7 (Ar-*C)*, 128.9 (Ar-*C)*, 128.8 (Ar-*C)*, 128.6 (Ar-*C)*, 128.4 (Ar-*C)*, 127.6 (Ar-*C)*, 126.9 (Ar-*C)*, 124.6 (Ar-*C)*, 120.3 (*ipso*-Ar-*C)*, 118.1 (Ar-*C)*, 117.1 (*ipso*-Ar-*C)*, 113.0 (Ar-*C),* 53.2 (CONH*C*H), 37.9 (CONHCH*C*$H_2$); *m/z* ($ES^+$) 512 ([$^{35}$Cl]$MH^+$), 514 ([$^{37}$Cl]$MH^+$); HRMS ($ES^+$) Found [$^{35}$Cl]$MH^+$, 512.1592 ($C_{27}H_{23}{}^{35}ClN_7O_2$ requires 512.1596).

**(S)-6-chloro-N-(1-oxo-3-phenyl-1-(2-(thiazol-2-yl)hydrazineyl)propan-2-yl)-2-phenylimidazo[1,2-*a*]pyridine-3-carboxamide 44Ej**

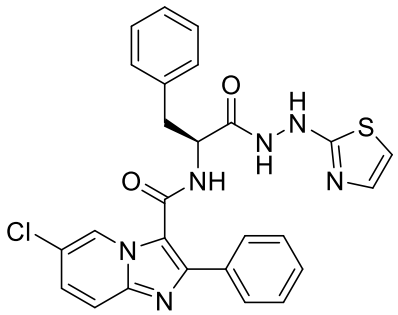


Using the standard procedure provided, *tert*-butyl (S)-(1-oxo-3-phenyl-1-(2-(thiazol-2-yl)hydrazineyl)propan-2-yl)carbamate **51Cj** (0.11 g, 0.30 mmol) was transformed following trituration with $Et_2O$ into the title compound as a white powder (50 mg, 37 %); $R_f$ 0.30 (DCM/EtOAc [1:2]); m.p. 230 - 233 °C; $\nu_{max}$ 3251 (N-H), 3035, 1674 (C=O), 1620 (C=O), 1538, 1493, 1450, 1419, 1386, 1324, 1229, 1166, 834, 698 $cm^{-1}$; $\delta_H$ (300 MHz, DMSO-$d_6$) 8.70 (1H, s, Ar-*H*), 8.67 (1H, d, *J* 7, CON*H*CH), 7.77 – 7.67 (2H, d, *J* 9, Ar-*H*), 7.67 – 7.57 (2H, dd, *J* 7, 1, Ar-*H*), 7.43 (1H, dd, *J* 9, 1, Ar-*H*), 7.39 – 7.22 (9H, m, Ar-*H*), 4.83 (1H, m, CONHC*H*), 3.16 (1H, dd, *J* 13, 4, CONHCHC$H_2$), 2.80 (1H, m, CONHCHC$H_2$); $\delta_C$ (75 MHz, DMSO-$d_6$) 173.1 (*C*ONHNH), 160.7 (*C*ONHCH), 145.1 (*ipso*-Ar-*C)*, 143.0 (*ipso*-Ar-*C)*, 138.3 (*ipso*-Ar-*C)*, 133.3 (*ipso*-Ar-*C)*, 130.4 (Ar-*C)*, 129.5 (Ar-*C)*, 128.9 (Ar-*C)*, 128.8 (Ar-*C)*, 128.6 (Ar-*C)*, 128.4 (Ar-*C)*, 127.9 (Ar-*C)*, 127.6 (Ar-*C)*, 126.8 (Ar-*C)*, 124.8 (Ar-*C)*, 120.3 (*ipso*-Ar-*C)*, 118.0 (Ar-*C)*, 117.3 (*ipso*-Ar-*C)*, 54.5 (C=ONH*C*H), 37.7 (C=ONHCH*C*$H_2$); *m/z* ($ES^+$) 517 ([$^{35}$Cl]$MH^+$), 519 ([$^{37}$Cl]$MH^+$); HRMS ($ES^+$) Found [$^{35}$Cl]$MH^+$, 517.1217 ($C_{26}H_{22}{}^{35}ClN_6O_2S$ requires 517.1208).

**(S)-6-chloro-N-(1-(2-(4-methylthiazol-2-yl)hydrazineyl)-1-oxo-3-phenylpropan-2-yl)-2-phenylimidazo[1,2-*a*]pyridine-3-carboxamide 44Ek**

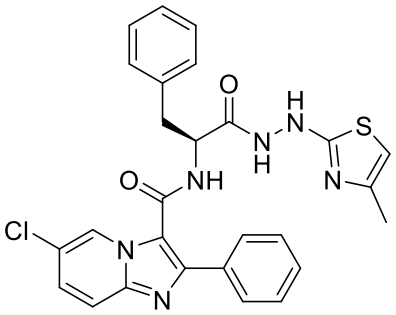

Using the standard procedure provided, *tert*-butyl (S)-(1-oxo-3-phenyl-1-(2-(4-methylthiazol-2-yl)hydrazineyl)propan-2-yl)carbamate **51Ck** (0.12 g, 0.31 mmol) was transformed using column chromatography (DCM /EtOAc [1:2]) into the title compound as a white powder (75 mg, 44 %); $R_f$ 0.30 (DCM/EtOAc [1:2]); m.p. 235 - 240 °C; $\nu_{max}$ 3259 (N-H), 3028 (N-H), 1671 (C=O), 1618 (C=O), 1534, 1492, 1419, 1385, 1322, 1226, 1166, 1079, 836, 742, 698 $cm^{-1}$; $\delta_H$ (300 MHz, DMSO-$d_6$) 8.81 (1H, s, Ar-*H*), 8.71 (1H, d, *J* 7, CON*H*CH), 7.77 – 7.63 (3H, m, Ar-*H*), 7.44 (1H, dd, *J* 9, 1, Ar-*H*), 7.33 – 7.24 (8H, m, Ar-*H*), 6.67 (1H, s, SC*H*C-$CH_3$), 6.05 (2H, s, CON*H*N*H*), 5.05 (1H, s, CONHC*H*), 3.51 (1H, dd, *J* 13, 4, CONHCHC$H_2$), 2.95 (1H, dd, *J* 13, 10, CONHCHC$H_2$), 2.29 (3H, s, SCHC-C$H_3$); $\delta_C$ (75 MHz, DMSO-$d_6$) 178.4 (*C*=ONHNH), 164.4 (NH*C*SCH), 160.5 (*C*=ONHCH), 145.2 (*ipso*-Ar-*C)*, 143.0 (*ipso*-Ar-*C)*, 138.8 (*ipso*-Ar-*C)*, 136.0 (SCH*C*-$CH_3$), 133.3 (*ipso*-Ar-*C)*, 129.5 (Ar-*C)*, 128.8 (Ar-*C)*, 128.6 (Ar-*C)*, 128.5 (Ar-*C)*, 127.6 (Ar-*C)*, 126.7 (Ar-*C)*, 124.9 (Ar-*C)*, 120.4 (*ipso*-Ar-*C)*, 118.0 (Ar-*C)*, 117.4 (*ipso*-Ar-*C)*, 102.1 (S*C*HC-$CH_3$), 57.4 (C=ONH*C*H), 38.0 (C=ONHCH*C*$H_2$), 13.5 (SCHC-*C*$H_3$); *m/z* ($ES^+$) 531 ([$^{35}$Cl]$MH^+$), 533 ([$^{37}$Cl]$MH^+$); HRMS ($ES^+$) Found [$^{35}$Cl]$MH^+$, 531.1359 ($C_{27}H_{24}{}^{35}ClN_6O_2S$ requires 531.1365).

**(S)-6-chloro-N-(1-oxo-3-phenyl-1-(2-(6-(trifluoromethyl)pyridin-3-yl)hydrazineyl)propan-2-yl)-2-phenylimidazo[1,2-*a*]pyridine-3-carboxamide 50El**

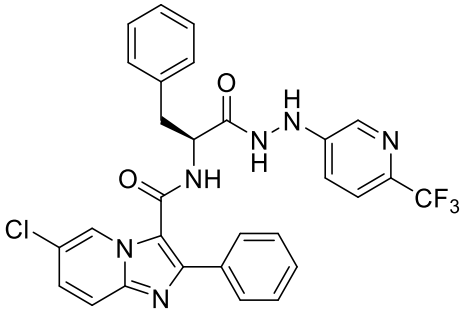

Using the standard procedure provided, *tert*-butyl (S)-(1-oxo-3-phenyl-1-(2-(6-(trifluoromethyl)propan-3-yl)hydrazineyl)propan-2-yl)carbamate **51Cl** (0.11 g, 0.25 mmol) was transformed using column chromatography (*n*-Hexane /EtOAc [2:1]) into the title compound as a white powder (65 mg, 43 %); $R_f$ 0.30 (*n*-Hexane /EtOAc [2:1]); m.p. 250 - 253 °C; $\nu_{max}$ 3252 (N-H), 3028 (N-H), 1672 (C=O), 1620 (C=O), 1591, 1533, 1492, 1450, 1419, 1386, 1341, 1224, 1166, 1085, 833, 698 $cm^{-1}$; $\delta_H$ (300 MHz, DMSO-$d_6$) 10.39 (1H, s, CON*H*NH), 8.91 (1H, d, *J* 7, CON*H*CH), 8.80 (1H, s, CONHN*H*), 8.55 (1H, s, Ar-*H*), 8.18 (1H, d, *J* 2, Ar-*H*), 7.76 – 7.62 (3H, m, Ar-*H*), 7.57 (1H, d, *J* 8, Ar-*H*), 7.45 (1H, dd, *J* 9, 1, Ar-*H*), 7.36 – 7.24 (8H, m, Ar-*H*), 7.07 (1H, dd, *J* 8, 2, Ar-*H*), 4.95 (1H, m, CONHC*H*), 3.18 (1H, dd, *J* 13, 4, CONHCHC$H_2$), 2.96 (1H, dd, *J* 13, 10, CONHCHC$H_2$); $\delta_C$ (75 MHz, DMSO-$d_6$) 171.4 (*C*=ONHNH), 161.1 (*C*=ONHCH), 147.9 (*ipso*-Ar-*C)*, 143.1 (*ipso*-Ar-*C)*, 137.7 (*ipso*-Ar-*C)*, 135.1 (Ar-*C)*, 133.3 (*ipso*-Ar-*C)*, 129.6 (Ar-*C)*, 128.8 (Ar-*C)*, 128.5 (Ar-*C)*, 127.7 (Ar-*C)*, 127.0 (Ar-*C)*, 124.5 (Ar-*C)*, 121.6 (Ar-*C)*, 120.3 (*ipso*-Ar-*C)*, 118.3 (Ar-*C)*, 118.1 (Ar-*C)*, 116.9 (*ipso*-Ar-*C)*, 53.9 (C=ONH*C*H), 37.4 (C=ONHCH*C*$H_2$); $\delta_F$ (282 MHz, DMSO-$d_6$) -64.9 (C$F_3$); *m/z* ($ES^+$) 578 ([$^{35}$Cl]$MH^+$), 280 ([$^{37}$Cl]$MH^+$); HRMS ($ES^+$) Found [$^{35}$Cl]$MH^+$, 578.1646 ($C_{29}H_{22}{}^{35}ClN_6O_2$ requires 578.1644).

**(S)-6-chloro-N-(1-(2-(6-chloropyridin-3-yl)hydrazineyl)-1-oxo-3-phenylpropan-2-yl)-2-phenylimidazo[1,2-*a*]pyridine-3-carboxamide 44Em**

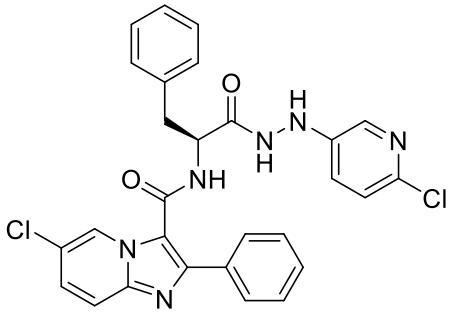


Using the standard procedure provided, *tert*-butyl (S)-(1-oxo-3-phenyl-1-(2-(6-chloropyridin-3-yl)hydrazineyl)propan-2-yl)carbamate **51Cm** (0.13 g, 0.30 mmol) was transformed using column chromatography (*n*-Hexane /EtOAc [1:1]) into the title compound as a white powder (65 mg, 42 %); $R_f$ 0.30 (*n*-Hexane /EtOAc [2:1]); m.p. 247 – 252 °C; $\nu_{max}$ 3252 (N-H), 3030 (N-H), 1673 (C=O), 1621 (C=O), 1537, 1492, 1387, 1341, 1228, 1165, 1086, 833, 699 $cm^{-1}$; $\delta_H$ (300 MHz, DMSO-$d_6$) 10.31 (1H, s, CON*H*NH), 8.86 (1H, d, *J* 7, CON*H*CH), 8.57 (1H, dd, *J* 2, 1, Ar-*H*), 8.34 (1H, s,

CONHN*H*), 7.86 (1H, d, *J* 3, Ar-*H*), 7.73 (1H, dd, *J* 9, 1, Ar-*H*), 7.70 – 7.65 (2H, dd, *J* 8, 2, Ar-*H*), 7.45 (1H, dd, *J* 9, 2, Ar-*H*), 7.37 – 7.25 (8H, m, Ar-*H*), 7.20 (1H, d, *J* 8, Ar-*H*), 7.05 (1H, dd, *J* 8, 2, Ar-*H*), 4.92 (1H, m, CONHC*H*), 3.16 (1H, dd, *J* 13, 4, CONHCHC$H_2$), 2.94 (1H, dd, *J* 13, 10, CONHCHC$H_2$); $\delta_C$ (75 MHz, DMSO-$d_6$) 171.4 (*C*=ONHNH), 161.0 (*C*=ONHCH), 145.5 (*ipso*-Ar-*C)*, 145.1 *ipso*-Ar-*C)*, 143.2 (*ipso*-Ar-*C)*, 139.5 (*ipso*-Ar-*C)*, 137.7 (*ipso*-Ar-*C)*, 134.5 (Ar-*C)*, 133.3 (*ipso*-Ar-*C)*, 129.6 (Ar-*C)*, 128.9 (Ar-*C)*, 128.8 (Ar-*C)*, 128.5 (Ar-*C)*, 127.8 (Ar-*C)*, 127.1 (Ar-*C)*, 124.6 (Ar-*C)*, 123.1 (Ar-*C)*, 120.4 (*ipso*-Ar-*C)*, 118.1 (Ar-*C)*, 117.0 (*ipso*-Ar-*C)*, 53.8 (C=ONH*C*H), 37.4 (C=ONHCH*C*$H_2$); *m/z* ($ES^+$) 545 ([$^{35,35}$Cl]$MH^+$), 547 ([$^{35,37}$Cl]$MH^+$), 549 ([$^{37,37}$Cl]$MH^+$); HRMS ($ES^+$) Found [$^{35,35}$Cl]$MH^+$, 545.1249 ($C_{28}H_{23}{}^{35,35}Cl_2N_6O_2$ requires 545.1254).

**(S)-6-chloro-N-(1-(2-(4-chloropyridin-2-yl)hydrazineyl)-1-oxo-3-phenylpropan-2-yl)-2-phenylimidazo[1,2-*a*]pyridine-3-carboxamide 44En**

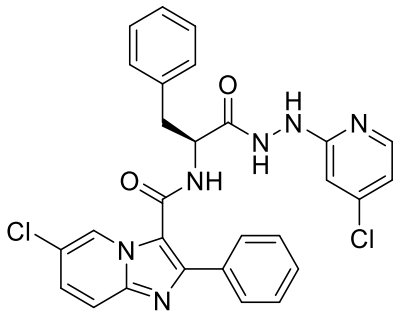


Using the standard procedure provided, *tert*-butyl (S)-(1-(2-(4-chloropyridin-2-yl)hydrazineyl)-1-oxo-3-phenylpropan-2-yl)carbamate **51Cn** (0.13 g, 0.33 mmol) was transformed using column chromatography (*n*-Hexane /EtOAc [1:1]) into the title compound as a white powder (83 mg, 46 %); $R_f$ 0.30 (*n*-Hexane /EtOAc [2:1]); m.p. 247 – 252 °C; $\nu_{max}$ 3259 (N-H), 3033 (N-H), 1670 (C=O), 1618 (C=O), 1535, 1493, 1450, 1419, 1386, 1322, 1251, 1228, 1166, 1126, 1078, 837, 687 $cm^{-1}$; $\delta_H$ (300 MHz, DMSO-$d_6$) 10.32 (1H, s, CON*H*NH), 8.98 (1H, s, CONHN*H*), 8.74 (1H, d, *J* 7, CON*H*CH), 8.57 (1H, dd, *J* 2, 1, Ar-*H*), 8.66 (1H, s, Ar-*H*), 7.91 (1H, d, *J* 5, Ar-*H*), 7.45 (1H, d, *J* 9, Ar-*H*), 7.72 – 7.64 (2H, d, *J* 7, Ar-*H*), 7.47 (1H, dd, *J* 9, 2, Ar-*H*), 7.38 – 7.23 (8H, m, Ar-*H*), 6.62 (1H, s, Ar-*H*), 6.55 (1H, d, *J* 5, Ar-*H*), 4.89 (1H, m, CONHC*H*), 3.14 (1H, dd, *J* 13, 4, CONHCHC$H_2$), 2.96 (1H, dd, *J* 13, 10, CONHCHC$H_2$); $\delta_C$ (75 MHz, DMSO-$d_6$) 171.2 (*C*ONHNH), 161.1 (*C*=ONHCH), 157.3 (*ipso*-Ar-*C)*, 151.5 (*ipso*-Ar-*C)*, 149.7 (Ar-*C)*, 145.9 (*ipso*-Ar-*C)*, 143.3 (*ipso*-Ar-*C)*, 137.5 (*ipso*-Ar-*C)*, 133.3 (*ipso*-

Ar-*C)*, 129.5 (Ar-*C)*, 128.9 (Ar-*C)*, 128.6 (Ar-*C)*, 127.9 (Ar-*C)*, 127.1 (Ar-*C)*, 124.7 (Ar-*C)*, 120.5 (*ipso*-Ar-*C)*, 118.2 (Ar-*C)*, 116.7 (*ipso*-Ar-*C)*, 107.0 (Ar-*C)*, 105.5 (Ar-*C)*, 53.9 (CONH*C*H), 37.3 (CONHCH*C*$H_2$); *m/z* ($ES^+$) 545 ([$^{35,35}$Cl]$MH^+$), 547 ([$^{35,37}$Cl]$MH^+$), 549 ([$^{37,37}$Cl]$MH^+$); HRMS ($ES^+$) Found [$^{35,35}$Cl]$MH^+$, 545.1245 ($C_{28}H_{23}{}^{35,35}Cl_2N_6O_2$ requires 545.1254).

**(S)-6-chloro-N-(1-(2-(2-chloropyridin-4-yl)hydrazineyl)-1-oxo-3-phenylpropan-2-yl)-2-phenylimidazo[1,2-*a*]pyridine-3-carboxamide 44Eo**

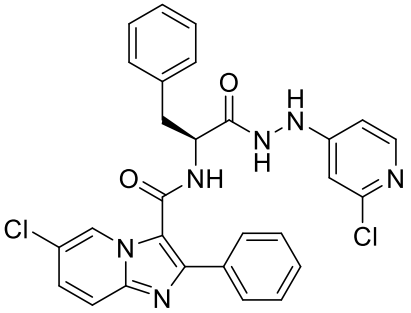

Using the standard procedure provided, *tert*-butyl (S)-(1-(2-(2-chloropyridin-4-yl)hydrazineyl)-1-oxo-3-phenylpropan-2-yl)carbamate **51Co** (0.13 g, 0.33 mmol) was transformed using column chromatography (*n*-Hexane /EtOAc [1:1]) into the title compound as a white powder (65 mg, 47 %); $R_f$ 0.30 (DCM/EtOAc [1:1]); m.p. 247 – 252 °C; $\nu_{max}$ 3251 (N-H), 3030, 1670 (C=O), 1618 (C=O), 1537, 1493, 1450, 1419, 1386, 1322, 1230, 1166, 1076, 988, 799, 696 $cm^{-1}$; $\delta_H$ (300 MHz, DMSO-$d_6$) 10.32 (1H, s, CON*H*NH), 8.98 (1H, s, CONHN*H*), 8.74 (1H, d, *J* 7, CON*H*CH), 8.66 (1H, s, Ar-*H*), 7.90 (1H, d, *J* 5, Ar-*H*), 7.74 (1H, d, *J* 9, Ar-*H*), 7.71 – 7.64 (2H, d, *J* 7, Ar-*H*), 7.47 (1H, dd, *J* 9, 2, Ar-*H*), 7.38 – 7.24 (8H, m, Ar-*H*), 6.62 (1H, s, Ar-*H*), 6.54 (1H, d, *J* 5, Ar-*H*), 4.91 (1H, m, CONHC*H*), 3.14 (1H, dd, *J* 13, 4, CONHCHC$H_2$), 2.95 (1H, dd, *J* 13, 10, CONHCHC$H_2$); $\delta_C$ (75 MHz, DMSO-$d_6$) 171.2 (*C*=ONHNH), 161.1 (*C*=ONHCH), 157.3 (*ipso*-Ar-*C)*, 151.5 (*ipso*-Ar-*C)*, 149.7 (Ar-*C)*, 145.9 (*ipso*-Ar-*C)*, 143.3 (*ipso*-Ar-*C)*, 137.5 (*ipso*-Ar-*C)*, 133.3 (*ipso*-Ar-*C)*, 129.5 (Ar-*C)*, 128.9 (Ar-*C)*, 128.8 (Ar-*C)*, 128.6 (Ar-*C)*, 127.9 (Ar-*C)*, 127.1 (Ar-*C)*, 124.7 (Ar-*C)*, 120.5 (*ipso*-Ar-*C)*, 118.2 (Ar-*C)*, 116.7 (*ipso*-Ar-*C)*, 107.0 (Ar-*C)*, 105.5 (Ar-*C)*, 53.9 (C=ONH*C*H), 37.3 (C=ONHCH*C*$H_2$); *m/z* ($ES^+$) 545 ([$^{35,35}$Cl]$MH^+$), 547 ([$^{35,37}$Cl]$MH^+$), 549 ([$^{37,37}$Cl]$MH^+$); HRMS ($ES^+$) Found [$^{35,35}$Cl]$MH^+$, 545.1249 ($C_{28}H_{23}{}^{35,35}Cl_2N_6O_2$ requires 545.1254).

**(S)-6-chloro-N-(1-(2-(6-methoxypyridin-3-yl)hydrazineyl)-1-oxo-3-phenylpropan-2-yl)-2-phenylimidazo[1,2-*a*]pyridine-3-carboxamide 44Ep**

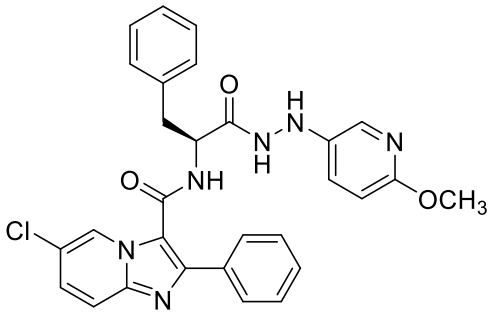

Using the standard procedure provided, *tert*-butyl (S)-(1-oxo-3-phenyl-1-(2-(6-methoypyridin-3-yl)hydrazineyl)propan-2-yl)carbamate **51** (0.10 g, 0.25 mmol) was transformed using column chromatography (DCM /EtOAc [1:1]) into the title compound as a white powder (62 mg, 44 %); $R_f$ 0.30 (DCM/EtOAc [1:1]); m.p. 242 – 245 °C; $\nu_{max}$ 3261 (N-H), 1666 (C=O), 1619 (C=O), 1537, 1490, 1383, 1322, 1224, 1164, 1031, 820, 685 $cm^{-1}$; $\delta_H$ (300 MHz, DMSO-$d_6$) 10.18 (1H, s, CON*H*NH), 8.85 (1H, d, *J* 7, CON*H*CH), 8.56 (1H, dd, *J* 2, 1, Ar-*H*), 8.34 (1H, s, CONHN*H*), 7.76 – 7.69 (2H, d, *J* 9, Ar-*H*), 7.69 – 7.61 (3H, m, Ar-*H*), 7.44 (1H, dd, *J* 9, 2, Ar-*H*), 7.36 – 7.23 (8H, m, Ar-*H*), 7.11 (1H, dd, *J* 9, 2, Ar-*H*), 6.63 (1H, d, *J* 8, Ar-*H*), 4.93 (1H, m, CONHC*H*), 3.73 (3H, s, Ar-OC*H*$_3$), 3.16 (1H, dd, *J* 13, 4, CONHCHC*H*$_2$), 2.92 (1H, dd, *J* 13, 10, CONHCHC*H*$_2$); $\delta_C$ (75 MHz, DMSO-$d_6$) 171.3 (*C*=ONHNH), 160.9 (*C*=ONHCH), 158.0 (*ipso*-Ar-*C)*, 145.4 (*ipso*-Ar-*C)*, 143.1 (*ipso*-Ar-*C)*, 137.8 (*ipso*-Ar-*C)*, 133.5 (Ar-*C)*, 133.2 (*ipso*-Ar-*C)*, 130.8 (Ar-*C)*, 129.6 (Ar-*C)*, 128.9 (Ar-*C)*, 128.8 (Ar-*C)*, 128.4 (Ar-*C)*, 127.7 (Ar-*C)*, 127.0 (Ar-*C)*, 125.8 (Ar-*C)*, 124.6 (Ar-*C)*, 120.4 (*ipso*-Ar-*C)*, 118.1 (Ar-*C)*, 117.0 (*ipso*-Ar-*C)*, 110.5 (Ar-*C)*, 53.7 (C=ONH*C*H), 53.4 (Ar-O*C*H$_3$), 37.6 (C=ONHCH*C*H$_2$); *m/z* (ES$^+$) 541 ([$^{35}$Cl]MH$^+$), 543 ([$^{37}$Cl]MH$^+$); HRMS (ES$^+$) Found [$^{35}$Cl]MH$^+$, 541.1744 ($C_{29}H_{26}{}^{35}ClN_6O_3$ requires 541.1749).

## 6.3 General Experimental Information- Biological evaluation

The mycobacterial strains and cell lines utilised in this research are shown in (Table 19).

### 6.3.1 Cell line

| Strain | Genotype | Comments |
|---|---|---|
| *Mtb* mc$^2$7902 | Δ*leuCD* Δ*panCD* Δ*argB* | mc$^2$6206 derived, arginine auxotroph[187] |
| *Mtb* mc$^2$8245 | Δ*panCD* Δ*leuCD* Δ*argB* Δ 2116169–2162530 | mc$^2$7902 derived, Δ2116169–2162530; INH-Resistant [187] |
| *Mtb* mc$^2$8247 | Δ*panCD* Δ*leuCD* Δ*argB* *rpoB* (H445Y) | mc$^2$7902 derived, *rpoB* His445 --> Lys; RIF resistant [187] |
| *Mtb* mc$^2$8250 | Δ*panCD* Δ*leuCD* Δ*argB r poB* (H445Y) Δ2122397–2170320 | mc$^2$8247 derived, Δ2122397–2170320; INH-Resistant, *rpoB* His445 --> Lys; RIF resistant [187] |
| *Mtb* mc$^2$8258 | Δ*panCD* Δ*leuCD* Δ*argB* *rpoB* (H445Y) *katG* (W43 8R) | mc$^2$8247 derived, *rpoB* His445 --> Lys; RIF resistant, *katG* Val1 --> Ala; INH-Resistant [187] |

Table 19. *Mtb* strains used in this work.

### 6.3.2 *In vitro* antibacterial assay

The inhibitory activity of compounds against *Mtb* strains was evaluated using a broth microdilution method in 96-well plates to determine minimum inhibitory concentrations. Mycobacterial cultures were maintained in either Middlebrook 7H10 agar or Middlebrook 7H9 broth, both supplemented with albumin–dextrose–catalase (ADC) or oleic acid–albumin–dextrose–catalase (OADC), along with 0.2% casamino acids, 0.2% glycerol, 1 µg/mL penicillin G, 10 µg/mL cycloheximide, and 24 µg/mL pantothenate. All culture components were sourced from BD Biosciences, and unless otherwise stated, additional reagents were purchased from Sigma-Aldrich (Gillingham, United Kingdom).

For MIC testing, bacteria were pre-cultured in 7H9OLAPp1k25c10 medium at 37 °C under 5% $CO_2$ for one week. The resulting suspensions were adjusted to a 0.5 McFarland standard and diluted 1:25 in fresh medium. Stock solutions of test compounds were prepared in sterile DMSO at 10 mg/mL, then serially diluted two-fold

(ranging from 64 to 0.062 µg/mL) in 7H9 medium. Each well of a sterile 96-well microplate received 100 µL of the diluted bacterial inoculum and 100 µL of the compound solution. Plates were sealed and incubated statically at 37 °C in a 5% $CO_2$ incubator.

Untreated cultures served as positive controls, while sterile medium served as a negative control. On day five of incubation, 10.5 µL of 0.1% (w/v) resazurin solution—prepared in phosphate-buffered saline (PBS) containing 0.02% Tween 80 was added to each well. The plates were incubated for an additional ~48 hours, after which color changes were observed to assess bacterial viability. The assay relies on metabolic reduction of blue, non-fluorescent resazurin into pink, fluorescent resorufin by viable cells.

Fluorescence was measured at excitation/emission wavelengths of 530/590 nm using a FLUOstar Optima plate reader (BMG Labtech). $MIC_{90}$ values were calculated using four-parameter logistic (4PL) regression in SigmaPlot™, and results were averaged across replicates for each compound.

# 7. References:


(1) World Health Organization. Global Tuberculosis Report; **2024**. https://tinyurl.com/tj9aya9w 2.

(2) Farhat, M.; Cox, H.; Ghanem, M.; Denkinger, C. M.; Rodrigues, C.; Abd El Aziz, M. S.; Enkh-Amgalan, H.; Vambe, D.; Ugarte-Gil, C.; Furin, J.; Pai, M. Drug-Resistant Tuberculosis: A Persistent Global Health Concern. *Nat Rev Microbiol* **2024**, *22* (10), 617–635. https://doi.org/10.1038/s41579-024-01025-1.

(3) Grüber, G. Introduction: Novel Insights into TB Research and Drug Discovery. *Prog Biophys Mol Biol* **2020**, *152*, 2–5. https://doi.org/10.1016/j.pbiomolbio.2020.02.003.

(4) Zhang, H.; Hsu, H. C.; Kahne, S. C.; Hara, R.; Zhan, W.; Jiang, X.; Burns-Huang, K.; Ouellette, T.; Imaeda, T.; Okamoto, R.; Kawasaki, M.; Michino, M.; Wong, T. T.; Toita, A.; Yukawa, T.; Moraca, F.; Vendome, J.; Saha, P.; Sato, K.; Aso, K.; Ginn, J.; Meinke, P. T.; Foley, M.; Nathan, C. F.; Darwin, K. H.; Li, H.; Lin, G. Macrocyclic Peptides That Selectively Inhibit the *Mycobacterium Tuberculosis* Proteasome. *J Med Chem* **2021**, *64* (9), 6262–6272. https://doi.org/10.1021/acs.jmedchem.1c00296.

(5) Guirado, E.; Schlesinger, L. S.; Chensue, S. W.; Taub, D. D. Modeling the *Mycobacterium Tuberculosis* Granuloma – the Critical Battlefield in Host Immunity and Disease. *Front. Immunol.* **2013**. https://doi.org/10.3389/fimmu.2013.00098.

(6) Bohórquez, J. A.; Jagannath, C.; Xu, H.; Wang, X.; Yi, G. T Cell Responses during Human Immunodeficiency Virus/*Mycobacterium Tuberculosis* Coinfection. *Vaccines (Basel)* **2024**, *12* (8), 1–16. https://doi.org/10.3390/vaccines12080901.

(7) Stewart, P.; Patel, S.; Comer, A.; Muneer, S.; Nawaz, U.; Quann, V.; Bansal, M.; Venketaraman, V. Role of B Cells in *Mycobacterium Tuberculosis* Infection. *Vaccines (Basel)* **2023**, *11* (5). https://doi.org/10.3390/vaccines11050955.

(8) Miggiano, R.; Rizzi, M.; Ferraris, D. M. Mycobacterium Tuberculosis Pathogenesis, Infection Prevention and Treatment. *Pathogens* **2020**, *9* (5), 10–13. https://doi.org/10.3390/pathogens9050385.

(9) Vu, A.; Glassman, I.; Campbell, G.; Yeganyan, S.; Nguyen, J.; Shin, A.; Venketaraman, V. Host Cell Death and Modulation of Immune Response against *Mycobacterium Tuberculosis* Infection. *Int J Mol Sci* **2024**, *25* (11). https://doi.org/10.3390/ijms25116255.

(10) Ramon-Luing, L. A.; Palacios, Y.; Ruiz, A.; Téllez-Navarrete, N. A.; Chavez-Galan, L. Virulence Factors of *Mycobacterium Tuberculosis* as Modulators of Cell Death Mechanisms. *Pathogens* **2023**, *12* (6). https://doi.org/10.3390/pathogens12060839.

(11) Liu, Y.; Li, H.; Dai, D.; He, J.; Liang, Z. Gene Regulatory Mechanism of *Mycobacterium Tuberculosis* during Dormancy. *Curr Issues Mol Biol* **2024**, *46* (6), 5825–5844. https://doi.org/10.3390/cimb46060348.

(12) Rahlwes, K. C.; Dias, B. R. S.; Campos, P. C.; Alvarez-Arguedas, S.; Shiloh, M. U. Pathogenicity and Virulence of Mycobacterium Tuberculosis. *Virulence* **2023**, *14* (1). https://doi.org/10.1080/21505594.2022.2150449.

(13) Silhavy, T. J.; Kahne, D.; Walker, S. The Bacterial Cell Envelope. *Cold Spring Harb. Perspect. Biol.* **2010** https://doi.org/10.1101/cshperspect.a000414.

(14) Maitra, A.; Munshi, T.; Healy, J.; Martin, L. T.; Vollmer, W.; Keep, N. H.; Bhakta, S. Cell Wall Peptidoglycan in *Mycobacterium Tuberculosis*: An Achilles' Heel for the TB-Causing Pathogen. *FEMS Microbiol Rev* **2019**, *43* (5), 548–575. https://doi.org/10.1093/FEMSRE/FUZ016.

(15) Vilchèze, C. Mycobacterial Cell Wall: A Source of Successful Targets for Old and New Drugs. *Appl. Sci.* **2020**, 10(*7*), 2278. https://doi.org/10.3390/app10072278.

(16) Seničar, M.; Lafite, P.; Eliseeva, S. V; Petoud, S.; Landemarre, L.; Daniellou, R. Molecular Sciences Galactofuranose-Related Enzymes: Challenges and Hopes. *Int. J. Mol. Sci.* **2020**, 21(*10*), 3465. https://doi.org/10.3390/ijms21103465.

(17) Chauhan, M.; Barot, R.; Yadav, R.; Joshi, K.; Mirza, S.; Chikhale, R.; Srivastava, V. K.; Yadav, M. R.; Murumkar, P. R. The Mycobacterium Tuberculosis Cell Wall: An Alluring Drug Target for Developing Newer Anti-TB Drugs—A Perspective. *Chem Biol Drug Des* **2024**, *104* (3). https://doi.org/10.1111/cbdd.14612.

(18) Raffetseder, J. *Phenotypes Interplay of Human Macrophages and Mycobacterium Tuberculosis Phenotypes*; PhD Thesis, Umeå University, **2019**. https://doi.org/10.3384/diss.diva-132321.

(19) Bendre, A. D.; Peters, P. J.; Kumar, J. Tuberculosis: Past, Present and Future of the Treatment and Drug Discovery Research. *Current Research in Pharmacology and Drug Discovery* **2021**, *2* (May), 100037. https://doi.org/10.1016/j.crphar.2021.100037.

(20) Fatima, S.; Kumari, A.; Das, G.; Dwivedi, V. P. Tuberculosis Vaccine: A Journey from BCG to Present. *Life Sci* **2020**, *252* (April). https://doi.org/10.1016/j.lfs.2020.117594.

(21) Stephanie, F.; Saragih, M.; Tambunan, U. S. F. Recent Progress and Challenges for Drug-Resistant Tuberculosis Treatment. *Pharmaceutics* **2021**, *13* (5). https://doi.org/10.3390/pharmaceutics13050592.

(22) Cho, T.; Khatchadourian, C.; Nguyen, H.; Dara, Y.; Jung, S.; Venketaraman, V. A Review of the BCG Vaccine and Other Approaches toward Tuberculosis Eradication. *Hum Vaccin Immunother*. **2021**. https://doi.org/10.1080/21645515.2021.1885280.

(23) Kuan, R.; Muskat, K.; Peters, B.; Lindestam Arlehamn, C. S. Is Mapping the BCG Vaccine-Induced Immune Responses the Key to Improving the Efficacy against Tuberculosis? *J Intern Med* **2020**, *288* (6), 651–660. https://doi.org/10.1111/JOIM.13191.

(24) Zhuang, L.; Ye, Z.; Li, L.; Yang, L.; Gong, W. Next-Generation TB Vaccines: Progress, Challenges, and Prospects. *Vaccines (Basel)* **2023**, *11* (8). https://doi.org/10.3390/vaccines11081304.

(25) Stewart, E.; Triccas, J. A.; Petrovsky, N. Adjuvant Strategies for More Effective Tuberculosis Vaccine Immunity. *Microorganisms* **2022**, *7* (8), 1–16. https://doi.org/10.3390/microorganisms7080255.

(26) Romano, M.; Squeglia, F.; Kramarska, E.; Barra, G.; Choi, H. G.; Kim, H. J.; Ruggiero, A.; Berisio, R. A Structural View at Vaccine Development against M. Tuberculosis. *Cells* **2023**, *12* (2). https://doi.org/10.3390/cells12020317.

(27) Kayukova, L. A.; Berikova, E. A. Modern Anti-Tuberculosis Drugs and Their Classification. Part I: First-Line Drugs. *Pharm Chem J* **2020**, *54* (6), 555–563. https://doi.org/10.1007/s11094-020-02239-2.

(28) Alsayed, S. S. R.; Gunosewoyo, H. Tuberculosis: Pathogenesis, Current Treatment Regimens and New Drug Targets. *Int J Mol Sci* **2023**, *24* (6). https://doi.org/10.3390/ijms24065202.

(29) Vilchèze, C.; Jacobs, W. R. The Isoniazid Paradigm of Killing, Resistance, and Persistence in Mycobacterium Tuberculosis. *Journal of Molecular Biology*. Academic Press August 23, **2019**, pp 3450–3461. https://doi.org/10.1016/j.jmb.2019.02.016.

(30) du Preez, I.; Loots, D. T. Novel Insights into the Pharmacometabonomics of First-Line Tuberculosis Drugs Relating to Metabolism, Mechanism of Action and Drug-Resistance. *Drug Metabolism Reviews*. Taylor and Francis Ltd October 2, **2018**, pp 466–481. https://doi.org/10.1080/03602532.2018.1559184.

(31) Shah, M. A.; Uddin, A.; Shah, M. R.; Ali, I.; Ullah, R.; Hannan, P. A.; Hussain, H. Synthesis and Characterization of Novel Hydrazone Derivatives of Isonicotinic Hydrazide and Their Evaluation for Antibacterial and Cytotoxic Potential. *Molecules* **2022**, *27* (19). https://doi.org/10.3390/molecules27196770.

(32) Kilic-Kurt, Z.; Acar, C.; Ergul, M.; Bakar-Ates, F.; Altuntas, T. G. Novel Indole Hydrazide Derivatives: Synthesis and Their Antiproliferative Activities through Inducing Apoptosis and DNA Damage. *Arch Pharm (Weinheim)* **2020**, *353* (8). https://doi.org/10.1002/ardp.202000059.

(33) Hu, Y. Q.; Zhang, S.; Zhao, F.; Gao, C.; Feng, L. S.; Lv, Z. S.; Xu, Z.; Wu, X. Isoniazid Derivatives and Their Anti-Tubercular Activity. *Eur J Med Chem* **2017**, *133*, 255–267. https://doi.org/10.1016/j.ejmech.2017.04.002.

(34) Alghamdi, S.; Qusty, N. F.; Atwah, B.; Alhindi, Z.; Alatawy, R.; Verma, S.; Asif, M. Isoniazid Analogs and Their Biological Activities as Antitubercular Agents ( A Review ). *Russ J Gen Chem*. **2024**, *94* (8), 2101–2141. https://doi.org/10.1134/S1070363224080231.

(35) Peloquin, C. A.; Davies, G. R. The Treatment of Tuberculosis. *Clin Pharmacol Ther* **2021**, *110* (6), 1455–1466. https://doi.org/10.1002/cpt.2261.

(36) Goldstein, B. P. Resistance to Rifampicin: A Review. *Journal of Antibiotics* **2014**, *67* (9), 625–630. https://doi.org/10.1038/ja.2014.107.

(37) Singh, V.; Chibale, K. Strategies to Combat Multi-Drug Resistance in Tuberculosis. *Acc Chem Res* **2021**, *54* (10), 2361–2376. https://doi.org/10.1021/acs.accounts.0c00878.

(38) Morgan, M.; Kalantri, S.; Flores, L.; Pai, M. A Commercial Line Probe Assay for the Rapid Detection of Rifampicin Resistance in *Mycobacterium Tuberculosis*: A Systemic Review and Meta-Analysis. *BMC Infect Dis* **2005**, *5* (1), 1–9. https://doi.org/10.1186/1471-2334-5-62/FIGURES/3.

(39) Adams, R. A.; Leon, G.; Miller, N. M.; Reyes, S. P.; Thantrong, C. H.; Thokkadam, A. M.; Lemma, A. S.; Sivaloganathan, D. M.; Wan, X.; Brynildsen, M. P. Rifamycin Antibiotics and the Mechanisms of Their Failure. *Journal of Antibiotics* **2021**, *74* (11), 786–798. https://doi.org/10.1038/s41429-021-00462-x.

(40) Nusrath Unissa, A.; Hanna, L. E.; Swaminathan, S. A Note on Derivatives of Isoniazid, Rifampicin, and Pyrazinamide Showing Activity Against Resistant Mycobacterium Tuberculosis. *Chem Biol Drug Des* **2016**, *87* (4), 537–550. https://doi.org/10.1111/cbdd.12684.

(41) Vernon, A.; Burman, W.; Benator, D.; Khan, A.; Bozeman, L. Acquired Rifamycin Monoresistance in Patients with HIV-Related Tuberculosis Treated with Once-Weekly Rifapentine and Isoniazid. *Lancet* **1999**, *353* (9167), 1843–1847. https://doi.org/10.1016/S0140-6736(98)11467-8.

(42) Schubert, K.; Sieger, B.; Meyer, F.; Giacomelli, G.; Böhm, K.; Rieblinger, A.; Lindenthal, L.; Sachs, N.; Wanner, G.; Bramkamp, M. The Antituberculosis Drug Ethambutol Selectively Blocks Apical Growth in CMN Group Bacteria. *mBio* **2017**, *8* (1). https://doi.org/10.1128/mBio.02213-16.

(43) Khawbung, J. L.; Nath, D.; Chakraborty, S. Drug Resistant Tuberculosis: A Review. *Comp Immunol Microbiol Infect Dis* **2021**, *74*, 101574. https://doi.org/10.1016/j.cimid.2020.101574.

(44) Peloquin, C. A.; Davies, G. R. The Treatment of Tuberculosis. *CLINICAL PHARMACOLOGY & THERAPEUTICS | VOLUME* **2021**, *110* (6). https://doi.org/10.1002/cpt.2261.

(45) Wang, X.; Hu, H.; Zhou, W.; Gongye, J.; Wang, T.; Xu, J. Pyrazinamide Analogs Designed for Rational Drug Designing Strategies Against Resistant Tuberculosis (A Review). *Russ J Bioorg Chem* **2024**, *50* (1), 8–27. https://doi.org/10.1134/S1068162024010242.

(46) Gopal, P.; Grüber, G.; Dartois, V.; Dick, T. Pharmacological and Molecular Mechanisms Behind the Sterilizing Activity of Pyrazinamide. *Trends Pharmacol Sci* **2019**, *40* (12), 930–940. https://doi.org/10.1016/J.TIPS.2019.10.005.

(47) Zhang, Y.; Shi, W.; Zhang, W.; Mitchison, D. Mechanisms of Pyrazinamide Action and Resistance. *Microbiol Spectr* **2014**, *2* (4). https://doi.org/10.1128/MICROBIOLSPEC.MGM2-0023-2013.

(48) Jean-Paul Ursul, D. N. Pharmacotherapeutic Evolution of Antituberculosis Drug—A Review. *World J Pharm Pharm Sci.* https://doi.org/10.20959/wjpps201812-12776.

(49) Ramachandran, G.; Swaminathan, S. Safety and Tolerability Profile of Second-Line Anti-Tuberculosis Medications. *Drug Saf.* **2015**. https://doi.org/10.1007/s40264-015-0267-y.

(50) Espinosa-Pereiro, J.; Sánchez-Montalvá, A.; Aznar, M. L.; Espiau, M. Medicina MDR Tuberculosis Treatment. *Medicina (Kaunas).* **2022**. https://doi.org/10.3390/medicina58020188.

(51) Pranger, A. D.; van der Werf, T. S.; Kosterink, J. G.; Alffenaar, · J W C. The Role of Fluoroquinolones in the Treatment of Tuberculosis in 2019. *Drugs.* **2019**, *79*, 161–171. https://doi.org/10.1007/s40265-018-1043-y.

(52) Espinosa-Pereiro, J.; Sánchez-Montalvá, A.; Aznar, M. L.; Espiau, M. MDR Tuberculosis Treatment. *Medicina (Lithuania)* **2022**, *58* (2), 1–34. https://doi.org/10.3390/medicina58020188.

(53) Ahmad, N.; Ahuja, S. D.; Akkerman, O. W. Treatment Correlates of Successful Outcomes in Pulmonary Multidrug-Resistant Tuberculosis: An Individual Patient Data Meta-Analysis. Lancet **2018**, 392 (10150), 821–834. https://doi.org/10.1016/S0140-6736(18)31644-1.

(54) World Health Organization. Treatment of Tuberculosis: *Guidelines for Treatment of Drug-Susceptible Tuberculosis and Patient Care*; WHO: Geneva, Switzerland, **2017**. https://www.who.int/publications/i/item/9789241550000

(55) World Health Organization. *Meeting Report of the WHO Expert Consultation on the Definition of Extensively Drug-Resistant Tuberculosis*; Geneva, Switzerland, **2020**. https://iris.who.int/bitstream/handle/10665/338776/9789240018662-eng.pdf

(56) Magnet, S.; Blanchard, J. S. Molecular Insights into Aminoglycoside Action and Resistance. *Chem Rev* **2005**, *105* (2), 477–497. https://doi.org/10.1021/cr0301088.

(57) Guthrie, O. W. Aminoglycoside Induced Ototoxicity. *Toxicology* **2008**, *249* (2–3), 91–96. https://doi.org/10.1016/j.tox.2008.04.015.

(58) Laborde, J.; Deraeve, C.; Duhayon, C.; Pratviel, G.; Bernardes-Génisson, V. Organic & Biomolecular Chemistry Ethionamide Biomimetic Activation and an Unprecedented Mechanism for Its Conversion into Active and Non-Active Metabolites †. *Org Biomol Chem* **2016**, *14*, 8848. https://doi.org/10.1039/c6ob01561a.

(59) World Health Organization. *WHO Consolidated Guidelines on Tuberculosis. Module 4: Treatment – Drug-Resistant Tuberculosis Treatment*. Geneva: WHO; **2020**. https://www.who.int/publications/i/item/9789240007048

(60) Khawbung, J. L.; Nath, D.; Chakraborty, S. Drug Resistant Tuberculosis: A Review. *Comp Immunol Microbiol Infect Dis* **2021**, *74*, 101574. https://doi.org/10.1016/J.CIMID.2020.101574.

(61) Lehmann, J. Para-Aminosalicylic Acid in the Treatment of Tuberculosis. *The Lancet* **1946**, *247* (6384), 15–16. https://doi.org/10.1016/S0140-6736(46)91185-3.

(62) Iseman, M. D. Tuberculosis Therapy: Past, Present and Future. *European Respiratory Journal, Supplement* **2002**, *20* (36), 87–94. https://doi.org/10.1183/09031936.02.00309102.

(63) Lee, A.; Xie, Y. L.; Barry, C. E.; Chen, R. Y. Current and Future Treatments for Tuberculosis. *The BMJ* **2020**, *368*. https://doi.org/10.1136/bmj.m216.

(64) Zheng, J.; Rubin, E. J.; Bifani, P.; Mathys, V.; Lim, V.; Au, M.; Jang, J.; Nam, J.; Dick, T.; Walker, J. R.; Pethe, K.; Camacho, L. R. Para-Aminosalicylic Acid Is a Prodrug Targeting Dihydrofolate Reductase in Mycobacterium Tuberculosis. *Journal of Biological Chemistry* **2013**, *288* (32), 23447–23456. https://doi.org/10.1074/jbc.M113.475798.

(65) Hegde, P. V.; Howe, M. D.; Zimmerman, M. D.; Boshoff, H. I. M.; Sharma, S.; Remache, B.; Jia, Z.; Pan, Y.; Baughn, A. D.; Dartois, V.; Aldrich, C. C. Synthesis and Biological Evaluation of Orally Active Prodrugs and Analogs of Para-Aminosalicylic Acid (PAS). *Eur J Med Chem* **2022**, *232*, 114201. https://doi.org/10.1016/j.ejmech.2022.114201.

(66) Wei, X.; Yue, L.; Zhao, B.; Jiang, N.; Lei, H.; Zhai, X. Recent Advances and Challenges of Revolutionizing Drug-Resistant Tuberculosis Treatment. *Eur J Med Chem* **2024**, *277* (June), 116785. https://doi.org/10.1016/j.ejmech.2024.116785.

(67) Samanta, S.; Kumar, S.; Aratikatla, E. K.; Ghorpade, S. R.; Singh, V. Recent Developments of Imidazo[1,2-a]Pyridine Analogues as Antituberculosis Agents. *RSC Med Chem* **2023**, *14* (4), 644–657. https://doi.org/10.1039/d3md00019b.

(68) Li, Y.; Sun, F.; Zhang, W. Bedaquiline and Delamanid in the Treatment of Multidrug-Resistant Tuberculosis: Promising but Challenging. *Drug Dev Res* **2019**, *80* (1), 98–105. https://doi.org/10.1002/ddr.21498.

(69) Appetecchia, F.; Consalvi, S.; Scarpecci, C.; Biava, M.; Poce, G. Sar Analysis of Small Molecules Interfering with Energy-Metabolism in Mycobacterium Tuberculosis. *Pharmaceuticals* **2020**, *13* (9), 1–33. https://doi.org/10.3390/ph13090227.

(70) Sutherland, H. S.; Tong, A. S. T.; Choi, P. J.; Blaser, A.; Conole, D.; Franzblau, S. G.; Lotlikar, M. U.; Cooper, C. B.; Upton, A. M.; Denny, W. A.; Palmer, B. D. 3,5-Dialkoxypyridine Analogues of Bedaquiline Are Potent Antituberculosis Agents with Minimal Inhibition of the HERG Channel. *Bioorg Med Chem* **2019**, *27* (7), 1292–1307. https://doi.org/10.1016/j.bmc.2019.02.026.

(71) Svensson, E. M.; Murray, S.; Karlsson, M. O.; Dooley, K. E. Rifampicin and Rifapentine Significantly Reduce Concentrations of Bedaquiline, a New Anti-TB Drug. *Journal of Antimicrobial Chemotherapy* **2014**, *70* (4), 1106–1114. https://doi.org/10.1093/jac/dku504.

(72) Tong, A. S. T.; Choi, P. J.; Blaser, A.; Sutherland, H. S.; Tsang, S. K. Y.; Guillemont, J.; Motte, M.; Cooper, C. B.; Andries, K.; Van Den Broeck, W.; Franzblau, S. G.; Upton, A. M.; Denny, W. A.; Palmer, B. D.; Conole, D. 6-Cyano Analogues of Bedaquiline as Less Lipophilic and Potentially Safer Diarylquinolines for Tuberculosis. *ACS Med Chem Lett* **2017**, *8* (10), 1019–1024. https://doi.org/10.1021/acsmedchemlett.7b00196.

(73) Van Heeswijk RPG, Dannemann B, Hoetelmans RMW. Bedaquiline: A Review of Human Pharmacokinetics and Drug-Drug Interactions. *J Antimicrob Chemother*. **2014**;69(9):2310–2318. https://doi.org/10.1093/jac/dku171.

(74) Chen, X.; Hashizume, H.; Tomishige, T.; Nakamura, I.; Matsuba, M.; Fujiwara, M.; Kitamoto, R.; Hanaki, E.; Ohba, Y.; Matsumoto, M. Delamanid Kills Dormant Mycobacteria in Vitro and in a Guinea Pig Model of Tuberculosis. *Antimicrob Agents Chemother* **2017**, *61* (6). https://doi.org/10.1128/AAC.02402-16.

(75) Cabrera-rivero, J. L.; Vargas-vasquez, D. E.; Gao, M.; Ph, D.; Awad, M.; Ch, B.; Park, S.; Ph, D.; Shim, T. S.; Ph, D.; Suh, G. Y. Delamanid for Multidrug Resistant Pulmonary Tuberculosis. *N. Engl. J. Med.* **2012**, 366 (*23*), 2151–2160. https://doi.org/10.1056/NEJMoa1112433.

(76) Conradie, F.; Diacon, A. H.; Ngubane, N.; Howell, P.; Everitt, D.; Crook, A. M.; Mendel, C. M.; Egizi, E.; Moreira, J.; Timm, J.; McHugh, T. D.; Wills, G. H.; Bateson, A.; Hunt, R.; Van Niekerk, C.; Li, M.; Olugbosi, M.; Spigelman, M. Treatment of Highly Drug-Resistant Pulmonary Tuberculosis. *New England Journal of Medicine* **2020**, *382* (10), 893–902. https://doi.org/10.1056/nejmoa1901814.

(77) Hanaki, E.; Hayashi, M.; Matsumoto, M. Delamanid Is Not Metabolized by Salmonella or Human Nitroreductases: A Possible Mechanism for the Lack of Mutagenicity. *Regulatory Toxicology and Pharmacology* **2017**, *84*, 1–8. https://doi.org/10.1016/j.yrtph.2016.12.002.

(78) Lee, B. M.; Harold, L. K.; Almeida, D. V.; Afriat-Jurnou, L.; Aung, H. L.; Forde, B. M.; Hards, K.; Pidot, S. J.; Ahmed, F. H.; Mohamed, A. E.; Taylor, M. C.; West, N. P.; Stinear, T. P.; Greening, C.; Beatson, S. A.; Nuermberger, E. L.; Cook, G. M.; Jackson, C. J. Predicting Nitroimidazole Antibiotic Resistance Mutations in Mycobacterium Tuberculosis with Protein Engineering. *PLoS Pathog* **2020**, *16* (2), 1–27. https://doi.org/10.1371/journal.ppat.1008287.

(79) World Health Organization, (WHO). *Consolidated Guidelines on Tuberculosis Treatment*; **2020**.

(80) Sloan, D. J.; Lewis, J. M. Management of Multidrug-Resistant TB: Novel Treatments and Their Expansion to Low Resource Settings. *Trans R Soc Trop Med Hyg* **2015**, *110* (3), 163–172. https://doi.org/10.1093/trstmh/trv107.

(81) Zhaojing Zong, a, c Wei Jing, a Jin Shi, b Shu'an Wen, a Tingting Zhang, a Fengmin Huo, a Yuanyuan Shang, a Qian Liang, a Hairong Huang, a Yu Pangarug-resistant, E. Crossm Comparison of *In Vitro* Activity and MIC Distributions Between. *Antimicrob Agents Chemother* **2018**, *62* (8), 1–8.

(82) Negatu, D. A.; Aragaw, W. W.; Cangialosi, J.; Dartois, V.; Dick, T. Side-by-Side Profiling of Oxazolidinones to Estimate the Therapeutic Window against Mycobacterial Infections. *Antimicrob Agents Chemother* **2023**, *67* (4). https://doi.org/10.1128/aac.01655-22.

(83) Chen, R. H.; Burke, A.; Cho, J. G.; Alffenaar, J. W.; Davies Forsman, L. New Oxazolidinones for Tuberculosis: Are Novel Treatments on the Horizon? *Pharmaceutics* **2024**, *16* (6), 1–27. https://doi.org/10.3390/pharmaceutics16060818.

(84) Cho, Y. L.; Jang, J. Development of Delpazolid for the Treatment of Tuberculosis. *Applied Sciences (Switzerland)* **2020**, *10* (7), 1–11. https://doi.org/10.3390/app10072211.

(85) Yuan, S.; Shen, D. D.; Bai, Y. R.; Zhang, M.; Zhou, T.; Sun, C.; Zhou, L.; Wang, S. Q.; Liu, H. M. Oxazolidinone: A Promising Scaffold for the Development of Antibacterial Drugs. *Eur J Med Chem* **2023**, *250* (January), 115239. https://doi.org/10.1016/j.ejmech.2023.115239.

(86) Tantry, S. J.; Markad, S. D.; Shinde, V.; Bhat, J.; Balakrishnan, G.; Gupta, A. K.; Ambady, A.; Raichurkar, A.; Kedari, C.; Sharma, S.; Mudugal, N. V.; Narayan, A.; Naveen Kumar, C. N.; Nanduri, R.; Bharath, S.; Reddy, J.; Panduga, V.; Prabhakar, K. R.; Kandaswamy, K.; Saralaya, R.; Kaur, P.; Dinesh, N.; Guptha, S.; Rich, K.; Murray, D.; Plant, H.; Preston, M.; Ashton, H.; Plant, D.; Walsh, J.; Alcock, P.; Naylor, K.; Collier, M.; Whiteaker, J.; McLaughlin, R. E.; Mallya, M.; Panda, M.; Rudrapatna, S.; Ramachandran, V.; Shandil, R.; Sambandamurthy, V. K.; Mdluli, K.; Cooper, C. B.; Rubin, H.; Yano, T.; Iyer, P.; Narayanan, S.; Kavanagh, S.; Mukherjee, K.; Balasubramanian, V.; Hosagrahara, V. P.; Solapure, S.; Ravishankar, S.; Hameed P, S. Discovery of Imidazo[1,2-a]Pyridine Ethers and Squaramides as Selective and Potent Inhibitors of Mycobacterial Adenosine Triphosphate (ATP) Synthesis. *J Med Chem* **2017**, *60* (4), 1379–1399. https://doi.org/10.1021/acs.jmedchem.6b01358.

(87) Abrahams, K. A.; Cox, J. A. G.; Spivey, V. L.; Loman, N. J.; Pallen, M. J.; Constantinidou, C.; Fernández, R.; Alemparte, C.; Remuiñán, M. J.; Barros, D.; Ballell, L.; Besra, G. S. Identification of Novel Imidazo[1,2-a]Pyridine Inhibitors Targeting *M. Tuberculosis* QcrB. *PLoS One* **2012**, *7* (12). https://doi.org/10.1371/journal.pone.0052951.

(88) Pethe, K.; Bifani, P.; Jang, J.; Kang, S.; Park, S.; Ahn, S.; Jiricek, J.; Jung, J.; Jeon, H. K.; Cechetto, J.; Christophe, T.; Lee, H.; Kempf, M.; Jackson, M.; Lenaerts, A. J.; Pham, H.; Jones, V.; Seo, M. J.; Kim, Y. M.; Seo, M.; Seo, J. J.; Park, D.; Ko, Y.; Choi, I.; Kim, R.; Kim, S. Y.; Lim, S.; Yim, S. A.; Nam, J.; Kang, H.; Kwon, H.; Oh, C. T.; Cho, Y.; Jang, Y.; Kim, J.; Chua, A.; Tan, B. H.; Nanjundappa, M. B.; Rao, S. P. S.; Barnes, W. S.; Wintjens, R.; Walker, J. R.; Alonso, S.; Lee, S.; Kim, J.; Oh, S.; Oh, T.; Nehrbass, U.; Han, S. J.; No, Z.; Lee, J.; Brodin, P.; Cho, S. N.; Nam, K.; Kim, J. Discovery of Q203, a Potent Clinical Candidate for the Treatment of Tuberculosis. *Nat Med* **2013**, *19* (9), 1157–1160. https://doi.org/10.1038/nm.3262.

(89) Bahuguna, A.; Rawat, S.; Rawat, D. S. QcrB in Mycobacterium Tuberculosis: The New Drug Target of Antitubercular Agents. *Med Res Rev* **2021**, *41* (4), 2565–2581. https://doi.org/10.1002/med.21779.

(90) Bahuguna, A.; Rawat, S.; Rawat, D. S. QcrB in Mycobacterium Tuberculosis: The New Drug Target of Antitubercular Agents. *Med Res Rev* **2021**, *41* (4), 2565–2581. https://doi.org/10.1002/med.21779.

(91) Kang, S.; Kim, Y. M.; Kim, R. Y.; Seo, M. J.; No, Z.; Nam, K.; Kim, S.; Kim, J. Synthesis and Structure-Activity Studies of Side Chain Analogues of the Anti-Tubercular Agent, Q203. *Eur J Med Chem* **2017**, *125*, 807–815. https://doi.org/10.1016/j.ejmech.2016.09.082.

(92) Wang, A.; Wang, H.; Geng, Y.; Fu, L.; Gu, J.; Wang, B.; Lv, K.; Liu, M.; Tao, Z.; Ma, C.; Lu, Y. Design, Synthesis and Antimycobacterial Activity of Less Lipophilic Q203 Derivatives Containing Alkaline

Fused Ring Moieties. *Bioorg Med Chem* **2019**, *27* (5), 813–821. https://doi.org/10.1016/j.bmc.2019.01.022.

(93) Kang, S.; Kim, Y. M.; Jeon, H.; Park, S.; Seo, M. J.; Lee, S.; Park, D.; Nam, J.; Lee, S.; Nam, K.; Kim, S.; Kim, J. Synthesis and Structure-Activity Relationships of Novel Fused Ring Analogues of Q203 as Antitubercular Agents. *Eur J Med Chem* **2017**, *136*, 420–427. https://doi.org/10.1016/j.ejmech.2017.05.021.

(94) Church, N. A.; McKillip, J. L. Antibiotic Resistance Crisis: Challenges and Imperatives. *Biologia (Bratisl)* **2021**, *76* (5), 1535–1550. https://doi.org/10.1007/s11756-021-00697-x.

(95) Chinemerem Nwobodo, D.; Ugwu, M. C.; Oliseloke Anie, C.; Al-Ouqaili, M. T. S.; Chinedu Ikem, J.; Victor Chigozie, U.; Saki, M. Antibiotic Resistance: The Challenges and Some Emerging Strategies for Tackling a Global Menace. *J Clin Lab Anal* **2022**, *36* (9), 1–10. https://doi.org/10.1002/jcla.24655.

(96) Khawbung, J. L.; Nath, D.; Chakraborty, S. Drug Resistant Tuberculosis: A Review. *Comp Immunol Microbiol Infect Dis* **2021**, *74*, 101574. https://doi.org/10.1016/j.cimid.2020.101574.

(97) Tiberi, S.; Utjesanovic, N.; Galvin, J.; Centis, R.; D'Ambrosio, L.; van den Boom, M.; Zumla, A.; Migliori, G. B. Drug Resistant TB – Latest Developments in Epidemiology, Diagnostics and Management. *International Journal of Infectious Diseases* **2022**, *124*, S20–S25. https://doi.org/10.1016/j.ijid.2022.03.026.

(98) Khawbung, J. L.; Nath, D.; Chakraborty, S. Drug Resistant Tuberculosis: A Review. *Comp Immunol Microbiol Infect Dis* **2021**, *74*, 101574. https://doi.org/10.1016/J.CIMID.2020.101574.

(99) Antonio, J.; Luna, C.; Mendoza, G. P.; Rodríguez De Castro, F. *Multi-Drug Resistant Tuberculosis, Ten Years Later*; **2021**; Vol. 156.

(100) WHO. Rapid Communication: Key Changes to the Treatment of Drug-Resistant Tuberculosis. *Who* **2022**, No. WHO/UCN/TB/2022.2., 6.

(101) Sachan, R. S. K.; Mistry, V.; Dholaria, M.; Rana, A.; Devgon, I.; Ali, I.; Iqbal, J.; Eldin, S. M.; Mohammad Said Al-Tawaha, A. R.; Bawazeer, S.; Dutta, J.; Karnwal, A. Overcoming Mycobacterium Tuberculosis Drug Resistance: Novel Medications and Repositioning Strategies. *ACS Omega* **2023**, *8* (36), 32244–32257. https://doi.org/10.1021/acsomega.3c02563.

(102) Nasiri, M. J.; Haeili, M.; Ghazi, M.; Goudarzi, H.; Pormohammad, A.; Fooladi, A. A. I.; Feizabadi, M. M. New Insights in to the Intrinsic and Acquired Drug Resistance Mechanisms in Mycobacteria. *Front Microbiol* **2017**, *8* (APR). https://doi.org/10.3389/fmicb.2017.00681.

(103) Lee, J. M.; Hammarén, H. M.; Savitski, M. M.; Baek, S. H. Control of Protein Stability by Post-Translational Modifications. *Nat Commun* **2023**, *14* (1), 1–16. https://doi.org/10.1038/s41467-023-35795-8.

(104) Ramazi, S.; Zahiri, J. Post-Translational Modifications in Proteins: Resources, Tools and Prediction Methods. *Database* **2021**, *2021* (7), 1–20. https://doi.org/10.1093/database/baab012.

(105) Shen, F.; Dassama, L. M. K. Opportunities and Challenges of Protein-Based Targeted Protein Degradation. *Chem Sci* **2023**, *14* (32), 8433–8447. https://doi.org/10.1039/d3sc02361c.

(106) Zhao, L.; Zhao, J.; Zhong, K.; Tong, A.; Jia, D. Targeted Protein Degradation: Mechanisms, Strategies and Application. *Signal Transduct Target Ther*. **2022**, *7* (1). https://doi.org/10.1038/s41392-022-00966-4.

(107) Alhasan, B. A.; Morozov, A. V.; Guzhova, I. V.; Margulis, B. A. The Ubiquitin-Proteasome System in the Regulation of Tumor Dormancy and Recurrence. *Biochim Biophys Acta Rev Cancer* **2024**, *1879* (4), 189119. https://doi.org/10.1016/j.bbcan.2024.189119.

(108) Çetin, G.; Klafack, S.; Studencka-Turski, M.; Krüger, E.; Ebstein, F. The Ubiquitin–Proteasome System in Immune Cells. *Biomolecules* **2021**, *11* (1), 1–23. https://doi.org/10.3390/biom11010060.

(109) Striebel, F.; Imkamp, F.; Özcelik, D.; Weber-Ban, E. Pupylation as a Signal for Proteasomal Degradation in Bacteria. *Biochim Biophys Acta Mol Cell Res* **2014**, *1843* (1), 103–113. https://doi.org/10.1016/j.bbamcr.2013.03.022.

(110) Regev, O.; Linder, H.; Gur, E. Pup-Click A New Chemoenzymatic Method for the Generation of Singly Pupylated Targets. *Bioconjug Chem.* **2019**. https://doi.org/10.1021/acs.bioconjchem.9b00611.

(111) Özcelik, D.; Barandun, J.; Schmitz, N.; Sutter, M.; Guth, E.; Damberger, F. F.; Allain, F. H. T.; Ban, N.; Weber-Ban, E. Structures of Pup Ligase PafA and Depupylase Dop from the Prokaryotic Ubiquitin-like Modification Pathway. *Nat Commun* **2012**, *3* (May). https://doi.org/10.1038/ncomms2009.

(112) Alhuwaider, A. A. H.; Truscott, K. N.; Dougan, D. A. Pupylation of PafA or Pup Inhibits Components of the Pup-Proteasome System. *FEBS Lett* **2018**, *592* (1), 15–23. https://doi.org/10.1002/1873-3468.12930.

(113) Festa, R. A.; McAllister, F.; Pearce, M. J.; Mintseris, J.; Burns, K. E.; Gygi, S. P.; Darwin, K. H. Prokayrotic Ubiquitin-like Protein (Pup) Proteome of *Mycobacterium Tuberculosis*. *PLoS One* **2010**, *5* (1). https://doi.org/10.1371/JOURNAL.PONE.0008589.

(114) Samanovic, M. I.; Li, H.; Darwin, K. H. The Pup-Proteasome System of *Mycobacterium Tuberculosis*. *Subcell Biochem* **2013**, *66*, 267–295. https://doi.org/10.1007/978-94-007-5940-4_10.

(115) Barandun, J.; Delley, C. L.; Ban, N.; Weber-Ban, E. Crystal Structure of the Complex between Prokaryotic Ubiquitin-like Protein and Its Ligase PafA. *J Am Chem Soc* **2013**, *135* (18), 6794–6797. https://doi.org/10.1021/ja4024012.

(116) von Rosen, T.; Keller, L. M. L.; Weber-Ban, E. Survival in Hostile Conditions: Pupylation and the Proteasome in Actinobacterial Stress Response Pathways. *Front Mol Biosci* **2021**, *8* (June), 1–17. https://doi.org/10.3389/fmolb.2021.685757.

(117) Zerbib, E.; Levin, R.; Gur, E. Tag Recycling in the Pup-Proteasome System Is Essential for Mycobacterium Smegmatis Survival Under Starvation Conditions. *Mol Microbiol* **2024**, 504–513. https://doi.org/10.1111/mmi.15312.

(118) Von Rosen, T.; Keller, L. M.; Weber-Ban, E. Survival in Hostile Conditions: Pupylation and the Proteasome in Actinobacterial Stress Response Pathways. *Front Mol Biosci*. **2021**;8:685757. https://doi.org/10.3389/fmolb.2021.685757..

(119) Darwin, K. H.; Ehrt, S.; Gutierrez-Ramos, J. C.; Weich, N.; Nathan, C. F. The Proteasome of Mycobacterium Tuberculosis Is Required for Resistance to Nitric Oxide. *Science (1979)* **2003**, *302* (5652), 1963–1966. https://doi.org/10.1126/science.1091176.

(120) Guzzo, M. B.; Li, Q.; Nguyen, H. V.; Boom, W. H.; Nguyen, L. The Pup-Proteasome System Protects Mycobacteria from Antimicrobial Antifolates. *Antimicrob Agents Chemother* **2021**, *65* (4). https://doi.org/10.1128/AAC.01967-20.

(121) Festa, R. A.; Mcallister, F.; Pearce, M. J.; Mintseris, J.; Burns, K. E. Prokayrotic Ubiquitin-Like Protein (Pup) Proteome of *Mycobacterium Tuberculosis*. *PLoS One* **2010**, *5* (1), 8589. https://doi.org/10.1371/journal.pone.0008589.

(122) Shi, X.; Festa, R. A.; Ioerger, T. R.; Butler-Wu, S.; Sacchettini, J. C.; Heran Darwin, K.; Samanovic, M. I. The Copper-Responsive RicR Regulon Contributes to Mycobacterium Tuberculosis Virulence. *mBio* **2014**, *5* (1). https://doi.org/10.1128/mBio.00876-13.

(123) Lin, G.; Li, D.; Chidawanyika, T.; Nathan, C.; Li, H. Fellutamide B Is a Potent Inhibitor of the Mycobacterium Tuberculosis Proteasome. *Arch Biochem Biophys* **2010**, *501* (2), 214–220. https://doi.org/10.1016/j.abb.2010.06.009.

(124) Lin, G.; Li, D.; De Carvalho, L. P. S.; Deng, H.; Tao, H.; Vogt, G.; Wu, K.; Schneider, J.; Chidawanyika, T.; Warren, J. D.; Li, H.; Nathan, C. Inhibitors Selective for Mycobacterial versus Human Proteasomes. *Nature* **2009**, *461* (7264), 621–626. https://doi.org/10.1038/nature08357.

(125) Gandotra, S.; Schnappinger, D.; Monteleone, M.; Hillen, W.; Ehrt, S. In Vivo Gene Silencing Identifies the *Mycobacterium Tuberculosis* Proteasome as Essential for the Bacteria to Persist in Mice. *Nat Med* **2007**, *13* (12), 1515–1520. https://doi.org/10.1038/nm1683.

(126) Li, C.; Liu, S.; Dong, B.; Li, C.; Jian, L.; He, J.; Zeng, J.; Zhou, Q.; Jia, D.; Luo, Y.; Sun, Q. Discovery and Mechanistic Study of *Mycobacterium Tuberculosis* PafA Inhibitors. *J Med Chem*. **2022**. https://doi.org/10.1021/acs.jmedchem.2c00289.

(127) Hecht, N.; Regev, O.; Dovrat, D.; Aharoni, A.; Gur, E. Proteasome Accessory Factor A (PafA) Transferase Activity Makes Sense in the Light of Its Homology with Glutamine Synthetase. *J Mol Biol* **2018**, *430* (5), 668–681. https://doi.org/10.1016/j.jmb.2018.01.009.

(128) Jiang, H. W.; Czajkowsky, D. M.; Wang, T.; Wang, X. De; Wang, J. bin; Zhang, H. N.; Liu, C. X.; Wu, F. L.; He, X.; Xu, Z. W.; Chen, H.; Guo, S. J.; Li, Y.; Bi, L. J.; Deng, J. Y.; Xie, J.; Pei, J. F.; Zhang, X. E.; Tao, S. C. Identification of Serine 119 as an Effective Inhibitor Binding Site of M. Tuberculosis Ubiquitin-like Protein Ligase PafA Using Purified Proteins and M. Smegmatis. *EBioMedicine* **2018**, *30*, 225–236. https://doi.org/10.1016/j.ebiom.2018.03.025.

(129) Jiang, H. W.; Czajkowsky, D. M.; Wang, T.; Wang, X. De; Wang, J. bin; Zhang, H. N.; Liu, C. X.; Wu, F. L.; He, X.; Xu, Z. W.; Chen, H.; Guo, S. J.; Li, Y.; Bi, L. J.; Deng, J. Y.; Xie, J.; Pei, J. F.; Zhang, X. E.; Tao, S. C. Identification of Serine 119 as an Effective Inhibitor Binding Site of *M. Tuberculosis* Ubiquitin-like Protein Ligase PafA Using Purified Proteins and M. Smegmatis. *EBioMedicine* **2018**, *30*, 225–236. https://doi.org/10.1016/j.ebiom.2018.03.025.

(130) Iyer, L. M.; Burroughs, A. M.; Aravind, L. Unraveling the Biochemistry and Provenance of Pupylation: A Prokaryotic Analog of Ubiquitination. *Biol Direct* **2008**, *3*, 1–7. https://doi.org/10.1186/1745-6150-3-45.

(131) Hecht, N.; Regev, O.; Dovrat, D.; Aharoni, A.; Gur, E. Proteasome Accessory Factor A (PafA) Transferase Activity Makes Sense in the Light of Its Homology with Glutamine Synthetase. *J Mol Biol* **2018**, *430* (5), 668–681. https://doi.org/10.1016/j.jmb.2018.01.009.

(132) Cui, H.; Müller, A. U.; Leibundgut, M.; Tian, J.; Ban, N.; Weber-Ban, E. Structures of Prokaryotic Ubiquitin-like Protein Pup in Complex with Depupylase Dop Reveal the Mechanism of Catalytic Phosphate Formation. *Nat Commun* **2021**, *12* (1). https://doi.org/10.1038/s41467-021-26848-x.

(133) Regev, O.; Korman, M.; Hecht, N.; Roth, Z.; Forer, N.; Zarivach, R.; Gur, E. An Extended Loop of the Pup Ligase, PafA, Mediates Interaction with Protein Targets. *J Mol Biol* **2016**, *428* (20), 4143–4153. https://doi.org/10.1016/j.jmb.2016.07.021.

(134) Mowbray, S. L.; Kathiravan, M. K.; Pandey, A. A.; Odell, L. R. Inhibition of Glutamine Synthetase: A Potential Drug Target in Mycobacterium Tuberculosis. *Molecules* **2014**, *19* (9), 13161–13176. https://doi.org/10.3390/molecules190913161.

(135) Mowbray, S. L.; Kathiravan, M. K.; Pandey, A. A.; Odell, L. R. Molecules Inhibition of Glutamine Synthetase: A Potential Drug Target in Mycobacterium Tuberculosis. *Molecules* **2014**, *19*, 13161–13176. https://doi.org/10.3390/molecules190913161.

(136) Odell, L. R.; Nilsson, M. T.; Gising, J.; Lagerlund, O.; Muthas, D.; Nordqvist, A.; Karlén, A.; Larhed, M. Functionalized 3-Amino-Imidazo[1,2-a]Pyridines: A Novel Class of Drug-like Mycobacterium Tuberculosis Glutamine Synthetase Inhibitors. *Bioorg Med Chem Lett* **2009**, *19* (16), 4790–4793. https://doi.org/10.1016/J.BMCL.2009.06.045.

(137) Jain, S.; Sen, D. J. Exploration of Indolo-Imidazo[1,2-*a*]Pyridine Compounds as Anti-Tubercular Agents through Docking, ADMET and Drug Likeliness Studies. *Life Sci Arch.* **2022**, *11* (2), 3350–3361. https://doi.org/10.33263/LIANBS112.33503361.

(138) Brown, A. K.; Aljohani, A. K. B.; Gill, J. H.; Steel, P. G.; Sellars, J. D. Identification of Novel Benzoxa-[2,1,3]-Diazole Substituted Amino Acid Hydrazides as Potential Anti-Tubercular Agents. *Molecules* **2019**, *24* (4), 1–14. https://doi.org/10.3390/molecules24040811.

(139) Brown, A. K.; Aljohani, A. K. B.; Alsalem, F. M. A.; Broadhead, J. L.; Gill, J. H.; Lu, Y.; Sellars, J. D. Identification of Substituted Amino Acid Hydrazides as Novel Anti-Tubercular Agents, Using a Scaffold Hopping Approach. *Molecules* **2020**, *25* (10), 1–24. https://doi.org/10.3390/molecules25102387.

(140) K, S. D.; Keri, R. S.; Reddy, D. S.; M, S. K.; Naik, L.; Kumar, A.; Kadam, N.; Patil, P. N.; H, S.; Padmashali, B. Design, Synthesis, Single-Crystal X-Ray and Docking Studies of Imidazopyridine Analogues as Potent Anti-TB Agents. *J Mol Struct* **2024**, *1295* (P2), 136540. https://doi.org/10.1016/j.molstruc.2023.136540.

(141) Narayan, A.; Patel, S.; B.baile, S.; Jain, S.; Sharma, S. Imidazo[1,2-A]Pyridine: Potent Biological Activity, SAR and Docking Investigations (2017-2022). *Infect Disord Drug Targets* **2024**, *24* (8). https://doi.org/10.2174/0118715265274067240223040333.

(142) Khatun, S.; Singh, A.; Bader, G. N.; Sofi, F. A. Imidazopyridine, a Promising Scaffold with Potential Medicinal Applications and Structural Activity Relationship (SAR): Recent Advances. *J Biomol Struct Dyn* **2022**, *40* (24), 14279–14302. https://doi.org/10.1080/07391102.2021.1997818.

(143) Samanta, S.; Kumar, S.; Aratikatla, E. K.; Ghorpade, S. R.; Singh, V. Recent Developments of Imidazo[1,2- a]Pyridine Analogues as Antituberculosis Agents . *RSC Med Chem* **2023**, 644–657. https://doi.org/10.1039/d3md00019b.

(144) Moraski, G. C.; Markley, L. D.; Cramer, J.; Hipskind, P. A.; Boshoff, H.; Bailey, M. A.; Alling, T.; Ollinger, J.; Parish, T.; Miller, M. J. Advancement of Imidazo[1,2-a]Pyridines with Improved Pharmacokinetics and NM Activity vs. Mycobacterium Tuberculosis. *ACS Med Chem Lett* **2013**, *4* (7), 675–679. https://doi.org/10.1021/ML400088Y.

(145) Agu, P. C.; Afiukwa, C. A.; Orji, O. U.; Ezeh, E. M.; Ofoke, I. H.; Ogbu, C. O.; Ugwuja, E. I.; Aja, P. M. Molecular Docking as a Tool for the Discovery of Molecular Targets of Nutraceuticals in Diseases Management. *Sci Rep* **2023**, *13* (1), 1–18. https://doi.org/10.1038/s41598-023-40160-2.

(146) Pagadala, N. S.; Syed, K.; Tuszynski, J. Software for Molecular Docking: A Review. *Biophys Rev* **2017**, *9* (2), 91–102. https://doi.org/10.1007/s12551-016-0247-1.

(147) Kang, S.; Kim, Y. M.; Kim, R. Y.; Seo, M. J.; No, Z.; Nam, K.; Kim, S.; Kim, J. Synthesis and Structure-Activity Studies of Side Chain Analogues of the Anti-Tubercular Agent, Q203. *Eur J Med Chem* **2017**, *125*, 807–815. https://doi.org/10.1016/j.ejmech.2016.09.082.

(148) Kang, S.; Kim, R. Y.; Seo, M. J.; Lee, S.; Kim, Y. M.; Seo, M.; Seo, J. J.; Ko, Y.; Choi, I.; Jang, J.; Nam, J.; Park, S.; Kang, H.; Kim, H. J.; Kim, J.; Ahn, S.; Pethe, K.; Nam, K.; No, Z.; Kim, J. Lead Optimization of a Novel Series of Imidazo[1,2-a]Pyridine Amides Leading to a Clinical Candidate (Q203) as a Multi- and Extensively-Drug-Resistant Anti-Tuberculosis Agent. **2014**. https://doi.org/10.1021/jm5003606.

(149) Popiołek, Ł. Hydrazide–Hydrazones as Potential Antimicrobial Agents: Overview of the Literature since 2010. *Medicinal Chemistry Research* **2017**, *26* (2), 287–301. https://doi.org/10.1007/s00044-016-1756-y.

(150) Majumdar, P.; Pati, A.; Patra, M.; Behera, R. K.; Behera, A. K. Acid Hydrazides, Potent Reagents for Synthesis of Oxygen-, Nitrogen-, and/or Sulfur-Containing Heterocyclic Rings. *Chem Rev* **2014**, *114* (5), 2942–2977. https://doi.org/10.1021/cr300122t.

(151) Montalbetti, C. A. G. N.; Falque, V. Amide Bond Formation and Peptide Coupling. *Tetrahedron* **2005**, *61* (46), 10827–10852. https://doi.org/10.1016/j.tet.2005.08.031.

(152) Valeur, E.; Bradley, M. Amide Bond Formation: Beyond the Myth of Coupling Reagents. *Chem Soc Rev* **2009**, *38* (2), 606–631. https://doi.org/10.1039/b701677h.

(153) Mahesh, S.; Tang, K. C.; Raj, M. Amide Bond Activation of Biological Molecules. *Molecules* **2018**, *23* (10). https://doi.org/10.3390/molecules23102615.

(154) Agami, C.; Couty, F. The Reactivity of the N-Boc Protecting Group: An Underrated Feature. *Tetrahedron* **2002**, *58* (14), 2701–2724. https://doi.org/10.1016/S0040-4020(02)00131-X.

(155) Han, S. Y.; Kim, Y. A. Recent Development of Peptide Coupling Reagents in Organic Synthesis. *Tetrahedron* **2004**, *60* (11), 2447–2467. https://doi.org/10.1016/j.tet.2004.01.020.

(156) Tamaki, M.; Hruby, V. J. Fast , Ef ® Cient and Selective Deprotection of the Group Using HCl / Dioxane. *Journal of Peptide Researc* **2001**, *58*, 338–341.

(157) Subbaiah, M. A. M.; Meanwell, N. A. Bioisosteres of the Phenyl Ring: Recent Strategic Applications in Lead Optimization and Drug Design. *J Med Chem* **2021**, *64* (19), 14046–14128. https://doi.org/10.1021/acs.jmedchem.1c01215.

(158) Meanwell, N. A. Applications of Bioisosteres in the Design of Biologically Active Compounds. *J Agric Food Chem* **2023**, *71* (47), 18087–18122. https://doi.org/10.1021/acs.jafc.3c00765.

(159) Faleye, O. S.; Boya, B. R.; Lee, J. H.; Choi, I.; Lee, J. Halogenated Antimicrobial Agents to Combat Drug-Resistant Pathogens. *Pharmacol Rev* **2024**, *76* (1), 90–141. https://doi.org/10.1124/pharmrev.123.000863.

(160) Talj, R.; Francis, C.; Talj, R.; Francis, C. An An Overview An Overview. *IFAC PapersOnLine* **2023**, *56* (2), 10971–10983.

(161) Fang, W. Y.; Ravindar, L.; Rakesh, K. P.; Manukumar, H. M.; Shantharam, C. S.; Alharbi, N. S.; Qin, H. L. Synthetic Approaches and Pharmaceutical Applications of Chloro-Containing Molecules for Drug Discovery: A Critical Review. *European Journal of Medicinal Chemistry*. Elsevier Masson SAS July 1, **2019**, pp 117–153. https://doi.org/10.1016/j.ejmech.2019.03.063.

(162) Machado, D.; Girardini, M.; Viveiros, M.; Pieroni, M. Challenging the Drug-Likeness Dogma for New Drug Discovery in Tuberculosis. *Frontiers in Microbiology*. Frontiers Media S.A. July 3, **2018**. https://doi.org/10.3389/fmicb.2018.01367.

(163) Meanwell, N. A. Fluorine and Fluorinated Motifs in the Design and Application of Bioisosteres for Drug Design. *J Med Chem* **2018**, *61* (14), 5822–5880. https://doi.org/10.1021/acs.jmedchem.7b01788.

(164) Abula, A.; Xu, Z.; Zhu, Z.; Peng, C.; Chen, Z.; Zhu, W.; Aisa, H. A. Substitution Effect of the Trifluoromethyl Group on the Bioactivity in Medicinal Chemistry: Statistical Analysis and Energy Calculations. *J Chem Inf Model* **2020**, *60* (12), 6242–6250. https://doi.org/10.1021/acs.jcim.0c00898.

(165) Hao, B. Y.; Han, Y. P.; Zhang, Y.; Liang, Y. M. New Synthetic Approaches toward OCF3-Containing Compounds. *Organic and Biomolecular Chemistry*. Royal Society of Chemistry May 22, **2023**, pp 4926–4954. https://doi.org/10.1039/d3ob00258f.

(166) Perveen, S.; Sharma, R. Screening Approaches and Therapeutic Targets: The Two Driving Wheels of Tuberculosis Drug Discovery. *Biochem Pharmacol* **2022**, *197* (January 2022), 114906. https://doi.org/10.1016/j.bcp.2021.114906.

(167) Perveen, S.; Kumari, D.; Singh, K.; Sharma, R. Tuberculosis Drug Discovery: Progression and Future Interventions in the Wake of Emerging Resistance. *Eur J Med Chem* **2022**, *229*, 114066. https://doi.org/10.1016/j.ejmech.2021.114066.

(168) Yeware, A.; Akhtar, S.; Sarkar, D. Probes and Techniques Used in Active and the Hypoxia-Based Dormant State of an Antitubercular Drug Screening Assay. *Med Drug Discov* **2022**, *13* (October 2021), 100115. https://doi.org/10.1016/j.medidd.2021.100115.

(169) Katawera, V.; Siedner, M.; Boum, Y. Evaluation of the Modified Colorimetric Resazurin Microtiter Plate-Based Antibacterial Assay for Rapid and Reliable Tuberculosis Drug Susceptibility Testing. *BMC Microbiol* **2014**, *14* (1). https://doi.org/10.1186/s12866-014-0259-6.

(170) Palomino, J. C.; Martin, A.; Portaels, F. Rapid Drug Resistance Detection in Mycobacterium Tuberculosis: A Review of Colourimetric Methods. *Clinical Microbiology and Infection* **2007**, *13* (8), 754–762. https://doi.org/10.1111/j.1469-0691.2007.01698.x.

(171) Chiodi, D.; Ishihara, Y. "Magic Chloro": Profound Effects of the Chlorine Atom in Drug Discovery. *J Med Chem* **2023**, *66* (8), 5305–5331. https://doi.org/10.1021/acs.jmedchem.2c02015.

(172) Chiodi, D.; Ishihara, Y. The Role of the Methoxy Group in Approved Drugs. *European Journal of Medicinal Chemistry*. Elsevier Masson s.r.l. July 5, **2024**. https://doi.org/10.1016/j.ejmech.2024.116364.

(173) Wang, X.; Wang, Y.; Li, X.; Yu, Z.; Song, C.; Du, Y. Nitrile-Containing Pharmaceuticals: Target, Mechanism of Action, and Their SAR Studies. *RSC Med Chem* **2021**, *12* (10), 1650–1671. https://doi.org/10.1039/d1md00131k.

(174) Komura, H.; Watanabe, R.; Mizuguchi, K. The Trends and Future Prospective of In Silico Models from the Viewpoint of ADME Evaluation in Drug Discovery. *Pharmaceutics* **2023**, *15* (11), 1–30. https://doi.org/10.3390/pharmaceutics15112619.

(175) Ekins, S.; Lane, T. R.; Urbina, F.; Puhl, A. C. In Silico ADME/Tox Comes of Age: Twenty Years Later. *Xenobiotica* **2024**, *54* (7), 352–358. https://doi.org/10.1080/00498254.2023.2245049.

(176) Dong, J.; Wang, N. N.; Yao, Z. J.; Zhang, L.; Cheng, Y.; Ouyang, D.; Lu, A. P.; Cao, D. S. Admetlab: A Platform for Systematic ADMET Evaluation Based on a Comprehensively Collected ADMET Database. *J Cheminform* **2018**, *10* (1), 1–11. https://doi.org/10.1186/s13321-018-0283-x.

(177) Lipinski, C. A. Lead- and Drug-like Compounds: The Rule-of-Five Revolution. *Drug Discovery Today: Technologies*. December 2004, pp 337–341. https://doi.org/10.1016/j.ddtec.**2004**.11.007.

(178) Soumyashree, D. K.; Keri, R. S.; Reddy, D. S.; M, S. K.; Naik, L.; Kumar, A.; Kadam, N.; Patil, P. N.; Shanavaz, H.; Padmashali, B. Design , Synthesis , Single-Crystal X-Ray and Docking Studies of Imidazopyridine Analogues as Potent Anti-TB Agents. *J Mol Struct* **2024**, *1295* (P2), 136540. https://doi.org/10.1016/j.molstruc.2023.136540.

(179) Josef J. Heterocycles in Medicinal Chemistry. *Molecules* **2019**, *24* (3839), 1–4.

(180) Gomtsyan, A. Heterocycles in Drugs and Drug Discovery. *Chem Heterocycl Compd (N Y)* **2012**, *48* (1), 7–10. https://doi.org/10.1007/s10593-012-0960-z.

(181) Atukuri, D.; Gunjal, R.; Holagundi, N.; Korlahalli, B.; Gangannavar, S.; Akkasali, K. Contribution of N-Heterocycles towards Anti-Tubercular Drug Discovery (2014–2019); Predicted and Reengineered Molecular Frameworks. *Drug Dev Res* **2021**, *82* (6), 767–783. https://doi.org/10.1002/ddr.21809.

(182) Dwivedi, A. R.; Jaiswal, S.; Kukkar, D.; Kumar, R.; Singh, T. G.; Singh, M. P.; Gaidhane, A. M.; Lakhanpal, S.; Prasad, K. N.; Kumar, B. A Decade of Pyridine-Containing Heterocycles in US FDA Approved Drugs: A Medicinal Chemistry-Based Analysis. *RSC Med Chem* **2024**, 12–36. https://doi.org/10.1039/d4md00632a.

(183) Nammalwar, B.; Bunce, R. A. Recent Advances in Pyrimidine-Based Drugs. *Pharmaceuticals*. **2024**;17(1). https://doi.org/10.3390/ph17010104.

(184) Petrou, A.; Fesatidou, M.; Geronikaki, A. Thiazole Ring—a Biologically Active Scaffold. *Molecules* **2021**, *26* (11). https://doi.org/10.3390/molecules26113166.

(185) Fesatidou, M.; Petrou, A.; Athina, G. Heterocycle Compounds with Antimicrobial Activity. *Curr Pharm Des* **2020**, *26* (8), 867–904. https://doi.org/10.2174/1381612826666200206093815.

(186) Bhanwala, N.; Gupta, V.; Chandrakar, L.; Khatik, G. L. Thiazole Heterocycle: An Incredible and Potential Scaffold in Drug Discovery and Development of Antitubercular Agents. *ChemistrySelect* **2023**, *8* (46). https://doi.org/10.1002/slct.202302803.

(187) Vilchèze, C.; Copeland, J.; Keiser, T. L.; Weisbrod, T.; Washington, J.; Jain, P.; Malek, A.; Weinrick, B.; Jacobs, W. R. Rational Design of Biosafety Level 2-Approved, Multidrug-Resistant Strains of

*Mycobacterium Tuberculosis* through Nutrient Auxotrophy. *mBio* **2018**, *9* (3). https://doi.org/10.1128/mBio.00938-18.

# 8. Appendix

## 8.1 MIC results of imidazo[1,2-*a*]pyridine analogues

### 8.1.1 First-series of compounds:

| | | | MIC (μM) | | | | |
|---|---|---|---|---|---|---|---|
| **Entry** | **Chemical structure** | **LogP** | **WT 7902** | **INH$^R$ 8245** | **RIF$^R$ 8247** | **RIF/INH$^R$ 8250** | **RIF/INH$^R$ 8258** |
| **44Aa** | 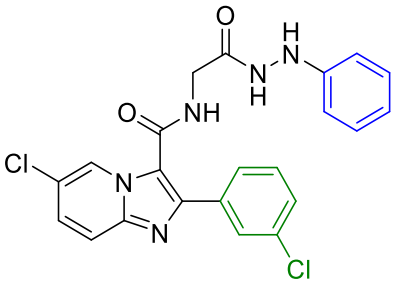 | 3.34 | - | - | - | - | - |
| **44Ab** | 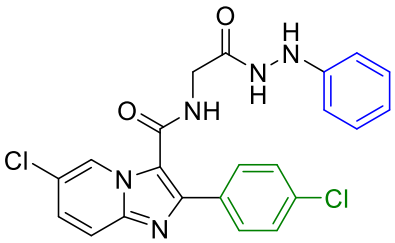 | 3.34 | - | - | - | - | - |
| **44Ac** | 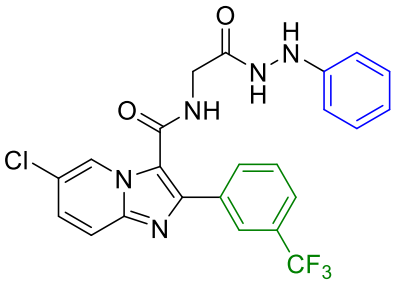 | 3.70 | - | - | - | - | - |
| **44Ad** | 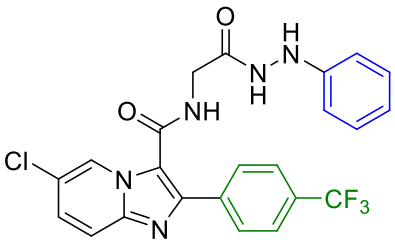 | 3.70 | 65.6 | 32.8 | 65.6 | 65.6 | 32.8 |
| **44Ae** | 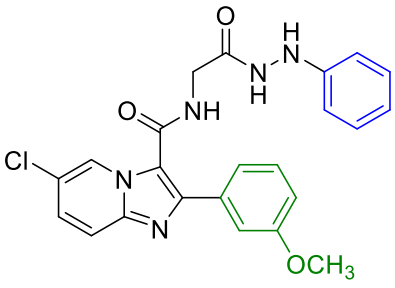 | 2.65 | - | - | - | - | - |

| | | | | | | | |
|---|---|---|---|---|---|---|---|
| **44Af** | 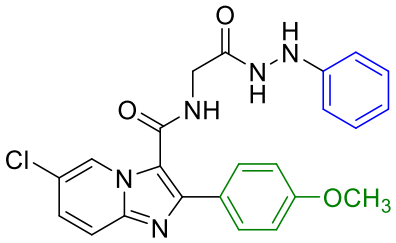 | 2.65 | - | - | - | - | - |
| **44Ag** | 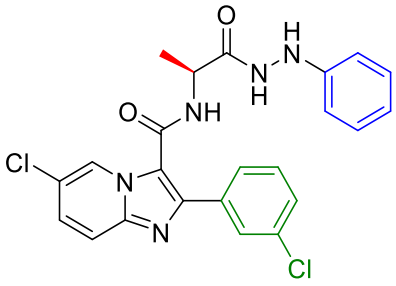 | 3.83 | - | - | - | - | - |
| **44Ah** | 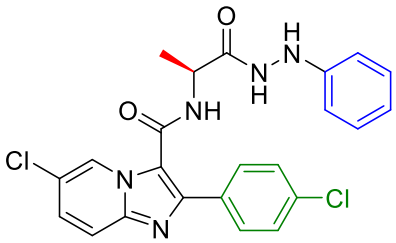 | 3.83 | - | - | - | - | - |
| **44Ai** | 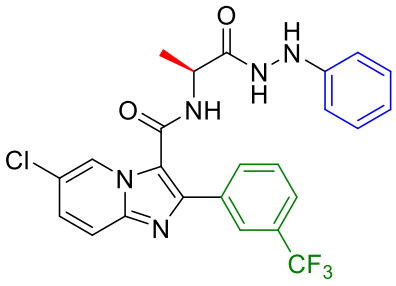 | 4.19 | - | - | - | - | - |
| **44Aj** | 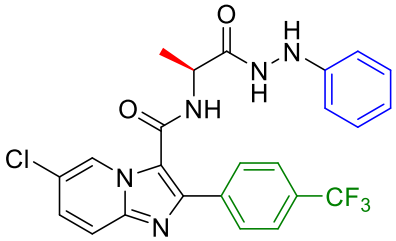 | 4.19 | - | - | - | - | - |
| **44Ak** | 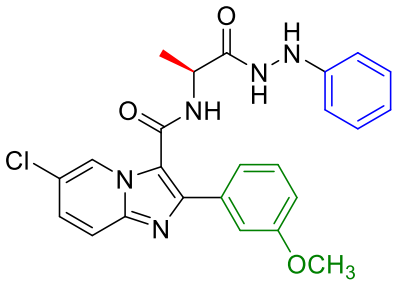 | 3.15 | - | - | - | - | - |

| | | | | | | | |
|---|---|---|---|---|---|---|---|
| **44Al** | 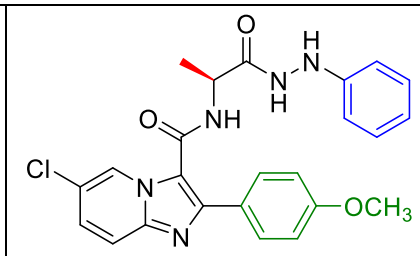 | 3.15 | - | - | - | - | - |
| **44Am** | 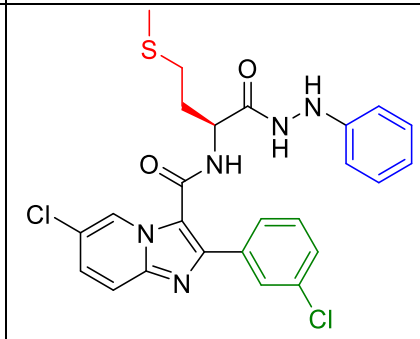 | 4.16 | - | - | - | - | - |
| **44An** | 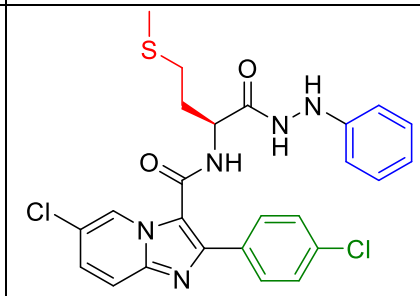 | 4.16 | - | - | - | - | - |
| **44Ao** | 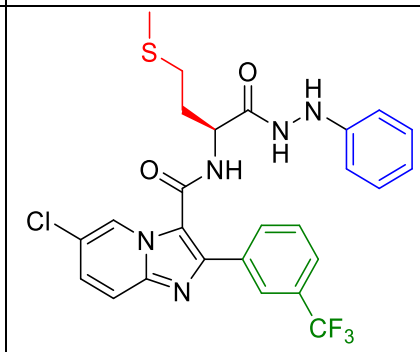 | 4.53 | - | - | - | - | - |
| **44Ap** | 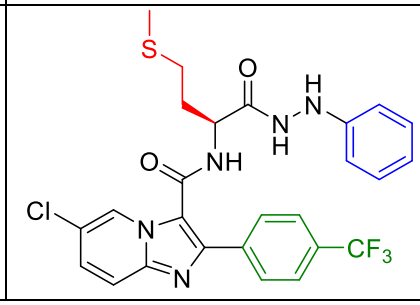 | 4.53 | - | - | - | - | - |

| | | | | | | | |
|---|---|---|---|---|---|---|---|
| **44Aq** | 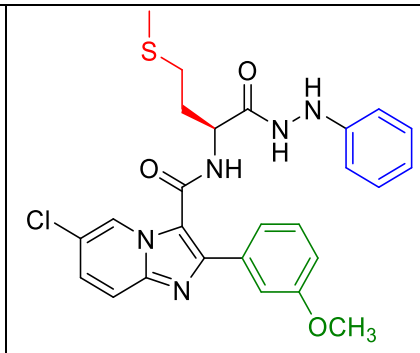 | 3.48 | - | - | - | - | - |
| **44Ar** | 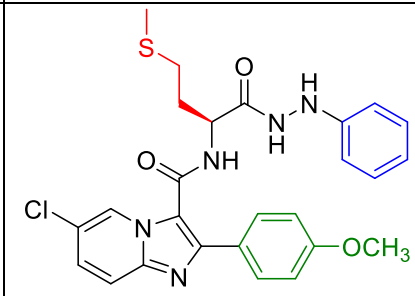 | 3.48 | - | - | - | - | - |
| **44As** | 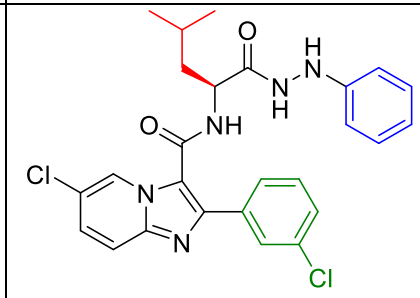 | 5.06 | - | - | - | - | - |
| **44At** | 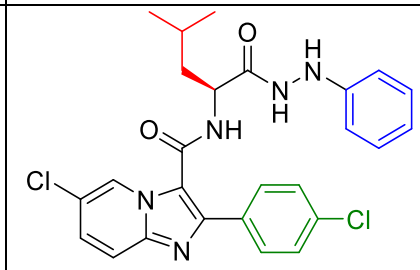 | 5.06 | - | - | - | - | - |
| **44Au** | 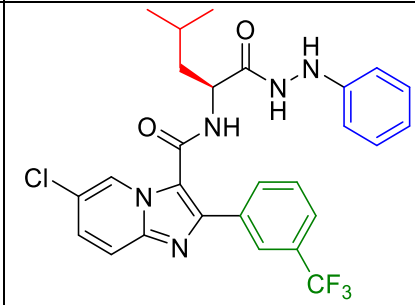 | 5.43 | - | - | - | - | - |
| **44Av** | 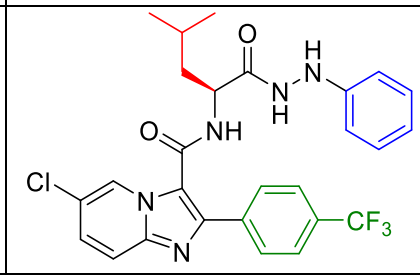 | 5.43 | - | - | - | - | - |

| | | | | | | | |
|---|---|---|---|---|---|---|---|
| **44Aw** | 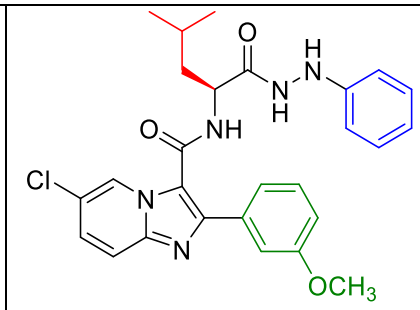 | 4.38 | - | - | - | - | - |
| **44Ax** | 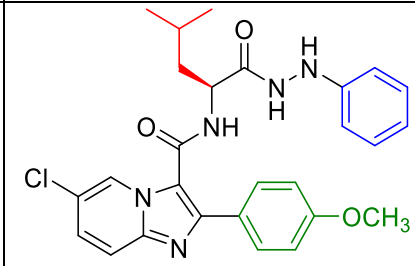 | 4.38 | - | - | - | - | - |
| **44Ay** | 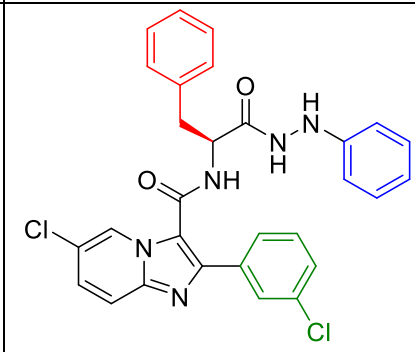 | 5.50 | 117.6 | 117.6 | - | 117.6 | 117.6 |
| **44Az** | 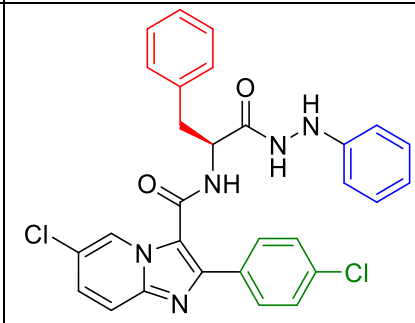 | 5.50 | - | - | - | - | - |
| **44Ba** | 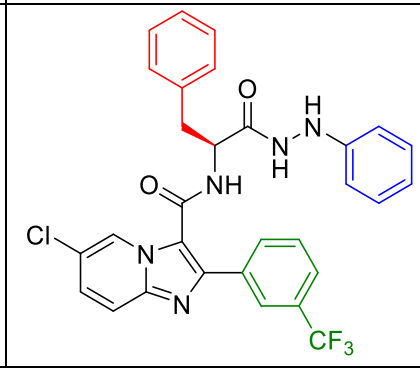 | 5.87 | - | - | - | - | - |

| | | | | | | | |
|---|---|---|---|---|---|---|---|
| **44Bb** | 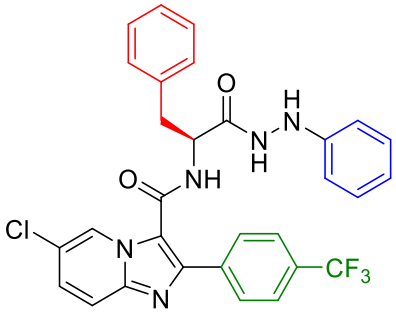 | 5.87 | - | - | - | - | - |
| **44Bc** | 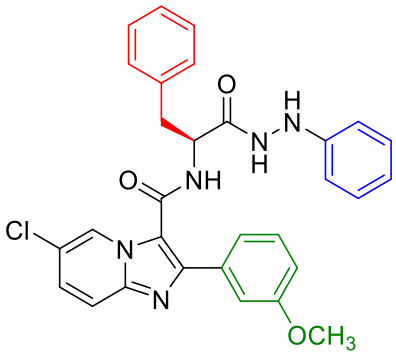 | 4.82 | - | 118.5 | - | 118.5 | 118.5 |
| **44Bd** | 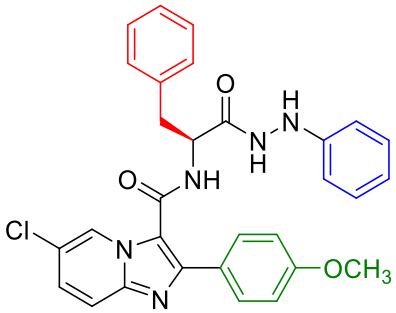 | 4.82 | - | - | - | - | - |

### 8.1.2 Second-series of compounds:

| | | | MIC (μM) | | | |
|---|---|---|---|---|---|---|
| Entry | Chemical structure | LogP | WT 7902 | INH$^R$ 8245 | RIF$^R$ 8247 | RIF/INH$^R$ 8250 |
| 44Be | 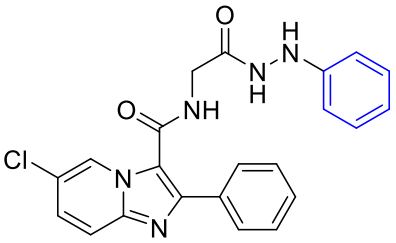 | 2.78 | 152.43 | 152.43 | 152.43 | 152.43 |
| 44Bf | 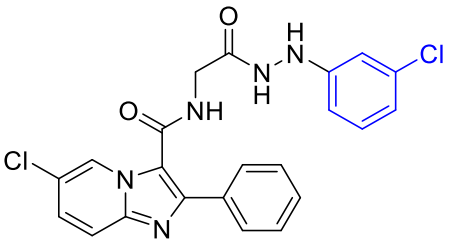 | 3.34 | 140.8 | 140.8 | 140.8 | 140.8 |
| 44Bg | 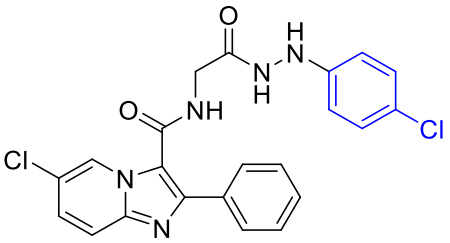 | 3.34 | 140.8 | 140.8 | 140.8 | 140.8 |
| 44Bh | 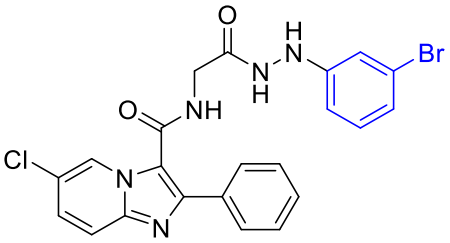 | 3.61 | 128.3 | 128.3 | 128.3 | 128.3 |
| 44Bi | 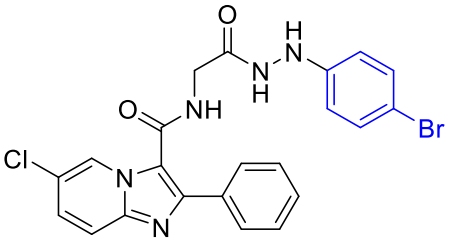 | 3.61 | 128.3 | 128.3 | 128.3 | 128.3 |
| 44Bj | 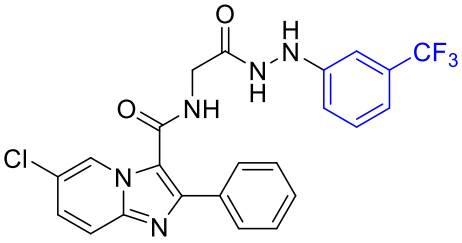 | 3.70 | 131.18 | 131.18 | 131.18 | 131.18 |

| | | | | | | |
|---|---|---|---|---|---|---|
| **44Bk** | 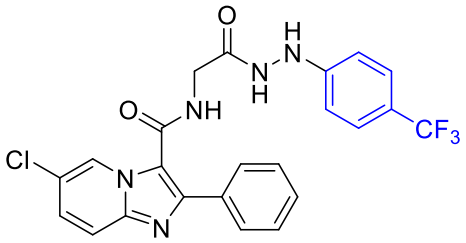 | 3.70 | 131.18 | 131.18 | 131.18 | 131.18 |
| **44Bl** | 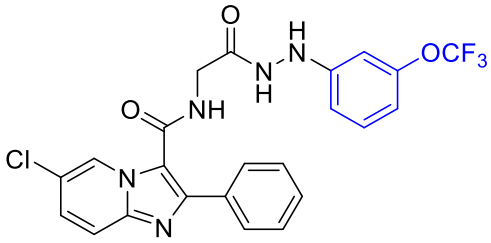 | 4.31 | 63.50 | 63.50 | 127.01 | 63.50 |
| **44Bm** | 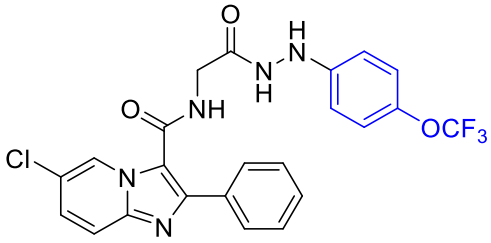 | 4.31 | 63.504 | 63.50 | 127.01 | 63.50 |
| **44Bn** | 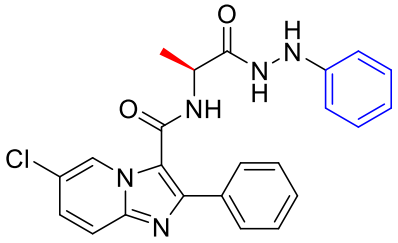 | 3.27 | 147.49 | 147.49 | 147.49 | 73.74 |
| **44Bo** | 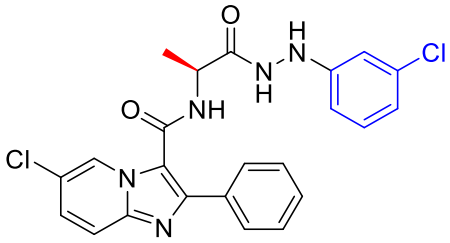 | 3.83 | 136.65 | 68.33 | 136.65 | 136.65 |
| **44Bp** | 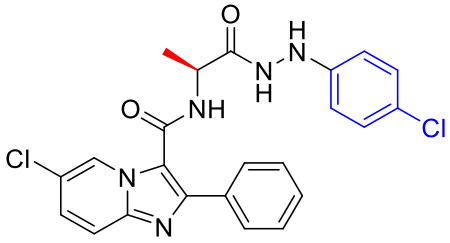 | 3.83 | 136.65 | 68.33 | 136.65 | 136.65 |
| **44Bq** | 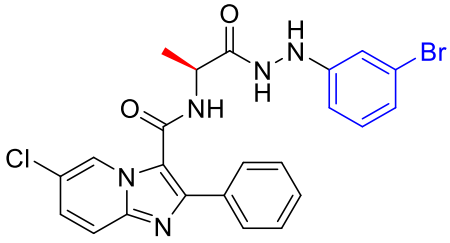 | 4.10 | 62.40 | 62.40 | 62.40 | 62.40 |

| | | | | | | |
|---|---|---|---|---|---|---|
| **44Br** | 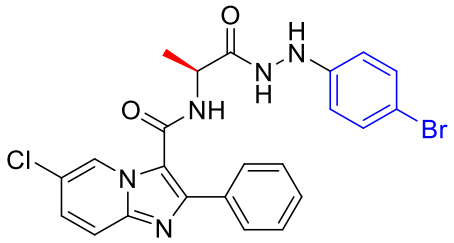 | 4.10 | 124.81 | 124.81 | 124.81 | 124.81 |
| **44Bs** | 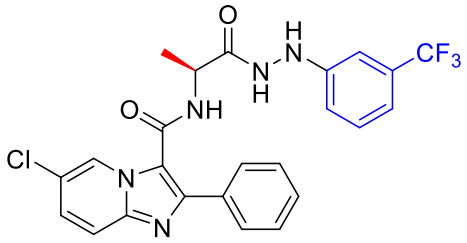 | 4.19 | 127.52 | 127.52 | 127.52 | 127.52 |
| **44Bt** | 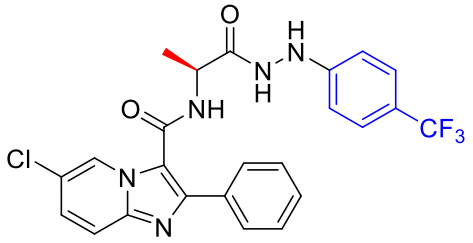 | 4.19 | 63.76 | 63.76 | 127.52 | 63.76 |
| **44Bu** | 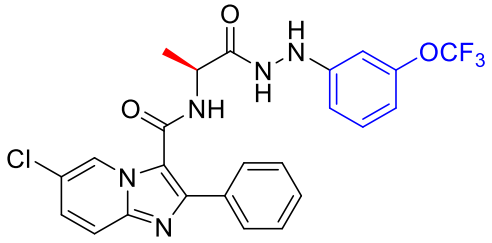 | 4.80 | 30.89 | 15.44 | 30.89 | 30.89 |
| **44Bv** | 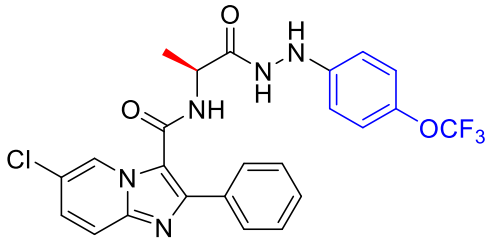 | 4.80 | 61.78 | 61.78 | 61.78 | 61.78 |
| **44Bw** | 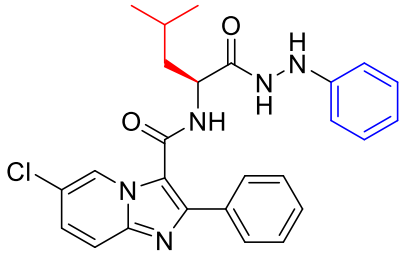 | 4.51 | 33.61 | 16.80 | 134.45 | 33.61 |
| **44Bx** | 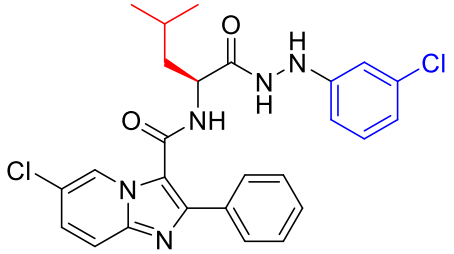 | 5.06 | 125.39 | 125.39 | 125.39 | 125.39 |

| | | | | | | |
|---|---|---|---|---|---|---|
| **44By** | 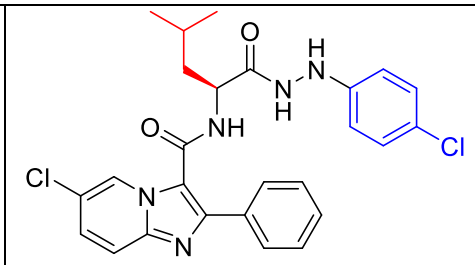 | 5.06 | 62.69 | 62.69 | 125.39 | 62.69 |
| **44Bz** | 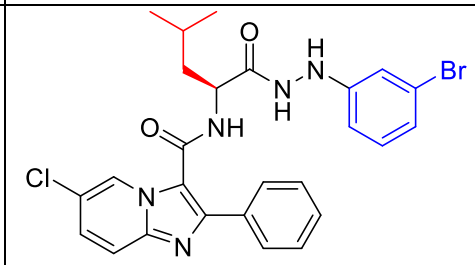 | 5.33 | 115.34 | 115.34 | - | 57.67 |
| **44Ca** | 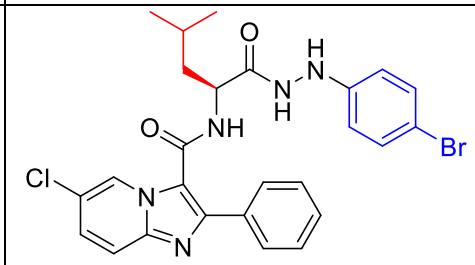 | 5.33 | 57.67 | 115.34 | - | 57.67 |
| **44Cb** | 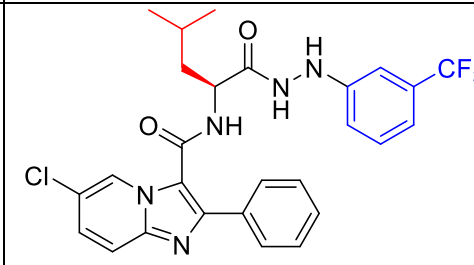 | 5.43 | - | 29.41 | - | 29.41 |
| **44Cc** | 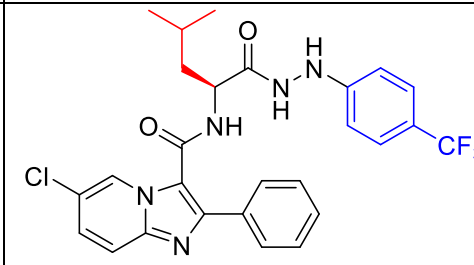 | 5.43 | - | 117.65 | - | 117.65 |
| **44Cd** | 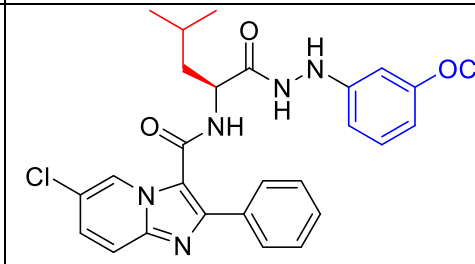 | 6.03 | - | 57.14 | - | 28.57 |
| **44Ce** | 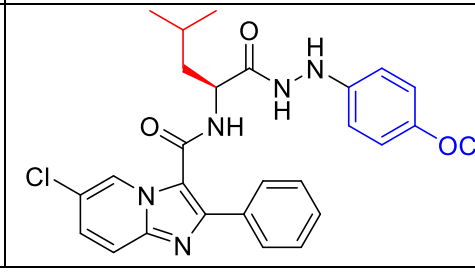 | 6.03 | 28.57 | 28.57 | - | 28.57 |

| | | | MIC (μM) | | | |
|---|---|---|---|---|---|---|
| **Entry** | **Chemical structure** | **LogP** | **WT 7902** | **INH$^R$ 8245** | **RIF/INH$^R$ 8250** | **RIF/INH$^R$ 8258** |
| **44Cf** | 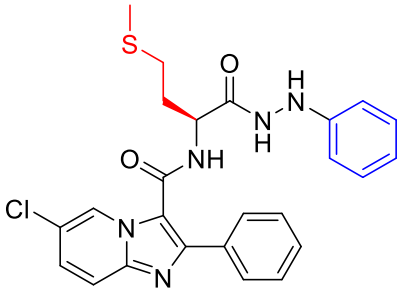 | 3.50 | 64.77 | 129.55 | 129.55 | 64.77 |
| **44Cg** | 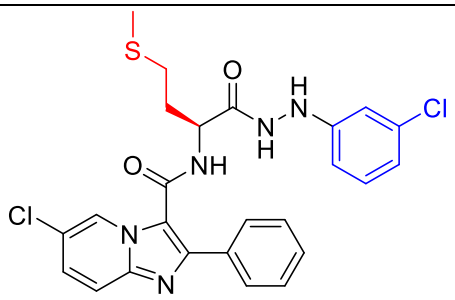 | 4.06 | 60.55 | 60.55 | 30.27 | 121.10 |
| **44Ch** | 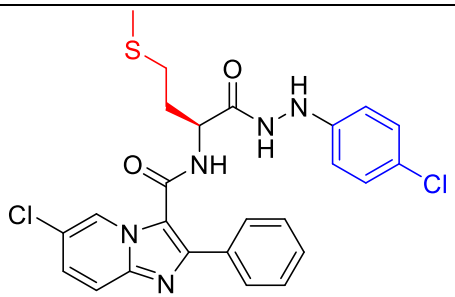 | 4.06 | 30.27 | 30.27 | 30.27 | 30.27 |
| **44Ci** | 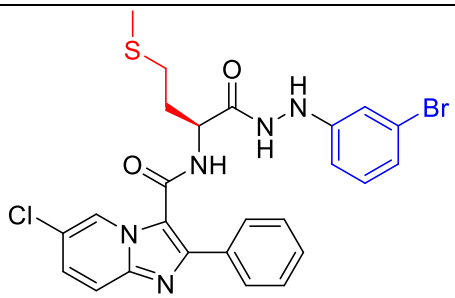 | 4.33 | 27.92 | 27.92 | 27.92 | 55.85 |
| **44Cj** | 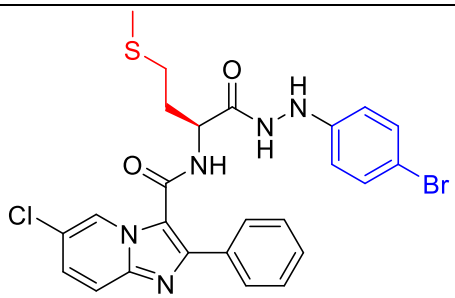 | 4.33 | 55.85 | 27.92 | 27.92 | 27.92 |

| | | | | | | |
|---|---|---|---|---|---|---|
| **44Ck** | 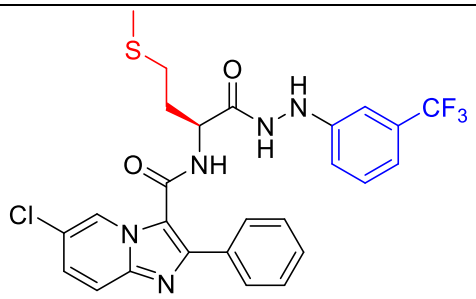 | 4.42 | 56.93 | 28.46 | 56.93 | 28.46 |
| **44Cl** | 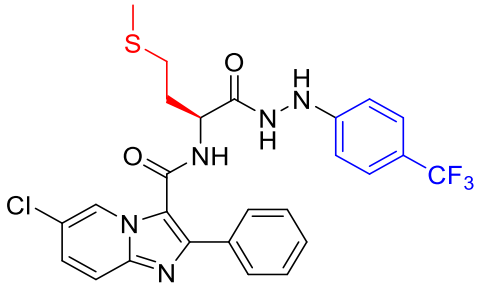 | 4.42 | 28.46 | 28.46 | 28.46 | 28.46 |
| **44Cm** | 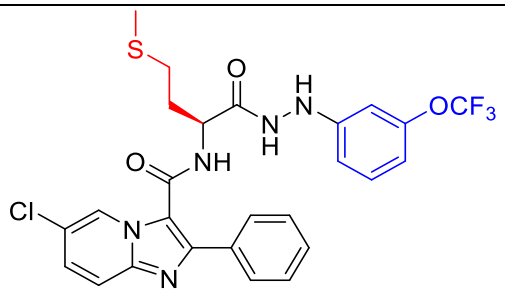 | 5.03 | - | - | - | 110.72 |
| **44Cn** | 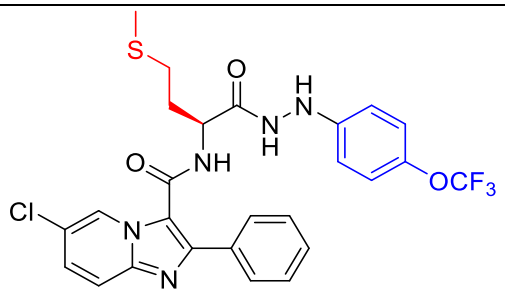 | 5.03 | 27.68 | 27.68 | 27.68 | 55.85 |
| **44Co** | 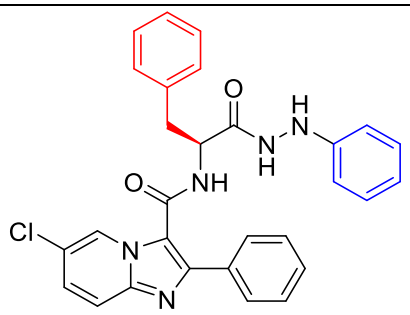 | 4.95 | 15.68 | 125.49 | 62.74 | 31.37 |
| **44Cp** | 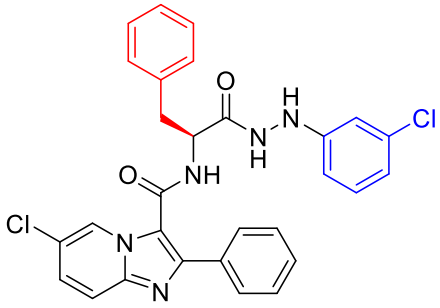 | 5.50 | 3.67 | 58.77 | 7.34 | 7.34 |

| | | | | | | |
|---|---|---|---|---|---|---|
| **44Cq** | 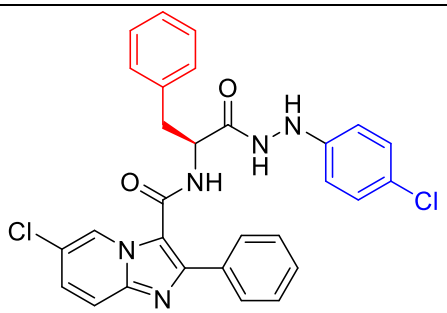 | 5.50 | 117.55 | - | - | 117.55 |
| **44Cr** | 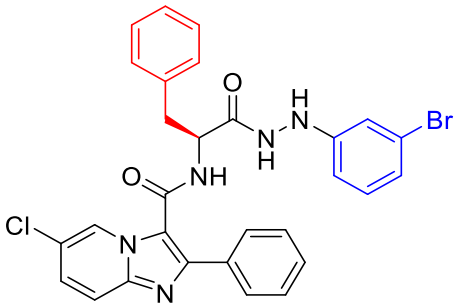 | 5.78 | 13.58 | 13.58 | 13.58 | 13.58 |
| **44Cs** | 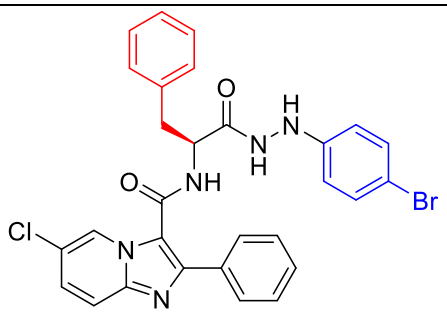 | 5.78 | 54.33 | 54.33 | 54.331 | 27.16 |
| **44Ct** | 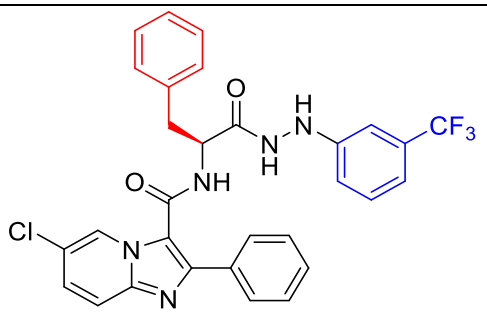 | 5.87 | 6.92 | 55.36 | 13.84 | 13.84 |
| **44Cu** | 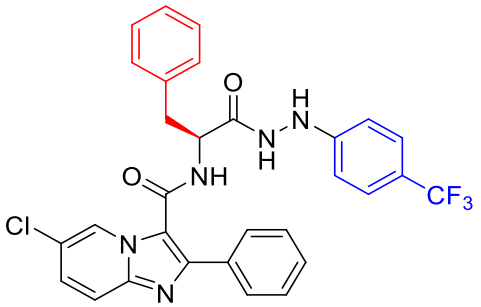 | 5.87 | 110.72 | 110.72 | - | 27.68 |

| | | | | | | |
|---|---|---|---|---|---|---|
| **44Cv** | 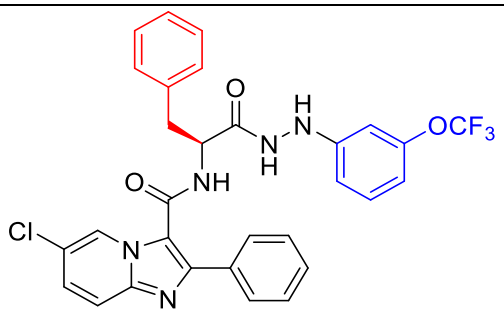 | 6.47 | 13.46 | 26.93 | 13.46 | 13.46 |
| **44Cw** | 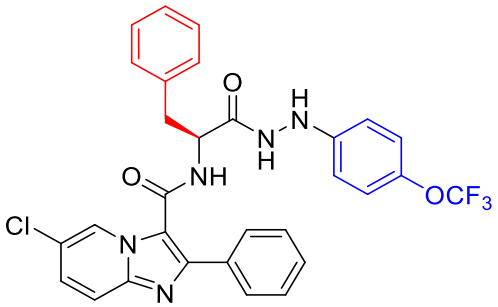 | 6.47 | 107.75 | 107.75 | - | 107.75 |
| **44Cx** | 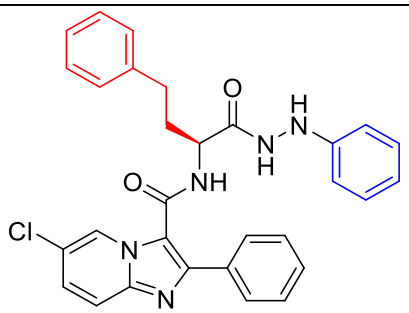 | 5.36 | - | - | - | - |
| **44Cy** | 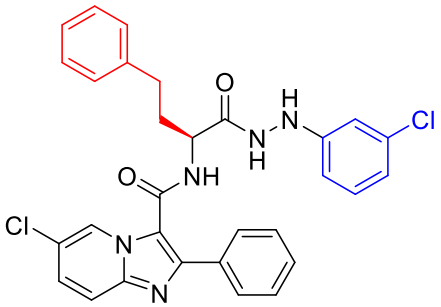 | 5.92 | - | - | - | - |
| **44Cz** | 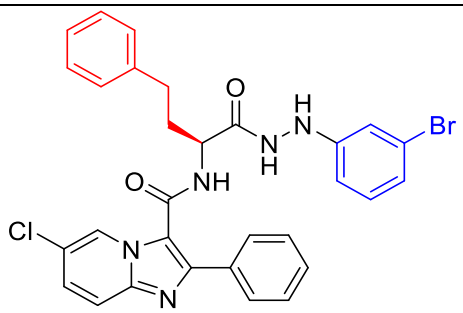 | 6.91 | - | - | - | - |

| | | | | | | |
|---|---|---|---|---|---|---|
| **44Da** | 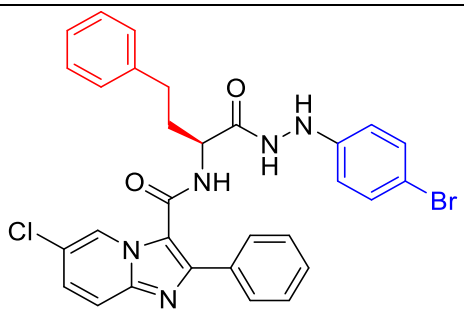 | 6.19 | - | - | - | - |
| **44Db** | 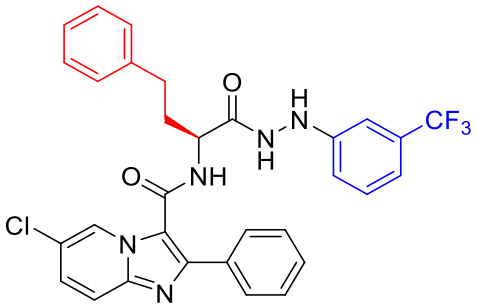 | 6.28 | - | - | - | - |
| **44Dc** | 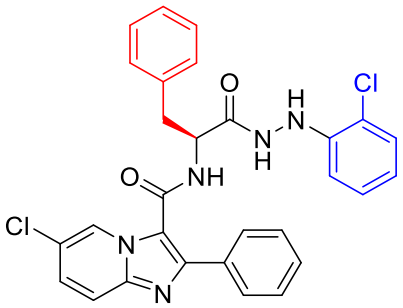 | 5.50 | - | - | 89.3 | 42.8 |
| **44Dd** | 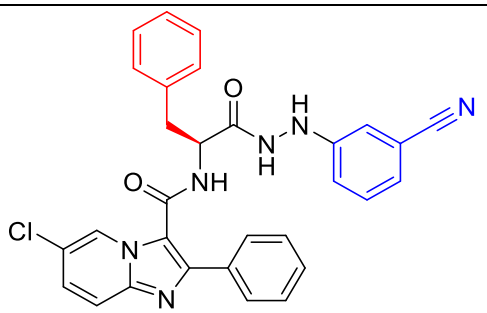 | 4.98 | - | - | - | - |
| **44De** | 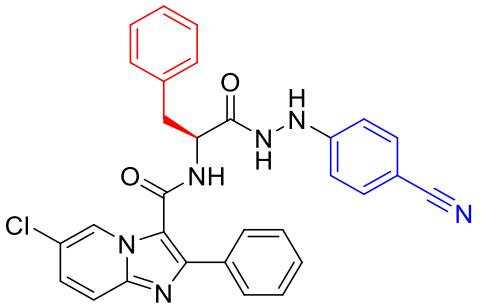 | 4.98 | - | - | - | - |

### 8.1.3 Third-series of compounds:

| | | | MIC (μM) | | | | |
|---|---|---|---|---|---|---|---|
| **Entry** | **Chemical structure** | **LogP** | **WT 7902** | **INH$^R$ 8245** | **RIF$^R$ 8247** | **RIF/INH$^R$ 8250** | **RIF/INH$^R$ 8258** |
| **44Df** | 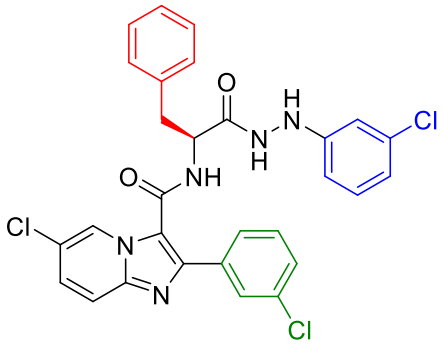 | 6.06 | 110.6 | 27.6 | 110.6 | 110.6 | 27.6 |
| **44Dg** | 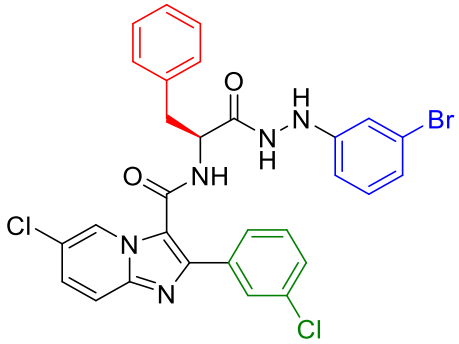 | 6.33 | - | 102.7 | - | 102.7 | 102.7 |
| **44Dh** | 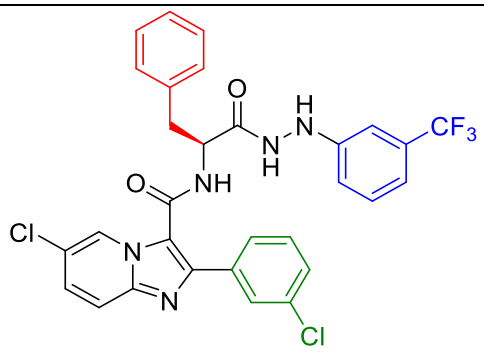 | 6.43 | - | 104.5 | - | 104.5 | 52.3 |

| | | | | | | | |
|---|---|---|---|---|---|---|---|
| **44Di** | 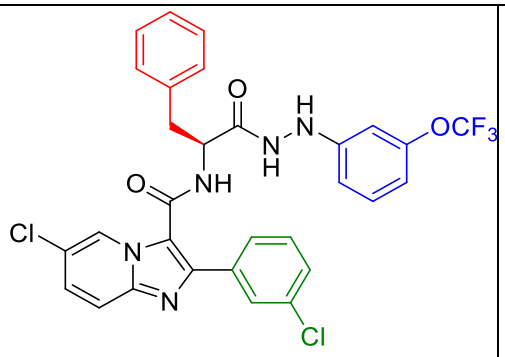 | 7.03 | - | - | - | - | - |
| **44Dj** | 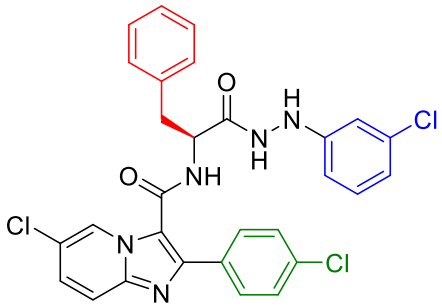 | 6.06 | 55.2 | - | 33.6 | - | - |
| **44Dk** | 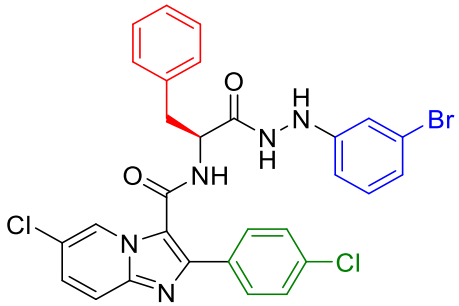 | 6.33 | 16.4 | 25.6 | 16.0 | 52.6 | 28.5 |
| **44Dl** | 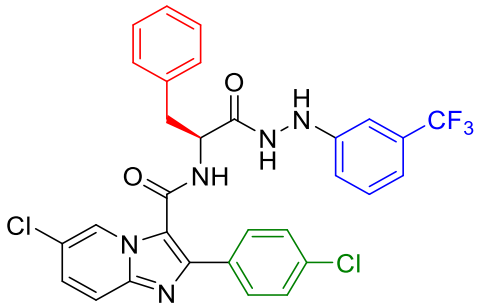 | 6.43 | 25.5 | 71.1 | 15.5 | 34.2 | 34.2 |
| **44Dm** | 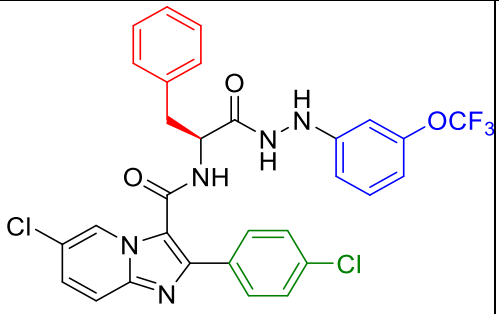 | 7.03 | 29.8 | 16.3 | 71.1 | - | 70.2 |

| | | | | | | | |
|---|---|---|---|---|---|---|---|
| **44Dn** | 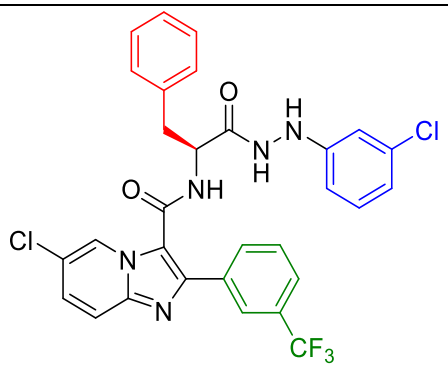 | 6.43 | - | - | - | - | - |
| **44Do** | 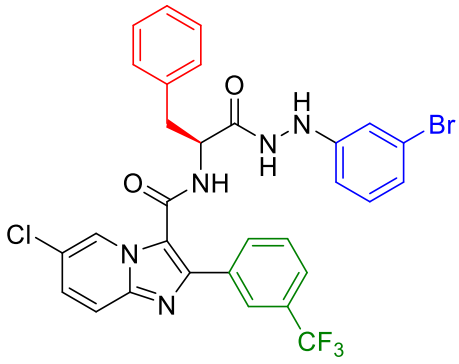 | 6.70 | - | 97.4 | - | - | 97.4 |
| **44Dp** | 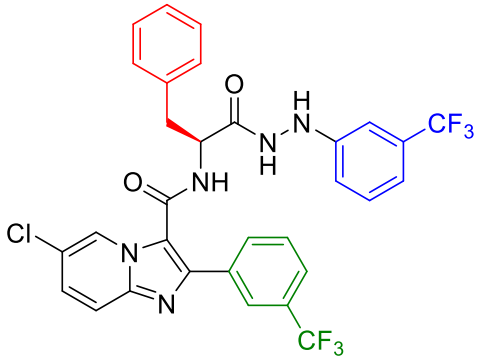 | 6.79 | - | 117.65 | - | 117.65 | 58.82 |
| **44Dq** | 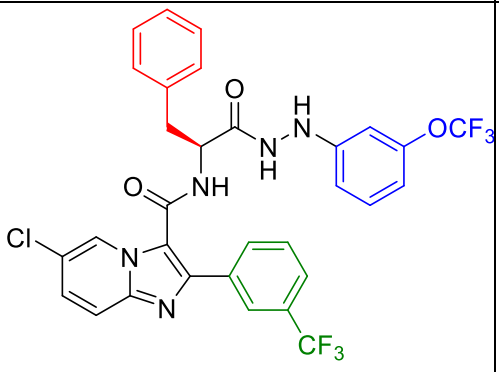 | 7.39 | - | 96.7 | - | - | 96.7 |

| | | | | | | | |
|---|---|---|---|---|---|---|---|
| **44Dr** | 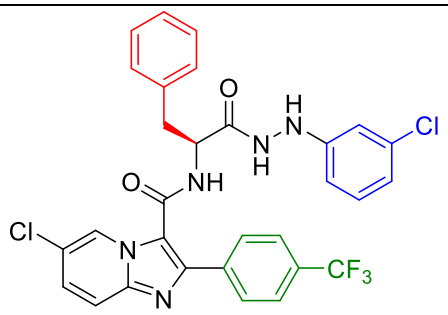 | 6.43 | 52.3 | 13.1 | 52.3 | 26.1 | 13.1 |
| **44Ds** | 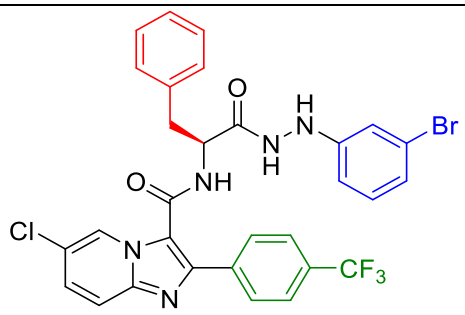 | 6.70 | 24.4 | 12.2 | 24.4 | 12.2 | 12.2 |
| **44Dt** | 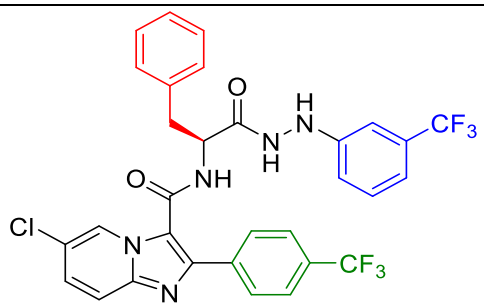 | 6.79 | - | 99.1 | - | - | - |
| **44Du** | 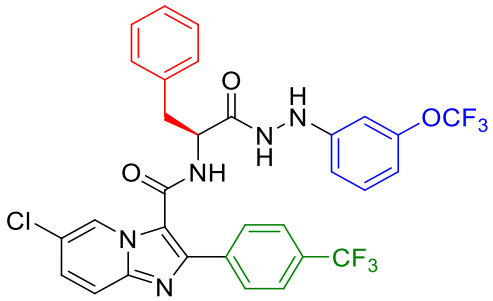 | 7.39 | - | - | - | - | - |
| **44Dv** | 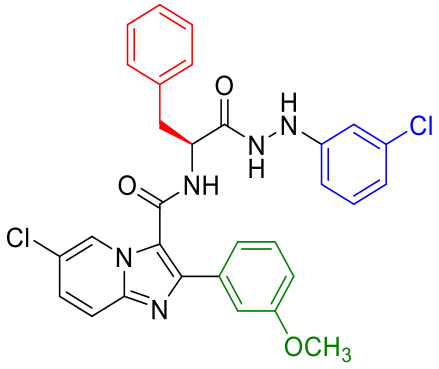 | 5.38 | - | 55.7 | - | 111.4 | 55.7 |

| | | | | | | | |
|---|---|---|---|---|---|---|---|
| **44Dw** | 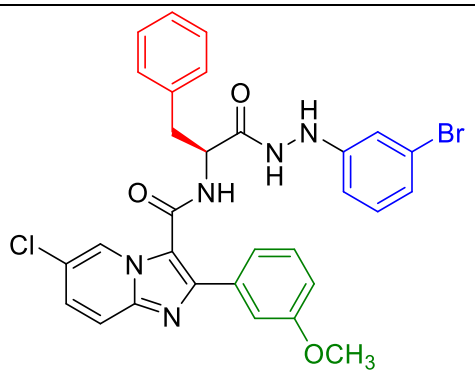 | 5.65 | - | 51.7 | - | 103.4 | 51.7 |
| **44Dx** | 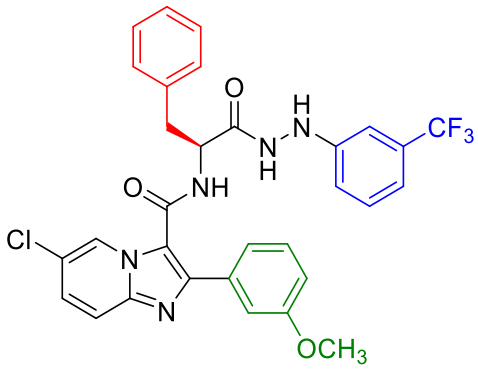 | 5.74 | - | 52.6 | - | 105.3 | 105.3 |
| **44Dy** | 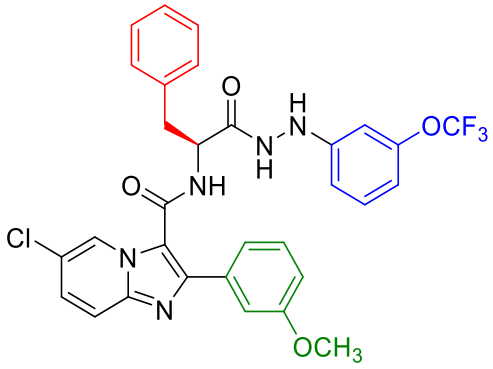 | 6.35 | - | 102.6 | - | 102.6 | 102.6 |
| **44Dz** | 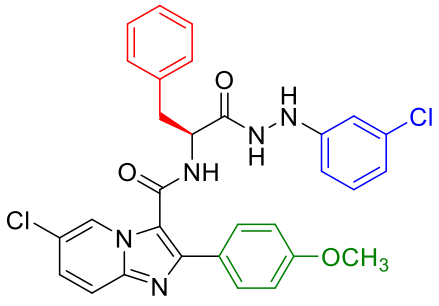 | 5.38 | - | - | 46.6 | - | - |

| | | | | | | | |
|---|---|---|---|---|---|---|---|
| **44Ea** | 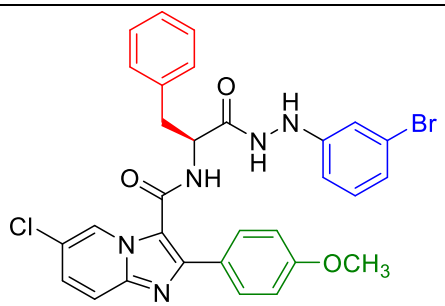 | 5.65 | 54.6 | - | 24.7 | 55.8 | 22.7 |
| **44Eb** | 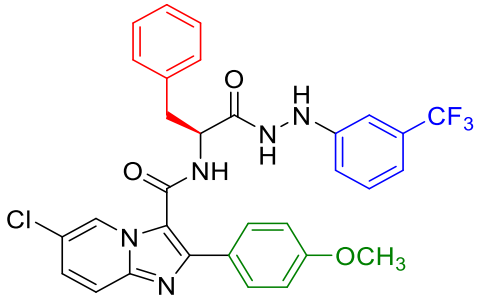 | 5.74 | 73.8 | - | 29.8 | - | 52.6 |
| **44Ec** | 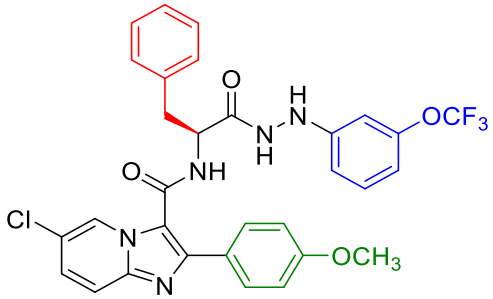 | 6.35 | - | - | 36.7 | 60.8 | - |

### 8.1.4 Heterocyclic compounds:

| | | | MIC (μM) | | | | |
|---|---|---|---|---|---|---|---|
| Entry | Chemical structure | LogP | WT 7902 | INH$^R$ 8245 | RIF$^R$ 8247 | RIF/INH$^R$ 8250 | RIF/INH$^R$ 8258 |
| 44Ed | 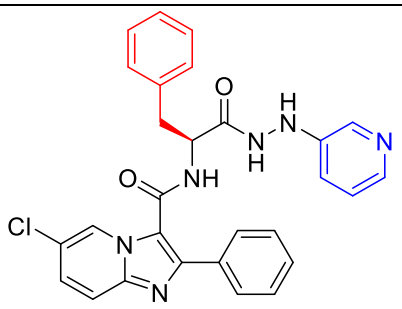 | 3.61 | - | - | - | - | - |
| 44Ee | 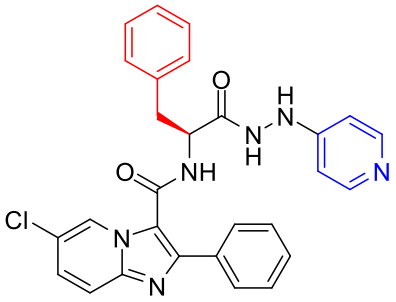 | 3.61 | - | - | - | - | - |
| 44Ef | 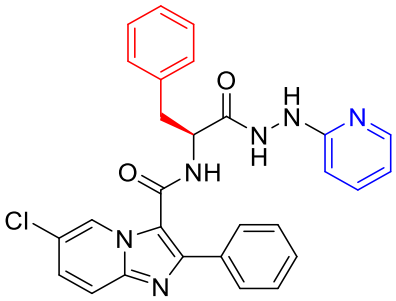 | 4.33 | - | - | - | - | - |
| 44Eg | 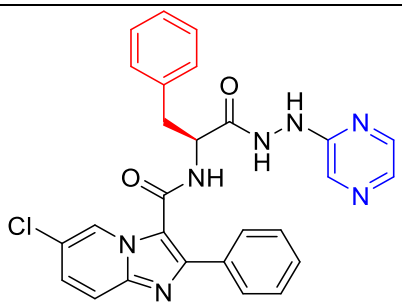 | 2.99 | - | - | - | - | - |
| 44Eh | 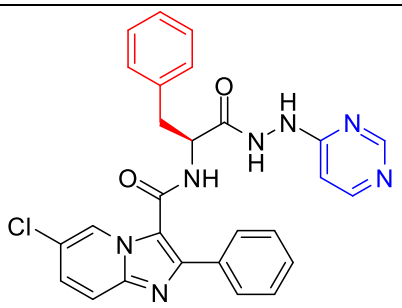 | 3.73 | - | - | - | - | - |

| | | | | | | | |
|---|---|---|---|---|---|---|---|
| **44Ei** | 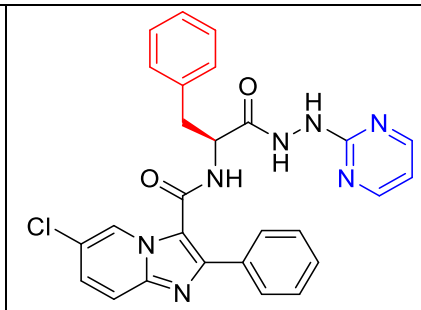 | 3.52 | - | - | - | - | - |
| **44Ej** | 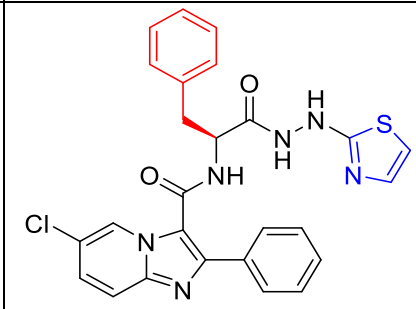 | 4.67 | - | - | - | - | - |
| **44Ek** | 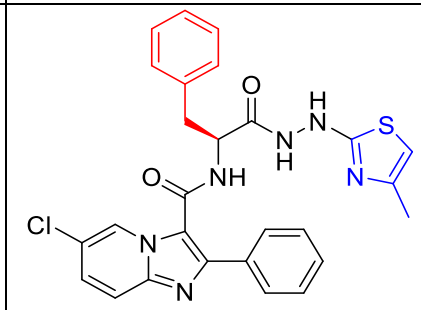 | 5.37 | - | - | - | - | - |
| **44El** | 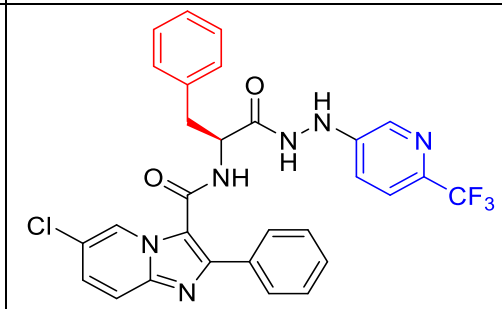 | 4.95 | - | - | - | - | - |
| **44Em** | 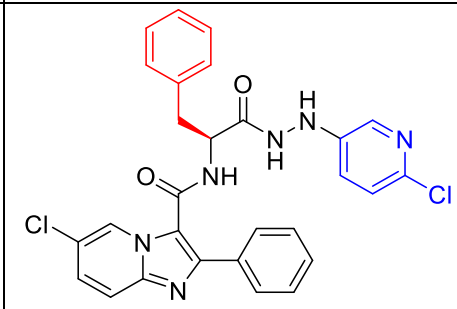 | 4.51 | - | - | - | - | - |
| **44En** | 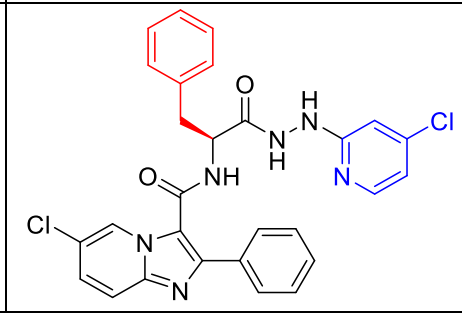 | 4.88 | 86.9 | 39.9 | 108 | 28.7 | 35.6 |

| | | | | | | | |
|---|---|---|---|---|---|---|---|
| **44Eo** | 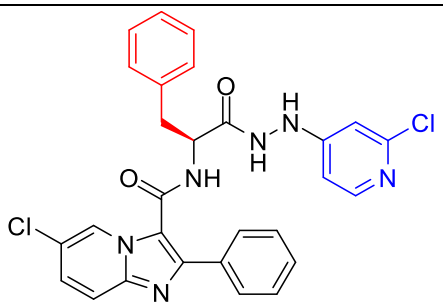 | 4.51 | 60.9 | 63.5 | 67.1 | 50.4 | 66.3 |
| **44Ep** | 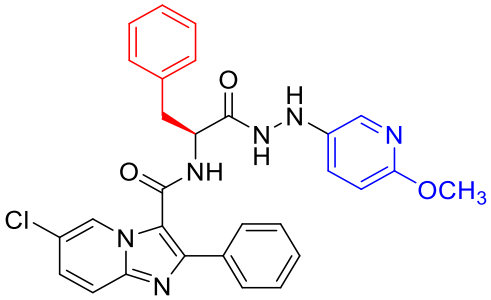 | 4.20 | - | - | - | - | - |

## 8.2 *In silico* ADME data:

### 8.2.1 First-series of imidazo[1,2-*a*]pyridine analogues

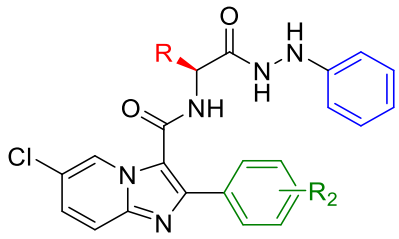


**44(Cb-De)**

| Entry | R | $R_2$ | Mwt | nRot | LogP | HBD | HBA | nLV | TPSA | LogS | HIA (%) | BBB |
|---|---|---|---|---|---|---|---|---|---|---|---|---|
| **INH** | - | - | 137.0 | 2 | -0.6 | 3 | 4 | 0 | 68.0 | -0.02 | High | no |
| **BDQ** | - | - | 554.1 | 8 | 7.5 | 1 | 4 | 2 | 45.5 | -5.1 | High | yes |
| **44Aa** | Gly | 3-Cl | 453.0 | 8 | 3.34 | 3 | 7 | 0 | 87.5 | -4.7 | High | yes |
| **44Ab** | | 4-Cl | 453.0 | 8 | 3.34 | 3 | 7 | 0 | 87.5 | -4.7 | High | yes |
| **44Ac** | | 3-CF3 | 487.1 | 9 | 3.70 | 3 | 7 | 0 | 87.5 | -4.8 | High | yes |
| **44Ad** | | 4-CF3 | 487.1 | 9 | 3.70 | 3 | 7 | 0 | 87.5 | -4.8 | High | yes |
| **44Ae** | | 3-$OCH_3$ | 449.1 | 9 | 2.65 | 3 | 8 | 0 | 96.7 | -4.7 | High | no |
| **44Af** | | 4-$OCH_3$ | 449.1 | 9 | 2.65 | 3 | 8 | 0 | 96.7 | -4.7 | High | no |
| **44Ag** | Ala | 3-Cl | 467.0 | 8 | 3.83 | 3 | 7 | 0 | 87.5 | -4.6 | High | yes |
| **44Ah** | | 4-Cl | 467.0 | 8 | 3.83 | 3 | 7 | 0 | 87.5 | -4.6 | High | yes |
| **44Ai** | | 3-CF3 | 501.1 | 9 | 4.19 | 3 | 7 | 0 | 87.5 | -5.1 | High | yes |
| **44Aj** | | 4-CF3 | 501.1 | 9 | 4.19 | 3 | 7 | 0 | 87.5 | -5.1 | High | yes |
| **44Ak** | | 3-$OCH_3$ | 463.1 | 9 | 3.15 | 3 | 8 | 0 | 96.7 | -4.8 | High | no |
| **44Al** | | 4-$OCH_3$ | 463.1 | 9 | 3.15 | 3 | 8 | 0 | 96.7 | -4.8 | High | no |
| **44Am** | Met | 3-Cl | 527.0 | 11 | 4.16 | 3 | 7 | 1 | 87.5 | -4.9 | High | no |
| **44An** | | 4-Cl | 527.0 | 11 | 4.16 | 3 | 7 | 1 | 87.5 | -4.9 | High | no |
| **44Ao** | | 3-CF3 | 561.1 | 12 | 4.53 | 3 | 7 | 1 | 87.5 | -5.2 | High | no |
| **44Ap** | | 4-CF3 | 561.1 | 12 | 4.53 | 3 | 7 | 1 | 87.5 | -5.2 | High | no |
| **44Aq** | | 3-$OCH_3$ | 523.1 | 12 | 3.48 | 3 | 8 | 1 | 96.7 | -4.9 | High | no |
| **44Ar** | | 4-$OCH_3$ | 523.1 | 12 | 3.48 | 3 | 8 | 1 | 96.7 | -4.9 | High | no |
| **44As** | Leu | 3-Cl | 509.1 | 10 | 5.06 | 3 | 7 | 0 | 87.5 | -5.2 | High | no |
| **44At** | | 4-Cl | 509.1 | 10 | 5.06 | 3 | 7 | 0 | 87.5 | -5.2 | High | no |
| **44Au** | | 3-CF3 | 543.1 | 11 | 5.43 | 3 | 7 | 1 | 87.5 | -5.4 | High | no |
| **44Av** | | 4-CF3 | 543.1 | 11 | 5.43 | 3 | 7 | 1 | 87.5 | -5.4 | High | no |
| **44Aw** | | 3-$OCH_3$ | 505.1 | 11 | 4.38 | 3 | 8 | 0 | 96.7 | -5.1 | High | no |
| **44Ax** | | 4-$OCH_3$ | 505.1 | 11 | 4.38 | 3 | 8 | 0 | 96.7 | -5.1 | High | no |
| **44Ay** | Phe | 3-Cl | 557.1 | 11 | 5.50 | 3 | 7 | 2 | 87.5 | -5.4 | High | No |

| | | | | | | | | | | | |
|---|---|---|---|---|---|---|---|---|---|---|---|
| **44Az** | 4-Cl | 557.1 | 11 | 5.50 | 3 | 7 | 2 | 87.5 | -5.4 | High | No |
| **44Ba** | 3-CF3 | 577.1 | 11 | 5.87 | 3 | 7 | 2 | 87.5 | -5.6 | High | No |
| **44Bb** | 4-CF3 | 577.1 | 11 | 5.87 | 3 | 7 | 2 | 87.5 | -5.6 | High | No |
| **44Bc** | 3-$OCH_3$ | 539.1 | 11 | 4.82 | 3 | 8 | 1 | 96.7 | -5.0 | High | No |
| **44Bd** | 4-$OCH_3$ | 539.1 | 11 | 4.82 | 3 | 8 | 1 | 96.7 | -5.0 | High | No |

### 8.2.2 Second-series of imidazo[1,2-*a*]pyridine analogues

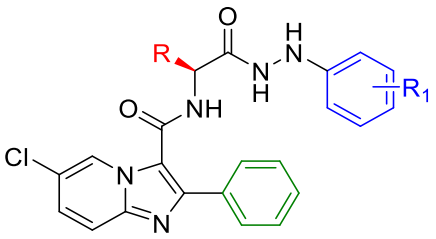


**44(Aa-Bx)**

| Entry | R | $R_1$ | Mwt | nRot | LogP | HBD | HBA | nLV | TPSA | LogS | HIA (%) | BBB |
|---|---|---|---|---|---|---|---|---|---|---|---|---|
| **INH** | - | - | 137.0 | 2 | -0.6 | 3 | 4 | 0 | 68.0 | -0.02 | High | no |
| **BDQ** | - | - | 554.1 | 8 | 7.5 | 1 | 4 | 2 | 45.5 | -5.1 | High | yes |
| **44Be** | Gly | H | 419.1 | 8 | 2.78 | 3 | 7 | 0 | 87.5 | -4.0 | High | yes |
| **44Bf** | | 3-Cl | 453.0 | 8 | 3.34 | 3 | 7 | 0 | 87.5 | -4.6 | High | yes |
| **44Bg** | | 4-Cl | 453.0 | 8 | 3.34 | 3 | 7 | 0 | 87.5 | -4.6 | High | yes |
| **44Bh** | | 3-Br | 497.0 | 8 | 3.61 | 3 | 7 | 0 | 87.5 | -4.7 | High | yes |
| **44Bi** | | 4-Br | 497.0 | 8 | 3.61 | 3 | 7 | 0 | 87.5 | -4.7 | High | yes |
| **44Bj** | | 3-$CF_3$ | 487.1 | 9 | 3.70 | 3 | 7 | 0 | 87.5 | -4.8 | High | yes |
| **44Bk** | | 4-$CF_3$ | 487.1 | 9 | 3.70 | 3 | 7 | 0 | 87.5 | -4.8 | High | yes |
| **44Bl** | | 3-$OCF_3$ | 503.1 | 10 | 4.31 | 3 | 8 | 0 | 96.7 | -5.2 | High | yes |
| **44Bm** | | 4-$OCF_3$ | 503.1 | 10 | 4.31 | 3 | 8 | 0 | 96.7 | -5.2 | High | yes |
| **44Bn** | Ala | H | 433.1 | 8 | 3.27 | 3 | 7 | 0 | 87.5 | -4.1 | High | yes |
| **44Bo** | | 3-Cl | 467.0 | 8 | 3.83 | 3 | 7 | 0 | 87.5 | -4.5 | High | yes |
| **44Bp** | | 4-Cl | 467.0 | 8 | 3.83 | 3 | 7 | 0 | 87.5 | -4.5 | High | yes |
| **44Bq** | | 3-Br | 511.0 | 8 | 4.10 | 3 | 7 | 1 | 87.5 | -4.6 | High | yes |
| **44Br** | | 4-Br | 511.0 | 8 | 4.10 | 3 | 7 | 1 | 87.5 | -4.6 | High | yes |
| **44Bs** | | 3-$CF_3$ | 501.1 | 9 | 4.19 | 3 | 7 | 0 | 87.5 | -4.9 | High | yes |
| **44Bt** | | 4-$CF_3$ | 501.1 | 9 | 4.19 | 3 | 7 | 0 | 87.5 | -4.9 | High | yes |
| **44Bu** | | 3-$OCF_3$ | 517.1 | 10 | 4.80 | 3 | 8 | 1 | 96.7 | -5.3 | High | no |
| **44Bv** | | 4-$OCF_3$ | 517.1 | 10 | 4.80 | 3 | 8 | 1 | 96.7 | -5.3 | High | no |
| **44Bw** | Leu | H | 475.1 | 10 | 4.51 | 3 | 7 | 0 | 87.5 | -4.5 | High | no |
| **44Bx** | | 3-Cl | 509.1 | 10 | 5.06 | 3 | 7 | 0 | 87.5 | -5.1 | High | yes |
| **44By** | | 4-Cl | 509.1 | 10 | 5.06 | 3 | 7 | 0 | 87.5 | -5.1 | High | yes |
| **44Bz** | | 3-Br | 553.0 | 10 | 5.33 | 3 | 7 | 2 | 87.5 | -5.2 | High | yes |
| **44Ca** | | 4-Br | 553.0 | 10 | 5.33 | 3 | 7 | 2 | 87.5 | -5.2 | High | yes |
| **44Cb** | | 3-$CF_3$ | 543.1 | 11 | 5.43 | 3 | 7 | 2 | 87.5 | -5.3 | High | yes |
| **44Cc** | | 4-$CF_3$ | 543.1 | 11 | 5.43 | 3 | 7 | 2 | 87.5 | -5.3 | High | yes |
| **44Cd** | | 3-$OCF_3$ | 559.1 | 12 | 6.03 | 3 | 8 | 2 | 96.7 | -5.8 | High | no |

| | | | | | | | | | | | | |
|---|---|---|---|---|---|---|---|---|---|---|---|---|
| **44Ce** | | 4-$OCF_3$ | 559.1 | 12 | 6.03 | 3 | 8 | 2 | 96.7 | -5.8 | High | no |
| **44Cf** | | H | 493.1 | 11 | 3.50 | 3 | 7 | 0 | 87.5 | -4.5 | High | no |
| **44Cg** | | 3-Cl | 527.0 | 11 | 4.06 | 3 | 7 | 1 | 87.5 | -4.7 | High | no |
| **44Ch** | | 4-Cl | 527.0 | 11 | 4.06 | 3 | 7 | 1 | 87.5 | -4.7 | High | no |
| **44Ci** | | 3-Br | 571.0 | 11 | 4.33 | 3 | 7 | 1 | 87.5 | -4.9 | High | no |
| **44Cj** | Met | 4-Br | 571.0 | 11 | 4.33 | 3 | 7 | 1 | 87.5 | -4.9 | High | no |
| **44Ck** | | 3-$CF_3$ | 561.1 | 12 | 4.42 | 3 | 7 | 1 | 87.5 | -5.1 | High | no |
| **44Cl** | | 4-$CF_3$ | 561.1 | 12 | 4.42 | 3 | 7 | 1 | 87.5 | -5.1 | High | no |
| **44Cm** | | 3-$OCF_3$ | 577.1 | 13 | 5.03 | 3 | 8 | 1 | 96.7 | -5.5 | High | no |
| **44Cn** | | 4-$OCF_3$ | 577.1 | 13 | 5.03 | 3 | 8 | 1 | 96.7 | -5.5 | High | no |
| **44Co** | | H | 509.1 | 10 | 4.95 | 3 | 7 | 0 | 87.5 | -4.3 | High | No |
| **44Cp** | | 3-Cl | 543.1 | 10 | 5.50 | 3 | 7 | 2 | 87.5 | -5.1 | High | No |
| **44Cq** | | 4-Cl | 543.1 | 10 | 5.50 | 3 | 7 | 2 | 87.5 | -5.1 | High | No |
| **44Cr** | | 3-Br | 587.0 | 10 | 5.78 | 3 | 7 | 2 | 87.5 | -5.2 | High | No |
| **44Cs** | Phe | 4-Br | 587.0 | 10 | 5.78 | 3 | 7 | 2 | 87.5 | -5.2 | High | No |
| **44Ct** | | 3-$CF_3$ | 577.1 | 11 | 5.87 | 3 | 7 | 2 | 87.5 | -5.6 | High | No |
| **44Cu** | | 4-$CF_3$ | 577.1 | 11 | 5.87 | 3 | 7 | 2 | 87.5 | -5.6 | High | No |
| **44Cv** | | 3-$OCF_3$ | 593.1 | 12 | 6.47 | 3 | 8 | 2 | 96.7 | -5.9 | High | No |
| **44Cw** | | 4-$OCF_3$ | 593.1 | 12 | 6.47 | 3 | 8 | 2 | 96.7 | -5.9 | High | No |
| **44Cx** | | H | 523.1 | 11 | 5.36 | 3 | 7 | 2 | 87.5 | -4.3 | High | No |
| **44Cy** | | 3-Cl | 557.1 | 11 | 5.92 | 3 | 7 | 2 | 87.5 | -5.1 | High | No |
| **44Cz** | Hph | 3-Br | 601.0 | 11 | 6.91 | 3 | 7 | 2 | 87.5 | -5.2 | High | No |
| **44Da** | | 4-Br | 601.0 | 11 | 6.91 | 3 | 7 | 2 | 87.5 | -5.2 | High | No |
| **44Db** | | 3-$CF_3$ | 591.1 | 12 | 6.28 | 3 | 7 | 2 | 87.5 | -5.7 | High | No |

### 8.2.3 Third-series of imidazo[1,2-*a*]pyridine analogues

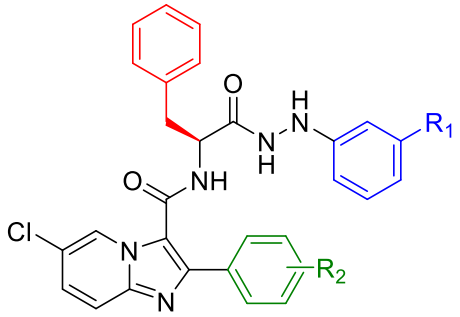


**44(Df-Ec)**

| Entry | $R_1$ | $R_2$ | Mwt | nRot | LogP | HB D | HB A | nLV | TPSA | LogS | HIA (%) | BBB |
|---|---|---|---|---|---|---|---|---|---|---|---|---|
| **44Df** | 3-Cl | 3-Cl | 591.1 | 11 | 6.06 | 3 | 7 | 2 | 87.5 | -5.7 | High | No |
| **44Dg** | 3-Br | | 635.0 | 11 | 6.33 | 3 | 7 | 2 | 87.5 | -5.8 | High | No |
| **44Dh** | 3-$CF_3$ | | 625.1 | 12 | 6.43 | 3 | 7 | 2 | 87.5 | -6.2 | High | No |
| **44Di** | 3-$OCF_3$ | | 641.1 | 13 | 7.03 | 3 | 8 | 2 | 96.7 | -6.5 | High | No |
| **44Dj** | 3-Cl | 4-Cl | 591.1 | 11 | 6.06 | 3 | 7 | 2 | 87.5 | -5.7 | High | No |
| **44Dk** | 3-Br | | 635.0 | 11 | 6.33 | 3 | 7 | 2 | 87.5 | -5.8 | High | No |
| **44Dl** | 3-$CF_3$ | | 625.1 | 12 | 6.43 | 3 | 7 | 2 | 87.5 | -6.2 | High | No |
| **44Dm** | 3-$OCF_3$ | | 641.1 | 13 | 7.03 | 3 | 8 | 2 | 96.7 | -6.5 | High | No |
| **44Dn** | 3-Cl | 3-$CF_3$ | 611.1 | 11 | 6.43 | 3 | 7 | 2 | 87.5 | -6.0 | High | No |
| **44Do** | 3-Br | | 655.0 | 11 | 6.70 | 3 | 7 | 2 | 87.5 | -6.0 | High | No |
| **44Dp** | 3-$CF_3$ | | 645.1 | 12 | 6.79 | 3 | 7 | 2 | 87.5 | -6.5 | High | No |
| **44Dq** | 3-$OCF_3$ | | 661.1 | 13 | 7.39 | 3 | 8 | 2 | 96.7 | -6.7 | High | No |
| **44Dr** | 3-Cl | 4-$CF_3$ | 611.1 | 11 | 6.43 | 3 | 7 | 2 | 87.5 | -6.0 | High | No |
| **44Ds** | 3-Br | | 655.0 | 11 | 6.70 | 3 | 7 | 2 | 87.5 | -6.0 | High | No |
| **44Dt** | 3-$CF_3$ | | 645.1 | 12 | 6.79 | 3 | 7 | 2 | 87.5 | -6.5 | High | No |
| **44Du** | 3-$OCF_3$ | | 661.1 | 13 | 7.39 | 3 | 8 | 2 | 96.7 | -6.7 | High | No |
| **44Dv** | 3-Cl | 3-$OCH_3$ | 573.1 | 11 | 5.38 | 3 | 8 | 2 | 96.7 | -5.4 | High | No |
| **44Dw** | 3-Br | | 617.0 | 11 | 5.65 | 3 | 8 | 2 | 96.7 | -5.5 | High | No |
| **44Dx** | 3-$CF_3$ | | 607.1 | 12 | 5.74 | 3 | 8 | 2 | 96.7 | -5.6 | High | No |
| **44Dy** | 3-$OCF_3$ | | 623.1 | 13 | 6.35 | 3 | 9 | 2 | 105.9 | -6.0 | High | No |
| **44Dz** | 3-Cl | 4-$OCH_3$ | 573.1 | 11 | 5.38 | 3 | 8 | 2 | 96.7 | -5.4 | High | No |
| **44Ea** | 3-Br | | 617.0 | 11 | 5.65 | 3 | 8 | 2 | 96.7 | -5.5 | High | No |
| **44Eb** | 3-$CF_3$ | | 607.1 | 12 | 5.74 | 3 | 8 | 2 | 96.7 | -5.6 | High | No |
| **44Ec** | 3-$OCF_3$ | | 623.1 | 13 | 6.35 | 3 | 9 | 2 | 105.9 | -6.0 | High | No |

## 8.3 The Crystal data and structure refinement

### Ethyl 6-chloro-2-(3-chlorophenyl)imidazo[1,2-*a*]pyridine-3-carboxylate 54c

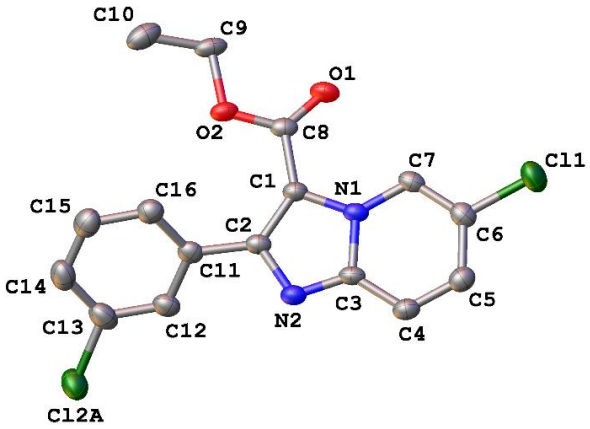


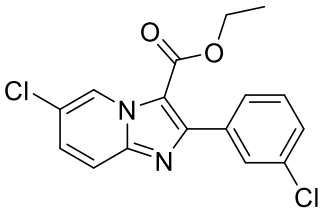


### Ethyl 6-chloro-2-phenylimidazo[1,2-*a*]pyridine-3-carboxylate 54a

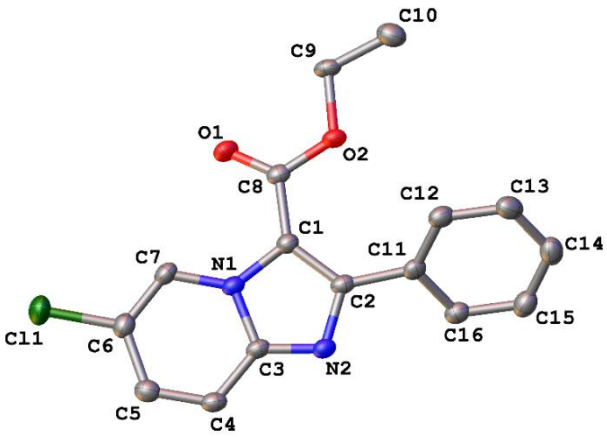


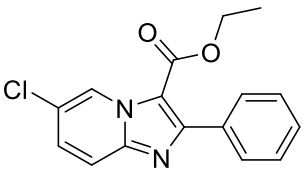


| Entry | 54c | 54a |
|---|---|---|
| Empirical formula | $C_{16}H_{12}Cl_2N_2O_2$ | $C_{16}H_{13}ClN_2O_2$ |
| Formula weight | 335.18 | 300.73 |
| Temperature/K | 150.0(2) | 150.0(2) |
| Crystal system | triclinic | triclinic |
| Space group | P-1 | P-1 |
| a/Å | 3.82048(5) | 3.8745(2) |

| | | |
|---|---|---|
| b/Å | 13.25773(15) | 12.5374(5) |
| c/Å | 15.36948(18) | 15.3482(5) |
| α/° | 75.6625(10) | 68.343(4) |
| β/° | 86.8302(10) | 86.388(4) |
| γ/° | 87.8706(10) | 86.912(3) |
| Volume/$Å^3$ | 752.856(16) | 691.17(5) |
| Z | 2 | 2 |
| $\rho_{calc}g/cm^3$ | 1.479 | 1.445 |
| $\mu/mm^{-1}$ | 3.953 | 2.500 |
| F(000) | 344.0 | 312.0 |
| Crystal size/$mm^3$ | 0.24 × 0.09 × 0.04 | 0.24 × 0.07 × 0.03 |
| Radiation | CuKα (λ = 1.54184) | CuKα (λ = 1.54184) |
| 2Θ range for data collection/° | 5.942 to 152.488 | 6.202 to 154.43 |
| Index ranges | -4 ≤ h ≤ 4, -16 ≤ k ≤ 16, -18 ≤ l ≤ 18 | -4 ≤ h ≤ 4, -15 ≤ k ≤ 15, -18 ≤ l ≤ 18 |
| Reflections collected | 27876 | 10007 |
| Independent reflections | 2976 [$R_{int}$ = 0.0384, $R_{sigma}$ = 0.0175] | 2691 [$R_{int}$ = 0.0391, $R_{sigma}$ = 0.0347] |
| Data/restraints/parameters | 2976/1/209 | 2691/0/191 |
| Goodness-of-fit on $F^2$ | 1.081 | 1.066 |
| Final R indexes [I>=2σ (I)] | $R_1$ = 0.0403, $wR_2$ = 0.1214 | $R_1$ = 0.0365, $wR_2$ = 0.0960 |
| Final R indexes [all data] | $R_1$ = 0.0423, $wR_2$ = 0.1232 | $R_1$ = 0.0409, $wR_2$ = 0.0999 |
| Largest diff. peak/hole / e $Å^{-3}$ | 0.46/-0.48 | 0.24/-0.28 |

**6-Chloro-2-phenylimidazo[1,2-*a*]pyridine-3-carboxylic acid 50a**

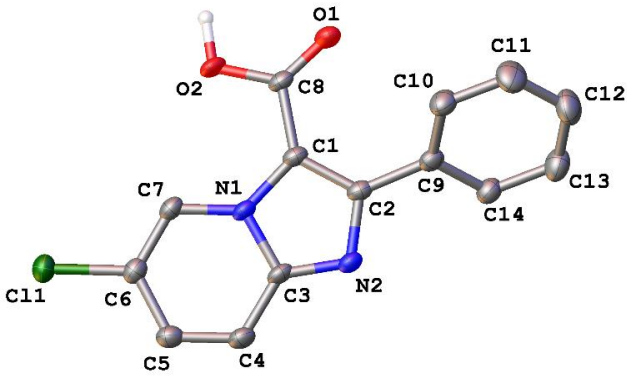


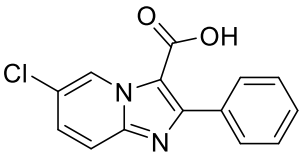


**6-chloro-2-(4-trifluoromethylphenyl)imidazo[1,2-*a*]pyridine-3-carboxylic acid 50f**

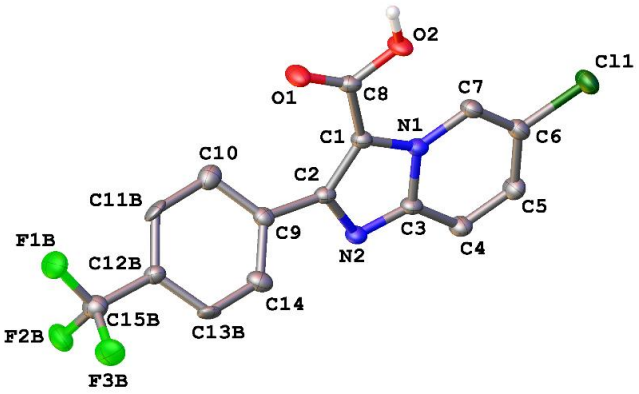


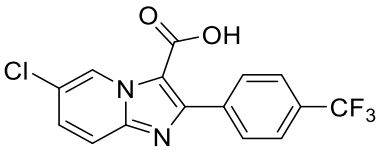


| **Entry** | **50a** | **50f** |
|---|---|---|
| Empirical formula | $C_{14}H_9ClN_2O_2$ | $C_{15}H_8ClF_3N_2O_2$ |
| Formula weight | 272.68 | 340.68 |
| Temperature/K | 150.0(2) | 150.0(2) |
| Crystal system | monoclinic | monoclinic |
| Space group | $P2_1/c$ | $P2_1/c$ |
| a/Å | 7.32490(10) | 3.89010(10) |
| b/Å | 14.07940(10) | 26.9704(9) |
| c/Å | 23.8701(2) | 12.9038(4) |
| α/° | 90 | 90 |

| | | |
|---|---|---|
| β/° | 98.7950(10) | 98.136(3) |
| γ/° | 90 | 90 |
| Volume/Å$^3$ | 2432.78(4) | 1340.21(7) |
| Z | 8 | 4 |
| $\rho_{calc}$g/cm$^3$ | 1.489 | 1.688 |
| μ/mm$^{-1}$ | 2.782 | 2.997 |
| F(000) | 1120.0 | 688.0 |
| Crystal size/mm$^3$ | 0.29 × 0.11 × 0.05 | 0.14 × 0.11 × 0.02 |
| Radiation | CuKα (λ = 1.54184) | CuKα (λ = 1.54184) |
| 2Θ range for data collection/° | 7.312 to 154.95 | 6.554 to 154.338 |
| Index ranges | -9 ≤ h ≤ 8, -17 ≤ k ≤ 17, -29 ≤ l ≤ 29 | -4 ≤ h ≤ 3, -33 ≤ k ≤ 33, -16 ≤ l ≤ 16 |
| Reflections collected | 44707 | 14561 |
| Independent reflections | 4846 [$R_{int}$ = 0.0452, $R_{sigma}$ = 0.0260] | 2666 [$R_{int}$ = 0.0328, $R_{sigma}$ = 0.0241] |
| Data/restraints/parameters | 4846/0/349 | 2666/463/274 |
| Goodness-of-fit on $F^2$ | 1.068 | 1.040 |
| Final R indexes [I>=2σ (I)] | $R_1$ = 0.0534, $wR_2$ = 0.1467 | $R_1$ = 0.0320, $wR_2$ = 0.0851 |
| Final R indexes [all data] | $R_1$ = 0.0579, $wR_2$ = 0.1509 | $R_1$ = 0.0364, $wR_2$ = 0.0876 |
| Largest diff. peak/hole / e Å$^{-3}$ | 1.08/-0.49 | 0.33/-0.24 |

**6-Chloro-N-(1-oxo-1-(2-(4-(trifluoromethyl)phenyl)hydrazineyl)propan-2-yl)-2-phenylimidazo[1,2-*a*]pyridine-3-carboxamide 44Bt**

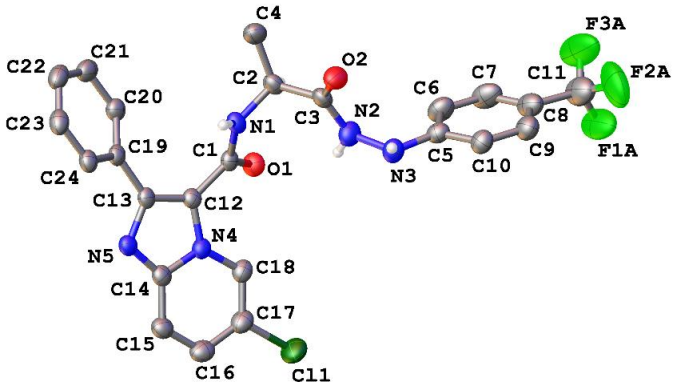


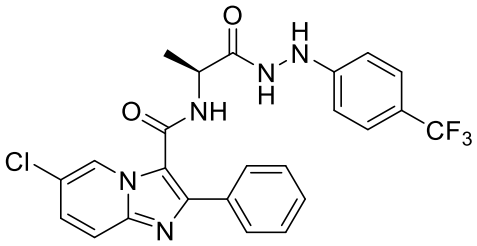


**(S)-6-chloro-N-(1-oxo-1-(2-phenylhydrazineyl)propan-2-yl)-2-(4-(trifluoromethyl)phenyl)imidazo[1,2-*a*]pyridine-3-carboxamide 44Aj**

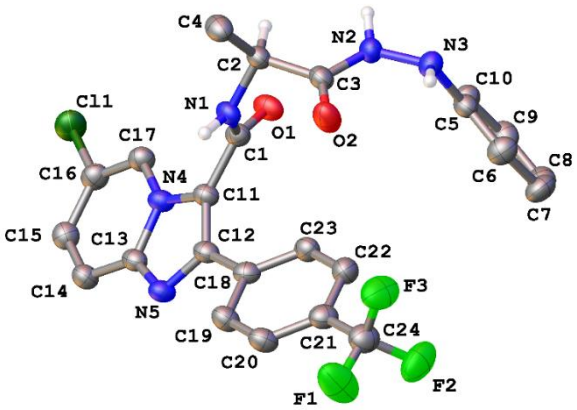


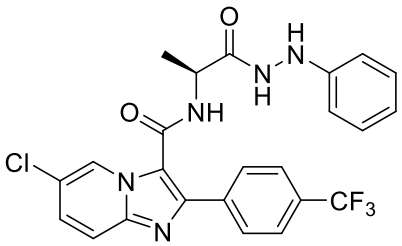


| **Entry** | **44Bt** | **44Aj** |
|---|---|---|
| Empirical formula | $C_{26}H_{25}ClF_3N_5O_3S$ | $C_{24}H_{19}ClF_3N_5O_2$ |
| Formula weight | 580.02 | 501.89 |
| Temperature/K | 150.0(2) | 150.0(2) |
| Crystal system | orthorhombic | monoclinic |
| Space group | $P2_12_12_1$ | $P2_1$ |
| a/Å | 6.98900(10) | 15.3171(6) |
| b/Å | 15.6967(3) | 7.4613(4) |

| | | |
|---|---|---|
| c/Å | 24.8546(6) | 19.7081(8) |
| α/° | 90 | 90 |
| β/° | 90 | 94.336(4) |
| γ/° | 90 | 90 |
| Volume/Å$^3$ | 2726.65(9) | 2245.90(18) |
| Z | 4 | 4 |
| $\rho_{calc}$g/cm$^3$ | 1.413 | 1.484 |
| μ/mm$^{-1}$ | 2.470 | 2.026 |
| F(000) | 1200.0 | 1032.0 |
| Crystal size/mm$^3$ | 0.16 × 0.11 × 0.02 | 0.35 × 0.05 × 0.03 |
| Radiation | CuKα (λ = 1.54184) | CuKα (λ = 1.54184) |
| 2Θ range for data collection/° | 6.66 to 154.312 | 4.496 to 154.33 |
| Index ranges | -8 ≤ h ≤ 8, -19 ≤ k ≤ 19, -30 ≤ l ≤ 30 | -18 ≤ h ≤ 19, -9 ≤ k ≤ 8, -23 ≤ l ≤ 24 |
| Reflections collected | 51109 | 38481 |
| Independent reflections | 5550 [$R_{int}$ = 0.0407, $R_{sigma}$ = 0.0203] | 8447 [$R_{int}$ = 0.0423, $R_{sigma}$ = 0.0366] |
| Data/restraints/parameters | 5550/357/391 | 8447/1/652 |
| Goodness-of-fit on $F^2$ | 1.054 | 1.076 |
| Final R indexes [I>=2σ (I)] | $R_1$ = 0.0312, $wR_2$ = 0.0850 | $R_1$ = 0.0408, $wR_2$ = 0.1021 |
| Final R indexes [all data] | $R_1$ = 0.0337, $wR_2$ = 0.0877 | $R_1$ = 0.0498, $wR_2$ = 0.1091 |
| Largest diff. peak/hole / e Å$^{-3}$ | 0.19/-0.27 | 0.28/-0.30 |
| Flack parameter | -0.013(5) | -0.009(8) |

***tert*-butyl (S)-(1-oxo-3-phenyl-1-(2-(pyridin-2-yl)hydrazineyl)propan-2-yl)carbamate 51Cf**

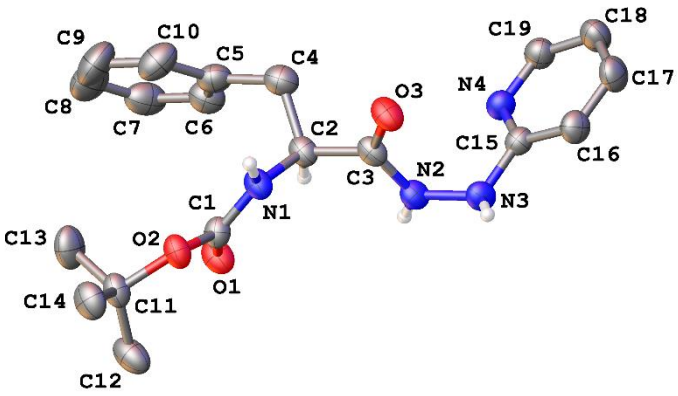


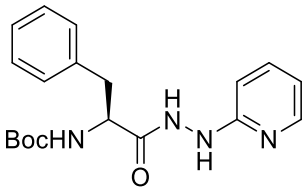


**(S)-6-chloro-N-(1-oxo-3-phenyl-1-(2-(pyridin-2-yl)hydrazineyl)propan-2-yl)-2-phenylimidazo[1,2-*a*]pyridine-3-carboxamide 44Ef**

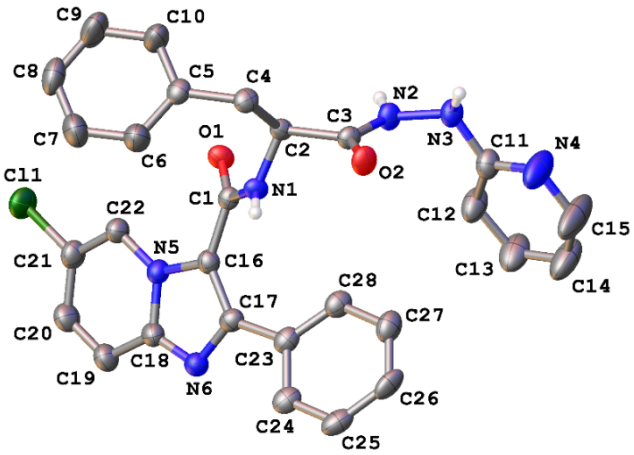


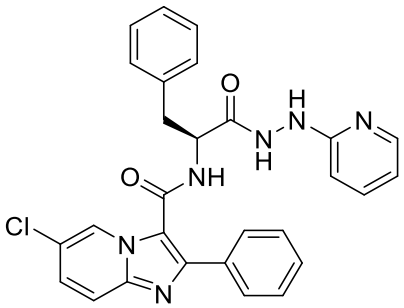


| Entry | 51Cf | 44Ef |
|---|---|---|
| Empirical formula | $C_{59}H_{76}Cl_2N_{12}O_9$ | $C_{28}H_{23}ClN_6O_2$ |
| Formula weight | 1168.21 | 510.97 |
| Temperature/K | 150.0(2) | 150.0(2) |
| Crystal system | orthorhombic | monoclinic |
| Space group | $P2_12_12_1$ | $P2_1$ |
| a/Å | 11.7479(3) | 4.9768(2) |
| b/Å | 18.8304(6) | 17.4331(7) |

| | | |
|---|---|---|
| c/Å | 28.7431(9) | 14.2282(5) |
| α/° | 90 | 90 |
| β/° | 90 | 99.488(4) |
| γ/° | 90 | 90 |
| Volume/Å$^3$ | 6358.5(3) | 1217.57(8) |
| Z | 4 | 2 |
| $\rho_{calc}$g/cm$^3$ | 1.220 | 1.394 |
| μ/mm$^{-1}$ | 1.425 | 1.711 |
| F(000) | 2480.0 | 532.0 |
| Crystal size/mm$^3$ | 0.31 × 0.05 × 0.02 | 0.23 × 0.05 × 0.01 |
| Radiation | CuKα (λ = 1.54184) | CuKα (λ = 1.54184) |
| 2Θ range for data collection/° | 5.61 to 154.688 | 6.298 to 154.766 |
| Index ranges | -14 ≤ h ≤ 5, -23 ≤ k ≤ 21, -34 ≤ l ≤ 34 | -6 ≤ h ≤ 5, -20 ≤ k ≤ 21, -17 ≤ l ≤ 17 |
| Reflections collected | 35564 | 17370 |
| Independent reflections | 12254 [$R_{int}$ = 0.0360, $R_{sigma}$ = 0.0371] | 4776 [$R_{int}$ = 0.0249, $R_{sigma}$ = 0.0232] |
| Data/restraints/parameters | 12254/672/812 | 4776/1/343 |
| Goodness-of-fit on $F^2$ | 1.038 | 1.054 |
| Final R indexes [I>=2σ (I)] | $R_1$ = 0.0380, $wR_2$ = 0.0908 | $R_1$ = 0.0394, $wR_2$ = 0.1007 |
| Final R indexes [all data] | $R_1$ = 0.0450, $wR_2$ = 0.0942 | $R_1$ = 0.0407, $wR_2$ = 0.1014 |
| Largest diff. peak/hole / e Å$^{-3}$ | 0.18/-0.30 | 0.38/-0.39 |
| Flack parameter | 0.017(7) | 0.016(5) |